

Fatigue Damage

Mechanical Vibration and Shock Analysis
second edition – volume 4

Fatigue Damage

Christian Lalanne

ISTE

 WILEY

First published in France in 1999 by Hermes Science Publications © Hermes Science Publications, 1999
First published in English in 2002 by Hermes Penton Ltd © English language edition Hermes Penton Ltd, 2002
Second edition published in Great Britain and the United States in 2009 by ISTE Ltd and John Wiley & Sons, Inc.

Apart from any fair dealing for the purposes of research or private study, or criticism or review, as permitted under the Copyright, Designs and Patents Act 1988, this publication may only be reproduced, stored or transmitted, in any form or by any means, with the prior permission in writing of the publishers, or in the case of reprographic reproduction in accordance with the terms and licenses issued by the CLA. Enquiries concerning reproduction outside these terms should be sent to the publishers at the undermentioned address:

ISTE Ltd
27-37 St George's Road
London SW19 4EU
UK

www.iste.co.uk

© ISTE Ltd, 2009

John Wiley & Sons, Inc.
111 River Street
Hoboken, NJ 07030
USA

www.wiley.com

The rights of Christian Lalanne to be identified as the author of this work have been asserted by him in accordance with the Copyright, Designs and Patents Act 1988.

Library of Congress Cataloging-in-Publication Data

Lalanne, Christian.

[Vibrations et chocs mécaniques. English]

Mechanical vibration and shock analysis / Christian Lalanne. -- 2nd ed.

v. cm.

Includes bibliographical references and index.

Contents: v. 1. Sinusoidal vibration -- v. 2. Mechanical shock -- v. 3. Random vibration -- v. 4. Fatigue damage -- v. 5. Specification development.

ISBN 978-1-84821-122-3 (v. 1) -- ISBN 978-1-84821-123-0 (v. 2) 1. Vibration. 2. Shock (Mechanics). I. Title.

TA355.L2313 2002

624.1'76--dc22

2009013736

British Library Cataloguing-in-Publication Data

A CIP record for this book is available from the British Library

ISBN: 978-1-84821-121-6 (Set of 5 Volumes)

ISBN: 978-1-84821-125-4 (Volume 4)

Printed and bound in Great Britain by CPI Antony Rowe, Chippenham and Eastbourne.



Table of Contents

Foreword to Series	xiii
Introduction	xvii
List of Symbols	xix
Chapter 1. Concepts of Material Fatigue	1
1.1. Introduction	1
1.2. Types of dynamic loads (or stresses)	2
1.2.1. Cyclic stress	2
1.2.2. Alternating stress	4
1.2.3. Repeated stress	5
1.2.4. Combined steady and cyclic stress	5
1.2.5. Skewed alternating stress	6
1.2.6. Random and transitory stresses	6
1.3. Damage arising from fatigue	7
1.4. Characterization of endurance of materials	10
1.4.1. S-N curve	10
1.4.2. Statistical aspect	13
1.4.3. Distribution laws of endurance	14
1.4.4. Distribution laws of fatigue strength	16
1.4.5. Relation between fatigue limit and static properties of materials	18
1.4.6. Analytical representations of S-N curve	21
1.5. Factors of influence	30
1.5.1. General	30
1.5.2. Scale	31
1.5.3. Overloads	32
1.5.4. Frequency of stresses	34
1.5.5. Types of stresses	34

1.5.6. Non-zero mean stress	35
1.6. Other representations of S-N curves	37
1.6.1. Haigh diagram.	37
1.6.2. Statistical representation of Haigh diagram	44
1.7. Prediction of fatigue life of complex structures.	44
1.8. Fatigue in composite materials	45
Chapter 2. Accumulation of Fatigue Damage	47
2.1. Evolution of fatigue damage.	47
2.2. Classification of various laws of accumulation.	48
2.3. Miner's method	49
2.3.1. Miner's rule	49
2.3.2. Scatter of damage to failure as evaluated by Miner.	53
2.3.3. Validity of Miner's law of accumulation of damage in case of random stress	57
2.4. Modified Miner's theory	59
2.4.1. Principle	59
2.4.2. Accumulation of damage using modified Miner's rule.	60
2.5. Henry's method	63
2.6. Modified Henry's method	65
2.7. Corten and Dolan's method	65
2.8. Other theories	67
Chapter 3. Counting Methods for Analyzing Random Time History	71
3.1. General	71
3.2. Peak count method	75
3.2.1. Presentation of method.	75
3.2.2. Derived methods	78
3.2.3. Range-restricted peak count method.	79
3.2.4. Level-restricted peak count method	79
3.3. Peak between mean-crossing count method.	81
3.3.1. Presentation of method.	81
3.3.2. Elimination of small variations.	83
3.4. Range count method	84
3.4.1. Presentation of method.	84
3.4.2. Elimination of small variations.	86
3.5. Range-mean count method.	87
3.5.1. Presentation of method.	87
3.5.2. Elimination of small variations.	90
3.6. Range-pair count method.	92
3.7. Hayes' counting method	96

3.8. Ordered overall range counting method	97
3.9. Level-crossing count method	100
3.10. Peak valley peak counting method	104
3.11. Fatigue-meter counting method	109
3.12. Rainflow counting method	111
3.12.1. Principle of method	111
3.12.2. Subroutine for rainflow counting	117
3.13. NRL (National Luchtvaart Laboratorium) counting method	120
3.14. Evaluation of time spent at a given level	123
3.15. Influence of levels of load below fatigue limit on fatigue life	124
3.16. Test acceleration	124
3.17. Presentation of fatigue curves determined by random vibration tests	126
Chapter 4. Fatigue Damage by One-degree-of-freedom Mechanical System	129
4.1. Introduction.	129
4.2. Calculation of fatigue damage due to signal versus time	130
4.3. Calculation of fatigue damage due to acceleration spectral density	132
4.3.1. General case	132
4.3.2. Approximate expression of the probability density of peaks	137
4.3.3. Particular case of a wide-band response, e.g. at the limit $r = 0$	138
4.3.4. Particular case of narrow band response	140
4.3.5. Rms response to narrow band noise G_0 of width Δf when $G_0 \Delta f = \text{constant}$	152
4.4. Equivalent narrow band noise	153
4.4.1. Use of relation established for narrow band response	153
4.4.2. Alternative: use of mean number of maxima per second.	155
4.4.3. Approximation to real maxima distribution using a modified Rayleigh distribution.	157
4.5. Calculation of fatigue damage from the probability density of domains	161
4.5.1. Differences between the probability of peaks and of ranges.	161
4.5.2. Wirsching's approach	166
4.5.3. Chaudhury and Dover's approach	169
4.5.4. Dirlik's probability density	172
4.5.5. Expression of the fatigue damage from the Dirlik probability density	178
4.6. Comparison of S-N curves established under sinusoidal and random loads.	179
4.7. Comparison of theory and experiment	183

4.8. Influence of shape of power spectral density and value of irregularity factor	189
4.9. Effects of peak truncation	189
4.10. Truncation of stress peaks	190
4.10.1. Particular case of a narrow band noise.	191
4.10.2. Layout of the S-N curve for a truncated distribution	199
Chapter 5. Standard Deviation of Fatigue Damage	205
5.1. Calculation of standard deviation of damage: Bendat's method	205
5.2. Calculation of standard deviation of damage: method of Crandall <i>et al.</i>	210
5.3. Comparison of Mark and Bendat's results.	214
5.4. Statistical S-N curves	220
5.4.1. Definition of statistical curves	220
5.4.2. Bendat's formulation.	221
5.4.3. Mark's formulation.	224
Chapter 6. Fatigue Damage using other Calculation Assumptions.	229
6.1. S-N curve represented by two segments of a straight line on logarithmic scales (taking into account fatigue limit)	229
6.2. S-N curve defined by two segments of straight line on log-lin scales.	232
6.3. Hypothesis of non-linear accumulation of damage.	235
6.3.1. Corten-Dolan's accumulation law	235
6.3.2. Morrow's accumulation model.	236
6.4. Random vibration with non-zero mean: use of modified Goodman diagram.	239
6.5. Non-Gaussian distribution of instantaneous values of signal.	241
6.5.1. Influence of distribution law of instantaneous values.	241
6.5.2. Influence of peak distribution.	242
6.5.3. Calculation of damage using Weibull distribution	243
6.5.4. Comparison of Rayleigh assumption/peak counting	246
6.6. Non-linear mechanical system.	247
Chapter 7. Low Fatigue Cycle	249
7.1. Overview	249
7.2. Definitions	250
7.2.1. Baushinger effect	250
7.2.2. Cyclic strain hardening	251
7.2.3. Properties of cyclic stress-strain curves	251
7.2.4. Stress-strain curve	251
7.2.5. Hysteresis and fracture by fatigue	254

7.2.6. Significant factors influencing hysteresis and fracture by fatigue	255
7.2.7. Cyclic stress-stress curve (or cyclic consolidation curve)	255
7.3. Behavior of materials experiencing strains in the oligocyclic domain	256
7.3.1. Types of behaviors	256
7.3.2. Cyclic strain hardening	257
7.3.3. Cyclic strain softening	258
7.3.4. Cyclically stable metals	260
7.3.5. Mixed behavior	260
7.4. Influence of the level application sequence	261
7.5. Development of the cyclic stress-strain curve.	262
7.6. Total strain	263
7.7. Fatigue strength curve	264
7.7.1. Basquin curve	265
7.8. Relation between plastic strain and number of cycles to fracture	265
7.8.1. Orowan relation	265
7.8.2. Manson relation	265
7.8.3. Coffin relation	266
7.8.4. Shanley relation	276
7.8.5. Gerberich relation.	276
7.8.6. Sachs, Gerberich, Weiss and Latorre relation	276
7.8.7. Martin relation	276
7.8.8. Tavernelli and Coffin relation	277
7.8.9. Manson relation	278
7.8.10. Ohji <i>et al.</i> relation	279
7.8.11. Bui-Quoc <i>et al.</i> relation	279
7.9. Influence of the frequency and temperature in the plastic field	279
7.9.1. Overview.	279
7.9.2. Influence of frequency.	280
7.9.3. Influence of temperature and frequency.	280
7.9.4. Effect of frequency on plastic strain range	282
7.9.5. Equation of generalized fatigue	283
7.10. Laws of damage accumulation.	284
7.10.1. Miner rule	284
7.10.2. Yao and Munse relation	285
7.10.3. Use of the Manson–Coffin relation.	287
7.11. Influence of an average strain or stress	287
7.11.1. Other approaches	289
7.12. Low cycle fatigue of composite material.	290
Chapter 8. Fracture Mechanics.	293
8.1. Overview	293

8.1.1. Definition: stress gradient	296
8.2. Fracture mechanism	296
8.2.1. Major phases	296
8.2.2. Initiation of cracks	297
8.2.3. Slow propagation of cracks	299
8.3. Critical size: strength to fracture	299
8.4. Modes of stress application	301
8.5. Stress intensity factor	302
8.5.1. Stress in crack root	302
8.5.2. Mode I	304
8.5.3. Mode II	307
8.5.4. Mode III	307
8.5.5. Field of equation use	308
8.5.6. Plastic zone	310
8.5.7. Other form of stress expressions	312
8.5.8. General form	313
8.5.9. Widening of crack opening	314
8.6. Fracture toughness: critical K value	315
8.6.1. Units	317
8.7. Calculation of the stress intensity factor	319
8.8. Stress ratio	322
8.9. Expansion of cracks: Griffith criterion	323
8.10. Factors affecting the initiation of cracks	326
8.11. Factors affecting the propagation of cracks	326
8.11.1. Mechanical factors	326
8.11.2. Geometric factors	328
8.11.3. Metallurgical factors	329
8.11.4. Factors linked to the environment	329
8.12. Speed of propagation of cracks	330
8.13. Effect of a non-zero mean stress	335
8.14. Laws of crack propagation	336
8.14.1. Head	336
8.14.2. Modified Head law	337
8.14.3. Frost and Dugdale	337
8.14.4. McEvily and Illg	338
8.14.5. Paris and Erdogan	339
8.15. Stress intensity factor	352
8.16. Dispersion of results	353
8.17. Sample tests: extrapolation to a structure	354
8.18. Determination of the propagation threshold K_S	354
8.19. Propagation of cracks in the domain of low cycle fatigue	356
8.20. Integral J	357

8.21. Overload effect: fatigue crack retardation	359
8.22. Fatigue crack closure	361
8.23. Rules of similarity	363
8.24. Calculation of a useful lifetime	363
8.25. Propagation of cracks under random load	366
8.25.1. Rms approach	366
8.25.2. Narrow band random loads	372
8.25.3. Calculation from a load collective	377
Appendix	383
Bibliography	397
Index	433
Summary of Other Volumes in the Series	437

Foreword to Series

In the course of their lifetime, simple items in everyday use such as mobile telephones, wristwatches, electronic components in cars or more specific items such as satellite equipment or flight systems in aircraft, can be subjected to various conditions of temperature and humidity, and more particularly to mechanical shock and vibrations, which form the subject of this work. They must therefore be designed in such a way that they can withstand the effects of the environmental conditions they are exposed to without being damaged. Their design must be verified using a prototype or by calculations and/or significant laboratory testing.

Sizing and testing are performed on the basis of specifications taken from national or international standards. The initial standards, drawn up in the 1940s, were often extremely stringent, blanket specifications, consisting of a sinusoidal vibration, the frequency of which was set to the resonance of the equipment. They were essentially designed to demonstrate a certain standard resistance of the equipment, with the implicit hypothesis that if the equipment survived the particular environment, it would withstand, undamaged, the vibrations to which it would be subjected in service. Sometimes with a delay due to a certain conservatism, the evolution of these standards followed that of the testing facilities: the possibility of producing swept sine tests, the production of narrow-band random vibrations swept over a wide range and finally the generation of wide-band random vibrations. At the end of the 1970s, it was felt that there was a basic need to reduce the weight and cost of on-board equipment and to produce specifications closer to the real conditions of use. This evolution was taken into account between 1980 and 1985 concerning American standards (MIL-STD 810), French standards (GAM EG 13) and international standards (NATO), which all recommended the *tailoring of tests*. Current preference is to talk of the *tailoring of the product to its environment* in order to assert more clearly that the environment must be taken into account from the very start of the project, rather than to check the behavior of the material *a*

posteriori. These concepts, originating with the military, are currently being increasingly echoed in the civil field.

Tailoring is based on an analysis of the life profile of the equipment, on the measurement of the environmental conditions associated with each condition of use and on the synthesis of all the data into a simple specification, which should be of the same severity as the actual environment.

This approach presupposes a correct understanding of the mechanical systems subjected to dynamic loads and knowledge of the most frequent failure modes.

Generally speaking, a good assessment of the stresses in a system subjected to vibration is possible only on the basis of a finite element model and relatively complex calculations. Such calculations can only be undertaken at a relatively advanced stage of the project once the structure has been sufficiently defined for such a model to be established.

Considerable work on the environment must be performed independently of the equipment concerned either at the very beginning of the project, at a time where there are no drawings available, or at the qualification stage, in order to define the test conditions.

In the absence of a precise and validated model of the structure, the simplest possible mechanical system is frequently used consisting of mass, stiffness and damping (a linear system with one degree of freedom), especially for:

- the comparison of the severity of several shocks (shock response spectrum) or of several vibrations (extreme response and fatigue damage spectra);
- the drafting of specifications: determining a vibration which produces the same effects on the model as the real environment, with the underlying hypothesis that the equivalent value will remain valid on the real, more complex structure;
- the calculations for pre-sizing at the start of the project;
- the establishment of rules for analysis of the vibrations (choice of the number of calculation points of a power spectral density) or for the definition of the tests (choice of the sweep rate of a swept sine test).

This explains the importance given to this simple model in this work of five volumes on *Vibration and Mechanical Shock*:

Volume 1 of this series is devoted to *sinusoidal vibration*. After several reminders about the main vibratory environments which can affect materials during their working life and also about the methods used to take them into account,

following several fundamental mechanical concepts, the responses (relative and absolute) of a mechanical one-degree-of-freedom system to an arbitrary excitation are considered, and its transfer function in various forms are defined. By placing the properties of sinusoidal vibrations in the contexts of the real environment and laboratory tests, the transitory and steady state response of a single-degree-of-freedom system with viscous and then with non-linear damping is evolved. The various sinusoidal modes of sweeping with their properties are described, and then, starting from the response of a one-degree-of-freedom system, the consequences of an unsuitable choice of the sweep rate are shown and a rule for the choice of this rate deduced from it.

Volume 2 deals with *mechanical shock*. This volume presents the shock response spectrum (SRS) with its different definitions, its properties and the precautions to be taken in calculating it. The shock shapes most widely used with the usual test facilities are presented with their characteristics, with indications how to establish test specifications of the same severity as the real, measured environment. A demonstration is then given on how these specifications can be produced with classic laboratory equipment: shock machines, electrodynamic exciters driven by a time signal or by a response spectrum, indicating the limits, advantages and disadvantages of each solution.

Volume 3 examines the analysis of *random vibration* which encompasses the vast majority of the vibrations encountered in the real environment. This volume describes the properties of the process, enabling simplification of the analysis, before presenting the analysis of the signal in the frequency domain. The definition of the power spectral density is reviewed, as well as the precautions to be taken in calculating it, together with the processes used to improve results (windowing, overlapping). A complementary third approach consists of analyzing the statistical properties of the time signal. In particular, this study makes it possible to determine the distribution law of the maxima of a random Gaussian signal and to simplify the calculations of fatigue damage by avoiding direct counting of the peaks (Volumes 4 and 5). The relationships that provide the response of a degree of freedom linear system to a random vibration are established.

Volume 4 is devoted to the calculation of *damage fatigue*. It presents the hypotheses adopted to describe the behavior of a material subjected to fatigue, the laws of damage accumulation and the methods for counting the peaks of the response (used to establish a histogram when it is impossible to use the probability density of the peaks obtained with a Gaussian signal). The expressions of mean damage and of its standard deviation are established. A few cases are then examined using other hypotheses (mean not equal to zero, taking account of the fatigue limit, non-linear accumulation law, etc.). The main laws governing low cycle fatigue and fracture mechanics are also presented.

Volume 5 is dedicated to presenting the method of *specification development* according to the principle of tailoring. The extreme response and fatigue damage spectra are defined for each type of stress (sinusoidal vibrations, swept sine, shocks, random vibrations, etc.). The process for establishing a specification from the lifecycle profile of the equipment is then detailed taking into account the uncertainty factor (uncertainties related to the dispersion of the real environment and of the mechanical strength) and the test factor (function of the number of tests performed to demonstrate the resistance of the equipment).

First and foremost, this work is intended for engineers and technicians working in design teams responsible for sizing equipment, for project teams given the task of writing the various sizing and testing specifications (validation, qualification, certification, etc.) and for laboratories in charge of defining the tests and their performance following the choice of the most suitable simulation means.

Introduction

Fatigue damage to a system with one degree of freedom is one of the two criteria adopted for comparing the severity of different vibratory environments, the second being the maximum response of the system.

This criterion is also used to create a specification reproducing the same effects on the equipment as all the vibrations to which it will be subjected in its useful lifetime. This book is not intended as a treatise on material fatigue. Instead, it is meant to provide the elements necessary for understanding the behavior of components or materials going through fatigue and to describe the methods that can be used specifically for calculating damage caused by random vibration.

This requires the following items:

- Knowledge of the fatigue behavior of the materials, characterized by the S-N curve (stress versus number of cycles), yields the number of cycles to failure of a specimen depending on the amplitude of the stress applied. The main laws used to represent the curve are quoted in Chapter 1, emphasizing the random nature of fatigue phenomena. This is followed by some measured values of the variation coefficients of the numbers of cycles to failure.

- The law of accumulation of the damage caused by all the stress cycles must be selected. The most common laws with their limitations are described in Chapter 2.

- The histogram of the peaks of the response stress, assumed here to be proportional to the relative displacement, is determined. When the signal is Gaussian stationary, as was seen in Volume 3, the probability density of its peaks can easily be obtained from only the power spectral density (PSD) of the signal. When this is not the case, the response of the given one-degree-of-freedom system must be calculated digitally and the peaks then counted directly. Numerous methods, ranging

from the simplest (counting of the peaks) to the most complex (rainflow) have been proposed and are presented, with their disadvantages, in Chapter 3.

All these data are used to estimate the damage – characterized statistically if the probability density of the peaks is available and deterministically otherwise (Chapter 4) – and its standard deviation (Chapter 5).

A few elements for damage estimation from other hypotheses are provided in Chapter 6. These concern the shape of the S-N curve, the existence of an endurance limit, the non-linear accumulation of damage, the law of distribution of peaks and the existence of a non-zero mean value.

The Wöhler curve describes three fields based on the level of stress: with unlimited endurance in which the useful lifetime is very long, or even infinite; limited endurance (considered in the first chapters of this book); and for when stress is close to yield stress (low cycle fatigue). Chapter 7 shows how the S-N curve can be characterized in this context by a strain – number of cycles to failure relation, and how calculation of fatigue damage can then be calculated.

All these approaches are “black box”, with no analysis of physical phenomena leading to failure. Experience shows that a crack will eventually appear in a part submitted to alternating stresses. This crack grows until the part fails. Several studies were carried out to understand and model propagation mechanisms in order to evaluate the remaining useful lifetime of cracked parts and to introduce an inspection and maintenance strategy, particularly in the aeronautics field. Chapter 8 discusses the major laws proposed to describe these phenomena and to evaluate a useful lifetime from these criteria.

The elements necessary for calculating the Gamma function and the different integrals involved in the relations established in this book are provided in the Appendix.

List of Symbols

The list below gives the most frequent definition of the main symbols used in this book. Some of the symbols can have locally another meaning which will be defined in the text to avoid any confusion.

a	One half of crack length	f_0	Natural frequency
b	Exponent in Basquin's relation ($N \sigma^b = C$) or exponent	G	Shear modulus
c	Viscous damping constant	$G(\)$	Power spectral density for $0 \leq f \leq \infty$
C	Constant in Basquin's relation ($N \sigma^b = C$)	h	Interval (f/f_0)
d	Damage associated with one half-cycle or Exponent in Corten-Dolan law or Plastic work exponent	$h(t)$	Impulse response
dof	Degree of freedom	$H(\)$	Transfer function
D	Damage by fatigue or Damping capacity ($D = J \sigma^n$)	i	$\sqrt{-1}$
D_t	Fatigue damage calculated using truncated signal	J	Damping constant
erf	Error function	k	Stiffness
E	Young's modulus	K	Constant of proportionality between stress and deformation
$E(\)$	Expectation of...	K_I	Stress intensity factor (Mode I)
f	Frequency	K_{IC}	Critical stress intensity factor (also mode I fracture toughness)
		m	Mass or mean or exponent (Paris law)
		M_n	Moment of order n

n	Number of cycles undergone by test-bar or a material or order of moment	t	Time
	Exponent of $D = J \sigma^n$ or Number of constant levels of a PSD	T	Duration of vibration
n'	Cyclic work hardening exponent	u	Ratio of peak a to rms value z_{rms} of $z(t)$
n_0	Mean number of zero-crossings per second	u_{rms}	Rms value of $u(t)$
n_0^+	Mean number of zero-crossings with positive slope per second (expected frequency)	$u(t)$	Generalized response
n_p^+	Mean number of maxima per second	v	Variation coefficient
N	Number of cycles to failure	V_N	Variation coefficient of number of cycles to failure by fatigue
	Number of dB per octave	\ddot{x}_{rms}	Rms value of $\ddot{x}(t)$
N_p	Number of peaks over duration T	$x(t)$	Absolute displacement of the base of a one-degree-of-freedom system
$p(\)$	Probability density	$\dot{x}(t)$	Absolute velocity of the base of a one-degree-of-freedom system
PSD	Power spectral density	$\ddot{x}(t)$	Absolute acceleration of the base of a one-degree-of-freedom system
q	$\sqrt{1 - r^2}$	z_p	Amplitude of peak of $z(t)$
$q(u)$	Probability density of maxima	z_{rms}	Rms value of $z(t)$
Q	Q factor (factor of quality)	$z(t)$	Relative response displacement of mass of one-degree-of-freedom system with respect to its base
r	Irregularity factor ($= n_0^+ / n_p^+$)	α	$2 \sqrt{1 - \xi^2}$
r_p	Distance from the crack tip	β	$2 \left(1 - 2 \xi^2 \right)$
rms	Root mean square (value)	Δ	Index of damage to failure
R	Stress ratio $\sigma_{min} / \sigma_{max}$	Δf	Frequency interval between half-power points or Width of narrow band noise
R_e	Yield stress	ΔK	Stress intensity factor range
R_m	Ultimate tensile strength	ΔK_S	Threshold stress intensity range
$R_z(\tau)$	Correlation function	$\Delta \epsilon$	Strain range
s	Standard deviation		
s_D	Standard deviation of damage		

$\Delta\sigma$	Stress range
$\Delta\tau$	Time of correlation
ε	Strain
ε_{el}	Elastic strain
ε_f	Fracture ductility
ε'_f	Necessary true strain to obtain a fracture with one cycle
ε_p	Plastic strain
$\gamma()$	Incomplete gamma function
$\Gamma()$	Gamma function
η	Exponent in Weibull's law
$\varphi(t)$	Signal of simple form
ν	Poisson's ratio

π	3.14159265...
σ	Stress
σ_a	Alternating stress
σ_D	Fatigue limit stress
σ_f	Necessary true stress to obtain a fracture with a cycle
σ_{rms}	Rms value of stress
σ_m	Mean stress
σ_t	Truncation level of stress
ω_0	Natural pulsation ($2 \pi f_0$)
Ω	Pulsation of excitation ($2 \pi f$)
ξ	Damping factor

Chapter 1

Concepts of Material Fatigue

1.1. Introduction

Fatigue phenomena, with formation and growth of cracks in machine elements subjected to repeated loads below ultimate strength, was discovered during the 19th century with the arrival of machines and freight vehicles functioning under dynamic loads larger than those encountered before [NEL 78].

According to H.F. Moore and J.B. Kommers [MOO 27], the first work published on failure by fatigue was by W. Albert. A German mining engineer, in 1829 he carried out repeated loading tests on welded chains of mine winches. S.P. Poncelet was perhaps the first to use the term *fatigue* in 1839 [TIM 53].

The most important problems of failure by fatigue were found about 1850 during the development of the European railroad (axes of car wheels). A first explanation was that metal crystallizes under the action of the repeated loads, until failure. The source of this idea is the coarsely crystalline appearance of many surfaces of parts broken by fatigue. This theory was disparaged by W.J. Rankine [RAN 43] in 1843. The first tests were carried out by Wöhler between 1852 and 1869 [WÖH 60].

The dimensioning of a structure to fatigue is more difficult than with static loads [LAV 69] because ruptures by fatigue depend on localized stresses. Since the fatigue stresses are in general too low to produce a local plastic deformation and the redistribution associated with the stresses, it is necessary to carry out a detailed analysis which takes into account both the total model of the stresses and the strong localized stresses due to the concentrations.

2 Fatigue Damage

On the other hand, analysis of static stresses only requires the definition of the total stress field, the high localized stresses being redistributed by local deformation. Three fundamental steps are necessary:

- definition of the loads;
- detailed analysis of the stresses; and
- consideration of the statistical variability of the loads and the properties of materials.

Fatigue damage depends strongly on the oscillatory components of the load, its static component and the order of application of the loads.

Fatigue can be approached in several ways and, in particular, by:

- the study of the Wöhler's curves (stress versus number of cycles, or S-N, curves);
- study of cyclic work hardening (low cycle fatigue); and
- study of the crack propagation rate (fracture mechanics).

The first of these approaches is the most used. We will present some aspects of them in this chapter.

1.2. Types of dynamic loads (or stresses)

The load applied to equipment can vary in different ways:

- periodic or *cyclic*;
- random; or
- quickly between two stationary states (*transitory*).

It can also be zero average, any average, constant or not.

1.2.1. *Cyclic stress*

In the simplest case, the load applied varies in a sinusoidal manner between σ_{\max} and σ_{\min} around the rest position (zero mean).

Consider a stress $\sigma(t)$ varying periodically in time; $\sigma(t)$ values over a period (the smallest part of the function periodically repeating) are called “cycle of stress”. The most common cycle is the sinusoidal cycle.

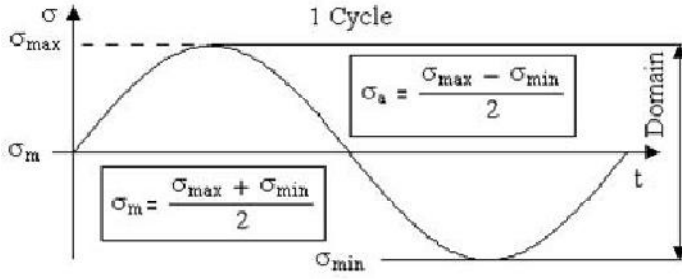


Figure 1.1. Non-zero mean sinusoidal cycle of stress

We refer to the largest algebraic value of the stress during a cycle as *maximum stress* σ_{\max} and the smallest algebraic value (the traction stress being positive) as the *minimum stress* σ_{\min} .

The *mean stress* σ_m is the permanent (or static) stress on which the cyclic stress is superimposed.

σ_a is the amplitude of the oscillatory stress $\sigma_a = \sigma_{\max} - \sigma_m$.

We define the *cycle coefficient* or *stress variation rate* (or “*stress ratio*”) as:

$$R = \frac{\sigma_{\min}}{\sigma_{\max}} \quad [1.1]$$

We also define another parameter A:

$$A = \frac{\sigma_a}{\sigma_m} \quad [1.2]$$

which relates the alternating stress amplitude to the mean stress. A and R are linked by equation [1.3]:

$$R = \frac{1-A}{1+A} \text{ or } A = \frac{1-R}{1+R} \quad [1.3]$$

We refer to the difference

$$\sigma_d = \sigma_{\max} - \sigma_{\min} = 2 \sigma_a \quad [1.4]$$

as the *range of stress*. σ_a is called the *purely alternating stress* when it varies between equal positive and negative values.

1.2.2. Alternating stress

An *alternating stress* evolves between a positive maximum and a negative minimum where absolute values are different.

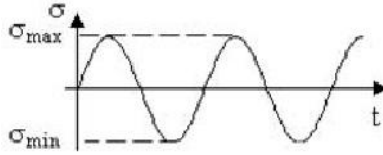


Figure 1.2. *Alternating stress*

In the case of a zero mean stress ($\sigma_m = 0$), we have $R = -1$ and the cycle is said to be *symmetric* or *alternating symmetric* [BRA 81] [CAZ 69] [RAB 80] [RIC 65b].

The cyclic load can also be superimposed on a constant static load σ_m . If σ_a is the cyclic load amplitude:

$$\sigma_{\max} = \sigma_m + \sigma_a$$

$$\sigma_{\min} = \sigma_m - \sigma_a$$

When σ_{\min} or σ_{\max} is zero, the cycle is said to be *pulsating* [FEO 69].

Two cycles are *similar* if they have the same R coefficient.

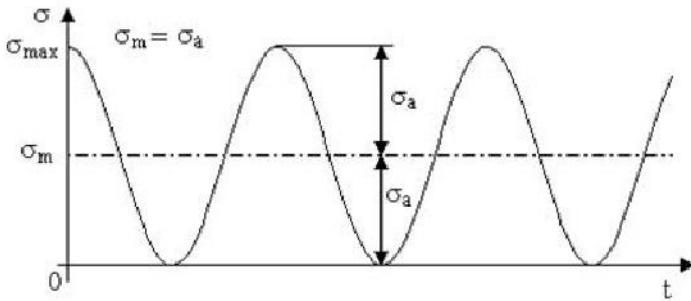


Figure 1.3. *Repeated stress*

When R is ordinary, we can consider that such a cycle is the superimposition of:

- a constant stress σ_m
- a symmetric cyclic stress of amplitude σ_a . We have:

$$\sigma_m = \frac{\sigma_{\max} + \sigma_{\min}}{2} \quad [1.5]$$

$$\sigma_a = \frac{\sigma_{\max} - \sigma_{\min}}{2} \quad [1.6]$$

It is considered that the endurance of a component does not depend on the law of variation in the interval $(\sigma_{\max}, \sigma_{\min})$. We also ignore the influence of the frequency of the cycle [RIC 65b].

1.2.3. *Repeated stress*

When the stress varies between 0 and $\sigma_{\max} > 0$, between 0 and $\sigma_{\min} < 0$, i.e. when $R = 0$, we say that the load is *repeated* ($\sigma_m = \sigma_a$).

1.2.4. *Combined steady and cyclic stress*

The stress is said to be combined steady and cyclic when $0 < R < 1$ ($\sigma_m > \sigma_a$), i.e. when σ_{\max} and σ_{\min} are similar.

1.2.5. Skewed alternating stress

In this case, $-1 < R < 0$ (with $0 < \sigma_m < \sigma_a$).

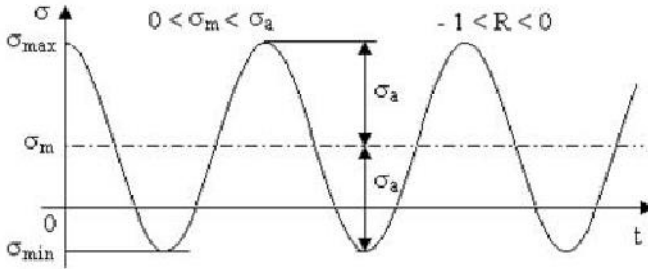


Figure 1.4. Skewed alternating stress

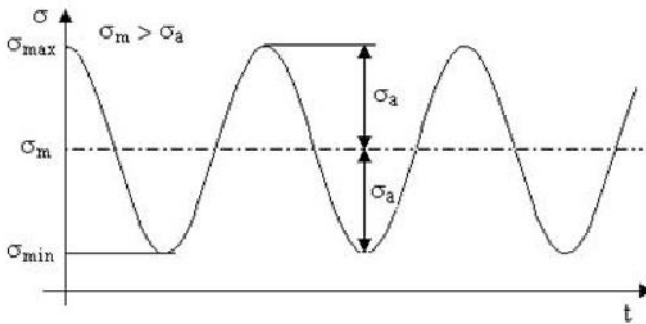


Figure 1.5. Combined steady and cyclic stress ($0 < R < 1$)

These cyclic loads can be encountered e.g. in rotating machines.

1.2.6. Random and transitory stresses

In many cases, we cannot consider vibrations as sinusoidal. For example, vibrations from an aircraft's floor or on missile devices are *random* vibrations with randomly variable amplitude in time. Energy is distributed in a wide frequency interval, instead of being centered on a given frequency (Volume 1, Chapter 1 and Volume 3).

Other phenomena such as shocks measured on an aircraft's landing gear, the starting or stopping of rotating machines, missile and launcher staging, etc. are all transitory, either centered on a given frequency or not.

All these loads lead to effects of fatigue that are much harder to evaluate experimentally, especially in a projected manner. In the following sections, we will show how we can estimate them.

1.3. Damage arising from fatigue

We define the modification of the characteristics of a material, primarily due to the formation of cracks and resulting from the repeated application of stress cycles, as *fatigue damage*. This change can lead to a failure.

We will not consider here the mechanisms of nucleation and growth of the cracks. We will simply state that fatigue starts with a plastic deformation, initially highly localized around certain macroscopic defects (inclusions, cracks of manufacture, etc.), under total stresses which can be lower than the yield stress of the material. The effect is extremely weak and negligible for only one cycle. If the stress is repeated, each cycle creates a new localized plasticity. After a number of variable cycles, depending on the level of the applied stress, ultra-microscopic cracks can be formed in the newly plastic area. The plastic deformation then extends from the ends of the cracks which increase until becoming visible with the naked eye, and lead to failure of the part. Fatigue damage is a cumulative phenomenon.

If the stress-strain cycle is plotted, the hysteresis loop obtained is an open curve whose form evolves depending on the number of applied cycles [FEO 69]. Each cycle of stress produces certain damage and the succession of the cycles results in a cumulative effect.

The damage is accompanied by modifications of the mechanical properties and, in particular, of a reduction of the static ultimate tensile strength R_m and of the fatigue limit strength.

This is generally local to the place of a geometrical discontinuity or a metallurgical defect. The fatigue damage is also related to metallurgical and mechanical phenomena, with appearance and cracks growth depending on the microstructural evolution and mechanical parameters (possibly with the effects of the environment).

The damage can be characterized by:

- evolution of a crack and energy absorption of plastic deformation in the plastic zone which exists at the ends of the crack;
- loss of strength in static tension;

- reduction of the fatigue limit stress up to a critical value corresponding to the failure; and
- variation of the plastic deformation which increases with the number of cycles up to a critical value.

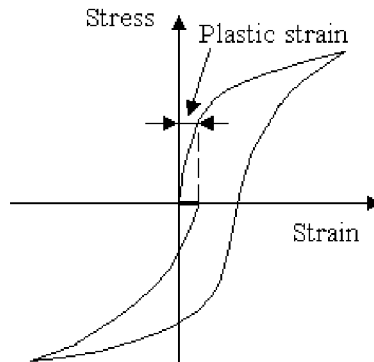


Figure 1.6. *Unclosed hysteresis loop*

We can suppose that fatigue is [COS 69]:

- the result of a dynamic variation of the conditions of load in a material;
- a statistical phenomenon;
- a cumulative phenomenon; and
- a function of material and of amplitude of the alternating stresses imposed on material.

There are several approaches to the problem of fatigue:

- establishing empirical relations taking experimental results into account;
- expressing in an equation the physical phenomena in the material, including microscopic cracks starting from intrusion defects and propagation of these microscopic cracks until macro-cracks and failure are obtained.

Cazaud *et al.* [CAZ 69] quote several theories concerning fatigue, the principal theories being:

- mechanical theories;
- theory of the secondary effects (consideration of the homogeneity of the material, regularity of the distribution of the effort);
- theory of hysteresis of pseudo-elastic deformations (discussion based on Hooke's law);
 - theory of molecular slip,
 - theory of work hardening,
 - theory of crack propagation, and
 - theory of internal damping;
- physical theories, which consider the formation and propagation of the cracks using models of dislocation starting from extrusions and intrusions;
- static theories, in which the stochastic character of the results is explained by the heterogeneity of materials, the distribution of the stress levels, cyclic character of loading, etc.;
- theories of damage; and
- low cycle plastic fatigue, in the case of failures caused by approximately $N < 10^4$ cycles.

The estimate of the lifetime of a test bar is carried out from:

- a curve characteristic of the material (which gives the number of cycles to failure according to the amplitude of stress), in general sinusoidal with zero mean (S-N curve); and
- a law of accumulation of damages.

The various elaborated theories are distinguished by the selected analytical expression to represent the curve of damage and the by the manner of cumulating the damages.

To avoid failures of parts by fatigue dimensioned in statics and subjected to variable loads, we were initially tempted to adopt arbitrary *safety factors*. If badly selected, i.e. insufficient or too large, these could lead to excessive dimensions and masses.

An ideal design would require use of materials in the elastic range. Unfortunately, the plastic deformations always exist at points of strong stress

concentration. The nominal deformations and stresses are elastic and linearly related to the applied loads. This is not the case for stresses and local deformations which exist in metal at critical points, and which control resistance to fatigue of the whole structure.

It therefore proved necessary to carry out tests on test bars for better estimating of the resistance to fatigue under dynamic load, beginning with the simplest, i.e. the sinusoidal load. We will see in the following chapters how the effects of random vibrations most frequently met in practice can be evaluated.

1.4. Characterization of endurance of materials

1.4.1. *S-N curve*

The endurance of materials is studied in the laboratory by subjecting until rupture test bars cut in the material to be studied to stresses (or strains) of amplitude σ , generally sinusoidal with zero mean.

Following the work of Wöhler [WÖH 60] [WÖH 70] carried out on axes of trucks subjected to rotary bending stresses, we note that for each test bar, the number N of cycles to failure (*endurance of the part or fatigue life*) depends on σ . The curve obtained in plotting σ against N is termed the *S-N curve* (stress versus number of cycles) or *Wöhler's curve* or *endurance curve*. The endurance is therefore the ability of a machine part to resist fatigue.

Taking into account the huge variations of N with σ , it is usual to plot $\log N$ (decimal logarithm in general) on abscissae. Logarithmic scales on abscissae and on ordinates are also sometimes used.

This curve is generally composed of three zones [FAC 72] [RAB 80] (Figure 1.7):

- zone AB: corresponding to *low cycle fatigue*, which corresponds to the largest stresses higher than the yield stress of material, where N varies from one-quarter of cycle with approximately 10^4 to 10^5 cycles (for mild steels). In this zone, we observe significant plastic deformation followed by failure of the test bar. The plastic deformation ε_p can be related here to the number of cycles to the failure by a simple relationship of the form:

$$N^k \varepsilon_p = C \quad [1.7]$$

where the exponent k is close to 0.5 for common metals (steels, light alloys) [COF 62].

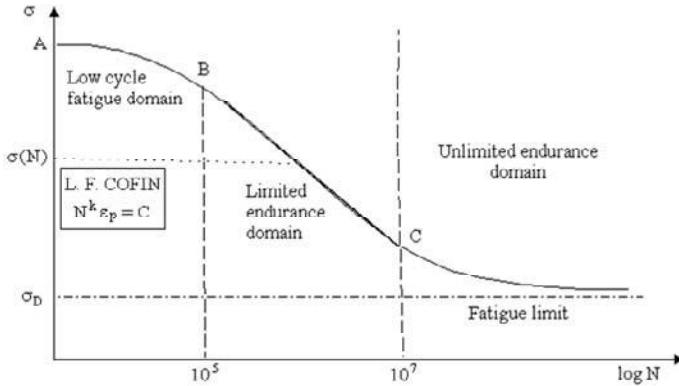


Figure 1.7. Main zones of the S-N curve

– zone BC: often approximates a straight line on log-linear scales (or sometimes on log-log scales), in which the fracture certainly appears under a stress lower than previously, without appearance of measurable plastic deformation. There are many relationships proposed between σ and N to represent the phenomenon in this domain where N increases and when σ decreases. This zone, known as the *zone of limited endurance*, lies between approximately 10^4 cycles and 10^6 to 10^7 cycles.

– zone CD: where D is a point which, for ferrous metals, is ad infinitum. The S-N curve generally presents a significant variation of slope around 10^6 to 10^7 cycles, followed in a way more or less clear, marked by a zone (CD) where the curve tends towards a limit parallel with the N axis. On this side of this limit, the value of σ is denoted σ_D ; there is never failure by fatigue whatever the number of cycles applied. σ_D is referred to as the *fatigue limit* and represents the stress with zero mean of greater amplitude for which we do not observe failure by fatigue after an infinite number of cycles. This stress limit does not exist or can be badly defined for certain materials [NEL 78] (e.g. high-strength steels, non-ferrous metals).

For sufficiently resistant metals, where it is not possible to evaluate the number of cycles which the test bar would support without damage [CAZ 69] (too large a test duration) and to take account of the scatter of the results, the concept of conventional fatigue limit or endurance limit is introduced. It is about the greatest amplitude of stress σ for which 50% of failures after N cycles of stress is observed.

It is denoted $\sigma_m = 0$, $\sigma_D(N)$. N can vary between 10^6 and 10^8 cycles [BRA 80a, b]. For steels, $N = 10^7$ and $\sigma_D(10^7) \approx \sigma_D$. The notation σ_D is used in this case.

NOTE:

Brittle materials do not have a well-defined fatigue limit [BRA 81] [FID 75].

For extra-hardened tempered steels (certainly titanium, copper or aluminum alloys), or when there is corrosion, this limit remains theoretical and without interest since the fatigue life is never infinite.

When the mean stress σ_m is different from zero, it is important to associate σ_m with the amplitude of the alternating stress. The fatigue limit can be written σ_a or σ_{aD} in this case.

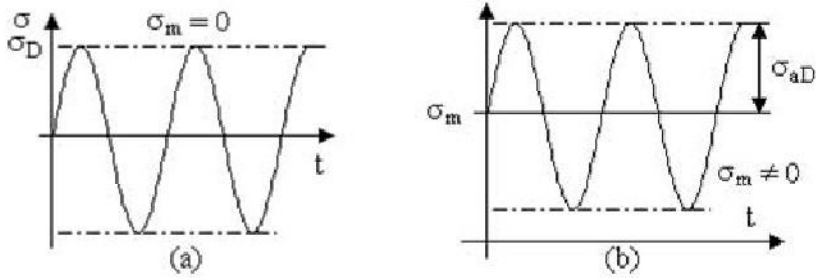


Figure 1.8. Sinusoidal stress with (a) zero and (b) non-zero mean

Definition

The *endurance ratio* is the ratio of the fatigue limit σ_D (normally at 10^7 cycles) to the ultimate tensile strength R_m of material:

$$R = \frac{\sigma_D(N)}{R_m} \quad [1.8]$$

NOTE: The *S-N curve* is sometimes plotted on reduced scales on axes $(\sigma/R_m, N)$, in order to be able to proceed more easily to comparisons between different materials.

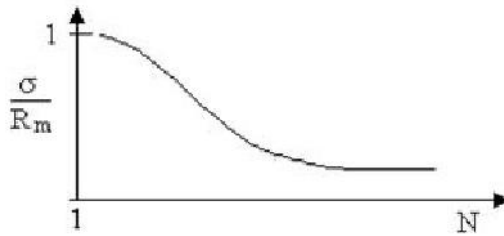


Figure 1.9. *S-N curve on reduced axes*

1.4.2. Statistical aspect

The S-N curve of a material is plotted by successively subjecting ten (or more) test bars to sinusoidal stresses of various amplitudes. The results show that there is considerable scatter in the results, in particular for the long fatigue lives. For a given stress level, the relationship between the maximum and the minimal value of the number of cycles to failure can exceed 10 [LAV 69] [NEL 78].

The dispersion of the results is related on the heterogeneity of materials, the surface defects, the machining tolerances and, in particular, to metallurgical factors. Among these factors, inclusions are most important. Scatter is in fact due to the action of fatigue in a metal, which is generally strongly localized. Contrary to the case of static loads, only a small volume of material is concerned. The rate of fatigue depends on the size, orientation and chemical composition of some material grains which are located in a critical zone [BRA 80b] [LEV 55] [WIR 76].

In practice, it is therefore not realistic to characterize the resistance to fatigue of a material by a S-N curve plotted from only one fatigue test at each stress level. It is more correct to describe this behavior by a curve in a statistical manner, the abscissae providing the endurance N_p for a survival of p percent of the test bars [BAS 75] [COS 69].

The median endurance curve (or *equiprobability curve*) denoted N_{50} (i.e. survival of 50% of the test bars), or sometimes the median curves with ± 1 to 3 standard deviations or other isoprobability curves, are generally given [ING 27].

Without other indication, the S-N curve is the median curve.

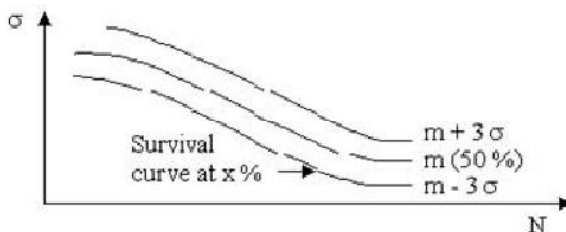


Figure 1.10. *Isoprobability S-N curves*

NOTE: The scatter of fatigue life of non-ferrous metals (aluminum, copper, etc.) is less than that of steels, probably because these metals have fewer inclusions and inhomogeneities.

1.4.3. Distribution laws of endurance

For high stress levels, endurance N follows a log-normal law [DOL 59] [IMP 65]. In other words, in scales where the abscissa carry $\log N$, the distribution of $\log N$ follows, in this stress domain, a roughly normal law (nearer to the normal law when σ is higher) with a scatter which decreases when σ increases. M. Matolcsy [MAT 69] considers that the standard deviation s can be related to the fatigue life at 50% by an expression of the form

$$s(N) = A N_{50}^{\beta} \quad [1.9]$$

where A and β are constant functions of material.

Example 1.1.

	β
Aluminum alloys	1.125
Steels	1.114–1.155
Copper wires	1.160
Rubber	1.125

Table 1.1. *Examples of values of the exponent β*

G.M. Sinclair and T.J. Dolan [SIN 53] observed that the statistical law describing the fatigue evolution is roughly log-normal and that the standard

deviation of the variable ($\log N$) varies with the amplitude of the applied stress according to an exponential law.

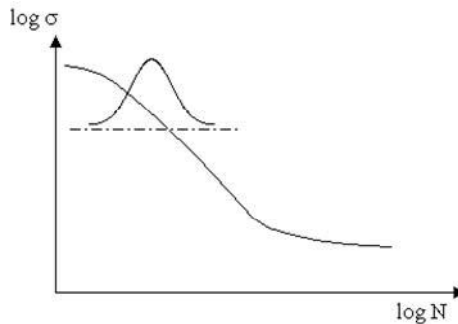


Figure 1.11. *Log-normal distribution of the fatigue life*

In the endurance zone, close to σ_D , F. Bastenaire [BAS 75] showed that the inverse $1/N$ of endurance follows a modified normal law (with truncated tail).

Other statistical models were proposed e.g. following [YAO 72] [YAO 74]:

- the normal law [AST 63];
- extreme value distribution;
- Weibull's law [FRE 53]; and
- the gamma law [EUG 65].

From a compilation of various experimental results, P.H. Wirshing [WIR 81] checked that, for welded tubular parts, the log-normal law is that which adapts best. It is this law which is most often used [WIR 81]. It has the following advantages:

- well-defined statistical properties;
- easy to use; and
- adapts to large variations in coefficient.

Tables 1.2 and 1.3 give values of the variation coefficient of the number of cycles to failure for some materials noted in the literature [LAL 87].

Value 0.2 of the standard deviation (on $\log N$) is often used for the calculation of the fatigue lives (for notched or other parts) [FOR 61] [LIG 80] [LUN 64] [MEH 53].

Authors	Materials	Conditions	V_N (%)
Whittaker and Besuner [WHIT 69]	Steels $R_m \leq 1650$ MPa (240 ksi) Steels $R_m > 1650$ MPa (240 ksi) Aluminum alloy Alloy titanium		36 48 27 36 (Log-normal)
Endo and Morrow [END 67] [WIR 82]	Steel 4340 7075-T6 2024-T4 Titanium 811	Low cycle fatigue ($N < 10^3$)	14.7 17.6 19.7 65.8
Swanson [SWA 68]	Steel SAE 1006 Maraging steel 200 grade Maraging steel Nickel 18%	Fatigue under narrow band random noise	25.1 38.6 69.0
Gurney [GUR 68]	Welded structures	Mean	52

Table 1.2. *Examples of values of the variation coefficient of the number of cycles to failure*

1.4.4. Distribution laws of fatigue strength

Another way of resolving the problem consists of studying *the fatigue strength* of the material [SCH 74], i.e. the stress which the material can resist during N cycles. This strength also has a statistical character; strength to p percent of survival and a median strength are also defined here.

The *response curve* represents the probability of failure during a test with duration limited to N cycles, depending on the stress σ [CAZ 69] [ING 27].

The experiment shows that the fatigue strength follows a roughly normal law whatever the value of N and is fairly independent of N [BAR 77]. This constancy is masked on the S-N diagrams by the choice of the log-linear or log-log scales, scatter appearing to increase with N . Some values of the variation coefficient of this law for various materials, extracted from the literature, can be found in [LAL 87].

Authors	Materials	Conditions	V_N (%)
Blake and Baird [BLA 69]	Aerospace components	Random loads	3 to 30
Epremian and Mehl [EPR 52]	Steels Log-normal law	s_{\log}/m_{\log}	2.04 to 8.81 Log-normal law
Ang and Munse [Ang 75]	Welding		52
Whittaker [WHIT 72]	Steel UTS \leq 1650 MPa Steel UTS $>$ 1650 MPa		36 48
	Aluminum alloys Titanium alloys		22 36
Wirsching [WIR 83b]	Welding (tubes)		70 to 150
Wirsching and Wu [WIR 83c]	RQC - 100 Q	Plastic strain Elastic strain	15 to 30 55
	Waspaloy B Super alloys Containing Nickel	Plastic strain Elastic strain	42 55
Wirsching [WIR 83a]	V_N , often about 30% to 40%, can reach 75% and even exceed 100%. Low cycle fatigue field: 20% to 40% for the majority of metal alloys. For N large, V_N can exceed 100%.		
Yokobori [YOK 65]	Steel Rotational bending or traction compression		28 to 130
Dolan and Brown [DOL 52]	Aluminum alloy 7075.T6 Rotational bending		44 to 80
Sinclair and Dolan [SIN 53]	Aluminum alloy 75.S-T Rotational bending		10 to 100
Levy [LEV 55]	Mild steel Rotational bending		43 to 75
Konishi and Shinozuka [KON 56]	Notched plates - Steel SS41 Alternate traction		18 to 43
Matolcsy [MAT 69]	Synthesis of various test results		20 to 90
Tanaka and Akita [TAN 72]	Silver/nickel wires Alternating bending		16 to 21

Table 1.3. Examples of values of the variation coefficient of the number of cycles to failure

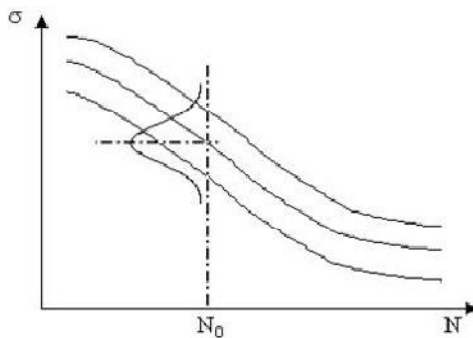


Figure 1.12. *Gaussian distribution of fatigue strength*

Authors	Materials	Parameter	V_N (%)
Ligeron [LIG 80]	Steels Various alloys	Fatigue limit stress	4.4 to 9.4
Yokobori [YOK 65]	Mild steel	Fatigue limit stress	2.5 to 11.3
Mehle [MEH 53]	Steel SAE 4340		20 to 95
Epremian [WIR 83a]	Large variety of metallic materials	Endurance stress (failure for given N)	5 to 15

Table 1.4. *Examples of values of the variation coefficient of the endurance strength for a given N*

For all the metals, J.E. Shigley [SHI 72] proposes a variation coefficient σ_D (ratio of the standard deviation to the mean) equal to 0.08 [LIG 80], a value which can be reduced to 0.06 for steels [RAN 49].

1.4.5. Relation between fatigue limit and static properties of materials

Some authors tried to establish empirical formulae relating the fatigue limit σ_D and its standard deviation to the mechanical characteristics of the material (Poisson coefficient, Young’s modulus, etc.). For example, the relations listed in Table 1.5 were proposed for steels [CAZ 69] [LIE 80].

After completing a large number of fatigue tests (rotational bending, on test bars without notches). A. Brand and R. Sutterlin [BRA 80a] noted that the best

correlation between σ_D and a mechanical strength parameter is that obtained with the ultimate strength R_m (tension):

$$\sigma_{D50\%} = R_m \left(0.57 - 1.2 \cdot 10^{-4} R_m \right) \text{ for } 800 \leq R_m \leq 1300 \text{ N/mm}^2$$

$$\sigma_D = R_m \left(0.56 - 1.4 \cdot 10^{-4} R_m \right) \text{ for } R_m < 800 \text{ N/mm}^2 \text{ or } R_m > 1300 \text{ N/mm}^2$$

All these relations only represent correctly the results of the experiments which made it possible to establish them, and therefore are not general. A. Brand and R. Sutterlin [BRA 80a] tried however to determine a more general relation, independent of the size of the test bars and stress, of the form:

$$\sigma_{DM} = a \log \chi + b$$

where a and b are related to R_m . σ_{DM} is the real fatigue limit related to the nominal fatigue limit σ_{Dnom} by

$$\sigma_{DM} = K_t \sigma_{Dnom}$$

where K_t = stress concentration factor. χ is the stress gradient, defined as the value of the slope of the tangent of the stress field at the notch root divided by the maximum value of the stress at the same point, i.e.

$$\chi = \lim_{x \rightarrow 0} \frac{1}{\sigma} \frac{d\sigma}{dx}.$$

The *variation coefficient* is defined:

$$v = \frac{s_{\sigma_D}}{\bar{\sigma}_D} = 6 \%$$

where v is independent of R_m . A. Brand and R. Sutterlin [BRA 80a] recommend a value of 10%.

Houdremont and Mailander	$\sigma_D = 0.25 (R_e + R_m) + 5$	R_e = yield stress R_m = ultimate stress
Lequis, Buchholtz and Schultz	$\sigma_D = 0.175 (R_e + R_m - A\% + 100)$	A% = lengthening, in percent.
Fry, Kessner and Öttel	$\sigma_D = \alpha R_m + \beta R_e$	α proportional to R_m and β inversely proportional
Heywood	$\sigma_D = \frac{R_m}{2}$ $\sigma_D = 150 + 0.43 R_e$	
Brand	$\sigma_D = 0.32 R_m + 121$	
Lieurade and Buthod [LIE 82]	$\sigma_D = 0.37 R_m + 77$ $\sigma_D = 0.38 R_m + 16$ $\sigma_D = 0.41 R_m + 2 A$ $\sigma_D = 0.39 R_m + S$	(to 15% near) S = striction, expressed in %
Jüger	$\sigma_D = 0.2 (R_e + R_m + S)$	
Rogers	$\sigma_D = 0.4 R_e + 0.25 R_m$	
Mailander	$\sigma_D = (0.49 \pm 20\%) R_m$ $\sigma_D = (0.65 \pm 30\%) R_e$	
Stribeck	$\sigma_D = (0.285 \pm 20\%) (R_e + R_m)$	
In all the above relations, σ_D , R_m and R_e are expressed in N / mm^2 .		
Feodossiev [FEO 69]	Steel, bending: $\sigma_D \approx 0.4$ to $0.5 R_m$ Very resistant steels: $\sigma_D \approx 4000 + \frac{1}{6} R_m$ (in kg / cm^2) Non-ferrous metals: $\sigma_D \approx 0.25$ to $0.5 R_m$	

Table 1.5. Examples of relations between the fatigue limit and the static properties of materials

1.4.6. Analytical representations of S - N curve

Various expressions have been proposed to describe the S - N curve representative of the fatigue strength of a material, often in the limited endurance domain (the definition of this curve has evolved over the years from a deterministic curve to a curve of statistical character).

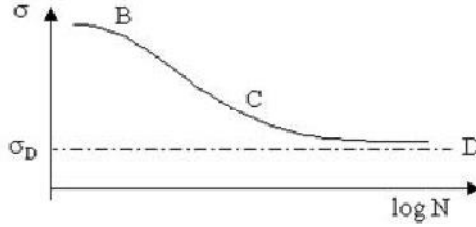


Figure 1.13. Representation of the S - N curve in semi-logarithmic scales

The S - N curve is generally plotted in semi-logarithmic scales of $\log N$ and σ , in which it presents a roughly linear part (around an inflection point), a curve characteristic of the material (BC) and an asymptote to the straight line $\sigma = \sigma_D$.

Among the many more or less complicated representations (none of which are really general), the following relations can be found [BAS 75] [DEN 71] [LIE 80].

1.4.6.1. Wöhler relation [WÖH 70]

$$\sigma = \alpha - \beta \log N \quad [1.10]$$

This relation does not describe the totality of the curve since σ does not tend towards a limit σ_D when $N \rightarrow \infty$ [HAI 78]. It represents only the part BC. It can also be written in the form:

$$N e^{a\sigma} = b \quad [1.11]$$

1.4.6.2. Basquin relation

The relation suggested by Basquin in 1910 [BAS 10] is of the form

$$\ln \sigma = \alpha - \beta \ln N \quad [1.12]$$

i.e.

$$N \sigma^b = C \quad [1.13]$$

where

$$\beta = \frac{1}{b} \text{ and } \ln C = \frac{\alpha}{\beta}$$

The parameter b is sometimes referred to as the *index of the fatigue curve* [BOL 84].

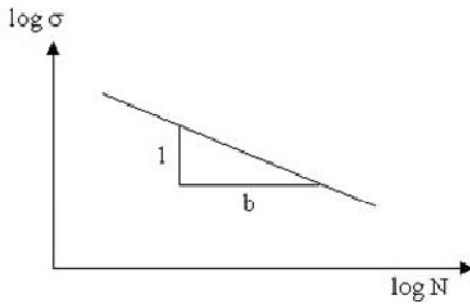


Figure 1.14. Significance of the parameter b of Basquin's relation

In these scales, the curve can be entirely linearized (upwards) by considering the amplitudes of the true stresses (and neither nominal). Expression [1.13] can also be written:

$$\sigma = \sigma_{RF} N^\beta \quad [1.14]$$

or

$$N \sigma^b = \sigma_{RF}^b \quad [1.15]$$

where σ_{RF} is the fatigue strength coefficient. This expression is generally valid for high values of N ($> 10^4$). If there is a non-zero σ_0 mean stress, constant C must be replaced by:

$$C \left(1 - \frac{\sigma_0}{R_m} \right)^m$$

where C is the constant used when $\sigma_0 = 0$ and R_m is the ultimate strength of the material [WIR 83a].

In the expression $N \sigma^b = C$, the stress tends towards zero when N tends towards the infinite. This relation is therefore representative of the S-N curve only for part BC. In addition, it represents a straight line in logarithmic scales and not in semi-logarithmic scales (log-linear). A certain number of authors presented the results of the fatigue tests in these scales (log-log) and showed that part BC is close to a straight line [MUR 52]. F.R. Shanley [SHA 52] considers in particular that it is preferable to choose these scales. H.P. Lieurade [LIE 80] notes that the representation of Basquin is less appropriate than that of the relation of Wöhler in the intermediate zone, and that the Basquin method is not better around the fatigue limit. It is very much used, however.

To take account of the stochastic nature of this curve, P.H. Wirsching [WIR 79] proposed treating constant C like a log-normal random variable of mean \bar{C} and standard deviation σ_C and provides the following values, in the domain of the great numbers of cycles:

- median: $1.55 \cdot 10^{12}$ (ksi)⁽¹⁾,
- variation coefficient: 1.36

(statistical study of S-N curves relating to connections between tubes).

Some numerical values of the parameter b in Basquin's relationship

Metals. The range of variation of b is 3–25. The most common values are between 3 and 10 [LEN 68]. M. Gertel [GER 61] [GER 62] and C.E. Crede and E.J. Lunney [CRE 56b] consider a value of 9 to be representative of most materials. It is probably a consideration of this order that led to the choice of 9 by standards such as MIL-STD-810, AIR, etc. This choice is satisfactory for most light alloys and copper but may be unsuitable for other materials. For instance, for steel, the value of b varies between 10 and 14 depending on the alloy. D.S. Steinberg [STE 73] mentions the case of 6144-T4 aluminum alloy for which $b = 14$ ($N \sigma^{14} = 2.26 \cdot 10^{78}$).

1. 1 ksi = 6.8947 MPa

b is approximately 9 for ductile materials and approximately 20 for brittle materials, whatever the ultimate strength of the material [LAM 80].

Material	Type of fatigue test	$\frac{\sigma_{\min}}{\sigma_{\max}}$	b
2024-T3 aluminum	Axial load	-1	5.6
2024-T4 aluminum	Rotating beam	-1	6.4
7075-T6 aluminum	Axial loading	-1	5.5
6061-T6 aluminum	Rotating beam	-1	7.0
ZK-60 magnesium			4.8
BK31XA-T6 magnesium	Axial load	0.25	8.5
	Rotating beam	-1	5.8
QE 22-T6 magnesium	Wöhler	-1	3.1
4130 steel			
Standardized	Axial load	-1	4.5
Hardened	Axial load	-1	4.1
6Al-4V Ti	Axial load	-1	4.9
Beryllium			
Hot pressed	Axial load	0	10.8
Block		0.2	8.7
		-1	12.6
Cross Rol Sheat	Axial load	0.2	9.4
Invar	Axial load		4.6
Anneal copper			11.2
1S1 fiberglass			6.7

Table 1.6. *Examples of values of the parameter b [DEI 72]*

The lowest values indicate that the fatigue strength drops faster when the number of cycles is increased, which is generally the case for the most severe geometric shapes. The lower the stress concentration, the higher the value of parameter b . Table 1.6 gives the value of b for a few materials according to the type of load applied: tension-compression, torsion, etc. and the value of the mean stress, i.e. the ratio $\sigma_{\min}/\sigma_{\max}$.

A few other values are given by R.G. Lambert [LAM 80] with no indication of the test conditions.

Material	b
Copper wire	9.28
Aluminum alloy 6061-T6	8.92
7075-T6	9.65
Soft solder (63-37 Tin - Lead)	9.85
4340 (BHN 243)	10.5
4340 (BHN 350)	13.2
AZ31B Magnesium alloy	22.4

Table 1.7. Examples of values of the parameter b [LAM 80]

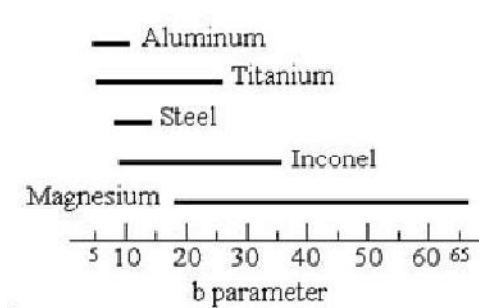


Figure 1.15. Examples of values of the parameter b [CAR 74]

It should be noted that the b parameter of an assembly can differ appreciably from that of the material of which it is composed. The b parameter defined in experiments for a steel ball bearing is, for example, close to 4. That of steel or aluminum welded parts has a b value between 3 and 6 [BRI 80] [EUR 93] [HAA 98] [LAS 05] [MAN 04] [SHE 05] [TVE 03].

It is therefore necessary to be very cautious when choosing the value of this parameter, especially when reducing the test times for constant fatigue damage testing.

Case of electronic components

The failures observed in electronic components follow the conventional fatigue failure model [HAS 64]. The equations established for structures are therefore applicable [BLA 78]. During initial tests on components such as capacitors, vacuum tubes, resistors, etc. and on equipment, it was observed that the failures (lead breakage) generally occurred near the frame resonance frequencies, generally below 500 Hz [JAC 56]. The analysis of tests conducted on components by D.L. Wrisley and W.S. Knowles [WRI] tends to confirm the existence of a fatigue limit.

Electronic components could be expected *a priori* to be characterized by a parameter b of around 8 or 9 for fatigue strength, at least in the case of discrete components with copper or light alloy leads. That is the value chosen by some authors [CZE 78].

Few data have been published on the fatigue strength of electronic components. C.A. Golueke [GOL 58] provides S-N curves plotted from the results of fatigue testing conducted at resonance on resistors, for setups such that the resonance frequency is between 120 Hz and 690 Hz. Its results show that the S-N curves obtained for each resonance are roughly parallel. On $\log N - \log \ddot{x}$ scales (acceleration), parameter b is very close to 2. Components with the highest resonance frequency have the longest life expectancy, which demonstrates the interest of decreasing the component lead length to a minimum.

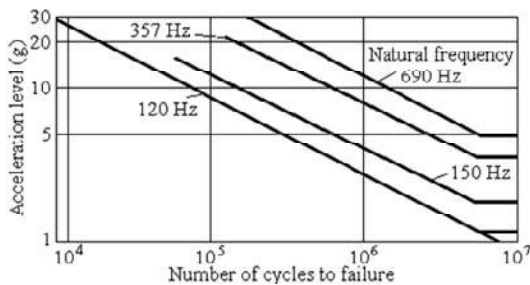


Figure 1.16. Examples of S-N curves of electronic components [GOL 58]

This work also reports that the most fragile parts regarding fatigue strength are the soldered joints and interconnections followed by capacitors, vacuum tubes, relays to a much lesser extent, transformers and switches.

M. Gertel [GER 61] [GER 62] writes the Basquin relation $N \sigma^b = C$ in the form

$$N \frac{\sigma^b}{\sigma_D^b} = \frac{C}{\sigma_D^b} = C_1 \quad [1.16]$$

where σ_D is the fatigue limit. If the excitation is sinusoidal [GER 61] and if the structure, comparable to a one-degree-of-freedom system, is subjected to tension-compression, the movement of mass m is such that

$$m \ddot{y} = \sigma S \quad [1.17]$$

where σ is stress in the part with cross-section S . If the structure is excited at resonance, we have:

$$\ddot{y} = Q \ddot{x} \quad [1.18]$$

and

$$\ddot{x} = \frac{\sigma S}{m Q} \quad [1.19]$$

Knowing that the specific damping energy D is related to the stress by

$$D = J \sigma^n \quad \begin{cases} n = 2.4 & \text{if } \sigma \leq 0.8 R_e \\ n = 8 & \text{if } \sigma > 0.8 R_e \end{cases} \quad [1.20]$$

and that the Q factor can be considered as the product:

$$Q = K_m K_v \quad [1.21]$$

where

$$K_m = \frac{\pi \sigma^2}{E D}$$

is the dimensionless factor of the material, E is Young's modulus, and where K_v is the dimensionless volumetric stress factor, we obtain

$$\ddot{x} = \frac{S \sigma}{m K_v K_m} = \frac{S \sigma}{m K_v} \frac{E D}{\pi \sigma^2}$$

$$\ddot{x} = \frac{S E}{m K_v \pi \sigma} J \sigma^n$$

$$\ddot{x} = \frac{S E J}{m K_v \pi} \sigma^{n-1} \quad [1.22]$$

If

$$\ddot{x}_e = \frac{S E J}{m K_v \pi} R_e^{n-1}$$

$$\frac{\ddot{x}}{\ddot{x}_e} = \left(\frac{\sigma}{R_e} \right)^{n-1}$$

and

$$N \frac{\sigma^b}{R_e^b} = C_1,$$

we obtain

$$N \left(\frac{\ddot{x}}{\ddot{x}_e} \right)^{\frac{b}{n-1}} = C_1, \quad [1.23]$$

yielding the value of the parameter b of resistors in N - σ axes (instead of N , \ddot{x}):

$$b = 2(n-1) \quad [1.24]$$

which, for $n = 2.4$, is equal to $2 \times 1.4 = 2.8$. These low values of b are confirmed by other authors [CRE 56b] [CRE 57] [LUN 58]. Some relate to different component technologies [DEW 86]. Among the published values are, for instance, that of C.E. Crede [GER 61] [GER 62]:

Resistors: $b = 2.4$ to 5.8

Vacuum tubes: $b = 0.6$,

those of E.J. Lunney and C.E. Crede [CRE 56b]:

Capacitors: $b = 3.6$ (leads)

Vacuum tubes: $b = 2.83$ to 2.13 ,

or, for weldings, $b = 5.7$ [GOP 89].

1.4.6.3. *Some other laws*

Other laws include that of C.E. Stromeyer [STR 14]:

$$\log(\sigma - \sigma_D) = \alpha - \beta \log N \quad [1.25]$$

or

$$\sigma = \sigma_D + \left(\frac{C}{N} \right)^{1/b} \quad [1.26]$$

or

$$(\sigma - \sigma_D)^b N = C \quad [1.27]$$

Here, σ tends towards σ_D when N tends towards infinity.

A. Palmgren [PAL 24] stated that

$$\sigma = \sigma_D + \left(\frac{C}{N + A} \right)^{1/b} \quad [1.28]$$

or

$$(\sigma - \sigma_D)^b (N + A) = C \quad [1.29]$$

a relation which is better adjusted using experimental curves than Stromeyer's relation.

According to W. Weibull [WEI 49],

$$\frac{\sigma - \sigma_D}{R_m - \sigma_D} = \left(\frac{C}{N + A} \right)^{1/b} \quad [1.30]$$

where R_m is the ultimate strength of studied material. This relation does not improve the preceding relation. It can be also written:

$$\sigma = \sigma_D + \frac{F}{(N + A)^{1/b}} \quad [1.31]$$

where F is a constant and A is the number of cycles (different from $1/4$) corresponding to the ultimate stress [WEI 52]. It was used in other forms, such as:

$$\sigma - \sigma_D = \left(\frac{C}{N} \right)^{1/n} \quad [1.32]$$

with $n = 1$ [PRO 48], $n = 2$ [FER 55] and

$$\frac{\sigma - \sigma_D}{R_m - \sigma} = b N^{-a} \quad [1.33]$$

where a and b are constants [FUL 63].

According to Corson [MIL 82],

$$(\sigma - \sigma_D) A^{\sigma - \sigma_D} = \frac{C}{N} \quad [1.34]$$

Bastenaire [BAS 75] stated that:

$$(N + B) (\sigma - \sigma_D) e^{A(\sigma - \sigma_D)} = C \quad [1.35]$$

1.5. Factors of influence

1.5.1. General

A great number of parameters affect fatigue strength and hence the S-N curve. The fatigue limit of a test bar can therefore be expressed in the form [SHI 72]:

$$\sigma_D = K_{sc} K_s K_\theta K_f K_r K_v \sigma'_D \quad [1.36]$$

where σ'_D is the fatigue limit of a smooth test bar and where the other factors make it possible to take into account the following effects:

K_{sc} scale effect

K_s	surface effect
K_θ	temperature effect
K_f	form effect (notches, holes, etc.)
K_r	reliability effect
K_v	various effects (loading rate, type of load, corrosion, residual stresses, stress frequency, etc.)

These factors can be classified as follows [MIL 82]:

- factors depending on the conditions of load (type of loads: tension/compression, alternating bending, rotational bending, alternating torsion, etc.);
- geometrical factors (scale effect, shape, etc.);
- factors depending on the conditions of surface;
- factors of a metallurgical nature; and
- factors of environment (temperature, corrosion etc).

We examine some of these parameters in the following sections.

1.5.2. *Scale*

For the sake of simplicity and minimizing cost, the tests of characterization of strength to fatigue are carried out on small test bars. The tacit and fundamental assumption is that the damage processes apply both to the test bars and the complete structure. The use of the constants determined with test bars for the calculation of larger parts assumes that the scale factor has little influence.

A scale effect can appear when the diameter of the test bar is increased, involving an increase in the concerned volume of metal and in the surface of the part, and thus an increase in the probability of cracking. This scale effect has as origins:

- mechanics: existence of a stress gradient in the surface layers of the part, variable according to dimensions, weaker for the large parts (case of the non-uniform loads, such as torsion or alternating bending);
- statistics: larger probability of existence of defects being able to start microscopic cracks in the large parts; and
- technological: surface quality and material heterogeneity.

It is noted in practice that the fatigue limit is smaller when the test bar is larger. With equal nominal stress, the greater the dimensions of a part, the greater its fatigue strength decreases [BRA 80b] [BRA 81] [EPR 52].

B.N. Leis [LEI 78] and B.N. Leis and D. Broek [LEI 81] demonstrated that, under conditions to ensure that similarity is respected strictly at the critical points (notch root, crack edges, etc.), precise structure fatigue life predictions can be made from laboratory test results. Satisfying conditions of similarity is sometimes difficult to achieve, however, since there is a lack of understanding of the factors controlling the process of damage rate.

1.5.3. Overloads

We will see that the order of application of loads of various amplitudes is an important parameter. It is observed in practice that:

1. For a smooth test bar, the effect of an overload leads to a reduction in the fatigue life. J. Kommers [KOM 45] showed that a material which was submitted to significant over-stress, then to under-stress, can break even if the final stress is lower than the initial fatigue limit. This is because the over-stress produces a reduction in the initial fatigue limit. By contrast, an initial under-stress increases the fatigue limit [GOU 24].

J.R. Fuller [FUL 63] noted that the S-N curve of a material which has undergone an overload turns in the clockwise direction with respect to the initial S-N curve, around a point located on the curve with ordinate of amplitude σ_1 of the overload.

The fatigue limit is reduced. If n_2 cycles are carried out on the level σ_2 after n_1 cycles at level σ_1 , the new S-N curve takes the position 3 (Figure 1.17).

Rotation is quantitatively related to the value of the ratio n_1/N_1 on the over-stress level σ_1 . J.R. Fuller defines a *factor of distribution* which can be written for two load levels:

$$\beta = \frac{1}{q} \log_{10} \frac{10^q N_A}{N_A + N_a} = 1 + \frac{1}{q} \log_{10} \frac{N_A}{N_A + N_a} \quad [1.37]$$

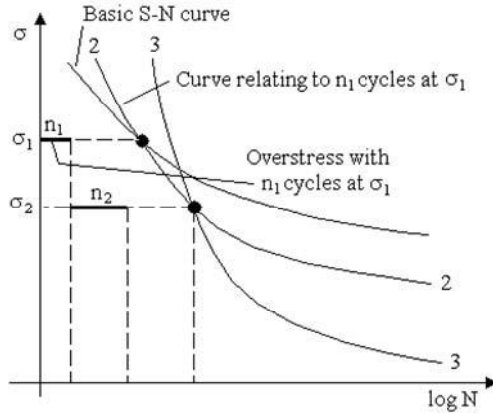


Figure 1.17. Rotation of the S-N curve of a material which has undergone an overload [FUL 63]

Rotation is quantitatively related to the value of the ratio n_1/N_1 on the over-stress level σ_1 . J.R. Fuller defines a *factor of distribution* which can be written for two load levels:

$$\beta = \frac{1}{q} \log_{10} \frac{10^q N_A}{N_A + N_a} = 1 + \frac{1}{q} \log_{10} \frac{N_A}{N_A + N_a} \quad [1.37]$$

where q is a constant generally equal to 3 (*notch sensitivity* of material to fatigue to the high loads), N_A is the number of cycles on the highest level σ_A and N_a is the number of cycles on the lower level σ_a .

If $\beta = 1$, all the stress cycles are carried out at the higher stress level ($N_a = 0$). This factor β enables the distribution of the peaks between the two limits σ_A and σ_a to be characterized and is used to correct the fatigue life of the test bars calculated under this type of load. It can be used for a narrow band random loading.

2. For a notched test bar, on which most of the fatigue life is devoted to the propagation of the cracks by fatigue, this same effect led to an increase in the fatigue life [MAT 71]. Conversely, an initial under-load accelerates cracking. This acceleration is all the more significant since the ensuing loads are larger. In the case of random vibrations, they are statistically not very frequent and of short duration so that the under-load effect can be neglected [WEI 78].

1.5.4. *Frequency of stresses*

The frequency, within reasonable limits of variation, is not important [DOL 57]. It is generally considered that this parameter has little influence as long as the heat created in the part can be dissipated and a heating does not occur which would affect the mechanical characteristics. (Stresses are considered here to be directly applied to the part with a given frequency. It is different when the stresses are due to the total response of a structure involving several modes [GRE 81]).

An assessment of the influence of the frequency shows [HON 83]:

- the results published are not always coherent, particularly because of corrosion effects;
- for certain materials, the frequency can be a significant factor when it varies greatly, acting differently depending on materials and load amplitude; and
- its effect is much more significant at high frequencies.

For the majority of steels and alloys, it is negligible for $f < 117$ Hz. In the low number of cycle fatigue domain, there is a linear relation between the fatigue life and the frequency on logarithmic scales [ECK 51]. Generally observed are:

- an increase in the fatigue limit when the frequency increases; and
- a maximum value of fatigue limit at a certain frequency.

For specific treatment of materials, unusual effects can be noted [BOO 70] [BRA 80b] [BRA 81] [ECK 51] [FOR 62] [FUL 63] [GUR 48] [HAR 61] [JEN 25] [KEN 82] [LOM 56] [MAS 66a] [MAT 69] [WAD 56] [WEB 66] [WHI 61]. I. Palfalvi [PAL 65] demonstrated theoretically the existence of a limiting frequency, beyond which the thermal release creates additional stresses and changes of state.

The effect of frequency seems more marked with the large numbers of cycles and decreases when the stress tends towards the fatigue limit [HAR 61]. It becomes paramount in the presence of a hostile environment (for example, corrosive medium, temperature) [LIE 91].

1.5.5. *Types of stresses*

The plots of the S-N curves are generally obtained by subjecting test bars to sinusoidal loads (tension and compression, torsion, etc.) with zero mean. It is also possible to plot these curves for random stress or even by applying repeated shocks.

1.5.6. Non-zero mean stress

Unless otherwise specified, it will be assumed in what follows that the S-N curve is defined by the median curve. The presence of a non-zero mean stress modifies the fatigue life of the test bar, in particular when this mean stress is relatively large compared to the alternating stress. A tensile mean stress decreases the fatigue life; a compressive stress increases it.

Since the amplitudes of the alternating stresses are relatively small in the fatigue tests with a great number of cycles, the effects of the mean stress are more important than in the tests with a low number of cycles [SHI 83].

If the stresses are large enough to produce significant repeated plastic strains, as in the case of fatigue with a small number of cycles, the mean strain is quickly released and its effect can be weak [TOP 69] [YAN 72].

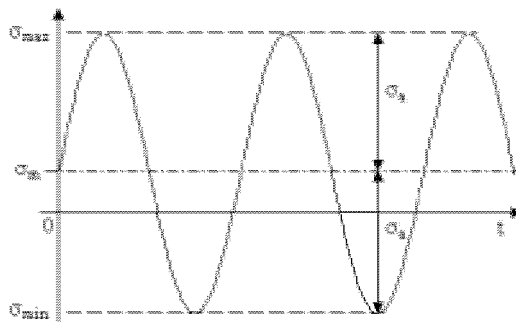


Figure 1.18. Sinusoidal stress with non-zero mean

When the mean stress σ_m is different from zero, the sinusoidal stress is generally characterized by two parameters from: σ_a , σ_{\max} , σ_{\min} and $R = \sigma_{\min} / \sigma_{\max}$.

Although this representation is seldom used, it is possible to use the traditional representation of the S-N curves with the logarithm of the number of cycles to failure on the abscissa axis and on the ordinate stress σ_{\max} , the curves being plotted for different values of σ_m or R [FID 75] [SCH 74].

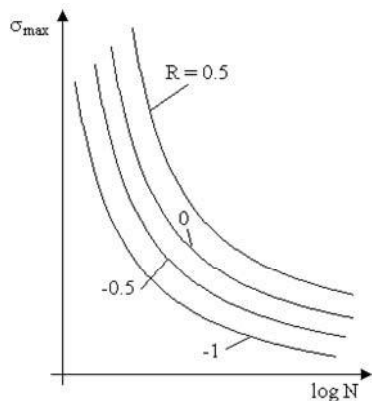


Figure 1.19. Representation of the S-N curves with non-zero mean versus R

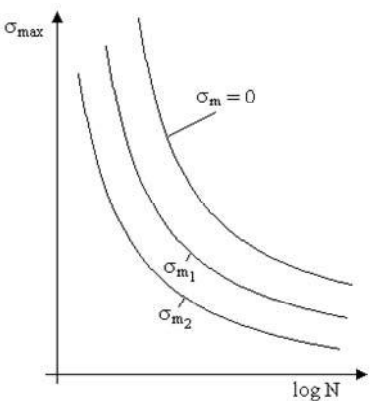


Figure 1.20. Representation of the S-N curves with non-zero mean versus the mean stress

Other authors plot S-N curves with σ_a versus N for various values of σ_m , and propose empirical relations between constants C and b of Basquin's relation ($N \sigma^b = C$) and σ_m [SEW 72]:

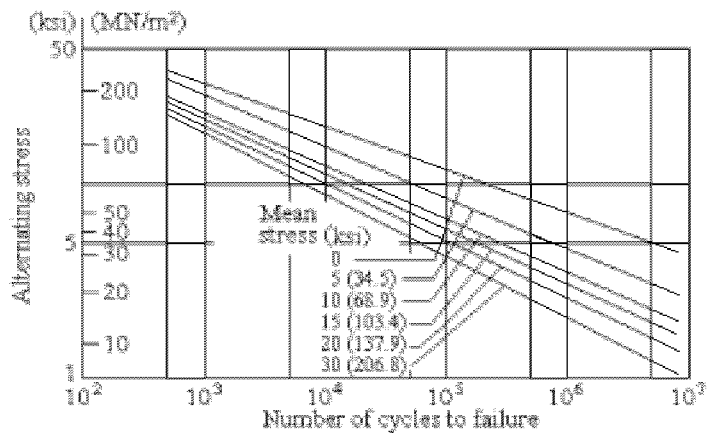


Figure 1.21. Example of S-N curves with non-zero mean

Example 1.2.

Aluminum alloy:

$$\begin{aligned}\log_{10} C &= 9.45982 - 2.37677 \sigma_m + 1.18776 \sigma_m^2 - 0.25697 \sigma_m^3 \\ b &= 3.96687 - 0.213676 \sigma_m - 0.04786 \sigma_m^2 + 0.00657 \sigma_m^3 \\ (\sigma_m \text{ in units of } 10 \text{ ksi})^{(2)}\end{aligned}$$

It is generally agreed to use material below its yield stress ($\sigma_{\max} < R_e$) only, which limits the influence of σ_m on the lifespan. The application of static stress leads to a reduction in σ_a (for a material, a stress mode and a given fatigue life). It is therefore interesting to know how σ_a varies with σ_m . Several relations or diagrams were proposed to this end.

For tests with given σ_m , we can correspond each value of the fatigue limit σ_D to each value of σ_m . All of these values σ_D are represented on diagrams known as “*endurance diagrams*” which, as for the S-N curves, can be drawn for given probabilities [ATL 86].

1.6. Other representations of S-N curves

1.6.1. Haigh diagram

The Haigh diagram is constructed by plotting the stress amplitude σ_a against the mean stress at which the fatigue test was carried out, for a given number N of cycles to failure [BRA 80b] [BRA 81] [LIE 82]. Tensions are considered as positive and compressions as negative.

Let σ_m be the mean stress, σ_a the alternating stress superimposed on σ_m , σ'_a the purely alternating stress (zero mean) which, applied alone, would lead to the same lifetime and σ_D the fatigue limit.

Point A represents the fatigue limit σ_D in purely alternating stress and point B corresponds to the ultimate stress during a static test ($\sigma_a = 0$). The straight lines starting from the origin (*radii*) represent couples σ_a and σ_m . They can be

2. 1 ksi = 6.8947 MPa.

parameterized according to the values of the ratio $R = \sigma_a / \sigma_m$. The coordinates of a point on the line of slope equal to 1 are (σ_m, σ_m) (*repeated stress* [SHI 72]).

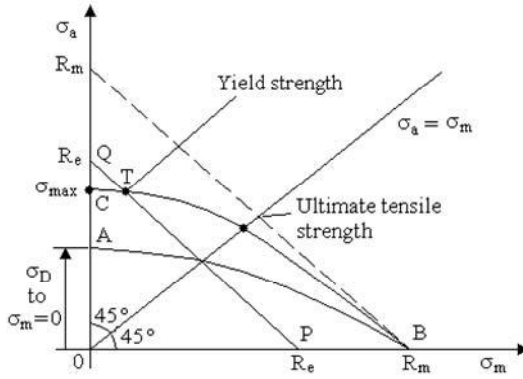


Figure 1.22. Haigh diagram

The locus of the fatigue limits observed during tests for various values of the couple (σ_m, σ_a) is an arc of curve crossing A and B. The domain delimited by arc AB and the two axes represents the couples (σ_m, σ_a) for which the fatigue life of the test bars is higher than the fatigue life corresponding to σ_D .

As long as $\sigma_{\max} (= \sigma_m + \sigma_a)$ remains lower than the yield stress R_e , the curve representing the variations of σ_a with σ_m is roughly a straight line. For $\sigma_{\max} \leq R_e$, we have, at the limit,

$$\sigma_{\max} = R_e = \sigma_m + \sigma_a$$

$$\sigma_a = R_e - \sigma_m.$$

This line crosses the axis $O\sigma_m$ at a point P on abscissa R_e and $O\sigma_a$ at a point Q on ordinate R_e . Let C be the point of $O\sigma_a$ having as ordinate $\sigma_{\max} (< R_e)$. The arc CB is the locus of the points (σ_m, σ_a) leading to the same fatigue life. This arc of curve crosses the straight line PQ at T. Only the arc (appreciably linear) crossing by T on the left of PQ is representative of the variations of σ_a varying with σ_m for $\sigma_{\max} \leq R_e$. On the right, the arc is no longer linear [SCH 74].

Curve AB has been represented by several analytical approximations, starting from the value of σ_D (for $\sigma_m = 0$), and from σ_a and σ_m , used to build this diagram *a priori* in an approximate way [BRA 80a] [GER 74] [GOO 30] [OSG 82]:

– *Modified Goodman line*:

$$\sigma_a = \sigma_D \left(1 - \frac{\sigma_m}{R_m} \right); \quad [1.38]$$

– *Söderberg line*:

$$\sigma_a = \sigma_D \left(1 - \frac{\sigma_m}{R_e} \right); \quad [1.39]$$

and

– *Gerber parabola*:

$$\sigma_a = \sigma_D \left[1 - \left(\frac{\sigma_m}{R_m} \right)^2 \right]. \quad [1.40]$$

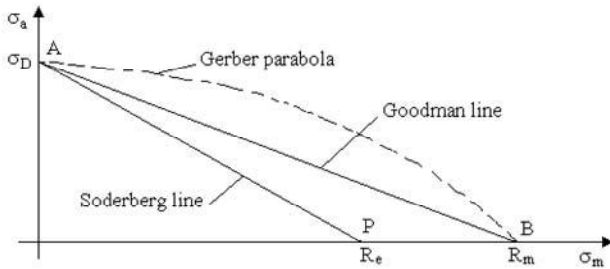


Figure 1.23. Haigh, Gerber, Goodman and Söderberg representations

The Haigh diagram is plotted for a given endurance N_0 , in general fixed at 10^7 cycles, but it can also be established for any number of cycles. In this case, curve CTB can similarly be represented depending on the case by:

Modified Goodman	Söderberg	Gerber
$\sigma_a = \sigma'_a \left(1 - \frac{\sigma_m}{R_m} \right) \quad [1.41]$	$\sigma_a = \sigma'_a \left(1 - \frac{\sigma_m}{R_e} \right) \quad [1.42]$	$\sigma_a = \sigma'_a \left[1 - \left(\frac{\sigma_m}{R_m} \right)^2 \right] \quad [1.43]$

These models make it possible to calculate the equivalent stress range $\Delta\sigma_{eq}$, taking into account the non-zero mean stress using the relation [SHI 83]:

$$\Delta\sigma_{eq} = \frac{1}{a} \Delta\sigma \quad [1.44]$$

where $\Delta\sigma$ is the total stress range, $a = 1 - \sigma_m/R_m$ (modified Goodman), σ_m is mean stress and R_m is ultimate tensile strength.

Relationships [1.41]–[1.43] can be written in the form

Modified Goodman	Söderberg	Gerber
$\frac{\sigma_a}{\sigma'_a} + \frac{\sigma_m}{R_m} = 1 \quad [1.45]$	$\frac{\sigma_a}{\sigma'_a} + \frac{\sigma_m}{R_e} = 1 \quad [1.46]$	$\frac{\sigma_a}{\sigma'_a} + \left(\frac{\sigma_m}{R_m} \right)^2 = 1 \quad [1.47]$

Depending on materials, one of the representations is best suited. The modified Goodman line leads to conservative results (and therefore also for over-sizing) [HAU 69] [OSG 82], except close to the points $\sigma_m = 0$ and $R_m = 0$. It is good for brittle materials and conservative for ductile materials.

The Gerber representation was proposed to correct this conservatism; it adapts better to the experimental data for $\sigma_a > \sigma_m$. The case $\sigma_m \gg \sigma_a$ can correspond to plastic deformations. The model is worse for $\sigma_m < 0$ (compression). It is satisfactory for ductile materials.

The Söderberg model eliminates this latter problem, but it is more conservative than that of J. Goodman. E.B. Haugen and J. A. Hritz [HAU 69] observe that:

- the modifications made by Langer (which exclude the area where the sum $\sigma_a + \sigma_m$ is higher than R_e) and by Sines are not significant;
- it is desirable to replace the static yield stress by the dynamic yield stress in this diagram; and

– the curves are not deterministic. It is preferable to use a Gerber parabola in statistical matter, of the form:

$$\frac{\sigma_a}{\bar{\sigma}_D} + \left(\frac{\sigma_m}{\bar{R}_m} \right)^2 = 1 \quad [1.48]$$

where $\bar{\sigma}_D$ and \bar{R}_m are mean values, like

$$\frac{\sigma_a}{\bar{\sigma}_D \pm 3 S_{\sigma_D}} + \left(\frac{\sigma_m}{\bar{R}_m \pm 3 S_{R_m}} \right)^2 = 1 \quad [1.49]$$

where S_{σ_D} and S_{R_m} are the standard deviations of σ_D and R_m , respectively [BAH 78].

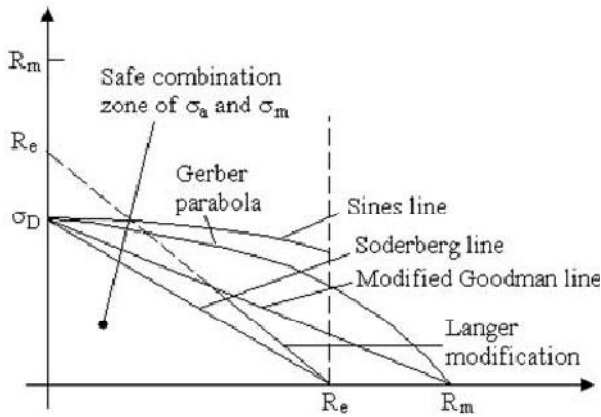


Figure 1.24. Haigh diagram. Langer and Sines modifications

NOTE: The Haigh diagram can be built from the $S-N$ curves plotted for several values of the mean stress σ_m (Figures 1.25 and 1.26)

A static test makes it possible to evaluate R_m . A test with zero mean stress yields σ'_a . For given N , the curves σ_{mi} have an ordinate equal to $\sigma_D(N)_i$.

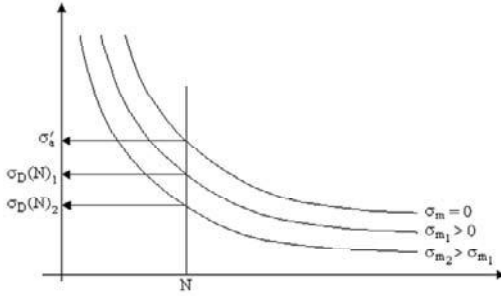


Figure 1.25. *S-N curves with non-zero mean stress, for construction of the Haigh diagram*

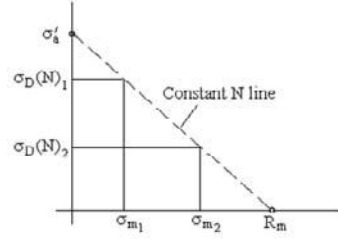


Figure 1.26. *Construction of the Haigh diagram*

Other relations

Von Settings-Hencky ellipse or Marin ellipse [MAR 56] is defined:

$$\left(\frac{\sigma_a}{\sigma'_a}\right)^2 + \left(\frac{\sigma_m}{R_m}\right)^2 = 1 \quad [1.50]$$

$$\frac{\sigma_a}{\sigma'_a} + \left(\frac{\sigma_m}{R_m}\right)^{ml} = 1 \quad [1.51]$$

where σ'_a is allowable stress when $\sigma_m = 0$, σ_a is allowable stress (for the same fatigue life N) for given $\sigma_m \neq 0$ and ml is a constant.

The case of $ml = 1$ (Goodman) is conservative. The experiment shows that $ml < 2$. A value of 1.5 is considered correct for the majority of steels [DES 75].

J. Bahuaud [MAR 56] states that:

$$\frac{\sigma_a}{\sigma_D} + \frac{1}{\rho} \left(\frac{\sigma_m}{R_t}\right)^2 + \left(1 - \frac{1}{\rho}\right) \frac{\sigma_m}{R_t} = 1 \quad [1.52]$$

where

$$\rho = \frac{R_{t\text{compression}}}{R_{t\text{tension}}}$$

and R_t is the true ultimate tensile and compressive strength.

If strength R_t is unknown, it can be approximated using

$$R_t = 0.92 R_m (1 + Z_u) \quad [1.53]$$

where Z_u is striction coefficient and R_m is conventional ultimate strength.

According to Dietmann,

$$\left(\frac{\sigma_a}{\sigma_D} \right)^2 + \frac{\sigma_m}{R_m} = 1 \quad [1.54]$$

All these relations can be gathered in the more general form

$$\left(\frac{\sigma_a}{k_1 \sigma'_a} \right)^{r_1} + \left(\frac{\sigma_m}{k_2 R_m} \right)^{r_2} = 1 \quad [1.55]$$

where k_1 , k_2 , r_1 and r_2 are constant functions of the chosen law.

	r_1	r_2	k_1	k_2
Söderberg	1	1	1	R_e/R_m
Modified Goodman	1	1	1	1
Gerber	1	2	1	1
Von Mises-Hencky	2	2	1	1
Marin	1	ml	1	1
Dietmann	2	1	1	1
Kececioglu	$b^{(*)}$	2	1	1

(*) b = factor function of the nature of material (close to 1)

Table 1.8. Values of the constants of the general law (Haigh diagram)

NOTE: In rotational bending, the following relation can be used in the absence of other data [BRA 80b]:

$$\sigma_{D \text{ rotative bending}} = \frac{\sigma_{D \text{ tension-compression}}}{0.9} \quad [1.56]$$

1.6.2. Statistical representation of Haigh diagram

We saw that in practice, the phenomena of fatigue are represented statistically. The Haigh diagram can take such a form.

For example, if the Gerber relation is chosen, parabolic curves are plotted on the axes σ_a , σ_m to describe the variations of a given stress σ_a corresponding to a given number of cycles to failure with given probability.

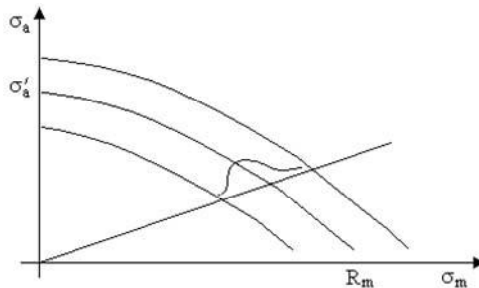


Figure 1.27. Statistical representation of the Haigh diagram

It has been shown that the distribution of the alternating stresses obtained while crossing the arcs of parabola by a straight line emanating from the origin O (slope σ_a/σ_m) is roughly Gaussian [ANG 75].

1.7. Prediction of fatigue life of complex structures

A very difficult problem in the calculation of the fatigue life of a structure is the multiplicity of the sites of initiation of cracks and the mechanisms which determine the life resulting from fatigue of the structure. It could be observed that these sites and mechanisms depend on the environment of service, the amplitude and the nature of the loads.

B.N. Leis [LEI 78] classes fatigue analysis methods into two principal categories:

- indirect approach, in which we try to predict the fatigue life (estimate and accumulation of damage) on the basis of deformation and stress acting far from the potential areas of initiation of the cracks by fatigue, depending on the external displacements and forces (*black box* approach); and

– the direct approach, in which we try to predict the fatigue life on the basis of stress and deformations acting on the potential sites of initiation. These stresses and deformations are local.

The first approach cannot take into account the local inelastic action at the site of initiation of fatigue, whereas the direct approaches can introduce this non-linearity.

The direct approach allows correct predictions of initiation of cracks in a structure provided that the multiplicity of the sites of initiation and mechanisms which control the life in fatigue are correctly taken into account.

1.8. Fatigue in composite materials

An essential difference between metals and composites lies in their respective fatigue behavior. Metals usually break by initiation and propagation of crack in a manner which can be predicted by the fracture mechanics. The composites present several modes of degradation such as the delamination, failure of fibers, disturbance of the matrix, presence of vacuums, failure of the matrix and failure of the composite. A structure can present one or several of these modes and it is difficult to say *a priori* which will prevail and produce the failure [SAL 71].

Another difference with metals relates to behavior due to low frequency fatigue. It is often admitted that metals follow, for a low number of cycles, *Coffin-Manson's* law relating the number of cycles to failure N to the strain range. This is of the form:

$$\Delta \varepsilon_p N^\beta = C \quad [1.57]$$

where $\beta \approx 0.5$. The composites are more sensitive to the strain range and more resistant to fatigue when undergoing large numbers of cycles than with a low number of cycles. A structure can break due to the part of the load spectrum relating to small stresses if it is metallic, whereas the same structure in composite would break because of high loads.

The fatigue strength of composite materials is affected by various parameters which can be classified as follows [COP 80]:

– factors specific to the material: low thermal conductivity, leading to an important increase in the temperature if the frequency is too high, defects related on the heterogenous structure of material and its implementation (bubbles, etc.), natural aging related to its conditions of storage, etc.;

– factors related to the geometry of the test bars:

- shape, holes, notches (stress concentration factors), as with metals;
- irregularities of surface being able to modify the thickness of the test bars in a significant way (important in the case of non-uniform stresses (torsion, bending, etc.);

– stress and environment conditions:

- mode of application of the stresses (torsion, etc.),
- frequency,
- mean stress,
- hygrothermic environment, and
- corrosion (surface deterioration of polymer comparable with corrosion).

For example, R. Cope and A. Balme [COP 80] show that a resin polyester-fiberglass composite or laminate obeys a fatigue degradation model because of:

- degradation of the interface fiber-resin;
- degradation by cracking and loss of the resin polyester; and
- progressive damage of the reinforcement.

They use an index of reference for damage evolution depending on the number n of cycles of the ratio G/G_0 (where G is rigidity modulus in torsion after n cycles and G_0 is the same modulus at the test commencement) and observe a threshold n_S . Beyond this threshold, the material starts to adapt in an irreversible way and undergo damage.

The effect of temperature results in a decrease of the threshold n_S for weak deformations and an increase in the number of cycles for failure (for $t > 60^\circ\text{C}$).

The presence of mean stress amplifies the fatigue damage in an important way.

It is often considered that Miner's rule strongly over-estimates the fatigue life of the structures in composites [GER 82].

Chapter 2

Accumulation of Fatigue Damage

2.1. Evolution of fatigue damage

From a fundamental point of view, the concept of fatigue damage is not well defined because of a lack of comprehension of the physical phenomena related to the material.

The constituent material of any part subjected to alternating stresses undergoes a deterioration of its properties. Depending on the stress level and the number of cycles carried out, this deterioration is partial or can continue until failure.

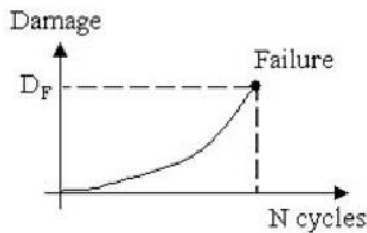


Figure 2.1. *Accumulation of fatigue damage until failure*

In order to follow the evolution of deterioration, we define the concept of *damage* undergone by the test bar, which can rise from zero to 100% at the instant of failure.

To follow the progress of damage over time, a first solution could consist, for example, of studying the evolution of specific physical properties of the test bar [LLO 63].

Strength in (static) tension decreases gradually as the number of stress cycles increases. Measurement of the evolution of these parameters encounters two difficulties: (1) its variation is very weak for most of the life of the test bar and (2) the test to be carried out for this measurement is destructive.

During the fatigue test, cracks appear which are propagated until failure of the test bar. Unfortunately, cracks become detectable and measurable only towards the end of the fatigue life of the test bar.

Additionally, the studies conducted to determine evolution of fatigue as a function of the characteristics of elasticity, plasticity, viscoelasticity and buckling showed that these parameters do not evolve during the application of alternating stress cycles [LEM 70].

Regarding this impossibility, it was conceived that laws of damage accumulation by fatigue could be based on other criteria. Many laws of this type were established, generally from experimental results.

2.2. Classification of various laws of accumulation

Some laws of accumulation of damage are independent of the stress level σ . Others are dependent on it: the $D(n)$ curve varies with values of σ [BUI 80] [LLO 63] [PRO 48]. For others, the $D(n)$ curve varies not only with σ , but also with the preceding series of alternating stresses applied to the material (damage *with interaction*).

In general, all these laws of damage accumulation relate to alternating loads with zero average applied to ordinary temperature. There are, however, publications treating these two particular problems (strong temperature or non-zero mean stress).

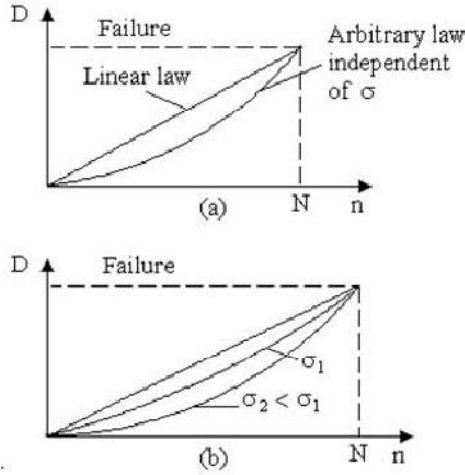


Figure 2.2. Various processes of stress accumulation

2.3. Miner's method

2.3.1. Miner's rule

One of the oldest, simplest and most-used rules is *Miner's rule* [MIN 45] (or *Palmgren-Miner*, because this rule was initially proposed by Palmgren [PAL 24] in 1924 then by Langer in 1937 [LAN 37]). It is based on the following assumptions:

- the damage accumulated by material during each cycle is a function only of the stress level σ ; for n cycles, we define *damage* (or *fraction of fatigue life*) at the level of sinusoidal stress σ :

$$d = \frac{n}{N} \quad [2.1]$$

where N is the number of cycles to the failure at level σ . If W is the stored energy at failure after N cycles at the stress level σ and w that absorbed after the application of n cycles at this same level, we have:

$$\frac{w}{W} = \frac{n}{N} \quad [2.2]$$

- the appearance of a crack, if it is observed, is regarded as a fracture [MIN 45];

– at this level of stress σ , failure intervenes (in a deterministic way) when $n = N$, i.e. when $d = 1$ (endurance). We will see that N could also correspond to the number of cycles with a failure rate of 50% (number of cycles for which half of the test bars tested are broken). This number N is given by the S-N curves previously defined (which are, in general, plotted starting from tests under sinusoidal stresses with constant amplitude). The stresses lower than the fatigue limit stress are not taken into account (N is infinite, therefore d is zero);

– the damages d are added linearly. If k sinusoidal stresses σ_i of equal or different amplitudes are applied successively in n_i cycles, the total damage undergone by the test bar is written:

$$D = \sum_{i=1}^k d_i = \sum_i \frac{n_i}{N_i} \quad [2.3]$$

It is assumed that the damage accumulates without an influence of one level on the other. In this case, the failure occurs for

$$D = \sum_i \frac{n_i}{N_i} = 1 \quad [2.4]$$

NOTE: *The assumption of linearity is not necessary to obtain*

$$\sum_i \frac{n_i}{N_i} = 1$$

for the failure. It is sufficient to suppose that the rate of damage is a function of n/N , independent of the amplitude of the cyclic stress [BLA 46].

Miner's rule therefore consists of calculating the sum of the fractions of fatigue life of the specimen consumed with each cycle and each stress level, where the damage corresponds to a cycle of stress σ being equal to $1/N$. It is therefore a linear law *independent of the stress level and without interaction*.

We will see that Miner's rule can also be used for a random excitation or even for shocks. In this case it is necessary to establish a histogram of the peaks of stress or a table indicating, for the period of validity of the stress, the number of peaks having a given amplitude (or included in a range of amplitudes). For a given amplitude σ_i , the partial damage relating to a peak (half-cycle) is:

$$d_i = \frac{1}{2 N_i} \quad [2.5]$$

yielding total damage for n_i peaks of amplitude σ_i :

$$D = \sum_i \frac{1}{2 N_i} n_i \quad [2.6]$$

Example 2.1.

Let us consider a test in which each test bar is subjected successively to the following three tests:

- a sinusoidal stress of amplitude 15 daN/mm², frequency 10 Hz, duration 1 hour,
- a sinusoidal stress of amplitude 20 daN/mm², frequency 20 Hz, duration 45 min,
- a sinusoidal stress of amplitude 12 daN/mm², frequency 15 Hz, duration 1 hour 30 min.

The S-N curve of the material considered is plotted in Figure 2.3.

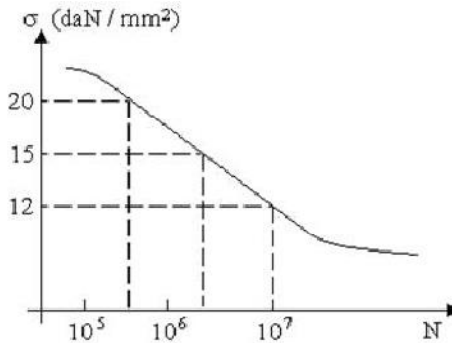


Figure 2.3. Example of S-N curve

For $\sigma_1 = 15$ daN/mm², the number of cycles to failure is equal to $N_1 = 3 \times 10^6$. For $\sigma_2 = 20$ daN/mm², $N_2 = 6 \times 10^5$ and for $\sigma_3 = 12$ daN/mm², $N_3 = 10^7$.

The numbers of cycles carried out at each level are equal to

$$n_1 = \underset{\text{(Hz)}}{f_1} \underset{\text{(s)}}{T_1} = 10 \times 3600 = 3.6 \times 10^4,$$

$$n_2 = 20 \times 2700 = 5.4 \times 10^4,$$

and

$$n_3 = 15 \times 5400 = 8.1 \times 10^4$$

respectively, yielding

$$D = \sum_i \frac{n_i}{N_i} = \frac{3.6 \times 10^4}{3 \times 10^6} + \frac{5.4 \times 10^4}{6 \times 10^5} + \frac{8.1 \times 10^4}{10^7}$$

$$D = 0.1101.$$

Continue the test until failure under the conditions of the third test. One duration of complementary test T_c is defined such that:

$$T_c = \frac{n_c}{f_3}$$

where n_c is given by

$$\frac{n_c}{N_3} = 1 - D$$

$$n_c = (1 - D) \cdot N_3 = (1 - 0.1101) 10^7 = 8.899 \times 10^6 \text{ cycles},$$

yielding

$$T = \frac{8.914 \times 10^6}{15} \approx 5.933 \times 10^5 \text{ s} \approx 164 \text{ hr } 48 \text{ min}$$

Application

If we consider that the S-N curve can be described analytically by Basquin's relationship $N \sigma^b = C$, we can write:

$$D = \sum_i \frac{n_i}{N_i} = \sum_i \frac{n_i}{C} \sigma_i^b$$

or

$$D = \frac{\sum_i n_i \sigma_i^b}{C} \quad [2.7]$$

yielding, for example, the expression of an equivalent alternating stress σ_e which would produce the same fatigue damage if it were applied during N_e cycles, i.e.

$$\sigma_e = \left(\frac{\sum_i n_i \sigma_i^b}{N_e} \right)^{1/b} \quad [2.8]$$

In this relation, the only characteristic parameter of the S-N curve is the exponent b .

Miner's rule for the estimate of the fatigue lifespan under stresses with variable amplitudes is easy to implement. Although much criticized, it is very frequently used in design calculations. Since fatigue is a complex process involving many factors, this rule, a simplified description of fatigue, does not provide very precise estimates. It seems, however, that it leads to results acceptable for the evaluation of the initiation of the cracks under random stresses [WIR 83b].

2.3.2. Scatter of damage to failure as evaluated by Miner

Many tests were carried out to confirm this law by experiment. They showed that actually, we observe a significant scatter in the value of D at the instant of failure [CUR 71] [GER 61]. In addition, M.A. Miner specifies that the value 1 is only an average.

The study of the scatter of the sum $\sum n_i/N_i$ to failure was the object of multiple works; see P.G. Forrest [FOR 74].

All these works showed that the order of application of the sinusoidal stresses influences the fatigue life of the test bars. In addition, it has been demonstrated that

the rate of cracking does not only depend on the amplitude of the loading at a given time, but also on the amplitudes during preceding cycles [BEN 46] [DOL 49] [KOM 45].

For decreasing levels ($\sigma_2 < \sigma_1$), there is generally failure for $D < 1$ (acceleration of cracking by overload effect), whereas failure occurs with $D > 1$ when the levels are increasingly applied ($\sigma_1 < \sigma_2$) (weaker cracking rate due to the under-load). This latter phenomenon, of much less significance than the former, is generally neglected [NEL 78] [WEI 78].

This difference in behavior can be explained by considering that when first applied, cycles of large amplitude create damage in the form of intergranular microscopic cracks that the following cycles at low level will continue to propagate.

Alternatively, at low levels, the first cycles cannot create microscopic cracks [NEU 91]. In certain cases however, and in particular for notched samples, one observes the opposite effect [HAR 60] [NAU 59].

D.N. Nelson [NEL 78] considers that the variations between real fatigue life and fatigue life estimated using Miner's law are related to the order of application of the loads and are, for the smooth parts, lower than or equal to $\pm 50\%$.

Calculations are often made using this law by assuming that any stress lower than the fatigue limit stress σ_D of material has no effect on the material, whatever the number N of cycles applied. However, the tests showed that this stress limit can be lowered when the test bar underwent cycles of fatigue at a higher level than σ_D , which is not taken into account by Miner's rule [HAI 78].

The damage D_F obtained with failure can in practice, depending on the material and the stress type, vary over a wide range. We find in the literature values of about 0.1–10 [HAR 63] [HEA 56] [TAN 70], 0.03–2.31 and even 0.18–23 [DOL 49]. The observed range is narrower, however, e.g. 0.5–2 [CZE 78] [FID 75].

These values are only examples among many others [BUC 77] [BUC 78] [COR 59] [DOL 49] [FOR 61] [GAS 65] [GER 61] [JAC 68] [JAC 69] [KLI 81] [LAV 69] [MIN 45] [STE 73] [STR 73] [WIR 76] [WIR 77]. Compilations of work by various authors showed that:

- Depending on the materials and test sequences, D_F does not generally deviate strongly from 1 and is most frequently larger than 0.3 when all the stress levels are greater than the fatigue limit stress [BUC 78]. The variation in the non-conservative direction is larger when the amplitude of the stresses close or lower than the fatigue

limit stress is larger than that of the stresses higher than this limit. In addition, it is noted that D_F is practically independent of the size of the specimens.

– With a cumulative damage less than 0.3, the probability of non-failure is equal to 95% (560 test results, without reference to the various types of loads and for a constant average stress, on various parts and materials) [BRA 80b] [JAC 68].

In practice, it would be more correct to set at failure:

$$D = \sum_i \frac{n_i}{N_i} = C \quad [2.9]$$

where C is a constant whose value is a function of the order of application of the stress levels. This approach assumes, however, that the damage on the same stress level is deterministic. However, the experiment shows that the test results carried out under the same conditions are scattered.

P.H. Wirsching [WIR 79] [WIR 83b] proposes a statistical formulation of the form:

$$D = \sum_i \frac{n_i}{N_i} = \Delta \quad [2.10]$$

where Δ is the index of damage to failure. Δ is a random variable of median value near 1 with a scatter characterized by the coefficient of variation V_Δ and has a distribution regarded as log-normal.

The purpose of this formulation is to quantify uncertainties associated with the use of a simple model to describe a complicated physical phenomenon. The author proposes separating the factors:

$$1 + V_\Delta^2 = \left(1 + V_N^2\right) \left(1 + V_0^2\right) \quad [2.11]$$

where V_N is the variation coefficient for cycles with constant amplitude until failure and V_0 is the variation coefficient related to the other effects (sequence, etc.).

Failure occurs for $D > \Delta$ with a probability given by:

$$P_f = P(D > \Delta) \quad [2.12]$$

Values recorded in the literature by P.H. Wirsching [WIR 79] are listed in Table 2.1.

	Mean of Δ	Median of Δ	Variation coefficient V_{Δ}
Aluminum (n = 389 specimens)	1.33	1.11	0.65
Steel (n = 90)	1.62	1.29	0.76
Steel (n = 87)	1.47	1.34	0.45
Composite (n = 479)	1.39	1.15	0.68
Composite	1.22	0.98	0.73

Table 2.1. Examples of statistical parameters characterizing the law of damage to failure

P.H. Wirsching [WIR 79] recommends, with a log-normal distribution, a median value equal to 1 and a variation coefficient equal to 0.70. He also quotes other results deviating from these values:

$$7075 \text{ alloy: } V_{\Delta} = 0.98$$

$$2024 \text{ T4 aluminum alloy: } V_{\Delta} = 0.161.$$

For sinusoidal loads or random sequences, W.T. Kirkby [KIR 72] deduced from a compilation of test results on aluminum alloys that:

$$\Delta = 2.42$$

$$V_{\Delta} = 0.98$$

$$\text{standard deviation} = 2.38.$$

Other authors [BIR 68] [SAU 69] [SHI 80] [TAN 75] proposed ascribing a statistical character to Miner's rule by considering in particular that:

– the number N_i of cycles to failure is a random variable with average \bar{N}_i at the stress level σ_i ;

– the expected value of the failure is given by:

$$E \left[\sum_{i=1}^k \frac{n_i}{N_i} \right] = 1 \quad [2.13]$$

– the probability density of the damage to failure

$$D = \sum_i \frac{n_i}{N_i} \quad [2.14]$$

follows a log-normal distribution [SHI 80] [WIR 76] [WIR 77] with mean μ_D and standard deviation equal to 1.

NOTE: *The above was defined for the case of stresses with zero average. If this is not the case, the method continues to apply by using the S-N curve plotted for the value of the mean stress considered.*

2.3.3. Validity of Miner's law of accumulation of damage in case of random stress

A.K. Head and F.H. Hooke [HEA 56] were the first to publish data from tests where the amplitude of the stress varies in a completely random way.

Miner's rule was sometimes regarded as inadequate and dangerous to apply for loads of random amplitude [OSG 69]. This opinion, however, is not commonly held and the majority of authors consider that this rule is even better for these loads. Since the order of application of the stresses is random, its influence is much weaker than in sinusoidal mode.

The results are often regarded as resolutely optimistic. Much work carried out on aluminum alloy test bars show that the Miner assumption led to predictions of fatigue lives longer than those observed in experiments, with variations in the ratio from 1 to 1.3 or 1 to 20 according to individual cases [CLE 65] [EXP 59] [FRA 61] [FUL 63] [HEA 56] [HIL 70] [JAC 68] [PLU 66] [SMI 63] [SWA 63]. There is therefore failure noted for

$$\sum \frac{n_i}{N_i} < 1.$$

On the contrary, other studies show that Miner's rule is pessimistic [EXP 59] [KIR 65a] [LOW 62]. In fact, this seems to be the case for loads with average tensile stress associated with an axial loading [MAR 66] or when there are frictional phenomena [KIR 65a].

The precision of the estimates is considered to be acceptable in the majority of cases [BOO 69] [BOO 70] [BOO 76] [KOW 59] [NEL 77] [TRO 58], however. Although Miner's rule leads to coarse results, varying considerably, many authors

consider that there is no rule more applicable than Miner's. The regularity of the results obtained with the other methods is not significantly better despite their increased complexity [EST 62] [FRO 75] [ING 27] [NEL 78] [WIR 77]. Miner's hypothesis remains a good first approximation confirmed by experiment. The error depends on the rule itself, but also on the precision of the S-N curve used [SCH 72a].

All other rules developed to make it more precise, to be discussed later, brought an additional complexity while not always using well-known constants; they only lead to better results in certain specific cases.

Miner's rule is very much used for mechanical structures and even for the calculation of strength to fatigue of electronic equipments. For these materials, D.S. Steinberg [STE 73] suggests calculating fatigue life using:

$$\sum_i \frac{n_i}{N_i} = 0.7$$

instead of 1 (and not 0.3 as sometimes proposed, a value which can lead to an increase in superfluous mass). W. Schutz [SCH 74] proposed $\sum \frac{n_i}{N_i} = 0.6$ and, at high temperatures, when the yield stress is definitely lower, $\sum \frac{n_i}{N_i} = 0.3$ (result of statistical studies [OSG 69]).

Miner's rule can also be used to make comparisons of the severity of several vibrations (the criterion being the fatigue damage). This use, which does not require that $\sum \frac{n_i}{N_i}$ is equal to unity at failure, gives good results [KIR 72] [SCH 72b] [SCH 74].

NOTE: *Alternatives very similar to Miner's rule were evaluated [BUC 78]:*

– the form $\sum \frac{n}{N_{min}} = 1$, where N_{min} is a value corresponding to a certain probability of survival (95% for example), is not always conservative; and

– the sum $\sum \frac{n}{N_{mean}}$ (N_{mean} = mean number of cycles to failure at a given stress level) does not give either a precise estimate of the fatigue life (sequence effect, non-linear accumulation law, etc.).

2.4. Modified Miner's theory

2.4.1. Principle

To try to correct the variations observed between the calculated fatigue lives starting from Miner's theory and the results of the tests, in particular during the application of sinusoidal stresses at several levels σ_i , it was planned to replace the linear accumulation law by a non-linear law of the form:

$$D = \sum_i \left(\frac{n_i}{N_i} \right)^x \quad [2.15]$$

where x is a constant assumed to be higher than 1.

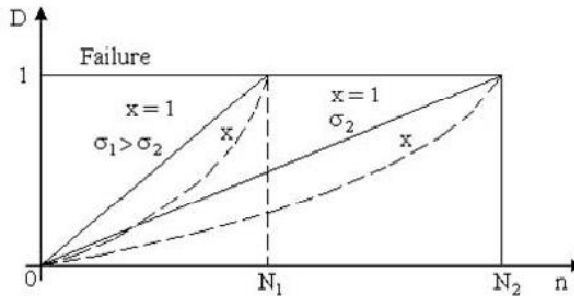


Figure 2.4. Damage versus the number of cycles, as function of stress amplitude

Figure 2.4 shows the variations of the damage D versus the number of cycles carried out at two stress levels σ_1 and σ_2 . For given σ , we assume that the test bar breaks when $D = 1$.

The number of cycles to failure is greater since σ is smaller. If the damage is linearly cumulative (Miner's hypothesis), the curve $D(n)$ is a straight line. With the modified law, the curve $D_x(n)$ is, at level σ , of the form:

$$D = a n^x \quad [2.16]$$

where a is a constant such that $D = 1$ when $n = N$:

$$a = \frac{1}{N^x} \quad [2.17]$$

For $x > 1$, $D_x(n)$ is below the straight line of the linear case (dotted curve).

2.4.2. Accumulation of damage using modified Miner's rule

Two methods can be considered [BAH 78] [GRE 81]:

- method of equivalent cycles; and
- method of equivalent stresses,

according to whether the damage is expressed as a function of the number of cycles brought back to only one level of stress or the damage d_i is calculated independently at each stress level σ_i before determining the total damage

$$D = \sum_i d_i .$$

The reasoning is based on the damage curves (damage D undergone by the test bar according to the number of cycles n) for a given stress level σ . As an example, we will consider two levels below σ_1 and σ_2 .

2.4.2.1. Method of equivalent cycles

We carry out:

- n_1 cycles at level σ_1 , failure occurring on this level for $n = N_1$ cycles; and
- n_2 cycles at level σ_2 (failure for N_2 cycles).

The damage d_2 created by these n_2 cycles at level σ_2 could be generated by n_1^* cycles at level σ_1 , n_1^* being such that

$$d_2 = \left(\frac{n_2}{N_2} \right)^x = \left(\frac{n_1^*}{N_1} \right)^x \quad [2.18]$$

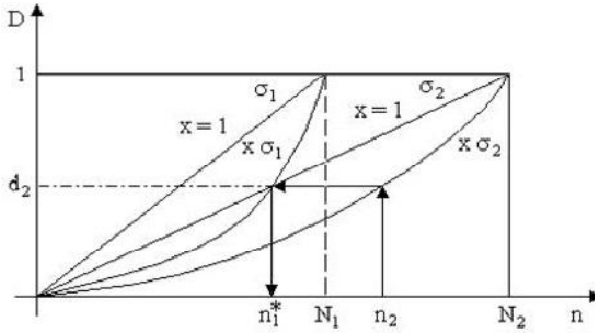


Figure 2.5. *Determination of equivalent number of cycles*

i.e., for any value of x , for

$$n_1^* = n_2 \frac{N_1}{N_2} \quad [2.19]$$

If it is assumed that the block composed of these n_1 and n_2 cycles of stress of amplitudes, equal to σ_1 and σ_2 , respectively, is repeated p times until failure, we will have then carried out n_{1R} cycles at level σ_1 and n_{2R} cycles at level σ_2 (i.e. n_{1R}^* equivalent cycles), yielding

$$n_{1R} + n_{1R}^* = N_1 \quad [2.20]$$

$$n_{1R} + n_{2R} \frac{N_1}{N_2} = N_1,$$

$$N_1 \left(\frac{n_{1R}}{N_1} + \frac{n_{2R}}{N_2} \right) = N_1,$$

$$\frac{n_{1R}}{N_1} + \frac{n_{2R}}{N_2} = 1 \quad [2.21]$$

If we set

$$\eta_1 = \frac{n_{1R}}{n_{1R} + n_{2R}} \text{ and } \eta_2 = \frac{n_{2R}}{n_{1R} + n_{2R}},$$

this relationship can also be written

$$(n_{1R} + n_{2R}) \left(\frac{\eta_1}{N_1} + \frac{\eta_2}{N_2} \right) = 1$$

i.e.

$$N_R \left(\frac{\eta_1}{N_1} + \frac{\eta_2}{N_2} \right) = 1 \quad [2.22]$$

while setting

$$N_R = n_{1R} + n_{2R} = p (n_1 + n_2) \quad [2.23]$$

The method can be extended to the study of a loading comprising an arbitrary number of levels. Calculation is easier if we use an analytical form of the damage curves.

2.4.2.2. Method of equivalent stresses

Instead of considering a number of cycles equivalent to the single level σ_1 , we calculate the partial damage created by each sequence [BAH 78, GRE 81]. With the same notation, we have (to failure):

$$D = d_1 + d_2 = \left(\frac{n_{1R}}{N_1} \right)^x + \left(\frac{n_{2R}}{N_2} \right)^x = 1 \quad [2.24]$$

yielding

$$N_R^x \left[\left(\frac{\eta_1}{N_1} \right)^x + \left(\frac{\eta_2}{N_2} \right)^x \right] = 1$$

and

$$N_R = \frac{1}{\sqrt[x]{\left(\frac{\eta_1}{N_1}\right)^x + \left(\frac{\eta_2}{N_2}\right)^x}} \quad [2.25]$$

Miner's theory is a particular case of this method, with linear damage curves. On this assumption, the two approaches (equivalent cycles and equivalent stresses) lead to the same results.

The modified Miner's rule therefore yields a fatigue life longer than the rule of origin, consequently nearer to the experiment when $\sigma_1 < \sigma_2$ (first stress level lower than the second). The improvement is however only partial, since it does not yield anything when $\sigma_1 > \sigma_2$. The modified Miner's rule is also *independent of the level of stress and without interaction*.

2.5. Henry's method

D.L. Henry [HEN 55] supposes that:

– the S-N curve of a steel specimen can be described by a relation of a hyperbolic type of the form

$$N(\sigma - \sigma_D) = C \quad [2.26]$$

where C is a constant and σ_D is the fatigue limit stress of material; and

– the two parameters C and σ_D are modified as the fatigue damage accumulates. The endurance to fatigue decreases and C varies proportionately to σ_D .

It is the author's opinion that relation [2.26] is correct as long as σ remains lower than $1.5 \sigma_D$. One of the interests of this representation is related to the introduction of a fatigue limit. With these assumptions, D.L. Henry shows that the damage D stored by a test bar, defined here like the relative variation of the fatigue limit

$$D = \frac{\sigma_D - \sigma'_D}{\sigma_D} \quad [2.27]$$

is written

$$D = \frac{\frac{n}{N}}{\sigma_D \left(1 - \frac{n}{N}\right) + \frac{\sigma - \sigma_D}{\sigma_D}} \quad [2.28]$$

i.e., if we set $\gamma = \frac{\sigma - \sigma_D}{\sigma_D} = \text{stress ratio}$ and $\beta = \frac{n}{N}$,

$$D = \frac{\beta}{1 + \frac{1}{\gamma}(1 - \beta)} \quad [2.29]$$

It is noted that for $\sigma'_D = 0$ we have $D = 1$ and that, when $\sigma \rightarrow \sigma_D$, $\gamma \rightarrow 0$ and $D \rightarrow 0$.

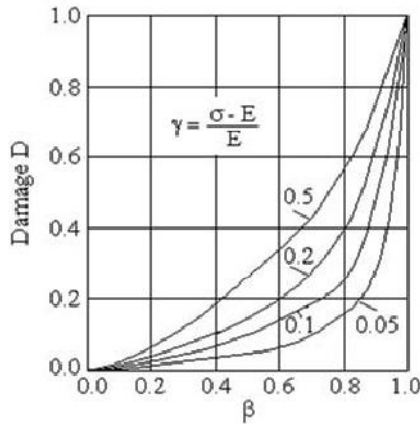


Figure 2.6. Accumulation of damage according to Henry's hypothesis

The curve $D(\beta)$ plotted for several values of γ shows that when γ increases (i.e. for the strong values of the stress), the law tends to a linear relationship.

For a given β ratio, the damage is larger since σ is higher.

This theory therefore supposes that fatigue damage is a function of applied stress level and of the order of application of the stresses (the law is *dependent on the level of the stresses and with interaction*).

2.6. Modified Henry's method

The Henry's relation was modified by addition of a term D_c [EST 62] [INV 60]:

$$\frac{D}{D_c} = \frac{\frac{n}{N}}{1 + \frac{\sigma_D}{\sigma - \sigma_D} \left(1 - \frac{n}{N}\right)} \quad [2.30]$$

where D_c is *critical fatigue damage* (damage at which the part breaks completely), in order to take into account the application of a load which exceeds the residual resistance of the item to the test. Calculations of fatigue life are carried out according to same process as that used for method EFD (equivalent fatigue damage [POP 62]) [EST 62]. The increments n/N are added along the curve of damage; the failure occurs when $D/D_c = 1$. This method requires the knowledge of an additional parameter, D_c .

Henry's rule and this modified rule have a limited use, the materials generally having a badly defined fatigue limit stress (aluminum and light alloys in particular).

2.7. Corten and Dolan's method

These authors propose a non-linear theory of cumulative damage, based on the number m of nuclei likely to be damaged and on the velocity r of propagation of the cracks [COR 56] [COR 59] [DOL 49] [DOL 57] [HIL 70] [LIU 59] [LIU 60]. The accumulated damage on the stress level i is written:

$$D_i = m_i r_i n_i^{a_i} \quad [2.31]$$

where a_i is an experimentally determined constant and m and r are constants for a given stress level.

Damage to failure occurs for $D = 1$. It is expressed as a function of the number of cycles according to

$$D_i = \left(\frac{n_i}{N_i} \right)^{a_i} \quad [2.32]$$

It is about a law *depending on the stress level, with interaction*. The effects of interaction are included in the concept of propagation of cracks. In a test, the cycle of maximum load is decisive for the initial damage since it determines the number of points where cracks will be formed. Once this number is established, we assume that the propagation is carried out according to a cumulative process without interaction.

Let α_i be the percentage of cycles carried out at level σ_{a_i} , d a constant, σ_1 the maximum amplitude of the sinusoidal stress for a fatigue life N_1 and N_g the total number of cycles of the test program. We have

$$\alpha_i N_g = n_i \quad [2.33]$$

yielding

$$\sum_i \alpha_i N_g \left(\frac{\sigma_{a_i}}{\sigma_{a_1}} \right)^d = N_1 \quad [2.34]$$

$$N_g = \frac{N_1}{\sum_i \alpha_i \left(\frac{\sigma_{a_i}}{\sigma_{a_1}} \right)^d} \quad [2.35]$$

or

$$\sum_i \frac{n_i}{N_1} \left(\frac{\sigma_{a_i}}{\sigma_{a_1}} \right)^d = 1 ,$$

$$\sum_i \frac{n_i}{N_i} \left[\frac{N_i}{N_1} \left(\frac{\sigma_{a_i}}{\sigma_{a_1}} \right)^d \right] = 1 \quad [2.36]$$

This relationship, comparable with that of A.M. Freudenthal and R.A. Heller [FRE 58], can be reduced to that of Miner by using a modified fatigue curve which, on $\log \sigma$, $\log N$ scales, intersects the y-axis at σ_1 and has a negative slope equal to $1/d$. The equation of this curve is then

$$N' \sigma^d = A \quad [2.37]$$

where N' is the fatigue life given by this modified curve. From equation [2.33], α_i can be substituted into equation [2.35] by taking account of equation [2.37], to calculate σ_1 and σ_i :

$$N'_i \sigma_i^d = N_1 \sigma_1^d \quad [2.38]$$

where $N_1 = 1$.

$$N_g = \frac{N_1}{\sum_i \frac{n_i}{N_g} \left(\frac{\sigma_i}{\sigma_1} \right)^d} = \frac{N_1}{\sum_i \frac{n_i}{N_g} \frac{1}{N'_i}}$$

$$\sum_i \frac{n_i}{N'_i} = N_1$$

yielding

$$\sum_i \frac{n_i}{N'_i} = 1.$$

B.M. Hillberry [HIL 70] shows that the Corten–Dolan theory, like that of Palmgren–Miner, over-estimates the fatigue lives under random stress (by a factor varying from 1.5 to 5 for Miner and approximately 2.5 for Corten–Dolan).

This result is compatible with those of other authors. It can be explained by noting that for random loads, according to these two theories, damage accumulates under a certain weighted average stress and that this same stress produces the failure. With such a load, however, the failure can occur earlier under one of the largest peaks present in a statistical way. This view of Nelson [NEL 77] is confirmed by the test results carried out by I.F. Gerks [GER 66].

2.8. Other theories

Taking into account their significant number, we will limit ourselves within the framework of this book to simply quoting theories and providing their respective references. This list does not claim to be exhaustive, in terms of both methods and references.

NOTE: Among all the models suggested, of which we will quote only a small number, little have found practical application. Miner's rule, with its imperfections, remains the simplest, most general and the most used by far [BLA 78], and is often sufficiently accurate. The other rules generally use several constants whose value is difficult to find and which complicate the analysis in a way not justified by the result. See [DEN 62] [FUL 6] [RIC 65b] for comparisons of these various methods.

Theory	Date	References
Miner modified by Haibach	1970	[HAI 70] [STR 73]
Marco and Starkey	1954	[MAR 54]
Shanley	1952/1953	[MAS 66b] [SHA 52]
Langer	1937	[LAN 37]
Kommers	1945	[KOM 45]
Richart and Newmark	1948	[COR 59] [[RIC 48]
Machlin	1949	[MAC 49]
Lunberg	1955	[LUN 55]
Head and Hooke	1956	[HEA 56]
Levy	1957	[LEV 57]
Freudenthal and Heller	1956–1960	[FRE 55] [FRE 56] [FRE 58] [FRE 60] [FRE 61]
Smith	1958–1964	[SMI 58] [SMI 64b]
Grover	1959	[GRO 59] [GRO 60]
Eshleman, Van Dyke and Belcher	1959	[ESH 59]
Parzen	1959	[PAR 59]
Gatts	1961–1962	[GAT 61] [GAT 62a] [GAT 62b]
Valluri	1961–1964	[VAL 61a] [VAL 61b] [VAL 63] [VAL 64]
Poppleton	1962	[POP 62]
Method of equivalent fatigue damage (EFD Method)	1962	[EST 62]
Serensen	1964	[SER 64]

Lardner	1966	[LAR 66]
Birnbaum and Saunders	1968–1969	[BIR 68] [BIR 69a] [BIR 69b]
Esin	1968	[ESI 68]
Filipino, Topper and Leipholz	1976	[PHI 76]
Kozin and Sweet	1964–1968	[ESI 68] [KOZ 68]
Marsh	1965	[MAR 65]
Heller and Heller	1965	[HEL 65]
Manson, Freche and Ensign	1967	[MAN 67]
Sorensen	1968	[SOR 68]
Caboche	1974	[CHA 74]
Dubuc, Bui-Quoc, Bazergui and Biron	1971–1982	[BUI 71] [BUI 82] [DUB 71]
Hashin and Rotom	1977	[HAS 77]
Tanaka and Akita	1975–1980	[TAN 75] [TAN 80]
Bogdanoff	1978–1981	[BOG 78a] [BOG 78b] [BOG 78c] [BOG 80] [BOG 81]
Wirsching	1979	[WIR 79] [WIR 83b]

Table 2.2. *Some theories of fatigue damage accumulation*

Chapter 3

Counting Methods for Analyzing Random Time History

3.1. General

Counting methods were initially developed for the study of fatigue damage generated in aeronautical structures. The signal measured, in general a random stress $\sigma(t)$, is not always made up of a single peak between two zero crossings. On the contrary, several peaks often appear which makes it difficult to determine the number of cycles undergone by the structure.

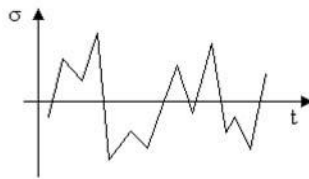


Figure 3.1. *Random stress*

The counting of peaks makes it possible to create a *histogram* of the peaks of the signal (number of events counted on the abscissa whose amplitude is shown on the ordinate) which can then be transformed into a *stress spectrum* (cumulative frequency distribution) giving the number of events (on abscissae) for lower than a given stress value (on ordinates), i.e. the number of peaks lower than a given threshold level versus the value of this threshold. The stress spectrum is therefore a

representation of the statistical distribution of the characteristic amplitudes of the signal as a function of time [SCH 72a]; it is used in two applications:

- to carry out estimated fatigue life calculations on the parts subjected to stresses measured; and
- to transform a complex random stress into a simpler test specification, comprising for example several *blocks* of sinusoidal vibrations of constant amplitude. Several test strategies are possible, such as the realization of sinusoidal cycles with constant amplitude in random sequence or the application of individual cycles in randomized sequence. The tests are carried out on material test bars with a control in force.

The importance of this analysis of the signal in these studies and its difficulty is easily understood, which explains the significant number of methods suggested.

The analyzed signal is a stress varying with time. Within the framework of this work, these same methods can be used to establish a peak histogram of the relative response displacement $z(t)$ of the mass of a system with one degree-of-freedom subjected to a vibration and to calculate the fatigue damage which results from it (the stress being assumed proportional to this relative displacement).

All the methods assume that the result of counting always includes an assumption of damage, which postulates that the same fatigue life is obtained with the original signal and the signal reconstituted from counting or, at least, that starting from the two signals. There exists a constant ratio of the fatigue lives for all the possible material combinations, stress concentrations, stress ratio, treatment of surfaces, etc.

Beyond this, it is certain that the evaluation of a result of counting is also related to the procedure of a specific test or to a theoretical method of fatigue life prediction (modification in the order of application of the stress levels can, for example, change the fatigue life) [BUX 73].

The evaluation of the fatigue damage is therefore carried out in three steps:

- counting of the cycles;
- choice of a relation cycle – generated damage; and
- summation of the damage generated by each cycle.

Various methods of counting were proposed, leading to different results and therefore (for some) to errors in the calculation of the fatigue lives:

1. peak count;
2. range-restricted peak count;
3. level-restricted peak count;
4. mean-crossing peak count;
5. range count;
6. range-mean count;
7. range-pair count;
8. ordered overall range method;
9. racetrack method;
10. level crossing count;
11. modified level crossing count;
12. peak valley pair (PVP) counting;
13. fatigue-meter count;
14. rainflow count;
15. NRL (National Luchtvaart Laboratorium) counting;
16. time spent at a given count level.

Schematically, these counting methods can be classified into two principal categories [WAT 76]:

- methods in which a counting of a signal characteristic not necessarily connected in a simple way to damage accumulation is carried out (peaks, level crossings, etc.); and

- methods using the stress or deformation ranges (range counting, range-mean counting, range-pair counting and rainflow). These latter methods are generally preferred, since they are using parameters which are more directly connected to the fatigue damage.

We will see that two methods (range-mean counting and rainflow counting) have the additional advantage of taking into account the mean stress level (or deformation) for each range.

In all these methods, it is necessary to be able to eliminate the small variations. This correction, initially intended to remove the background noise of the measuring equipment, also aims to transform long duration signals into signals easier to use [CON 78]. This simplification results in the definition of a threshold value below which the peaks or ranges are not counted.

As an example, let us consider the signal sample $\sigma(t)$ in Figure 3.2. The signal has peaks A, B,..., F from which ranges can be defined: AB, BC, CD, ..., EF, with amplitudes equal to r_1, r_2, r_3, r_4, r_5 respectively and with means m_1, \dots, m_5 .

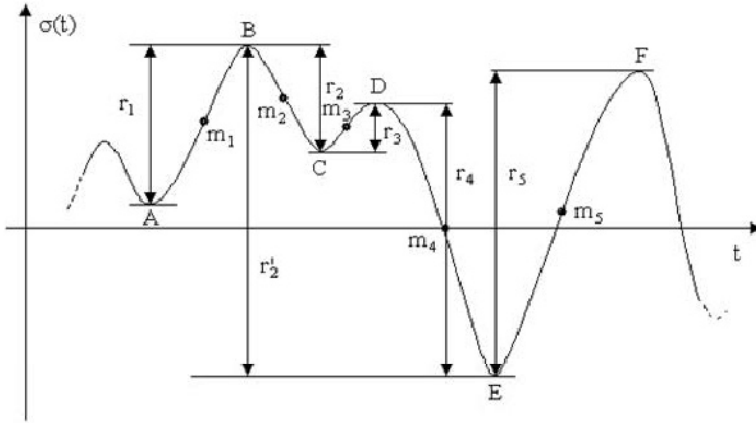


Figure 3.2. *Elimination of small variation ranges*

The small variations such as CD can be neglected by imposing a threshold for counting. In this case, the ranges BC, CD and DE are replaced by the single range BE (r'_2).

Taking into account the expression for the fatigue damage, in which the peak amplitude is raised to the power b , if the linear part of the S-N curve is represented by the Basquin's relation:

$$N \sigma = \text{Constant}$$

then it is seen easily that the total damage is much smaller when it is calculated by taking account of the small variations than when they are removed. Total damage is equal to

$$D = \sum_i \frac{n_i}{N_i} = \frac{n_i \sigma_i^b}{C} \quad [3.1]$$

$$\left(r_1^b + r_2^b + r_3^b + r_4^b \right) < r_2'^b \quad [3.2]$$

independent of the mean stress. This is true only because the small variations are possibly below the fatigue limit and can therefore be neglected [DOW 72] [WAT 76].

A reduction of the counting threshold, which results in considering more ranges of small amplitude, can therefore lead to a weaker expected damage and *vice versa*. This phenomenon is not systematic and can be negligible depending on the shape of the signal (for example, when the small cycles are dominating). P. Watson and B.J. Dabell [WAT 76] observe that, to guard against this problem, a solution can consist of successively calculating the damage with several thresholds to retain only the greatest value. The effect of omission of small variations has been studied by several authors [CON 78] [KID 77] [POT 73]. It often appears that the cycles of loads below the fatigue limit can generally be ignored if the load peak levels of the remainder of the curve versus time ($\varepsilon(t)$ or $\sigma(t)$) are not too large.

A study by A. Conle and H.T. Topper [CON 78] showed that, even with the rainflow method, the damage neglected by using a signal without small variations is much larger than predicted. When the signal has very high levels (load or deformation), it is necessary to be very careful during the elimination of the smallest variations. J.M. Potter [POT 73] observed in experiments that the suppression of the levels which, according to a conventional analysis of fatigue damage, do not lead to any damage, leads (in experiments) to an increase in the fatigue life.

We will describe in the following sections the methods quoted.

3.2. Peak count method

3.2.1. Presentation of method

This method is undoubtedly the simplest and oldest. The values considered as significant here are the maxima and the minima, which are observed over the duration T of the signal [BUX 66] [DEJ 70] [NEL 78] [RAV 70] [SCH 63] [SCH 72a] [STR 73].

A peak located above the mean is regarded as positive; below, it is negative. The ordinate axis can be divided in order to define classes and build a histogram.

We can choose to count only the peaks above a certain threshold value (in absolute value) or to decide that small stress variations lower than a given value are negligible; these small variations are defined as for the variation between a maximum and a minimum (or the reverse). In Figure 3.3, for example, the peaks marked by the symbol \square are not counted [HAA 62].

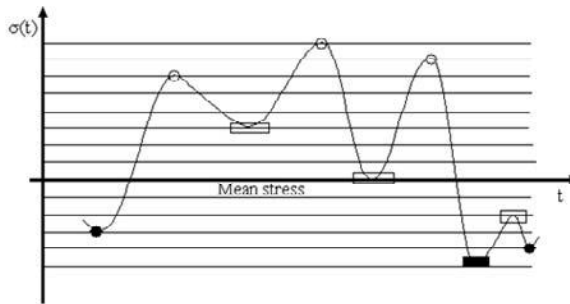


Figure 3.3. *Stress time history peaks*

The results can be expressed either in the form of the maximum (or minimum) number:

- having a given amplitude;
- located above a given threshold, this threshold being variable to cover all the range of the amplitudes; or
- by curves giving the peak occurrence frequency versus their amplitude.

The curves giving the maxima and the minima are generally symmetric (but not necessarily). It is the case for a normal process [RAV 70].

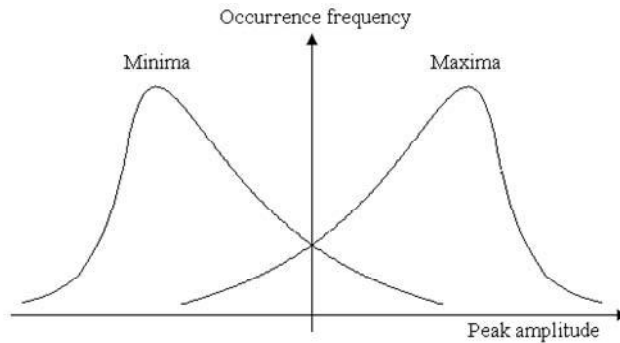


Figure 3.4. *Occurrence frequency of maxima and minima*

With this method, any information on the sequence of load, on the order of appearance of the peaks is completely lost [VAN 71].

After counting, it is not possible to know if a counted peak is associated with a small or with a great load variation. The interpretation of the load spectrum formed using this method can therefore be disturbed by small load variations.

When counting is finished, a signal is reconstituted from this peak histogram by associating a positive peak with a negative peak of the same amplitude to constitute a complete cycle [HAA 62]. Consequently, it can be seen that the real total length of the excursion of the signal is generally less than that obtained by reconstituting the signal from the histogram.

Peaks such as A and B in Figure 3.5, for example, are treated both as starting from zero and returning to zero.

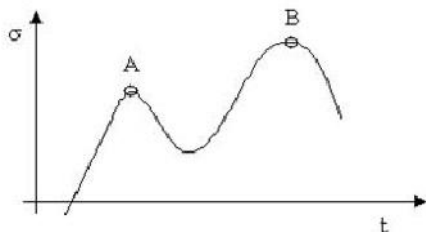


Figure 3.5. Peaks counted as complete half-cycles

The reconstituted signal is therefore more severe than the real signal [WEB 66]. This method of counting is often named *total peak count* as opposed to the *net peak count* method, in which the peaks are defined as the algebraic sum of the extrema, the valleys (minima) being counted negatively. The lengths of excursions tend to be equal in this case.

Another way of counting the extrema can consist of retaining only the positive maxima and the negative minima. An alternative to this process is frequently used for the study of the vibrations measured during fighter aircraft operations [LEY 63]. The sorting of the extrema can be carried out from the results of the above method.

The peak count method is also sometimes referred to as the *simple peak count method* [GOO 73] as opposed to the *peak count method* in which the extrema between two passages by the mean value are taken (described in section 3.3). Each peak is noted. It is the least restrictive of all the methods. It can be used as means of characterization of the signal by comparing the extrema distribution with a given distribution (Rayleigh's law, for example).

3.2.2. Derived methods

The present maxima in each class of amplitude are counted (Figure 3.6). The reconstituted signal does not account for the peak order or for the frequency. The small strain variations are amplified. To reduce their influence, a secondary condition can be introduced, intended to neglect the extrema which are associated with a load variation lower than a given value (hatched zone / / / / in Figure 3.6).

Another possibility is to count the minimal values in addition to the maximal values, but this leads to a very great number of combinations to reconstitute the signal and is therefore not a suitable method [WEB 66].

It is also sometimes decided to count only the maxima above a specified level (or minima below some level). This modification does not improve the validity of the results.

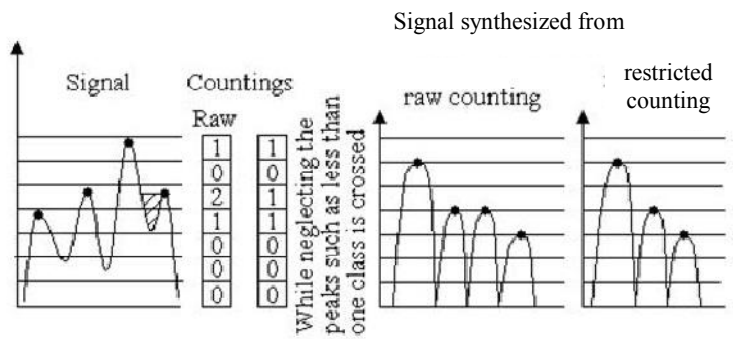


Figure 3.6. *Omission of small variations below a given threshold*

O. Buxbaum [BUX 66] suggests neglecting all the signal variations lower than 5% of the maximum value, which do not have any influence on the fatigue life. F.E. Kiddle and J. Darts [KID 77] observed that, on a specimen with bolted connection, the progressive omission of the peaks of small amplitude above the fatigue limit does not have an appreciable effect on the mean endurance. This effect is independent of the maximum load present in the spectrum. The endurance of this same specimen is, on the other hand, sensitive to the greatest loads.

3.2.3. Range-restricted peak count method

The objective here is to count only the most significant peaks associated with the greatest load variations [MOR 67] [WEL 65]. Counts are limited to the peaks beyond mean thresholds (for example, if it is an acceleration, the minima which are below 0 g and the maxima above 2 g) and which are at the same time preceded and followed by a minimal variation of the amplitude (1 g, for example), or which exceed a given percentage of the incremental peak value (for example, 50%) (the largest of the two results is chosen).

Here the incremental peak value is defined as the difference between the peak value and the mean load level [GOO 73] [MOR 67] [WEL 65].

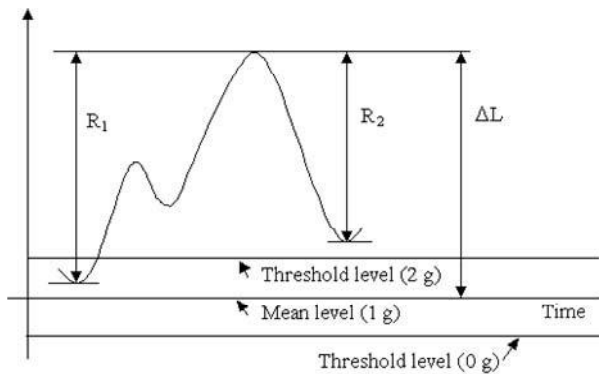


Figure 3.7. Counting of ranges higher than a given value

In Figure 3.7, for example, the ranges R_1 and R_2 are higher than the threshold $R_0 = 1$ g or 50% of ΔL . The intermediate fluctuations are neglected with this method, as well as some fluctuations which are not really of any importance. However, counting relating to largest maxima and the smallest minima assume more importance.

3.2.4. Level-restricted peak count method

After having defined classes, the procedure is as follows:

- a maximum (*primary peak*) is accepted only if the signal falls below a larger value than a specified threshold [VAN 71] [WEL 65] (all crossings prior to this primary level being forgotten); and

– the value attributed to the peak is that of the threshold crossed just before the peak.

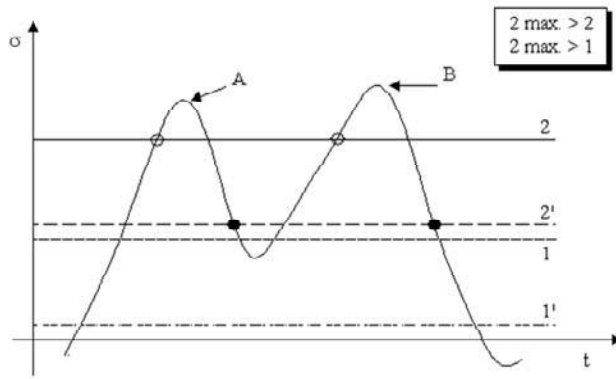


Figure 3.8. *Elimination of peaks not followed by sufficient amplitude variation*

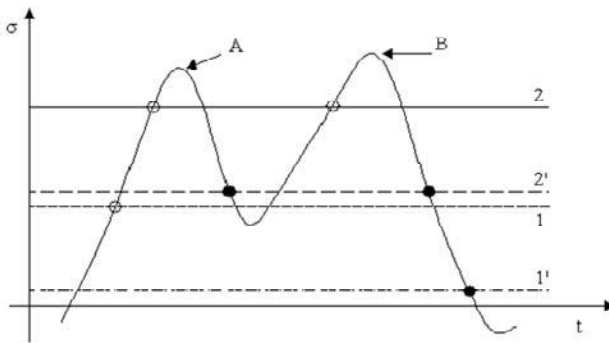


Figure 3.9. *Counting of all threshold crossings (fatigue-meter method)*

For example, peak A (Figure 3.8) is counted because the signal crosses threshold 2' after having crossed the larger threshold level 2 before passing through the maximum value at A. This method uses the same type of threshold specification as the fatigue-meter method. Only the peaks which are preceded and followed by the necessary threshold are considered [GOO 73]. However, in contrast to the fatigue-meter method, all the other passages across the threshold below 2 are not considered. As an example, for the same signal, the fatigue-meter method would lead to the result in Figure 3.9.

3.3. Peak between mean-crossing count method

This method may be called *mean-crossing peak count method* or *maximum peaks between zero crossing* or *peak-count method* [GOO 73] [SEW 72] (the latter being ambiguous with the above method).

3.3.1. Presentation of method

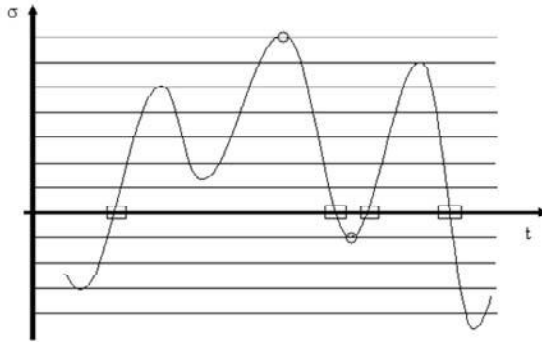


Figure 3.10. Counting of largest peaks between two passages through mean value

Only the largest maximum or minimum between two passages through an average value is counted, which is equivalent to completely neglecting the stress variations between two passages through zero, even if they are important [SCH 72a] [WEB 66]. The signal is therefore reduced to only one peak between two passages through zero. With an identical signal, the number of peaks counted is therefore smaller than for the first method [BUX 66] [HAA 62] [STR 73] [VAN 71] and the total duration of the reconstituted signal from this histogram of peaks is shorter than that of the initial real signal.

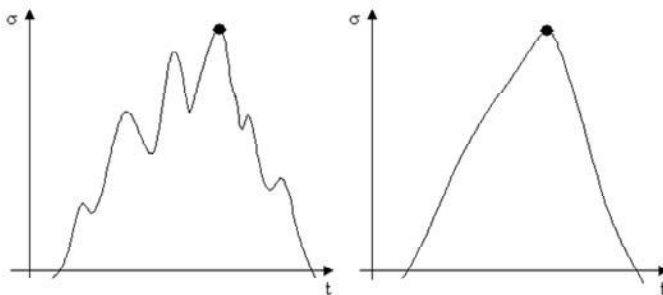


Figure 3.11. Suppression of all small variations not crossing the mean

The values of this count can be deduced from the results of the first method (with elimination of approximately 25% of the initially counted peaks) [LEY 63] [RAV 70]. This method is similar to that sometimes used to count the turbulence loads observed by transport aircraft [DEJ 70].

This type of counting can lead to incorrect results. If the signals in Figure 3.12 are considered, for example, the same count is obtained in both cases whereas signal (b) is certainly more severe than signal (a).

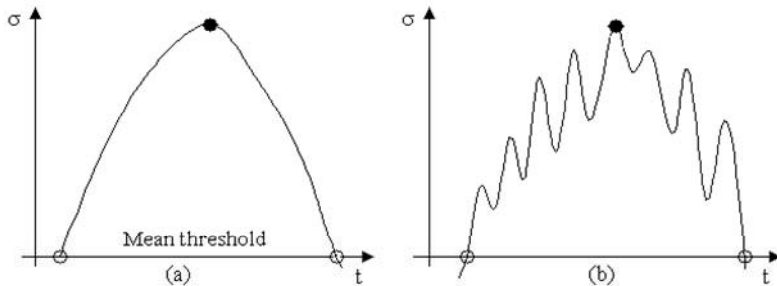


Figure 3.12. Example of two different signals leading to the same counting result

All the secondary variations of the load between two zeros and the maximum level are neglected by assumption. Some of these secondary load variations can, however, be very significant with respect to their contribution to the total fatigue damage [SEW 72].

NOTE: A specific measuring instrument – the VGH-Recorder (NACA) – has been developed to carry out these counts [WAL 58] [WEB 66].

This is equivalent to counting the number of up-crossings through the mean value of the signal which allows, for narrow band signals, calculation of the mean frequency of the signal (the narrow band signals have the same number of zero threshold crossings and of peaks). It is therefore recommended to use this method only in this case.

If the distribution of the instantaneous values of the signal is, in addition, Gaussian, this measurement of the mean frequency provides access to the peak distribution or to the curve of level crossings. It is indeed shown that in this case, the number of crossings of a level a with a positive slope is given by (Volume 3, equation [5.57]):

$$N^+ = N_0^+ e^{-\frac{a^2}{2\sigma_{rms}^2}}$$

where

$$N_0^+ = n_0^+ T,$$

T is signal duration and n_0^+ is mean frequency.

3.3.2. Elimination of small variations

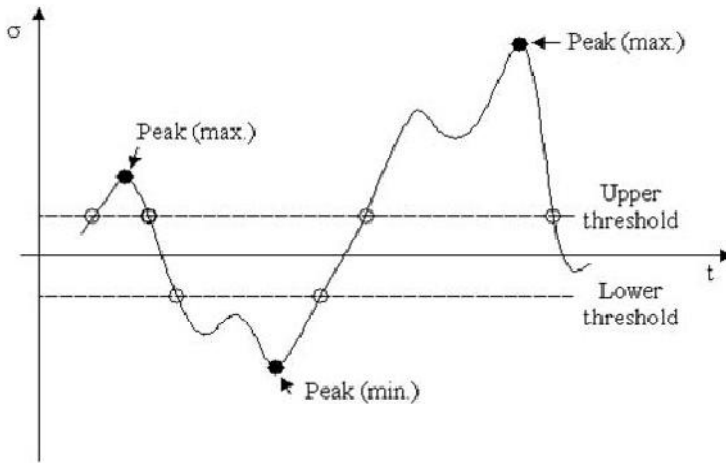


Figure 3.13. *Elimination of small variations around the mean*

Two mean threshold levels of reference are fixed: one positive and the other negative. We retain the largest maximum between two arbitrary successive crossings of the higher threshold and the smallest minimum between two crossings of the lower threshold (Figure 3.13) [DON 67]. With this modification, the peaks associated with small variations around the static value are neglected. In addition, smaller maxima are neglected and smaller minima will be neglected.

3.4. Range count method

This method is also referred to as *amplitudes regardless of mean*.

3.4.1. Presentation of method

The range is defined as the difference between two extreme values of the stress (or the deformation) with a sign according to direction of the transition (minimum \rightarrow maximum: +, maximum \rightarrow minimum: -) [BUX 66] [DEJ 70] [GRE 81] [NEL 78] [RAV 70] [SCH 63] [SCH 72a] [STR 73] [VAN 71] [WEB 66].

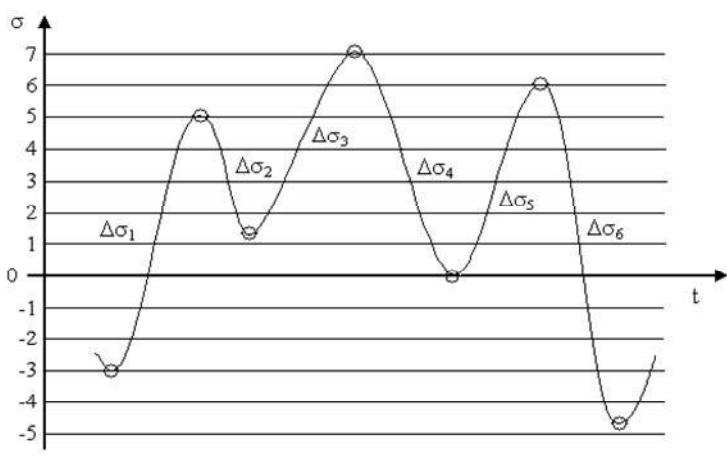


Figure 3.14. Range counting

$\Delta\sigma_1 = 8$	$\Delta\sigma_2 = -3.5$
$\Delta\sigma_3 = 5.5$	$\Delta\sigma_4 = -7$
$\Delta\sigma_5 = 6$	$\Delta\sigma_6 = -10.5$

As opposed to the above methods, here we obtain information about the real variations of the stress on the sequence (but not on the maximum amplitude) [LEY 63] [WEB 66]. All the ranges counted are considered as symmetric with respect to the zero axis [HAA 62]. The damage is then calculated from these ranges by considering them as half-cycles of sinusoidal stress using a S-N curve or its representation (for example, Basquin), and with a accumulation rule (for example, Miner) by considering (or not) the effect of the mean stress of each half-cycle (Goodman, Gerber, Söderberg criteria) [STA 57].

Several methods were proposed to take into account the effect of non-zero mean stress. For example, curves stress/number of cycles to the rupture are given, where the y axis represents (instead of σ or $\Delta\sigma$) the quantity

$$\frac{\Delta\sigma / 2}{1 - \sigma_m / R_m}$$

[SMI 42] or

$$\frac{\Delta\sigma / 2}{1 - \sigma_m / R_f}$$

[MOR 64], where $\Delta\sigma$ is stress range, σ_m is mean stress, R_m is ultimate tensile strength and R_f is true ultimate tensile strength (load to the fracture divided by the minimal cross-section after fracture).

The calculation of damage by this process is relatively easy when the signal is periodic, since the counting of the ranges is carried out over one period. If the signal is random, calculations are more difficult and it can be worthwhile to consider the statistical properties of the signal. For a Gaussian signal, for example, it can be shown that the mean value $\Delta\sigma_m$ of the ranges $\Delta\sigma$ is equal to:

$$\Delta\sigma_m = \dot{\sigma}_{\text{rms}}^2 \sqrt{\frac{2\pi}{\sigma_{\text{rms}}^2}} = \sqrt{2\pi} \sigma_{\text{rms}} \frac{n_0}{n_p} \quad [3.3]$$

where σ_{rms} is the rms value of the stress σ , $\dot{\sigma}_{\text{rms}}$ is rms value of the first derivative of σ , and

$$\Delta\sigma_m = \sqrt{2\pi} \sigma_{\text{rms}} r \quad [3.4]$$

where r is irregularity factor, n_0 is the number of zero crossings (centered signal) per unit time and n_p is the number of extrema per unit time.

3.4.2. Elimination of small variations

The method does not make it possible to take into account the stress variations lower than a given threshold and not considered important for the fatigue process. J.B. De Jonge [DEJ 70] noted that this method has a serious disadvantage.

Given the signal depicted in Figure 3.15, three ranges can be counted:

$$\Delta\sigma_1 = \sigma_2 - \sigma_1;$$

$$\Delta\sigma_2 = \sigma_3 - \sigma_2;$$

and

$$\Delta\sigma_3 = \sigma_4 - \sigma_3.$$

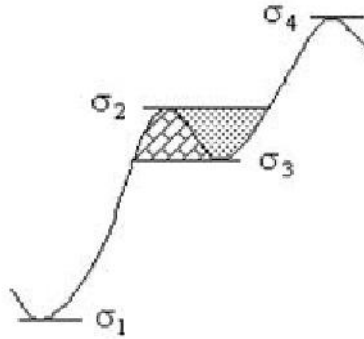


Figure 3.15. *Elimination of small variations*

If as a consequence of an unspecified filtering, the small variations such as $\sigma_2 - \sigma_3$ are removed, counting will give only $\sigma_4 - \sigma_1$ instead of the first three already quoted ranges. The result of counting depends greatly on the amplitude of the small load variation considered. In addition, there is always the possibility of not being able to pair the positive and negative ranges if both are counted.

The range counting method detects variations which actually occur, but neglects the variations of the mean load. By centering all the ranges on the zero value, it tends without reason to support the number of the smallest loads in the spectrum [RAV 70] [SCH 63]. A characterization of the endurance to fatigue requires knowledge of the range and its mean value (or the maximum and minimum values) [WEB 66].

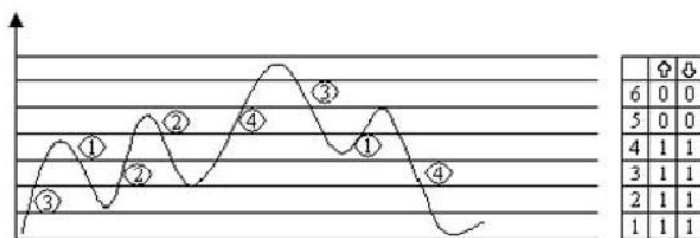


Figure 3.16. Example of range counting

NOTE: In the case of a Gaussian process, the plotting of the load spectrum can be carried out from an approximation of the distribution law of the ranges (increasing or decreasing direction), rather than by counting. The exact determination of this distribution in a continuous random process is very difficult [RIC 65a]. However, there are techniques which enable an approximate relation to be obtained, such as:

- H.P. Schjelderup and A.E. Galef [SCH 61a], which treats the particular case of Gaussian processes for which the PSD is composed of narrow peaks of very remote frequencies;

- J. Kowaleski [KOW 59], which gives a distribution law for a Gaussian process without demonstration (however, this law was considered to be incorrect by Rice et al. [RIC 65a]); and

- J.R. Rice and F.P. Beer [RIC 64] [RIC 65a], which proposes a relation calling upon the autocorrelation function of the signal and its first four derivatives.

3.5. Range-mean count method

This method is also referred to as *range-mean pair count method* or *means and amplitudes*.

3.5.1. Presentation of method

This method was proposed in 1939 by A. Teichmann [TEI 41]. Here, a gap in the range counting method (the absence of measurement of the mean value of the signal) is eliminated. The ranges are counted as with the above method and the mean value of the range is noted complementary to $\Delta\sigma$ [BUX 66] [FAT 77] [NEL 78] [RAV 70] [SCH 63] [VAN 71].

	i	$\Delta\sigma_i$	σ_{mi}
AB	1	8	1
BC	2	-3.5	3.25
CD	3	5.5	4.25
OF	4	-7	3.25
EF	5	6	3
FG	6	-10.5	0.75

Table 3.1. Example of statement of ranges and means

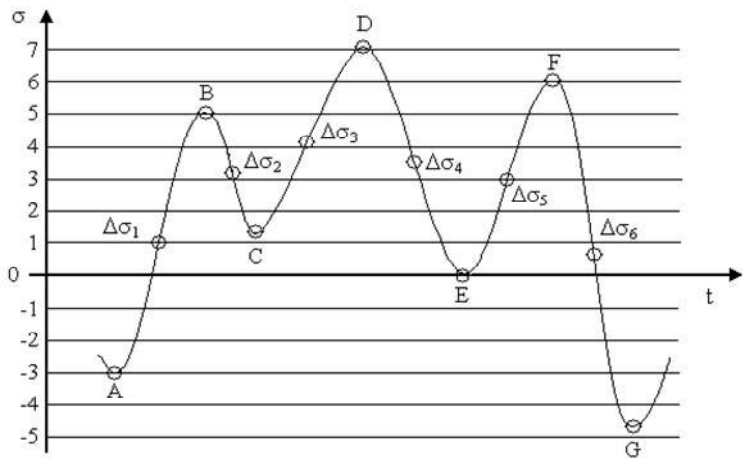


Figure 3.17. Counting of ranges and means

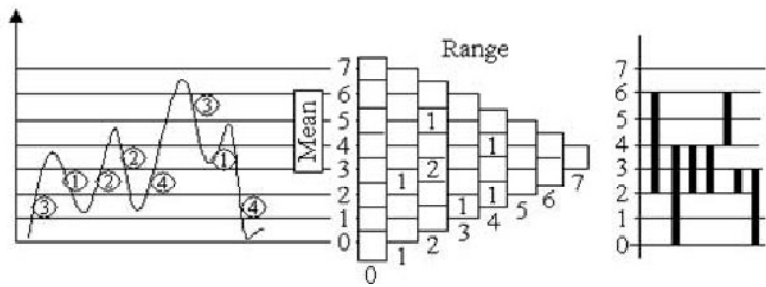


Figure 3.18. Example of range and mean counting

Some authors prefer to consider $\Delta\sigma_1 / 2$. These values make it possible to create a histogram with two dimensions (each mean corresponds to a list of ranges) [STR 73]. Since the information collected is highly fertile, it can be used to derive the results of some of the other methods [WEB 66]: the range counting method is a particular case of the range-mean count method. In the same way, the results of this counting can be transformed to determine those of the peaks counting method or the level-crossing count method.

The mean is defined as the algebraic half-sum of two successive extrema:

$$\sigma_m = \frac{\sigma_{\max} + \sigma_{\min}}{2} \quad [3.5]$$

The amplitude is the algebraic half-difference between these extrema.

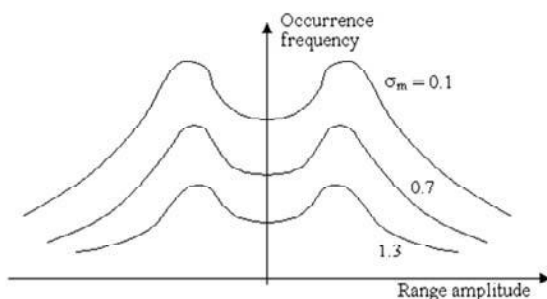


Figure 3.19. Example of presentation of results of a count

The results can be presented in the shape of curves giving, for a given mean σ_{mj} , the occurrence frequency versus the range amplitude (or the half-amplitude). The distributions thus obtained have the same form whatever the mean σ_{mj} .

This method is generally regarded as most significant in fatigue [LEY 63]. It takes into account the assumption that the fatigue behavior is mainly a function of the amplitude of the stresses around the mean value [GRE 81] [RAV 70].

The reason for the non-utilization of this method is two-fold [HAA 62]:

- the instrumentation necessary is complicated. Equipment was, however, developed for this use (*strain analyser*) [VER 56] [WEB 66]; and
- reproduction of the loads counted is not easy.

3.5.2. Elimination of small variations

As with the above method, the suppression of small variations of σ is not simple since it results in modifying the preceding and following ranges. It is the weak point of these methods, sensitive to the smallest range neglected [WEB 66]. Elimination is carried out by removing all the variations of less than a given value. On the curve where these small variations occur, the mean and the interval between the peaks are calculated immediately before and after these small fluctuations.

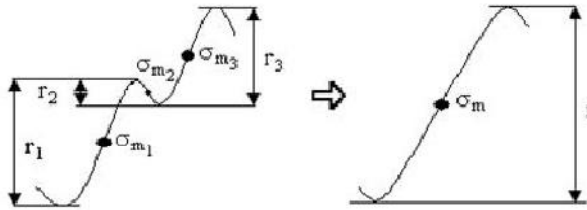


Figure 3.20. *Elimination of small variations*

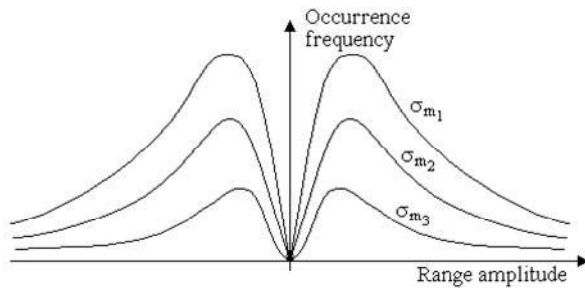


Figure 3.21. *Frequency of event after elimination of small variations*

In general, this treatment results in particular of the removal the small variations close to the mean, which have little effect on fatigue.

From these results, it is possible to carry out a calculation of fatigue damage as follows [STA 57]. Let us consider, as an example, the signal in Figure 3.22(a). This signal can be smoothed to eliminate the small irregularities (Figure 3.22(b)).

The signal is then broken up into 4 ranges AB, BC, CD and DE which are used to define cycles ABB', BCC', etc. (Figure 3.22(c)).

The damage due to the signal (a) will be half of that due to the complete cycles of (c). The cycles are centered with respect to the zero mean value, by modifying the amplitudes obeying a rule such as Gerber or modified Goodman (Figure 3.22(d)).

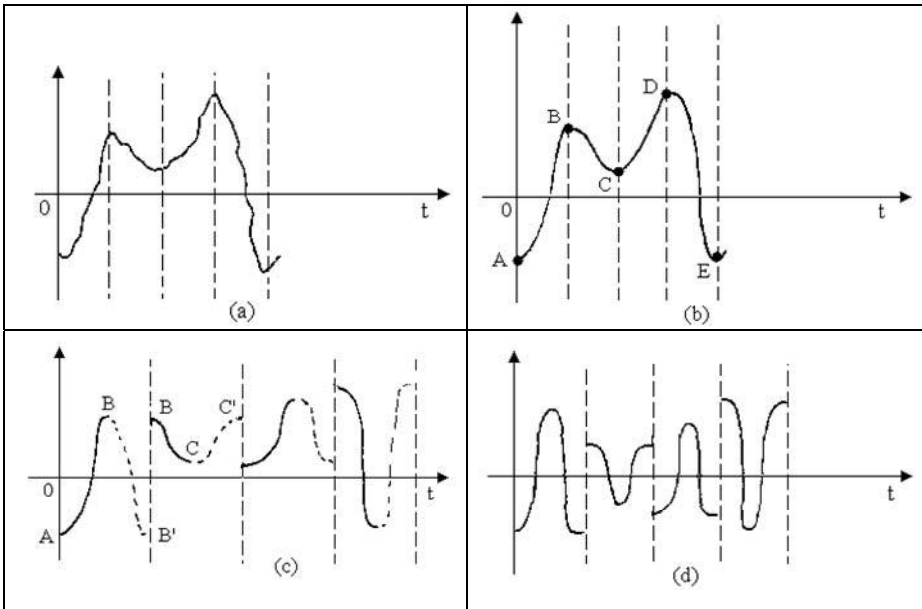


Figure 3.22.(a) to (d) *Decomposition in ranges*

By translation according to the time axis, a continuous signal is reconstituted (Figure 3.23) producing a damage double of (a), which can then be evaluated using, for example, Miner's rule.

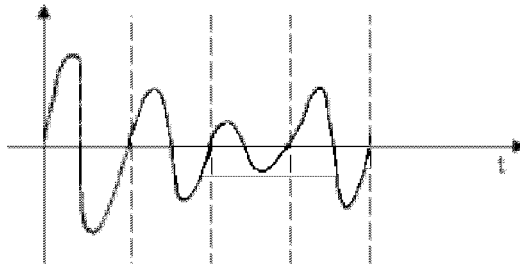


Figure 3.23. *Process of cycle reconstitution*

3.6. Range-pair count method

This is also referred to as *range-pair cycles counting* or *range-pair exceedance count method*.

This method, which has several variants [BUR 56] [BUX 66] [FUC 80] [GRO 60] [JAC 72] [RAV 70] [SCH 63] [SCH 72a] [VAN 71], consists of counting a stress (or strain) range as a cycle if it can be paired with a subsequent stress (or strain) range of equal amplitude in the opposite direction.

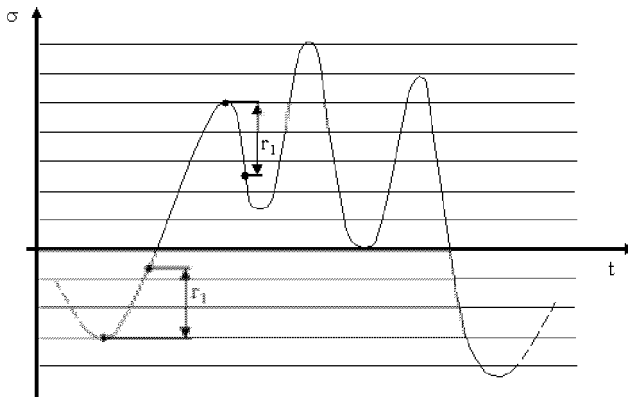


Figure 3.24. *Counting of range-pairs*

The ranges are therefore counted per pair. A range is defined here as a load variation starting from an extremum. A counting is carried out if the positive range exceeds a certain value r and if it is followed by a negative range exceeding the same value r [STR 73] [TEI 55] [VAN 71]. The intermediate variations (r_e) are neglected.

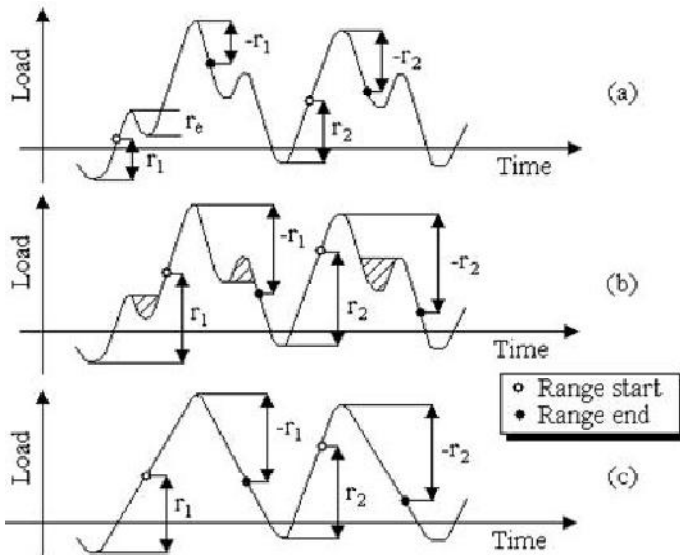


Figure 3.25. Process of counting of ranges by pairs

The procedure of counting is repeated for other values of r .

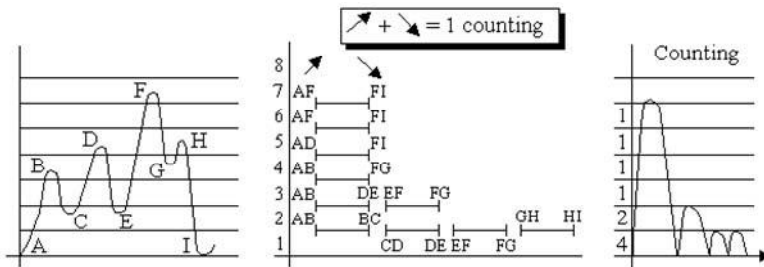


Figure 3.26. Example of counting of ranges by pairs

The result of counting can be expressed in the form of the number of range pairs exceeding a given value r . This method counts mainly the greatest fluctuations. The small fluctuations are regarded as superimposed on the largest. If the pairs of ranges are counted for $|r| > r_2$, the intermediate positive or negative ranges for which $|r| < r_2$ do not affect the result of counting. They can therefore be eliminated.

This method takes into account the sequence of load and is insensitive to the amplitude of the smallest load ranges considered (counting thresholds). The small ranges can therefore be counted or neglected at will, without any effect on the large ranges [DEJ 70] [WEB 66]. The method combines the greatest load increments with the smallest following decrements, which is important from the damage point of view.

Any information is stored in the mean value of the counted cycles. The ranges are paired without respect to their occurrence time. Each counted element is insensitive to the ranges other than those of its own previously chosen level. All the load excursions are not fully counted.

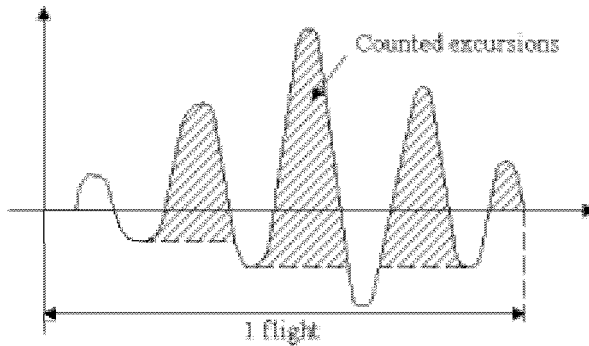


Figure 3.27. *Combination of stress increments*

This method can be used in the plastic range by associating the pairs of plastic deformation ranges with the pairs of stress ranges [KIK 71].

The measuring instrument used in this method is the *strain range counter* [TEI 55] [WEB 66].

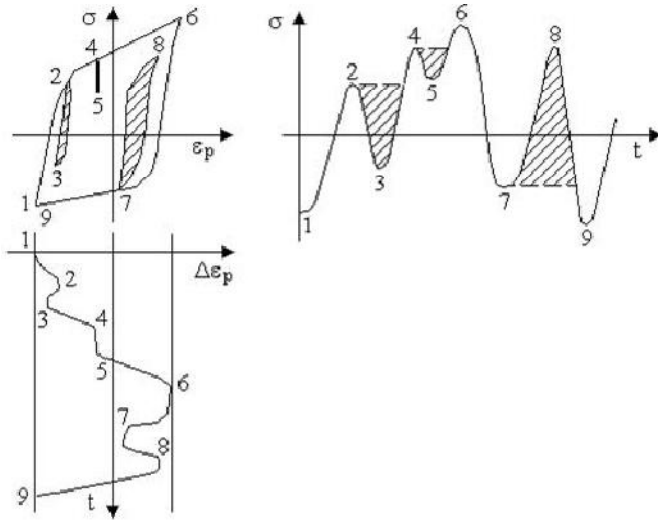


Figure 3.28. Association of deformation and stress ranges

NOTES:

1. *N.E. Dowling [DOW 7] proposes carrying out counting according to the procedure described below, based on Figure 3.29.*

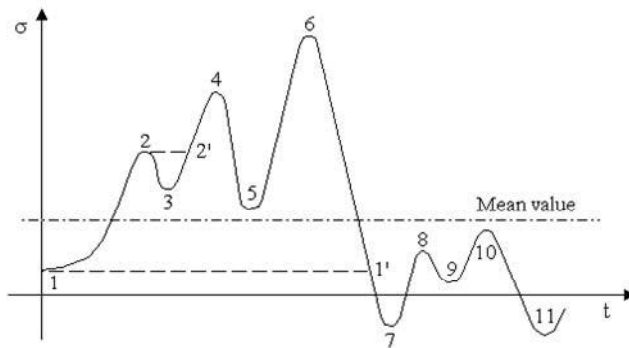


Figure 3.29. Counting according to *N.E. Dowling [DOW 7]*

Starting from a minimum (1), the signal increases to the largest peak (6), which is for the moment the only one selected. The descent from 6 to 1' of the same amplitude is associated with this rise from 1 to 6. When we start from peak 2 the signal decreases according to 2o 3 and we associate 3o 2 with this variation.

The result is close to that of the rainflow counting method (section 3.2)

2. O. Buxbaum [BM66] (or T.J. Ravishankar [RAV70]) defines classes of range r_i , r_1 being the smallest amplitude chosen for the counting and the lower values being neglected.

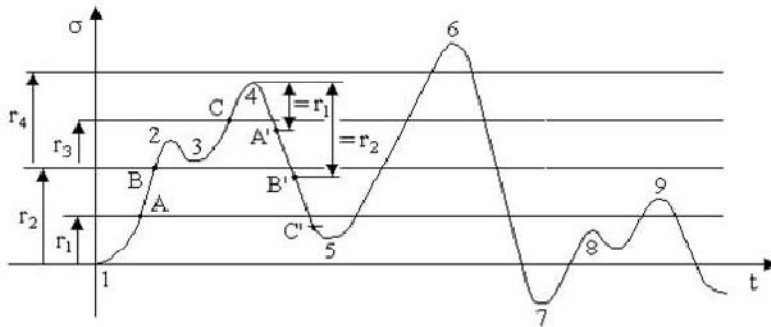


Figure 3.30. Counting according to O. Buxbaum [BM66]

Starting from minimum 1, we will have a range each time the signal crosses a limit of class with positive slope. The range is closed when a negative variation of the same amplitude is crossed. For example, we open range AA' in A, BB' in B, CC' in C and we close these same ranges in A', B' and C'.

These cuttings per pair of ranges are however artificial and, if the stresses are in the plastic range, can lead to an inaccurate description of the stress-strain cycles, i.e. to an error in the calculated damage [WAT 6].

3.7. Hayes' counting method

This is a similar method to that of the rainflow, but easier to visualize [FUC 77] [FUC 80] [NEL 78]. We start here by counting the cycles of smaller amplitude, then they are removed from the curve to count the cycles of greater amplitude. Let us consider, as an example, the signal in Figure 3.31(a).

Hayes first identifies small ranges such as BC and DE, which are *interruptions* of a larger range (AF). There is interruption:

- for a peak-valley pair such as BC when the following peak D is higher than the peak B;
- for a valley-peak pair, such as GH, when the next valley I is of smaller amplitude than the valley G.

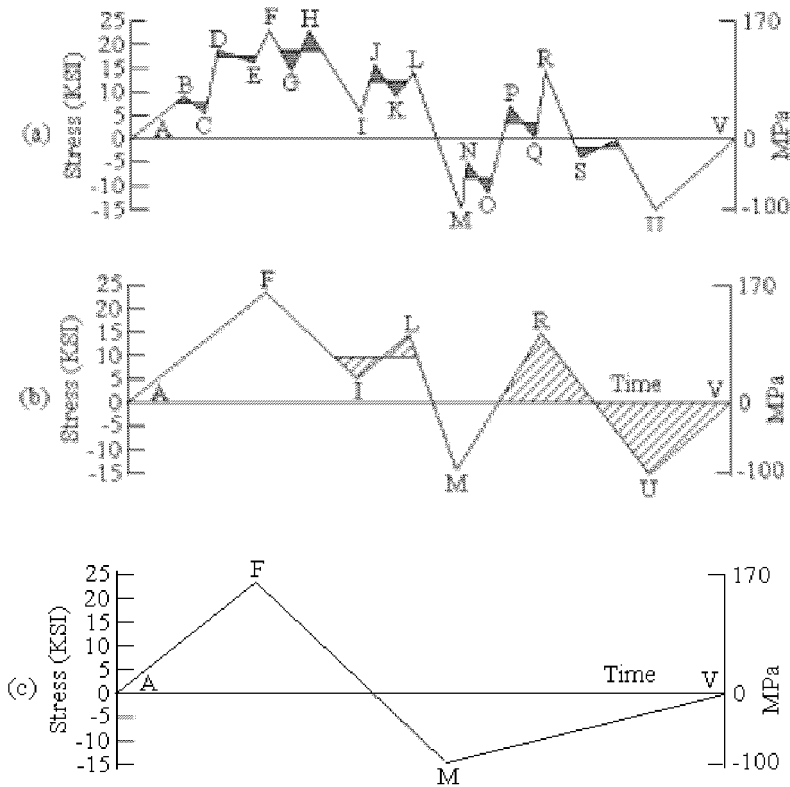


Figure 3.31. Hayes counting procedure

The hatched surface corresponds to the cycles relating to the ranges selected. In Figure 3.31, 20 alternations (20 peaks) are counted. Among these peaks, 14 are retained to form 7 pairs materialized by the hatchings, then eliminated from the curve (Figure 3.31(b)). There remain 6 alternations (6 extrema) with 3 peaks and 3 valleys. The two hatched cycles I–L and R–U are counted, then are removed to obtain the curve in Figure 3.31(c) in which there only remains the peak F and the valley M. The result of this counting can be expressed in the shape of a table of occurrence of the ranges possibly with their mean value.

3.8. Ordered overall range counting method

This is also referred to as the *racetrack counting method*.

To illustrate the method, let us consider the signal in Figure 3.32(a) which will be treated to obtain that in Figure 3.32(c). The elimination of the smallest ranges is carried out as indicated in Figure 3.32(b) [FUC 80] [NEL 77].

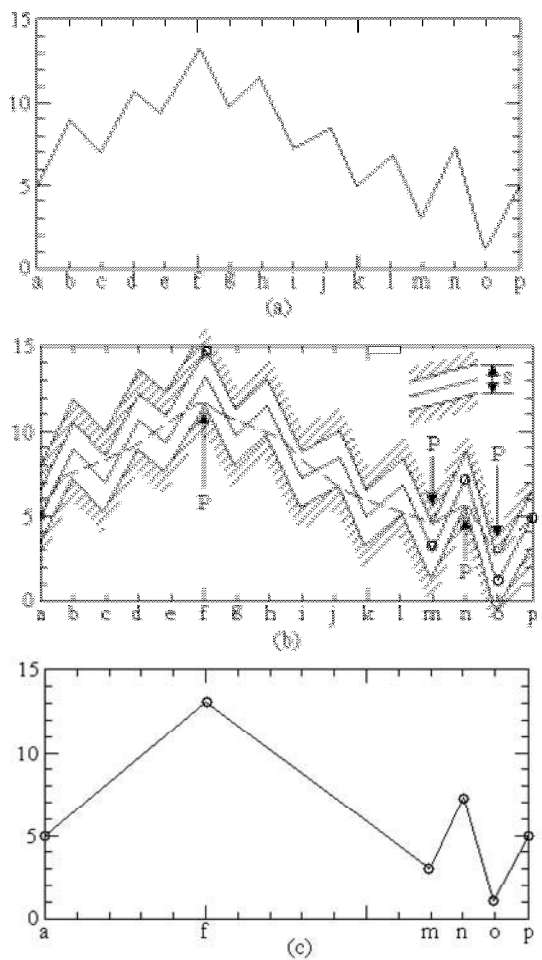


Figure 3.32. *Racetrack counting method*

The method consists of defining a *track* of width S , limited by *barriers* which have the same profile as the signal. We retain as extremum only those for which a *racing driver* would have to change direction from top to bottom as in f and n , or from bottom to top as in m and o . The width S of the track determines the number of alternations which will be counted.

This method was originally named *ordered overall range method* [FUC 77] [NEL 78]. Its aim is to condense a long and complex signal into a signal that is simpler to use.

The procedure used is based on the assumption that the most significant part of the signal is the maximum range, i.e. the interval between the largest peak and the lowest valley.

The distance between the second lowest valley and the second largest peak is the next most important element, provided that this second range crosses the first (between the largest peak and the smallest valley) or that it is outside the interval of time defined by the extreme values of the first range. By continuing the process in this manner, we can either exhaust the counting of all alternations or stop counting at a selected threshold and regard all the smaller peaks and valleys as negligible.

The results can be presented in two ways:

- in the form of a histogram, of a spectrum or a list giving the range amplitudes and their occurrence frequency. If counting is carried out until exhaustion of the peaks and valleys, this method leads to the same result as a rainflow type counting and to a result very close to the range-pair count method. The racetrack method makes it possible to stop counting before exhaustion of the extrema and to take into account only a fraction of the ranges. In many cases, that led to the same result as an exhaustive counting of alternations;

- in the form of a synthesized curve in which the essential peaks and valleys are the subject of a list with their origin sequence. If the procedure is continued until exhaustion of all the extrema, we then reproduce the initial curve in all its details. If counting is limited, small variations of the curve are omitted but we retain alternations which produce the greatest ranges.

The condensed curve contains more information than the spectrum. It includes the sequence of events, which can be important if the deformation produces residual stresses which remain active during the following alternating. This method initially chooses the greatest ranges and preserves them in a correct temporal sequence. It is useful to condense curves by preserving only a few events (e.g. 10%) which produce most of the damage, usually more than 90% [FUC 77]. These condensed curves make it possible to reduce the duration of calculations and the tests and to focus the attention on a reduced number of the most significant events.

3.9. Level-crossing count method

This is also referred to as the *simple level-crossing method*.

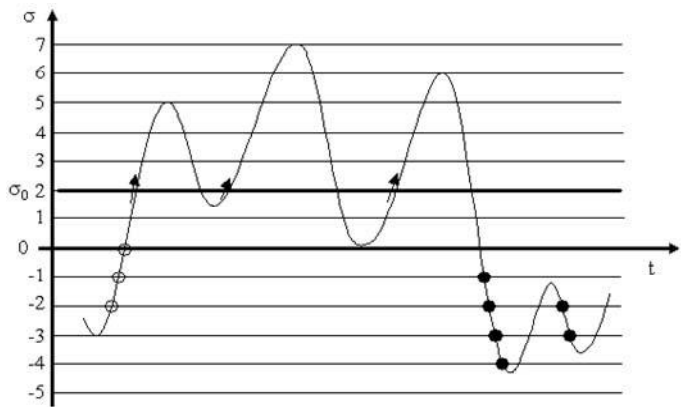


Figure 3.33. Counting of level crossings

Here, we count the number of times that the signal crosses a given level σ_0 with a positive slope, depending on σ_0 [BUX 66] [GOO 73] [NEL 78] [RAV 70] [SCH 63] [SEW 72] [VAN 71].

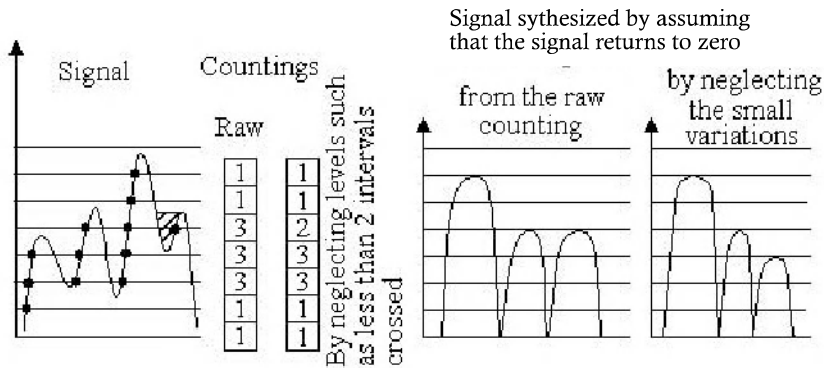


Figure 3.34. Example of level-crossing counting

The instrument developed for this measurement is the *contact extensometer* (Svenson) [SVE 52] [WEB 66]. We can expect that the mean level (zero in general) is the most-often crossed, since the number of crossings of threshold falls when the

threshold increases. Counts can be carried out with positive slope or negative slope above and below the mean (the results being the same) [GOO 73].

If the signal has a symmetric distribution, it is enough to choose a direction and to count only above the mean [STR 73]. The passages below a certain threshold can be eliminated. If they are very few, the small load variations can be neglected without appreciable effect on the number of up-crossings. Very different models of load can lead to the same counting result [GOO 73]. The inadequacy of the method is shown in Figure 3.35 [VAN 71].

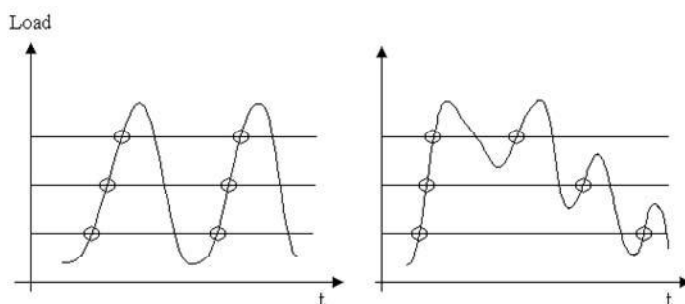


Figure 3.35. *Different signals having the same number of level crossings*

Although very different, the two signals above lead to the same number of crossings of each level. The small load variations, which are of less importance in the fatigue process, increase counting. To compensate (at a certain point) for this source of error, level crossings associated with load variations lower than a given threshold can be neglected [GOO 73] (see the fatigue-meter method). This is equivalent to defining classes of amplitude σ_i , $\sigma_i + \Delta\sigma$ of width $\Delta\sigma$ such that any oscillation included inside a class is not counted, by suitable choice of $\Delta\sigma$ [BUX 66].

Not all of the small oscillations disappear. We continue to take into account those which cross the limit between two classes.

Neglecting small alternations can, however, have an influence on the results [WEB 66].

The level-crossing counting method can be used to compare the signal distribution with that of a Gaussian signal [BUX 66] [GRE 81].

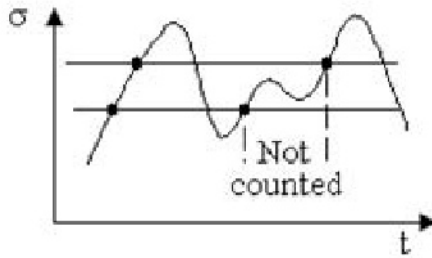


Figure 3.36. *Elimination of small alternations*

This counting is sometimes used to calculate the number of peaks between two levels, by difference of the up-crossings of these two levels.

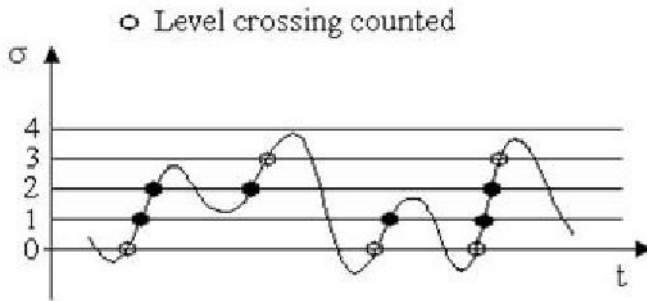


Figure 3.37. *Example of error in the calculation of the number of peaks from a level-crossing counting*

This step can lead to errors [SCH 63] [SCH 72a] [SVE 52] [VAN 71].

H.A. Leybold and E.C. Naumann [LEY 63] show that in a given interval of amplitude, the calculation of the number of peaks carried out from the up-crossings of levels can be false because of a certain compensation of maxima and minima.

An example is given using the signal of Figure 3.37; no peak is detected by difference of crossings of thresholds 2 and 1 although there actually is one. As a consequence, we note that the number of peaks calculated in the interval close to the mean is very weak.

This method of calculation of the number of the peaks can, however, be used provided that the signal is: stationary; Gaussian; with narrow band; and that the threshold is sufficiently large compared to the rms value.

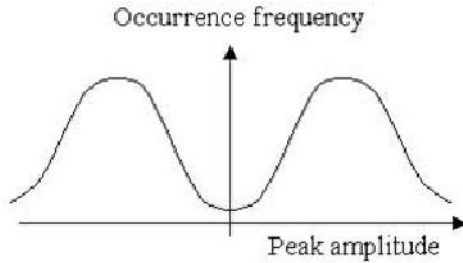


Figure 3.38. Frequency of event of peaks deduced from counting of crossings of threshold

It is also sometimes used to plot the curve of occurrence frequency versus peak amplitude [LEY 63].

Modified level-crossing method

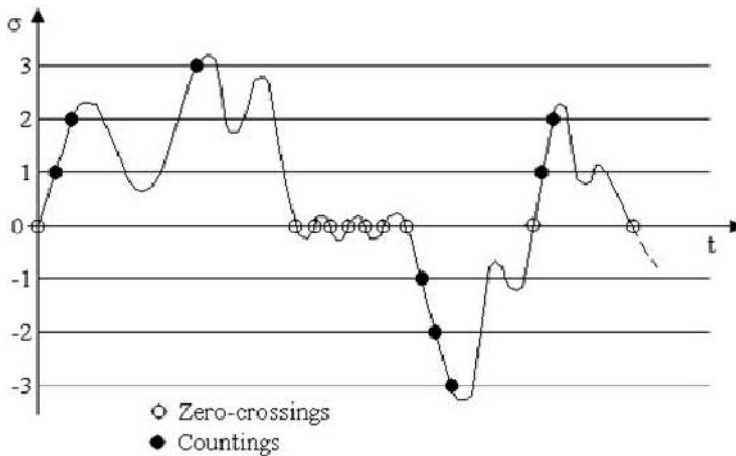


Figure 3.39. Level-crossing counting method modified to eliminate small variations

This method, sometimes used in the car industry, consists of:

- choosing load levels (stress, deformation, etc.);
- between several consecutive zero-crossings, recording only one counting each time that a level is exceeded (a level can be exceeded several times between two passages by zero, but only the first level up-crossing is counted).

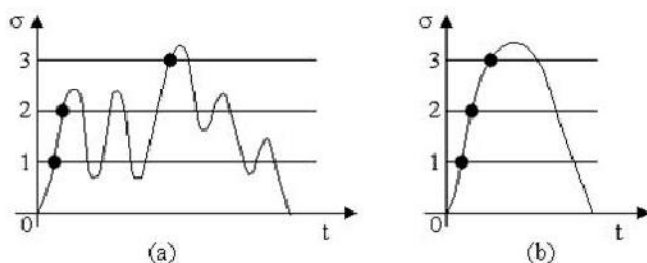


Figure 3.40. Example of very different signals leading to the same result using the modified level-crossing counting method

This method also has its limits. It will produce, for example, the same counts for signals (a) and (b) in Figure 3.40. In this case, (a) is probably much more damaging than (b). This method is not appropriate for detecting the important differences between such loads.

3.10. Peak valley peak counting method

This is also referred to as the *PP* method.

The direct reproduction of the signal (stress or deformation) is not very practical as it is too long to expect reliable statistics [HOL 73].

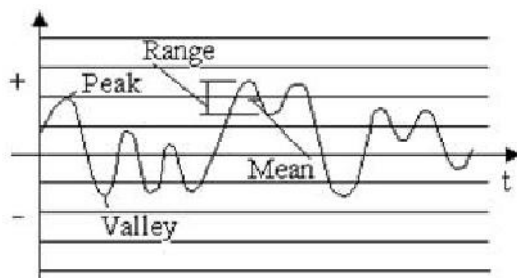


Figure 3.41. Definitions

During fatigue tests of materials on test bars, methods related to the use of a stress spectrum generally result in carrying out *blocks* of sinusoids not very representative of reality (fluctuations of amplitudes and of half-cycle durations). The histograms do not give information on the sequence or on the mean-range interactions, which have an effect on the fatigue life.

The PVP method takes account of these elements and makes it possible to reduce the test duration in a notable manner. The steps of the method are as follows:

- analyze the signal measured and plot:
 - a histogram of the range mean (row),
 - a histogram of the ranges;

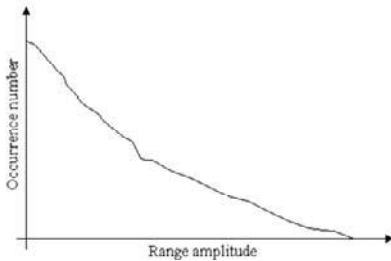


Figure 3.42. *Histogram of the ranges*

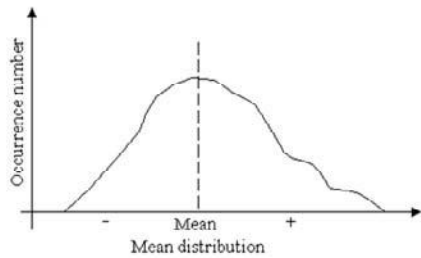


Figure 3.43. *Histogram of the means*

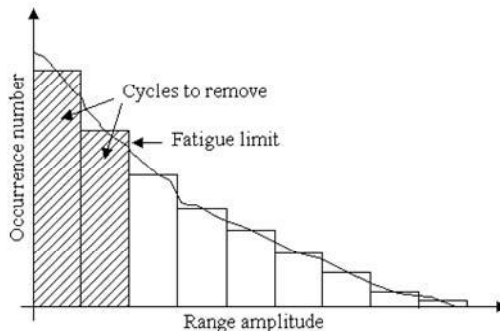


Figure 3.44. *Histogram of the ranges after suppression of events below fatigue limit*

– modify this last histogram by eliminating levels lower than the fatigue limit and consider this as without effect;

– reconstitute a signal from the remaining blocks. The method which would result in considering blocks of sinusoids by respecting the levels and numbers of cycles is not used as it is not considered to be representative here.

Instead, the PVP method uses a matrix such as depicted in Figure 3.45 including, according to each axis, classes located by their *medium* level with the values of the peaks on the vertical axis and those of the valleys on the horizontal axis.

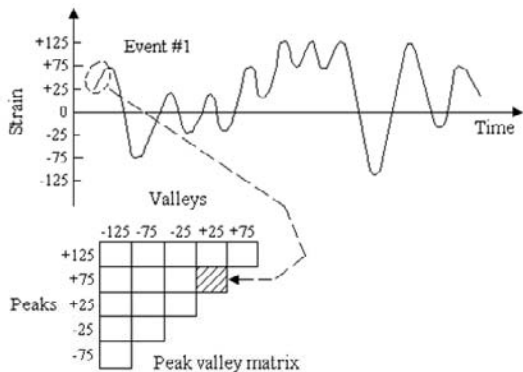


Figure 3.45. Constitution of the peak and valley matrix

Each event is placed in the appropriate cell. This matrix therefore makes it possible to describe the signal using the two parameter ranges: mean value, since diagonal “1” is at a constant mean, and diagonal “2” is at constant range.

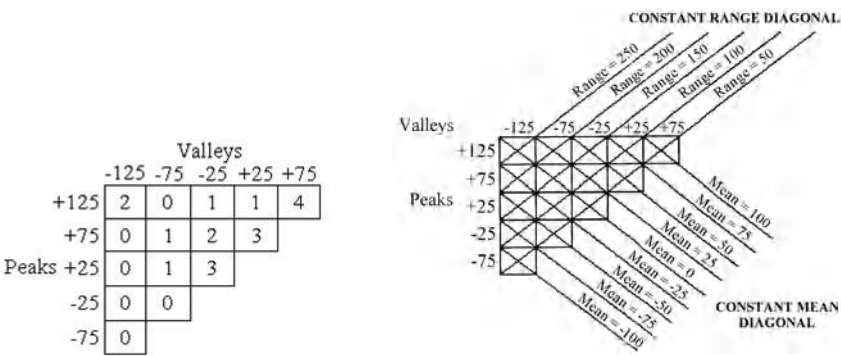


Figure 3.46. Example of matrix

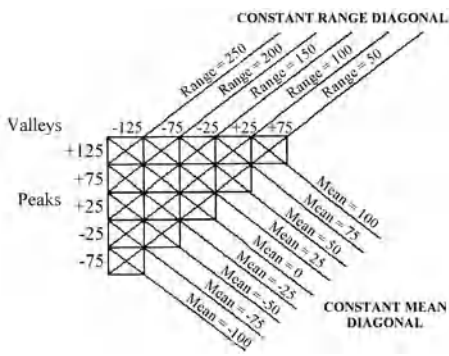


Figure 3.47. Diagonals of the matrix [HOL 73]

By using the properties of materials under fatigue, the authors propose a method of elimination of the levels lower than the fatigue limit, leading to a very important reduction of time (90% in the given example). The procedure involves the following steps:

- note the fatigue limit of materials used and its ultimate strength ($\sigma_D \approx \frac{R_m}{2}$);
- plot the Goodman diagram (with the range on ordinates and the mean on abscissae) in order to determine the boxes of the matrix which are below σ_D . This results in eliminating at the same time values in the histogram of ranges and of averages;
- generate a random signal. We generally start from a valley and choose a valley-peak range in the matrix: 25 and 75 for example (Figure 3.50). We miss the number of occurrences indicated in the box by 1.

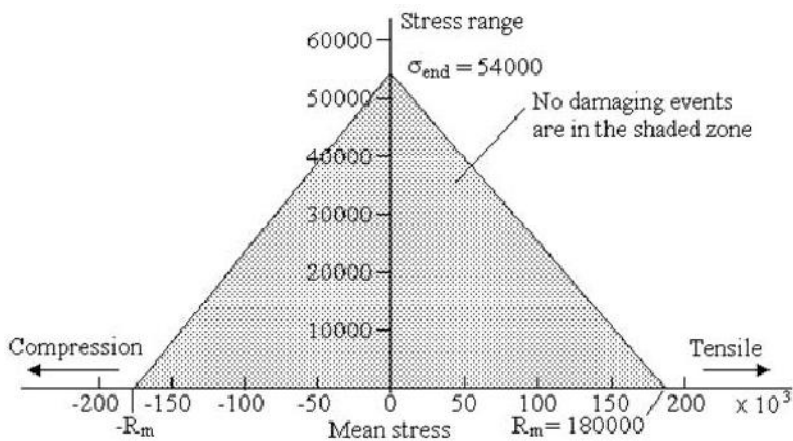


Figure 3.48. Goodman diagram

It is then necessary to search a range starting from a peak of amplitude 75; this choice can be carried out in one of hatched boxes in Figure 3.49.

In the example treated, the possible valleys following +75 are -75, -25 and +25 (five ranges on the whole), the probabilities being $1/5$, $2/5$ and $2/5$. We therefore choose the following range taking into account these last values. Let us suppose that the selected transition is (+75, -25). The following transition will go towards a peak and will have to be selected in the third column (Figure 3.52). There are two possibilities - 125 and 75 - with the same probability.

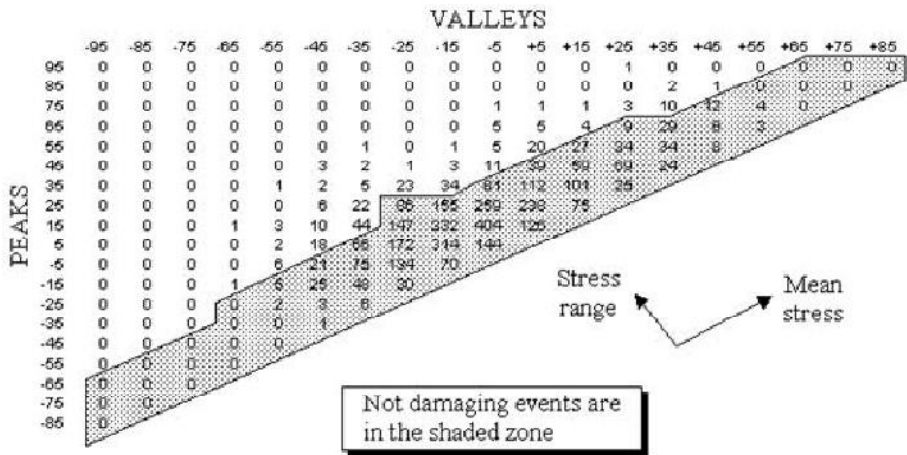


Figure 3.49. Example of matrix

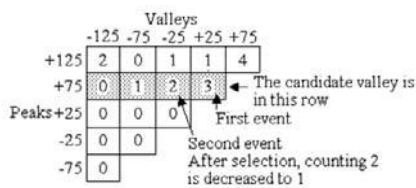


Figure 3.50. Choice of first range

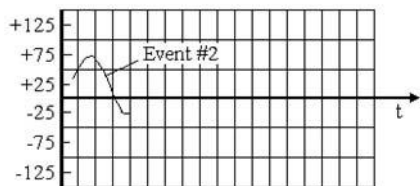


Figure 3.51. Constitution of a signal

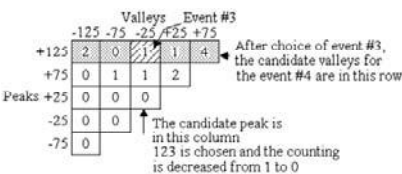


Figure 3.52. Choice of second range

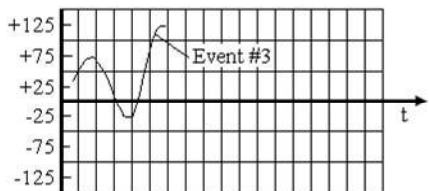


Figure 3.53. Addition of range to the signal

If 125 is chosen, the next valley will have to be taken in the hatched line and we proceed in this way until the table is empty. Towards the end of the signal, it may occur that direct connections are impossible as some boxes are already empty. In this case, we will connect the arcs continuously.

Frequencies

We saw that the life in fatigue is, to a certain extent, independent of the frequency. This parameter is therefore not taken into account. Rather, the authors use the velocity limitations of the actuators to determine the duration of each event.

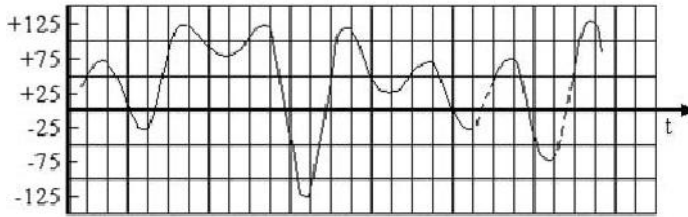


Figure 3.54. Connections of un-joined arcs

3.11. Fatigue-meter counting method

This is also referred to as the *level crossings eliminating small fluctuations* or *restricted level-crossing count method* or *variable reset method*.

The *fatigue-meter* was developed for fatigue studies, especially in aeronautics to measure and record vertical accelerations in the center of gravity of aircraft in flight [LAM 73] [MEA 54] [RID 77]. Use of this equipment, such as the *GH recorder* or *fatigue-meter* (RAE) [TAY 53], is limited apart from this particular application [HAA 62]. This material uses a level-crossings counting method with elimination of the small load variations.

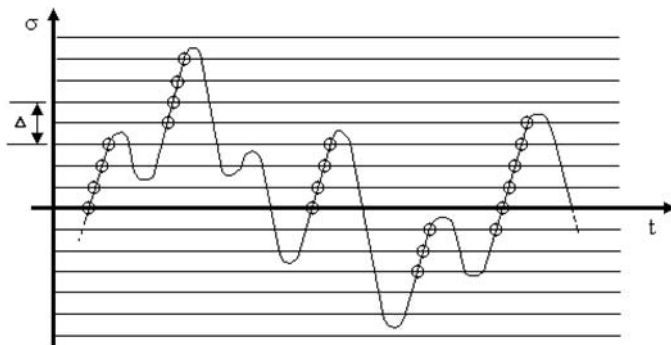


Figure 3.55. Fatigue-meter counting

A count of a level up-crossing above the mean stress is retained only if the stress is crossed before at least one interval Δ previously chosen with a positive slope [GOO 73] [NEL 78] [RAV 70] [SEW 72] [SCH 63] [SCH 72a] [STR 73] [TAY 50].

This increment Δ corresponds to a stress interval below the fatigue limit stress and is therefore negligible from the point of view of fatigue [LEY 63]. It is equivalent to saying that a *rearmament threshold* is used when:

- for the levels higher than the mean, counting is started at the time of the passage of a given level;
- a new passage on this same level gives place to a counting only if the signal has descended rather low and crossed at a lower level fixed in advance with a negative slope before ascending [NEL 78] [RAV 70].

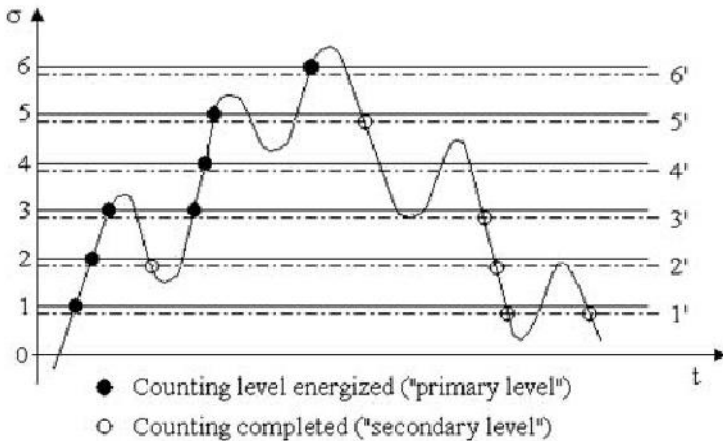


Figure 3.56. *Counting with elimination of small variations*

Counting is similar for the levels lower than the mean. This method therefore introduces a new parameter, the *release threshold*, which can vary according to the level (all the larger since the level is higher) [GRE 81]. It has the advantage of recording the majority of the secondary load variations of some importance [SEW 72]. It results in neglect of certain small variations. There is loss of information on the sequences, however the small variations do not influence counting. The number of peaks calculated in each class by subtracting the number of up-crossings of a level i from the number of up-crossings of the following threshold $i + 1$ is not exact, as with the preceding level-crossing count method.

With this method, very different signals can still lead to the same result [VAN 71].

Example 3.1.

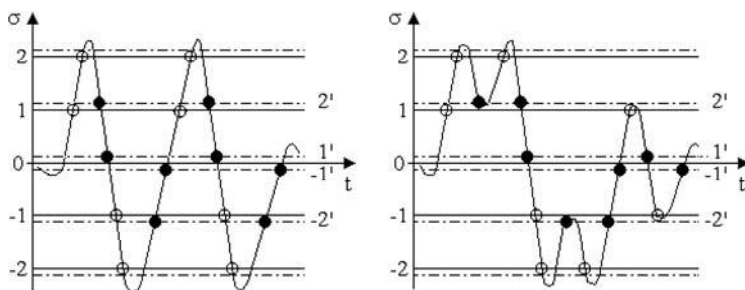


Figure 3.57. Example of signals leading to the same number of crossings

This problem here is also related to small variations in stress.

Example of threshold levels [GOO 73]

	Acceleration levels in g										
Primary	0.05	0.10	0.15	0.20	0.25	0.30	0.35	0.40	0.45	0.50	0.55
Secondary	0.00	0.05	0.05	0.10	0.10	0.15	0.15	0.20	0.20	0.25	0.25

Table 3.2. Examples of primary and secondary threshold values

It is seen that the higher the primary level, the higher the secondary level (and thus the threshold).

3.12. Rainflow counting method

This is also referred to as the *Pagoda roof method*.

3.12.1. Principle of method

This method [DOW 72] [DOW 87] [FAT 93] [FUC 80] [KRE 83] [LIN 87] [NEL 78] [RYC 87] [SHE 82] [SOC 83] [WIR 77] was initially proposed by

M. Matsuiski and T. Endo [END 74] [MAT 68] to count the cycles or the half-cycles of strain-time signals. Counting is carried out on the basis of the stress-strain behavior of the material considered [STR 73]. The extracted cycles conform with those of the tests of constant amplitude from which the predictions of fatigue life are generally carried out.

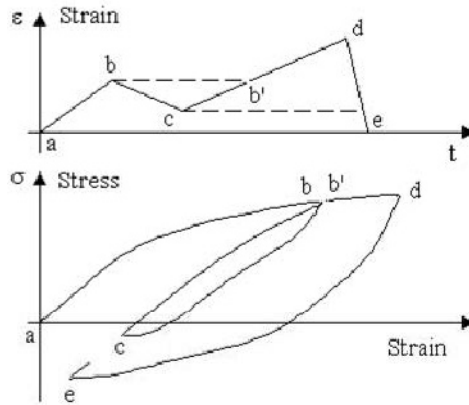


Figure 3.58. *Stress-strain cycles*

This is illustrated in Figure 3.58. In this example, the response $\epsilon(t)$ can be divided into two half-cycles ad and de and into a complete cycle $bc b'$, which can be considered as an interruption of a larger half-cycle.

To describe this method and explain the origin of its name, let us imagine that the time axis is vertical and that the signal $\sigma(t)$ represents a series of roofs on which water falls. The rules of the flow are described in the following.

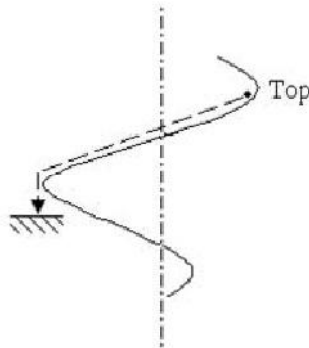


Figure 3.59. *The drop is released from the largest peak*

The origin of the signal is placed on the axis at the abscissa of the largest peak of the signal (this condition is not necessary for certain algorithms derived from this method) [FUC 80]. Water drops are sequentially released at each extrema. By convention, the tops of the roofs are on the right of the axis and the bottoms of the roofs are on the left.

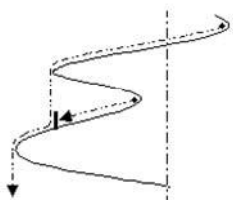


Figure 3.60. *Flow rule of the drop from a peak*

If the fall starts from a peak:

- (a) the drop will stop if it meets an opposing peak larger than that of departure;
- (b) it will stop if it meets the path traversed by another drop, previously determined; and
- (c) the drop will fall onto another roof and continue to slip according to rules (a) and (b).

NOTE: *A new path cannot start before its predecessor has finished.*

If the fall begins from a valley [END 74] [NEL 78]:

- (d) the fall will stop if the drop meets a valley deeper than that of departure;
- (e) the fall will stop if it crosses the path of a drop coming from a preceding valley; and
- (f) the drop can fall onto another roof and continue according to rules (d) and (e).

The horizontal length of each *rainflow* defines a range which can be regarded as equivalent to a half-cycle of a constant amplitude load.



Figure 3.61. *Drop departure from a valley*

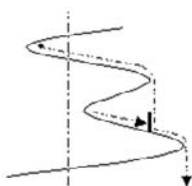


Figure 3.62. *Flow rule of the drop from a valley*

Example 3.2.

Let us consider the signal in Figure 3.63, the time axis being plotted vertically.

On this figure, pairs of ranges can be identified which, taken together, are equivalent to whole cycles:

- | | |
|--------------------------|-------------------------------|
| a) $(1 - 8) + (8 - 11):$ | largest cycle of the sequence |
| b) $(2 - 5) + (5 - C)$ | } cycles of intermediate size |
| c) $(6 - 7) + (7 - B)$ | |
| d) $(3 - 4) + (4 - A)$ | } the smallest cycles |
| $(9 - 10) + (10 - D)$ | |

The damage can be calculated from these cycles. Intermediate ranges (2–5) and (5–C) are simply interruptions of a larger range (1–8). Small ranges (3–4) and (4–A) are, in their turn, the interruptions of the intermediate range (2–5), etc.

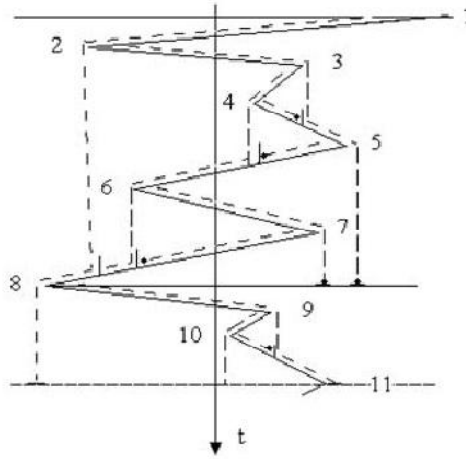


Figure 3.63. Example of signal for a rainflow counting

This method lends itself with difficulty to an analytical formulation [KRE 83]. Several algorithms were developed to carry out counting (see section 3.12.2) [DOW 82] [DOW 87] [FAT 93] [RIC 74] [SOC 77]. It is currently well established that this method gives the best estimates of fatigue life in the case of cycles of strain under load of variable amplitude [DOW 72] [TUC 77].

Example 3.3.

Figure 3.64(a) shows a signal and the part of this signal retained in a first passage. The left ranges are those of Figure 3.64(b).

The procedure is still applied to the remaining peaks and there only remains the peak of Figure 3.64(c). The result of this counting gives the half-cycles (25; -14), (14; 5), (16; -12) and (7; 2).

The rainflow counting yields the same result as the range-pair count method, except for the small additional half-cycle (7; 2) counted here.

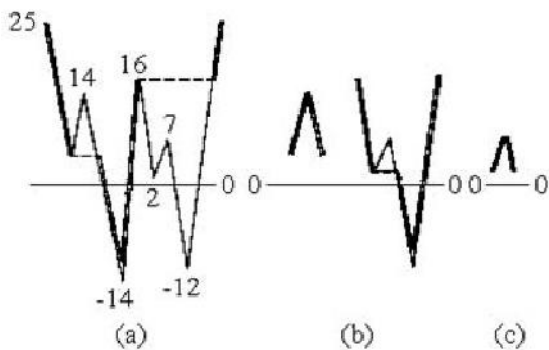


Figure 3.64. Application example of the rainflow counting process

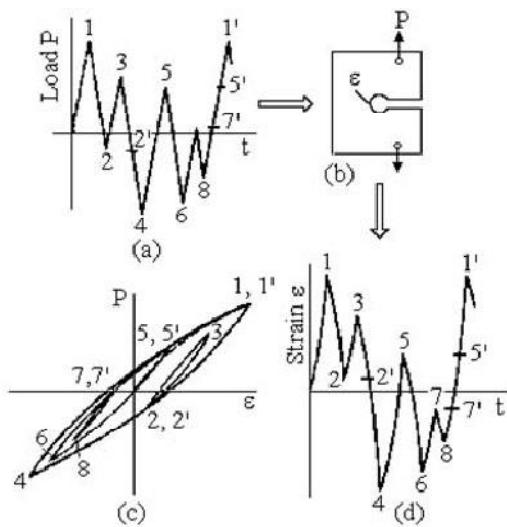


Figure 3.65. Rainflow method combined with strain analysis [MR 65]

The rainflow method is interesting when it is combined with a strain analysis [FUC 80]. Let us consider, for example, the case in Figure 3.65. The damage can be calculated for each cycle as soon as it is identified in the counting procedure.

Each part of strain time history $\epsilon(t)$ is counted only once. The damage created by a great variation of the strain is not affected by an interruption which produces a small cycle.

For each cycle of stress, we follow a closed hysteresis loop returning at the initial point of the beginning of cycle, the preceding curve continuing as if this cycle had not existed. There is simply addition of the damage. The signal $\epsilon(t)$ can therefore be broken up into half-cycles with known terminals from which we can calculate the mean value. These data make it possible to calculate the damage undergone with an accumulation law [WAT 76].

NOTES:

1. There are methods very similar to this (the "maximum–minimum procedure," the pattern classification procedure) [EN 7] which give the same results.

2 The rainflow method is very similar to the range-pair counting method. If we consider again Figure 3, the difference between these two methods can be explained by considering the half-cycle 1–6. In the case of the range-pair counting, the half-cycle which is complementary for it is 6–1' and the part 1'–7 is lost. With the present method, when the range which could constitute the second half-cycle has a range larger than 6–1' (which is the case here, with 6–7), counting 1–6 is suspended (on standby of another later complementary half-cycle) and a new counting 6–7 is opened.

In addition, the residual half-cycles are preserved here (those which could not be paired), whereas the range-pair counting method is unaware of them.

3.12.2. Subroutine for rainflow counting

The routine below makes it possible to determine the ranges of a signal to use for the calculation of the fatigue damage according to this method. The signal must be first modified in order to start and finish by the largest peak. The total number of peaks and valleys must be even and an array of the peaks and valleys (*Extrema()*) must be composed of the signal prepared in this way.

The boundaries of the ranges from the peaks are provided in arrays *PeakM()* and *PeakM()* and those of the ranges resulting from the valleys in *ValleyM()* and *ValleyM()*. These values make it possible to calculate the two types of ranges *RangePeak()* and *RangeValley()*, as well as their mean value $\frac{PeakM(i) + PeakM(i)}{2}$ and $\frac{ValleyM(i) + ValleyM(i)}{2}$.

' Procedure RAINFLOW of peaks counting (GFA-BASIC)*'According to D.VEISON**'The procedure uses as input/output data:**' Extremum(Nbr_Extrema%+2)= array giving the list of Nbr_Extrema% extrema**' successive and starting from the largest peak**' At output, we obtain:**' Peak_Max(Nbr_Peaks%) and Peak_Min(Nbr_Peaks%)= limits of the ranges of the peaks**' Valley_Max(Nbr_Peaks%) and Valley_Min(Nbr_Peaks%)= limits of the valley ranges**' These values make it possible to calculate the ranges and their mean value.**' Range_Peak(Nbr_Peaks%)= array giving the listed ranges relating to the peaks**' Range_Valley(Nbr_Peaks%)= array of the ranges relating to the valleys*

,

PROCEDURE rainflow (Nbr_Extrema%,VAR Extremum())

LOCAL i%,n%,Q%,Output&,m%,j%,k%

' Separation of peaks and valleys

Nbr_Peaks% = (Nbr_Extrema% + 1) / 2

FOR i% = 1 TO Nbr_Peaks%

Peak(i%) = Extremum(i% * 2 - 1)

NEXT i%

FOR i% = 2 TO Nbr_Peaks%

Valley(i%) = Extremum(i% * 2 - 2)

NEXT i%

' Research of deepest valley

Valley_Min = Valley(2)

FOR i% = 2 TO Nbr_Peaks%

IF Valley(i%) < Valley_Min

Valley_Min = Valley(i%)

ENDIF

NEXT i%

Valley(Nbr_Peaks% + 1) = 1.01 * Valley_Min

' Treatment of valleys

FOR i% = 2 TO Nbr_Peaks% // Initialization of the tables with Peak(1)

L(i%) = Peak(1)

LL(i%) = Peak(1)

NEXT i%

FOR i% = 2 TO Nbr_Peaks%

n% = 0

Q% = i%

Output& = 0

DO /Calculation of the Ranges relating to the valleys

IF LL(i% + n%) < Peak(i% + n%)


```

Range_Valley(i%) = ABS(LL(i% + n%) - Valley(i%)) / Array of the llleys
Ranges
Valley_Max(i%) = LL(i% + n%) / Array of the llleys
Valley_Min(i%) = Valley(i%) / Array of the llleys
Output& = 1
ELSE
IF Valley(i% + n% + 1) < Valley(i%)
Range_Valley(i%) = ABS(Peak(Q%) - Valley(i%))
Valley_Max(i%) = Peak(Q%)
Valley_Min(i%) = Valley(i%)
Output& = 1
ELSE
IF Peak(i% + n% + 1) < Peak(Q%)
L(i% + n% + 1) = Peak(Q%)
n% = n% + 1
ELSE
L(i% + n% + 1) = Peak(Q%)
Q% = i% + n% + 1
n% = n% + 1
ENDIF
ENDIF
ENDIF
LOOP UNTIL Output& = 1
m% = i% + 1
IF m% <= Q%
FOR j% = m% TO Q%
LL(j%) = L(j%)
NEXT j%
ENDIF
NEXT i%
' Treatment of peaks
FOR i% = 2 TO Nbr_Peaks% + 1 // Initialization of the arrays with llleyM
L(i%) = Valley_Min
LL(i%) = Valley_Min
NEXT i%
FOR i% = 1 TO Nbr_Peaks%
n% = 0
k% = i% + 1
Q% = k%
Output& = 0
DO
IF LL(k% + n%) > Valley(k% + n%)
Range_Peak(i%) = ABS(Peak(i%) - LL(k% + n%)) / Array of the Ranges of the
Peaks

```

```

Peak_Max(i%) = Peak(i%) /Array of the Mimum of the Ranges of the Peaks
Peak_Min(i%) = LL(k% + n%) /Array of the Mimum of the Ranges of the Peaks
Output& = 1
ELSE
IF Peak(k% + n%) > Peak(i%)
Range_Peak(i%) = ABS(Peak(i%) - Valley(Q%))
Peak_Max(i%) = Peak(i%)
Peak_Min(i%) = Valley(Q%)
Output& = 1
ELSE
IF Valley(k% + n% + 1) > Valley(Q%)
L(k% + n% + 1) = Valley(Q%)
n% = n% + 1
ELSE
L(k% + n% + 1) = Valley(Q%)
Q% = k% + n% + 1
n% = n% + 1
ENDIF
ENDIF
ENDIF
LOOP UNTIL Output& = 1
m% = k% + 1
IF m% <= Q%
FOR j% = m% TO Q%
LL(j%) = L(j%)
NEXT j%
ENDIF
NEXT i%
RETURN

```

3.13. NRL (National Luchtvaart Laboratorium) counting method

This method is also known as the *range-pair-range count method*.

This section concerns an extension of the range-pair counting method, taking into account information on the mean value and therefore making it possible to characterize the extreme levels correctly [SCH 72a].

The procedure of counting is applied in two steps. In the first, all the intermediate cycles of load are detected and counted by noting the associated mean values. Each cycle of intermediate load counted is then eliminated from the signal varying with time [VAN 71]. The procedure is repeated until the signal does not present any more cycles of intermediate load. The signal obtained at the end of this

first step is of oscillatory type with a narrow band with cycles of variable amplitude, each extremum preceded and followed by a zero-crossing. In the second step, the residual load is analyzed according to the range-mean count method.

Example 3.4.

Let us consider the sample of signal in Figure 3.66(a).

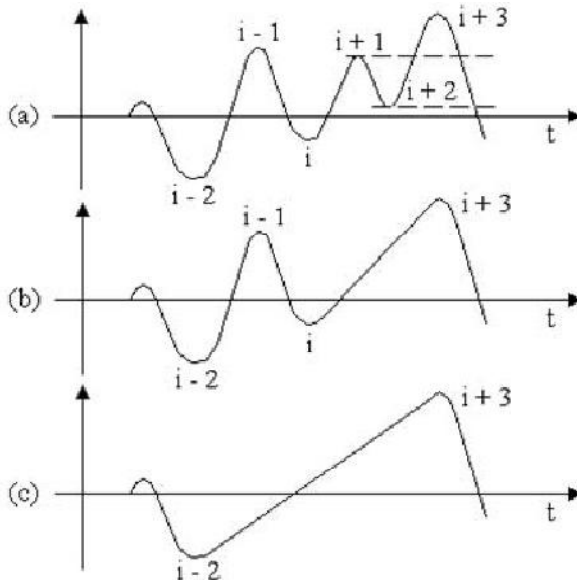


Figure 3.66. Principle of the RLC counting method (step no. 1)

Step no. 1

Four successive peaks i to $i+3$ are considered. If x_{i+1} and x_{i+2} are within the interval x_i, x_{i+3} , two half-cycles of amplitude $\frac{x_{i+1} - x_{i+2}}{2}$ and mean $\frac{x_{i+1} + x_{i+2}}{2}$ are counted.

The values x_{i+1} and x_{i+2} are then removed from signal (b). The procedure is repeated for the peaks x_{i-2} , x_{i-1} , x_i and x_{i+3} , and leads, after counting and removal of the range x_{i-1}, x_i , to the signal (c) [DEJ 70].

The repetition of this procedure on the whole signal leads to a new signal of the form of that of Figure 3.67 at the end of step no. 1.

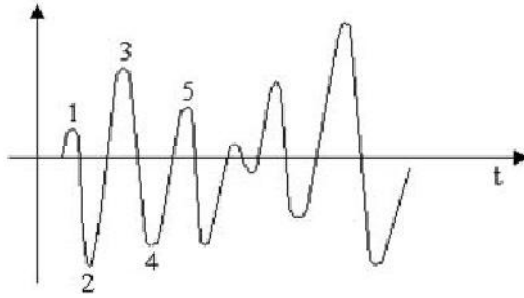


Figure 3.67. *Signal obtained at end of step no. 1*

Step no. 2

Counting according to the range-mean method consists of noting the pairs

$$\left| \frac{x_1 - x_2}{2} \right| \text{ and } \frac{x_1 + x_2}{2}$$

$$\left| \frac{x_2 - x_3}{2} \right| \text{ and } \frac{x_2 + x_3}{2}.$$

These countings are added to those of step no. 1.

The total result can be described as the number of cycles (range $\Delta\sigma$, mean σ_m) for each combination of $\Delta\sigma$ and σ_m . This representation is not very convenient because of its 2D character. As fatigue is primarily due to the amplitude of the load (range) and, with the second order, to the mean, we calculate a mean value $\bar{\sigma}_m(\Delta\sigma)$ for each value of amplitude $\Delta\sigma$ and preserve the standard deviation of the mean as information on the variations of the value σ_m , i.e.

$$s_m(\Delta\sigma) = \sqrt{\sigma_m^2(\Delta\sigma) - [\bar{\sigma}_m(\Delta\sigma)]^2} \quad [3.6]$$

This description makes it possible to represent the result in a mono-dimensional form. For each amplitude of range $\Delta\sigma$, we obtain [DEJ 70]:

- the number of cycles;

- the mean value of these cycles $\bar{\sigma}_m(\Delta\sigma)$; and
- the standard deviation of the mean $s_m(\Delta\sigma)$.

It is considered that this method gives more significant information from the fatigue point of view than the other methods described (except for the rainflow, to which it is close [VAN 71]). It has the same advantages as the range-pair counting method without having its previously discussed disadvantages [SCH 72a].

3.14. Evaluation of time spent at a given level

The range of variation of the signal is broken up into sections of small width $\Delta\sigma_i$. Given one of these sections included between the levels σ_i and σ_{i+1} , we count the times Δt_j during which the signal remains inside this section. The sum of these Δt_j is a fraction of total time T of the signal studied.

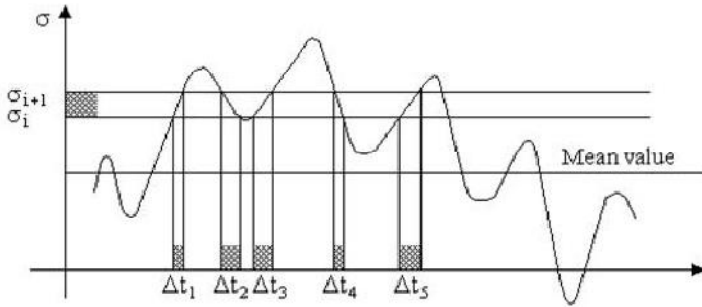


Figure 3.68. *Time of staying at a given level*

This fraction is all the larger since the section is broader. To eliminate this disadvantage, we weight it by the width $\Delta\sigma_i$.

The results so obtained make it possible to calculate the probability density:

$$p = \lim_{\Delta\sigma_i \rightarrow 0} \left[\frac{1}{\Delta\sigma_i} \frac{\sum_j \Delta t_j}{T} \right] \quad [3.7]$$

Very often, this density can be approximated by that of a Gaussian law.

This method, which is based on the time spent in a section $\Delta\sigma$, is very dependent on the first derivative of the signal. The result will be very different according to whether the signal varies quickly or slowly. It poorly represents the frequency of appearance of the levels, and is therefore seldom used [BUX 66].

3.15. Influence of levels of load below fatigue limit on fatigue life

From a synthesis of much work carried out on alloys 2024-T3 and 7075-T6, T.J. Ravishankar [RAV 70] showed that the low levels, lower than the fatigue limit, produce damage while contributing to the propagation of the fissure if started. Their omission therefore increases the lifetime.

3.16. Test acceleration

We can be led by this objective to increase the amplitudes of the sequence. It is advisable to be careful and only increase those cycles of average size; an increase in the amplitude of the strongest levels can modify the fatigue life of the test bar [SCH 74].

Let us consider a signal whose instantaneous values are distributed according to a Gaussian law and peaks according to Rayleigh's law:

1. The spectrum is maintained linearly by increasing the probability uniformly.

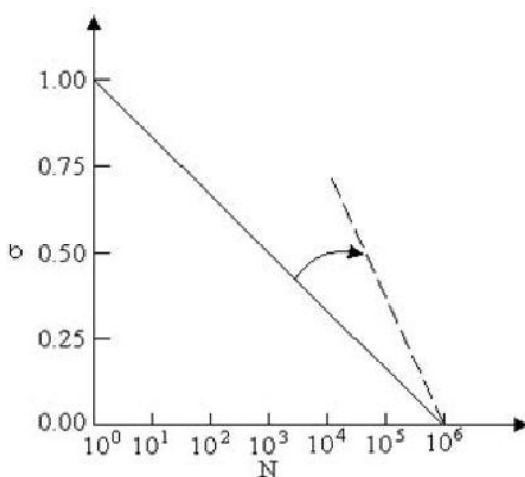


Figure 3.69. *Reduction of the duration of a test by increasing all the stresses*

The highest load levels occur more frequently while the smallest loads are less affected. This case is similar to the *in situ* situation where the segments of the worst road are traversed with a frequency higher than the normal [BUS 72].

W. Schütz [SCH 72b] considers that if a test must be accelerated, that should not be carried out by increasing the stresses, but rather by neglecting the stresses of low amplitude.

In order that a test is representative, it is necessary to simulate the real stresses as accurately as possible with respect to the sequences and the amplitudes.

The reduction of the duration of a test by increasing the frequency (central frequency of the narrow band noise) does not have a beneficial effect since there is an accompanying increase in the fatigue life of the material [KEN 82].

2. Another method can consist of neglecting the low levels [SCH 74] (loads lower than a certain percentage of the static ultimate load, e.g. 2%).

Tedford *et al.* [TED 73] note that the levels of stress lower than 1.75 times the rms stress do not have any significant effect on the fatigue damage. Their elimination makes it possible to reduce the duration of test considerably (note that M.N. Kenefeck [KEN 82] gives 2.5 times the rms value as a limit). It is, on the other hand, important to have a good knowledge of the highest levels of the environment since they produce the damage.

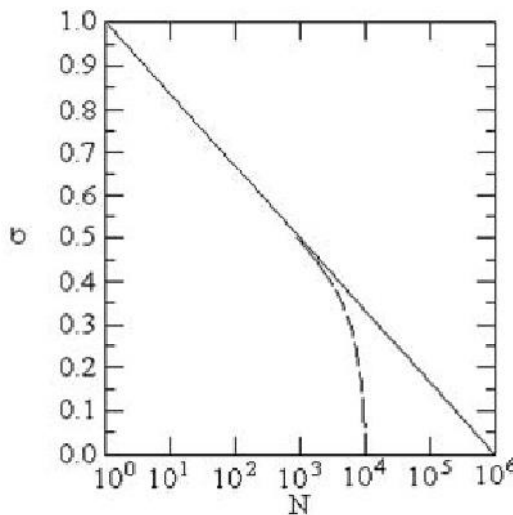


Figure 3.70. Reduction of test duration by elimination of the lowest stresses

The method consists of distorting the low part of the load spectrum by considering that the low levels do not contribute to fatigue. This is equivalent to considering that the vehicle does not run on the best parts of the road.

NOTE: A combination of the two methods (rotation of the spectrum and suppression of the low levels) is possible and is analogous to bumping along roads where potholes and paving stones are present [BS77].

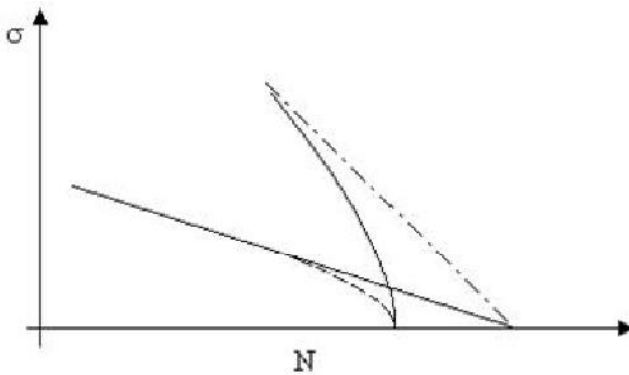


Figure 3.71. Reduction of duration of a test by suppression of the lowest stresses and by an increase in other stresses

Although we can think a priori that such a suppression has little consequence, this step must however be applied with prudence [N64].

A synthesis of various publications shows indeed that the low levels, lower than the fatigue limit, contribute to the damage. Their omission increases the fatigue life. They take part in the propagation of the fissure (dominating phenomenon under random loading) when this is started [JAC 66] [RA77].

3.17. Presentation of fatigue curves determined by random vibration tests

The S-N curves plotted for sinusoidal loads give the number N of cycles to rupture (on the abscissae) against amplitude of the stress σ (on the ordinates). If the load is a random vibration, the load amplitude is no longer constant and the most significant parameter (for constant PSD shape) is the rms value [BOO 70] [BOO 76] [KEN 82] [PER 74] for a given value of the mean stress.

The number of cycles is generally badly defined (except for the narrow band noises for which there is one peak between two through-zero passages). Two possibilities exist and are used:

- the number of passages through zero with positive slope [BOO 66,] [BOO 70] [BOO 76] [KEN 82] [RAV 70], when this parameter is representative of the number of cycles (r close to 1); and

- the number of peaks above the mean value (if the signal has symmetric positive and negative distributions) [BOO 66] [HIL 70] [PER 74] [RAV 70]. This number of peaks can be evaluated either from the counting methods, or from a statistical calculation using its PSD if the signal is Gaussian.

In the case of a sinusoidal signal, these two definitions are equivalent.

We note in these tests that, contrary to the case of a sinusoidal load, a fatigue limit is not observed for steels. This result is explained easily since, for a given rms value, there is in the signal peaks of amplitude equal to several times this rms value. According to the characteristics of the test control system, the peak factor (ratio of the largest peak to the rms value) can be about 4–4.5.

The comparison of the results obtained under sinusoidal and random loads can therefore be carried out only by modifying the representation of the curves plotted in sinusoidal mode on the stress axis. Several representations exist, including [PER 74]:

- instead of σ_a (amplitude of the sinusoidal alternating stress), we use

$$\sigma_{\text{rms}} = \sqrt{\frac{\sigma_a^2}{2} + \sigma_m^2} \quad [3.8]$$

(σ_m = mean stress);

- we use $\frac{\sigma_a}{\sqrt{2}}$ [RUD 75] in sine and σ_{rms} calculated on the centered signal, the two values for σ_m being given (the most usual method).

Chapter 4

Fatigue Damage by One-degree-of-freedom Mechanical System

4.1. Introduction

In this chapter we propose considering the damage by fatigue created by a random vibration on a one-degree-of-freedom (one-dof) linear system, of natural frequency f_0 and quality factor Q , and provide all the relations necessary to the layout of the fatigue damage spectra (Volume 5). This calculation can be carried out directly from a sample of the vibratory signal defined in the time domain or in a statistical manner (mean and standard deviation of the damage) from an acceleration spectral density of the vibration.

Unless otherwise specified, we will make the following assumptions:

- the S-N curve is represented by Basquin's relation (of the form $N \sigma^b = C$);
- a linear accumulation law of the fatigue damage (Miner's rule);
- a vibration of zero mean; and
- a Gaussian distribution of the instantaneous values of the vibratory signal.

We will however examine at the end of this volume (Chapter 6) some different assumptions:

- an S-N curve having an ultimate endurance stress;
- a linear S-N curve in logarithmic-linear scales;

- a truncated signal;
- a damage accumulation law of Corten-Dolan;
- non-zero mean stress; and
- other probability distribution laws governing instantaneous values of excitation.

4.2. Calculation of fatigue damage due to signal versus time

Let us consider a random vibration with zero mean applied to a one-degree-of-freedom linear mechanical system of natural frequency f_0 and damping ratio ξ . If the excitation is defined by acceleration $\ddot{x}(t)$ in the time domain, in analog or numerical form, it is possible to calculate, over duration T corresponding to the duration of the signal, the response of the one-degree-of-freedom mechanical system, characterized by the relative displacement $z(t)$ between the mass and its support.

If the damping ratio ξ is sufficiently small, the response appears as an oscillation around the zero average value, generally passing through positive and negative peaks successively with a randomly varying amplitude. The frequency of the response is very close to the natural frequency f_0 of the system (narrow band noise).

In this simple case, the response can be broken up into half-cycles which are classified and counted according to their amplitude (histogram). If the response has a more complex form, the histogram of the peaks must be established using a peak counting method such as the *rainflow* method [LAL 92] (Chapter 3).

Since the system is linear, the stress created in the elastic element is proportional to the relative displacement z_p corresponding to each extremum of $z(t)$ ($\dot{z} = 0$ at these points):

$$\sigma = K z_p.$$

If the S-N curve of the material can be treated using Basquin's analytical expression [LAL 92],

$$N \sigma^b = C \tag{4.1}$$

where N is the number of cycles to failure of a test bar under sinusoidal stress of amplitude σ and b and C are constants characteristic of the material (Chapter 1 provides some values of the b parameter). We therefore have:

$$N (K z_p)^b = C \quad [4.2]$$

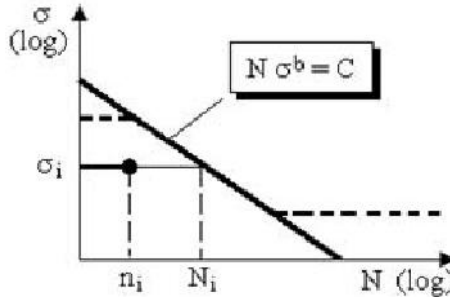


Figure 4.1. Representation of the S - N curve

The damage undergone by the system during the application of a half-cycle of stress σ_i is:

$$\delta_i = \frac{1}{2 N_i} = \frac{\sigma_i^b}{2 C} \quad [4.3]$$

and, for n_i half-cycles on the stress level σ_i ,

$$d_i = \frac{n_i}{2 N_i} = \frac{n_i \sigma_i^b}{2 C} = \frac{K^b}{2 C} n_i z_{p_i}^b \quad [4.4]$$

In this relation, N_i is the number of cycles to failure at level σ_i , n_i is the number of half-cycles counted at this level σ_i (which explains the factor 2). If we defined m classes of levels z_{p_i} , the generated total damage can be written (according to the Miner's linear rule of accumulation):

$$D = \sum_{i=1}^m d_i = \sum_i \frac{n_i \sigma_i^b}{2 C} \quad [4.5]$$

$$D = \frac{K^b}{2 C} \sum_{i=1}^m n_i z_{p_i}^b \quad [4.6]$$

NOTE: *J.W. Miles [MIL 54] shows that, in the case of a structure subjected to random vibrations, Miner's hypothesis can be regarded as correct for the estimate of fatigue life. A non-linear hypothesis of damage accumulation leads to an unimportant variation of the fatigue life when the amplitudes of the stresses are distributed continuously over a broad range.*

4.3. Calculation of fatigue damage due to acceleration spectral density

4.3.1. General case

Let us consider a record $\ddot{x}(t)$ of a random vibration (acceleration) representative of a stationary ergodic process with mean zero, duration T and PSD $G(f)$. Let us set $q(z_p)$ as the peak probability density of the stress response of the system to this vibration. The mean number of maxima (positive or negative) is equal to:

$$N_p = n_p^+ T \quad [4.7]$$

and the mean number of peaks (maxima + minima) is equal to $2 N_p$. The number of peaks dn of the stress response whose amplitude is included, in absolute value, between σ_p and $\sigma_p + d\sigma_p$ is, over duration T :

$$dn = 2 n_p^+ T q(\sigma_p) d\sigma_p \quad [4.8]$$

The amplitude of the stress is assumed to be proportional to relative strain level z :

$$\sigma_p = K z_p \quad [4.9]$$

The damage by fatigue dD generated by these dn peaks is, according to Miner's rule [CRA 63]:

$$dD = \frac{dn}{2 N(\sigma)} \quad [4.10]$$

$$dD = n_p^+ T \frac{q(\sigma)}{N(\sigma)} d\sigma \quad [4.11]$$

The mean damage D (or expected damage, also denoted $E(D)$ in the following pages) is the sum of the partial damages for all the positive values of σ [BRO 68a] [HIL 70] [LIN 72] (we are not interested in negative maxima or the positive minima):

$$D = n_p^+ T \int_0^{+\infty} \frac{q(\sigma)}{N(\sigma)} d\sigma \quad [4.12]$$

NOTES:

1. *The mean damage per peak is equal to*

$$\bar{d} = \frac{D}{2 n_p^+ T} \quad [4.13]$$

2. *The expected fatigue life T is obtained by setting $D = 1$, yielding:*

$$T = \frac{1}{n_p^+ \int_0^{+\infty} \frac{q(\sigma)}{N(\sigma)} d\sigma} \quad [4.14]$$

If the S-N curve of the material can be approached using Basquin's relation $N \sigma^b = C$, it can be written [PER 74]:

$$D = \frac{n_p^+ T}{C} \int_0^{+\infty} \sigma^b q(\sigma) d\sigma \quad [4.15]$$

If the relation between the stress and the strain is linear ($\sigma = K z_p$), it becomes

$$D = \frac{K^b}{C} n_p^+ T \int_0^{+\infty} z_p^b q(z_p) dz_p \quad [4.16]$$

If we set

$$u = \frac{z_p}{z_{rms}} = \frac{\sigma_p}{\sigma_{rms}} \quad [4.17]$$

where z_{rms} is the rms value of $z(t)$ and σ_{rms} that of $\sigma(t)$. Since

$$Q(z) = \int_{-\infty}^z q(z) dz = Q(u) = \int_{-\infty}^u q(u) du \quad [4.18]$$

and

$$q(z) = \frac{q(u)}{z_{\text{rms}}} \quad [4.19]$$

we have

$$D = \frac{K^b}{C} n_p^+ T z_{\text{rms}}^b \int_0^{+\infty} u^b q(u) du \quad [4.20]$$

or

$$D = \frac{n_p^+ T}{C} \sigma_{\text{rms}}^b \int_0^{+\infty} u^b q(u) du \quad [4.21]$$

The calculation of the mean damage D uses the rms value of the relative displacement z_{rms} (or the rms stress) and an integral. We saw in Chapter 1 how z_{rms} can be evaluated starting from a PSD defined by straight line segments.

Let us suppose that the distribution of the instantaneous values of the input signal $\ddot{x}(t)$ (applied to the base of the one-dof system) is Gaussian. The response of the system is then itself Gaussian and the probability density $p(z_p)$ of the maxima z_p of the response can be expressed analytically in the form of the sum of a Gaussian distribution and Rayleigh's distribution (Volume 3, Chapter 6) [LAL 92]:

$$q(u) = \frac{\sqrt{1-r^2}}{\sqrt{2\pi}} e^{-\frac{u^2}{2(1-r^2)}} + u r e^{-\frac{u^2}{2}} \left[1 - \frac{1}{\sqrt{\pi}} \int_{\frac{u r}{\sqrt{2(1-r^2)}}}^{\infty} e^{-\lambda^2} d\lambda \right] \quad [4.22]$$

where r is the irregularity factor $= n_0^+ / n_p^+$, ratio of the expected frequency to the mean number of maxima per second. This expression can be also written in the form

$$q(u) = \frac{\sqrt{1-r^2}}{\sqrt{2\pi}} e^{-\frac{u^2}{2(1-r^2)}} + \frac{ur}{2} e^{-\frac{u^2}{2}} \left[1 + \operatorname{erf}\left(\frac{ur}{\sqrt{2(1-r^2)}}\right) \right] \quad [4.23]$$

where

$$\operatorname{erf}(x) = \frac{2}{\sqrt{\pi}} \int_0^x e^{-\lambda^2} d\lambda$$

or

$$q(\sigma) = \frac{q(u)}{\sigma_{\text{rms}}} = \frac{\sqrt{1-r^2}}{\sigma_{\text{rms}} \sqrt{2\pi}} e^{-\frac{\sigma^2}{2(1-r^2)\sigma_{\text{rms}}^2}} + \frac{r\sigma}{2\sigma_{\text{rms}}^2} e^{-\frac{\sigma^2}{2\sigma_{\text{rms}}^2}} \left[1 + \operatorname{erf}\left(\frac{r\sigma}{\sigma_{\text{rms}} \sqrt{2(1-r^2)}}\right) \right]. \quad [4.24]$$

From equations [4.15] and [4.24],

$$D = \frac{n_p^+ T}{\sigma_{\text{rms}}} \int_0^{+\infty} \left\{ \frac{\sqrt{1-r^2}}{\sigma_{\text{rms}} \sqrt{2\pi}} e^{-\frac{\sigma^2}{2(1-r^2)\sigma_{\text{rms}}^2}} + \frac{r\sigma}{2\sigma_{\text{rms}}^2} e^{-\frac{\sigma^2}{2\sigma_{\text{rms}}^2}} \left[1 + \operatorname{erf}\left(\frac{r\sigma}{\sigma_{\text{rms}} \sqrt{2(1-r^2)}}\right) \right] \right\} \frac{d\sigma}{N(\sigma)} \quad [4.25]$$

Knowing that $\sigma = K z$ and that $N = \frac{C}{\sigma^b}$, we have

$$D = \frac{K^b n_p^+ T}{C z_{\text{rms}}} \int_0^{+\infty} z_p^b \left\{ \frac{\sqrt{1-r^2}}{\sqrt{2\pi}} e^{-\frac{z_p^2}{2(1-r^2)z_{\text{rms}}^2}} + \frac{r z_p}{2 z_{\text{rms}}} e^{-\frac{z_p^2}{2 z_{\text{rms}}^2}} \left[1 + \operatorname{erf}\left(\frac{r z_p}{z_{\text{rms}} \sqrt{2(1-r^2)}}\right) \right] \right\} dz_p \quad [4.26]$$

NOTES:

1. Depending on the value of r , the response has peaks which follow a Gaussian or Rayleigh distribution or intermediary. In the case of the Rayleigh distribution, corresponding to a low damping, the response is of narrow band type and resembles a sinusoid of randomly modulated amplitude. Each positive peak is followed by a negative peak, itself followed by a positive peak and so on.

All the authors agree that, for a given rms stress level and a given expected frequency, the most severe loading case (one-dof system) is that for which the peaks of the response have a Rayleigh distribution [BRO 70a] [SCH 61b].

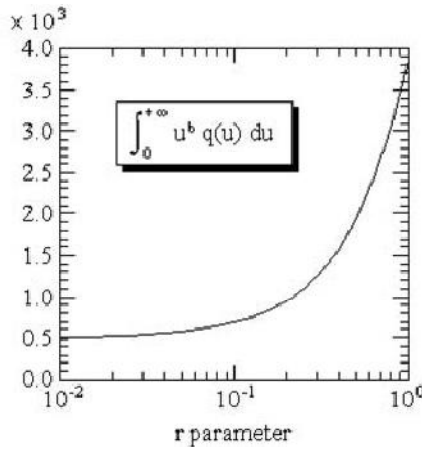


Figure 4.2. Variations of damage versus irregularity factor of response

Figure 4.2 shows the variations of the integral of relation [4.21] versus parameter r , for $b = 10$.

It is checked that for a constant number $n_p^+ T$ of peaks, the damage increases with r , i.e. when the peak distribution tends towards Rayleigh's law.

2. The calculation of D requires the evaluation of integrals of the form

$$\int_0^{\infty} y^b e^{-a y^2} dy.$$

There are approximate expressions available facilitating this calculation [SYL 81] (see Appendix A3.6).

4.3.2. Approximate expression of the probability density of peaks

L. Pierrat [PIE 04] considers the expression of the peaks probability density [4.24] and identifies the error function to the quadratic exponential form:

$$\text{erf}(x) \approx 1 - \frac{1}{n} \sum_{i=1}^n \exp \left[- \left(A_{n,i} x \right)^2 \right] \quad [4.27]$$

yielding an expression of damage of the form:

$$D = \frac{n_p^+ T}{C} \left(\sqrt{2} \sigma_{\text{rms}} \right)^b \left\{ \frac{q^{b+2}}{2 \sqrt{\pi}} \Gamma \left(\frac{b+1}{2} \right) + LP_n(r, b) \Gamma \left(\frac{b}{2} + 1 \right) \right\} \quad [4.28]$$

in which $LP_n(r, b)$ is a corrective function calculated to respect the asymptotic solutions corresponding to, on the one hand, wideband processes ($r = 0$) and narrow band processes ($r = 1$) and, on the other hand, the identity of the mean values of the approximate and exact error function.

To zero order, this function is a constant independent of r and b . The corrective functions to order one and two can be written

$$LP_n = 1 - \frac{1}{2n} \sum_{i=1}^n C_{n,i} \quad [4.29]$$

where the coefficients $C_{n,i}$ and $A_{n,i}$ are related by

$$C_{n,i} = \left[1 + \left(\frac{A_{n,i} r}{q} \right)^2 \right]^{- (1+b/2)} \quad [4.30]$$

and coefficients $A_{n,i}$ are equal to

$$\left\{ \begin{array}{l} A_{1,1} = \frac{\pi}{2} \approx 1.571 \\ A_{2,1} = \frac{2\pi}{4 + \sqrt{2\pi^2 - 16}} \approx 1.059 \\ A_{2,2} = \frac{2\pi}{4 - \sqrt{2\pi^2 - 16}} \approx 3.104 \end{array} \right. \quad [4.31]$$

and the error can be estimated by the ratio

$$p = \frac{D_{LP}}{D} = \frac{\left(\frac{\sqrt{1-r^2}}{2\sqrt{\pi}}\right)^{b+2} \Gamma\left(\frac{1+b}{2}\right) + LP(r, b) \Gamma\left(1+\frac{b}{2}\right)}{\int_0^{+\infty} u^b q(u) du} \quad [4.32]$$

The error made with this approximation was evaluated for b ranging between 3 and 25, the largest error corresponding to 25 (Figures 4.3 and 4.4). To zero order, the coefficient of the Gamma function,

$$LP_0 = 1 - \frac{1}{2\sqrt{\pi}} \approx 0.718,$$

is close to that of G.K. Chaudhury and W.D. Dover [CHA 85] (0.75) (see section 4.5.3, equation [4.92]). This leads to a significant error, about 28% for $r = 1$. The approximation of order one allows the error to be limited to 5% and of order two to 2% (for $3 \leq b \leq 25$).

4.3.3. Particular case of a wide-band response, e.g. at the limit $r = 0$

In this case [CHA 85] we have that

$$D = \frac{n_p^+ T}{C} \int_0^{+\infty} \sigma^b q(\sigma) d\sigma$$

with

$$q(\sigma) = \frac{1}{\sigma_{rms} \sqrt{2\pi}} e^{-\frac{\sigma^2}{2\sigma_{rms}^2}} \quad [4.33]$$

Let us set

$$\alpha = \frac{\sigma^2}{2\sigma_{rms}^2};$$

then the above equation becomes

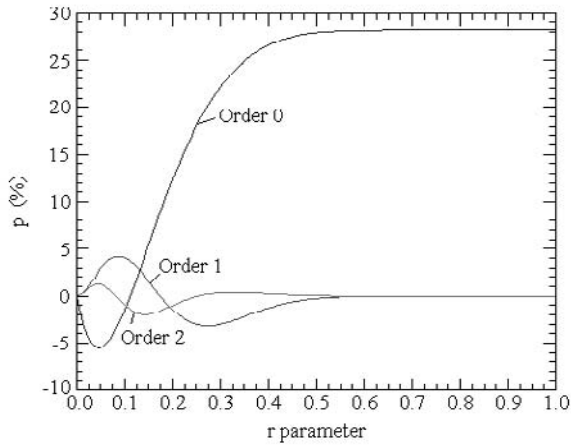


Figure 4.3. Error according to r parameter for an approximation of order 0, 1 and 2 ($b = 25$)

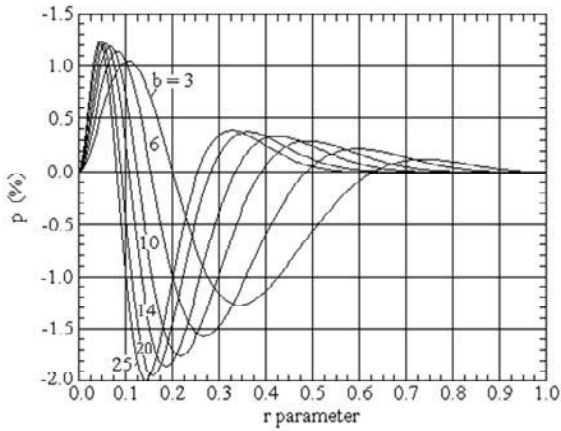


Figure 4.4. Error according to r parameter for an approximation of order 2 ($b = 3, 6, 10, 14, 20$ and 25)

$$D = \frac{n_p^+ T}{2 C \sqrt{\pi}} (\sqrt{2} \sigma_{\text{rms}})^b \int_0^{+\infty} \alpha^{\frac{b-1}{2}} e^{-\alpha} d\alpha.$$

The integral

$$\int_0^{+\infty} \alpha^{\frac{b-1}{2}} e^{-\alpha} d\alpha$$

is the gamma function (Appendix A1):

$$\Gamma(x) = \int_0^{\infty} \alpha^{x-1} e^{-\alpha} d\alpha \quad [4.34]$$

where $x = \frac{b+1}{2}$; yielding

$$D = \frac{n_p^+ T}{2 C \sqrt{\pi}} (\sqrt{2} \sigma_{\text{rms}})^b \Gamma\left(\frac{b+1}{2}\right) \quad [4.35]$$

4.3.4. Particular case of narrow band response

4.3.4.1. Expression for expected damage

From the expression for the damage [4.25], we can write:

$$\begin{aligned} D = \frac{n_p^+ T}{\sigma_{\text{rms}}} & \left[\int_0^{+\infty} \frac{\sqrt{1-r^2}}{\sigma_{\text{rms}} \sqrt{2\pi}} \frac{\sigma^b}{C} e^{-\frac{\sigma^2}{2\sigma_{\text{rms}}^2(1-r^2)}} d\sigma \right. \\ & + \int_0^{+\infty} \frac{r}{2\sigma_{\text{rms}}^2} \frac{\sigma^{b+1}}{C} e^{-\frac{\sigma^2}{2\sigma_{\text{rms}}^2}} d\sigma \\ & \left. + \int_0^{+\infty} \frac{r}{2\sigma_{\text{rms}}^2} \frac{\sigma^{b+1}}{C} \operatorname{erf}\left[\frac{\sigma}{\sigma_{\text{rms}}} \sqrt{\frac{r^2}{2(1-r)}}\right] e^{-\frac{\sigma^2}{2\sigma_{\text{rms}}^2}} d\sigma \right] \end{aligned}$$

It can be shown that, if x is large,

$$\operatorname{erf}(x) \approx 1 - \frac{1}{x\sqrt{\pi}} e^{-x^2} \quad [4.36]$$

The development in series of the error function can be limited to two terms without too much error only if $x \geq 0.9$, the approximation then being greater than 90% of the true value. From this, we obtain the condition

$$\frac{\sigma}{\sigma_{\text{rms}}} \frac{r}{\sqrt{2(1-r^2)}} \geq 0.9.$$

In addition, it has been shown [PUL 67] that 90% of the damage is produced by the reduced stresses $\sigma/\sigma_{\text{rms}}$ when higher than 1.85 when the signal presents a Rayleigh peak distribution, yielding

$$1.85 \frac{r}{\sqrt{2(1-r^2)}} \geq 0.9$$

$$r^2 \geq 0.3213$$

i.e.

$$r \geq 0.567 \quad [4.37]$$

NOTE: If $r^2 = 0.16$, the series limited to two terms gives approximately half the real value.

If this condition is observed, then after replacement of the error function by its approximate value and after simplification D can be written:

$$D \approx n_p^+ T \int_0^{+\infty} \frac{r}{\sigma_{\text{rms}}^2} \frac{\sigma^{b+1}}{C} e^{-\frac{\sigma^2}{2\sigma_{\text{rms}}^2}} d\sigma.$$

Let us set $\alpha = \frac{\sigma^2}{2\sigma_{\text{rms}}^2}$. We have $d\alpha = \frac{\sigma d\sigma}{\sigma_{\text{rms}}^2}$, yielding [HAL 78]:

$$D \approx n_p^+ T \frac{r}{C} (\sqrt{2} \sigma_{\text{rms}})^b \int_0^{+\infty} \alpha^{b/2} e^{-\alpha} d\alpha \quad [4.38]$$

The integral of this relation has the form of the gamma function with $x = 1 + \frac{b}{2}$, yielding [MIL 53]:

$$D \approx \frac{n_p^+ T}{C} r \left(\sqrt{2} \sigma_{rms} \right)^b \Gamma \left(1 + \frac{b}{2} \right) \quad [4.39]$$

Knowing that $n_0^+ = r n_p^+$ (relation [6.45], Volume 3), it becomes [BRO 68a] [CRA 63] [LIN 67]:

$$D \approx \frac{n_0^+ T}{C} \left(\sqrt{2} \sigma_{rms} \right)^b \Gamma \left(1 + \frac{b}{2} \right) \quad [4.40]$$

Since $\sigma = K z$,

$$D \approx \frac{K^b}{C} n_0^+ T \left(\sqrt{2} z_{rms} \right)^b \Gamma \left(1 + \frac{b}{2} \right) \quad [4.41]$$

If the excitation has a PSD made up of straight line segments, the damage D can be written (equation [8.79], Volume 3):

$$D \approx \frac{K^b}{C} \frac{n_0^+ T}{\left[4 \xi (2 \pi f_0)^3 \right]^{b/2}} \Gamma \left(1 + \frac{b}{2} \right) \left(\sum_{i=1}^n a_i G_i \right)^{b/2} \quad [4.42]$$

If the straight line segments are horizontal, we have, starting from equation [4.41] and from equation [8.86] (Volume 3):

$$D \approx \frac{K^b}{C} \frac{n_0^+ T \left(\sqrt{2} \right)^b}{\left[(2 \pi)^4 f_0^3 \right]^{b/2}} \Gamma \left(1 + \frac{b}{2} \right) \left\{ \frac{\pi}{4 \xi} \sum_{i=1}^n G_i \left[I_0(h_{i+1}) - I_0(h_i) \right] \right\}^{b/2} \quad [4.43]$$

NOTES:

1. Relationships [8.57], [8.58] and [8.59] of Volume 3 are used to calculate z_{rms} , \dot{z}_{rms} and \ddot{z}_{rms} and then n_0^+ and r if the PSD is composed of broken straight

lines. Relationships [8.61], [8.63] and [8.64] (Volume 3) are used if the PSD of excitation is constant in the frequency interval considered.

2. Calculation of the true value of the damage D is made difficult by ignorance of the coefficients K and C . They are therefore set equal to 1 in practice when calculating D , which is therefore obtained to a near arbitrary multiplicative coefficient. This choice is in general without consequence since this damage is evaluated in order to compare the severity of several stresses on the same structure, therefore for given K and C .

3. Basquin's relation can be also written:

$$N \sigma^b = A^b \quad [4.44]$$

The mean fatigue damage then becomes, on the assumptions selected:

$$D = \left(\frac{K}{A} \right)^b n_0^+ T \left(\sqrt{2} z_{rms} \right)^b \Gamma \left(1 + \frac{b}{2} \right) \quad [4.45]$$

a relation in which $n_0^+ T$ is the number N of alternate loadings to failure. The mean time to reach failure is such that $D = 1$, yielding:

$$\left(\frac{K}{A} \right)^b N \left(\sqrt{2} z_{rms} \right)^b \Gamma \left(1 + \frac{b}{2} \right) = 1$$

or

$$N (K z_{rms})^b = \left(\frac{A}{\sqrt{2}} \right)^b \frac{1}{\Gamma \left(1 + \frac{b}{2} \right)} = (A')^b \quad [4.46]$$

Equation [4.46] is Basquin's relation for random fatigue of a weakly damped system with one degree-of-freedom. On logarithmic scales, the S - N curve for random fatigue is a line with the slope $-1/b$, the same as for alternating fatigue, and A' can be interpreted as the ultimate stress ($N = 1$).

Particular case where the input noise is white noise

The rms displacement response to a vibration $\ell(t)$ of constant power spectral density varying with the pulsation Ω between zero and infinite is (Chapter 8, Volume 3):

$$z_{\text{rms}} = u_{\text{rms}} = \sqrt{\frac{\pi}{2} \omega_0 Q G_{\ell_0}(\Omega)} \quad [4.47]$$

If the PSD is defined with respect to frequency f ,

$$z_{\text{rms}} = \sqrt{\frac{\omega_0}{4} Q G_{\ell_0}(f)} \quad [4.48]$$

In the latter case, if the input is an acceleration, since $\ell(t) = -\frac{\ddot{x}(t)}{\omega_0^2}$,

$$z_{\text{rms}} = \sqrt{\frac{Q G_{\ddot{x}_0}(f)}{4 \omega_0^3}} \quad [4.49]$$

Finally, we can consider that the response is narrow band ($r = 1$):

$$D = \frac{K^b}{C} n_0^+ T \left(\frac{Q G_{\ddot{x}}}{2 \omega_0^3} \right)^{b/2} \Gamma\left(1 + \frac{b}{2}\right) \quad [4.50]$$

Fatigue life

The failure by fatigue takes place, according to Miner's assumption, when $D = 1$, yielding the expression for the fatigue life:

$$T = \frac{C}{K^b} \frac{1}{n_p^+ \int_0^\infty z_p^b q(z_p) dz_p} \quad [4.51]$$

If the response can be regarded as a narrow band noise,

$$T = \frac{C}{K^b} \frac{1}{n_0^+ \left(\sqrt{2} z_{\text{rms}}\right)^b \Gamma\left(1 + \frac{b}{2}\right)} \quad [4.52]$$

and, if the input is a white noise,

$$T = \frac{C}{K^b} \frac{1}{n_0^+ \left(\frac{G_{\ddot{x}}}{4 \omega_0^3} \right)^{\frac{b}{2}} \Gamma \left(1 + \frac{b}{2} \right)} \quad [4.53]$$

4.3.4.2. Notes

1. On the Rayleigh hypothesis, the damage can also be calculated from expression [4.3] $\delta_i = \frac{\sigma_i^b}{2C}$ relating to a half-cycle using

$$D = \sum_{i=1}^{N_T} \delta_i = \frac{1}{2C} \sum_{i=1}^{N_T} s_i^b \quad [4.54]$$

where N_T is the total number of half-cycles. If N_T is large, the expected value $E(\sigma^b)$ of σ^b is equal to

$$E(\sigma^b) \approx \frac{1}{N_T} \sum_{i=1}^{N_T} \sigma_i^b \quad [4.55]$$

yielding [WIR 83b]:

$$D = \frac{N_T}{2C} E(\sigma^b) = \frac{n_p^+ T}{C} E(\sigma^b) \quad [4.56]$$

2. Relationship [4.41] is exact when $r = 1$, the stresses then being distributed according to Rayleigh's law. We will see that for r close to unity, we obtain a very satisfactory approximation of damage with this expression.

3. When $r = 1$, i.e. for a narrow band stress response, relation [4.41] can be demonstrated more directly from the probability density of the Rayleigh distribution [BEN 64] [BRO 68a]:

$$q(\sigma) = \frac{\sigma}{\sigma_{rms}^2} e^{-\frac{\sigma^2}{2\sigma_{rms}^2}} \quad [4.57]$$

The narrow band response of a mechanical system to one degree-of-freedom is carried out at a mean frequency close to the natural frequency of the system ($n_0^+ \approx f_0$).

There is only one peak associated with each crossing of the mean value with positive slope [BER 77]. The mean damage per maximum (or half-cycle, since $r = \frac{n_0^+}{n_p^+} = 1$) is [POW 58]:

$$E(d) = \frac{1}{\sigma_{rms}^2} \int_0^\infty \frac{\sigma}{N(\sigma)} e^{-\frac{\sigma^2}{2\sigma_{rms}^2}} d\sigma \quad [4.58]$$

and, for n_0^+ T cycles,

$$E(D) = \frac{n_0^+ T}{\sigma_{rms}^2} \int_0^\infty \frac{\sigma}{N(\sigma)} e^{-\frac{\sigma^2}{2\sigma_{rms}^2}} d\sigma \quad [4.59]$$

where $N(\sigma) = \frac{C}{\sigma^b}$, yielding:

$$E(D) = \frac{n_0^+ T}{\sigma_{rms}^2 C} \int_0^\infty \sigma^{b+1} e^{-\frac{\sigma^2}{2\sigma_{rms}^2}} d\sigma \quad [4.60]$$

which leads, after transformation, to relation [4.41].

4. If N^* is the number of cycles to failure at the rms stress level σ_{rms} [POW 58], the expected damage [4.59]

$$E(D) = \frac{n_0^+ T}{\sigma_{rms}^2} \int_0^\infty \frac{\sigma}{N(\sigma)} e^{-\frac{\sigma^2}{2\sigma_{rms}^2}} d\sigma$$

can be also written, while setting $u = \frac{\sigma}{\sigma_{rms}}$,

$$E(D) = \frac{n_0^+ T}{N^*} \int_0^\infty \frac{N^*}{N(\sigma)} u e^{-\frac{u^2}{2}} du \quad [4.61]$$

Let us set

$$\frac{1}{\eta} = \int_0^\infty \frac{N^*}{N(\sigma)} u e^{-\frac{u^2}{2}} du \quad [4.62]$$

The damage to failure is, assuming

$$E(D) = \frac{n_0^+ T}{\eta N^*} = 1,$$

yielding another expression of time-to-failure

$$T = \eta \frac{N^*}{n_0^+} = \frac{N_e}{n_0^+} \quad [4.63]$$

where $N_e = \eta N^*$ is the number of cycles to failure corresponding to the stress σ_{rms} . This formulation makes it possible to build the S-N curves for random stresses starting from traditional S-N curves.

5. The quantity $\pi(\sigma) = \frac{q(\sigma)}{N(\sigma)}$ can be regarded as a (scaled) probability density indicating how the fatigue damage is distributed as a function of stress:

$$\pi(\sigma) = \frac{C}{\sigma_{rms}^2} \sigma^{b+1} e^{-\frac{\sigma^2}{2\sigma_{rms}^2}} \quad [4.64]$$

Figure 4.5 shows the variations of $\pi(\sigma)$ for $b = 10, 8$ and 6 , $C = 1$ and $\sigma_{rms} = 1$.

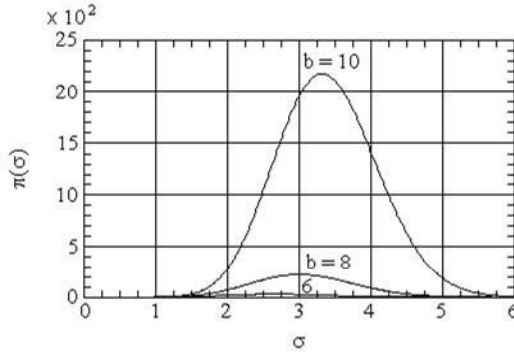


Figure 4.5. Density of probability of the damage

This law has the following characteristics:

$$\text{mode: } \sigma_{rms} \sqrt{1+b} \quad [4.65]$$

$$\text{mean: } \sqrt{2} \sigma_{rms} \frac{\Gamma\left(1 + \frac{b+1}{2}\right)}{\Gamma\left(1 + \frac{b}{2}\right)} \quad [4.66]$$

$$\text{variance: } 2 \sigma_{rms}^2 \left[\frac{\Gamma\left(1 + \frac{b+2}{2}\right)}{\Gamma\left(1 + \frac{b}{2}\right)} - \left(\frac{\Gamma\left(1 + \frac{b+1}{2}\right)}{\Gamma\left(1 + \frac{b}{2}\right)} \right)^2 \right] \quad [4.67]$$

The mode, the mean and the standard deviation are linear functions of σ_{rms} and functions of the b parameter [LAM 76].

Figure 4.6 gives the variations of these three quantities according to b for $\sigma_{rms} = 1$. It can be seen that the standard deviation varies very little with b and is approximately equal to 0.7.

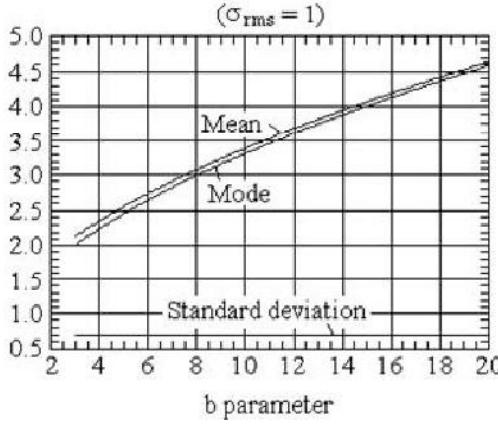


Figure 4.6. Mode, mean and standard deviation of the damage

These expressions can be written in an a -dimensional form by dividing them by the constant of standardization:

$$\frac{\frac{b}{2^2} \sigma_{rms}^b}{C} \Gamma\left(1 + \frac{b}{2}\right).$$

6. The expression of $E(D)$ for $r = 1$ is also sometimes written in the form [LIN 67] [SHE 83]:

$$E(D) = T \left(\frac{M_2}{M_0} \right)^{\frac{1}{2}} M_0^{\frac{b}{2}} \frac{2^{\frac{b}{2}}}{\sigma_1^b N_1} \int_0^{\infty} x^{\frac{b}{2}} e^{-x} dx \quad [4.68]$$

where M_0 and M_2 are the moments of order 0 and 2 of the excitation, respectively and σ_1 and N_1 are the co-ordinates at a particular point of the curve $N \sigma^b = C$.

7. The method of calculation of D leading to expression [4.40]

$$D = \frac{n_0^+ T}{C} \left(\sqrt{2} \sigma_{rms} \right)^b \Gamma\left(1 + \frac{b}{2}\right)$$

is sometimes named Crandall's method [TAN 70]. Other methods were proposed later, such as those of M. Shinozuka [SHI 66] and D. Karnopp and T.D. Scharton [KAR 66].

8. It is noted that the damage D varies with T and σ_{rms}^b . A small variation of σ_{rms} , i.e. of the amplitude of the excitation, is therefore much more sensitive than a variation of the duration T . In addition, since the stress level depends on power b , the damage is primarily created by the highest levels (in practice about four times the rms value [POW 58]).

4.3.4.3. Calculation of gamma function

If b is an even positive integer number, it is shown that

$$\Gamma\left(1 + \frac{b}{2}\right) = \frac{b}{2} ! \quad [4.69]$$

If b is odd integer, $b = 2\beta + 1$,

$$\Gamma\left(1 + \frac{b}{2}\right) = \Gamma\left(\frac{1}{2} + \beta\right) = \frac{1.3 \cdots (2\beta + 1)}{2^\beta} \sqrt{\pi} \quad [4.70]$$

and

$$\Gamma\left(\frac{1}{2}\right) = \sqrt{\pi}.$$

If b is arbitrary, we have:

$$\Gamma\left(1 + \frac{b}{2}\right) = \frac{b}{2} \Gamma\left(\frac{b}{2}\right) = \frac{b}{2} \left(\frac{b}{2} - 1\right) \Gamma\left(\frac{b}{2} - 1\right)$$

and

$$\Gamma\left(1 + \frac{b}{2}\right) = \frac{b}{2} \left(\frac{b}{2} - 1\right) \left(\frac{b}{2} - 2\right) \cdots \left(\frac{b}{2} - n\right) \Gamma\left(\frac{b}{2} - n\right) \quad [4.71]$$

where $b/2 - n$ lies between 1 and 2. Tables give $\Gamma(b/2 - n)$ for $b/2 - n \in [1, 2]$ [ABR 70].

b	$\Gamma(1+b/2)$	b	$\Gamma(1+b/2)$	b	$\Gamma(1+b/2)$	b	$\Gamma(1+b/2)$
1.25	0.8966	8.50	35.2116	15.75	3.09×10^4	23.00	1.37×10^8
1.50	0.9191	8.75	42.8625	16.00	4.03×10^4	23.25	1.87×10^8
1.75	0.9534	9.00	52.3428	16.25	5.27×10^4	23.50	2.55×10^8
2.00	1.0000	9.25	64.1193	16.50	6.91×10^4	23.75	3.50×10^8
2.25	1.0595	9.50	78.7845	16.75	9.07×10^4	24.00	4.79×10^8
2.50	1.1330	9.75	97.0916	17.00	1.19×10^5	24.25	6.57×10^8
2.75	1.2223	10.00	120.0000	17.25	1.57×10^5	24.50	9.03×10^8
3.00	1.3293	10.25	148.7344	17.50	2.07×10^5	24.75	1.24×10^9
3.25	1.4569	10.50	184.8610	17.75	2.74×10^5	25.00	1.71×10^9
3.50	1.6084	10.75	230.3860	18.00	3.63×10^5	25.25	2.36×10^9
3.75	1.7877	11.00	287.8853	18.25	4.81×10^5	25.50	3.26×10^9
4.00	2.0000	11.25	360.6710	18.50	6.39×10^5	25.75	4.50×10^9
4.25	2.2514	11.50	453.0107	18.75	8.50×10^5	26.00	6.23×10^9
4.50	2.5493	11.75	570.4130	19.00	1.13×10^6	26.25	8.63×10^9
4.75	2.9029	12.00	720.0000	19.25	1.51×10^6	26.50	1.20×10^{10}
5.00	3.3234	12.25	910.9983	19.50	2.02×10^6	26.75	1.66×10^{10}
5.25	3.8245	12.50	1155.3813	19.75	2.71×10^6	27.00	2.31×10^{10}
5.50	4.4230	12.75	1468.7106	20.00	3.63×10^6	27.25	3.21×10^{10}
5.75	5.1397	13.00	1871.2545	20.25	4.87×10^6	27.50	4.48×10^{10}
6.00	6.0000	13.25	2389.4457	20.50	6.55×10^6	27.75	6.24×10^{10}
6.25	7.0355	13.50	3057.8220	20.75	8.82×10^6	28.00	8.72×10^{10}
6.50	8.2851	13.75	3921.5895	21.00	1.19×10^7	28.25	1.22×10^{11}
6.75	9.7971	14.00	5040.0000	21.25	1.61×10^7	28.50	1.70×10^{11}
7.00	11.6317	14.25	64.9010^3	21.50	2.17×10^7	28.75	2.39×10^{11}
7.25	13.8636	14.50	8.38×10^3	21.75	2.94×10^7	29.00	3.35×10^{11}
7.50	16.5862	14.75	1.08×10^4	22.00	3.99×10^7	29.25	4.70×10^{11}
7.75	19.9162	15.00	1.40×10^4	22.25	5.42×10^7	29.50	6.60×10^{11}
8.00	24.0000	15.25	1.82×10^4	22.50	7.37×10^7	29.75	9.29×10^{11}
8.25	29.0214	15.50	2.37×10^4	22.75	1.00×10^8	30.00	1.31×10^{12}

Table 4.1. Values of the function $\Gamma(1+b/2)$ **Example 4.1.**

$$\Gamma(6.44) = 5.44 \Gamma(5.44)$$

$$\Gamma(6.44) = 5.44 \cdot 4.44 \cdot 3.44 \cdot 2.44 \cdot 1.44 \Gamma(1.44)$$

with $\Gamma(1.44) = 0.8858$, yielding $\Gamma(6.44) \approx 258.6$.

The gamma function can also be approximated from a series development (see Appendix A1). In Table 4.1, values of $\Gamma(1+b/2)$ as a function of b varying between 1.25 and 30 are listed.

4.3.5. Rms response to narrow band noise G_0 of width Δf when $G_0 \Delta f = \text{constant}$

Let us consider a noise of constant power spectral density G_0 and of width Δf centered around a frequency f_m limited by the frequencies f_1 and f_2 such that $f_1 = f_m - \frac{\Delta f}{2}$ and $f_2 = f_m + \frac{\Delta f}{2}$, i.e. with the reduced co-ordinates $h = \frac{f}{f_0}$, $h_1 = h_m - \frac{\Delta h}{2}$ and $h_2 = h_m + \frac{\Delta h}{2}$. Relationships [8.61] and [A6.20] of Volume 3 allow the rms response z_{rms} to be calculated. If Δh is small, we obtain

$$z_{\text{rms}}^2 \approx \frac{G_0 \Delta f}{(2\pi)^4 f_0^3 [h_m^4 + (2 - \alpha^2) h_m^2 + 1]} \quad [4.72]$$

where $\alpha = 2\sqrt{1 - \xi^2}$, or

$$\omega_0^4 z_{\text{rms}}^2 \approx \frac{G_0 \Delta f}{h_m^4 + (2 - \alpha^2) h_m^2 + 1},$$

It is noted that z_{rms}^2 varies with the product $G_0 \Delta h$. When f_m is small with respect to f_0 and, for the usual values of damping, it is seen that the quantity $\omega_0^2 z_{\text{rms}}$ is close to the rms value \ddot{x}_{rms} of the excitation. We saw that for a narrow band noise,

$$D = \frac{K^b}{C} n_0^+ T \left(\sqrt{2} z_{\text{rms}} \right)^b \Gamma \left(1 + \frac{b}{2} \right).$$

In addition, all things being equal, the damage D is a function of the product $(G_0 \Delta h)^{b/2}$. If this product is constant, z_{rms}^2 is constant like D . If $h_m = 1$,

$$\omega_0^4 z_{\text{rms}}^2 \approx \frac{G_0 \Delta f}{4 - \alpha^2}.$$

If $Q = 1$, $\alpha^2 = 3$ and

$$\omega_0^4 z_{\text{rms}}^2 \approx \frac{G_0 \Delta f}{h_m^4 - h_m^2 + 1}.$$

Finally, if $h_m = 1$ and $Q = 1$,

$$\omega_0^4 z_{rms}^2 \approx G_0 \Delta f .$$

4.4. Equivalent narrow band noise

The estimate of the fatigue damage requires the calculation of a histogram of the peaks of the response. In the previous sections, the probability density of the peaks of the response was estimated from the statistical properties of the signal. We can also use one of the many direct peak counting methods, the most current being the *rainflow* method.

Another approach is that of the *equivalent narrow band noise*. It is based on the simplified relation established on the assumption of a Rayleigh peak distribution ($r \approx 1$) with several alternatives:

- use of relation [4.41] obtained for a Rayleigh peak distribution (r being supposed equal to 1), whatever the real distribution;
- the same assumption and replacing the expected frequency n_0^+ by the mean number of peaks per unit time n_p^+ ; or
- transformation of the real law of peak probability density into a Rayleigh distribution.

4.4.1. Use of relation established for narrow band response

Even when the distribution of the peaks does not exactly follow a Rayleigh distribution, current practice to simplify the calculation is to assume that r is equal to 1. The response $z(t)$ is therefore assumed to be a narrow band noise [CHA 85], which allows relation [4.41] to be applied:

$$D = \frac{K^b}{C} n_0^+ T \left(\sqrt{2} z_{rms} \right)^b \Gamma \left(1 + \frac{b}{2} \right)$$

by considering that it is still correct whatever the true value of r .

It is therefore supposed that a narrow band stress which has at the same time the same rms value and the same number of zero crossings (n_0^+) as the real broad band stress provides an acceptable estimate of the damage. The interest of this assumption, if it is verified, lies in the facility of using analytical relation [4.41],

which makes it possible to avoid rainflow type counting and heavier numerical calculations of integration.

Error due to the Rayleigh distribution approximation

Relation [4.41] is a good approximation of the damage for $0.567 \leq r \leq 1$ (section 4.3.4.1). We propose considering, depending on the parameter r , up to what point and with which error we can use for all the cases (r arbitrary) of the Rayleigh law to calculate the fatigue damage. Let us calculate the ratio p of the damage $E(D)$ obtained with a Rayleigh peak probability density $q(u)$ and the damage D deduced from the most general law $q(u)$:

$$p = \frac{\frac{K^b}{C} n_0^+ T (\sqrt{2})^b z_{\text{rms}}^b \Gamma\left(1 + \frac{b}{2}\right)}{\frac{K^b}{C} n_p^+ T z_{\text{rms}}^b \int_0^{+\infty} u^b q(u) du} \quad [4.73]$$

$$p = \frac{r (\sqrt{2})^b \Gamma\left(1 + \frac{b}{2}\right)}{\int_0^{+\infty} u^b q(u) du} \quad [4.74]$$

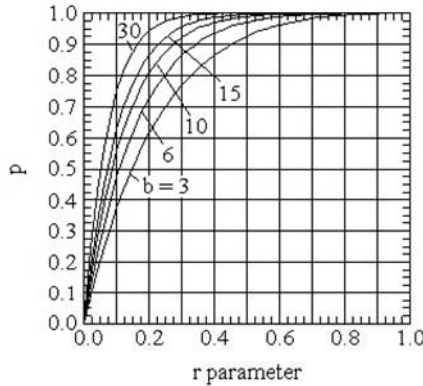


Figure 4.7. Ratio of the damage calculated using Rayleigh's law and the complete formulation

Figure 4.7 shows that p tends towards 1 when r tends towards 1, more quickly for large values of b . The error arising, assuming the Rayleigh law, remains lower

than 4% for $b \in [3, 30]$ and $r \geq 0.6$ (Figure 4.8), thus confirming Bernstein's calculation [BER 77].

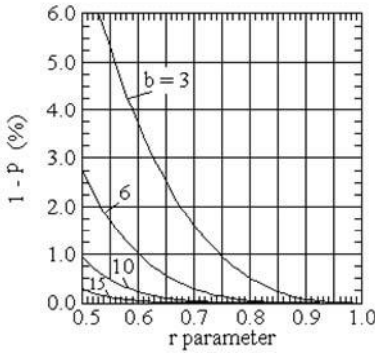


Figure 4.8. Error due to use of the Rayleigh law

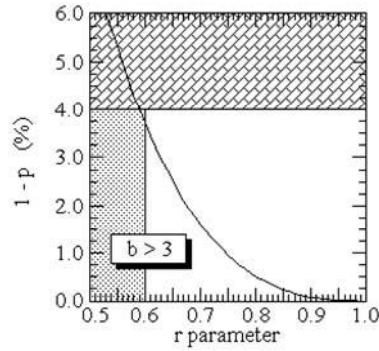


Figure 4.9. Range in which the approximation using the Rayleigh law is acceptable

The damage D calculated using the Rayleigh law is always lower than the damage obtained with the more general formulation (whatever the value of b and r).

NOTE: *L.P. Pook [POO 78] states that for problems of fatigue, a process can be considered as a narrow band process if $q \leq 0.14$ where $q = \sqrt{1 - r^2}$, i.e. for $r \geq 0.99$, a condition which seems very severe from the above curves.*

4.4.2. Alternative: use of mean number of maxima per second

The comparison between the complete formulation and Rayleigh formulation was made above beginning with expression of the damage [4.41]:

$$D = \frac{K^b}{C} n_0^+ T (\sqrt{2})^b z_{\text{rms}}^b \Gamma\left(1 + \frac{b}{2}\right)$$

in which the expected frequency n_0^+ equals, for $r = 1$, the mean number of maxima n_p^+ per unit times. J.T. Broch [BRO 68b] [SCH 61b] showed by experiment that, although n_0^+ and σ_{rms} (or z_{rms}) are the same, two tests carried out with different values of r lead to different fatigue lives. This tendency is confirmed by other

authors [BER 77] [FUL 62]. If r is different from 1, replacing n_0^+ by n_p^+ in the relation [4.41] is justified since the damage is related to the number of peaks. The comparison of the expression obtained:

$$D = \frac{K^b}{C} n_p^+ T (\sqrt{2})^b z_{\text{rms}}^b \Gamma\left(1 + \frac{b}{2}\right) \quad [4.75]$$

with that resulting from a complete formulation, carried out under the same conditions as previously, leads to the curves of Figure 4.10.

The damage calculated in a simplified way is therefore larger than that obtained with the complete formulation. This result is logical since the selected assumption results in regarding each peak as a well-formed half-cycle, which is obviously not the case for $r < 1$.

Approximation of the narrow band type has the principal disadvantage of overestimating the probability of occurrence of the largest peaks and therefore leads to a conservative evaluation of the damage [BER 77] [CHA 85] [EST 62]; when the distribution of the peaks is close to a Gaussian law (r small), its use is debatable.

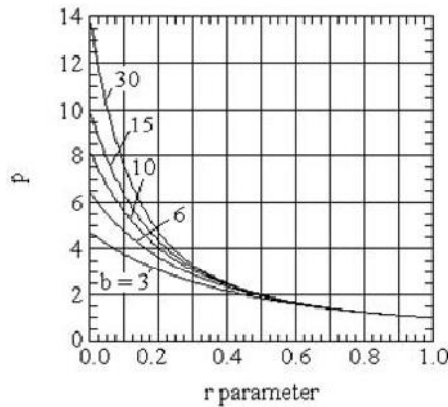


Figure 4.10. Ratio of damage calculated with a mean number of peaks and the Rayleigh law hypothesis with the complete formulation

In many practical cases, however, the results obtained are sufficiently accurate [PHI 65] [RUD 75] [SCH 61a].

4.4.3. Approximation to real maxima distribution using a modified Rayleigh distribution

The response of a linear one-degree-of-freedom system to a Gaussian random vibration is itself Gaussian, with a probability density of maxima [4.23]:

$$q(u) = \frac{\sqrt{1-r^2}}{\sqrt{2\pi}} e^{-\frac{u^2}{2(1-r^2)}} + \frac{ur}{2} e^{-\frac{u^2}{2}} \left[1 + \operatorname{erf}\left(\frac{ur}{\sqrt{2(1-r^2)}}\right) \right].$$

The parameter r of a narrow band response (or of a stress directly in a structure) is close to 1 and $q(u)$ tends towards a Rayleigh distribution which, we saw, led to much simpler calculations.

In the general case, $q(u)$ versus u is represented by a curve which has an arc for $u < 0$ and, depending on r , an arc relatively close to a Rayleigh curve for $u \geq 0$. To approach Rayleigh's law, it would first be necessary to remove the negative part and to multiply $q(u)$ by a standardization factor so that the new probability density $q^*(u)$ has an area under the curve equal to unity. We established that, if $Q(u_0)$ is the probability such that $u > u_0$,

$$Q(u_0) = \int_{u_0}^{\infty} q(u) du$$

i.e.

$$Q(u_0) = \frac{1}{2} \left\{ \left[1 - \operatorname{erf}\left(\frac{u_0}{\sqrt{2(1-r^2)}}\right) \right] + r e^{-\frac{u_0^2}{2}} \left[1 + \operatorname{erf}\left(\frac{ur}{\sqrt{2(1-r^2)}}\right) \right] \right\} \quad [4.76]$$

For $u_0 = 0$, $Q(u_0)$, equal to

$$Q(0) = \frac{1+r}{2} \quad [4.77]$$

corresponds to an area under the curve $q(u)$ for $u > 0$, yielding

$$P(0) = 1 - Q(0) = \frac{1-r}{2} \quad [4.78]$$

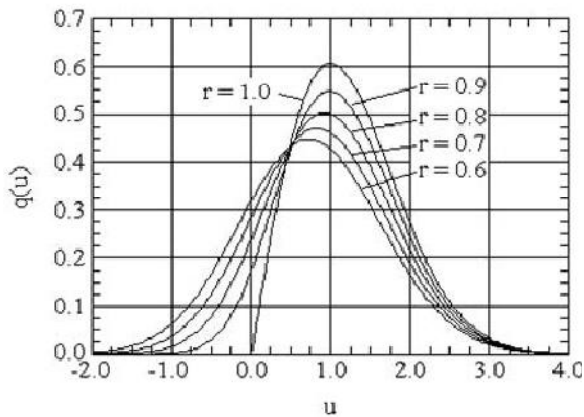


Figure 4.11. *Probability density of the maxima*

which is represented by the area on the left of the vertical axis (Figure 4.12).

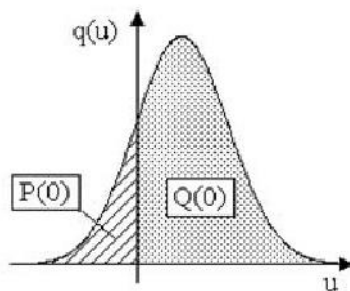


Figure 4.12. *Suppression of negative part of probability density of maxima*

Since $r = \frac{n_0^+}{n_p^+}$,

$$Q(0) = \frac{n_p^+ + n_0^+}{2 n_p^+} \tag{4.79}$$

and

$$P(0) = \frac{n_p^+ - n_0^+}{2 n_p^+} \quad [4.80]$$

In order that the new density $q^*(u)$ is standardized, it is necessary [HIL 70] [KAC 76] that:

$$q^*(u) = \frac{2}{r+1} q(u) \quad [4.81]$$

Figure 4.13 depicts $q^*(u)$ for $r = 0.6, 0.75, 0.8, 0.9$ and 1 , plotted in its definition interval $(0, \infty)$. Calculation of the fatigue damage requires that the number of maxima dn lying between the stress levels σ and $\sigma + d\sigma$ is:

$$dn = n_p^+ T q(\sigma) d\sigma = n_p^+ T q(u) du \quad [4.82]$$

where n_p^+ is the mean number of positive maxima per second. When the response is of narrow band, $r = 1$ and $n_p^+ = n_0^+$. We prefer in this case to use n_0^+ whose calculation assumes knowledge of only of z_{rms} and \dot{z}_{rms} (that of n_p^+ requires evaluation of the parameters \dot{z}_{rms} and \ddot{z}_{rms}). To preserve this facility, we can write

$$dn = n_p^+ T \left[\frac{1+r}{2} q^*(u) \right] du = n_0^+ T \left[\frac{1+r}{2r} q^*(u) \right] du = n_0^+ T q^{**}(u) du \quad [4.83]$$

Figure 4.14 shows, for the same values of r as above, the variations of $q^{**}(u) = \frac{q(u)}{r}$. After these two corrections, we see that the maxima lower than z_{rms} are more numerous than those expected from Rayleigh's law. Taking into account a Rayleigh distribution could therefore seem slightly conservative, if it were not known that the low level maxima have a quasi-negligible contribution to the total damage.

When $z > 2 z_{rms}$, all the distribution laws are almost confused with Rayleigh's law for $0.6 \leq r \leq 1$, an interval which includes almost all the values found in practice in structures with one or several degrees of freedom [KAC 76].

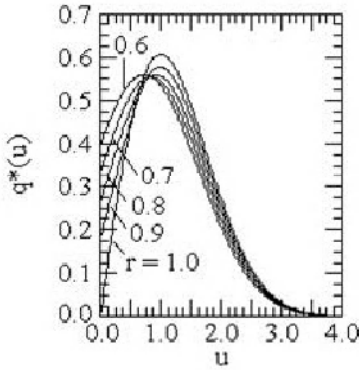


Figure 4.13. Truncated and standardized probability density of maxima

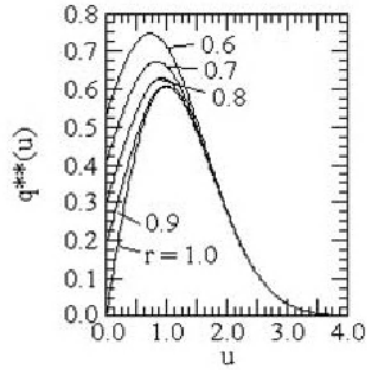


Figure 4.14. Truncated, standardized and modified probability density of maxima for using expected frequency

NOTE: B.M. Hillberry [HIL 70] proposes another approach based on relation [4.21]:

$$D = \frac{n_p^+ T}{C} \sigma_{rms}^b \int_0^{+\infty} u^b q(u) du$$

where $u = \frac{\sigma}{\sigma_{rms}}$. When r is arbitrary between 0 and 1, the curve $q(u)$ presents values for $u < 0$ (Figure 4.15).

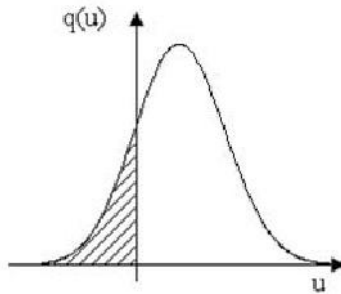


Figure 4.15. Suppression of negative maxima

To standardize the new peak probability density obtained after suppression of negative maxima, B.M. Hillberry writes the damage D in the form:

$$D = \frac{n_{p>0}^+ T \sigma_{rms}^b \int_0^\infty u^b q(u) du}{C \int_0^\infty q(u) du} \quad [4.84]$$

4.5. Calculation of fatigue damage from the probability density of domains

4.5.1. Differences between the probability of peaks and of ranges

When the fatigue damage is calculated from a signal according to time, we saw in the previous chapter that the most advanced methods of counting are those in which a histogram of the peak-valley and valley-peak ranges (ordinary ranges) is established. The method considered as most satisfactory is that of rainflow, which allows the definition of closed stress-strain cycles. The result of counting is a histogram of the ranges (rainflow ranges) from which the average of ranges and the amplitude of peaks (half-ranges) are determined.

For a Gaussian signal, the damage can be calculated starting from the PSD of the signal. In this case, analytical relations make it possible to obtain an expression of the peaks probability density of the response of a one-dof system [4.23].

To bring the two methods of calculation closer, it would be necessary to have an analytical expression of the probability density of ranges, an expression which was not established theoretically.

T. Dirlik [DIR 85] showed that the probability density of ordinary half-ranges differs from that of maxima [4.23]. When the factor of irregularity r is close to unity, this histogram is very close to a Rayleigh law. When r decreases, it remains close to the Rayleigh probability density except for the larger values.

The rainflow probability density of half-ranges has the same shape as that of the ordinary half-ranges, with the following differences:

- close to the origin, the rainflow density of half-ranges is larger than that of the ordinary half-ranges;
- for the values close to its peak, the rainflow density of half-ranges is smaller than that of the ordinary half-ranges; and
- for the large values, the rainflow density of half-ranges can become larger and tend less quickly towards zero, even for the small values of r .

Example 4.2.

Let us consider a Gaussian acceleration signal generated from the power spectral density of Figure 4.16. The Gaussian nature of this signal can be checked by comparing the histogram of its instantaneous values with a Gaussian probability density (Figure 4.17).

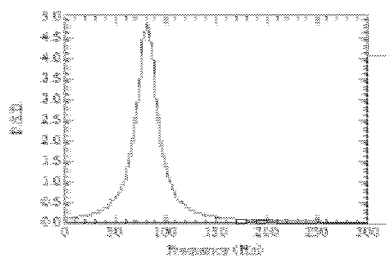


Figure 4.16. PSD of the analyzed signal

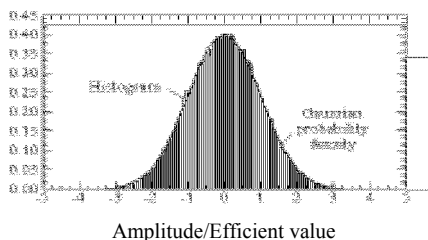


Figure 4.17. Reduced histogram of the instantaneous values of the signal

Figure 4.18 makes it possible to compare:

- the histogram of ordinary half-ranges calculated starting from the signal;
- the theoretical Rayleigh probability density [4.57] defined for the rms value of the studied signal; and
- the complete probability density of peaks [4.23].

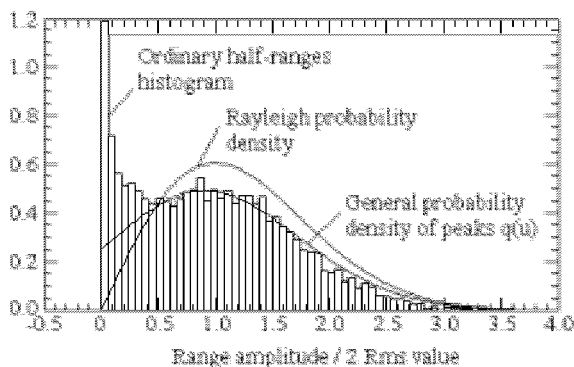


Figure 4.18. Reduced histogram of the ordinary half-ranges, complete probability of peaks and Rayleigh probability density

The difference between the histogram and the two densities for the small amplitudes can be observed.

The complete probability density of peaks is however closer to the histogram, except for low levels which have little influence on the fatigue damage (in this example, where the r parameter is equal to 0.775).

The histogram of ranges defined from a rainflow counting also has significant differences from the Rayleigh density (Figure 4.19) and is closer to the complete probability density.

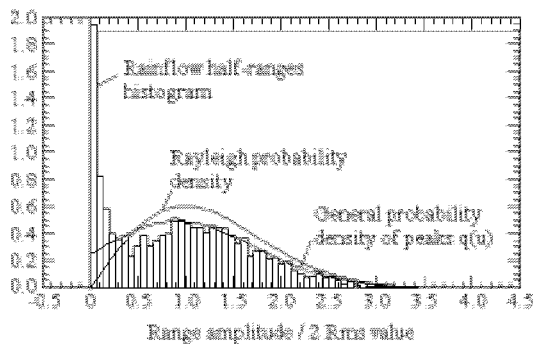


Figure 4.19. *Reduced histogram of the rainflow half-ranges, complete probability of peaks and Rayleigh probability density*

Example 4.3.

This example considers a signal which is characterized by a small r parameter, equal to 0.328.

For this value of r , the histogram of ordinary half-ranges (Figure 4.21) and the histogram of the rainflow half-ranges (Figure 4.22) are very different from the probability density of peaks (complete formulation) and from the Rayleigh density.

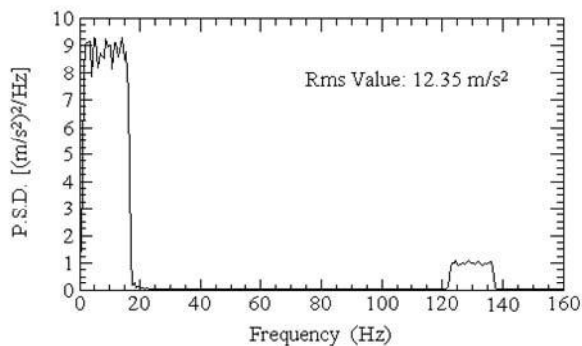


Figure 4.20. Power spectral density of the signal analyzed in example no. 2

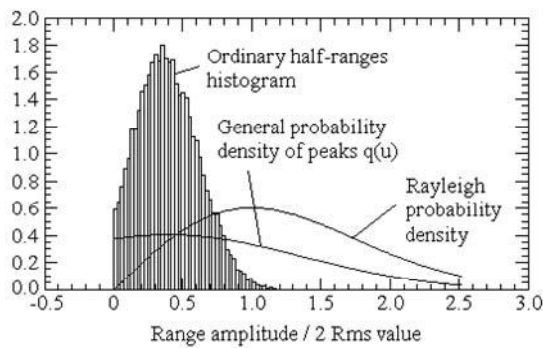


Figure 4.21. Reduced histogram of ordinary half-ranges, complete probability density of peaks $q(u)$ and Rayleigh probability density

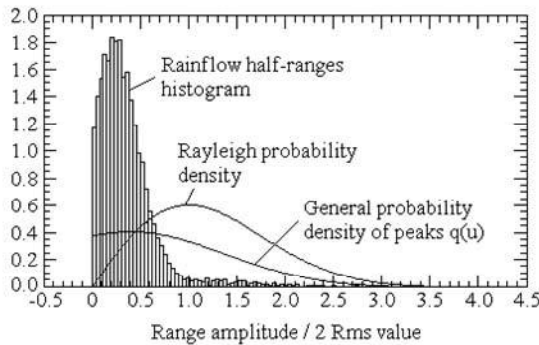


Figure 4.22. *Reduced histogram of rainflow half-ranges, complete probability density of peaks $q(u)$ and Rayleigh probability density*

Several approximations of the density of half-ranges were proposed to better represent the rainflow half-ranges histogram, and therefore correct the conservatism of the Rayleigh peaks probability density, which leads to values of fatigue damage larger than the rainflow counting. Certain values are adapted for the wideband processes; others for the narrow band processes. The signals are assumed Gaussian. The Rayleigh density is generally used as a base because of its simplicity.

Among these formulations, we find:

- that of P.H. Wirsching, which is relation [4.41] modified by a factor λ ;
- that of G.K. Chaudhury and W.D. Dover, which is also based on the relation [4.41] with a correction by a term function of b and r ; and
- an empirical expression suggested by Dirlik using the first moments of the power spectral density of stress.

Some empirical expressions of the probability density of rainflow half-ranges were published, such as those of T. Dirlik [DIR 85], W.W. Zhao and M.J. Baker [ZHA 92], G. Petrucci [PET 99] [PET 00] [PET 04] and D. Benasciutti and R. Tovo [BEN 05]. These methods are based on statistical models utilizing combinations of distributions such as Rayleigh, Weibull, exponential and with coefficient functions of the first moments of the power spectral density of the stress. Comparisons carried out by Bouyssy *et al.* [BOU 93] and D. Benasciutti [BEN 04] showed that the expression of T. Dirlik leads to the best results for the estimate of lifetimes.

4.5.2. Wirsching's approach

After a study intended to compare several counting methods, P.H. Wirsching [WIR 80a] [WIR 80b] [WIR 80c] [WIR 83b] defined the parameter

$$\lambda_X = \frac{\text{fatigue damage calculated from the "x" method}}{\text{fatigue damage calculated from the "equivalent narrow band" method}}$$

and plotted curves of λ_X against r (or $q = \sqrt{1 - r^2}$) for various values of b , using several methods:

λ_R : rainflow type counting;

λ_P : counting of the peaks of the response;

λ_Z : counting of zero crossings; and

λ_N : simplified relation ($r = 1$).

The curves obtained are depicted in Figure 4.23. They are plotted for $b = 3$, but their shape aspect is the same whatever the value of b (the variation between the curves increases, but their relative position remains the same).

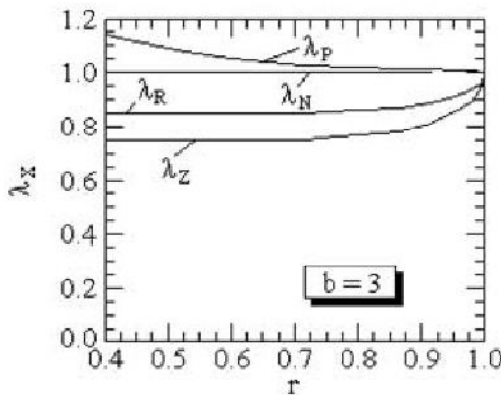


Figure 4.23. Ratios of damage obtained with various peak counting methods

Whatever the value of b and whatever the method, $\lambda_X \rightarrow 1$ when $r \rightarrow 1$.

By comparison with the rainflow method, considered in general to be the most precise, P.H. Wirsching shows that the method of peak counting and the equivalent narrow band method are conservative. The zero-crossing counting method gives non-conservative results.

From four particular forms of power spectral densities, an empirical relation from this study is deduced. By starting from the simplified *narrow band* relation, calculation of the damage which would be obtained with rainflow counting can be made. If D_{NB} is the *narrow band* damage and D is that given by rainflow counting,

$$D = \lambda_R D_{NB} \quad [4.85]$$

The empirical relation between λ_R , b and r is

$$\lambda_R(b, r) = A(b) + [1 - A(b)] [1 - \varepsilon]^{B(b)} \quad [4.86]$$

where

$$\left. \begin{aligned} A(b) &= 0.926 - 0.033 b \\ B(b) &= 1.587 b - 2.323 \end{aligned} \right\} \quad [4.87]$$

If $r = 1$, $\lambda_R = 1$ and if $r = 0$, $\lambda_R = A(b)$. Figures 4.24 and 4.25 show the variations of λ_R with r and b . It is noted that for a given b , λ_R varies little with r if $r < 0.9$.

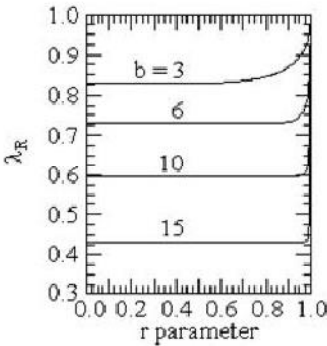


Figure 4.24. Factor of correction of damage calculated on a narrow band assumption (versus r)

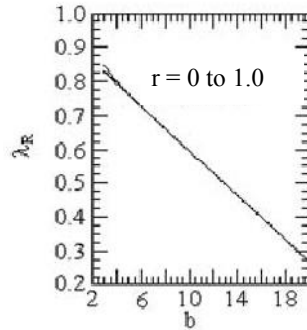


Figure 4.25. Factor of correction of damage calculated on a narrow band assumption (versus b)

The study was carried out for loads resulting from the action of waves on offshore structures, for which $q > 0.50$ ($r < 0.866$) and $b \approx 3$ (welded joints). In this range, λ_R varies little and only b is influential. For small b , the narrow band model provides a reasonably conservative estimate of the lifetime.

The accuracy of this approximation can also be evaluated by considering the ratio

$$p = \frac{\text{damage according to Wirsching}}{\text{damage from the general relation } q(u)}$$

i.e.

$$p = \frac{\lambda_R \frac{K^b}{C} \left(\sqrt{2} z_{rms} \right)^b n_0^+ T \Gamma\left(1 + \frac{b}{2}\right)}{\frac{K^b}{C} n_p^+ T z_{rms}^b \int_0^{+\infty} u^b q(u) du}$$

$$p = \frac{\lambda_R \left(\sqrt{2} \right)^b r \Gamma\left(1 + \frac{b}{2}\right)}{\int_0^{+\infty} u^b q(u) du} \quad [4.88]$$

If $r \rightarrow 0$, the damage calculated from the most general expression of $q(u)$ is equal to

$$D = \frac{K^b n_p^+ T}{2 C \sqrt{\pi}} \left(\sqrt{2} z_{rms} \right)^b \Gamma\left(\frac{b+1}{2}\right)$$

and

$$p \approx \frac{A(b) r \Gamma\left(1 + \frac{b}{2}\right)}{\Gamma\left(\frac{b+1}{2}\right)} 2 \sqrt{\pi} \rightarrow 0.$$

Figure 4.26 shows the variations of $1 - p$ with r , for $b = 3, 6, 10$ and 15 .

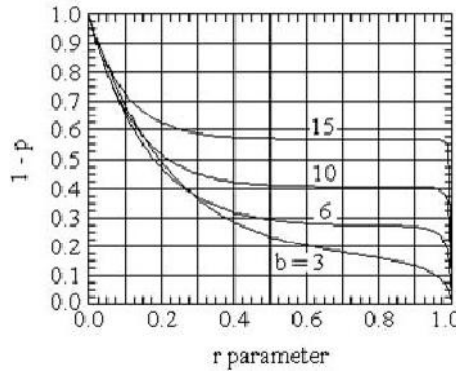


Figure 4.26. Error related to the use of the Wirsching relation

4.5.3. Chaudhury and Dover's approach

This approach [CHA 85] proposes a method derived from the general expression of the peak probability [4.24]:

$$q(\sigma) = \frac{q}{\sigma_{\text{rms}} \sqrt{2\pi}} e^{-\frac{\sigma^2}{2\sigma_{\text{rms}}^2 q^2}} + \frac{r \sigma}{2\sigma_{\text{rms}}^2} \left[1 + \text{erf} \left(\frac{\sigma}{\sigma_{\text{rms}}} \frac{r}{q\sqrt{2}} \right) \right] e^{-\frac{\sigma^2}{2\sigma_{\text{rms}}^2}}$$

where $q = \sqrt{1 - r^2}$.

By replacing σ with $x \sigma_{\text{rms}} \sqrt{2} \frac{q}{r}$, we obtain

$$q(x) = \frac{q}{\sigma_{\text{rms}} \sqrt{2\pi}} e^{-\left(\frac{x}{r}\right)^2} + \frac{x q}{\sigma_{\text{rms}} \sqrt{2}} \left[1 + \text{erf}(x) \right] e^{-\left(\frac{q x}{r}\right)^2} \quad [4.89]$$

The error function $\text{erf}(x)$ (which varies between 0 and 1 according to x) can be approximated to 1/2:

$$q(x) = \frac{q}{\sigma_{\text{rms}} \sqrt{2\pi}} e^{-\left(\frac{x}{r}\right)^2} + \frac{x q}{\sigma_{\text{rms}} \sqrt{2}} \frac{3}{2} e^{-\left(\frac{q x}{r}\right)^2} \quad [4.90]$$

yielding mean damage:

$$D = \frac{n_p^+ T}{C} \int_0^{+\infty} \sigma^b q(\sigma) d\sigma \quad [4.91]$$

and

$$D = \frac{n_p^+ T}{C} \left(\sqrt{2} \sigma_{\text{rms}} \right)^b \left\{ \frac{q^{b+2}}{2 \sqrt{\pi}} \Gamma\left(\frac{b+1}{2}\right) + 0.75 r \Gamma\left(\frac{b}{2} + 1\right) \right\} \quad [4.92]$$

If $r \rightarrow 0$ ($q \rightarrow 1$), D tends towards

$$D = \frac{n_p^+ T}{C} \left(\sqrt{2} \sigma_{\text{rms}} \right)^b \frac{1}{2 \sqrt{\pi}} \Gamma\left(\frac{b+1}{2}\right)$$

(relation already obtained in [4.35]) and if $r \rightarrow 1$ ($q \rightarrow 0$), D tends towards

$$D = \frac{n_0^+ T}{C} \left(\sqrt{2} \sigma_{\text{rms}} \right)^b 0.75 \Gamma\left(1 + \frac{b}{2}\right) \quad [4.93]$$

($n_p^+ = n_0^+$). This relation gives a value lower by 25% than that of a theoretical narrow band process. The difference comes from the choice of the value of the error function. Calculations seem to follow the experimental results in the case treated by the authors (stresses in tubular offshore structures) with peak counting using the rainflow method. To take account of the results of these countings, they correct and readjust relation [4.40] established using Rayleigh's hypothesis, i.e.

$$D = \frac{n_0^+ T}{C} \left(\sqrt{2} \sigma_{\text{rms}} \right)^b \Gamma\left(1 + \frac{b}{2}\right)$$

or

$$D = \frac{n_p^+ T}{C} S^b \quad [4.94]$$

where

$$\frac{S}{\sigma_{\text{rms}}} = \sqrt{2} \left[\Gamma \left(1 + \frac{b}{2} \right) \right]^{\frac{1}{b}} \text{ and } n_p^+ = n_0^+ \quad [4.95]$$

If the peak distribution is Rayleigh in the form

$$\frac{S}{\sigma_{\text{rms}}} = \sqrt{2} \left[\frac{1}{2\sqrt{\pi}} \Gamma \left(\frac{b+1}{2} \right) \right]^{\frac{1}{b}} \quad [4.96]$$

and, if this distribution is Gaussian,

$$\frac{S}{\sigma_{\text{rms}}} = \left\{ \sqrt{2} \left[\frac{1}{2\sqrt{\pi}} \Gamma \left(\frac{b+1}{2} \right) \right]^{\frac{1}{b}} + 0.42 \right\} + 4.2 \frac{r - 0.5}{b + 0.5} \quad [4.97]$$

in the general case, for $0.5 < r < 1$.

The relationship between the damage calculated by G.K. Chaudhury and W.D. Dover and that estimated using Rayleigh's hypothesis makes it possible to compare these two approaches (Figure 4.27).

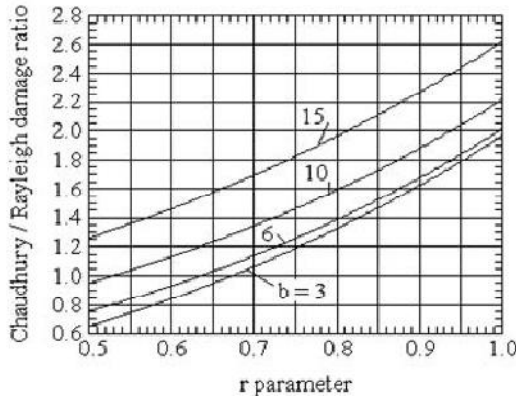


Figure 4.27. Comparison of damage calculated using the Chaudhury and Rayleigh assumptions

$$\frac{D_{CH}}{D_R} = \frac{\left[\left\{ \sqrt{2} \left[\frac{1}{2\sqrt{\pi}} \Gamma\left(\frac{b+1}{2}\right) \right]^{1/b} + 0.42 \right\} + 4.2 \frac{r-0.5}{b+0.5} \right]^b}{(\sqrt{2})^b \Gamma\left(1 + \frac{b}{2}\right)} \quad [4.98]$$

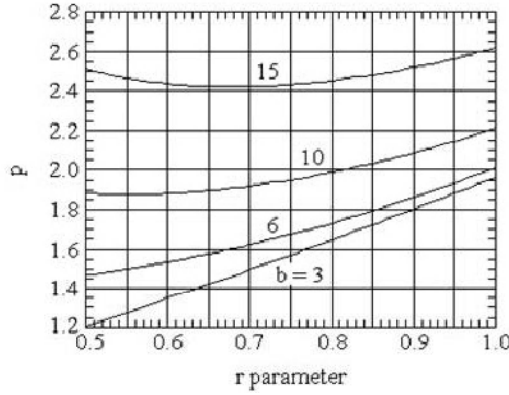


Figure 4.28. Comparison of damage calculated on the Chaudhury assumption and with complete formulation

The value of this method can also be evaluated by taking as a reference the damage calculated using the general formulation of $q(u)$ (Figure 4.28):

$$p = \frac{D_{CH}}{D} = \frac{\left[\left\{ \sqrt{2} \left[\frac{1}{2\sqrt{\pi}} \Gamma\left(\frac{b+1}{2}\right) \right]^{1/b} + 0.42 \right\} + 4.2 \frac{r-0.5}{b+0.5} \right]^b}{\int_0^{+\infty} u^b q(u) du} \quad [4.99]$$

4.5.4. Dirlik's probability density

T. Dirlik [DIR 85] established empirical expressions of the probability density of the ordinary half-ranges and those counted with the rainflow method using a digital simulation. The method involved:

– giving itself *a priori* an expression of the density, utilizing the spectral moments of order 0, 1, 2 and 4 of the power spectral density of the stress; and

– then determining the coefficients by minimization of the differences between this density and the histograms determined by considering signals generated starting from 70 spectral PSD of various shapes.

To facilitate the comparisons, the PSD had the same rms value and led to the same mean number of peaks per second (Volume 3, relation [6.31]).

It should be noted that in this study, the PSD considered are those of (Gaussian) stress signals, and therefore represent directly the mechanical responses of systems and not the PSD applied to a one-dof system. To be consistent with the previous sections, we will assume below that the treated signal is the relative response displacement of a one-dof system (proportional to the stress by hypothesis).

Let $z(t)$ be the response of a one-dof system (f_0, ξ) to a Gaussian signal, z_{rms} the rms value of $z(t)$, δ a range defined starting from a counting and u the reduced variable corresponding to a half-cycle, such as

$$u = \frac{\delta}{2 z_{\text{rms}}} \quad [4.100]$$

4.5.4.1. Probability density of ordinary half-ranges

T. Dirlik proposes the following expression for the probability of ordinary half-ranges:

$$p_R(u) = \frac{C_1}{A} e^{-\frac{u}{A}} + C_2 \frac{u}{B^2} e^{-\frac{u^2}{2B^2}} \quad [4.101]$$

where $C_1 + C_2 = 1$. The coefficients are calculated by minimizing the error between the histograms established for several types of signals and the empirical expression, i.e.

$$\begin{aligned} C_1 = \frac{C - x_{\min}}{r^2} & \quad \left| \quad C_2 = 1 - \frac{C - x_{\min}}{r^2} \right| & \quad x_{\min} = \frac{r(1+r^2)}{2} \\ A = 0.02 + \frac{2(C - x_{\min})}{r} & \quad \left| \quad B = r + \frac{C - x_{\min}}{r} \right. \\ C = \frac{M_1}{M_0} \sqrt{\frac{M_2}{M_4}} & = \frac{M_1}{2\pi n_p^+ z_{\text{rms}}^2} = \frac{r M_1}{\sqrt{M_0 M_2}} \end{aligned}$$

where $r = \frac{M_2}{\sqrt{M_0 M_4}} = \frac{n_0^+}{n_p^+}$, n_0^+ and n_p^+ are the irregularity factor, the mean number of zero-crossings per second with a positive slope and the mean number of maxima per second, respectively (Volume 3, equations [6.6], [5.73] and [6.13]).

M_n is the moment of order n of the PSD of the response $G_z(f)$ (Volume 3, equation [5.74]):

$$M_n = \int_0^\infty \Omega^n G_z(\Omega) d\Omega = (2\pi)^n \int_0^\infty f^n G_z(f) df .$$

Example 4.4.

Figures 4.29 to 4.32 allow the Dirlik density and the histogram of ordinary half-ranges to be compared for each of the two previous examples.

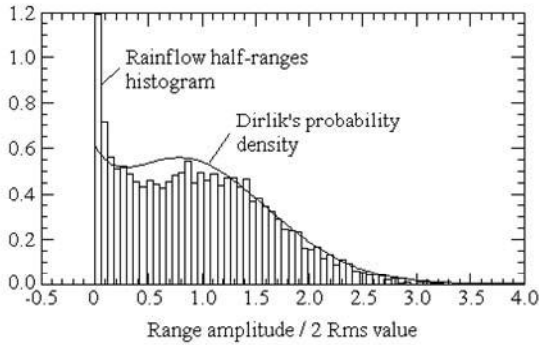


Figure 4.29. *Reduced histogram of ordinary ranges and Dirlik probability density (example 4.2)*

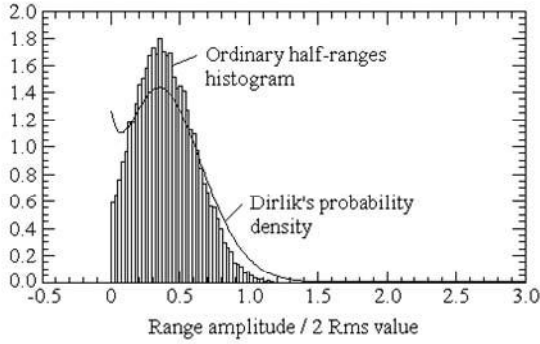


Figure 4.30. *Reduced histogram of ordinary ranges and Dirlik probability density (example 4.3)*

In the case of the response of a one-dof system, the moments M_0 , M_1 , M_2 and M_4 can be calculated using the integrals I_n (Appendix A6, Volume 3).

If f_1 and f_2 are the frequency limits of an interval where the PSD $G_{\ddot{x}}(f)$ of the excitation $\ddot{x}(t)$ is defined by a straight line segment of arbitrary slope (linear axes):

$$M_1 = 2 \pi \int_{f_1}^{f_2} f G_z(f) df = 2 \pi \int_{f_1}^{f_2} f H_{\ddot{x}z}^2(f) G_{\ddot{x}}(f) df \quad [4.102]$$

the transfer function of the linear one-dof system $H_{\ddot{x}z}(f)$ is equal to

$$H_{\ddot{x}z}(f) = \frac{1}{\omega_0^2 \sqrt{(1-h^2)^2 + (2\xi h)^2}}$$

where $h = \frac{f}{f_0}$.

Since, by assumption, the PSD is represented by straight line segments in linear axes, it can be written $G_{\ddot{x}} = a f + b$, yielding

$$M_1 = \frac{2 \pi}{\omega_0^4} \int_{f_1}^{f_2} \frac{a f^2}{(1-h^2)^2 + (2\xi h)^2} df + \frac{2 \pi}{\omega_0^4} \int_{f_1}^{f_2} \frac{b f}{(1-h^2)^2 + (2\xi h)^2} df \quad [4.103]$$

$$M_1 = \frac{2\pi}{\omega_0^4} a f_0^3 \int_{f_1}^{f_2} \frac{h^2}{(1-h^2)^2 + (2\xi h)^2} dh + \frac{2\pi}{\omega_0^4} b f_0^2 \int_{f_1}^{f_2} \frac{h}{(1-h^2)^2 + (2\xi h)^2} dh \quad [4.104]$$

Knowing that $I_1 = \frac{4\xi}{\pi} \int_{f_1}^{f_2} \frac{h}{(1-h^2)^2 + (2\xi h)^2} dh$ (Volume 3, Appendix A6)

and that $I_2 = \frac{4\xi}{\pi} \int_{f_1}^{f_2} \frac{h^2}{(1-h^2)^2 + (2\xi h)^2} dh$, we obtain

$$M_1 = \frac{\pi}{4\xi(2\pi)^3 f_0} \left(a I_2 + \frac{b I_1}{f_0} \right) \quad [4.105]$$

4.5.4.2. Probability density of rainflow half-ranges

The probability density of Dirlik is expressed

$$p_R(u) = \frac{D_1}{A} e^{-\frac{u}{A}} + D_2 \frac{u}{B^2} e^{-\frac{u^2}{2B^2}} + D_3 u e^{-\frac{u^2}{2}} \quad [4.106]$$

where $D_1 + D_2 + D_3 = 1$; the other coefficients are calculated as above.

The coefficients thus obtained are the following:

$$\begin{aligned} D_1 &= \frac{2(C-r^2)}{1+r^2} & B &= \frac{r-C-D_1^2}{1-r-D_1+D_1^2} & D_2 &= \frac{1-r-D_1+D_1^2}{1-B} \\ A &= 1.25 \frac{r-D_3-D_2 B}{D_1} & C &= \frac{M_1}{M_0} \sqrt{\frac{M_2}{M_4}} \end{aligned}$$

Example 4.5.

Figures 4.31 and 4.32 demonstrate the good fit between the rainflow half-ranges histogram and the Dirlik expression for the two examples of section 4.5.1

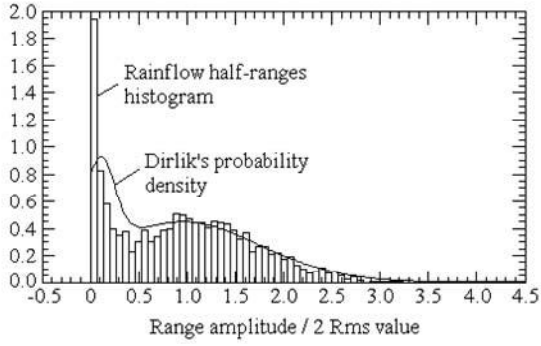


Figure 4.31. Reduced histogram of rainflow half-ranges and Dirlik probability density (example 4.2)

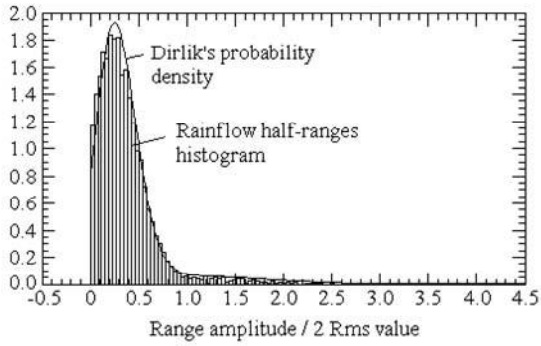


Figure 4.32. Reduced histogram of rainflow half-ranges and Dirlik probability density (example 4.3)

4.5.4.3. Distribution function of rainflow half-ranges

The distribution function is obtained by integrating equation [4.106], since

$$P_R(u) = \int_0^u p_R(u) du$$

$$P_R(u) = D_1 \left(1 - e^{-\frac{u}{A}} \right) + D_2 \left(1 - e^{-\frac{u^2}{2B^2}} \right) + D_3 \left(1 - e^{-\frac{u^2}{2}} \right) \quad [4.107]$$

This expression can be used to calculate the extreme response spectrum (ERS) (Volume 5).

The function $P_R(u)$ is normalized since it tends towards 1 when u tends towards infinity. It is equal to zero when $u = 0$.

NOTE: *Spectra centered around one or two frequencies (observed for example on windmills) lead, with the Dirlik density, to lifetimes larger than those calculated starting from wideband spectra (having the same spectral moments) [HEN 03]. After a study based on a great number of spectra, a correction function was proposed to reduce the error. This correction does not hold, however, due to the harmonics of the discrete components which can have an influence on the damage according to the relations of phase [BIS 95] [BUR 01] [MOR 90].*

4.5.5. Expression of the fatigue damage from the Dirlik probability density

It was shown that the damage can be written in the form [4.20], i.e.

$$D = \frac{K^b}{C} n_p^+ T z_{rms}^b \int_0^{+\infty} u^b q(u) du$$

With the peak probability density [4.23], we have for $r = 1$:

$$\int_0^{+\infty} u^b q(u) du = 2^{b/2} \Gamma\left(1 + \frac{b}{2}\right) \quad [4.108]$$

With the Dirlik density, this expression becomes:

$$D = \frac{K^b}{C} n_p^+ T z_{rms}^b \int_0^{+\infty} u^b p_R(u) du \quad [4.109]$$

The integral is equal to

$$\int_0^{+\infty} u^b p_R(u) du = D_1 A^b \Gamma(1+b) + 2^{b/2} (D_2 B^b + D_3) \Gamma\left(1 + \frac{b}{2}\right), \quad [4.110]$$

yielding

$$D = \frac{K^b}{C} n_p^+ T z_{rms}^b \left[D_1 A^b \Gamma(1+b) + 2^{b/2} (D_2 B^b + D_3) \Gamma\left(1 + \frac{b}{2}\right) \right]. \quad [4.111]$$

If the excitation has a PSD composed of straight line segments in linear axes, the damage D can be written (Volume 3, equation [8.79]):

$$D \approx \frac{K^b}{C} \frac{n_p^+ T}{\left[4 \xi (2 \pi f_0)^3 \right]^{b/2}} \left(\sum_{i=1}^n a_i G_i \right)^{b/2} \frac{D_1 A^b \Gamma(1+b) + 2^{b/2} (D_2 B^b + D_3) \Gamma\left(1 + \frac{b}{2}\right)}{2^{b/2}}. \quad [4.112]$$

NOTE: *The use of the Dirlik probability density allows the ranges histogram established by a rainflow counting to be better represented. It makes it possible in certain cases (often when the r parameter is low, but this is not a general rule) to calculate the fatigue damage with a better precision than the traditional density of peaks for certain shapes of the PSD of the signal.*

This result particularly relates to the case of a strain or a stress directly used for the calculation of the fatigue damage. When the treated signal is an acceleration applied to a one-dof system, no significant difference between the damage calculated with the Dirlik expression and the complete probability density of the peaks is generally noted.

4.6. Comparison of S-N curves established under sinusoidal and random loads

The analytical expression selected to describe the S-N curve in its linear part (logarithmic scales) is that of Basquin ($N \sigma^b = C$) which can be written, if the stress is characterized by its rms value instead of its amplitude:

$$N \sigma_{rms}^b = \frac{C}{(\sqrt{2})^b} = C_1 \quad [4.113]$$

The above results make it possible to write, in the case of a test bar excited by a narrow band stress [4.41]:

$$D = \frac{n_0^+ T}{C} (\sqrt{2} \sigma_{rms})^b \Gamma\left(1 + \frac{b}{2}\right).$$

There is failure by fatigue, on average, when $D = 1$. Then [ROO 64]:

$$N \sigma_{rms}^b = \frac{C}{(\sqrt{2})^b \Gamma\left(1 + \frac{b}{2}\right)} = A \quad [4.114]$$

where $N = n_0^+ T$ (mean number of cycles to failure), yielding:

$$A = \frac{C}{(\sqrt{2})^b \Gamma\left(1 + \frac{b}{2}\right)} = \frac{C_1}{\Gamma\left(1 + \frac{b}{2}\right)} \quad [4.115]$$

The S-N curve thus evaluated for a random loading is therefore a line having the same slope as that obtained under sinusoidal stress, with a smaller ordinate at the origin. (The ordinate at the origin is defined here as the ordinate of the point $N = 1$, i.e. the theoretical ultimate stress of the material [ROO 64]. It is known that the approximation of the S-N curve by a line in this zone of low numbers of cycles is not correct.)

All the parameters appearing in the right-hand side of relation [4.114] are known from the results of the fatigue tests in sinusoidal mode: this relation allows the extrapolation of the S-N curves obtained with sine loads to the case of random loads.

NOTE: *If it is assumed that the peak distribution of the response follows a Gaussian distribution (instead of a Rayleigh distribution), i.e. that $r = 0$, we obtain in the same way:*

$$n_p^+ T \sigma_{rms}^b = \frac{2 \sqrt{\pi} C}{(\sqrt{2})^b \Gamma\left(\frac{b+1}{2}\right)} \quad [4.116]$$

We set here $N = n_p^+ T$.

Example 4.6.

7075-T6 aluminum alloy

$$b = 9.65$$

$$C = 5.56 \cdot 10^{87} \text{ (SI unit)}$$

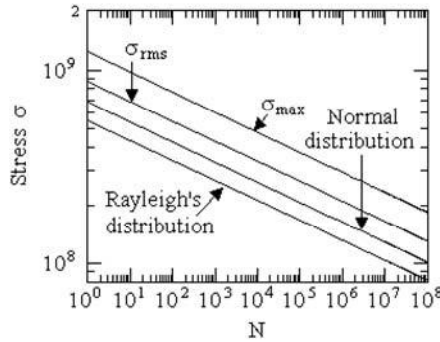
**Figure 4.33.** Comparison of S-N curves

Figure 4.33 depicts the curves $\sigma(N)$ plotted under the following conditions:

$$N \sigma^b = C \quad (\sigma = \text{maximum stress in sinusoidal mode})$$

$$N \sigma_{rms}^b = \frac{C}{(\sqrt{2})^b} \quad [4.117]$$

random, Rayleigh distribution [4.114]

random, Gaussian distribution [4.116]

The variation between the initial S-N curve (in sinusoidal mode) and the curve relating to random (Rayleigh) assumption is a function of the value of the parameter b .

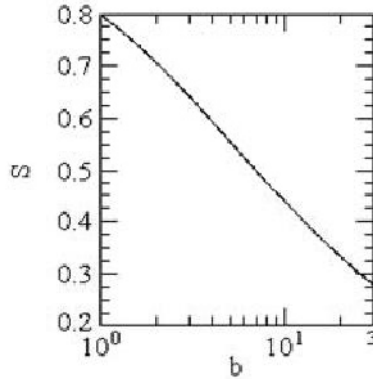


Figure 4.34. Variation between the *S-N* curve in sinusoidal mode and random [ROO 64]

Figure 4.34 shows the variations of the ratio $\frac{\sigma_{\text{rms random}}}{\sigma_{\text{max sine}}} = S$ versus parameter b :

$$S = \frac{1}{\sqrt{2} \left[\Gamma \left(1 + \frac{b}{2} \right) \right]^{\frac{1}{b}}} \quad [4.118]$$

NOTE: The fatigue calculations carried out for a peak distribution close to a Gaussian law are in general non-conservative (r is small, therefore many cycles of low amplitude (under-cycles) are superimposed on the cycles between two zero crossings). R.G. Lambert [LAM 93] proposes modifying relation [4.115] to take account of this phenomenon and to correct it simply, as follows:

$$A = \frac{C}{1.2 \left(\sqrt{2} \right)^b \Gamma \left(1 + \frac{b}{2} \right)} \quad [4.119]$$

More general case

We saw that the expected damage by fatigue is given by equation [4.21]:

$$D = \frac{n_p^+ T}{C} \sigma_{rms}^b \int_0^{+\infty} u^b q(u) du = \frac{n_0^+ T}{r C} \sigma_{rms}^b \int_0^{+\infty} u^b q(u) du$$

where $q(u)$ is the probability density function of maxima, represented by equation [4.22] if the distribution of the instantaneous values of the random excitation is Gaussian. If we set $N = n_0^+ T$, we obtain for $D = 1$ a relation between σ_{rms} and N of the form:

$$N \sigma_{rms}^b = \frac{C r}{\int_0^{+\infty} u^b q(u) du} \quad [4.120]$$

If we preserve $N = n_p^+ T$ [LAM 76], we obtain:

$$N \sigma_{rms}^b = \frac{C}{\int_0^{+\infty} u^b q(u) du} \quad [4.121]$$

Figures 4.35 and 4.36 show the curves $\sigma_{rms}(N)$ plotted for $r = 0.25, 0.50, 0.75$ and 1, with reference to the curve established in sine mode ($b = 10$, $C = 10^{80}$), when $n_0^+ T$ or $n_p^+ T$ is carried on the abscissa axis.

It is noted that these curves are (randomly) very tight and therefore not very sensitive to the variations of r . According to the choice of the definition of N and according to the value of r , a calculation carried out using Rayleigh's assumption can be slightly optimistic ($N = n_0^+ T$) or pessimistic ($N = n_p^+ T$).

4.7. Comparison of theory and experiment

We find in the bibliography test results carried out in various configurations, e.g. under stationary random stresses with or without zero average, used for the layout of S-N curves and for fatigue life calculations [GAS 65] [KIR 65a]. The conclusions are not always homogenous and sometimes vary according to the author. Generally, it seems that the parameter considered as most representative of fatigue under random stress is the rms value of the stress (confirmation of the theory) [CLE 66] [CLE 77] [KIR 65a].

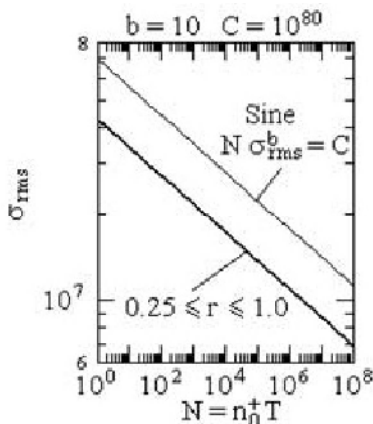


Figure 4.35. *S-N curve into random plotted as a function of the number of zero-crossings with positive slope, for various values of the irregularity factor*

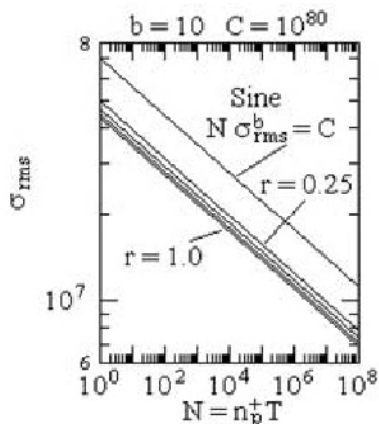


Figure 4.36. *S-N curve into random plotted as a function of the peak number, for various values of the irregularity factor*

S-N curves

The Miner/Rayleigh method for the determination of S-N curves was checked experimentally, and demonstrated a reasonable scatter of fatigue damage [MCC 64] [ESH 64].

The rms stress versus the number of cycles to failure curves are straight lines on logarithmic scales (note that we find the two definitions of N, i.e. $n_0^+ T$ and $n_p^+ T$, perhaps allowing some differences in the results to be explained).

The majority of authors agree to locate the S-N curve for random loads on the left of the curve obtained for sine [BRO 70b] [CLE 66] [CLE 77] [ELD 61] [HEA 56] [LAM 76] [MAR 68] [MCCL 64] [PER 74] [ROO 64] [SMI 63]; the fatigue lives are shorter for random than for sine for equal rms stress values. This result is logical since the damage by fatigue is primarily produced by large peaks which can exceed the rms value for random by a factor of five.

The difference observed is sometimes larger at low levels [PER 74] [SMI 63]. R.G. Lambert [LAM 76] provides some experimental results listed in Table 4.2, which we reproduce as an indication.

The values of the ultimate stress ratio R_s/R_A (stresses for $N = 1$ in the Basquin relation) obtained for a sinusoidal stress and a random stress, respectively, are close

to 2 for ductile materials and 3 for relatively brittle materials (the materials are more brittle when their b parameter is larger).

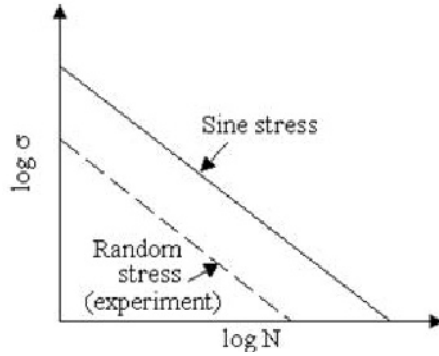


Figure 4.37. Comparison between the S - N curves determined for sinusoidal and random stress

However, some authors obtain a longer fatigue life for high random stress levels and a shorter fatigue life for low levels [KIR 65b] [FRA 59] [LOW 62].

J.R. Fuller [FUL 61], S.R. Swanson [SWA 63] and H.C. Schelderup and A.E. Galef [SCH 61a] have noted that the S - N curves plotted on logarithmic scales with sine stresses and narrow band random stresses (distribution of the peaks close to Rayleigh's law) are roughly straight lines of different slopes, the curve in random mode being deduced from that in sine mode by a clockwise rotation centered on the axis $N = 1$ (Figure 4.38). To take account of this remark, L. Fiderer [FID 75] proposes representing the S - N curve by a relation derived from Basquin's ($N \sigma^b = C = 1. \sigma_1^b$, where σ_1^b is a fictitious stress level and, since $\sigma_1 > R_m$, stress to rupture for 1 cycle i.e. in statics) of the form:

$$N \sigma^{\lambda b} = \sigma_1^{\lambda b}$$

where the constant λ takes account of observed rotation. The relative position of the theoretical S - N curves thus obtained and of the experimental curves is not so clearly established.

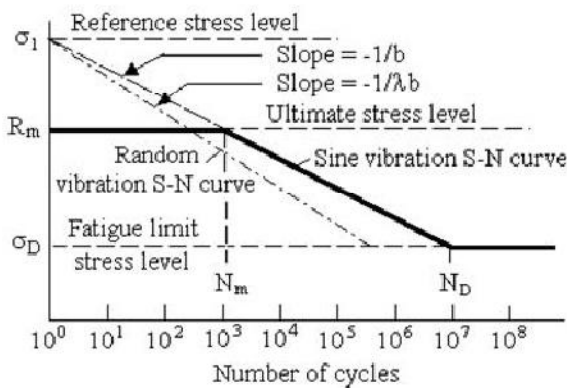


Figure 4.38. Transformation of the *S-N* curve in sine mode to the *S-N* curve into random mode

Material	b	Sinusoidal stress		Random stress		
		Ultimate stress R_S (Pa)	Constant C (SI unit)	Ultimate stress R_A (Pa)	Constant A (Pa)	Ratio $\frac{R_S}{R_A}$
Aluminum alloy 6061-T6	8.92	7.56×10^8	⁽¹⁾ 1.57×10^{79}	3.43×10^8	1.36×10^{76}	2.20
Copper Wire	9.28	5.65×10^8	1.66×10^{81}	2.54×10^8	9.93×10^{77}	2.22
Aluminum alloy 7075-T6	9.65	12.38×10^8	5.56×10^{87}	5.51×10^8	2.25×10^{84}	2.25
G10 Epoxy Fiberglass	12.08	5.58×10^8	4.56×10^{105}	2.28×10^8	9.20×10^{100}	2.45
Wrought Steel SAE 4130 BHN267	17.54	12.13×10^8	2.14×10^{159}	4.27×10^8	2.39×10^{151}	2.84
Magnesium alloy AZ31B	22.37	2.99×10^8	3.99×10^{189}	9.38×10^7	2.18×10^{178}	3.19

Table 4.2. Examples of constants in Basquin's relation for sinusoidal and random stresses [LAM 76]

1. $[7.56 \times 10^8]^{8.92}$

Work carried out by C. Perruchet and P. Vimont [PER 74] shows an important diversity in conclusions:

- the tests confirm the estimated lifetimes relatively well:
 - whatever the stress level [ELD 61] [KOW 61] [MAR 68],
 - only at low stress levels, real fatigue lives being longer than those estimated for high levels [ELD 61] [FRA 59] [KIR 65b] [LOW 62], and
 - only at high levels, real fatigue lives being shorter than the expectation for low levels [CLE 66] [CLE 77];
- the experimental fatigue lives are smaller by a factor of 2 to 10 [BOO 69] [BRO 70b] [CLE 66] [FUL 62] [HEA 56] [MAR 68] [PER 74] [SMI 63] whatever the stress level; and
- the experimental fatigue lives are longer by a factor of 2 to 3 approximately (between 10^4 and 10^7 cycles) whatever the stress level [ELD 61] [ROO 64].

Generally, it is considered that the estimates of fatigue life carried out using Miner's rule are rather good for random vibrations, the shape of the estimated S-N curve being correct [BRO 70b] [MAR 68]. This rule, relatively simple to use, provides adequate evaluations when an approximate result is required [BOO 69].

NOTE: *McClymonds and J.K. Ganoug [MCC 64] made a comparison of the SN curves established for random, sine and swept sine (for Miner's and Rayleigh's assumptions). Swept sine produces significant damage only during the time for which the excitation frequency crosses the frequency interval between the half-power points at each system resonance.*

Random loading creates damage by fatigue for each resonance over all the test duration. While referring the S-N curves to the load corresponding to the resonance peak for swept sine and to the rms load for random, they observe, at a given stress level, a longer fatigue life for swept sine than for sine and longer for sine than random.

This tendency is confirmed by calculation. Figure 4.39 shows the S-N curves plotted using the following relations:

sine [4.113]:

$$N \sigma_{rms}^b = \frac{C}{(\sqrt{2})^b}$$

random [4.114]:

$$N \sigma_{rms}^b = \frac{C}{(\sqrt{2})^b \Gamma\left(1 + \frac{b}{2}\right)}$$

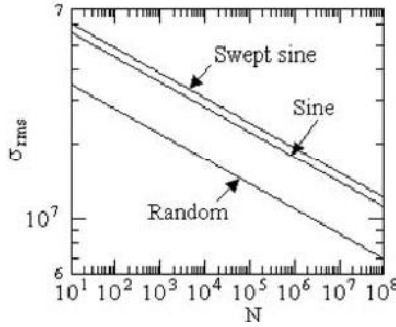


Figure 4.39. Comparison of the S-N curves established experimentally under sine and random stresses

For the swept sine, the relation is established using the approximation suggested by M. Gertel [GER 61] for the calculation of fatigue damage undergone by a one-dof system excited by a linear swept sine. It is shown [LAL 82] (Volume 5, Chapter 3):

$$D \approx \frac{\Delta N}{5} \frac{\sigma_{max}^b}{C} \Sigma_b \quad [4.122]$$

where ΔN is the number of cycles performed between the half-power points (function of the sweep rate):

$$\Sigma_b = 0.996^b + 0.959^b + 0.895^b + 0.82^b + 0.744^b \quad [4.123]$$

yielding, for $D = 1$,

$$\Delta N \sigma_{rms}^b = \frac{5 C}{(\sqrt{2})^b \Sigma_b} \quad [4.124]$$

4.8. Influence of shape of power spectral density and value of irregularity factor

The shape of the PSD and the bandwidth are generally regarded as not very influential parameters [BRO 68b] [HIL 70] [LIN 72]. Studies carried out to evaluate the importance of the factor r lead however to more moderate conclusions:

- The parameter r has little influence for $0.63 \leq r \leq 0.96$ (it was seen that the narrow band approximation is acceptable in this range) [CLE 66] [CLE 77] [FUL 62].

- The parameter r has little influence, except when it is very weak, about 0.3. We then observe an increase in the fatigue lives for notched samples [GAS 72] [GAS 77].

- The parameter r has a notable influence (except if the probability density functions of the peaks are comparable) [BRO 68b] [LIN 72] [NAU 65].

- The fatigue life is larger when r is smaller, both from the point of view of crack initiation and their propagation [GAS 76]. For S.L. Bussa [BUS 67], this effect is particularly sensitive for $r < 0.8$;

- S.R. Swanson [SWA 69] and J. Kowalewski [KOW 63] arrive at qualitatively similar results regarding the influence of the parameter r , without a law-binding r and the fatigue life being able to be truly established.

4.9. Effects of peak truncation

Since the fatigue damage is narrowly dependent on the number and the amplitude of the peaks of stress undergone by the part, it is interesting to speculate about the effect of a truncation of the peaks. This truncation can have several origins.

In theory, calculations take into account a law of peak distribution $q(u)$ without limitation, thus being able statistically to include very large peaks. In practice, it is rare to observe peaks higher than 6 standard deviations (rms value) in the real environment. During simulation tests in laboratory, the control system often cut the peaks higher than 4.5 times the rms value.

Before anticipating the analysis, it is wise to specify the nature of the truncated control signal. This signal can be:

1. an acceleration, a force or any other quantity imposed on a structure, the stress at a point being the result of this excitation only; or

2. a stress or a deformation directly measured on the part or the result of force applied directly to the part (case of tests on test bars).

Depending on the case, the results are different. We will consider in the following section only the latter case. The influence of a truncation of the acceleration signal will be examined in Chapter 4 of Volume 5.

4.10. Truncation of stress peaks

Let us suppose that the S-N curve can be represented by the analytical Basquin expression $N \sigma^b = C$ and that we use Miner's rule.

Under these assumptions, we saw that the fatigue damage can be written, without truncation:

$$D = \frac{n_p^+ T}{C} \int_0^{+\infty} \sigma^b q(\sigma) d\sigma.$$

If the peaks are truncated at stress level σ_t , the damage becomes:

$$D = \frac{n_p^+ T}{C} \int_0^{\sigma_t} \sigma^b q(\sigma) d\sigma \quad [4.125]$$

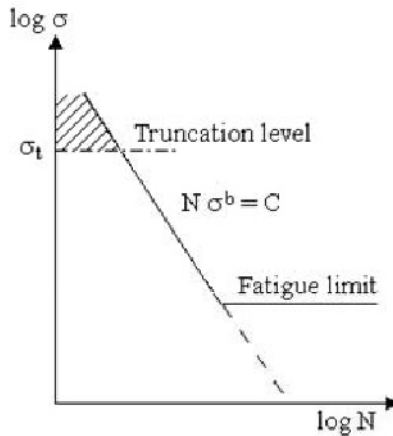


Figure 4.40. Truncation level of peaks on the S-N curve

4.10.1. Particular case of a narrow band noise

If the peak distribution of $\sigma(t)$ can be represented by Rayleigh's law ($r \approx 1$), expression [4.125] of the damage can be written [POO 78]

$$D = \frac{n_0^+ T}{C \sigma_{rms}^2} \int_0^{\sigma_t} \sigma^{b+1} e^{-\frac{\sigma^2}{2 \sigma_{rms}^2}} d\sigma \quad [4.126]$$

If we take into account a fatigue limit σ_D , this damage becomes:

$$D = \frac{n_0^+ T}{C \sigma_{rms}^2} \int_{\sigma_D}^{\sigma_t} \sigma^{b+1} e^{-\frac{\sigma^2}{2 \sigma_{rms}^2}} d\sigma .$$

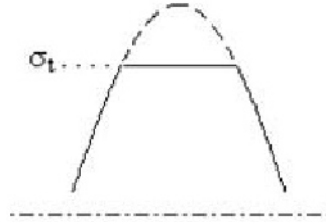


Figure 4.41. *Truncated peak*

Since the peaks are truncated at value σ_t , the amplitudes higher than this value are fixed at $\sigma = \sigma_t$ for calculation of the damage when $N \sigma^b = C$ [POO 78]. This damage

$$dD = n_0^+ T \frac{q(\sigma)}{N(\sigma)} d\sigma$$

therefore becomes

$$dD = \frac{n_0^+ T}{C} \sigma_t^b q(\sigma) d\sigma,$$

yielding

$$D_{\sigma > \sigma_t} = \frac{n_0^+ T}{C \sigma_{rms}^2} \sigma_t^b \int_{\sigma_t}^{\infty} \sigma e^{-\frac{\sigma^2}{2 \sigma_{rms}^2}} d\sigma \quad [4.127]$$

NOTE: This result can be arrived at by considering that truncation to σ_t is equivalent to the addition of a Dirac delta function at $\sigma = \sigma_t$ which restores the truncated area under the curve $q(\sigma)$ to the value 1. This area is equal to [LAM 76]:

$$a_t = \int_{\sigma_t}^{\infty} q(\sigma) d\sigma = \int_{\sigma_t}^{\infty} \frac{\sigma}{\sigma_{rms}^2} e^{-\frac{\sigma^2}{2 \sigma_{rms}^2}} d\sigma$$

$$a_t = e^{-\frac{\sigma_t^2}{2 \sigma_{rms}^2}} \quad [4.128]$$

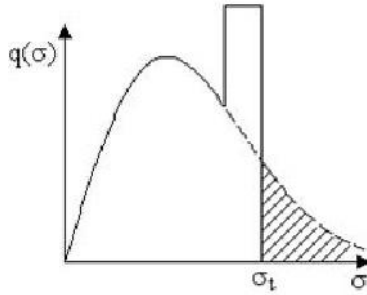


Figure 4.42. Addition of a Dirac delta function to the probability density of peaks to compensate for the area removed by truncation

The truncated probability density then becomes

$$q(\sigma) = \frac{\sigma}{\sigma_{rms}^2} e^{-\frac{\sigma^2}{2 \sigma_{rms}^2}} + a_t \delta(\sigma - \sigma_t) \quad [4.129]$$

where $0 \leq \sigma \leq \sigma_t$, and damage by fatigue relating to larger peaks than σ_t is:

$$\frac{n_0^+}{C} \frac{T}{\sigma_t} \underbrace{\int_{\sigma_t}^{\infty} \frac{a_t}{N(\sigma)} \delta(\sigma - \sigma_t) d\sigma}_{\text{Value of the function for } \sigma = \sigma_t} = \frac{n_0^+}{C} \frac{T}{\sigma_t^b} e^{-\frac{\sigma_t^2}{2 \sigma_{rms}^2}}.$$

The total damage in the presence of a fatigue limit stress is therefore:

$$\begin{aligned} D_t &= \frac{n_0^+}{C} \frac{T}{\sigma_{rms}^2} \int_0^{\sigma_t} \sigma^{b+1} e^{-\frac{\sigma^2}{2 \sigma_{rms}^2}} d\sigma - \frac{n_0^+}{C} \frac{T}{\sigma_{rms}^2} \int_0^{\sigma_D} \sigma^{b+1} e^{-\frac{\sigma^2}{2 \sigma_{rms}^2}} d\sigma \\ &+ \frac{n_0^+}{C} \frac{T}{\sigma_t^b} \int_{\sigma_t}^{\infty} \sigma e^{-\frac{\sigma^2}{2 \sigma_{rms}^2}} d\sigma. \end{aligned} \quad [4.130]$$

Knowing that the term

$$\int_0^{\sigma_t} \frac{\sigma^{b+1}}{\sigma_{rms}^2} e^{-\frac{\sigma^2}{2 \sigma_{rms}^2}} d\sigma$$

can be written in the form

$$\begin{aligned} &\left(\sqrt{2} \sigma_{rms}\right)^b \int_0^{\frac{\sigma_t^2}{2 \sigma_{rms}^2}} \alpha^{B-1} e^{-\alpha} d\alpha = \left(\sqrt{2} \sigma_{rms}\right)^b \int_0^{\tau} \alpha^{B-1} e^{-\alpha} d\alpha \\ &= \left(\sqrt{2} \sigma_{rms}\right)^b \gamma[B, \tau] \end{aligned}$$

where $\gamma[B, \tau]$ is the incomplete gamma function, it becomes, with $B = 1 + \frac{b}{2}$ and

$$\tau = \frac{\sigma_t^2}{2 \sigma_{rms}^2} :$$

$$D_t = \frac{n_0^+}{C} \frac{T}{\sigma_{rms}^2} \left(\sqrt{2} \sigma_{rms}\right)^b \left[\gamma\left(1 + \frac{b}{2}, \frac{\sigma_t^2}{2 \sigma_{rms}^2}\right) \right]$$

$$-\gamma\left(1 + \frac{b}{2}, \frac{\sigma_D^2}{2\sigma_{rms}^2}\right) + \frac{n_0^+ T}{C} \sigma_t^b e^{-\frac{\sigma_t^2}{2\sigma_{rms}^2}} \quad [4.131]$$

and

$$\frac{D_t}{D_\infty} = \frac{\gamma\left(1 + \frac{b}{2}, \frac{\sigma_t^2}{2\sigma_{rms}^2}\right) - \gamma\left(1 + \frac{b}{2}, \frac{\sigma_D^2}{2\sigma_{rms}^2}\right) + \frac{\sigma_t^b}{(\sqrt{2}\sigma_{rms})^b} e^{-\frac{\sigma_t^2}{2\sigma_{rms}^2}}}{\Gamma\left(1 + \frac{b}{2}\right) - \gamma\left(1 + \frac{b}{2}, \frac{\sigma_D^2}{2\sigma_{rms}^2}\right)} \quad [4.132]$$

The function γ is tabulated and can be calculated from approximate relations. If $\sigma_t \rightarrow \infty$ [BUS 67] [SWA 69], $\gamma\left(1 + \frac{b}{2}, \infty\right) = \Gamma\left(1 + \frac{b}{2}\right)$ and

$$D_t \rightarrow \frac{n_0^+ T}{C} (\sqrt{2}\sigma_{rms})^b \left[\Gamma\left(1 + \frac{b}{2}\right) - \gamma\left(1 + \frac{b}{2}, \frac{\sigma_D^2}{2\sigma_{rms}^2}\right) \right] \quad [4.133]$$

NOTES:

1. Expression [4.131] can also be written [WHI 69]:

$$D_t = \frac{n_0^+ T}{C} (\sqrt{2}\sigma_{rms})^b \Gamma\left(1 + \frac{b}{2}\right) \left\{ P\left[\left(\frac{\sigma_t}{\sigma_{rms}}\right)^2, b+2\right] - P\left[\left(\frac{\sigma_D}{\sigma_{rms}}\right)^2, b+2\right] \right\} + \frac{n_0^+ T}{C} \sigma_t^b e^{-\frac{\sigma_t^2}{2\sigma_{rms}^2}} \quad [4.134]$$

(the function P is tabulated).

2. If we set $\sigma_D = 0$ (no fatigue limit) in relationship [4.133], we find the Crandall expression [4.40].

The effect of truncation is to reduce the damage in the ratio $\frac{D_t}{D_\infty}$, which is related to b .

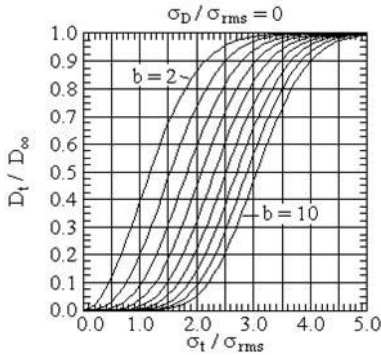


Figure 4.43. Effect of truncation on the damage in the absence of fatigue limit

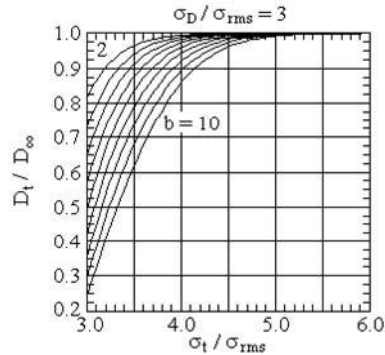


Figure 4.44. Effect of truncation on the damage for a fatigue limit equal to 3 times the rms value

Figures 4.43 and 4.44 show the variations of this ratio for $\sigma_D = 0$ and $\frac{\sigma_D}{\sigma_{rms}} = 3$ versus $\frac{\sigma_t}{\sigma_{rms}}$, parameterized by b (variable between 2 and 10 per step of 1).

For $\sigma_D = 0$, we note that if $b < 7$, truncation for $\frac{\sigma_t}{\sigma_{rms}} > 4$ has a negligible effect. However, if $b \geq 7$, at least 50% of the total damage by fatigue is produced by the peaks of the response exceeding $3\sigma_{rms}$, in spite of their infrequent occurrence [SMA 65]. Although the damage created by the peaks between $2\sigma_{rms}$ and $3\sigma_{rms}$ is important [POO 78], it appears clearly that a truncation of the response signal to $3\sigma_{rms}$ modifies the resulting damage a lot.

In certain cases (observed for “missile” environments), the responses greater than $3\sigma_{rms}$ can occur much more frequently than for a Gaussian noise; peaks higher than $5\sigma_{rms}$ are very probable.

The damage produced is then more significant than that envisaged with a Gaussian assumption. To avoid this problem, a method could consist of adjusting the total amplitude of the random noise created during the test laboratory so that the response peaks produced are similar to those in the real environment.

For $b < 7$ and $\sigma_D \neq 0$, truncation has little effect if $\frac{\sigma_t}{\sigma_{rms}} > 4$ and if $\frac{\sigma_D}{\sigma_{rms}} = 1$ and 2 [WHI 69].

For $b < 10$ and $\frac{\sigma_D}{\sigma_{rms}} > 4$ (Figure 4.45), the reduction of the damage is weak as long as $\frac{\sigma_t}{\sigma_{rms}} > \frac{\sigma_D}{\sigma_{rms}} + 1$. The level σ_g at which the greatest damage takes place is obtained while searching σ_g such that $\frac{dD}{d\sigma}$ is a maximum, i.e. for $\frac{d^2D}{d\sigma^2} = 0$, yielding

$$\frac{\sigma_t}{\sigma_{rms}} = \frac{\sigma_g}{\sigma_{rms}} \left[\frac{\left(\frac{\sigma_g}{\sigma_{rms}} \right)^2 - 1}{b + 1 - \left(\frac{\sigma_g}{\sigma_{rms}} \right)^2} \right]^{\frac{1}{b}} \quad [4.135]$$

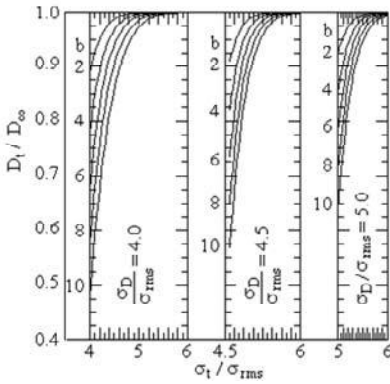


Figure 4.45. Effect of truncation on the damage as a function of fatigue limit

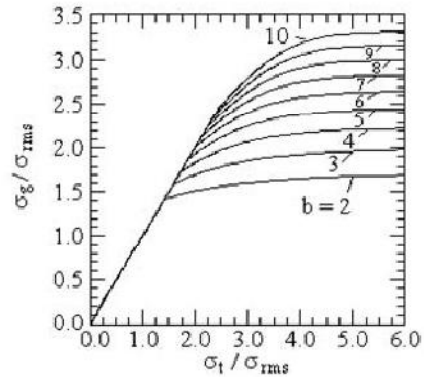


Figure 4.46. Stress leading to greatest damage

If $\sigma_t \rightarrow \infty$,

$$\frac{\sigma_g}{\sigma_{rms}} \rightarrow \sqrt{b + 1} \quad [4.136]$$

If $\frac{\sigma_t}{\sigma_{rms}} = \frac{\sigma_g}{\sigma_{rms}}$, we have

$$\frac{\sigma_g}{\sigma_{rms}} = \left(\frac{b}{2} + 1 \right)^{\frac{1}{2}} \quad [4.137]$$

For $\frac{\sigma_t}{\sigma_{rms}}$ small (Figure 4.46), there is a field for each value of b in which the level $\frac{\sigma_g}{\sigma_{rms}}$ is equal to $\frac{\sigma_t}{\sigma_{rms}}$. These curves are valid only if $\sigma_D < \sigma_g$ (there is no damage if $\sigma_D > \sigma_t$) [WHI 69].

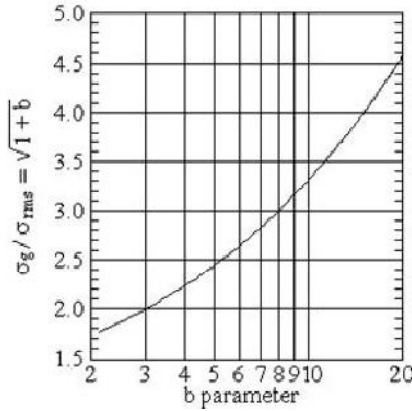


Figure 4.47. Stress leading to greatest damage in the absence of truncation

These results show that the effect of truncation generally cannot be neglected *a priori*. It is therefore important to specify, by test, the value of σ_t . The truncation of the peaks larger than $2.5 \sigma_{rms}$ has a notable influence, leading to longer fatigue lives.

The truncation of the peaks above $\pm 3.5 \sigma_{rms}$ has little influence on the experimental results [BOO 69].

The predictions of fatigue lives carried out using Miner's hypothesis and a truncated signal are good with a truncation between $4 \sigma_{rms}$ and $5.5 \sigma_{rms}$, worse with $3.5 \sigma_{rms}$ and very poor with $2.5 \sigma_{rms}$ [BOO 69].

Relation [4.136] established in the absence of truncation shows, in addition, that the maximum damage is brought about by the peaks located between 2 and 4.5 times the rms value, this maximum being a function of the parameter b (Figure 4.47).

NOTE: *A.J. Curtis [CUR 82] presents the calculation in a slightly different way. Given a Rayleigh distribution truncated for $\sigma \geq \sigma_l$ and a fatigue limit σ_D , it states the damage by fatigue D is of the form:*

$$D = \sum_i \frac{n_i}{N_i} = \frac{1}{C} \int_{\sigma_D/\sigma_{rms}}^{\sigma_l/\sigma_{rms}} \sigma^b n\left(\frac{\sigma}{\sigma_{rms}}\right) d\left(\frac{\sigma}{\sigma_{rms}}\right)$$

$$D = \frac{n_0^+ T}{C} \frac{\int_{\sigma_D/\sigma_{rms}}^{\sigma_l/\sigma_{rms}} \sigma^b q\left(\frac{\sigma}{\sigma_{rms}}\right) d\left(\frac{\sigma}{\sigma_{rms}}\right)}{\int_0^{\sigma_l/\sigma_{rms}} q\left(\frac{\sigma}{\sigma_{rms}}\right) d\left(\frac{\sigma}{\sigma_{rms}}\right)}$$

yielding

$$D = \frac{n_0^+ T}{C} s^b \frac{\int_{u_D}^{u_l} u^{b+1} e^{-\frac{u^2}{2}} du}{1 - e^{-\frac{u_l^2}{2}}}$$

where $u = \frac{\sigma}{\sigma_{rms}}$ and $u_D = \frac{\sigma_D}{\sigma_{rms}}$, or

$$D = \frac{n_0^+ T}{C} \frac{\sigma_{rms}^b 2^{\frac{b}{2}}}{1 - e^{-\frac{u_l^2}{2}}} \left[\gamma\left(\frac{b}{2} + 1, \frac{u_l^2}{2}\right) - \gamma\left(\frac{b}{2} + 1, \frac{u_D^2}{2}\right) \right] \quad [4.138]$$

where

$$\gamma\left(\frac{b}{2} + 1, \frac{u_l^2}{2}\right) = \int_0^{u_l} u^{b+1} e^{-\frac{u^2}{2}} du \quad [4.139]$$

$\gamma\left(\frac{b}{2} + 1, \frac{u_t^2}{2}\right)$					
u_t	$b = 3.0$	$b = 6.5$	$b = 9.0$	$b = 25.0$	$1 - e^{-u_t^2/2}$
.10	0.0000	0.000	0.000	0.000	0.005
0.20	0.0000	0.000	0.000	0.000	0.020
0.30	0.0002	0.000	0.000	0.000	0.044
0.40	0.0007	0.000	0.000	0.000	0.077
0.50	0.0020	0.000	0.000	0.000	0.118
0.60	0.0048	0.000	0.000	0.000	0.165
0.70	0.0100	0.000	0.000	0.000	0.217
0.80	0.0185	0.001	0.000	0.000	0.274
0.90	0.0314	0.004	0.001	0.000	0.333
1.00	0.0498	0.008	0.003	0.000	0.393
1.10	0.0746	0.017	0.007	0.000	0.454
1.20	0.1065	0.033	0.016	0.000	0.513
1.30	0.1460	0.059	0.035	0.000	0.570
1.40	0.1932	0.099	0.072	0.000	0.625
1.50	0.2478	0.159	0.136	0.000	0.675
1.60	0.3092	0.244	0.243	0.000	0.722
1.70	0.3763	0.359	0.413	0.000	0.764
1.80	0.4479	0.510	0.672	0.000	0.802
1.90	0.5227	0.702	1.048	256	0.836
2.00	0.5990	0.937	1.575	256	0.865
2.10	0.6753	1.217	2.284	512	0.890
2.20	0.7501	1.542	3.210	1,280	0.911
2.30	0.8222	1.908	4.380	3,328	0.929
2.40	0.8903	2.310	5.816	8,448	0.944
2.50	0.9536	2.744	7.528	19,968	0.956
2.60	1.0115	3.199	9.517	45,312	0.966
2.70	1.0635	3.667	11.770	98,304	0.974
2.80	1.1096	4.140	14.260	204,288	0.980
2.90	1.1498	4.606	16.950	406,528	0.985
3.00	1.1844	5.058	19.791	776,448	0.989
3.10	1.2136	5.488	22.729	1,427,456	0.992
3.20	1.2380	5.890	25.704	2,530,560	0.994
3.30	1.2581	6.259	28.656	4,333,056	0.996
3.40	1.2744	6.592	31.531	7,179,264	0.997
3.50	1.2874	6.888	34.277	11,527,168	0.998
3.60	1.2978	7.146	36.852	17,960,704	0.998
3.70	1.3058	7.368	39.224	27,195,392	0.999
3.80	1.3120	7.556	41.372	40,066,816	0.999
3.90	1.3167	7.712	43.283	57,502,976	1.000
4.00	1.3202	7.841	44.956	80,484,608	1.000
$\Gamma(1 + b/2)$					
$b = 3.0$		$b = 6.5$		$b = 25.0$	
1.3293		8.285		52.343	
				1.711 10 ⁹	

Table 4.3. Values of the incomplete gamma function [CUR 82]

A.J. Curtis [CUR 82] shows that the fatigue life is more modified when b is larger (for small u_D and $\frac{\sigma_t}{\sigma_{rms}} = \pm 3$). Table 4.3 gives, for u_t ranging between 1.10 and 4.00, the values of:

– the function $\gamma\left(\frac{b}{2} + 1, \frac{u_t^2}{2}\right)$ for b equal to 3.0, –6.5, –9.0 and 25.0; and

– the expression $1 - e^{-u_t^2/2}$.

$$\gamma\left(\frac{b}{2} + 1, \frac{u_t^2}{2}\right) = \int_0^{u_t} u^{b+1} e^{-\frac{u^2}{2}} du \quad [4.139]$$

4.10.2. Layout of the S-N curve for a truncated distribution

If $\sigma_D = 0$, σ_t is arbitrary and $N_t = n_0^+ T$, we have:

$$N_t \left[\left(\sqrt{2} \sigma_{rms} \right)^b \gamma\left(1 + \frac{b}{2}, \frac{\sigma_t^2}{2 \sigma_{rms}^2}\right) + \sigma_t^b e^{-\frac{\sigma_t^2}{2 \sigma_{rms}^2}} \right] = C \quad [4.140]$$

The ratio of fatigue life with and without truncation is therefore [LAM 76]:

$$\frac{N_t}{N} = \frac{\Gamma\left(1 + \frac{b}{2}\right)}{\gamma\left(1 + \frac{b}{2}, \frac{\sigma_t^2}{2 \sigma_{rms}^2}\right) + \left(\frac{\sigma_t^2}{2 \sigma_{rms}^2}\right)^{\frac{b}{2}} e^{-\frac{\sigma_t^2}{2 \sigma_{rms}^2}}} \quad [4.141]$$

This ratio depends only on $\frac{\sigma_t}{\sigma_{rms}}$ and on the parameter b . To compensate for the truncation and to produce the same damage, it would be necessary to multiply the rms value of the stress by the factor

$$\lambda = \left(\frac{N_t}{N} \right)^{\frac{1}{b}} \quad [4.142]$$

and the amplitude of the PSD by λ^2

$$\lambda = \left[\frac{\Gamma\left(1 + \frac{b}{2}\right)}{\gamma\left(1 + \frac{b}{2}, \tau\right) + \tau^{b/2} e^{-\tau}} \right]^{\frac{1}{b}} \quad [4.143]$$

where

$$\tau = \frac{\sigma_t^2}{2 \sigma_{rms}^2}.$$

Table 4.4 gives the values of λ for different values of b and $\frac{\sigma_t}{\sigma_{rms}}$.

Figures 4.48 and 4.49 show the variations of λ with b and $\frac{\sigma_t}{\sigma_{rms}}$. It is noted that λ increases with b and decreases when σ_t increases.

b	$\frac{\sigma_t}{\sigma_{\text{rms}}}$				
	3	3.5	4	4.5	5
3	1.01	1.0022	1.000377	1.000048	1.00000142
4	1.0159	1.0039348	1.000756	1.00011146	1.0000126
5	1.02336	1.000643	1.001375	1.000224	1.0000279
6	1.032285	1.00976	1.00231	1.000417	1.0000569
7	1.04248	1.01398	1.00364	1.000724	1.000108
8	1.05377	1.0191	1.00543	1.001185	1.000194
9	1.066	1.0250	1.00772	1.0018425	1.000331
10	1.0789	1.03178	1.01055	1.002738	1.000536
11	1.0924	1.0392	1.01393	1.00391	1.000833
12	1.10644	1.04732	1.01784	1.00539	1.001245

Table 4.4. Values of the compensation factor of truncation λ

NOTE: We could also consider the ratio of the damage of the truncated signal D_t to the damage of complete signal D . This ratio is equal to

$$\frac{D_t}{D} = \mu = \frac{N}{N_t} = \frac{1}{\lambda^b} \quad [4.144]$$

It is important to recall here that the truncation considered in this section relates to the stress and not to the acceleration signal applied to the base of the reference one-dof system. Some examples show that in this latter case, truncation has little effect when it is greater than 3 times the rms value of the signal (Volume 5).

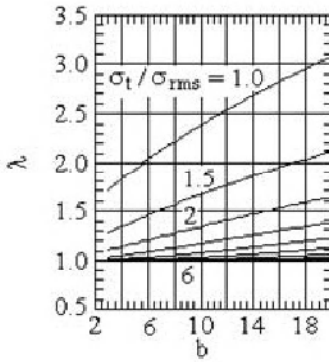


Figure 4.48. Compensation factor λ versus the parameter b

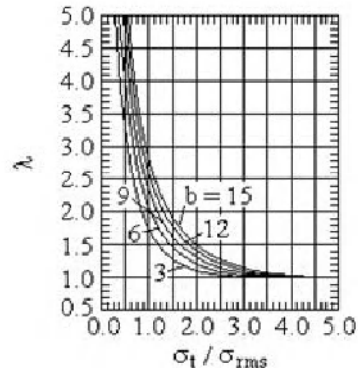


Figure 4.49. Compensation factor λ versus the truncation threshold

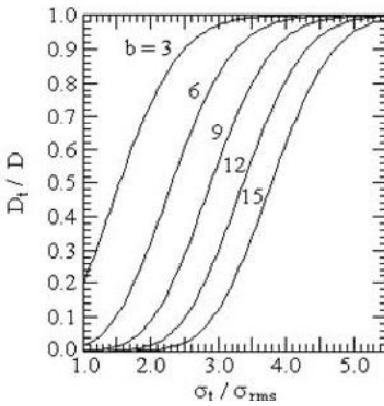


Figure 4.50. Ratio of damage of truncated and untruncated signals versus the truncation threshold

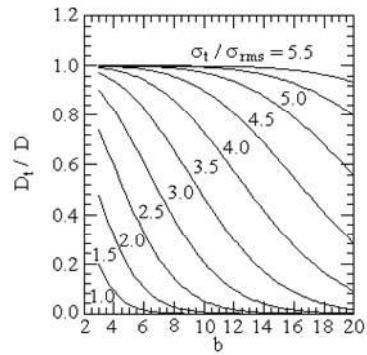


Figure 4.51. Ratio of the damage of the truncated and untruncated signals versus the parameter b

Chapter 5

Standard Deviation of Fatigue Damage

In previous chapters it was seen how fatigue damage undergone by a one-degree-of-freedom system can be calculated starting from the characteristics of random stress, Miner's rule and parameters of the S-N curve. When the peak distribution of the response can be represented analytically, we can obtain damage expectation $E(D)$. To this mean damage can be applied a standard deviation s_D (or variance s_D^2) characterizing scatter related to the random aspect of the excitation. Several methods have been proposed to approximately calculate s_D assuming a Rayleigh peak distribution.

5.1. Calculation of standard deviation of damage: Bendat's method

Assume that the signal is stationary and ergodic and assume the form of the autocovariance function of the damage created by each half-cycle of the response is equal to $s_d^2 e^{-2\pi k \xi}$, where $s_d^2 = E(d^2) - E^2(d)$ and d is the damage associated with the half-cycle k . J.S.Bendat [BEN 64] then showed that the variance of the damage undergone by a single-dof linear system can be written

$$s_D^2 = s_d^2 \left[N_p + \sum_{k=1}^{N_p-1} (N_p - k) e^{-2k\pi\xi} \right] \quad [5.1]$$

where

$$N_p = 2 n_p^+ \quad T = 2 N_p^+ \quad [5.2]$$

and

$$\sum_{k=1}^{N_p-1} (N_p - k) e^{-2k\pi\xi} = F(\pi\xi) = \frac{(N_p - 1) e^{2\pi\xi} - N_p + e^{-2(N_p-1)\pi\xi}}{(e^{2\pi\xi} - 1)^2} \quad [5.3]$$

$$s_d^2 = \left(\frac{K^b}{2C} \right)^2 \int_0^{+\infty} z_p^{2b} q(z_p) dz_p - \left[\frac{E(D)}{N_p} \right]^2 \quad [5.4]$$

with

$$\begin{aligned} \frac{E(D)}{N_p} &= \frac{K^b}{2C} \int_0^{+\infty} z_p^b q(z_p) dz_p \\ s_D^2 &= \left[\left(\frac{K^b}{2C} \right)^2 \int_0^{+\infty} z_p^{2b} q(z_p) dz_p - \left(\frac{E(D)}{N_p} \right)^2 \right] \\ &\quad \left[N_p + 2 \frac{(N_p - 1) e^{2\pi\xi} - N_p + e^{-2(N_p-1)\pi\xi}}{(e^{2\pi\xi} - 1)^2} \right] \end{aligned} \quad [5.5]$$

i.e.

$$\begin{aligned} s_D^2 &= \left[\left(\frac{K^b}{2C} \right)^2 z_{rms}^{2b} \int_0^{+\infty} u^{2b} q(u) du - \left(\frac{E(D)}{N_p} \right)^2 \right] \\ &\quad \left[N_p + 2 \frac{(N_p - 1) e^{2\pi\xi} - N_p + e^{-2(N_p-1)\pi\xi}}{(e^{2\pi\xi} - 1)^2} \right] \end{aligned} \quad [5.6]$$

where $u = \frac{z_p}{z_{rms}}$.

The variation coefficient v is given by:

$$v^2 = \frac{s_D^2}{E^2(D)} = \frac{N_p + 2 F(\pi\xi)}{E^2(D)} s_d^2 \quad [5.7]$$

$$v^2 = \frac{N_p + 2 F(\pi\xi)}{N_p^2} \frac{s_d^2}{\left[\frac{K^b}{2C} \int_0^{+\infty} z^b q(z_p) dz_p \right]^2} \quad [5.8]$$

Example 5.1.

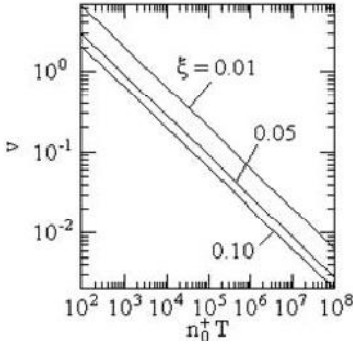


Figure 5.1. Variation coefficient of damage versus number of cycles [BEN 64]

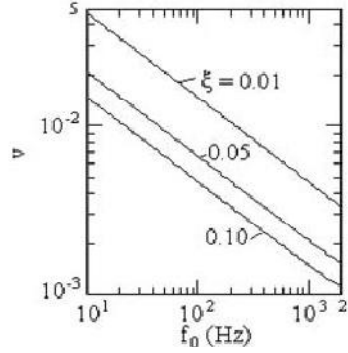


Figure 5.2. Variation coefficient of damage versus natural frequency [BEN 64]

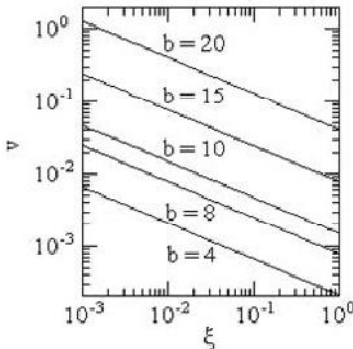


Figure 5.3. Variation coefficient of damage versus damping [BEN 64]

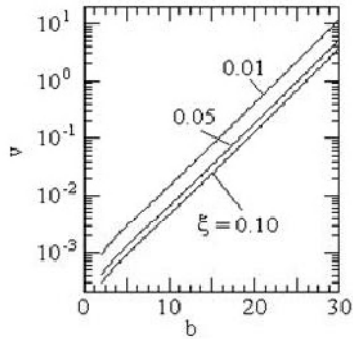


Figure 5.4. Variation coefficient of damage versus parameter b [BEN 64]

Figures 5.1–5.4 show the variations of v with b , f_0 , n_0^+ T and ξ in the case of a one-dof system of natural frequency 100 Hz subjected to a random noise of constant PSD equal to $1.65 \text{ (m/s}^2\text{)}^2/\text{Hz}$ between 1 Hz and 2000 Hz, with duration $T = 3600 \text{ s}$, under the following conditions: $b = 10$, $C = 10^{80}$, $K = 6.3 \times 10^{10}$ (SI units).

Since the peak distribution is assumed to follow a Rayleigh distribution,

$$\int_0^\infty z_p^{2b} q(z_p) dz_p = \frac{1}{z_{\text{rms}}^2} \int_0^\infty z_p^{2b+1} e^{-\frac{z_p^2}{2 z_{\text{rms}}^2}} dz_p = (z_{\text{rms}} \sqrt{2})^{2b} \Gamma(1+b) \quad [5.9]$$

$$\frac{E(D)}{N_p} = \frac{K^b}{2 C} (\sqrt{2} z_{\text{rms}})^b \Gamma\left(1 + \frac{b}{2}\right),$$

yielding

$$s_d^2 = \frac{K^{2b}}{4 C^2} (z_{\text{rms}} \sqrt{2})^{2b} \left[\Gamma(1+b) - \Gamma^2\left(1 + \frac{b}{2}\right) \right] \quad [5.10]$$

$$s_D^2 = s_d^2 \left[N_p + 2 F(\pi \xi) \right] \quad [5.11]$$

and

$$v^2 = \frac{N_p + 2 F(\pi \xi)}{N_p^2} \frac{\Gamma(1+b) - \Gamma^2\left(1 + \frac{b}{2}\right)}{\Gamma\left(1 + \frac{b}{2}\right)} \quad [5.12]$$

Lastly, if $2 n_p^+ T \xi$ is large, we have

$$F(\pi \xi) \approx \frac{n_p^+ T}{\pi \xi} \quad [5.13]$$

yielding

$$v^2 \approx \frac{1}{2 \pi \xi n_p^+ T} \frac{s_d^2}{\left[\frac{K^b}{2 C} \int_0^\infty z_p^b q(z_p) dz_p \right]^2} \quad [5.14]$$

and

$$v^2 \approx \frac{1}{2 \pi \xi n_p^+ T} \frac{\Gamma(1+b) - \Gamma^2\left(1 + \frac{b}{2}\right)}{\Gamma^2\left(1 + \frac{b}{2}\right)} \quad [5.15]$$

As an example, Table 5.1 lists some values of v calculated as a function of b and the product $2 \pi \xi n_p^+ T$ ($n_p^+ = n_0^+$ since $r = 1$).

$\frac{b}{2 \pi \xi n_0^+ T}$	2	4	6	8	10	12	14
10	$3.162 \cdot 10^{-1}$	$7.071 \cdot 10^{-1}$	$1.378 \cdot 10^0$	$2.627 \cdot 10^0$	$5.010 \cdot 10^0$	$9.601 \cdot 10^0$	$18.523 \cdot 10^0$
25	$2.000 \cdot 10^{-1}$	$4.472 \cdot 10^{-1}$	$8.718 \cdot 10^{-1}$	$1.661 \cdot 10^0$	$3.169 \cdot 10^0$	$6.076 \cdot 10^0$	$11.715 \cdot 10^0$
50	$1.414 \cdot 10^{-1}$	$3.162 \cdot 10^{-1}$	$6.164 \cdot 10^{-1}$	$1.175 \cdot 10^0$	$2.241 \cdot 10^0$	$4.297 \cdot 10^0$	$8.284 \cdot 10^0$
75	$1.155 \cdot 10^{-1}$	$2.582 \cdot 10^{-1}$	$5.033 \cdot 10^{-1}$	$9.592 \cdot 10^{-1}$	$1.829 \cdot 10^0$	$3.508 \cdot 10^0$	$6.764 \cdot 10^0$
100	$1.000 \cdot 10^{-1}$	$2.236 \cdot 10^{-1}$	$4.359 \cdot 10^{-1}$	$8.307 \cdot 10^{-1}$	$1.584 \cdot 10^0$	$3.038 \cdot 10^0$	$5.858 \cdot 10^0$
250	$6.325 \cdot 10^{-2}$	$1.414 \cdot 10^{-1}$	$2.757 \cdot 10^{-1}$	$5.254 \cdot 10^{-1}$	$1.002 \cdot 10^0$	$1.922 \cdot 10^0$	$3.705 \cdot 10^0$
500	$4.472 \cdot 10^{-2}$	$1.000 \cdot 10^{-1}$	$1.950 \cdot 10^{-1}$	$3.715 \cdot 10^{-1}$	$7.085 \cdot 10^{-1}$	$1.359 \cdot 10^0$	$2.620 \cdot 10^0$
750	$3.652 \cdot 10^{-2}$	$8.165 \cdot 10^{-2}$	$1.592 \cdot 10^{-1}$	$3.033 \cdot 10^{-1}$	$5.785 \cdot 10^{-1}$	$1.109 \cdot 10^0$	$2.139 \cdot 10^0$
1 000	$3.162 \cdot 10^{-2}$	$7.071 \cdot 10^{-2}$	$1.378 \cdot 10^{-1}$	$2.627 \cdot 10^{-1}$	$5.010 \cdot 10^{-1}$	$9.607 \cdot 10^{-1}$	$1.852 \cdot 10^0$
2 500	$2.000 \cdot 10^{-2}$	$4.472 \cdot 10^{-2}$	$8.718 \cdot 10^{-2}$	$1.661 \cdot 10^{-1}$	$3.167 \cdot 10^{-1}$	$6.075 \cdot 10^{-1}$	$1.172 \cdot 10^0$
5 000	$1.414 \cdot 10^{-2}$	$3.162 \cdot 10^{-2}$	$6.164 \cdot 10^{-2}$	$1.175 \cdot 10^{-1}$	$2.241 \cdot 10^{-1}$	$4.297 \cdot 10^{-1}$	$8.284 \cdot 10^{-1}$
7 500	$1.155 \cdot 10^{-2}$	$2.582 \cdot 10^{-2}$	$5.033 \cdot 10^{-2}$	$9.592 \cdot 10^{-2}$	$1.830 \cdot 10^{-1}$	$3.508 \cdot 10^{-1}$	$6.764 \cdot 10^{-1}$
10 000	$1.000 \cdot 10^{-2}$	$2.236 \cdot 10^{-2}$	$4.359 \cdot 10^{-2}$	$8.307 \cdot 10^{-2}$	$1.584 \cdot 10^{-1}$	$3.038 \cdot 10^{-1}$	$5.858 \cdot 10^{-1}$
25 000	$6.325 \cdot 10^{-3}$	$1.414 \cdot 10^{-2}$	$2.757 \cdot 10^{-2}$	$5.254 \cdot 10^{-2}$	$1.002 \cdot 10^{-1}$	$1.922 \cdot 10^{-1}$	$3.705 \cdot 10^{-1}$
50 000	$4.472 \cdot 10^{-3}$	$1.000 \cdot 10^{-2}$	$1.949 \cdot 10^{-2}$	$3.715 \cdot 10^{-2}$	$7.085 \cdot 10^{-2}$	$1.359 \cdot 10^{-1}$	$2.620 \cdot 10^{-1}$
100 000	$3.162 \cdot 10^{-3}$	$7.071 \cdot 10^{-3}$	$1.378 \cdot 10^{-2}$	$2.627 \cdot 10^{-2}$	$5.010 \cdot 10^{-2}$	$9.607 \cdot 10^{-2}$	$1.852 \cdot 10^{-1}$
500 000	$1.414 \cdot 10^{-3}$	$3.162 \cdot 10^{-3}$	$6.164 \cdot 10^{-3}$	$1.175 \cdot 10^{-2}$	$2.241 \cdot 10^{-2}$	$4.297 \cdot 10^{-2}$	$8.284 \cdot 10^{-2}$
1 000 000	$1.000 \cdot 10^{-3}$	$2.236 \cdot 10^{-3}$	$4.359 \cdot 10^{-3}$	$8.307 \cdot 10^{-3}$	$1.584 \cdot 10^{-2}$	$3.038 \cdot 10^{-2}$	$5.858 \cdot 10^{-2}$

Table 5.1. *Values of the variation coefficient of the damage [BEN 64]*

5.2. Calculation of standard deviation of damage: method of Crandall *et al.*

Crandall *et al.* calculate the variance of the damage in the following two ways [CRA 62] [MAR 61] [YAO 72]:

- (a) by assuming the amplitude of the stress cycles and the number of cycles in $[0, T]$ is random; and
- (b) by starting from an approximation considering only the random aspect of the stress amplitude.

These two approaches converge in extreme cases when the bandwidth tends towards zero. The problem in both cases is related to strong correlation in the incremental damage of successive cycles. It is necessary to carry out approximations which are valid only when T is large compared to the decrease in time of correlation.

NOTE: *There is a modified method of calculation of the variance [SHI 66] which assumes a normally distributed load (mathematically simpler than another distribution law).*

We make the following assumptions:

- the excitation is of white noise type and the peaks of the response are distributed according to Rayleigh's law;
- the excited system is linear, with only one dof, with a damping ratio very much lower than unity (in practice, less than or equal to 0.05); and
- the mean number of cycles of the response for the length of time T is very large compared to $1/2\xi$.

The approximate analytical expressions of the variance established in cases (a) and (b) converge towards the same expression when damping ξ tends towards zero (the mean damage $E(D)$ is the same for the two assumptions, in that $n_0^+ \approx f_0$).

By assuming the amplitude of the half-cycles and their number to be random, the variance can be written:

$$s_D^2 \approx \frac{K^{2b}}{C^2} \frac{n_0^+ T}{\xi} (\sqrt{2} z_{\text{rms}})^{2b} \Gamma^2\left(1 + \frac{b}{2}\right) \left\{ f_1(b) - \frac{f_2(b)}{\xi n_0^+ T} + \frac{\xi f_3(b)}{n_0^+ T} \right\} \quad [5.16]$$

where

$$f_1(b) = \frac{1}{2\pi} \left[\frac{\left(-\frac{b}{2}\right)^2}{1(1!)^2} + \frac{\left(-\frac{b}{2}\right)^2 \left(-\frac{b}{2} + 1\right)^2}{2(2!)^2} + \dots \right. \\ \left. + \frac{\left(-\frac{b}{2}\right)^2 \left(-\frac{b}{2} + 1\right)^2 \dots \left(-\frac{b}{2} + n - 1\right)^2}{n(n!)^2} + \dots \right], \quad [5.17]$$

$$f_2(b) = \frac{1}{8\pi^2} \left[\frac{\left(-\frac{b}{2}\right)^2}{1^2(1!)^2} + \frac{\left(-\frac{b}{2}\right)^2 \left(-\frac{b}{2} + 1\right)^2}{2^2(2!)^2} + \dots + \frac{\left(-\frac{b}{2}\right)^2 \left(-\frac{b}{2} + 1\right)^2 \dots \left(-\frac{b}{2} + n - 1\right)^2}{n^2(n!)^2} + \dots \right] \quad [5.18]$$

and

$$f_3(b) = \frac{1}{16} \frac{\Gamma(1+b)}{\Gamma^2\left(1+\frac{b}{2}\right)} \quad [5.19]$$

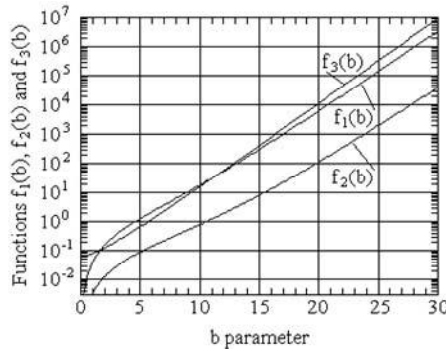


Figure 5.5. Variations of functions $f_1(b)$, $f_2(b)$ and $f_3(b)$

Figure 5.5 shows the variations of $f_1(b)$, $f_2(b)$ and $f_3(b)$ versus b . Table 5.2 lists some numerical values of these three functions for b varying between 3 and 20.

b	f₁(b)	f₂(b)	f₃(b)	b	f₁(b)	f₂(b)	f₃(b)
3.0	0.370	0.029	0.212	12.0	54.980	1.928	57.750
3.5	0.522	0.040	0.281	12.5	72.866	2.427	80.087
4.0	0.716	0.054	0.375	13.0	96.799	3.067	111.146
4.5	0.964	0.070	0.503	13.5	128.886	3.890	154.356
5.0	1.280	0.090	0.679	14.0	171.982	4.951	214.500
5.5	1.684	0.115	0.920	14.5	229.961	6.326	298.256
6.0	2.202	0.144	1.250	15.0	308.087	8.110	414.946
6.5	2.868	0.179	1.704	15.5	413.520	10.433	577.590
7.0	3.730	0.223	2.328	16.0	556.003	13.466	804.375
7.5	4.846	0.275	3.188	16.5	748.811	17.435	1,120.719
8.0	6.300	0.340	4.375	17.0	1,010.046	22.641	1,562.149
8.5	8.198	0.420	6.013	17.5	1,364.413	29.485	2,178.339
9.0	10.686	0.518	8.278	18.0	1,845.653	38.502	3,038.750
9.5	13.956	0.641	11.411	18.5	2,499.884	50.405	4,240.558
10.0	18.268	0.794	15.750	19.0	3,390.189	66.146	5,919.723
10.5	23.971	0.987	21.763	19.5	4,602.919	87.000	8,266.515
11.0	31.533	1.230	30.102	20.0	6,256.346	114.676	11,547.250
11.5	41.586	1.537	41.676				

Table 5.2. Values of functions $f_1(b)$, $f_2(b)$ and $f_3(b)$

We determine the variation coefficient [CRA 63] to be:

$$v \equiv \frac{s_D}{E(D)} = \frac{1}{\sqrt{n_0^+ T \xi}} \left[f_1(b) - \frac{f_2(b)}{n_0^+ T \xi} + \frac{\xi f_3(b)}{n_0^+ T} \right]^{1/2} \quad [5.20]$$

It should be noted that, while $E(D)$ varies linearly with duration T of the vibration, the standard deviation s_D varies with \sqrt{T} .

Example 5.2.

Figures 5.6 and 5.7 show the variations of v with ξ , b or f_0 in the particular case where the input is a white noise $G = 1 \text{ (m/s}^2\text{)}^2/\text{Hz}$ between 1 Hz and 2,000 Hz, applied during 3,600 s.

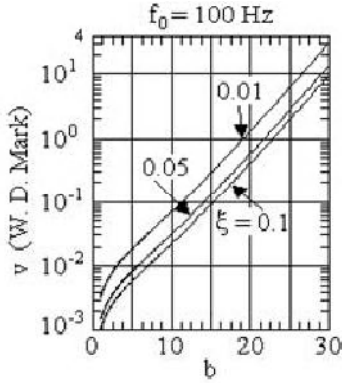


Figure 5.6. Variation coefficient of damage versus parameter b [MAR 61]

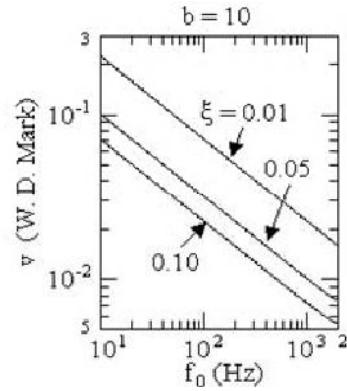


Figure 5.7. Variation coefficient of damage versus natural frequency [MAR 61]

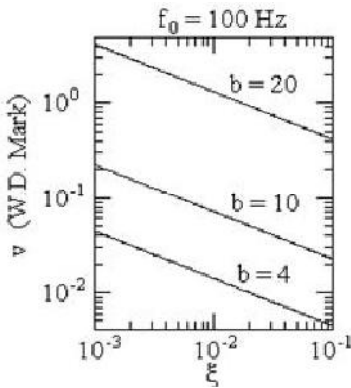


Figure 5.8. Variation coefficient of damage versus damping [MAR 61]

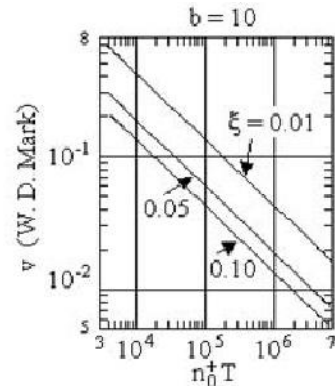


Figure 5.9. Variation coefficient of damage versus number of cycles [MAR 61]

These curves, plotted from expression [5.20], show that v :

- is an increasing function of b ;
- decreases when f_0 increases; and
- decreases when ξ increases.

Figure 5.9 shows that v decreases when time T (and therefore the number of cycles $N = n_0^+ T$) increases.

In many practical cases, it can be considered that $\xi n_0^+ T$ is large compared to unity. The last two terms of the bracket are then negligible and we have

$$s_D^2 \approx \frac{K^{2b}}{C} \frac{n_0^+ T}{\xi} \left(\sqrt{2} z_{\text{rms}} \right)^{2b} \Gamma^2 \left(1 + \frac{b}{2} \right) f_1(b) \quad [5.21]$$

The variation coefficient (or *relative dispersion*) is then written:

$$v = \frac{s_D}{E(D)} \approx \sqrt{\frac{f_1(b)}{\xi n_0^+ T}} \quad [5.22]$$

This ratio is then larger [CRA 63] since:

– ξ is smaller;

– $n_0^+ \approx f_0$ is smaller (i.e. since $\xi n_0^+ \approx \frac{f_0}{2Q} = \frac{\Delta f}{2}$, half of the interval between the half-power points is smaller); and

– T is smaller.

It can be seen that $E(D)$ is related to T and that s_D varies with \sqrt{T} .

5.3. Comparison of Mark and Bendat's results

We studied the variations of the ratio $\frac{V(\text{Bendat})}{V(\text{Mark})}$ with f_0 , b , ξ and $n_0^+ T$ in the case of the example already treated. This ratio is written, for a narrow band response:

$$\rho = \frac{\frac{1}{\sqrt{2\pi}\sqrt{\xi n_0^+ T}} \left[\Gamma(1+b) - \Gamma^2 \left(1 + \frac{b}{2} \right) \right]^{1/2}}{\frac{1}{\sqrt{\xi n_0^+ T}} \left[f_1(b) - \frac{f_2(b)}{\xi n_0^+ T} + \frac{\xi f_3(b)}{n_0^+ T} \right]^{1/2}},$$

$$\rho = \frac{1}{\Gamma\left(1 + \frac{b}{2}\right)} \sqrt{\frac{\Gamma(1+b) - \Gamma^2\left(1 + \frac{b}{2}\right)}{f_1(b) - \frac{f_2(b)}{\xi n_0^+ T} + \frac{\xi f_3(b)}{n_0^+ T}}} \quad [5.23]$$

We note the following:

– Figures 5.11 and 5.12 demonstrate that ρ does not in practice vary with ξ ; it is higher since b is bigger;

– Figures 5.10 and 5.13 demonstrate that ρ tends towards a constant value when f_0 increases from 10 Hz to 2,000 Hz (the increase is faster if ξ is larger). This limiting value is obtained by neglecting the terms of the denominator in n_0^+ ($n_0^+ \approx f_0$) yielding:

$$\rho_\ell = \frac{1}{\Gamma\left(1 + \frac{b}{2}\right)} \sqrt{\frac{\Gamma(1+b) - \Gamma^2\left(1 + \frac{b}{2}\right)}{2 \pi f_1(b)}} \quad [5.24]$$

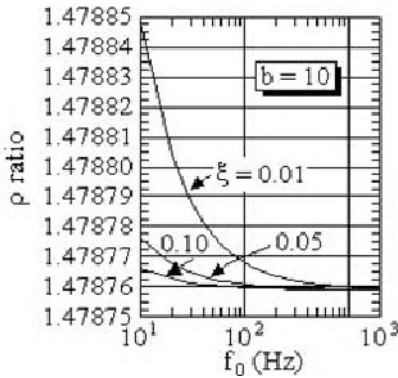


Figure 5.10. Ratio of variation coefficients calculated by J.S. Bendat [BEN 64] and W.D. Mark [MAR 61] versus natural frequency

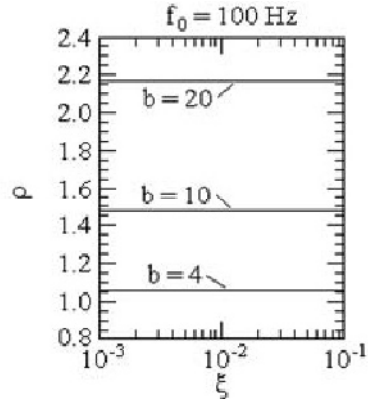


Figure 5.11. Ratio of variation coefficients calculated by J.S. Bendat [BEN 64] and W.D. Mark [MAR 61] versus damping ratio

Example 5.3.

For $b = 10$:

$$\rho_\ell = \frac{1}{120} \sqrt{\frac{3628800 - 120^2}{2\pi 18.26833488}},$$

$$\rho_\ell \approx 1.47876.$$

In the same way, ρ tends towards constant ρ_ℓ when $n_0^+ T$ tends towards infinity (Figure 5.13).

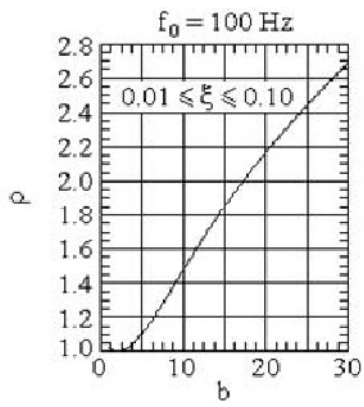


Figure 5.12. Ratio of variation coefficients calculated by J.S. Bendat [BEN 64] and W.D. Mark [MAR 61] versus parameter b

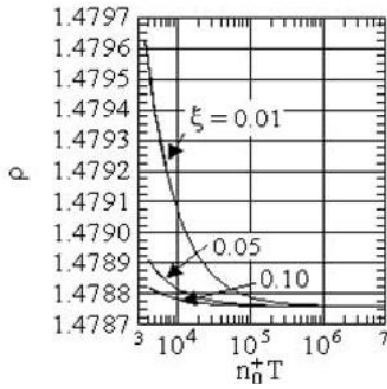


Figure 5.13. Ratio of variation coefficients calculated by J.S. Bendat [BEN 64] and W.D. Mark [MAR 61] versus number of cycles, for $b = 10$

– Figure 5.14 indicates that the ratio ρ varies very little with $n_0^+ T$. It is larger since b is larger.

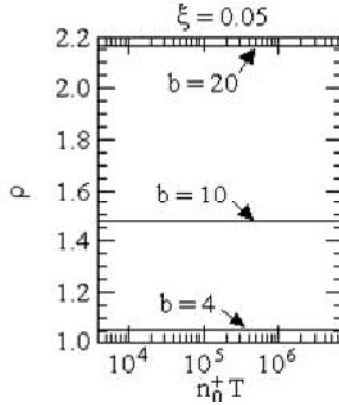


Figure 5.14. Ratio of variation coefficients calculated by J.S. Bendat [BEN 64] and W.D. Mark [MAR 61] versus number of cycles for $\xi = 0.05$

NOTE: J.P. Tang [TAN 78] shows that a limit of the failure probability is given by:

$$P(D > I) \leq \sqrt{I + \frac{\sqrt{2}[1 - E(D)]}{\sqrt{s_D^2}}} \exp \left\{ -\frac{[1 - E(D)]}{\sqrt{2 s_D^2}} \right\} \quad [5.25]$$

where D is the damage, $E(D)$ is the mean damage and s_D is the standard deviation of the damage.

Example 5.4.

Let us consider a steel structure working in tension compression, which can be comparable with a one-dof linear system, natural frequency $f_0 = 100$ Hz and relative damping $\xi = 0.05$.

Let us assume that the stress σ is related to the peak relative displacement z_p by $\sigma = K z_p$ with $K = 6.3 \cdot 10^{10}$ Pa/m and that steel has a S-N curve characterized by a parameter b equal to 10, with a constant $C = 10^{80}$ (SI units).

Finally, let us assume that this structure is subjected to a random acceleration applied to its base defined by a constant acceleration spectral density of amplitude $G_{\ddot{x}} = 1.65 \text{ (m/s}^2\text{)}^2/\text{Hz}$ between 1 Hz and 2,000 Hz.

We aim to calculate:

- the fatigue damage D after 50 hours of vibrations; and
- the standard deviation of the damage s_D .

For a system of natural frequency 100 Hz, the excitation can at first approximation (since regarded as a white noise) yield:

$$\begin{aligned} z_{\text{rms}} &= 1.29 \cdot 10^{-4} \text{ m} & r &= 0.664 \\ \dot{z}_{\text{rms}} &= 0.0809 \text{ m/s} & n_p^+ &= 150.47 \\ \ddot{z}_{\text{rms}} &= 76.48 \text{ m/s}^2 & n_0^+ &= 99.87 \\ \ddot{y}_{\text{rms}} &= 51.147 \text{ m/s}^2 & & \left[\approx (2\pi f_0)^2 z_{\text{rms}} \right]. \end{aligned}$$

Using the approximate relations mentioned above:

D : relation [4.26]: 0.86270
Rayleigh: 0.86196

s_D : relation [5.6]: 0.00577
Bendat relation: 0.00575
Mark relation: 0.003886

v : s_D Mark / $E(D)$ Rayleigh: 0.004508
 s_D Bendat / $E(D)$ Rayleigh: 0.0066666
Relation [5.6]/ D relation [4.26]: 0.006693

$P(D > 1) : < 2.48 \times 10^{-7}$ for s_D Bendat

$< 8.83 \times 10^{-11}$ for Mark

$< 2.93 \times 10^{-7}$ for s_D Bendat [5.6] and [4.26]

The mean damage calculated using Rayleigh's assumption is therefore slightly lower than the value obtained with relation [4.26]. The approximate Bendat expression gives a value of s_D very close to that deduced from relation [5.6]. The Mark relation definitely leads to a lower result. This variation is not due to neglecting the assumptions selected to establish these expressions ($r = 0.664$ instead of 1); since a difference is still observed if the coefficient r is very near to unity.

Mean fatigue life:

$$T = \frac{50 \text{ hours}}{D} \approx 57.9 \text{ hours.}$$

Mean numbers of cycles to failure (under random vibrations):

$$n_0^+ T = 99.87 \cdot 57.9 \cdot 3600 \approx 2.08 \cdot 10^7 \text{ cycles.}$$

Rms values:

$$\ddot{x}_{\text{rms}} = \sqrt{(2000 - 1) \cdot 1.65} = 57.43 \text{ m/s}^2,$$

$$z_{\text{rms}} = \frac{\ddot{x}_{\text{rms}}}{\omega_0^2 \left\{ \left[1 - \left(\frac{80}{100} \right)^2 \right]^2 + \frac{1}{10^2} \left(\frac{80}{100} \right)^2 \right\}^{\frac{1}{2}}},$$

$$z_{\text{rms}} \approx 3.94 \cdot 10^{-4} \text{ m, and}$$

$$z_m \approx \sqrt{2} z_{\text{rms}} \approx 5.58 \cdot 10^{-4} \text{ m.}$$

Number of cycles to failure under a sinusoidal stress having the same rms value and a frequency equal to 80 Hz:

$$N (K z_m)^b = 10^{80},$$

$$N = \frac{10^{80}}{\left(6.3 \cdot 10^{10} \cdot 5.58 \cdot 10^{-4}\right)^{10}}, \text{ and}$$

$$N \approx 34\,694 \text{ cycles.}$$

Now let us calculate the number of cycles to failure under sinusoidal stress, which creates the same rms response as the random vibration.

The random vibration generates at 100 Hz a rms response of (for $Q = 10$):

$$z_{\text{rms}} = 1.29 \cdot 10^{-4} \text{ m}$$

To obtain this response with a sinewave excitation of frequency 80 Hz (for example), an amplitude would be needed equal to

$$\ddot{x}_m = \ddot{x}_{\text{rms}} \sqrt{2} = \frac{\omega_0^2 z_{\text{rms}} \sqrt{2}}{Q},$$

$$\ddot{x}_m = \frac{(2\pi \cdot 80)^2 \cdot 1.29 \cdot 10^{-4} \sqrt{2}}{10} \approx 4.61 \text{ m/s}^2,$$

$$z_m = z_{\text{rms}} \sqrt{2} \approx 1.82 \cdot 10^{-4} \text{ m,}$$

yielding

$$N = \frac{10^{80}}{\left(6.3 \cdot 10^{10} \cdot 1.82 \cdot 10^{-4}\right)^{10}} \approx 2.55 \cdot 10^9 \text{ cycles.}$$

5.4. Statistical S-N curves

5.4.1. Definition of statistical curves

We showed that, for Gaussian random excitation and a narrow band response ($r = 1$), the damage can be expressed in form [4.41]:

$$E(D) = \frac{K^b}{C} n_0^+ T \left(\sqrt{2} z_{\text{rms}} \right)^b \Gamma \left(1 + \frac{b}{2} \right)$$

and the standard deviation s_D by the approximate relations:

Bendat [5.15]:

$$s_D = \frac{E(D)}{\sqrt{2 \pi \xi n_0^+ T}} \left[\frac{\Gamma(1+b) - \Gamma^2\left(1 + \frac{b}{2}\right)}{\Gamma^2\left(1 + \frac{b}{2}\right)} \right]^{1/2},$$

and

Mark [5.20]:

$$s_D = \frac{E(D)}{\sqrt{\xi n_0^+ T}} \left[f_1(b) - \frac{f_2(b)}{\xi n_0^+ T} + \frac{\xi f_3(b)}{n_0^+ T} \right]^{1/2}.$$

In the following, we will consider the curves defined by the fatigue damage $E(D) - \alpha s_D$ and $E(D) + \alpha s_D$ where the constant α is a function of the selected degree of confidence, for a given distribution law of the damage (the most frequently used law being the log-normal distribution).

For a given stress level, these values of the damage allow the calculation of the number of cycles $n_0^+ T$ for which failure can take place. These curves consider only the random aspect of the stress and do not take into account the scatter of the fatigue strength of material; more important and studied elsewhere (Chapter 1).

5.4.2. Bendat's formulation

The equation of the first curve, defined by

$$D = E(D) - \alpha s_D \quad [5.26]$$

for $D = 1$ (failure) can be also written

$$E(D) (1 - \alpha v) = 1 \quad [5.27]$$

i.e.

$$E(D) \left[1 - \frac{\alpha}{\sqrt{2 \pi \xi n_0^+ T}} \sqrt{\frac{\Gamma(1+b) - \Gamma^2\left(1 + \frac{b}{2}\right)}{\Gamma^2\left(1 + \frac{b}{2}\right)}} \right] = 1 \quad [5.28]$$

Let us set $N = n_0^+ T$,

$$A = \frac{K^b}{C} (\sqrt{2} z_{\text{rms}})^b \Gamma\left(1 + \frac{b}{2}\right) \quad [5.29]$$

and

$$B = \frac{\Gamma(1+b) - \Gamma^2\left(1 + \frac{b}{2}\right)}{\Gamma^2\left(1 + \frac{b}{2}\right)} \quad [5.30]$$

This becomes

$$N = \frac{(2+F) \pm \sqrt{F(F+2)}}{2A} \quad [5.31]$$

with

$$F = \frac{AB\alpha^2}{2\pi\xi} \quad [5.32]$$

The second equation ($E(D)(1 + \alpha v) = 1$) leads to the same result.

Example 5.5.

Let us consider a random noise of constant PSD between 1 Hz and 2,000 Hz with an amplitude G such that $1 \leq G \leq 9$ and then $2 \leq G \leq 30$ (to explore two ranges of stresses).

Let us suppose that:

$$b = 10,$$

$$\xi = 0.05,$$

$$f_0 = 100 \text{ Hz},$$

$$K = 6.3 \cdot 10^{10} \text{ Pa/m and}$$

$$C = 10^{80} \text{ (SI units).}$$

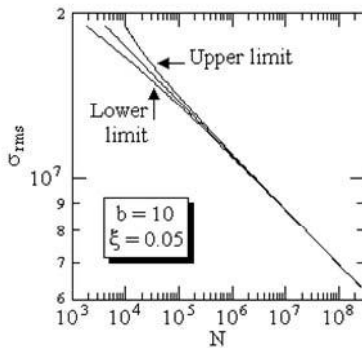


Figure 5.15. Mean ± 3 standard deviations S - N curves for high values of N

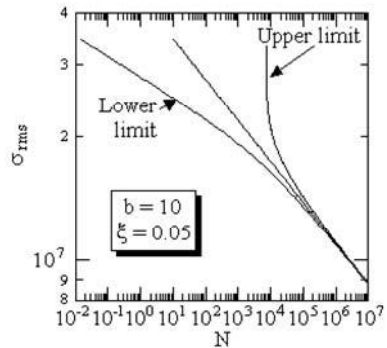


Figure 5.16. Mean ± 3 standard deviations S - N curves for low values of N

Figures 5.15 and 5.16 show the $s(N)$ curves obtained from these data for $E(D) = 1$, $E(D) - 3 s_D = 1$ and $E(D) + 3 s_D = 1$.

It is seen that, when the rms stress σ_{rms} is large, the curves corresponding to $E(D) + 3 s_D$ tend towards a limit which can be calculated as follows.

When G is large, A becomes large and

$$N [E(D) + \alpha \sigma_D] \rightarrow \frac{B \alpha^2}{2 \pi \xi}$$

whereas $N [E(D) - \alpha s_D] \rightarrow 0$. For $\alpha = 3$, $\xi = 0.05$ and $b = 10$, we have $B = 251$ and the limit is equal to 7,191 cycles. This limit increases very quickly with b and decreases when ξ increases (Figure 5.17).

We must however point out one of the assumptions in calculating s_D which supposes that $2 \pi n_0^+ T \xi$ is large.

For $N = 1000$, we have $2 \pi N \xi = 314$. It is at least necessary that $2 \pi n_0^+ T \xi = 10^4$, i.e. that $N > 3 \cdot 10^4$, since this eliminates this limit, which does not have any physical reality.

Figures 5.15 and 5.16 show that dispersion is stronger for the high levels of excitation (contrary to dispersion related to the fatigue strength of material).

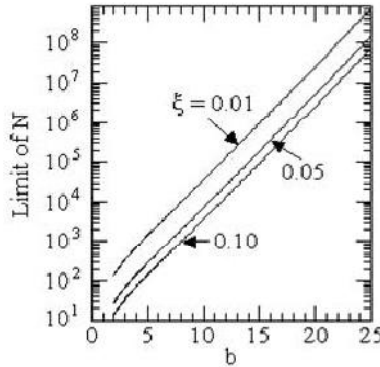


Figure 5.17. Limit of number of cycles to failure for $\alpha = 3$

5.4.3. Mark's formulation

As previously, let us write that, to failure:

$$E(D) - \alpha s_D = E(D) (1 - \alpha v) = 1$$

yielding

$$\frac{K^b}{C} n_0^+ T (\sqrt{2} z_{\text{rms}})^b \Gamma\left(1 + \frac{b}{2}\right) \left\{ 1 - \frac{\alpha}{\sqrt{\xi n_0^+ T}} \left[f_1(b) - \frac{f_2(b)}{\xi n_0^+ T} + \frac{\xi f_3(b)}{n_0^+ T} \right]^{1/2} \right\} = 1.$$

Let us also set

$$N = n_0^+ T$$

and

$$A = \frac{K^b}{C} (\sqrt{2} z_{\text{rms}})^b \Gamma\left(1 + \frac{b}{2}\right).$$

We then have:

$$N = \frac{\left[2 + \frac{\alpha^2 A}{\xi} f_1(b) \right] \pm \sqrt{\left[2 + \frac{\alpha^2 A}{\xi} f_1(b) \right]^2 - 4 \left\{ 1 + \frac{\alpha^2 A^2}{\xi} \left[\frac{f_2(b)}{\xi} - \xi f_3(b) \right] \right\}}}{2 A} \quad [5.33]$$

provided that the discriminant is positive or zero or that:

$$\alpha^2 A f_1^2(b) + 4 A f_3(b) \xi^2 + a f_1(b) \xi - 4 A f_2(b) \geq 0 \quad [5.34]$$

It can be shown that this expression is always positive. The condition $E(D) + \alpha s_D = 1$ leads to the same expression of N .

Example 5.6.

With the numerical conditions of the previous example, we obtain for $1 \leq G \leq 9$ the curves in Figure 5.18, which show the same tendency of the scatter to increase with σ_{rms} . Comparison of Figures 5.18 and 5.19 allows the influence of damping to be evaluated.

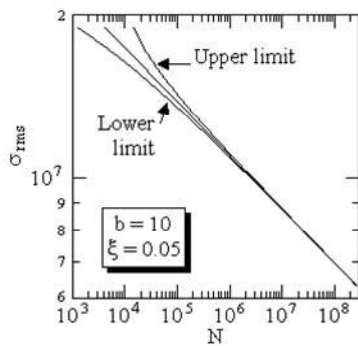


Figure 5.18. Mean ± 3 standard deviations S-N curves for $b = 10$ and $\xi = 0.05$ [MAR 61]

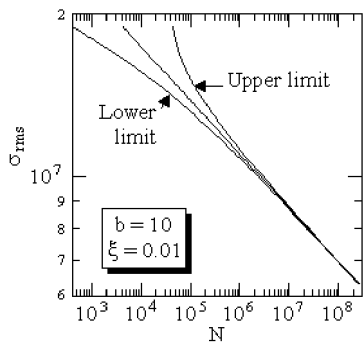


Figure 5.19. Mean ± 3 standard deviations S-N curves for $b = 10$ and $\xi = 0.01$ [MAR 61]

With the same calculation criteria but with $\xi = 0.01$ (instead of 0.05), to obtain the same curve $E(D)$ it is necessary that $0.2 \leq G \leq 1.8$, i.e. a weaker excitation. Scatter on the other hand tends to increase.

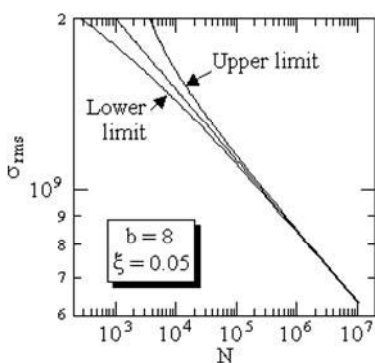


Figure 5.20. Mean ± 3 standard deviations S-N curves, for $b = 8$ and $\xi = 0.05$ [MAR 61]

Lastly, the same study carried out with $b = 8$ instead of 10 shows that, to obtain the same damage, the amplitude G of the PSD of the excitation must be greater (Figure 5.20, for $\xi = 0.05$).

NOTE: As previously, all these curves should not be plotted (with this formulation) for too large a value of G , i.e. for a low numbers of cycles.

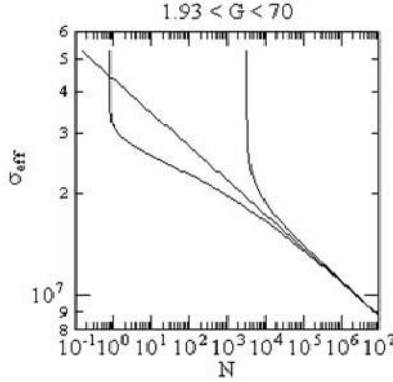


Figure 5.21. *S-N curves for low numbers of cycles [MAR 61]*

By considering the first example ($b = 10$, $\xi = 0.05$), we note that if G is too large (between 2 and 10), the number of cycles corresponding to $E(D) \pm 3 s_D = 1$ also tends towards a (not physical) limit equal to (Figure 5.21):

$$N [E(D) - 3 s_D] \rightarrow 0.65,$$

$$N [E(D) + 3 s_D] \rightarrow 3288 \text{ cycles.}$$

This limit can be found by calculation from relation [5.33] (for $\alpha = 3$):

$$N = \frac{1}{A} + \frac{9}{2} \frac{f_1(b)}{\xi} \pm \sqrt{\left[\frac{1}{A} + \frac{9}{2} \frac{f_1(b)}{\xi} \right]^2 - \left[\frac{1}{A^2} + \frac{9}{\xi} \left(\frac{f_2(b)}{\xi} - \xi f_3(b) \right) \right]} \quad [5.35]$$

When G becomes large, and therefore also A , we have

$$N \approx \frac{9}{2} \frac{f_1(b)}{\xi} \pm \sqrt{\left[\frac{9}{2} \frac{f_1(b)}{\xi} \right]^2 - \frac{9}{\xi} \left[\frac{f_2(b)}{\xi} - \xi f_3(b) \right]}. \quad [5.36]$$

The upper limit increases with b ; it is weaker when damping is larger. The lower limit decreases with b . Curves in Figure 5.21 are plotted out of the range of approximations used for the calculation of s_D . It was seen that $N \gg \frac{1}{2\xi}$ is needed, i.e. in our example $N \gg 10$.

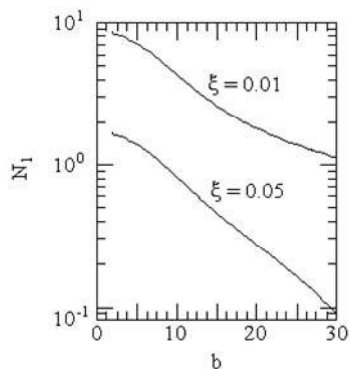


Figure 5.22. Limit of number of cycles relating to mean damage minus 3 standard deviations

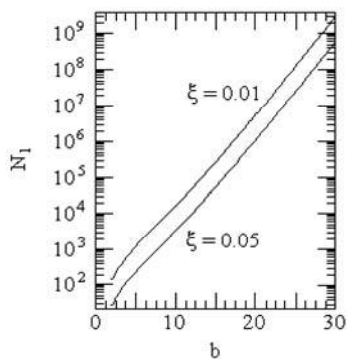


Figure 5.23. Limit of number of cycles relating to mean damage plus 3 standard deviations

In Figures 5.22 and 5.23, we note that N must be somewhat larger than 104 cycles for the upper limit.

Chapter 6

Fatigue Damage using other Calculation Assumptions

6.1. S-N curve represented by two segments of a straight line on logarithmic scales (taking into account fatigue limit)

It is assumed that the S-N curve is defined by:

- $N \sigma^b = C$ for $\sigma > \sigma_D$; or
- $\sigma = \sigma_D$ for $\sigma \leq \sigma_D$.

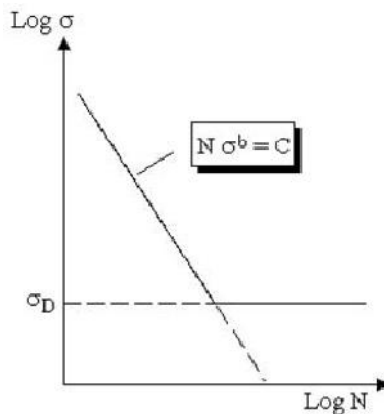


Figure 6.1. S-N curve with fatigue limit (logarithmic scales)

The damage is equal to

$$D = \int_0^{+\infty} \frac{dn}{N} = \int_0^{+\infty} \frac{n_p^+ T}{N} q(\sigma) d\sigma,$$

$$D = \frac{n_p^+ T}{C} \int_{\sigma_D}^{+\infty} \sigma^b q(\sigma) d\sigma \quad [6.1]$$

the probability density $q(\sigma)$ described by equation [4.24] for a Gaussian excitation. If we can consider that the peak distribution of the response follows a Rayleigh distribution, we have:

$$q(\sigma) = \frac{\sigma}{\sigma_{rms}^2} e^{-\frac{\sigma^2}{2\sigma_{rms}^2}} \quad [6.2]$$

and

$$D = \frac{n_0^+ T}{C} \int_{\sigma_D}^{\infty} \frac{\sigma^{b+1}}{\sigma_{rms}^2} e^{-\frac{\sigma^2}{2\sigma_{rms}^2}} d\sigma \quad [6.3]$$

Let us set

$$\alpha = \frac{\sigma^2}{2\sigma_{rms}^2},$$

$$d\alpha = \frac{\sigma d\sigma}{\sigma_{rms}^2}$$

We have

$$D = \frac{n_0^+ T}{C} \left(\sigma_{rms} \sqrt{2} \right)^b \int_{\tau_D}^{\infty} \alpha^{\frac{b}{2}} e^{-\alpha} d\alpha \quad [6.4]$$

with

$$\tau_D = \frac{\sigma_D^2}{2\sigma_{rms}^2}.$$

The integral

$$\gamma(a, x) = \int_0^a \alpha^{x-1} e^{-\alpha} d\alpha \quad [6.5]$$

is the incomplete gamma function (with $x = 1 + \frac{b}{2}$):

$$D = \frac{n_0^+ T}{C} (\sigma_{\text{rms}} \sqrt{2})^b \left[\int_0^\infty \alpha^{b/2} e^{-\alpha} d\alpha - \int_0^{\tau_D} \alpha^{b/2} e^{-\alpha} d\alpha \right],$$

$$D = \frac{n_0^+ T}{C} (\sigma_{\text{rms}} \sqrt{2})^b \left[\Gamma\left(1 + \frac{b}{2}\right) - \gamma\left(\tau_D, 1 + \frac{b}{2}\right) \right]$$

and

$$D = \frac{n_0^+ T (\sigma_{\text{rms}} \sqrt{2})^b}{C} \Gamma\left(1 + \frac{b}{2}\right) \left[1 - \frac{\gamma\left(\tau_D, 1 + \frac{b}{2}\right)}{\Gamma\left(1 + \frac{b}{2}\right)} \right] \quad [6.6]$$

While setting $\sigma = K z_p$,

$$D = \frac{K^b}{C} n_0^+ T (z_{\text{rms}} \sqrt{2})^b \Gamma\left(1 + \frac{b}{2}\right) \left[1 - \frac{\gamma\left(\tau_D, 1 + \frac{b}{2}\right)}{\Gamma\left(1 + \frac{b}{2}\right)} \right] \quad [6.7]$$

It is noted that if τ_D tends towards zero, expression [6.7] tends towards relation [4.41].

J.W. Miles [MIL 54] estimates that it is possible to neglect the fatigue limit when the stresses are distributed over a broad range.

Figure 6.2 shows the variations of the ratio

$$\frac{\text{damage with fatigue limit}}{\text{damage whitout limit}} = 1 - \frac{\gamma\left(\tau_D, 1 + \frac{b}{2}\right)}{\Gamma\left(1 + \frac{b}{2}\right)}$$

plotted versus the ratio τ_D for various values of b . It is noted that the damage decreases when the endurance limit increases; the rate of decrease is faster when b is smaller.

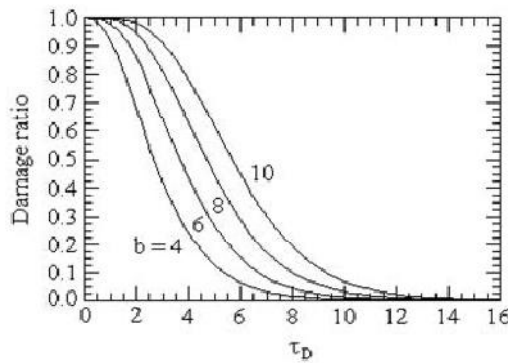


Figure 6.2. Ratio of the damage calculated with and without taking into account fatigue limit

6.2. S-N curve defined by two segments of straight line on log-lin scales

The S-N curves published in the literature are often plotted in logarithmic-linear scales and then are comparable with two segments of straight line. The horizontal part corresponds to the fatigue limit.

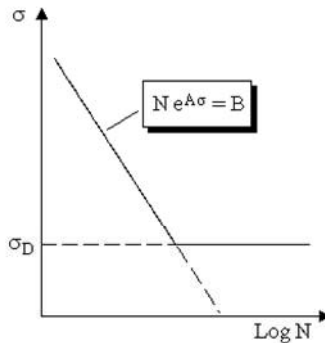


Figure 6.3. S-N curve with fatigue limit in semi-logarithmic scales

With this representation, this curve can be described analytically by [MUS 60]:

$$\left. \begin{array}{ll} N e^{A\sigma} = B & \text{for } \sigma > \sigma_D \\ \sigma = \sigma_D & \text{elsewhere} \end{array} \right\} \quad [6.8]$$

where A and B are constants characteristic of the material. The damage is then equal to

$$D = \int_0^{+\infty} \frac{dn}{N} = \int_{\sigma_D}^{\infty} n_p^+ \frac{T}{N} q(\sigma) d\sigma \quad [6.9]$$

$$D = \frac{n_p^+ T}{B} \int_{\sigma_D}^{\infty} q(\sigma) e^{A\sigma} d\sigma \quad [6.10]$$

where $q(\sigma)$ is the probability density function of stress peaks, given by equation [4.24]. While comparing this distribution with Rayleigh's law, this becomes:

$$q(\sigma) = \frac{\sigma}{\sigma_{rms}^2} e^{-\frac{\sigma^2}{2\sigma_{rms}^2}},$$

$$D = \frac{n_0^+ T}{B \sigma_{rms}^2} \int_{\tau_D}^{\infty} \sigma e^{\left(A\sigma - \frac{\sigma^2}{2\sigma_{rms}^2}\right)} d\sigma \quad [6.11]$$

Let us set $\tau^2 = \frac{\sigma^2}{2\sigma_{rms}^2}$. This implies that $d\tau = \frac{d\sigma}{\sqrt{2}\sigma_{rms}}$, yielding

$$D = 2 \frac{n_0^+ T}{B} \int_{\tau_D}^{\infty} \tau e^{(a - \tau^2)} d\tau$$

with $\tau_D = \frac{\sigma_D}{\sqrt{2}\sigma_{rms}}$ and $a = A\sqrt{2}\sigma_{rms}$.

However,

$$\int_{\tau_D}^{\infty} \tau e^{(a - \tau^2)} d\tau = \int_0^{\infty} \tau e^{(a - \tau^2)} d\tau - \int_0^{\tau_D} \tau e^{(a - \tau^2)} d\tau = I_1 - I_2$$

$$I_1 = \int_0^{\infty} \tau e^{(a - \tau^2)} d\alpha = e^{\frac{a^2}{4}} \int_0^{\infty} \tau e^{-\left(\tau - \frac{a}{2}\right)^2} d\tau$$

Let us set $u = \tau - \frac{a}{2}$

$$I_1 = e^{\frac{a^2}{4}} \int_0^\infty \left(u + \frac{a}{2}\right) e^{-u^2} du$$

$$I_1 = e^{\frac{a^2}{4}} \int_0^\infty u e^{-u^2} du + \frac{a}{2} e^{\frac{a^2}{4}} \int_0^\infty e^{-u^2} du = e^{\frac{a^2}{4}} \left(-\frac{e^{-u^2}}{2} \right)_0^\infty + \frac{a}{2} e^{\frac{a^2}{4}} \left[\frac{\sqrt{\pi}}{2} \right]$$

$$I_1 = \frac{e^{a^2/4}}{2} \left(1 + \frac{a\sqrt{\pi}}{2} \right).$$

In addition,

$$I_2 = \int_0^{\tau_D} \tau e^{(a\tau - \tau^2)} d\tau = \int_0^{\tau_D} \tau e^{\frac{a^2}{4} - \left(\tau - \frac{a}{2}\right)^2} d\tau$$

$$I_2 = e^{\frac{a^2}{4}} \int_0^{\tau_D} \tau e^{-\left(\tau - \frac{a}{2}\right)^2} d\tau$$

$$I_2 = e^{\frac{a^2}{4}} \int_{-\frac{a}{2}}^{\tau_D - \frac{a}{2}} \left(u + \frac{a}{2}\right) e^{-u^2} du$$

$$I_2 = e^{\frac{a^2}{4}} \left[\int_{-\frac{a}{2}}^{\tau_D - \frac{a}{2}} u e^{-u^2} du + \frac{a}{2} \int_{-\frac{a}{2}}^{\tau_D - \frac{a}{2}} e^{-u^2} du \right]$$

$$I_2 = e^{\frac{a^2}{4}} \left[\left(-\frac{e^{-u^2}}{2} \right)_{-\frac{a}{2}}^{\tau_D - \frac{a}{2}} + \frac{a}{2} \left(\int_{-\frac{a}{2}}^0 e^{-u^2} du + \int_0^{\tau_D - \frac{a}{2}} e^{-u^2} du \right) \right].$$

This yields

$$D = \frac{n_0^+ T}{B} e^{\frac{a^2}{4}} \left[1 + e^{-\left(\tau_D - \frac{a}{2}\right)^2} - e^{-\frac{a^2}{4}} + \frac{a\sqrt{\pi}}{2} \left(1 - \operatorname{erf}\left(\tau_D - \frac{a}{2}\right) - \operatorname{erf}\left(\frac{a}{2}\right) \right) \right]. \quad [6.12]$$

If $\tau_D = 0$,

$$D = \frac{n_0^+ T}{B} e^{\frac{a^2}{4}} \left[1 + \frac{a\sqrt{\pi}}{2} \right],$$

$$D = \frac{n_0^+ T}{B} e^{\frac{A^2 \sigma_{rms}^2}{2}} \left[1 + A \sigma_{rms} \sqrt{\frac{\pi}{2}} \right] \quad [6.13]$$

6.3. Hypothesis of non-linear accumulation of damage

6.3.1. Corten-Dolan's accumulation law

Miner's rule is most frequently utilized for the calculation of fatigue damage. Some attempts have been made to use other assumptions [SYL 81], such as Corten-Dolan's [COR 56] [COR 59], which assume that the damage is added in a non-linear way according to

$$N_g = \frac{N_1}{\sum_{i=1}^j \alpha_i \left(\frac{\sigma_i}{\sigma_1} \right)^d} \quad [6.14]$$

where α_i and d are constants.

Knowing that the S-N curve can be represented by

$$N' \sigma^d = A \quad [6.15]$$

we have, for random stress,

$$D = \frac{n_p^+ T}{A} \sigma_{rms}^d \int_0^\infty u^d q(u) du \quad [6.16]$$

where $u = \frac{\sigma}{\sigma_{\text{rms}}}$. H. Corten and T. Dolan showed that d is a constant when σ_1 varies. It is therefore the constant A which is related to σ_1 .

For untruncated random loadings or if the largest peaks do not exceed the yield stress of material, the value of σ_1 depends on the rms stress level. Let us set $\sigma_1 = \sigma'_1$, σ'_1 being the stress threshold exceeded by the largest peak in an interval containing m peaks. When m is large, σ'_1 is approximately equal to the largest peak.

The modified fatigue curve intersects the traditional curve in σ'_1 , so that the expressions $N(\sigma) = \frac{C}{\sigma^b}$ and $N' \sigma^d = A$ can be identified for $\sigma = \sigma'_1$; yielding

$$A = C (\sigma'_1)^{d-b} \quad [6.17]$$

Substituting this value in equation [6.16], we have:

$$D = \frac{n_p^+ T}{C} (u'_1)^{d-b} \sigma_{\text{rms}}^b \int_0^\infty u^d q(u) du \quad [6.18]$$

where $u'_1 = \frac{\sigma'_1}{\sigma_{\text{rms}}}$. Since u'_1 and the integral are constants for a given rms level, this expression differs from that obtained with Miner's rule only by one constant.

If the stress is truncated, or if the peaks of stress exceed the yield stress (a form of truncation), σ_1 is fixed for the various levels of rms stress and the expression [6.16] is applicable with A constant such that

$$A = \sigma_1^{d-b} C \quad [6.19]$$

When there is truncation, the random fatigue curve is parallel to the modified curve. If there is no truncation, it is parallel to that established in sinusoidal mode.

6.3.2. Morrow's accumulation model

R.G. Lambert [LAM 88] uses the accumulation damage model developed by J.D. Morrow [MOR 83] in the form:

$$D_{\sigma} = \frac{n_{\sigma}}{N_{\sigma}} \left(\frac{\sigma}{\sigma_{\max}} \right)^d \quad [6.20]$$

where σ is the amplitude of the stress, σ_{\max} is the value of the greatest stress, n_{σ} is the number of cycles of stress at level σ , N_{σ} is the number of cycles to failure at level σ and d is the plastic work exponent.

We saw from equation [4.11] that, in the linear case, the elementary damage dD can be written

$$dD = \frac{dn}{N} = \frac{n_p^+ T}{N} q(\sigma) d\sigma$$

where $N = \frac{C}{\sigma^b}$. Using the non-linear accumulation law [6.20], we have:

$$dD = \left(\frac{\sigma}{\sigma_{\max}} \right)^d \frac{dn}{N},$$

$$dD = \frac{n_p^+ T}{C} q(\sigma) \sigma^b \left(\frac{\sigma}{\sigma_{\max}} \right)^d d\sigma$$

where σ_{rms} is the rms stress. Let us denote $F = \frac{\sigma_{\max}}{\sigma_{\text{rms}}}$ as the crest factor, then:

$$\frac{\sigma}{\sigma_{\max}} = \frac{\sigma}{\sigma_{\text{rms}}} \frac{\sigma_{\text{rms}}}{\sigma_{\max}} = \frac{\sigma}{F \sigma_{\text{rms}}}$$

$$dD = \frac{n_p^+ T}{C} \frac{\sigma^{b+d}}{F^d \sigma_{\text{rms}}^d} q(\sigma) d\sigma$$

$$D = \frac{n_p^+ T}{C F^d \sigma_{\text{rms}}^d} \int_0^{+\infty} \sigma^{b+d} q(\sigma) d\sigma \quad [6.21]$$

Let us set $u = \frac{\sigma}{\sigma_{\text{rms}}}$ as previously. Then,

$$D = \frac{n_p^+ T}{C F^d} \sigma_{\text{rms}}^b \int_0^{\infty} u^{b+d} q(u) du \quad [6.22]$$

(alternatively, the integral can be calculated between the limits 0 and σ_{max} .) If $\sigma = K z$,

$$D = \frac{K^b n_p^+ T}{C F^d} z_{\text{rms}}^b \int_0^{\infty} u^{b+d} q(u) du \quad [6.23]$$

The parameter d varies between -0.25 and -0.20 . Integration can be carried out in practice between 0 and 8. The damage calculated under these conditions is higher than that obtained under a linear assumption of approximately 10% to 15%. Suppose that $q(u)$ is the probability density of a Rayleigh distribution.

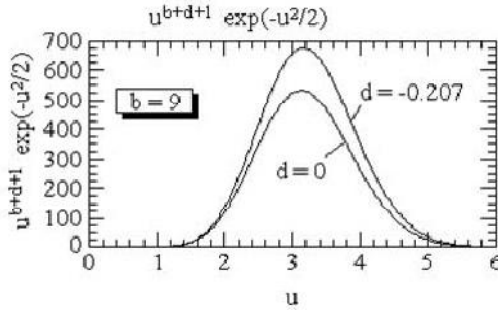


Figure 6.4. Probability density of damage using non-linear damage accumulation law of Corten-Dolan

Figure 6.4 shows the variations of the probability density $u^{b+d+1} / e^{u^2/2}$ for $d = 0$ (linear case) and $d = -0.207$ (non-linear case). It is noted that the damage is primarily created by the stress peaks between 2 and 5 times the rms value σ_{rms} .

When peaks larger than $5 \sigma_{\text{rms}}$ occur, they are extremely damaging. The peaks lower than $2 \sigma_{\text{rms}}$ are very frequent, but contribute little to the damage.

6.4. Random vibration with non-zero mean: use of modified Goodman diagram

It was assumed until now that the mean stress is zero. When this is not the case, H.C. Schjelderup [SCH 59] proposes using the modified diagram of Goodman or that of Gerber [LAL 92] (Chapter 1). These diagrams can be represented analytically by

$$\frac{\Delta\sigma}{R_m} = \frac{\Delta\sigma_0}{R_m} \left[1 - \left(\frac{\sigma_m}{R_m} \right)^n \right] \quad [6.24]$$

where R_m is the ultimate stress, $\Delta\sigma_0$ is the amplitude of the zero mean sinusoidal fluctuation, $\Delta\sigma$ is the amplitude of the non-zero mean sinusoidal stress fluctuation, σ_m is the mean stress (> 0 if it is about a tension, < 0 if it is a compression) and n is a constant ($=1$ for the Goodman relation and $=2$ for the Gerber relation).

This relation can be written

$$\Delta\sigma_0 = \frac{\Delta\sigma}{1 - \left(\frac{\sigma_m}{R_m} \right)^n} \quad [6.25]$$

If $N(\Delta\sigma_0)$ represents the S-N curve with zero mean stress, the S-N curve with mean stress σ_m is such that

$$N_m(\Delta\sigma) = N_0 \left[\frac{\Delta\sigma}{1 - (\sigma_m/R_m)^n} \right] \quad [6.26]$$

This result can be applied to the problem of random vibrations by making the following assumptions:

- the distribution of the peaks of stress is not modified by the variations of the mean stress; and
- Miner's rule constitutes a satisfactory tool for the calculation of the fatigue life for a mean stress.

In this case, relation [6.24] can be transformed for application to the random vibrations according to

$$\frac{\sigma_{\text{rms}}}{R_m} = \frac{\sigma_{0\text{rms}}}{R_m} \left[1 - \left(\frac{\sigma_m}{R_m} \right)^n \right] \quad [6.27]$$

where σ_{rms} is the rms stress for a non-zero mean and $\sigma_{0\text{rms}}$ is the rms stress for a zero mean.

The effects of the non-zero mean stress are taken into account while replacing σ_{rms} by $\frac{\sigma_{\text{rms}}}{1 - (\sigma_m/R_m)^n}$. We can therefore expect similar tendencies in fatigue with random vibrations and sinusoidal vibrations. The restrictions imposed by the selected assumptions limit this result to the modes of fatigue at long lifetime, low stress levels.

An experimental study by S.L. Bussa [BUS 67], carried out on notched samples subjected to random vibrations having various spectral shapes, shows that the effect of the mean stress is in accordance with the Goodman relation. This result is confirmed by work of R.G. Lambert [LAM 93].

NOTE: *Another way of taking into account the influence of the mean stress using the same principles consists of modifying the constant C_1 in relation [4.115] according to [LAM 93]:*

$$C_{1m} = C_1 \left[1 - \left(\frac{\sigma_m}{\sigma'_f} \right)^n \right]^b \quad [6.28]$$

or to directly correct the damage by fatigue as in

$$D_m = D \left[1 - \left(\frac{\sigma_m}{\sigma'_f} \right)^n \right]^{-b} \quad [6.29]$$

In these relations, σ_m must be lower than σ'_f . If this is not the case, failure takes place statically before the application of the alternate stress. σ'_f is the true ultimate stress, causing the failure for dynamics cycle.

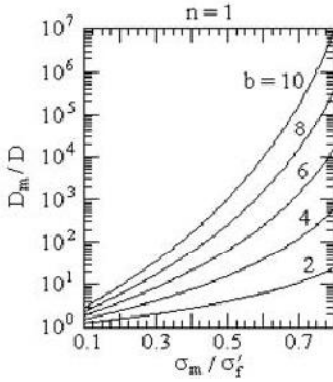


Figure 6.5. Ratio of the damage calculated with a non-zero mean stress and with a zero mean stress, for $n = 1$

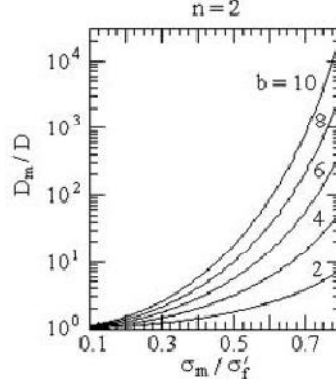


Figure 6.6. Ratio of the damage calculated with a non-zero mean stress and with a zero mean stress, for $n = 2$

6.5. Non-Gaussian distribution of instantaneous values of signal

The assumption is generally made that the distribution of the instantaneous values of the signal of excitation (and thus of the response) follows a Gaussian law and, consequently, that the distribution of the peaks of the response of the excited system follows a Rayleigh distribution [BEL 59] [MIL 54] [SCH 58].

6.5.1. Influence of distribution law of instantaneous values

A study by R.T. Booth and M.N. Kenefick [BOO 76], carried out on steel test bars, allowed the comparison of the results obtained with three distributions, characterized by their crossings curve of the form:

$$N = N_0 e^{-B \left(\frac{\sigma}{\sigma_{rms}} \right)^A} \quad [6.30]$$

where $N_0 = n_0^+ T$. For a Gaussian distribution, $A = 2$ and $B = 0.5$ and, for an exponential distribution, $A = 1$ and $C = \sqrt{2}$. The three laws considered are characterized as follows:

- Gaussian distribution truncated to 4 times the rms value (σ_{rms});

– a distribution close to that observed experimentally from measurements in the real environment on a vehicle suspension device ($A = 1.384$, $B = 0.955$) with truncation to $5.5 \sigma_{\text{rms}}$; and

– a distribution obtained in the real environment measured on dampers ($A = 1.19$, $B = 1.098$), with a truncation at $6.5 \sigma_{\text{rms}}$.

The irregularity coefficient is identical in the three cases, about 0.96 (PSD of the same shapes) and the S-N curve is plotted with σ_{rms} on ordinates:

$$N_0 (\sigma_{\text{rms}} - \sigma_D)^b = C \quad [6.31]$$

where σ_D is fatigue limit stress. These authors note the following points:

– The changes of distribution law have a significant influence on the fatigue strength: the distribution of the instantaneous values of the signal is therefore an important factor. The assumption of a Gaussian signal can lead to significant errors if it is not checked.

– The results obtained with the Miner rule are always optimistic (there is failure under test below $\sum_i \frac{n_i}{N_i} = 1$), but not unreasonable taking into account the scatter observed in the fatigue tests.

– The calculations carried out under the Gaussian assumption differ from the experimental results by a factor of about 2 if the distribution is Gaussian. If the distribution is not Gaussian, the error can reach a factor equal to 9, when the real distribution contains a greater number of stress peaks of greater amplitude.

6.5.2. Influence of peak distribution

A study carried out by R.G. Lambert [LAM 82] on the influence of the distribution law of the peaks of the response of the system (i.e. of the stress) on fatigue damage shows that:

– In a general way, the damage is primarily produced by the peaks with amplitude greater than twice the rms value σ_{rms} . For a Rayleigh distribution, they are the peaks between $2 \sigma_{\text{rms}}$ and $4 \sigma_{\text{rms}}$, while for an exponential law, they are the peaks of between $5 \sigma_{\text{rms}}$ and $15 \sigma_{\text{rms}}$.

– Because of the larger presence of peaks of great amplitude, the exponential law is more severe than a Rayleigh distribution.

6.5.3. Calculation of damage using Weibull distribution

The fatigue damage can be written, according to the Miner rule [NOL 76] and [WIR 77]:

$$D = \sum_i \frac{n_i}{N_i}$$

Knowing that $N \sigma^b = C$ and that $\sigma = K z^g$ if the stress-strain relationship is not linear, this becomes

$$D = \frac{K^b}{C} \sum_i n_i z^{bg} \quad [6.32]$$

i.e. in the continuous case,

$$D = \frac{K^b}{C} \int z^{bg} dn$$

with

$$dn = n_p^+ T q(z) dz \quad [6.33]$$

and

$$D = \frac{K^b}{C} n_p^+ T \int_0^{+\infty} z^{bg} q(z) dz \quad [6.34]$$

The integral can be regarded as the (bg) th moment of $q(z)$. Let us denote the distribution function of z as $Q(z)$, then

$$q(z) dz = dQ(z) \quad [6.35]$$

If the distribution of the peaks follows a Weibull distribution,

$$Q(z) = 1 - \exp \left[- \left(\frac{z}{\delta} \right)^\eta \right] \quad [6.36]$$

for $z > 0$, where η is a constant characterizing the form of the law ($\eta = 1$ for an exponential distribution and $\eta = 2$ for a Rayleigh distribution). Then we have

$$q(z) dz = \eta u^{\eta-1} \exp(-u^\eta) du \quad [6.37]$$

if $u = \frac{z}{\delta}$, yielding

$$E(D) = \frac{K^b}{C} n_p^+ T \delta^{bg} \eta \int_0^\infty u^{bg+\eta-1} \exp(-u^\eta) du \quad [6.38]$$

With $a = bg + \eta - 1$ and $b = \eta$, and knowledge that

$$\int_0^\infty X^a \exp(-X^\gamma) dX = \frac{1}{\gamma} \Gamma\left(\frac{a+1}{\gamma}\right) \quad [6.39]$$

this becomes

$$D = \frac{K^b}{C} n_p^+ T \delta^{bg} \Gamma\left(1 + \frac{bg}{\eta}\right) \quad [6.40]$$

NOTE: K.G. Nolte and J.E. Hansford [NOL 76] established this relation to study fatigue of immersed structures subjected to waves of height H . It is sufficient to replace z by H to treat this particular case. The distribution wave height is generally approximated by a Rayleigh distribution for which $\eta = 2$ and $\delta = \frac{H_s}{\sqrt{2}}$ (H_s = wave height, indicative of the state of the sea).

This yields

$$D = \frac{K^b}{C} \frac{n_p^+ T H_s^{bg}}{2^{\frac{bg}{2}}} \Gamma\left(1 + \frac{bg}{2}\right) \quad [6.41]$$

where $n_p^+ T$ is the total number of waves.

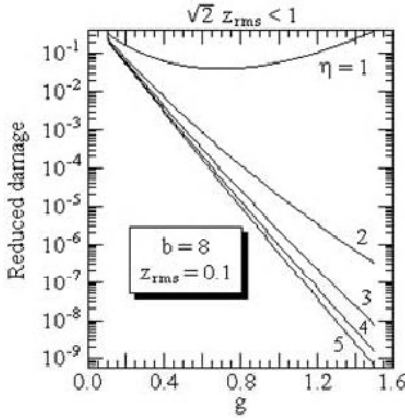


Figure 6.7. Reduced damage for Weibull peak distribution

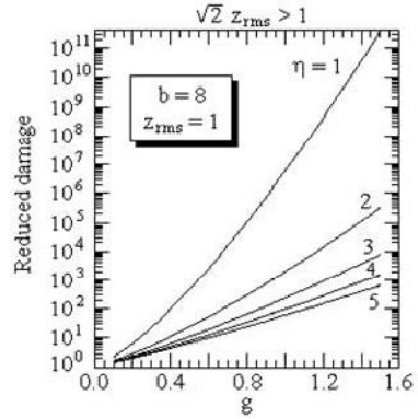


Figure 6.8. Reduced damage for Weibull peak distribution

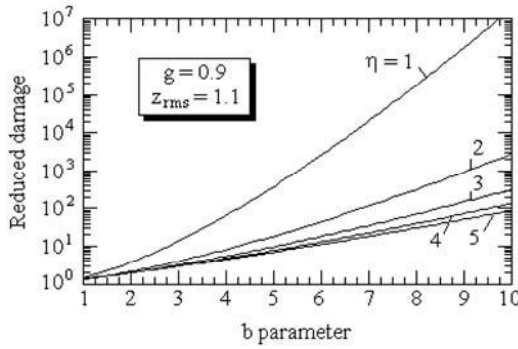


Figure 6.9. Reduced damage for Weibull peak distribution versus parameter b

Figures 6.7–6.9 show the variations in the quantity

$$\frac{C}{K^b} \frac{D}{n_p^+ T} = \left(\sqrt{2} z_{rms} \right)^{bg} \Gamma \left(1 + \frac{b g}{\eta} \right)$$

depending on b or g for various values of η , in order to highlight the influence of non-linearity (for $\sqrt{2} z_{rms}$ lower, then higher, than 1).

6.5.4. Comparison of Rayleigh assumption/peak counting

H.C. Schjelderup [SCH 61b] proposed using a method close to the *range-mean* counting method (Chapter 3) and assumes that:

- the mean stress follows a normal distribution

$$f_1(\sigma_m) = \frac{1}{\sigma_M \sqrt{2\pi}} e^{-\frac{1}{2} \left(\frac{\sigma_m}{\sigma_M} \right)^2} \quad [6.42]$$

- the alternate stress around this mean also follows a normal distribution:

$$f_2(\sigma_a) = \frac{1}{\sigma_A \sqrt{2\pi}} e^{-\frac{1}{2} \left(\frac{\sigma_a - \bar{\sigma}_a}{\sigma_A} \right)^2} \quad [6.43]$$

where σ is the standardized stress $\frac{\sigma}{\bar{\sigma}}$, σ_M is the standard deviation of the standardized mean stress, σ_A is the standard deviation of the standardized alternating stress and $\bar{\sigma}_a$ is the mean of the standardized alternating stress.

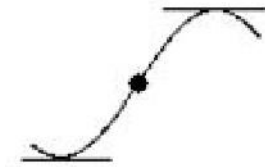


Figure 6.10. Alternating stress around the mean

The probability of occurrence of a mean stress σ_m and an alternating stress σ_a is

$$P(\sigma_m, \sigma_a) = f_1(\sigma_m) f_2(\sigma_a) d\sigma_m d\sigma_a \quad [6.44]$$

The number dn of cycles (σ_m, σ_a) among N cycles is equal to

$$dn = N P(\sigma_m, \sigma_a) \quad [6.45]$$

yielding damage dD created by these dn cycles:

$$dD = \frac{N P(\sigma_m, \sigma_a)}{N(\sigma_m, \sigma_a)} \quad [6.46]$$

where $N(\sigma_m, \sigma_a)$ is the number of cycles to failure for (σ_m, σ_a) . The total number of cycles to failure N is that for which $D = 1$, yielding:

$$\frac{1}{N} = \int_{\sigma_a} \int_{\sigma_m} \frac{f_1(\sigma_m) f_2(\sigma_a) d\sigma_m d\sigma_a}{N(\sigma_m, \sigma_a)} \quad [6.47]$$

The function $N(\sigma_m, \sigma_a)$ can be obtained from the modified Goodman diagram:

$$N(\sigma_m, \sigma_a) = N_0 \frac{\sigma_a}{1 - \frac{\sigma_m}{R_m}} \quad [6.48]$$

where R_m is ultimate strength.

From this formulation, H.C. Schjelderup presents an example to show that the Rayleigh distribution gives more severe results and that this method seems to adapt better to the experimental results.

6.6. Non-linear mechanical system

It is assumed that Basquin's distribution applies ($N \sigma^b = C$) and that the non-linearity is of the form $\sigma = K z^g$. Then,

$$D = \sum_i \frac{n_i}{N_i}$$

$$D = \frac{K^b}{C} \sum_i n_i z_i^{bg}$$

and, in the continuous case,

$$D = \frac{K^b}{C} \int_0^{+\infty} z^{bg} dn$$

where

$$dn = n_p^+ T q(z) dz$$

$$D = \frac{K^b}{C} n_p^+ T \int_0^{+\infty} z^{bg} q(z) dz \quad [6.49]$$

$$\text{If } u = \frac{z}{z_{rms}},$$

$$D = \frac{K^b}{C} n_p^+ T z_{rms}^{bg} \int_0^{+\infty} u^{bg} q(u) du. \quad [6.50]$$

Finally, if the peak distribution follows a Rayleigh distribution,

$$E(D) = \frac{K^b}{C} n_0^+ T \left(\sqrt{2} z_{rms} \right)^{bg} \Gamma \left(1 + \frac{bg}{2} \right). \quad [6.51]$$

NOTE: In the D. Karnopp and T.D. Scharton method [KAR 66], the authors approach the response of a non-linear hysteretic system slightly damped subjected to a random excitation by an artificial linear process [KAR 66] [TAN 70]. They calculate, starting from this process, the mean value of the displacement higher than a specific limit as an approximation to plastic deformation. Finally, they use the Coffin criterion to evaluate the mean fatigue life of the system under loads belonging to the low cycle fatigue domain.

Chapter 7

Low Cycle Fatigue

7.1. Overview

The first studies on low cycle fatigue, called *oligocyclic fatigue*, were carried out by Sachs, Liu, Lyngh and Ripling [LIU 48] [LIU 69].

When the (sinusoidal) stress increases, the number of cycles to failure decreases. Fatigue fracture slowly transforms into a static fracture. The conditions for which static properties become predominant are unclear. Their influence becomes significant for approximately 10^4 to 10^5 useful lifetime cycles. They are predominant for $N < 100$ cycles [MAT 71]. We therefore consider that the oligocyclic field is between 1/4 of a cycle and approximately 10^5 . In this field, the Wöhler curve slope decreases when the stress increases and the curve can therefore no longer be comparable to a line in general axes. In this case, materials work in the plastic field.

For most materials, cyclic stresses required for fracture with $N < 100$ cycles are close to static fracture values. The development of low cycle fracture requires significant amplitude of the part's cyclic plastic strain, large enough so that there is great non-linearity between the applied stress and the resulting strain [COF 62]. This fact has two consequences:

- The tests can be carried out with controlled stress or strain, since one parameter no longer makes it possible to control the other such as in the elastic field ($\sigma = E \epsilon$). Controlled stress test results are generally presented in the form of traditional S-N curves. These tests are not as easy to analyze as controlled strain tests, for which we could observe a linear relation between the fracture cycle number

and the plastic deformation in logarithmic axes. We prefer to control strain in this field.

– In this type of load, load frequency can be much lower than in the traditional fatigue case (1 cycle per day or even per week). Because of this, temperature variations can be a frequent source of large plastic strains (differential expansions) and thus low cycle fatigue fractures [MAN 65] [GOE 60]. Similarly, loads can be applied quasi-statically or dynamically in tests.

We will see that materials can support more dynamic load cycles than static load cycles [JU 69].

7.2. Definitions

7.2.1. Baushinger effect

Consider the material's stress-strain curve. If we stop stress at point D in the first part of the diagram, and relax the stress to zero, the stress and strain return to zero such that at each moment, the point (ϵ, σ) remains on the OD arc. If, on the contrary, we stop at point B in the second part of the diagram, and decrease σ , the point (ϵ, σ) describes segment BC parallel to OS.

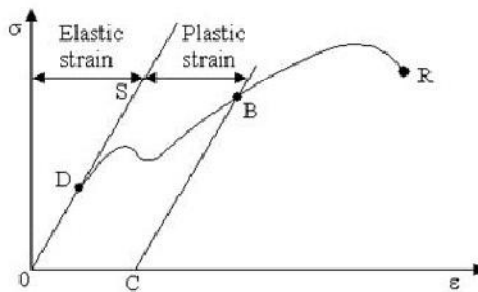


Figure 7.1. Stress-strain curve: strain hardening phenomenon

If we increase σ once again, point (ϵ, σ) describes CB then BR.

Everything occurs as if the higher elastic limit was increased: this is the phenomenon called *work hardening*. Experience shows that, consequently, the higher elastic compression limit decreases: this is the *Baushinger effect* [BAU 81].

7.2.2. *Cyclic strain hardening*

Under the imposed cyclic strains, we can observe a cyclic work hardening of the type (depending on the case):

- isotropic, such that the elastic limit increases in both directions;
- kinematic, such that the elastic limit in tension or in compression remains constant and equal to the raw component; or
- an intermediate between these two extremes.

7.2.3. *Properties of cyclic stress-strain curves*

We can observe that there is not much difference between the curves obtained with programmed block and random vibration testing; both curves are optimistic in relation to useful lifetime under real loads. The curve drawn with sinusoidal loads is very different from the previous curves.

The relation between endurance under sine and random loads is homogenous with results from J. Kowalewski [KOW 59], S.A. Clevenston and R. Steiner [CLE 65], S.R Swanson [SWA 63], and K.J. Marsh and J.A. Mackinnon [MAR 66].

7.2.4. *Stress-strain curve*

With cyclic loads corresponding to the low cycle fatigue field, the stress-strain curve appears as an open hysteresis loop and maximum stresses very slightly vary during the first cycles.

The alternating stress-strain loop of a metal that was initially work hardened increasingly opens during fatigue to become a sort of stabilized mode.

If the load is applied in alternating stress with constant amplitude $2\sigma_{m0}$, the amplitude of the stabilized alternating strain $2\varepsilon_m$ is higher than its initial value $2\varepsilon_{m0}$.

If we impose an alternating strain $2\varepsilon_{m0}$, the stabilized stress $2\sigma_{ms}$ is lower than its initial value $2\sigma_{m0}$ [BAR 77].

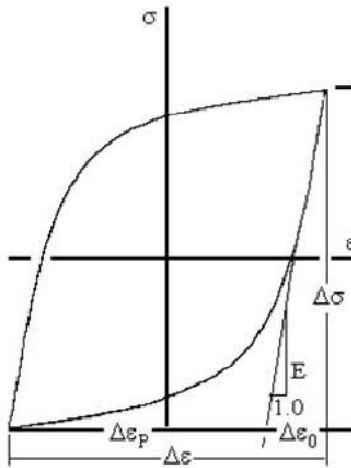


Figure 7.2. *Strain and stress ranges*

The curve in Figure 7.2 shows:

- the range $\Delta\epsilon$ of total imposed strain, cycle amplitude being $\epsilon_a = \frac{\Delta\epsilon}{2}$; and
- the total stress range $\Delta\sigma$ of amplitude $\sigma_a = \frac{\Delta\sigma}{2}$.

The first tension load provides the arc AB (Figure 7.3). The unloading gives BC, where the elastic part is generally parallel to AB [NEL 78].

The compression load yields CD. The elastic compression limit is decreased (Baushinger effect) [BAU 81]. The unloading from D results in DE. Re-stressing corresponds to the EF arc. If we continue a new constant load amplitude cycle, we create a closed loop i.e. the *hysteresis loop*.

If several test bars go through cycles, each with different strain amplitudes (or if a single test bar goes through different strain amplitude cycles), we then create a series of hysteresis loops. The stress-strain curve is defined as the locus of stable hysteresis loop peaks [MOR 64a].

During consecutive stress cycles, this loop tends to stabilize and close (Figure 7.6) [MAN 65] [PIN 80] [RAB 80]. The tensile stress then decreases until the test bar fails (Figure 7.5).

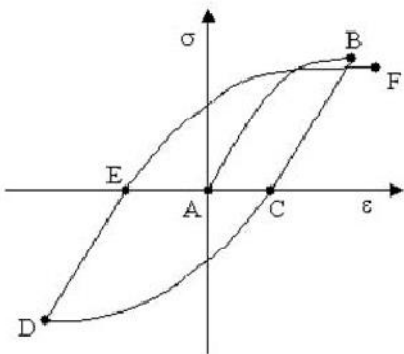


Figure 7.3. Hysteresis loop

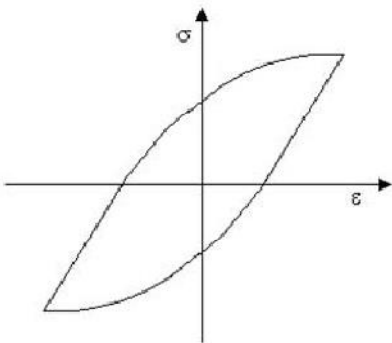


Figure 7.4. Closed hysteresis loop

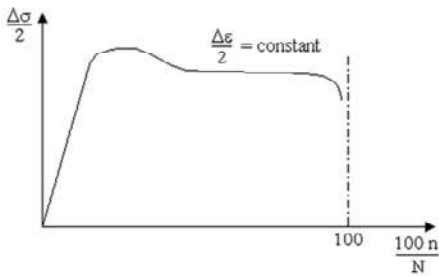


Figure 7.5. Evolution of the tensile stress to fracture

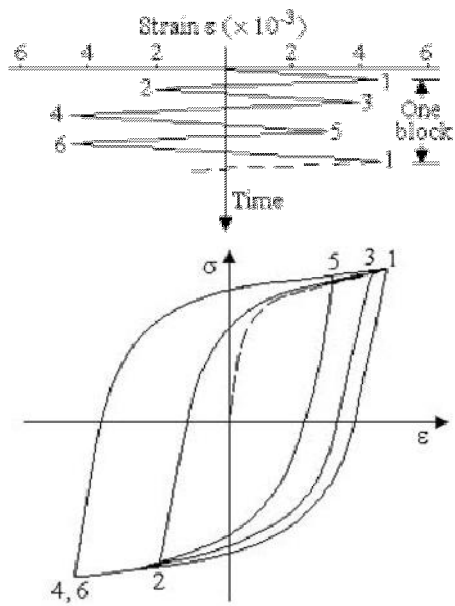


Figure 7.6. Evolution of the hysteresis loop

7.2.5. Hysteresis and fracture by fatigue

Why associate strain hysteresis and fracture by fatigue?

The product of the load by strain is proportional to the work done or the energy stored in the test item [FEL 59]:

$$\sigma \epsilon = \frac{F}{S} \frac{\Delta l}{l} = \frac{F \Delta l}{V} = \frac{dW}{V} \quad [7.1]$$

where V is the volume of the part.

We have seen that, regardless of the stress amplitude, even below the elastic limit, strain does not return to its initial value after a cycle (even if this strain is very small). A thermocouple would show elevation of temperature in the test item. All the energy stored in the test item is therefore not conserved. If the stress is small, the energy lost is obviously very low.

A test bar experiencing cycles of stress lower than the elastic limit may break, because the sub-microscopic connections are gradually broken. This fracture requires energy which corresponds to that linked to hysteresis.

7.2.6. Significant factors influencing hysteresis and fracture by fatigue

These factors are as follows:

- amplitude of the stress: effect described by the Wöhler curve.

The energy dissipated is given by (Volume 1):

$$D = J \sigma^n \quad [7.2]$$

where $n = 3$ [BRO 36] [ROW 13], $n = 4$ [HOP 12] or $n = 2$ [KIM 26];

- distribution of stresses: agreement with different distributions;
- frequency
 - this has very little, if any, effect on the quantity of energy absorbed by the cycle at a rate between 500 and 2,000 cycles/min [KIM 26],
 - FH Vitovec and B.J. Lazan [VIT 53] note a significant effect on plastic strain: if the frequency increases, damping energy decreases. The useful lifetime is therefore larger at higher frequencies (if the plastic strain is a criterion of fatigue);
- temperature: for strong stresses, an increase in temperature leads to an increase of the energy absorbed per cycle, and consequently, to a greater plastic strain. For the small stresses, we can observe an effect similar to the effect of frequency;
- the form of the test bar;
- surface conditions, internal imperfections; and
- composition, size of grains, thermal treatments, etc.

7.2.7. Cyclic stress-strain curve (or cyclic consolidation curve)

This is a curve obtained by connecting the peaks of stable hysteresis loops obtained for different strain values (applied to identical test bars).

This curve provides the stabilized stress according to the stabilized strain (to be distinguished from the stress strain curve during a cycle).

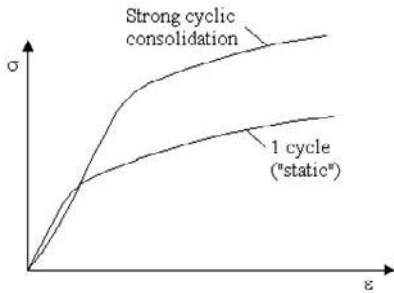


Figure 7.7. *Static and cyclic stress-strain curve*

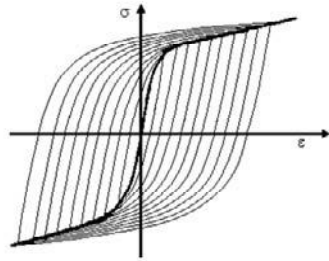


Figure 7.8. *Cyclic stress-strain curve*

This cyclic consolidation can be such that the material sometimes greatly supports strength to static tension.

The cyclic stress strain diagram characterizes the stable state of strains of a material experiencing cyclic stresses. By comparison with the traditional stress-strain diagram, it is possible to deduct the material's behavior.

7.3. Behavior of materials experiencing strains in the oligocyclic domain

7.3.1. *Types of behaviors*

We can distinguish in the useful lifetime of a test bar experiencing oligocyclic strains the following phases:

- accommodation: imposed plastic strain leads to stresses with amplitude varying significantly during the first cycles, then seems to stabilize and very slowly evolve with the number of cycles. This accommodation represents 10 to 50% of the general useful lifetime;
- cracking (initiating): this follows or overlaps the previous phase, in which surface micro-cracks appear (the longest phase); and
- propagation: one of the cracks propagates more rapidly and in a more stable way than others, and accelerates at the end of its life to fracture (discussed later).

High strain static or alternating loads tend to modify the state of metal strain hardening [BAR 77].

We can observe several types of behaviors with such loads. Because the stress-strain curve is modified by consecutive plastic strains based on the process which

the material has experienced (hardening and tempering, annealing, hardened, etc.), these differences are represented by an adaptation (*accommodation*) of the component. When it exists, this can be:

- with *softening* (case of a component that is initially work hardened experiencing alternating stresses);
- with *hardening* (case of an initially soft material);
- with *stable behavior*; or
- with a *mixed behavior* (hardening, softening) according to the field of strain.

The existence of this accommodation makes it possible to associate a strain to an imposed deformation in this field.

7.3.2. Cyclic strain hardening

Consider a test bar of a material submitted to alternating strains (zero mean) of imposed amplitude; let us examine the evolution of the stress.

A first possible behavior may consist of an increase of the stress amplitude over time to stabilization [LIG 80].

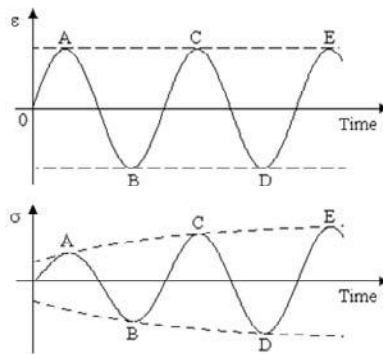


Figure 7.9. Alternating strain and resulting stress

The stress-strain curve is presented in Figure 7.10.

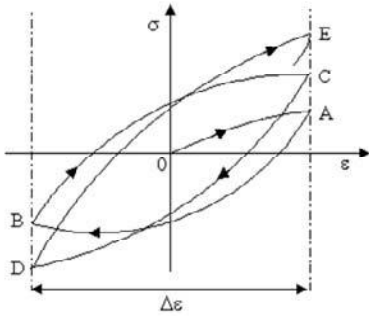


Figure 7.10. Stress-strain cycles with hardening

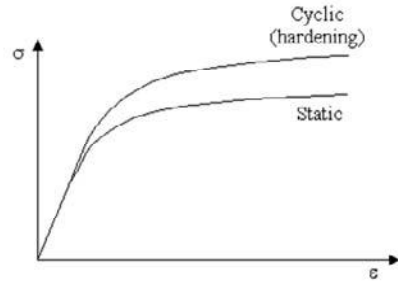


Figure 7.11. Stress-strain curve with hardening

The maximum σ_{\max} stress increases at each cycle carried out at constant maximum ϵ_{\max} strain. The slope of the curve $\sigma(\epsilon)$ increases, there is material hardening. This behavior is characteristic of annealing metals (copper).

Smith, Hirschberg and Manson [LIG 80] state that we can observe a hardening for materials such as $\frac{R_m}{R_e} > 1.4$ (where R_m is ultimate tensile strength and R_e is the yield stress).

Morrow provides the strain hardening coefficient n as a characteristic parameter. Hardening occurs for $n > 0.1$ [LIG 80].

7.3.3. Cyclic strain softening

Under the same conditions, some metals display the opposite behavior and experience a decrease of their characteristics.

The cyclic stress-strain curve is above the static stress-strain curve. With the above criteria, there is softening when, according to authors, $\frac{R_m}{R_e} < 1.2$ or $n < 0.1$.

For $1.2 < \frac{R_m}{R_e} < 1.4$, there can be hardening or softening.

The use of properties established in static for cyclic behavior calculations can lead to an error, particularly an unexpected plastic deformation [LIG 80].

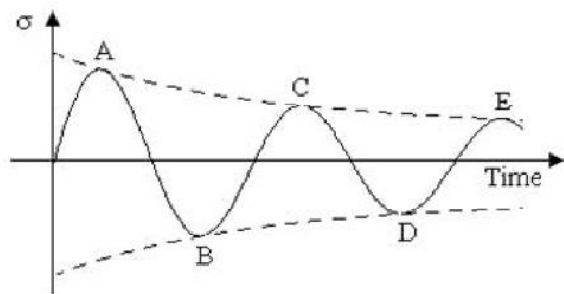


Figure 7.12. Evolution of stress in the case of cyclic strain hardening

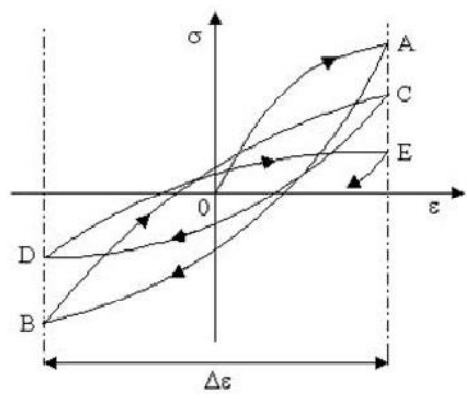


Figure 7.13. Stress-strain loop in the case of hardening

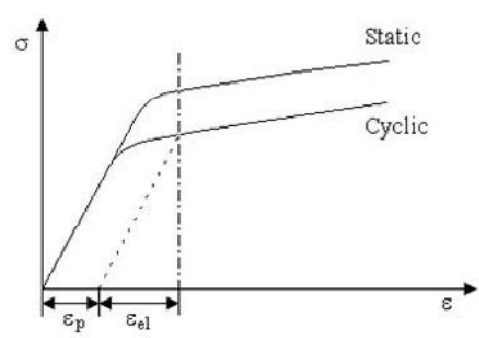


Figure 7.14. Cyclic stress-strain curve during softening

7.3.4. *Cyclically stable metals*

Certain metals behave in a stable manner in strain cycles.

In general, they stabilize very quickly after a rapid hardening or softening evolution under constant amplitude (20% to 40% of life in fatigue) and no longer evolve.

An overload can greatly modify the material's behavior, however [LIG 80].

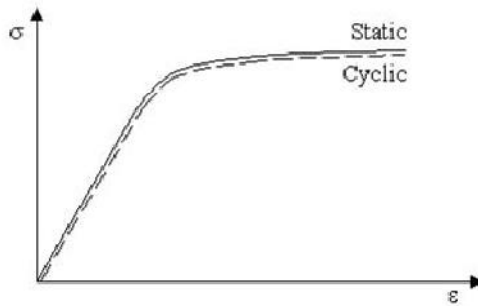


Figure 7.15. *Cyclic and static stress-strain curve of a stable material*

7.3.5. *Mixed behavior*

Depending on the value of ϵ , there is softening or hardening. Cyclic and static stress-strain curves cross each other.

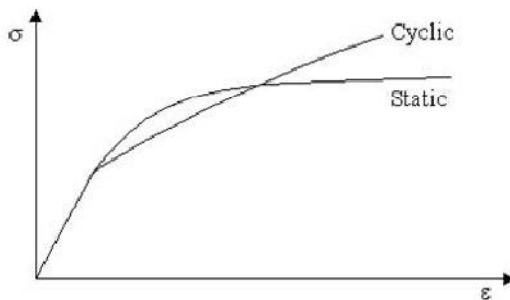


Figure 7.16. *Cyclic stress-strain curve of a mixed behavior material*

7.4. Influence of the level application sequence

We have shown that the stress σ -strain ϵ curve drawn in static load could be different from that of cyclic load, depending on the material.

Consider the case of a material softening in cyclic load and submitted to a load σ_{a1} during a few cycles, then submitted to a few $\sigma_{a2} > \sigma_{a1}$ cycles.

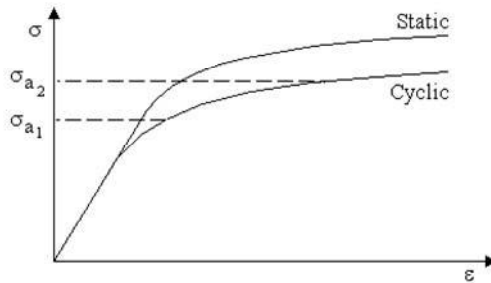


Figure 7.17. *Static and cyclic stress-strain curve in the case of softening*

Under stress σ_{a1} , the material works in the elastic field and follows the static curve. If the number of cycles achieved is sufficient, the hysteresis loop (a) (Figure 7.18) is stabilized, and its peak corresponds to a point in the cyclic curve with some plasticity.

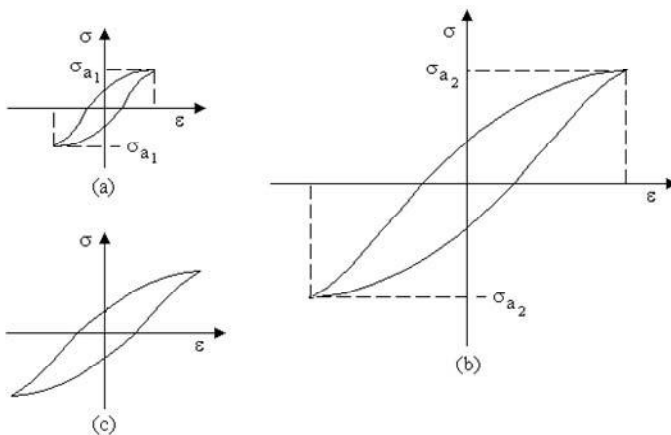


Figure 7.18. *Hysteresis loop*

If we apply cycles at level σ_{a2} , following a few cycles at level σ_{a1} , we obtain the same hysteresis loop (b) as if σ_{a1} had never been applied.

If, on the contrary, we start with level σ_{a2} , we can immediately observe the development of a large hysteresis loop. Curve $\sigma(\epsilon)$ is stabilized on the cyclic curve and the future application of lower level σ_{a1} cycles will produce the loop (c), different from (a), with a much larger plastic strain. The useful lifetime in this case is much shorter.

7.5. Development of the cyclic stress-strain curve

Because of the transitory nature of the evolution of the stress-strain curve (or *strain hardening curve*), and as stabilization generally occurs after a small percentage of the test bar's useful lifetime, the curve (σ, ϵ) is developed from tests on several test bars with different deformation amplitudes. We consider that stabilization is obtained at approximately 50% of the useful lifetime. Each test makes it possible to draw a hysteresis loop for a given $\Delta\epsilon$ amplitude.

Curve (σ, ϵ) is obtained by transposing on a diagram the peak coordinates of stabilized hysteresis loops.

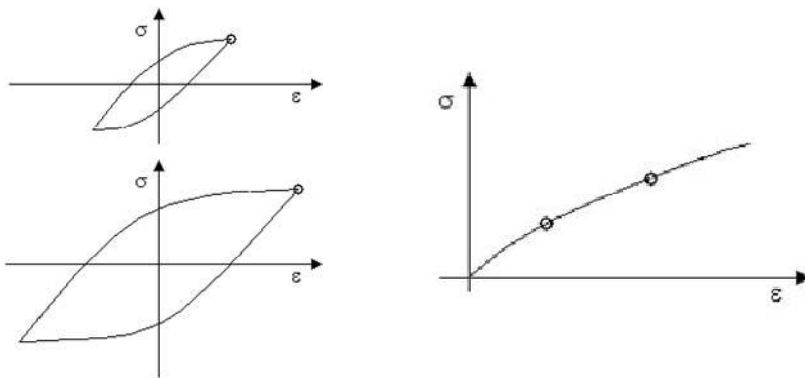


Figure 7.19. *Development of the stress-strain curve*

Other methods can be used to draw this curve [MOR 64a] from a single test bar submitted to several levels of vibration.

We show that this curve can be approximated in logarithmic axes by an equation line of the form:

$$\sigma = K' \varepsilon_p^{n'} \quad [7.3]$$

where σ is the amplitude of the “stable” alternating stress, ε_p is the amplitude of the real plastic strain, K' is the “cyclic strength” coefficient (real stress for real unit strain) and n' is *cyclic strain hardening* coefficient. n' is a constant (straight line slope) which varies in practice between 0.10 and 0.20. For most metals, n' is close to 0.15 regardless of their initial state [MOR 64a].

J.C. Ligeron [LIG 80] gives $0.07 < n' < 0.18$. For Jo Dean Morrow and F.R. Tuler [ING 27], we have $0.15 < n' < 0.18$ for many nickel-based alloys.

Relation [7.3] can also be written in terms of stress and strain ranges:

$$\frac{\Delta\sigma}{2} = K' \left(\frac{\Delta\varepsilon_p}{2} \right)^{n'} \quad [7.4]$$

7.6. Total strain

Total strain ε_t can be broken down into an elastic strain ε_{el} and a plastic strain ε_p . In the linear zone of the stress-strain diagram, we have $\Delta\sigma = E \Delta\varepsilon_{el}$. This linear zone is often very small.

The cyclic stress-strain curve can therefore be approximated by the relation:

$$\frac{\Delta\varepsilon_t}{2} = \frac{\Delta\varepsilon_{el}}{2} + \frac{\Delta\varepsilon_p}{2} = \frac{\Delta\sigma}{2E} + \frac{\Delta\varepsilon_p}{2} \quad [7.5]$$

$$\frac{\Delta\varepsilon_t}{2} = \frac{\Delta\sigma}{2E} + \frac{1}{2} \left(\frac{\Delta\sigma}{K'} \right)^{1/n'} \quad [7.6]$$

We have seen that the stabilization of the cycle to a given level of stress (or strain) is not instant. For irregular loads, stabilized behavior is only an idealistic concept.

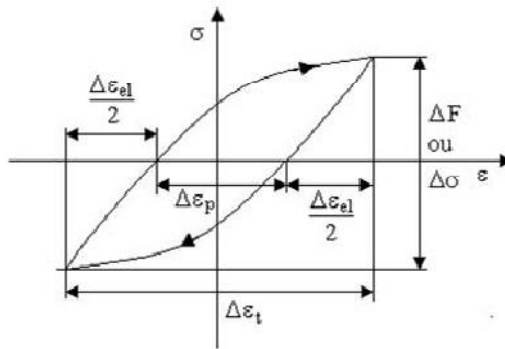


Figure 7.20. Cyclic stress-strain diagram

For sinusoidal vibration, the hysteresis loop slowly varies with cycles. $\Delta\epsilon_{el}$ and $\Delta\epsilon_p$ therefore vary, with $\Delta\epsilon_t$ remaining constant. These variations are very small and often neglected. When $\Delta\epsilon_t$ is small ($\leq 1\%$), $\Delta\sigma$ is often generally constant over a few thousand cycles and $\Delta\epsilon_p$ varies very little. When $\Delta\epsilon_t$ is small, the loop becomes very narrow and $\Delta\epsilon_p$ is difficult to determine with precision. When $\Delta\epsilon_t$ is larger ($\approx 10\%$), $\Delta\sigma$ significantly increases, but since $\Delta\epsilon_{el}$ is much smaller than $\Delta\epsilon_p$, $\Delta\epsilon_p$ is approximately equal to $\Delta\epsilon_t$ and is therefore about constant [GOE 60].

7.7. Fatigue strength curve

In the oligocyclic domain, since fatigue mainly depends on strain and the stress necessary to a given strain is variable, damage by fatigue is generally studied by controlled strain tests, and total strain ϵ_t can be broken down into an elastic strain and a plastic strain.

The endurance curve is then described in number of cycles to failure strain axes. The fatigue strength curve provides, for a given material, the number of cycles to fracture under a given imposed strain [PIN 80].

In calculations, we sometimes transform this plastic strain into a fictional “equivalent” elastic stress by multiplying the plastic strain by the Young E material modulus.

This diagram can be drawn by separating the total, elastic and plastic strains (*Coffin-Manson curves*) (see section 7.8.9).

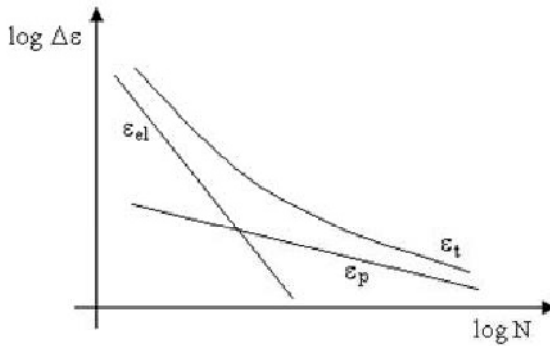


Figure 7.21. Coffin-Manson fatigue strength curves

7.7.1. Basquin curve

The curve of endurance drawn by using the equivalent stress based on the number of cycles to fracture generally connects well to traditional curves of endurance. As with traditional endurance, the low cycle fatigue strength curve was the subject of empirical analytical representations.

7.8. Relation between plastic strain and number of cycles to fracture

Several representations have been proposed.

7.8.1. Orowan relation

E. Orowan [ORO 52] proposed the relation

$$\epsilon N = \text{constant} \quad [7.7]$$

where ϵ is total deformation and N is the number of cycles to fracture under cyclic load.

7.8.2. Manson relation

S.S. Manson [MAN 54], followed by J.H. Gross and R.D. Stout [GRO 55], used a modified form of the previous relation:

$$\epsilon N^m = \text{constant}. \quad [7.8]$$

7.8.3. Coffin relation

7.8.3.1. Coffin law

According to L.F. Coffin [BAL 57] [COF 54] [COF 69a] [COF 71],

$$N^\beta \Delta \epsilon_p = c \quad [7.9]$$

where $\Delta \epsilon_p$ is the range of variation of the plastic strain (peak-to-peak amplitude) and β and c are constants based on the material. β also depends on temperature.

In practice, β varies very little and has a value that is close to 0.5 (β can be between 0.5 and 0.7). Constant c is directly linked to real strain during fracture.

Future proposed variations of the L.F. Coffin relation often involve the definition of constant c . This constant is directly linked to real strain during tensile fracture. The ultimate strength is generally considered as strength to fatigue to the lowest number of cycles and corresponds to the tensile test. According to the authors, this number can be equal to 1/4, 1/2 or 1 cycle [YAO 62].

The low cycle S-N curve starts at the ultimate strength. It is initially concave towards the bottom, then the top, the point of inflexion varying with the material, geometry, frequency, nature of the stress applied and temperature.

L.F. Coffin considers that, in logarithmic axes, the straight line $\epsilon_p N^{1/2} = c$ goes through the point of static tensile test corresponding to 1/4 cycle. Constant c could be calculated from static data. In the oligocyclic field, endurance depends on ductility of the material. L.F. Coffin expresses c as a function of ϵ_f (tensile strain fracture).

If ϵ_f is ductility to fracture (real fracture deformation), the author shows that if at fracture $N = \frac{1}{4}$ cycle,

$$\left(\frac{1}{4}\right)^{1/2} \epsilon_f = c \quad [7.10]$$

i.e.

$$c = \frac{\epsilon_f}{2} \quad [7.11]$$

We therefore have

$$\epsilon N^{1/2} = \frac{\epsilon_f}{2} \quad [7.12]$$

or $\Delta\epsilon N^{1/2} = \epsilon_f$.

The use ductility to fracture ϵ_f measured at 1/4 of a tensile cycle is conservative [PRO 48].

B. Barthememy [BAR 80] provides the relation

$$c = 2^{1-\beta} \log \frac{S_0}{S} \quad [7.13]$$

where S_0 is the initial cross-section and S is the cross-section at fracture.

This law is confirmed when imposed plastic strain has amplitude higher than 1/100.

The constant c can also be determined from the value of necking Σ in a tensile test [OSG 82]:

$$\Sigma = \frac{S_0 - S}{S_0} 100 \quad [7.14]$$

$$\log \frac{100 - \Sigma}{100} = \log \frac{S}{S_0} = \epsilon_f \quad [7.15]$$

We therefore have:

$$c = \frac{1}{2} \log \frac{100}{100 - \Sigma} \quad [7.16]$$

The Coffin relation is also written as

$$N^\beta \frac{\Delta\epsilon_p}{2} = \epsilon'_f \quad [7.17]$$

where ϵ'_f is the fatigue ductility coefficient (real strain required to obtain fracture with a cycle).

For small numbers of fracture cycles, we can generally replace $\Delta\epsilon_p$ by $\Delta\epsilon_t$, since $\Delta\epsilon_{el}$ is small compared to $\Delta\epsilon_p$.

If we consider that fracture ductility is defined for $N = \frac{1}{2}$ cycle, we have [MAR 61a]:

$$c = \frac{\epsilon_f}{\sqrt{2}} \quad [7.18]$$

In cyclic torsion, we also have [HAL 61]:

$$N_f \Delta\gamma_p = \gamma_f \quad [7.19]$$

where $\Delta\gamma_p$ is the strain range of plastic shear and γ_f is the monotonous shear strain at fracture.

More generally, since $\epsilon = \epsilon_{el} + \epsilon_p$ we can say:

$$\epsilon = \frac{\sigma}{E} + \frac{\epsilon'_f}{N^\beta} \quad [7.20]$$

From the Basquin law in the form:

$$N \sigma^b = C = \sigma_f'^b, \quad [7.21]$$

where σ_f' is the strength to fracture coefficient (real stress required to obtain fracture with a cycle), we have:

$$\epsilon = \frac{\sigma_f'}{E N^{1/b}} + \frac{\epsilon'_f}{N^\beta} \quad [7.22]$$

There is equality in elastic and plastic strains when N is equal to N_t such that

$$\frac{\sigma_f'}{E N_t^{1/b}} = \frac{\epsilon'_f}{N_t^\beta}$$

or

$$N_t = \left(\frac{E \epsilon'_f}{\sigma'_f} \right)^{\frac{b}{b\beta-1}} \quad [7.23]$$

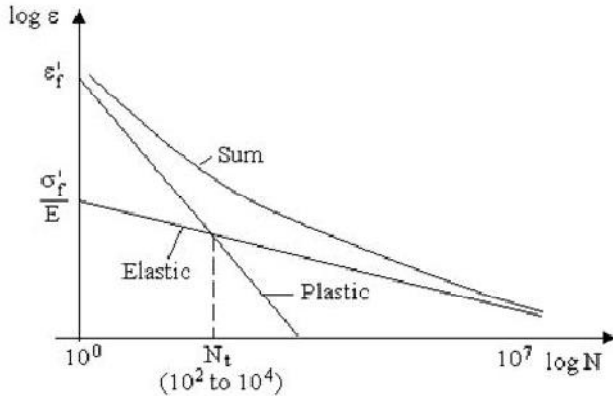


Figure 7.22. Composition of the strain versus number of cycles curve at fracture from Coffin and Basquin laws

For short useful lifetimes, plastic strain predominates and ductility coefficient is the important parameter. For large N , elastic strain is the most important and strength to fatigue is the vital parameter.

An ideal material would have high ductility and high strength simultaneously. These two properties are generally incompatible and a compromise must be chosen based on each specific case.

These relations apply to machined metals. When the part has internal faults (casting, welding, etc.), it is better to use relations of fracture mechanics.

Parameters ϵ'_f , σ'_f , b and β are linked to parameters n' and K' of the cyclic stress-strain curve [7.3] by:

$$n' = \frac{1}{b\beta} \quad [7.24]$$

and

$$K' = \frac{\sigma'_f}{\epsilon_f^{n'}} \quad [7.25]$$

In fact, knowing that

$$N \sigma^b = \sigma_f'^b, \quad [7.26]$$

we have

$$\varepsilon = \frac{\sigma_f'}{E N^{1/b}} + \frac{\varepsilon_f'}{N^\beta} = \frac{\sigma}{E} + \varepsilon_f' \left(\frac{\sigma}{\sigma_f'} \right)^{b\beta} \quad [7.27]$$

We have seen that $n' \approx 0.15$. In most cases, we can consider that parameters ε_f' and σ_f' are approximately equal to real ductility and strength to fracture [MOR 64a] [TAV 59].

From the surface of a hysteresis loop drawn in axes going through O' (Figure 7.23), whose area ΔW is equal to

$$\Delta W = 2 \sigma_a \Delta \varepsilon_p - 2 \int_0^{2\sigma_a} \varepsilon_{pO'} d\sigma \quad [7.28]$$

where σ_a is the amplitude of the alternating stress, Jo Dean Morrow [MOR 64a] shows that

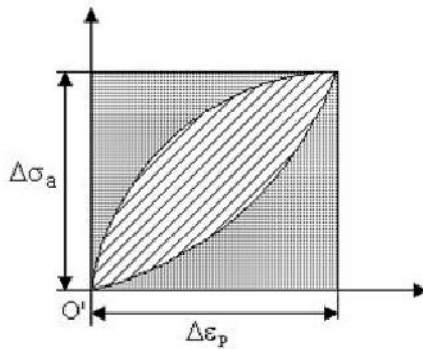


Figure 7.23. *Hysteresis loop*

$$\Delta W = 2 \sigma_a \Delta \varepsilon_p \frac{1-n'}{1+n'} \quad [7.29]$$

where $\varepsilon_{pO'}$ is equal to $\Delta\varepsilon_p \left(\frac{\sigma'_O}{2\sigma_a} \right)^{1/n'}$.

Knowing that

$$\frac{\Delta\varepsilon_p}{2} = \varepsilon'_f \left(\frac{\sigma_a}{\sigma'_f} \right)^{1/n'}, \quad [7.30]$$

it was deduced that

$$\Delta W = \frac{4 \varepsilon'_f \frac{1-n'}{1+n'}}{\frac{1}{\sigma'^{n'}}_f} \sigma_a^{n'}. \quad [7.31]$$

The energy ΔW absorbed by a cycle can equal the specific damping energy expressed by B.J. Lazan [LAZ 68] in the form:

$$D = J \sigma_a^n = \Delta W \quad [7.32]$$

We can observe, by identifying these relations, that exponent n is only a function of n' . If $n' = 0.15$, we obtain $n \approx 7.7$ to compare with value 8 given by B.J. Lazan for most metals under strong cyclic stresses (conversely, $n = 8$ would give $n' = 0.14286$).

7.8.3.2. Useful lifetime in fatigue in terms of energy dissipation

From relations [7.24, 7.26] and [7.31], we can write [MOR 64a]:

$$N^{-\frac{1}{b}-\beta} = \frac{\Delta W}{4 \sigma'_f \varepsilon'_f \frac{b\beta-1}{b\beta+1}}, \quad [7.33]$$

$$N = \left(\frac{\Delta W}{W'_f} \right)^{-\frac{b}{1+\beta b}} \quad [7.34]$$

or

$$\Delta W = W'_f N^{-\frac{1+\beta b}{b}} \quad [7.35]$$

with

$$W'_f = 4 \sigma'_f \epsilon'_f \frac{b \beta - 1}{b \beta + 1}, \quad [7.36]$$

where W'_f corresponds to energy ΔW required to break with $N = 1$ cycle. This relation links fatigue life N and strain energy ΔW by cycle.

Knowing that $n' = \frac{1}{b \beta}$, these relations can be written:

$$\Delta W = W'_f N^{\frac{1+n'}{b n'}} \quad [7.37]$$

7.8.3.3. Total energy required for fracture by fatigue

Since the energy dissipated by cycle is about constant during the fatigue test, the total plastic strain energy at fracture can be approximated by [MOR 64a]:

$$W_f = \Delta W N. \quad [7.38]$$

We therefore have

$$W_f = W'_f N^{1 - \frac{1+\beta b}{b}}, \quad [7.39]$$

$$W_f = W'_f N^{\frac{b-1-\beta b}{b}} \quad [7.40]$$

and

$$N = \left(\frac{W_f}{W'_f} \right)^{\frac{b}{b-1-\beta b}}. \quad [7.41]$$

Total energy at fracture increases with useful lifetime. It can be much greater than the energy required to break the test bar in a static tensile test.

Example 7.1.

For a steel test bar, $b = 12$, $n' = 0.15$ and $N = 10^5$ cycles, hence

$$\frac{b-1-\beta b}{b} = 1 - \frac{1}{b} - \frac{1}{n' b} = 0.361$$

and

$$\frac{W_f}{W'_f} = (10^5)^{0.361} \approx 64.$$

W_f is therefore 64 times larger than energy W'_f required to break the test bar in static.

NOTE:

The relations above are very often written in terms of quantities $\frac{\Delta \varepsilon}{2}$ and $2 N$ in order to resolve in half-cycle numbers. For example, total alternating strain ε_a is expressed

$$\varepsilon_a = \frac{\Delta \varepsilon}{2} = \frac{\sigma'_f}{E} \frac{1}{(2 N)^{1/b}} + \frac{\varepsilon'_f}{(2 N)^\beta} \quad [7.42]$$

where σ'_f , ε'_f , b and β are constants characteristic of material properties under cyclic load, measured from imposed strain tests.

This relation can also be written as [JOH 78] [MOR 64a] [NEL 78] [SMI 69] [WIR 83a]:

$$\varepsilon_a = \frac{\sigma'_f}{E} (2 N)^B + \varepsilon'_f (2 N)^c \quad [7.43]$$

where B is an exponent of fatigue strength, expressed

$$B = -\frac{1}{b} = -n' \beta = n' c$$

where c is a fatigue ductility exponent ($\neq \beta$) and N is the number of cycles to fracture.

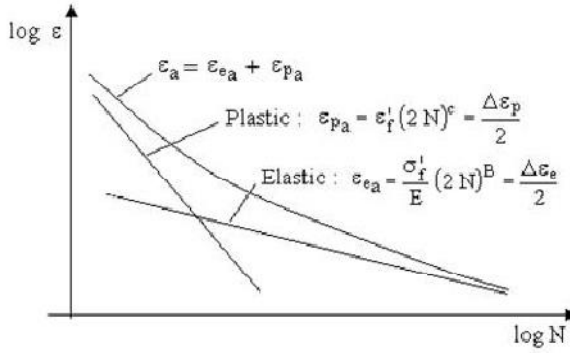


Figure 7.24. Strain versus number of cycles to fracture

The values of parameters B , c , and ϵ'_f characteristic of behavior at fatigue are tabulated [LW 72] [TQ4] for many common materials.

Constant c can be approximated by [MOR 64a]:

$$c \approx -\frac{1}{1 + 5n}, \quad [7.44]$$

where n is the exponent defined by relation [7.24].

According to the above equations, plastic strains are preponderant in the calculation of damage for short and average useful lifetimes. In this case, knowing that $D = \frac{1}{2N}$ for a half-cycle, relation [7.43] becomes

$$\epsilon_a = \epsilon'_f (2N)^c = \frac{\epsilon'_f}{(2N)^\beta} \quad [7.45]$$

D varies with $\left(\frac{\Delta\epsilon_p}{2}\right)^{1/\beta}$ i.e., since parameter β is close to 0.5, with $\left(\frac{\Delta\epsilon_p}{2}\right)^2$.

For longer useful lifetimes, elastic strains dominate in such a way that D varies with $\left(\frac{\Delta\epsilon_{el}}{2}\right)^b$. With b typically of the order 10, D varies with $\left(\frac{\Delta\epsilon_{el}}{2}\right)^{10}$. b estimation errors can have much greater consequences than errors in estimating c [MOR 64a].

NOTE:

Maximum stress relative to a purely alternating load is equal to σ_a :

$$\sigma_{max} = \sigma'_f (2 N_f)^b \quad [7.46]$$

By multiplying both members of equation [7.43] by σ_{max} , we have:

$$\sigma_{max} \Delta\epsilon = 2 \frac{\sigma'^2_f (2 N_f)^{2b}}{E} + 2 \sigma'_f \epsilon'_f (2 N_f)^{b+c} \quad [7.47]$$

i.e.

$$\sigma_{max} \Delta\epsilon = A \left(2 N_f \right)^{2b} + D \left(2 N_f \right)^d \quad [7.48]$$

where A and D are elastic and plastic damage coefficients (ordinates at the basis of elastic and plastic curves at one cycle) and a and d are slopes of elastic and plastic damage curves in logarithmic axes.

In order to evaluate damage relating to a given alternation, range $\Delta\epsilon$ is determined by the value of the last element to calculate whereas the stress is equal to the final alternating stress. These values are multiplied together and used to calculate $2 N_f$. The inverse of $2 N_f$ yields the damage of this alternation. Damages are then added.

J.G. Sessler and V. Weiss [SES 63] show that the Coffin relation predicts the useful lifetime, but cannot be used to evaluate damage progress during testing. Damage process is controlled by at least two processes which may be interdependent:

- loss of available ductility caused by hardening; and
- formation and growth of cracks leading to fracture.

7.8.4. *Shanley relation*

The Shanley relation [SHA 59] is based on the following hypotheses:

- controlled strain test;
- the crack is initiated at the beginning of the load;
- cracking speed depends on the amplitude of the cyclic plastic strain and, to a lesser degree, of the shear stress normal to the slide plane in which the crack propagates;
- the fracture corresponds to a critical cracking surface arbitrarily defined; and
- the variation of the area based on the number of cycles is given by

$$\frac{dS}{dN} = C (\Delta\epsilon)^2 \quad [7.49]$$

where C is a constant.

7.8.5. *Gerberich relation*

W. W. Gerberich [GER 59] takes a mean strain ϵ_m into consideration:

$$N = \left(\frac{\epsilon'_f - \epsilon_m}{\Delta\epsilon_p} \right)^2 \quad [7.50]$$

where ϵ'_f is the apparent fracture ductility.

7.8.6. *Sachs, Gerberich, Weiss and Latorre relation*

These authors [MAT 71] proposed a modification of the Gerberich relation by replacing $\Delta\epsilon_p$ by $\Delta\epsilon_t$ (total strain range).

7.8.7. *Martin relation*

The proposed relation is based on a low cycle fatigue energy criterion in the plastic field:

$$N^{1/2} \Delta\epsilon_p = C. \quad [7.51]$$

D.D. Martin [MAR 61a] explains the form of the Coffin relation with a theory based on the energy dissipated by hysteresis and finds the relation except for one difference for the value of the constant (ordinate at the origin of the curve).

The constant C is evaluated from a static test by comparing the work necessary to fatigue fracture with the work required by static fracture. If ϵ_f is the real fracture strain, we have:

$$C = \frac{\epsilon_f}{\sqrt{2}}. \quad [7.52]$$

The Coffin relation:

$$\epsilon N^{1/2} = \frac{\epsilon_f}{2} \quad [7.53]$$

seems more appropriate in the case of high temperature bending tests. Martin's is preferable for ambient temperature axial strain [YAO 62].

7.8.8. Tavernelli and Coffin relation

This is given by:

$$\sigma = \frac{E C}{2 N^{1/2}} + \sigma_D = E \frac{\Delta \epsilon_t}{2} \quad [7.54]$$

where σ_D is the fatigue limit, E is the elasticity module, C is a constant, equal to $\frac{\epsilon_f}{2}$, ϵ_f is fracture ductility and

$$\Delta \epsilon_t = \Delta \epsilon_p + 2 \frac{\sigma_D}{E},$$

$$\Delta \epsilon_p = \frac{C}{N^{1/2}} \text{ (Coffin relation).}$$

J.F. Tavernelli and L.F. Coffin [TAV 62] show that the phenomena can be described with precision with ϵ_p instead of $\epsilon_t = \epsilon_{el} + \epsilon_p$.

7.8.9. Manson relation

S.S. Manson [MAN 65] expresses the $\Delta\epsilon$ deformation in terms of $\Delta\epsilon_{el}$ and $\Delta\epsilon_p$ and shows that the variations of these two terms in relation to N can be represented by straight lines in logarithmic axes. They therefore have the form:

$$N^{k_1} \Delta\epsilon_{el} = C_1 \quad [7.55]$$

and

$$N^{k_2} \Delta\epsilon_p = C_2 \quad [7.56]$$

where C_1 is a function of $\frac{R_m}{E}$, R_m is the ultimate tensile strength, C_2 is a function of ductility $\delta = -\frac{1}{2} \ln \frac{100 - \Sigma}{100}$ and Σ is the necking. Note that

$$\Delta\epsilon_t = 3.5 \frac{R_m}{E} N^{-0.12} + \delta^{0.6} N^{-0.6}, \quad [7.57]$$

where N is the number of cycles to fracture.

These results were obtained from a study involving 29 materials.

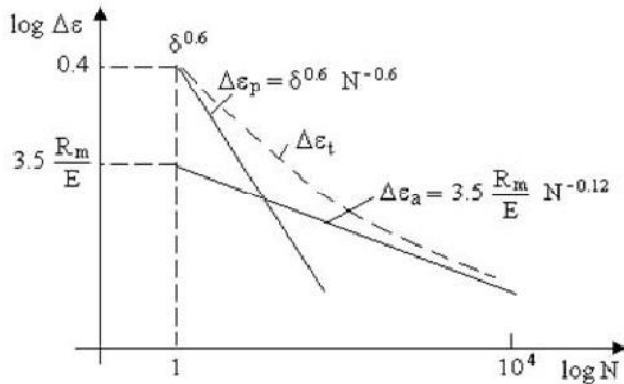


Figure 7.25. Strain versus number of cycles to fracture curve [MM 65]

We can observe, in general and from Figure 7.25, the following:

- with the low number of N cycles, the strength defined by ϵ_t is very closely linked to ductility δ of the material (the term $\Delta\epsilon_p(N)$ is predominant); and
- with the large number of N , the strength is greatly based on the yield strength and tensile strength ($\Delta\epsilon_{el}(N)$ is predominant) [PIN 80].

7.8.10. Ohji et al. relation

In this case, we consider that the damage is cumulative in a linear way for high stress fatigue, with a small number of cycles (a few 10^3 cycles) and zero (or other) mean strain [OHJ 66].

Damage per cycle is equal to ϵ^a , where a is a constant based on the material.

Fracture occurs when the accumulated damage equals $\frac{(2\epsilon_F)^a}{4}$, since tensile and compression strains have the same effect of damage, ϵ_F is a constant based on the material. We then have:

$$\epsilon_p^a N = \frac{(2\epsilon_F)^a}{4} \quad [7.58]$$

7.8.11. Bui-Quoc et al. relation

This is a unified theory [DUB 71a] with a similar approach to that used in the case of controlled stress damage [BUI 71], assuming that the accumulation of damage leads to a material ductility decrease (zero or positive mean strain).

7.9. Influence of the frequency and temperature in the plastic field

7.9.1. Overview

Low cycle fatigue is more sensitive to load frequency than traditional fatigue. Because of the high level of stresses and large strains imposed to the part in the low cycle field, it would be preferable not to carry out tests with the frequencies used in

the traditional fatigue field, which would lead to very high localized warming modifying the phenomena.

The tests show that resistance to fatigue decreases when test speed (or frequency) decreases in the case of frequencies lower than approximately 16 Hz [YAO 62]. A recommended speed for tests is between 0.8 and 1.7 Hz to avoid the excessive production of heat, to maintain a reasonable test time and to decrease the effect of frequency to a minimum [BEN 58].

Low cycle fatigue was the subject of frequency and temperature sensitivity studies.

A. Coles and D. Skinner [COL 65] observed from steel Cr - Mo - V test bars that the Coffin relation $\Delta\epsilon_p N^{1/2} = C$ overestimates useful lifetime at regular temperature and at high temperature (up to 565°C). The gap increases with temperature (creep influence).

7.9.2. Influence of frequency

J.F. Eckel [ECK 51] has shown from lead sample tests in bending that there is a relation between useful lifetime and frequency, of the form

$$\log T = \log b - m \log f \quad [7.59]$$

where T is useful lifetime, f is frequency, b is useful lifetime for $f = 1$ and m is a constant. Alternatively,

$$T = \frac{b}{f^m} . \quad [7.60]$$

This relation was established for very low frequencies (of approximately a cycle per day). For other metals besides lead, J.F. Eckel suggests that at high temperature we may have the same type of relation.

7.9.3. Influence of temperature and frequency

L.F. Coffin [COF 69] [COF 69b] provided the relation

$$C_1^\beta \Delta\epsilon_p = C_2 \quad [7.61]$$

where $C_1 = f^k T = N_f f^{k-1}$, k is an independent parameter describing plastic strain (based on temperature and generally lower than one), f is test frequency, T is total test time (or time to fracture), β and C_2 are constants based on the material, β is an increasing function of temperature (but not of frequency) and N_f is useful lifetime in number of cycles.

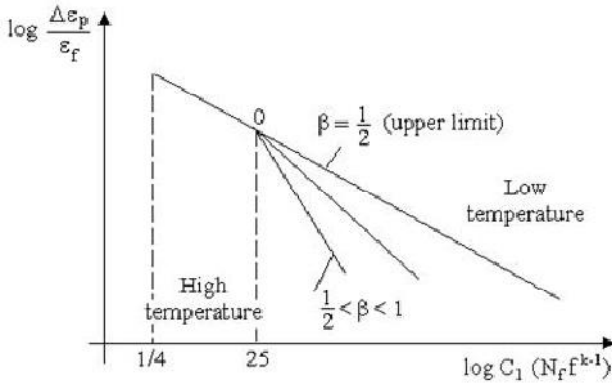


Figure 7.26. Variation of $\frac{\Delta \epsilon_p}{\epsilon_f}$ according to C_1

For a specific material tested at different temperatures, curves representing variations of $\frac{\Delta \epsilon_p}{\epsilon_f}$ according to C_1 (or $N_f f^{k-1}$) are straight lines converging at the abscissa C_1 point between 25 and 100 (if time is expressed in minutes) in logarithmic axes.

Between this C_1 value and $C_1 = \frac{1}{4}$, lines merge into one, defined for $\beta = \frac{1}{2}$ (tensile ductility).

When $C_1 = \frac{1}{4}$ [BAR 65a],

$$\frac{\Delta \epsilon_p}{\epsilon_f} = 1.$$

At low temperature, $k = 1$, $N_f = \frac{1}{4}$ and $\Delta\epsilon_p = \epsilon_f \left(\frac{\Delta\epsilon_p}{\epsilon_f} N_f^{1/2} = \frac{1}{4} = C_2 \right)$.

At high temperature, we have

$$\Delta\epsilon_p = C_2 N_f^{-\beta} f^{\frac{1-k}{\beta}} \quad [7.62]$$

or [COF 69]

$$N_f = \left(\frac{C_2}{\Delta\epsilon_p} \right)^{\frac{1}{\beta}} f^{1-k}$$

where C_2 depends on ϵ_f and O coordinates. The value of the constant k tends toward zero at high temperatures.

J.F. Barnes and G.P. Tilly [BAR 65a], however, note that relation $C_1 = N_f f^{k-1}$ does not always correctly describe the behavior of the material in all frequency and temperature conditions.

7.9.4. Effect of frequency on plastic strain range

At regular temperature and for low cycle fatigue, applied plastic strain range $\Delta\epsilon_p$ and resulting stress range $\Delta\sigma$ (peak-to-peak amplitude) are connected by the following relation [MOR 64a]

$$\Delta\sigma = A \left(\Delta\epsilon_p \right)^n \quad [7.63]$$

where A is range of stress for $\Delta\epsilon_p = 1$ and n is cyclic strain hardening exponent.

This relation is independent of the frequency. At high temperatures, frequency can influence the value of the stress range for a given plastic strain range. L.F. Coffin [COF 69b] takes this behavior into consideration by modifying relation [7.63] as follows:

$$\Delta\sigma = A \left(\Delta\epsilon_p \right)^n f^{k_1} \quad [7.64]$$

where k_1 is a constant at high temperature ($0.05 < k_1 < 0.15$), negative in certain cases.

If the material is insensitive to the frequency, $k_1 = 0$. The range of elastic strain can be obtained from this relation, by dividing $\Delta\sigma$ by the Young E modulus.

7.9.5. Equation of generalized fatigue

From the relations in section 7.8.3, we have [COF 69b]:

$$\Delta\epsilon = \frac{\Delta\sigma}{E} + \Delta\epsilon_p \quad [7.65]$$

$$\Delta\epsilon = \frac{A \left(\Delta\epsilon_p \right)^n f^{k_1}}{E} + C_2 N_f^{-\beta} f^{(1-k)\beta} \quad [7.66]$$

i.e., by eliminating $\Delta\epsilon_p$ with the help of relation $\left(N_f f^{k-1} \right)^\beta \Delta\epsilon_p = C_2$,

$$\Delta\epsilon = \frac{A}{E} f^{k_1} \frac{C_2^n}{N_f^{n\beta} f^{n(k-1)\beta}} + C_2 N_f^{-\beta} f^{(1-k)\beta} \quad [7.67]$$

$$\Delta\epsilon = \frac{A}{E} C_2^n N_f^{-n\beta} f^{k_1 - n(k-1)\beta} + C_2 N_f^{-\beta} f^{(1-k)\beta} \quad [7.68]$$

We then have a generalized fatigue equation that can apply to high and low temperatures simultaneously. At high temperatures, constants A , C_2 , n , β , k and k_1 must be determined for each temperature.

We derive the Manson equation at regular temperatures by assuming that the frequency has no effect: $k = 0$ and $k_1 = 0$.

If we let $\beta = 0.6$, $n = 0.2$, $C_2 = \delta^{0.6}$ (ϵ_f = tensile ductility) and $A = 3.5 \frac{R_m}{\epsilon_f^{0.12}}$

(R_m = ultimate stress), we have

$$\Delta \epsilon = \frac{3.5 R_m}{E} N_f^{-0.12} + \epsilon_f^{0.6} N_f^{-0.6} \quad [7.69]$$

which is the relation given by Manson.

If $k = 1$, $\beta = 0.5$, $C_2 = 0.5 \epsilon_f$, $k_1 = 0$, $n = 0$ and $A = 2 \sigma_D$, (σ_D = fatigue limit of the material), we find the relation proposed by Langer:

$$\Delta \epsilon = \frac{2 \sigma_D}{E} + \frac{\epsilon_f}{2 N_f^{1/2}} \quad [7.70]$$

7.10. Laws of damage accumulation

7.10.1. Miner rule

Several authors attempted to link the energy dissipated by hysteresis to fatigue (this is the case with Miner, for example) by suggesting that fracture by fatigue occurs when the quantity of energy absorbed by the specimen reaches a critical value [LIE 78] [YAO 62]. However, this criterion was often questioned as the energy absorbed by the complete system cannot exactly represent the energy required for a highly localized fatigue fracture. We could show that all the mechanical hysteresis energy does not lead to material damage and that there is hysteresis below the limit of fatigue that, when produced by an inelastic deformation of the material, does not generate fatigue damage.

The Miner rule is used, however. Each level $\Delta \epsilon_i$ cycle creates damage $\frac{1}{N_i}$ and total damage is written as

$$D = \sum_i \frac{1}{N_i} . \quad [7.71]$$

Fracture occurs (in theory) when $D = 1$.

J.G. Sessler and V. Weiss [SES 63] have shown that at fracture, quantity

$$D = \sum_i \frac{n_i}{N_i} \quad [7.72]$$

can vary from 0.6 to 1.6 (A302 and 4340 steels) and is sensitive to the sequence of strain application when several levels are applied consecutively.

Considering the Coffin relation, this expression of damage can also be written as

$$D = \frac{1}{C^{1/\beta}} \sum_i \Delta \varepsilon_{p_i}^{1/\beta} . \quad [7.73]$$

i.e., if $\beta = \frac{1}{2}$,

$$D = \frac{1}{C^2} \sum_i \Delta \varepsilon_{p_i}^2 . \quad [7.74]$$

This law can be better verified by experience than with the Miner rule applied in the field of elastic fatigue [BAR 80].

Several authors use the Miner rule, and note that the sequence of strain application also has an influence in this field, since damage D is greater than that for LO-HI sequences [COF 62].

Ju *et al.* [JU 69] provide the following rule for shear stress:

$$\sum_{i=1}^n \left(\frac{\Delta \gamma_i}{\gamma_u} \right)^p = 1.0 \quad [7.75]$$

where $\Delta \gamma_i$ is the range of variation of plastic shear strain for cycle i , γ_u is shear fracture strain for one load cycle and p is an empirical constant, based on the material and load speed (frequency).

For light alloy test bars (6061 - T6), $p = 1.26$ for dynamic tests and $p = 1.06$ for static tests. Specimens can therefore support more dynamic load cycles than static load cycles [COF 62].

7.10.2. Yao and Munse relation

J.T.P. Yao and W.H. Munse [YAO 62a] established a relation describing the accumulation of fatigue by plastic strain for steel for useful lifetimes lower than 1,000 cycles:

$$\sum_{i=1}^n \left[\left(\frac{\Delta q_t}{\Delta q_{t_i}} \right)^{1/m} \right] = 1 \quad [7.76]$$

where Δq_t is the variation of the real tensile cyclic plastic strain, Δq_{t_i} is the value of Δq_t for $n = 1$, m is a constant equal to the slope of $\Delta \varepsilon_t(N)$ in logarithmic axes, n is the number of applied cycles and $\Delta \varepsilon_t$ is the variation of calculated plastic cyclic strain.

Relation $N^\beta \Delta \varepsilon_p = C$ can be used to calculate damage, by accepting that damage is based on plastic strain accumulated in the part. At each cycle, we have [LIE 82a]:

$$\frac{dD}{dn} = \left(\frac{\Delta \varepsilon_p}{C} \right)^{1/\alpha} \quad [7.77]$$

where $\alpha \approx \frac{1}{2}$ [KIK 71] and C is a constant of the material approximately proportional to fracture ductility ε_f .

There is a fracture if $D = 1$, i.e. if

$$D = \frac{1}{2} \sum_{i=1}^{2N} \left(\frac{|\Delta \varepsilon_{pi}|}{C} \right)^{1/\alpha} = 1 \quad [7.78]$$

which results from applying the Miner rule to imposed strain amplitude tests (cumulative linear law). $|\Delta \varepsilon_{pi}|$ is the value of the plastic strain range for each half cycle. M. Kikukawa and M. Jono [KIK 71] observe that this hypothesis provides a good approximation of the useful lifetime measured for smooth specimens for many materials under different load conditions.

This method makes it possible to forecast a useful lifetime in imposed strain or load, by measuring total strain. By subtracting elastic strain $\frac{\Delta \sigma}{E}$, we have $\Delta \varepsilon_p$ hence damage D .

This relation does not consider the order of sequence or cycle application. It therefore only applies if over- or under-load effects are insignificant.

7.10.3. Use of the Manson–Coffin relation

From relation [7.23], we can note the damage per cycle in the form [LIE 82a]:

$$\frac{dD}{dN} = \frac{1}{2 N_t} \left(\frac{\Delta \epsilon_p}{\Delta \epsilon_e} \right)^{\frac{1}{\beta - \frac{1}{b}}} \quad [7.79]$$

where $2 N_t$ (number of half cycles) is the abscissa of the point of intersection of *elastic* and *plastic* straight lines in the Manson–Coffin diagram.

7.11. Influence of an average strain or stress

If we carry out a test in which strain ϵ varies between two values ϵ_{\min} and ϵ_{\max} such as mean strain,

$$\epsilon_{\text{mean}} = \frac{\epsilon_{\min} + \epsilon_{\max}}{2} \quad [7.80]$$

must be non-zero, the presence of this mean strain has very little influence on the behavior of the specimen: after significant initial stretching during the first cycle, the mean stress relaxes and the test continues as if the mean strain was zero.

A decrease of endurance (useful lifetime) can sometimes be observed in some sequences where ϵ_{mean} varies without the mean stress ever completely relaxing.

If the test is carried out with non-zero mean imposed stress, a strain is gradually created and tends to stabilize or not according to the amplitude of the imposed stress. There is a *limit of accommodation* beyond which there is no stabilization any longer and we very quickly reach fracture [PLE 68].

The simultaneous application of a cyclic strain and a permanent strain increases fracture ductility for many types of metals [COF 62].

J.G. Sessler and V. Weiss [SES 63] showed that a mean strain and a pre-strain are equivalent in low cycle fatigue tests.

G. Sachs *et al.* [MAT 71] could verify that the Coffin expression is correct for completely alternating strains for which the ratio $R = \frac{\epsilon_{\min}}{\epsilon_{\max}}$ is equal to -1 .

For $R \neq -1$, we have a pre-strain requiring the modification of the Coffin relation as follows:

$$N = \left(\frac{\epsilon'_f - \epsilon_0}{\Delta\epsilon} \right)^{1/\beta} \quad [7.81]$$

or

$$N^\beta \Delta\epsilon = \epsilon'_f - \epsilon_0 \quad [7.82]$$

where:

$$\epsilon_0 = \frac{1}{2}(\epsilon_{\max} + \epsilon_{\min}) = \text{pre-deformation};$$

$$\Delta\epsilon = \epsilon_{\max} - \epsilon_{\min} = \text{range of strain};$$

$$\epsilon'_f = \text{apparent fracture ductility obtained by extrapolation for } N = \frac{1}{4} \text{ cycle; and}$$

$$\beta = \text{constant close to } 0.5.$$

T.H. Topper and B.I. Sandor [TOP 70] conclude after an experimental study that:

– a plastic pre-strain significantly decreases useful lifetime measured in elastic strains, but has little effect on useful lifetime in plastic strains; and

– pre-strain tensile and compression effects can be correctly represented by an empirical relation of the form:

$$\frac{\Delta\sigma^*}{2} = \frac{\Delta\sigma}{2} + \frac{\sigma_0^\alpha}{E} \quad [7.83]$$

where E is Young's modulus. T.H. Topper and B.I. Sandor [TOP 70] then combine damages according to the Miner rule.

We have seen that the mean stress has little influence, because the material adapts in the plastic field. The presence of mean stress σ_{mean} only occurs on the “elastic” part of the relation [DEV 86].

The modified stress-strain relation [7.43] from Manson–Coffin can also take the form

$$\frac{\Delta \varepsilon}{2} = \frac{\sigma'_f - \sigma_{\text{mean}}}{E} (2N)^B + \varepsilon'_f (2N)^c \quad [7.84]$$

This expression provides similar results to Goodman’s (strength to fracture is replaced by σ'_f) [DEV 86] [LIE 82a] [NEL 78].

7.11.1. Other approaches

7.11.1.1 Modification of the strength to fracture coefficient

We consider that a mean stress alters the value of the strength to fracture coefficient in the stress-strain relation. If tension is involved, it decreases strength to fatigue; if compression is involved, it increases it.

In the case of a tensile mean stress, we have

$$\sigma_a = (\sigma'_f - \sigma_{\text{mean}}) N^b \quad [7.85]$$

and in the case of a compression mean stress

$$\sigma_a = (\sigma'_f + \sigma_{\text{mean}}) N^b \quad [7.86]$$

By substituting these values into relation [7.22], we have

$$\varepsilon = \frac{(\sigma'_f \mp \sigma_{\text{mean}})}{E N^{1/b}} + \frac{\varepsilon'_f}{N^{\beta}}. \quad [7.87]$$

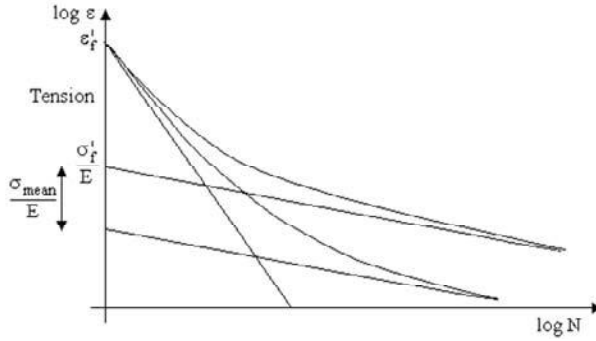


Figure 7.27. Influence of a non-zero mean stress

7.11.1.2. Smith relation

Smith *et al.* [SMI 69] propose the relation

$$\frac{\Delta \varepsilon}{2} = \frac{\sigma_f' (2 N_f)^b}{\sigma_{\max}} \left[\frac{\sigma_f'}{E} (2 N_f)^b + \varepsilon_f' (2 N_f)^c \right] \quad [7.88]$$

According to Morrow [MOR 64a]:

$$\varepsilon_a = \left(\frac{\sigma_f'}{E} \right) (2 N_f)^b + \varepsilon_f' (2 N_f)^c \quad [7.89]$$

and

$$\sigma_a = \sigma_f' (2 N_f)^b. \quad [7.90]$$

7.12. Low cycle fatigue of composite material

This subject will not be developed here because of the wide range of composite materials. We will only mention an experimental study by B.D. Agarwal and J.W. Dally [AGA 75] on composite material (SCOTCHPLY - 1000, fiberglass reinforced plastic) that has shown that:

– the relation of the form

$$N^k \Delta \varepsilon = C \quad [7.91]$$

correctly applies ($\Delta\epsilon$ being total strain, since there is no plastic strain with this material);

– controlled stress and controlled strain tests lead to the same results, on the condition that data be normalized considering $\frac{\Delta\epsilon}{R_m}$ and $\frac{\Delta\epsilon}{\epsilon_f}$ ratios where ϵ_f is the ultimate fracture strain and R_m is the ultimate fracture stress; and

– we observe a progressive decrease of modulus $E = \frac{\Delta\sigma}{\Delta\epsilon}$ in a linear way according to $\log N$. This variation is caused by progressive fractures of strands.

A synthesis carried out by A.W. Cardrick [CAR 73a] from a few studies also shows that the Miner rule can apply to a certain number of composite materials and that it offers a dispersion in relation to a $D = 1$ fracture that is no more significant than for metals and alloys.

Chapter 8

Fracture Mechanics

8.1. Overview

Wöhler curves are often used in fatigue studies in order to define a fatigue limit under which there is no fracture by fatigue and therefore for which cracking does not become initiated.

Certain parts may, however, have manufacturing problems from which a crack can appear which will propagate until fracture, even if the stress is lower than the limit of fatigue [LIE 82].

A large number of studies were carried out to attempt to predict the propagation of cracks in aeronautical structures experiencing repeated loads. Among the most important reasons noted in these studies is the need to:

- evaluate as accurately as possible the useful lifetime of airplane parts in service in which cracks or other damage were detected and defining inspection intervals;
- manage airplane security considering possible evolutions during use; and
- satisfy project specifications in relation to damage tolerances imposed by civilian and military users. This type of specification may, for example, require that all major structures, from a security standpoint, be designed so that the damage that may have occurred initially and which may have been ignored during a service inspection cannot reach a critical dimension and produce a fracture or the loss of a plane during a certain period of time [WOO 73].

The behavior of a part in fatigue can be studied from endurance curves (Wöhler) and, with the crack propagation aspect, curves of endurance can be checked to ensure they do not distinguish.

We will see that, after initiation in a smooth specimen, propagation of a crack is a short phase in the specimen's lifespan in relation to its total lifetime: less than 5%, according to the level of stress.

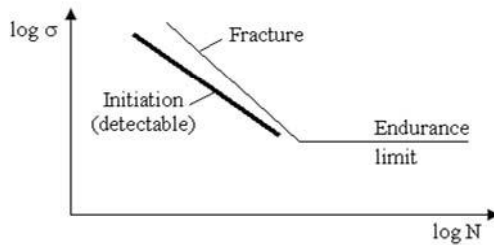


Figure 8.1. *S-N curve*

However, for a pre-cracked part (elements of some structures can only work in these conditions because of the stresses imposed), this phase is often predominant and can almost constitute the complete useful lifetime of the part; hence its importance and the necessity of a complementary study [LIE 82].

Fracture mechanics was developed from the brittle fracture: i.e. the catastrophic fracture of a structure composed of a generally ductile material under insignificant stress, lower than the yield stress calculated for the complete area and with no notable plastic strain.

A *brittle fracture* is a fracture that occurs suddenly and that is not preceded by a large increase in strain [JOH 53].

A perfectly brittle material would be a material for which complete fracture would occur at the same moment as fracture at the most fragile point (where there is a concentration of stresses).

Fracture occurs when the load to fracture is exceeded without prior plastic strain.

A *plastic fracture*, on the contrary, is a fracture preceded by large strains. A perfectly plastic material would have unlimited amplitude to support strains, with resistance that is equal to strength to fracture [JOH 53].

Between these two extremes, we find materials with intermediate characteristics with all possible cases.

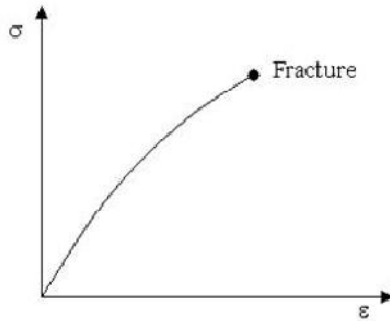


Figure 8.2. *Stress-strain curve of a brittle material*

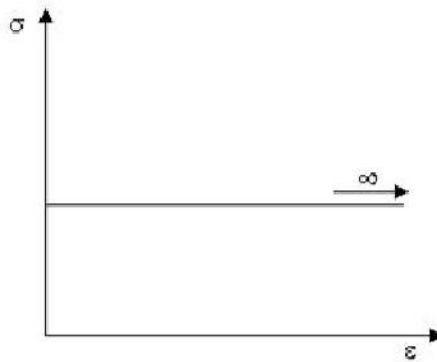


Figure 8.3. *Stress-strain curve of a perfectly plastic material*

Experience shows that brittle fractures always come from cracks developed during the part's lifetime, or from cracks in welds that can have occurred during manufacturing [POO 70].

Fracture mechanics is mainly used in aeronautics and for studies of pressurized tank behavior, for which cracks can lead to leaks (for example, space vehicles).

8.1.1. Definition: stress gradient

Stress gradient χ is by definition the tangent slope of the root of notch stress field, reported to the maximum value of the stress in the same location [BRA 80a]:

$$\chi = \lim_{x \rightarrow 0} \frac{1}{\sigma_{\max}} \frac{d\sigma}{dx} \text{ (mm}^{-1}\text{)} \quad [8.1]$$

8.2. Fracture mechanism

8.2.1. Major phases

From faults in the material (faults or circumstances favorable to a local decohesion of the material because of a high concentration of stresses, inhomogenities in a polycrystalline metal, etc.), alternating stresses create micro-cracks that quickly increase to a few surface micrometers (after a few 10^6 cycles). Progression then becomes slower before accelerating once more at the end of the lifetime between part fracture [RAB 80]. The propagation phase from a micro-crack to fracture can last 90% longer than the part's total useful lifetime [HAR 61].

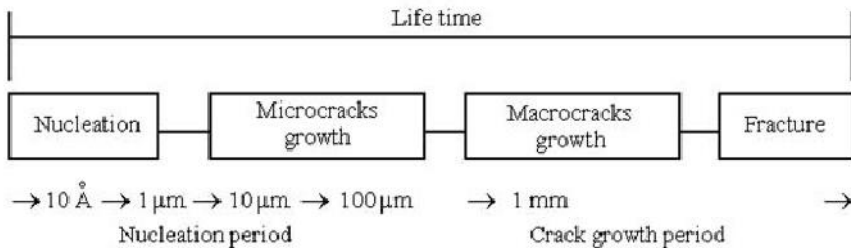


Figure 8.4. *Fracture mechanism [SOB 92]*

Damage can then be considered as a progressive change in the material's microstructure, all the way to nucleation and propagation of cracks by localized action of tension/compression alternating stresses and plastic strains.

The useful lifetime of a part submitted to cyclic loads leading to fracture by fatigue can be schematically broken down into three phases [BAR 80] [HEA 53] [MAR 58] [PAR 62] [RAB 80]:

- initiation of the crack;

- slow propagation of the crack. Some authors distinguish between the propagation of micro-cracks and cracks (macro-cracks). In general, the phase involving macro-cracks is the second phase; and
- sudden propagation leading to fracture (propagation of the crack caused by, for example, static load [IRW 58]).

8.2.2. Initiation of cracks

In the first fatigue phase, damage is expressed by the formation of isolated micro-cracks from an initial defect, ensuring relaxation of high strain incompatibility zones [FRE 68]. In general, cracks appear on the surface of parts for many reasons: greater surface stresses under certain load conditions (torsion, bending, etc.), corrosion, machining faults, fillets, piercing, notches, etc.

During the nucleation step, the process of damage occurs at a level that is greatly influenced by the random nature of the micro-structure: the damage model should therefore be probabilistic in this phase.

The probability of initiating a crack in a given zone of a part mainly depends on the local dynamic stress in this zone. Any geometric, physical or metallurgical phenomenon which increases the amplitude of the stress to a point has significant influence on the behavior at fatigue.

Resistance to the initiation of cracks for large numbers of N fracture cycles is directly linked to the mechanical strength to the material characterized by the ultimate stress R_m . For small N values, ductility is an important factor.

Different methods for predicting the number of cycles necessary for initiating cracks were developed, based on local strain amplitude, on the Neuber coefficient or on the stress intensity factor. These methods only involve a limited number of parameters, probably much lower than the actual number. Because of this uncertainty and the almost general observation of the presence of quasi-macroscopic faults in structures within manufacturing, it appears that this number of cycles should be considered zero [BAR 80].

Time of crack initiation can also be considered as the number of stress (or strain) cycles producing, for example, a 1 mm long crack (a micro-crack is a crack that can reach 0.5 to 1 mm) [MUR 83].

We most often consider that when a crack reaches a length of 0.1 mm [PAR 63] [RAB 80], it regularly propagates in the section. This length (0.1 mm) is

conventional and, according to the authors, there are different values in the literature: 0.05 mm [HEA 53], 0.5 mm [NOW 63], 50 to 100 μm [LIE 82], 10 mm [SCH 70]. G. Glinka and R.I. Stephens [BER 83] choose 0.25 mm, by specifying that this value is convenient but that the exact value is not the most important for the calculation of the total useful lifetime (in a reasonable field).

The initial dimension of cracks, a , is sometimes considered as a random variable [HAR 83]. Probability densities are chosen by considering the fact that the crack cannot be larger than the initial thickness h of the part.

Example 8.1.

The *exponential Marshall law* [MAR 76] is of the form:

$$p(a) = \frac{e^{-a/\mu}}{\mu (1 - e^{-h/\mu})} \quad [8.2]$$

where $\mu = 6.25$ mm.

The *log-normal Becher and Hansen law* [BEC 81] [JOH 83] is expressed:

$$p(a) = \frac{1}{\mu a H \sqrt{2\pi}} e^{-\frac{\left(\ln \frac{a}{\lambda}\right)^2}{2\mu^2}} \quad [8.3]$$

where

$$H = 1 - \frac{1}{2} \operatorname{erfc} \left(\frac{\ln \frac{h}{\lambda}}{\mu \sqrt{2}} \right),$$

$\mu = 0.82$ and $\lambda = 1.3$ mm.

For welded structures, the mean value of a equals $\bar{a} = 0.15$ mm and standard deviation $\sigma_a = 0.083$ mm.

By considering variable $\alpha = \ln a$, α obeys a normal law defined by $N[-2.031 ; 0.267]$.

With this angle, the fatigue limit can be defined as the minimum stress leading to the initiation of a crack or to a crack that propagates. This definition is arbitrary and could be different whether we consider the appearance of a micro-crack or a micro-structural evolution of the material.

8.2.3. *Slow propagation of cracks*

Propagation of the crack is generally slow depending on the material's ductility properties.

The growth of cracks in the metal depends on their crystalline structure, the environment and the distribution of stresses in a zone close to the crack.

Microscopically, we observe grooves; each groove can be associated with a load cycle in the case of variable load amplitude tests [MIL 67].

The emergence of a small crack is not always the sign of a future fracture. The crack sometimes stops or progresses very slowly. However, since we cannot predict for sure if the crack will stop, it would be wise to presume that it will continue to fracture and, if the part is vital, it should be replaced.

Linear elastic fracture mechanics is based on the analytical result that elastic stresses surrounding the root of the crack have a distribution that is independent from the applied load and geometry [PAR 65]. The intensity of the stress field around the root of the crack can however be uniquely described according to these two parameters.

8.3. Critical size: strength to fracture

Consider a cracked part experiencing a sinusoidal σ stress; the size of the crack will increase over time until it reaches a critical value a_c at which time the part will break. The location of a_c values when σ changes (Figure 8.5) characterizes *strength to fracture* of the material.

This parameter measures the strength of the material to fractures with load. For a given σ stress, this curve results in a_c and conversely [WEI 78].

The potential strength of a material is therefore defined by the size of the dominant crack present in the part and by the material's strength to fracture.

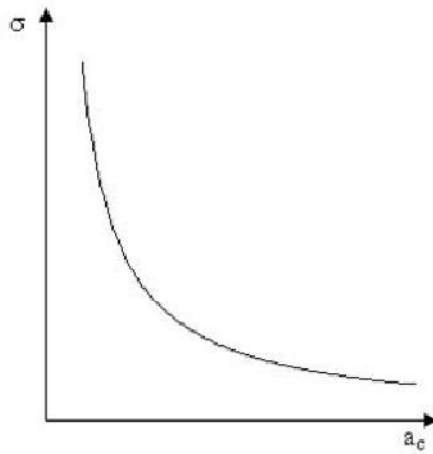


Figure 8.5. *Stress versus critical size curve*

Contrary to the traditional approach of fatigue analysis, the fracture mechanics approach focuses on the *growth of the fatigue crack* step instead of on the initiation or the initiation/propagation group step. Here we assume the presence of an initial crack. This methodology and corresponding hypotheses are well justified through experience [TIF 65].

Fracture mechanics focuses on the propagation of the crack from an initial size a_i to the size to fracture for a critical size a_c according to the number of cycles N (Figure 8.6).

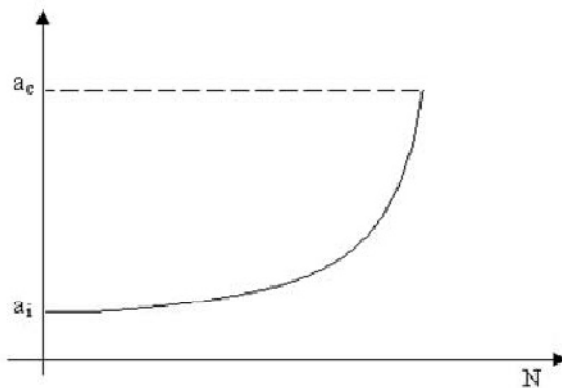


Figure 8.6. *Size of the crack according to the number of cycles (for a sinusoidal constant amplitude stress)*

Cracks spread with the appearance of grooves and ripples described by C. Laird [LAI 66], followed by B. Tomkins and W.D. Biggs [TOM 69].

Over time, as the crack increases, we can observe a decrease in the part's strength (Figure 8.7).

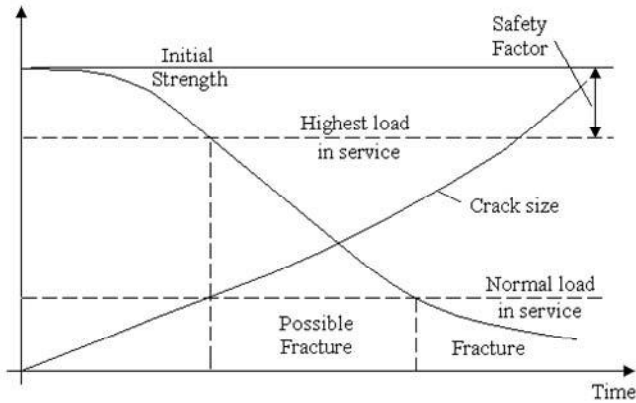


Figure 8.7. *Evolution of strength according to time [BRO 78]*

After a certain amount of time, the part's strength is such that it can no longer support the greatest service load. If this load does not appear, strength continues to decrease until fracture occurs during load.

The duration of each step varies. For smooth specimens duration of phase I can be between 50 and 95% of the part's total useful lifetime, for useful lifetimes between 10^3 and 10^5 cycles [LIE 82], and can reach 99% for longer useful lifetimes.

8.4. Modes of stress application

Stresses can increase the size of a crack in several modes; they can be applied [BRO 78] [MCC 64] [POO 70] [SHE 83a] [TAD 73]:

- from YY' axis, where they then open the crack (mode I);
- from XX' axis (movement of crack edges to plane) (mode II); or
- from ZZ' axes (tear) (mode III), perpendicular to the crack's plane.

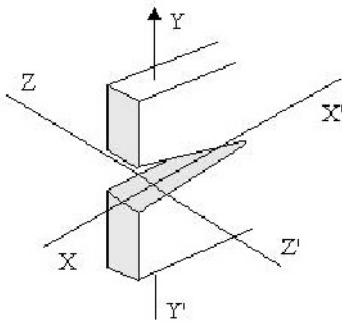


Figure 8.8. *Axes of the crack*

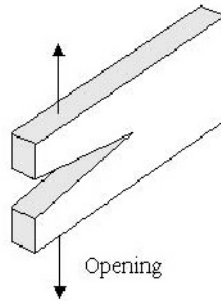


Figure 8.9. *Mode I*

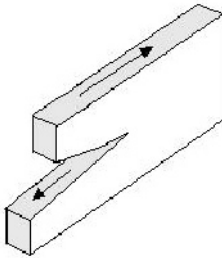


Figure 8.10. *Mode II*

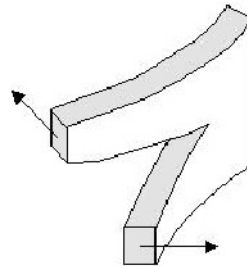


Figure 8.11. *Mode III*

Superposition of these three modes is sufficient to describe the more general case of crack opening. It is traditional to add roman numbers I, II and III to the different symbols used in calculations to indicate the mode. The fracture of isotropic brittle materials usually occurs in mode I, which explains the close attention paid to this mode [POO 70].

8.5. Stress intensity factor

8.5.1. *Stress in crack root*

The distribution of stresses in the neighborhood of the tip of a crack was studied by L.N. Sneddon [SNE 46], followed by G.R. Irwin [IRW 57] [IRW 58a], using a calculation method proposed by H.M. Westergaard [EFT 72] [WES 39] and M.I. Williams [WIL 57].

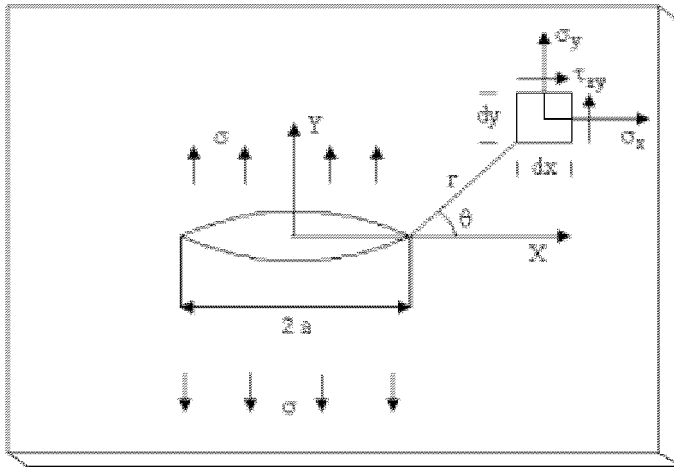


Figure 8.12. *Plate element in the crack root neighborhood*

Consider a cracked plate (Figure 8.12) and suppose that all stresses in the plate remain in the elastic field in the first place.

In the vicinity of any point of the contour of the crack, stresses tend towards infinity.

A $dx\,dy$ element of the plate located at a distance r from the root of the crack, with a θ angle in relation to the crack plane, experiences normal stresses σ_x and σ_y in the X and Y directions and shear stresses τ_{xy} .

The singular part of the field of stress only depends on three parameters K_I , K_{II} and K_{III} corresponding to the three modes listed above.

The distribution of stresses for a given geometric form and given loads can be established by the traditional elastic theory, under the condition that the values of calculated stresses are purely elastic and that corresponding strains are small.

In practice, stresses which are too great result in plastic strains which, in turn, increase the limit of elasticity by hardening.

Despite these limitations, the elastic theory is very useful if it is associated with experimental results.

We show that the field of stresses is given by the following asymptotic developments (mode I) [BRO 78] [PAR 61] [PAR 62] [PAR 65] [TAD 73]:

$$\sigma_x \approx \sigma \sqrt{\frac{a}{2r}} \cos \frac{\theta}{2} \left(1 - \sin \frac{\theta}{2} \sin \frac{3\theta}{2} \right) \quad [8.4]$$

$$\sigma_y \approx \sigma \sqrt{\frac{a}{2r}} \cos \frac{\theta}{2} \left(1 + \sin \frac{\theta}{2} \sin \frac{3\theta}{2} \right) \quad [8.5]$$

and

$$\tau_{xy} \approx \sigma \sqrt{\frac{a}{2r}} \sin \frac{\theta}{2} \cos \frac{\theta}{2} \cos \frac{3\theta}{2}. \quad [8.6]$$

According to the ZZ' axis perpendicular to plane XY , we have:

$$\sigma_z = 0 \text{ (plane stress)}$$

or

$$\sigma_z = \nu (\sigma_x + \sigma_y) \text{ (plane strain)} \quad [8.7]$$

where ν is Poisson's ratio (approximations are obtained by eliminating the higher-order terms in r).

The stresses are always plane to the surface. The plane strain hypothesis can be used within a plate. In this case, the stress perpendicular to the plane has an amplitude that varies from zero at surface to the corresponding value at the plane strain within the plate. The plastic zone is therefore more important at the center than at the surface.

8.5.2. Mode I

Elastic stress fields [POO 70] are defined:

$$\sigma_x = \frac{K_I}{\sqrt{2\pi r}} \cos \frac{\theta}{2} \left(1 - \sin \frac{\theta}{2} \sin \frac{3\theta}{2} \right), \quad [8.8]$$

$$\sigma_y = \frac{K_I}{\sqrt{2\pi r}} \cos \frac{\theta}{2} \left(1 + \sin \frac{\theta}{2} \sin \frac{3\theta}{2} \right) \quad [8.9]$$

and

$$\tau_{xy} = \frac{K_I}{\sqrt{2\pi r}} \sin \frac{\theta}{2} \cos \frac{\theta}{2} \cos \frac{3\theta}{2}. \quad [8.10]$$

Plane strain is described by:

$$\sigma_z = \nu (\sigma_x + \sigma_y) \quad [8.11]$$

and

$$\tau_{xy} = \tau_{yz} = 0$$

where, for plane stress, $\sigma_z = 0$. Displacements corresponding to X, Y and Z directions are represented:

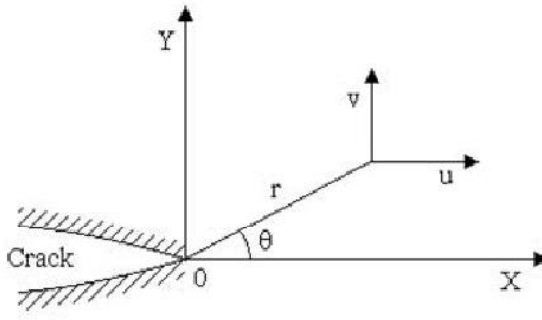


Figure 8.13. Displacement notation at distance r from the root of the crack

$$u = \frac{K_I}{G} \sqrt{\frac{r}{2\pi}} \cos \frac{\theta}{2} \left(1 - 2\nu + \sin^2 \frac{\theta}{2} \right), \quad [8.12]$$

$$v = \frac{K_I}{G} \sqrt{\frac{r}{2\pi}} \sin \frac{\theta}{2} \left(2 - 2\nu - \cos^2 \frac{\theta}{2} \right) \quad [8.13]$$

and $w = 0$, where $G = \frac{E}{2(1+\nu)}$ (shear modulus).

These relations can also be written as

$$u = \frac{K_I}{4\mu} \sqrt{\frac{2r}{\pi}} \left[(K-1) \cos \frac{\theta}{2} + \sin \theta \sin \frac{\theta}{2} \right], \quad [8.14]$$

$$v = \frac{K_I}{4\mu} \sqrt{\frac{2r}{\pi}} \left[(K-1) \sin \frac{\theta}{2} - \sin \theta \cos \frac{\theta}{2} \right] \quad [8.15]$$

where

$$2\mu = \frac{E}{1-\nu}. \quad [8.16]$$

In plane strain,

$$K = 3 - 4\nu, \quad [8.17]$$

$$\frac{K-1}{4\mu} = \frac{(1-2\nu)(1+\nu)}{E} \quad [8.18]$$

and

$$\frac{K+1}{2\mu} = \frac{2(1-\nu^2)}{E}. \quad [8.19]$$

In plane stress, we have

$$K = \frac{3-\nu}{1+\nu}, \quad [8.20]$$

$$\frac{K-1}{4\mu} = \frac{1-\nu}{E} \quad [8.21]$$

and

$$\frac{K+1}{2\mu} = \frac{2}{E}. \quad [8.22]$$

8.5.3. Mode II

$$\sigma_x = -\frac{K_{II}}{\sqrt{2\pi r}} \sin \frac{\theta}{2} \left(2 + \cos \frac{\theta}{2} \cos \frac{3\theta}{2} \right) \quad [8.23]$$

$$\sigma_y = \frac{K_{II}}{\sqrt{2\pi r}} \sin \frac{\theta}{2} \cos \frac{\theta}{2} \cos \frac{3\theta}{2} \quad [8.24]$$

$$\tau_{xy} = \frac{K_{II}}{\sqrt{2\pi r}} \cos \frac{\theta}{2} \left(1 - \sin \frac{\theta}{2} \sin \frac{3\theta}{2} \right) \quad [8.25]$$

In plane strain,

$$\sigma_z = \nu (\sigma_x + \sigma_y) \quad [8.26]$$

$$\tau_{xy} = \tau_{yx} = 0$$

(in plane stress, $\sigma_z = 0$).

$$u = \frac{K_{II}}{G} \sqrt{\frac{r}{2\pi}} \sin \frac{\theta}{2} \left(2 - 2\nu + \cos^2 \frac{\theta}{2} \right) \quad [8.27]$$

$$v = \frac{K_{II}}{G} \sqrt{\frac{r}{2\pi}} \cos \frac{\theta}{2} \left(-1 + 2\nu + \sin^2 \frac{\theta}{2} \right) \quad [8.28]$$

$$w = 0$$

8.5.4. Mode III

$$\tau_{xy} = -\frac{K_{III}}{\sqrt{2\pi r}} \sin \frac{\theta}{2} \quad [8.29]$$

$$\tau_{yz} = \frac{K_{III}}{\sqrt{2\pi r}} \cos \frac{\theta}{2} \quad [8.30]$$

$$\sigma_x = \sigma_y = \sigma_z = \tau_{xy} = 0 \quad [8.31]$$

$$w = \frac{K_{III}}{G} \sqrt{\frac{2r}{\pi}} \sin \frac{\theta}{2} \quad [8.32]$$

$$u = v = 0$$

8.5.5. Field of equation use

These equations were established for static or slowly progressing cracks from serial developments of fields of stress, by ignoring the highest order terms in r . These are good approximations when r is small in relation to the other part dimensions in the plane (x, y) . They tend to be exact when r tends towards zero.

For $\theta = 0$, we have:

$$\sigma_y = \sigma \sqrt{\frac{a}{2r}} = \sigma_x. \quad [8.33]$$

When $r \rightarrow \infty$, $\sigma_y \rightarrow 0$ (instead of σ) and when $r \rightarrow 0$, $\sigma_y \rightarrow \infty$.

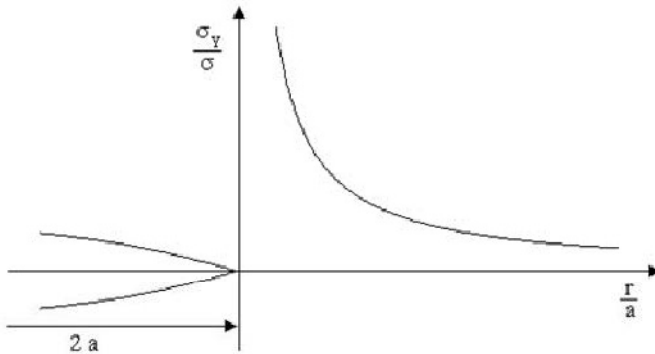


Figure 8.14. Stress versus distance r

The above equations can only be used around the root, albeit with a modification to take into consideration the fact that, when r tends towards zero, the stress cannot be infinite by remaining in the elastic field.

For $\theta = 0$, the shear stress τ_{xy} is zero. Principal stresses σ_1 and σ_2 are equal to σ_x and σ_y , respectively. The third principal stress is perpendicular to the plate ($\sigma_3 \equiv \sigma_z$).

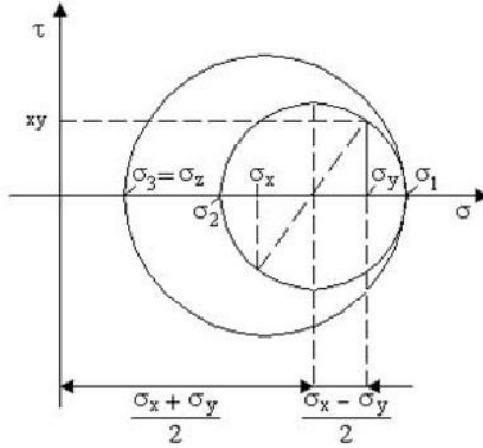


Figure 8.15. Mohr's circle: principal stresses (any θ)

If θ is ordinary, principal stresses at any point can be calculated from the Mohr circle:

$$\sigma_{1,2} = \frac{\sigma_x + \sigma_y}{2} \pm \sqrt{\left(\frac{\sigma_x - \sigma_y}{2}\right)^2 + \tau_{xy}^2}. \quad [8.34]$$

By replacing σ_x and σ_y with their expression given by relations [8.4] to [8.7], we have

$$\sigma_1 = \frac{K_I}{\sqrt{2\pi r}} \cos \frac{\theta}{2} \left(1 + \sin \frac{\theta}{2}\right), \quad [8.35]$$

$$\sigma_2 = \frac{K_I}{\sqrt{2\pi r}} \cos \frac{\theta}{2} \left(1 - \sin \frac{\theta}{2}\right) \quad [8.36]$$

and

$$\sigma_3 = 0$$

or

$$\sigma_3 = \frac{2 \gamma K_I}{\sqrt{2 \pi r}} \cos \frac{\theta}{2} . \quad [8.37]$$

8.5.6. Plastic zone

G.R. Irwin developed a method for evaluating the size of the plastic zone at the tip of the crack in a specimen to a single monotonous load [IRW 60].

If we remain in the field of elastic stresses, relations [8.4] to [8.7] are approximately correct to the limit of the plastic zone, which must make it possible to evaluate the position of the elastic and plastic field border.

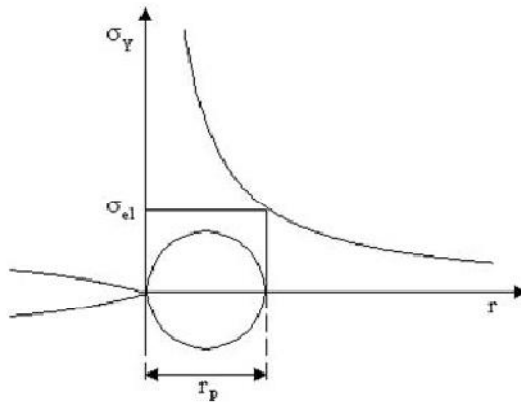


Figure 8.16. Plastic zone at the tip of the crack

We have seen that, in the case of elastic stresses, the solution leads to a curve $\sigma_y(r)$ which can be infinite when $r \rightarrow 0$. Physically, such a behavior is impossible since the stress cannot increase indefinitely without transferring into the plastic field.

A small volume of metal at the root of the notch or at the edge of the crack is submitted to very high stresses and is therefore the subject of a quick plastic evolution during fatigue. At the limits of this field, deformations remain slightly elastic and are imposed by the behavior of the rest of the specimen. The small plastic zone works in imposed strain mode, leading to a decrease of local alternating stresses if the metal is initially work hardened [BAR 77].

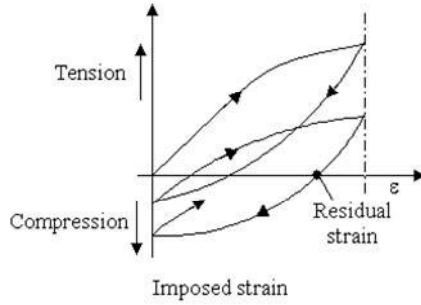


Figure 8.17. Variation of the local alternating stress in imposed strain

At the root of the crack, a plastic zone of length r_p (Figure 8.16) is established and can be approximated from the relation

$$\sigma_y = R_c = \frac{K_I}{\sqrt{2\pi r_p}}, \quad [8.38]$$

hence

$$r_p = \frac{K_I^2}{2\pi R_c^2} \quad [8.39]$$

in plane stress. In practice, the plastic stress zone cannot be greater than r_p .

The plane plastic strain zone r_p^* is smaller than the plane plastic stress zone, because the effective yield stress for plane strains is greater than the yield stress depending on an axis [BRO 78].

Irwin [IRW 60a] shows that the factor making it possible to go from r_p to r_p^* is equal to $\sqrt{2\sqrt{2}} \approx 1.68$, hence the length of plane plastic strain is

$$r_p^* \approx \frac{K_I^2}{6\pi R_c^2}. \quad [8.40]$$

8.5.7. Other form of stress expressions

Relations [8.4] to [8.7] stresses can be expressed as:

$$\sigma_r = \frac{K_I}{\sqrt{2 \pi r}} \cos \frac{\theta}{2} \left(1 + \sin^2 \frac{\theta}{2} \right), \quad [8.41]$$

$$\sigma_\theta = \frac{K_I}{\sqrt{2 \pi r}} \cos \frac{\theta}{2} \left(1 - \sin^2 \frac{\theta}{2} \right) \quad [8.42]$$

and

$$\tau_{r\theta} = \frac{K_I}{\sqrt{2 \pi r}} \sin \frac{\theta}{2} \cos^2 \frac{\theta}{2}. \quad [8.43]$$

In the case of mode II, we show that we have [EFT 72] [PAR 65] [TAD 73]:

$$\left. \begin{aligned} \sigma_r &= \frac{K_{II}}{\sqrt{2 \pi r}} \left(-\frac{5}{4} \sin \frac{\theta}{2} + \frac{3}{4} \sin \frac{3\theta}{2} \right) \\ \sigma_\theta &= \frac{K_{II}}{\sqrt{2 \pi r}} \left(-\frac{3}{4} \sin \frac{\theta}{2} - \frac{3}{4} \sin \frac{3\theta}{2} \right) \\ \tau_{r\theta} &= \frac{K_{II}}{\sqrt{2 \pi r}} \left(\frac{1}{4} \cos \frac{\theta}{2} + \frac{3}{4} \cos \frac{3\theta}{2} \right) \end{aligned} \right\} \quad [8.44]$$

$$\sigma_z = \nu (\sigma_x + \sigma_y) \quad [8.45]$$

and

$$\tau_{xz} = \tau_{yz} = 0.$$

For an infinite cracked plate with a shear stress τ in the plane at infinite,
 $K_{II} = \tau \sqrt{\pi a}$.

For mode III:

$$\sigma_x = \sigma_y = \sigma_z = \tau_{xy} = 0,$$

$$\tau_{xz} = -\frac{K_{III}}{\sqrt{2\pi r}} \sin \frac{\theta}{2} \quad [8.46]$$

and

$$\tau_{yz} = \frac{K_{III}}{\sqrt{2\pi r}} \cos \frac{\theta}{2}. \quad [8.47]$$

8.5.8. General form

Equations [8.4] to [8.7] can be written in the generalized form

$$\sigma_{ij} = \frac{K_I}{\sqrt{2\pi r}} f_{ij}(\theta) \quad [8.48]$$

where

$$K_I = \sigma \sqrt{\pi a} \quad [8.49]$$

for a plate of infinite width.

For a finite dimension part, we show that we have

$$K_I = \sigma \alpha \sqrt{\pi a} \quad [8.50]$$

where α is a function of the part's geometry and load conditions.

Index I is a reminder that these expressions were obtained for mode I (tension based on axis YY').

We note that σ_{ij} is proportional to load σ , which is the result of the elasticity hypothesis.

The notch root stress is at its highest when radius r is equal to radius ρ of the notch and has a value of

$$\sigma_{\max} = \frac{2 K_I}{\sqrt{\pi \rho}}. \quad [8.51]$$

$\frac{K_I}{\rho}$ is therefore the important parameter in the initiation of cracks.

We show that there is a limit value of this relation beyond which no crack can initiate [BAR 80].

K_I is called “*stress intensity factor*” (not to be confused with the *stress concentration factor* defined as the $K_t = \frac{\sigma_{\max}}{\sigma_{\text{nom}}}$ ratio between the maximum root of notch real stress σ_{\max} and nominal stress σ_{nom} in the same section) [ERD 83].

This factor is important and widely used in fracture mechanics. K_I can be considered as a measure of the load effect and the effect of the part’s geometry on the stress intensity close to the tip of the crack, a measure of the singularity of stresses at the root of the crack [POO 70].

When the load varies and geometry changes because of the expansion of the crack, the instant K_I value reflects the effects of these changes at the root of the crack [PAR 61].

When the size of the plastic zone at this point is small in relation to the length of the crack, factor K_I can provide a good indication of the state of root of notch stresses.

8.5.9. Widening of crack opening

For an elliptical crack, this widening e has a value of

$$e = \frac{4 \sigma a}{E} \quad [8.52]$$

and at the center

$$e_{\max} = \frac{4 \sigma a}{E} . \quad [8.53]$$

From the definition of K , we can observe that two cracks have the same K of $\sigma \sqrt{a} = \text{constant}$.

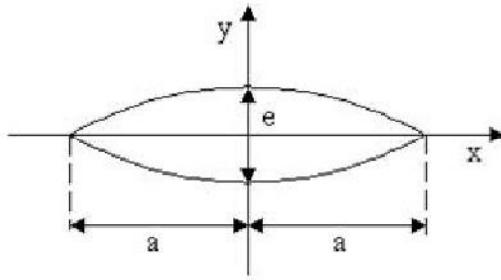


Figure 8.18. *Elliptical crack*

We have seen that the elastic model leads to an infinite elastic stress that is unrealistic close to the bottom of the crack. We can actually observe at that place a plastic deformation in a zone where the size can be evaluated by calculating distance r_p (from the root of crack) to which the elastic stress σ_y exceeds the elasticity limit R_e . From equations [8.33] and [8.49], we obtain for $\theta = 0$ [MCC 64]:

$$r_p = \frac{K_I^2}{2\pi R_e^2} = \frac{\sigma^2 a}{2 R_e^2} \quad [8.54]$$

i.e. r_p only depends on K_I and R_e .

In reality, the plastic zone is larger than is indicated by this relation [BRO 78].

Because of this relation, cracks with the same K_I will have the same behavior. This is true even if we consider the plastic zone around extremities, reinforcing the interest of this parameter, which is a measure of stresses and strains.

8.6. Fracture toughness: critical K value

Two conditions are necessary and sufficient for the growth of a crack under static load:

- there must be a large enough stress to jeopardize an appropriate fracture mechanism; and
- the strain energy triggered by a crack growth increment must be equal to or greater than the energy required to form the new surfaces of the crack [POO 70].

Under an increasing load, a crack starts to grow when stresses and strains at its extremities reach a critical value, or when K_I reaches a critical value K_{Ic} . It continues to grow as long as K_I is higher than K_{Ic} .

K_{Ic} can then be considered as a property of the material appropriately characterizing its resistance to the brittle fracture.

There are tables providing this toughness to fracture for different materials [HOF 68]. K_{Ic} is determined experimentally by resistance to fracture tests, in a similar way to tests intended for measuring the ultimate tensile stress [COF 69].

In the ideal case of an infinite plate with central crack $2a$ long submitted to plane stresses σ acting in a uniform way and perpendicular to the crack [LIA 73], we have [8.49]:

$$K_I = \sigma \sqrt{\pi a}$$

where

$$\sigma = \sigma_m \pm \sigma_a \quad [8.55]$$

σ_m is mean stress and σ_a is alternating stress.

The critical value therefore has the value

$$K_{Ic} = \sigma_c \sqrt{\pi a} . \quad [8.56]$$

K_{Ic} is a parameter characteristic of the material. It is a measure of its toughness to fracture. Two cracked parts of a single material will have the same behavior if they have the same K_{Ic} .

In fact, these relations are established for parts of infinite dimensions. In practice however, we have [TAD 73]:

$$K_I = \sigma \sqrt{\pi a} f\left(\frac{a}{L}\right) \quad [8.57]$$

where L is the width of the plate.

K_{Ic} is a function of $\frac{a}{L}$, tending towards the unit when L becomes very large.

Function $f\left(\frac{a}{L}\right)$ can be expressed in the form of a polynomial in $\frac{a}{L}$.

For a band in tension, C.E. Feddersen [FED 67] provides the following relation (developed from that of M. Isida [ISI 55]):

$$K_I = \sigma \sqrt{\pi a} \sqrt{\sec\left(\frac{\pi a}{L}\right)} \quad [8.58]$$

where $\sec = \frac{1}{\cos}$.

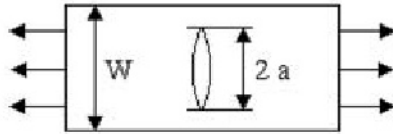


Figure 8.19. *Cracked band in tension*

We have also presumed that the plate has a large enough volume so that displacements in this direction are low (plane strain). If that is not the case (plane stresses), K_{Ic} depends on the size [BRO 78].

Low K_{Ic} materials can only tolerate small cracks.

8.6.1. Units

K_{Ic} is expressed in $\text{MPa} \sqrt{\text{m}}$ or in $\text{MN} / \text{m}^{3/2}$, with the following unit conversions:

$$1 \text{ MN} / \text{m}^{3/2} = 3.23 \text{ kg} / \text{mm}^{3/2} \left(= 0.925 \text{ ksi} \sqrt{\text{in}} \right)$$

$$1 \text{ kg} / \text{mm}^{3/2} = 0.31 \text{ MN} / \text{m}^{3/2} \left(= 0.287 \text{ ksi} \sqrt{\text{in}} \right)$$

$$1 \text{ ksi} \sqrt{\text{in}} = 1.081 \text{ MN} / \text{m}^{3/2} = 3.49 \text{ kg} / \text{mm}^{3/2}.$$

Example 8.2.

For aluminum alloy 7075 - T6,

$$R_m = 560 \text{ MN} / \text{m}^2,$$

$$R_e = 500 \text{ MN} / \text{m}^2$$

and

$$K_{Ic} = 32 \text{ MN} / \sqrt{\text{m}}.$$

Relation [8.56] makes it possible to calculate resistance based on length $2a$ of the crack:

$$\sigma_c = \frac{K_{Ic}}{\sqrt{\pi a}} = \frac{\sqrt{2} K_{Ic}}{\sqrt{2 a \pi}} \quad [8.59]$$

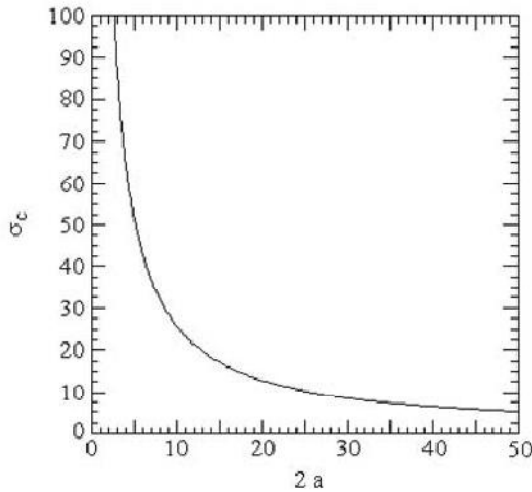


Figure 8.20. Resistance versus $2a$ ($K_{Ic} = 32 \text{ MN} / \sqrt{\text{m}}$)

The resistance decreases by half when $\sigma_c = \frac{R_m}{2}$, when

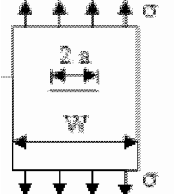
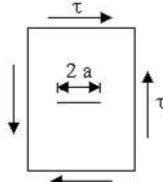
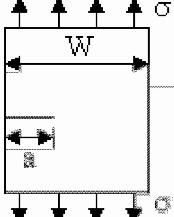
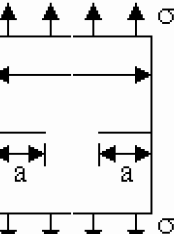
$$a = \frac{4 K_{Ic}^2}{\pi R_m^2} = 0.00416 \text{ m},$$

$$2a = 8.315 \text{ mm}.$$

For $a = 0$, relation [8.59] leads to infinite σ_c . We must correct this relation for small a so that we have $\sigma_c = R_m$.

8.7. Calculation of the stress intensity factor

The calculation problem of parameter K_I is linked to the consideration of conditions to limits. Approximate solutions were obtained in a few cases, particularly for metallic bands with finite width, cracked at the center or on one of the edges loaded in tension (one crack).

	$K_I = \sigma \sqrt{\pi a} \left(\sec \frac{\pi a}{W} \right)^{1/2}$ $K_I = \tau \sqrt{\pi a} \left(\frac{a}{W} \text{ small} \right)$	
	$K_I = 1.12 \sigma \sqrt{\pi a} \left(\frac{a}{W} \text{ small} \right) \text{ or } K_t = Y \sigma \sqrt{a}$ <p style="text-align: center;">with</p> $Y = 1.99 - 0.41 \frac{a}{W} + 18.7 \left(\frac{a}{W} \right)^2 - 38.48 \left(\frac{a}{W} \right)^3 + 53.85 \left(\frac{a}{W} \right)^4$ $(1.99 = 1.12 \sqrt{\pi})$	
	$K_I = 1.12 \sigma \sqrt{\pi a} \left(\frac{a}{W} \text{ small} \right) \text{ or } K_t = Y \sigma \sqrt{a}$ <p style="text-align: center;">with</p> $Y = 1.99 + 0.76 \frac{a}{W} - 8.48 \left(\frac{a}{W} \right)^2 + 27.36 \left(\frac{a}{W} \right)^3$ $(1.99 = 1.12 \sqrt{\pi})$	

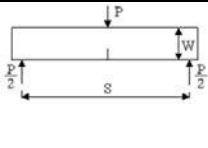
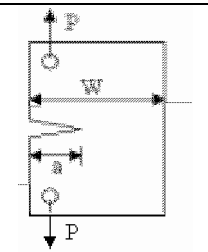
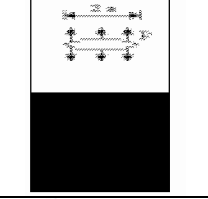
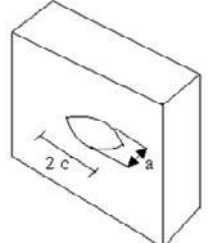
	<p>B width</p> $K_I = \frac{P S}{B W^{3/2}} \left[2.9 \left(\frac{a}{W} \right)^{1/2} - 4.6 \left(\frac{a}{W} \right)^{3/2} + 21.8 \left(\frac{a}{W} \right)^{5/2} - 37.6 \left(\frac{a}{W} \right)^{7/2} + 38.7 \left(\frac{a}{W} \right)^{9/2} \right]$
	<p>B width</p> $K_I = \frac{P}{B W^{3/2}} \left[29.6 \left(\frac{a}{W} \right)^{1/2} - 185.5 \left(\frac{a}{W} \right)^{3/2} + 655.7 \left(\frac{a}{W} \right)^{5/2} - 1017 \left(\frac{a}{W} \right)^{7/2} + 63.9 \left(\frac{a}{W} \right)^{9/2} \right]$
	<p>p by unit width</p> $K_I = p \sqrt{\pi a}$
	$K_{I\max} = 1.12 \frac{\sigma}{\Phi} \sqrt{\pi a}$ $K_{I\max} = 1.12 \frac{\sigma}{\Phi} \sqrt{\pi a^2 / c}$ $\Phi = \int_0^{\pi/2} \left[1 - \frac{c^2 - a^2}{c^2} \sin^2 \varphi \right] d\varphi \approx \frac{3\pi}{8} + \frac{\pi a^2}{8 c^2}$

Table 8.1. Some K_I values

Somewhat detailed tables provide K_I factors [HOF 68] [PAR 65] [ROO 76] [SIH 73] [TAD 73]. Table 8.1 provides some values [BRO 78]. There are a certain number of methods and software for their calculation [BRO 78] [CAR 73] [EDW 77]:

– Analytical methods can be used in the case of geometries and simple limit conditions [IRW 58] [PAR 61]. In two-dimensional problems, factor K_I can be obtained analytically by using common stress analysis methods. Solutions are available for a large number of shapes and load conditions [POO 70]:

- Westergaard stress functions,
- complex stress functions,

- stress concentrations, and
- Green functions.

If there is an internal crack $2a$ in length far from specimen edges, factor K can be obtained from the knowledge of stresses in the uncracked part in the plane of the crack to come, using Green's function [POO 70]:

$$K_I = \frac{1}{\sqrt{\pi a}} \int_{-a}^a \sigma_y(x, 0) \left(\frac{a+x}{a-x} \right)^{1/2} dx. \quad [8.60]$$

The distribution of stresses can be obtained in an experimental way, or analytically:

- integral transform [CAR 73]; or
- using a method based on continuous dislocation models;
- numerical methods are sometimes not so simple [PAR 61]:
 - finite elements, when geometry and stresses applied are complex,
 - “*boundary collocation*” method, and
 - *conformal mapping method*, etc.;
- experimental methods use a relation between K and a measurable parameter (strain, rigidity):
 - compliance (measure of the load applied, the displacement resulting in the load application point, length of the simulated crack, strain gauges, etc.),
 - photoelasticity, and
 - growth rate of fatigue cracks, etc.;
- approximate methods use a combination of intensity factors determined in other configurations and are known with error less than 10% [CAR 74a]

NOTES:

As with other fatigue characteristics, parameter K obeys statistical laws [JOH 82]. The variations observed are caused by metallurgical aspects, impurities or by the manufacturing process [WOO 71], etc.

When there is no clarification, the values given are average values (probability of fracture equal to 50%) [SCH 74]. The literature provides statistical evaluations of K values for certain materials [HEY 70]. H. Leis and W. Schütz [LEI 69] [LEI 70] showed that an envelope value of the standard deviation of resistance to

fracture K_{Ic} of a large number of materials used in aeronautics is equal to 0.05 for samples extracted from a single plate. If that is not the case, the dispersion can be much greater [WOO 71].

Other methods of stress analysis surrounding cracks or notches were proposed by some authors for use with a criterion of fracture [BAR 62] [KUH 64] [MET 76].

These methods, as those described earlier, are based on an elastic stress analysis to recalculate the load distribution around the crack. They all consider a specific phenomenon which, when it reaches a critical value, very quickly leads to fracture and, in this case, are equivalent to the theory using factor K [PAR 65].

Parameter K_I varies with the temperature of the material. Different relations linking it to temperature were proposed [JOH 83].

To simplify the notation, index I will be omitted in the following sections.

8.8. Stress ratio

According to the definitions introduced in section 1.2, the ratio of stresses R is equal to:

$$R = \frac{\sigma_{\min}}{\sigma_{\max}} = \frac{\sigma_{\text{mean}} - \sigma_a}{\sigma_{\text{mean}} + \sigma_a} \quad [8.61]$$

where $\sigma_{\min} = \sigma_{\text{mean}} - \sigma_a$. If $R = 0$, $\sigma_{\min} = 0$ and $\sigma_{\max} = 2 \sigma_a$.

The range of variation of the stress intensity ΔK is

$$\Delta K = K_{\max} - K_{\min} \quad [8.62]$$

and we have

$$R = \frac{K_{\min}}{K_{\max}}. \quad [8.63]$$

If $R = 0$, $\Delta K = K_{\max}$.

Case of an infinite plate

$$K = \sigma \sqrt{\pi a} \quad [8.64]$$

Neglecting index I (for simplification), we have

$$K_{\max} = \sigma_{\max} \sqrt{\pi a} , \quad [8.65]$$

$$K_{\max} = (\sigma_{\text{mean}} + \sigma_a) \sqrt{\pi a} \quad [8.66]$$

and, for $R = 0$,

$$\Delta K = K_{\max} = 2 \sigma_a \sqrt{\pi a} , \quad [8.67]$$

$$K_{\max} = \frac{\Delta K}{1 - R} \quad [8.68]$$

and

$$K_{\min} = R K_{\max} = R \frac{\Delta K}{1 - R} . \quad [8.69]$$

8.9. Expansion of cracks: Griffith criterion

With an infinite plate, one unit wide, cracked $2a$ long, submitted to a tension stress σ (Figure 8.21) and set at extremities, we can plot the load-deformation curve in the form of Figure 8.22 in the elastic field.

Under load C_1 , we obtain line OA with which we can associate an elastic strain energy stored in the plate characterized by area OAD_1 .

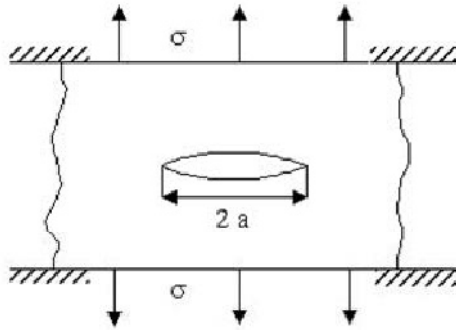


Figure 8.21. Cracked plate set at extremities

When the size of the crack increases by an increment of da , the rigidity of the part decreases and the straight line representing the load-deformation relation becomes OB . Since the two extremities of the plate are fixed, a part of the load is relaxed.

The elastic energy is now represented by the OBD_1 area and the energy variation corresponding to da by OAB (released energy). If the load increases (C_2), a larger quantity of energy is freed if the size of the crack increases with the same (OEF) increment.

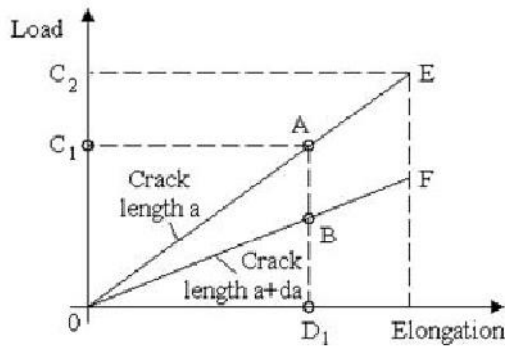


Figure 8.22. Evolution of the load-deformation relation according to the size of the crack

A.A. Griffith [GRI 21] [GRI 25] assumed that the cracks develop if energy U triggered by the growth of the crack is sufficient to provide all W energy required for this growth.

The condition for growth is therefore:

$$\frac{dU}{da} = \frac{dW}{da} . \quad [8.70]$$

From the results established by C.E. Inglis [ING 13] in the case of an elliptical crack, A.A. Griffith obtained:

$$\frac{dU}{da} = \frac{2 \pi \sigma^2 a}{E} \quad [8.71]$$

by the unit of width of the plate where E is Young's modulus.

The *elastic energy release rate* (or *crack extension force*) quantity is defined [BRO 78]:

$$G = \frac{1}{2} \frac{dU}{da} = \frac{\pi \sigma^2 a}{E} . \quad [8.72]$$

The energy absorbed by propagation is equal to $R_F = \frac{dW}{da}$ (*crack resistance*).

In order for cracking to happen, by supposing that R is the same for all da increments, $2 G \geq R_F$ must occur.

Since R_F is constant, G must then be higher than a critical value G_{IC} such that

$$G_{IC} = \frac{\pi \sigma_c^2 a}{E} . \quad [8.73]$$

G_{IC} can be calculated from a measure of σ_c required to break a plate presenting a crack of length $2a$.

For brittle materials (glass), R_F is a surface energy. For ductile materials (metals), R_F is mainly the plastic energy necessary to deform the material at the edge of the crack during each da increment.

D. Broek notes that this energy criterion, used by A.A. Griffith to model propagation, is linked to the criterion based on stresses developed in the previous sections (factor K) and that we have, from equations [8.49] and [8.73]:

$$G = \frac{K^2}{E} \quad [8.74]$$

for plane stresses and, in the case of plane strains,

$$G_I = \frac{K^2}{(1-\nu^2) E} . \quad [8.75]$$

8.10. Factors affecting the initiation of cracks

These factors include the following:

- the presence of inclusions,;
- size of grains;
- sharp angles;
- holes;
- welding faults;
- surface faults (machining, etc.); and
- environment (corrosion, etc.).

8.11. Factors affecting the propagation of cracks

The propagation of cracks is sensitive to many parameters, among which we can mention [WEI 78] mechanical, geometric or metallurgical factors or factors linked to the environment.

8.11.1. Mechanical factors

These include:

- the type of load;
- maximum stress σ_{\max} (or K_{\max});
- $\Delta\sigma$ (or ΔK);
- stresses R ratio (this is an important effect [PAR 62], but not in zone II of crack propagation [HAU 80]); propagation speed increases with R; and
- frequency.

A study by Schijve *et al.* [SCH 61c] shows that high frequencies lead to longer useful lifetimes, or a lower cracking speed (the speed studied was approximately 0.3 Hz to 37 Hz for the material alloy ALCLAD 2024). This effect is not very pronounced, so simulating a low frequency service load with a higher frequency test is possible.

A.J. McEvily and W. Illg [MCE 58] provide results in which the frequency plays a significant role (aluminum alloy 2024 - T3) or, on the contrary, in which its influence is very low (aluminum alloy 7075 - T6).

8.11.1.1. *Other results*

W. Weibull [WEI 60] observed the same effect as J. Schijve, except that it was clearly more pronounced for the material aluminum alloy 2024.

Other tests by J. Schijve [SCH 71] [SCH 72c] at 10 Hz, 1 Hz and 0.1 Hz on light alloys demonstrated that frequency has a small influence on fatigue life and was not completely systematic.

J. Branger [BRA 71] demonstrated a slightly shorter fatigue life at 1.6 Hz than at 2.9 Hz. However, the opposite result was obtained in another series of tests at 3.5, 0.7 and 0.09 Hz (longer life at lower frequency) [PAR 62].

K.C. Valanis [VAL 81] showed analytically that a decrease in the frequency decreases the useful lifetime (fatigue properties decrease with the frequency of the hardening increase with deformation speed).

The form of the wave or cycles also has an effect.

H.P. Lieurade and P. Rabbe [LIE 72] noticed that this effect is insignificant (for sine, rectangle and triangle form cycles).

The effect of the sequence [FUC 80] (overload), occurs with the same principles:

- in the initiation of cracks; and
- in the propagation of cracks.

We have seen that the fatigue life of smooth specimens is reduced more than expected by the linear accumulation law if some large stress cycles are applied before lower stress testing.

This effect is very weak compared to the effect observed in notched specimens.

With cracked specimens, on the contrary [LIE 82], fatigue life can be 10 to 100 times greater if the overload is applied at the beginning of the sequence instead of at the end. Cracking slowdown is less important when R increases. It is low if the overload is lower than 10% of the load. The sequence is important, however, especially the direction of the last overload before low stresses.

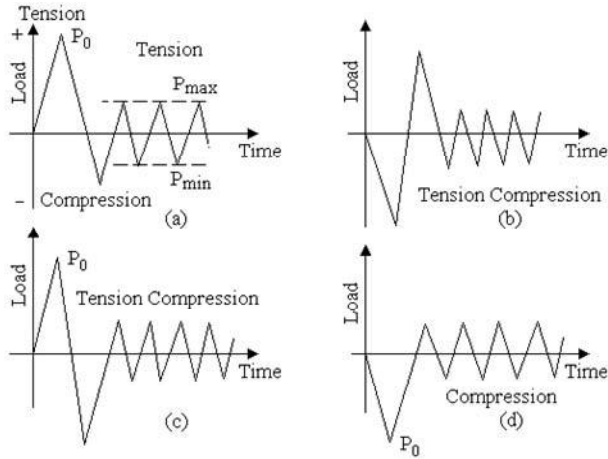


Figure 8.23. Four different overload models: (a) tension, (b) tension compression, (c) tension compression, (d) compression

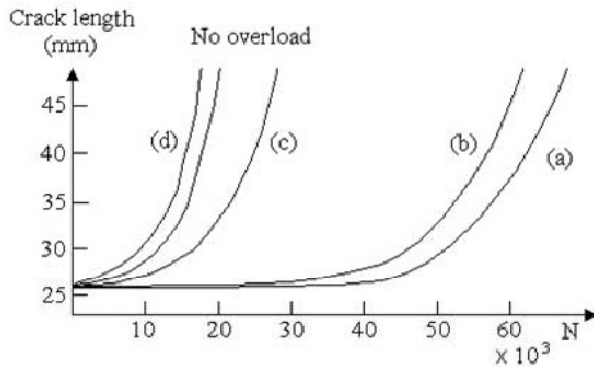


Figure 8.24. Length of the crack according to the number of cycles with and without overload

8.11.2. Geometric factors

This effect is insignificant as long as the plastic zone created in the neighborhood of the extremity of the crack is not very important [LIE 72]:

$$r_h = \frac{(\Delta K)^2}{2 \pi (2 R_e)^2} \quad [8.76]$$

where R_e is the yield stress.

The width of the test bar must be such that

$$B > 2.5 \left(\frac{\Delta K}{2 R_e} \right)^2 \quad [8.77]$$

or we must limit ΔK based on $\Delta K < 2 R_e \sqrt{\frac{B}{2.5}}$.

If this condition is met, width B has little influence on the propagation of cracks.

8.11.3. *Metallurgical factors*

These include:

- alloy composition;
- distribution of alloy elements;
- impurities;
- thermal treatments;
- mechanical treatments;
- mechanical properties; and
- texture (orientation of grains).

8.11.4. *Factors linked to the environment*

These include

- temperature;
- gas, liquid environments, etc.;
- environmental gas pressure;
- pH;
- viscosity of the environment;
- humidity; and
- corrosion.

The characteristics of the growth of cracks with corrosion (in steels, for example in the case of offshore drilling) are different for a factor of stress intensity lower or higher than the static load threshold from which the crack appears (K_{ISCC}).

The fatigue is called *real corrosion fatigue* in the case where $K < K_{ISCC}$ and, for $K > K_{ISCC}$, *stress corrosion fatigue* [AUS 78].

Real corrosion fatigue occurs for materials that do not corrode in static conditions.

Stress corrosion fatigue is the result of corrosion with cyclical loads.

The effect of the corrosion increases when the frequency decreases, with a threshold value of 10 Hz, below which the frequency has little effect [LIE 82].

Finally, we can observe that:

- for given ΔK , the propagation speed decreases when Young's modulus E increases; and
- the limit of elasticity of the material has little influence for certain materials (for example, steel and brass).

8.12. Speed of propagation of cracks

We have seen that for static loads in mechanics [8.51], we define the linear elastic fracture i.e. the stress intensity factor K by equation [8.49]:

$$K = \sigma \sqrt{\pi a}$$

where σ is the nominal stress and a is the length of the crack.

When the size of the plastic zone at the root of the crack is small compared to the length of the crack, the stress intensity factor can be a good indication of the state of the stresses at the root of the crack, or the rate of propagation of the crack.

The growth speed of cracks, expressed in the form of a variation of crack length by number of cycles, is characterized by the number of stress cycles $\frac{da}{dN}$. This is generally expressed according to the range of stress intensity:

$$\Delta K = K_{\max} - K_{\min} \quad [8.78]$$

We have

$$\frac{da}{dN} = f(\Delta K) = f\left[(\sigma_{\max} - \sigma_{\min}) \sqrt{\pi a}\right] = f\left[2 \sigma_a \sqrt{\pi a}\right] \quad [8.79]$$

where σ_{\max} , σ_{\min} are the maximum and minimum stresses in a cycle and σ_a is the amplitude of the alternating stress [PAR 61].

In cyclic loads, the size of the cracks can increase to a critical size and therefore lead to a decrease of its performance or even to a fracture. Since it may not be possible to prevent cracks from happening during service, it is necessary to have a method of evaluation of their effect in a given structure. This method will help to minimize their action and estimate the behavior of a cracked structure during propagation to fracture [ROO 76].

In all modes proposed, we assume that $\frac{da}{dN}$ is a continuous function of the external load, part dimensions and properties of the material [ERD 68].

ΔK can be written in the form

$$\Delta K = \text{constant} \times \Delta \sigma \sqrt{\pi a} = A \Delta \sigma \sqrt{\pi a} \quad [8.80]$$

where the constant A (dimensionless) is a function of geometric dimensions of the part and crack and $\Delta \sigma$ is the peak-to-peak amplitude of the sinusoidal dynamic stress and is half as long as the crack.

Example 8.3.

The part of width $2b$ (Figure 8.25) submitted to tension stresses [LAM 78] [LAM 80a] can be expressed:

$$A = \sqrt{\pi} \sqrt{\sec\left(\frac{\pi a}{2b}\right)} \quad [8.81]$$

where $\sec = \frac{1}{\cos}$.

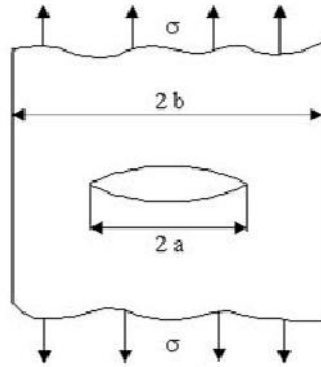


Figure 8.25. *Cracked part under tension stress*

Experience shows that $\frac{da}{dn}$ varies according to ΔK based on a law that is represented graphically as in Figure 8.26. This law is not well known. We distinguish three fields of cracking [SAN 77]:

1. The initial fracture does not propagate (or propagates very slowly) below a certain threshold ΔK_s :

$$\Delta K = A \Delta \sigma \sqrt{a_i} \leq \Delta K_s \quad [8.82]$$

where a_i is the initial half-length of the crack.

This threshold makes it possible to determine the dimensions of tolerable defects that cannot be at the origin of a propagating crack ($\frac{da}{dn} \leq 10^{-7}$ mm/cycle) [LIG 80].

The experimental determination of this threshold is not easy [BRO 78]. J.P. Harrison [BAR 80] [HAR 70] shows that, for a large number of materials, it is included between 2.4×10^{-5} and $2.9 \times 10^{-5} E m^{0.5}$ (where E is Young's modulus). Different empirical formulae linking ΔK_s to R and to ΔK_{s0} (value of ΔK_s for $R = 0$) were established [BAR 80].

In this zone, the microstructure, mean stress and the environment have a strong influence.

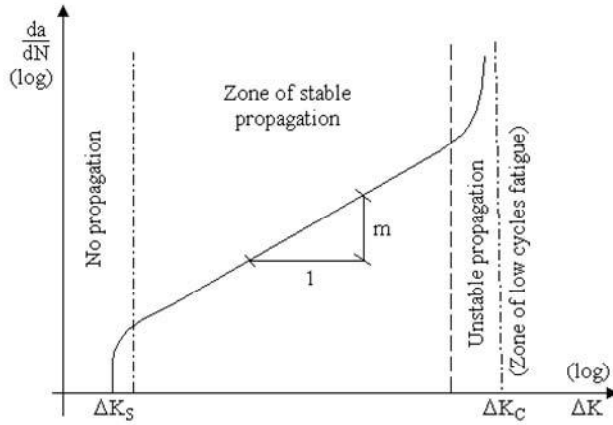


Figure 8.26. *Cracking zones*

2. For large values of ΔK , we observe a zone in which the crack has an unstable behavior for a critical value ΔK_{Ic} , with very quick growth to fracture of the part. There is also a strong influence of the microstructure and mean stress as well as the size of the part. Environmental conditions have very little consequences.

3. Between these two limits, there is a zone of stable crack growth which can be represented in logarithmic axes by a straight line of equation [LAM 78] [PAR 63] [PAR 64] [SHE 83a]:

$$\frac{da}{dN} = C \Delta K^m \text{ (meters/cycle)} \quad [8.83]$$

where C and m are constants for material, given load (R) and the environmental conditions.

This representation, referred to as the Paris relation, is the most widely used. It is however not the only one and, as a rough guide, we will mention some other formulations proposed by different authors without being exhaustive. Some of these relations are functions of σ , others of ΔK alone or of ΔK and R (or, the equivalent of ΔK and K_{max}). For $R < 0$ (compression), we have [BRO 78]

$$\frac{da}{dN} = f(K_{max}). \quad [8.84]$$

The Paris relation only involves the intermediate growth rates of cracks and does not include the initial and final phases [AUS 78].

R was defined as the $\sigma_{\min}/\sigma_{\max}$ ratio. From relations [8.63] and [8.78], we have

$$\Delta K = K_{\max} - K_{\min} = \left(1 - \frac{K_{\min}}{K_{\max}}\right) K_{\max}, \quad [8.85]$$

$$\Delta K = (1 - R) K_{\max}. \quad [8.86]$$

In this zone, we observe a slight influence of the microstructure, mean stress, the environment and size.

NOTE:

The acoustic transmission (when a material is plastically deformed by external or internal stresses) can be used for detecting the presence and propagation of fatigue cracks. It is directly linked to the stress intensity factor [DUN 68] by a relation in the form

$$N = A K^m \quad [8.87]$$

where A characterizes the acoustic transmission, K is the stress intensity factor, A is a constant and μ is a constant for a given material and thickness. μ varies from 4 to 8 (experimental values); value 4 is given by a simplified theoretical model linking acoustic transmission, the volume of the plastic zone at the top of the crack and the size of the plastic zone to K .

Knowing that

$$\frac{da}{dN} = C \hat{K}^q \quad [8.88]$$

where $q \in [2, 6]$ and that $K = \sigma \sqrt{\pi a}$, we obtain

$$a = a_0 \left[1 - \frac{q-2}{2} a_0^{\frac{q-2}{2}} C \sigma_w^q \pi^{q/2} n \right]^{-\frac{2}{q-2}} \quad [8.89]$$

where σ_w is work stress and

$$N = A (K_p^m - K_w^m) = A \left[\left(\sigma_p \sqrt{\pi a} \right)^m - \left(\sigma_w \sqrt{\pi a} \right)^m \right] \quad [8.90]$$

where σ_p is periodic over-stress ($> \sigma_w$), which gives us

$$N = A \pi^{m/2} \sigma_p^m \left[1 - \left(\frac{\sigma_w}{\sigma_p} \right)^m \right] a_0^{m/2} \left[1 - \frac{q-2}{2} a_0^{\frac{q-2}{2}} C \sigma_w^q \pi^{q/2} n \right]^{-\frac{m}{q-2}} \quad [8.91]$$

Ae for K lower than K_w were neglected due to the irreversibility of the acoustic transmission.

If $m = \mu = 4$ (frequent value), we have

$$N = A \pi^2 a_0^2 \left(\sigma_p^4 - \sigma_w^4 \right) \left(1 - a_0 C \sigma_w^4 \pi^2 n \right) \quad [8.92]$$

In practice, the expression of K is more complicated than $\sigma \sqrt{\pi a}$ and a corrective factor must be calculated according to the geometry of the component studied. A good theory was determined by Harris et al. [HAR], known as the experience correlation.

8.13. Effect of a non-zero mean stress

The effects of the presence of a non-zero mean stress are:

- to decrease the duration of the step during which there is initiation of the crack (the crack appears quicker if the mean stress is large) [FAC 72]; and
- to increase the speed of crack propagation [PRI 72] and therefore to decrease the useful lifetime.

D. Broek and J. Schijve [BRO 63] note that the speed of propagation is proportional to a mean stress power (of approximately 1.5).

N.E. Dowling [DOW 72] confirms that a mean tension stress shortens the useful lifetime, but that a compression stress extends it.

Based on the mean stress, we can obtain for low ΔK values different values of exponent m of the Paris relation [RIC 72]:

$$\frac{da}{dN} = C \Delta K^m. \quad [8.93]$$

8.14. Laws of crack propagation

A general law of crack propagation should consider several factors [PEL 70]:

- geometry (component dimensions, length of the crack, etc.);
- loads (amplitude, direction, etc.);
- properties of the material (elastic resistance, resistance to fracture, Young's modulus, ductility, etc.);
- time (number of cycles); and
- the environment.

Most relations listed in the previous sections only take the latter two factors into consideration.

The laws proposed have four major origins [PEL 70]:

- theoretical laws based on the dimensional analysis;
- theoretical relations derived from a stress hardening and fatigue damage model;
- theoretical equation linking the growth rate to the displacement of the crack root opening; or
- semi-empirical laws.

There is no single empirical law to explain all the experimental results. Each law has its field of application and must be chosen by the user [WOO 73].

In the following, we find some of the laws proposed to represent the speed of crack propagation.

8.14.1. Head [HEA 53a]

This first theoretical model considers the plastic zone at the root of the crack and the elastic behavior over the rest of an infinite plate. It supposes that the material hardens in the plastic zone in strain, until it breaks by loss of ductility:

$$\frac{da}{dN} = \frac{C_1 \sigma^3 a^{3/2}}{(R_e - \sigma) \Gamma_p^{1/2}} \quad [8.94]$$

where C_1 is the function of hardening to strain of the part, the yield stress and the ultimate stress, R_e is the yield stress of the material, a is the half-length of the crack

and r_p is the size of the plastic zone close to the extremity of the crack, assumed constant during crack propagation.

8.14.2. *Modified Head law*

N.E. Frost [FRO 58] notes that the size of this plastic zone increases in direct proportion with the length of the crack.

G.R. Irwin [IRW 60] showed that

$$r_p \approx \sigma^2 a, \quad [8.95]$$

yielding

$$\frac{da}{dN} = \frac{C_1 \sigma^2 a}{R_e - \sigma}. \quad [8.96]$$

8.14.3. *Frost and Dugdale [FRO 58]*

N.F. Frost and D.S. Dugdale propose a new approach of propagation laws by noting that the modified Head law is a function of a . From a dimensional analysis, they arrive at the relation

$$\frac{da}{dN} = B a \quad [8.97]$$

where B (a constant) is a function of stresses applied. To satisfy their experimental results, they conclude that

$$B = \frac{\sigma^3}{C_4} \quad [8.98]$$

hence

$$\frac{da}{dN} = \frac{\sigma^3 a}{C_4} = \text{Constant} \times \sigma^3 a \quad [8.99]$$

where C_4 is a parameter characteristic of the material. This law was generalized in the form

$$\frac{da}{dN} = \frac{\sigma^n a}{N_s} \quad [8.100]$$

where N_s is constant for a given material and a mean stress and n is a constant ($= 3$ for light alloys and soft steel), yielding

$$\frac{da}{dN} = (P + Q \bar{\sigma}) \Delta \sigma^3 a \quad [8.101]$$

where P and Q are constants, $\Delta \sigma$ is the stress variation range and a is the length of the crack.

8.14.4. *McEvily and Illg*

Starting from

$$\frac{da}{dN} = f(K_n, \sigma_n) \quad [8.102]$$

where K_n is the factor of theoretical elastic stress concentration by Neuber, we have

$$K_n = 1 + 2 \left(\frac{a}{\rho_1} \right)^{1/2} = \frac{\sigma_0}{\sigma} \quad [8.103]$$

where ρ_1 is the radius of curvature of the root of the crack and σ_n is the stress in cracked section. We therefore have

$$\sigma_n = \frac{\sigma}{1 - \lambda} \quad [8.104]$$

where $\lambda = \frac{2a}{w}$, w is the size of the specimen and σ is the stress in the non-cracked section. A.J. McEvily and W. Illg [MCE 58] therefore propose the empirical law:

$$\log_{10} \left(\frac{da}{dN} \right) = 0.00509 K_n \sigma_n - 5.472 - \frac{34}{K_n \sigma_n - 34} \quad [8.105]$$

8.14.5. *Paris and Erdogan*

We have

$$\frac{da}{dN} = C (\Delta K)^m, \quad [8.106]$$

where ΔK is the domain of variation of the stress intensity factor K and C and m are constants for a given material.

This law, the most widely used in practice, does not highlight Young's modulus, the stress hardening coefficient or the yield stress (non-influential parameters) [PAR 62] [PAR 63] [PAR 64].

We consider that, for steels,

$$2 \leq m \leq 10 \quad [8.107]$$

and, for light alloys,

$$3 \leq m \leq 5 \quad [8.108]$$

H.P. Lieurade [LIE 82] gives

$$2 \leq m \leq 7 \quad [8.109]$$

whereas W.G. Clark and E.T. Wessel [CLA 70] note that, for steels,

$$1.4 \leq m \leq 10 \quad [8.110]$$

and

$$2 \cdot 10^{-51} \leq C \leq 2.9 \cdot 10^{-12} \quad [8.111]$$

if ΔK is in $\text{psi} \sqrt{\text{inch}}$ and $\frac{da}{dN}$ in inches/cycle.

The value $m = 4$ gives good results in many cases, except with high propagation speeds. Other authors estimate that the value 3 applies with few errors to many situations [FRO 75].

When the size of the plastic zone is small in comparison with the length of the crack and the size of the plate, we can show that $m = 2$ from considerations in the

stress and strain experienced by the material facing the root of the crack (ΔK small). For large ΔK , m is larger and can reach 5 [PAR 64].

Tables provide C values for different materials [HAU 80].

J.F. Throop and G.A. Miller [THR 70] attempted to measure the dispersion of parameter m of the Paris relation, written in the form

$$\frac{da}{dN} = C K_{max}^m \cdot \tag{8.112}$$

The mean value of the 69 values measured is equal to 3.5 and the standard deviation to 0.65.

Material	Range of m	\bar{m}
Low and average resistance steel	2.3–5.2	3.5
High resistance steel	2.2–6.7	3.3
Titanium	3.3–3.7	3.5
Alloy 2024-T3	2.7–3.8	3.4
Stainless steel 305	2.8–4.5	3.3
70-30 brass	3.6–4.9	4.1
	Range: 2.2–6.7	Average: 3.5

Table 8.2. Some values of exponent m

From a study on the dependence of constant C in relation to mechanical properties, J.F. Throop and G.A. Miller concluded that

$$C = \frac{B}{E R_e K_C} \tag{8.113}$$

for steel 4340, where $K > 40 \text{ ksi} \sqrt{\text{inch}}$, B is a constant, R_e is the yield stress and E is Young's modulus.

Different expressions were proposed to calculate an approximate value of constant C of the law of Paris based on static or dynamic mechanical characteristics of materials, including [LIG 80]:

$$C = \frac{0.76}{\rho_i E^2 R_m^2 \epsilon_f^2} = \frac{\text{constant}}{E^2 R_m^2 \epsilon_f^2} \quad [8.114]$$

according to F.A. McClintock [MCC 63] and

$$C = \frac{16 \cdot 10^6 (1+\gamma)^4 \left[1 - (1-\gamma)^2 \right]}{7 E^3 K_C^2 n} \quad [8.115]$$

according to J.M. Krafft [KRA 65], where R_m is ultimate tensile stress (ksi), R_e is yield stress at 0.2 % (ksi), K_C is the stress intensity factor (ksi $\sqrt{\text{inch}}$), ϵ_f is strain at fracture, n is stress hardening coefficient, $\gamma = \frac{\Delta K}{K_{\max}}$ and ρ_i is the inclusive interval.

A.J. Evily and T.L. Johnston [MCE 65] stated that

$$C = \frac{\text{constant}}{\frac{R_e + R_m}{2} \epsilon_u R_m^2 E} \quad [8.116]$$

where ϵ_u is strain at the tensile strength.

According to B.S. Pearson [PEA 66],

$$C = \frac{\text{constant}}{E^{3.6}}. \quad [8.117]$$

We also find

$$m = 20 n' \quad [8.118]$$

where n' is the cyclical stress hardening coefficient of the material [LIE 78] (defined in relation [7.3]: $\sigma = K' \epsilon_p^{n'}$).

Virkler *et al.* [VIR 78] provide an expression of C according to m established after a study of 68 value pairs and, with the help of a line of regression, they obtain

$$\log C = b_0 + b_1 \log m, \quad [8.119]$$

where $b_0 = -5.7792$ and $b_1 = -4.6150$.

A relation between m and C in the same form was also proposed by V.M. Radhakrishnan [RAD 80] for aluminum alloys and by T.R. Gurney [GUR 79] for steels:

$$\log C = -q m + r \quad [8.120]$$

where q and r are constants of the material, which can incorporate a stress ratio or an effect of the temperature.

For steels, F. Koshiga and M. Kawahara [KOS 74] provide an example for $q = 1.84$ and $r = -4.32$. Some other values are combined in Table 8.3, where stresses in units of kg/mm^2 and crack lengths are in mm.

Material	q	r	Reference
Average resistance steels	1.25	-4.30	[KOS 74]
	1.74	-4.30	[KIT 71]
Carbon steels, alloy steels	1.84	-4.07	[NIS 77]
Aluminum alloys	1.25	-4.00	[KOS 74]
	1.74	-4.00	[KIT 71]
Very high resistance steels	1.35	-4.03	[LIE 78]

Table 8.3. Some values of constants q and r [KOS 74]

NOTE:

Several studies show that the distribution of times (or numbers of cycles) necessary to reach a given crack length follows a statistical law.

The Paris law can be considered as a statistical law, as constants C and m were in this case random variables [JOH 83]. In fact, experience shows that these two parameters are linked and that only one distribution is necessary.

After an analysis of different published results, T.R. Gurney [GUR 79] considered that the best relation between C and m is

$$C = \frac{1.315 \cdot 10^{-4}}{(895.4)^m}. \quad [8.121]$$

G.O. Johnston [JOH 83] supposes that the C distribution is the same for given m, and consequently he only studied the case where $m = 3$. He obtained a log-normal distribution of paramaters for C:

$$\mu = -29.31$$

and

$$\sigma = 0.24$$

where μ and σ are the mean and standard deviation of $\log C$, respectively.

G.O. Johnston notes that, for $m = 2$, the C distribution can be approximated by the normal law $N[1.716 \times 10^{-10}; 1.588 \times 10^{-21}]$, but he notes that the log-normal law would be better.

E.K. Walker [WAL 83] concludes that the law is approximately log-normal (standard deviation $\sigma_{\log} < 0.20$ at a level of confidence 0.90).

Table 8.4 combines expressions of the speed of crack propagation proposed by different authors (note that this list is not exhaustive).

Author	Relation	Equ.	Comments
Weibull [WEI 54]	$\frac{da}{dN} = k \sigma_n^b$	[8.122]	k and b are constants for given material, σ_n is the nominal stress in the section presumed without cracks
Paris [PAR 57]	$\frac{da}{dN} = f(\sigma a^{1/2})$	[8.123]	
Walker [IRW 60a] Erdogan [ERD 67]	$\frac{da}{dN} = C K_{\max}^m \Delta K^p$ then $\frac{da}{dN} = C \overline{\Delta K}$ where $\overline{\Delta K} = S_{\max} (1-R)^m \sqrt{\pi a}$	[8.124] [8.125] [8.126]	
Liu [LIU 61]	$\frac{da}{dN} = f(\Delta\sigma, \sigma_m) a$	[8.127]	f is a function of the range of stress and mean stress

	<p>Modifiel Liu law</p> <p>H.W. Liu [LIU 63] shows, from a propagation model using a plastic elastic idealized strain stress diagram and a concept of energy absorption by hysteresis, that $f(\) = C \sigma^2$. Hence,</p> $\frac{da}{dN} = C \sigma^2 a \quad [8.128]$ <p>P.C. Paris and F. Erdogan [PAR 63] note that Head, Frost, Dugdale, Liu and Paris, Gomez and Anderson laws [PAR 61] can be written in the more general form</p> $\frac{da}{dN} = \frac{\sigma^n a^m}{\sigma_0} \quad [8.129]$		
McEvily and Boettner [MCE 63]	$\frac{da}{dN} = A \sigma^{2n} a^n$	[8.130]	A is a constant, 2a is the length of crack, σ is stress, n is a constant where $1 \leq n \leq 3$
Liu [LIU 63a]	$\frac{da}{dN} = A \Delta \sigma^2 a,$ <p>then</p> $\frac{da}{dN} = A \Delta \sigma^2 \frac{W}{\pi} \tan \frac{\pi a}{W}$	[8.131] [8.132]	A is a constant (not necessarily independent of the stress), 2a is the length of the crack, $\Delta \sigma$ is the range of stress, W is the width of specimen
McClintock [MCC 63]	$\frac{1}{\rho} \frac{da}{dN} = \frac{7.5}{16} \frac{(\Delta K)^4}{\epsilon_f E^2 R_e^2 \rho^2}$	[8.133]	The model is based on an analysis of stress hardening and the accumulation of fatigue damage with plastic strain around the root of the crack (Coffin law). R_e is yield stress, E is Young's modulus, ρ is the radius of the plastic zone at the root of the crack (in which propagation occurs), ϵ_f is ductility, where according to the Coffin Law, $N^{1/m} \epsilon_p = \frac{\epsilon_f}{2}$
Valluri <i>et al.</i> [VAL 63] [VAL 64]	$\frac{1}{C} \frac{da}{dN} = (\sigma_p - \sigma_i)^2 (\sigma_p - \sigma'_p)^2 \frac{W}{\pi} \tan \frac{\pi a}{W}$ $\frac{1}{C} \frac{da}{dN} = (K_n \sigma - \sigma')^2 (K_n \sigma_p - \sigma'_p)^2 a$	[8.134] [8.135]	C is a constant, K_n is a factor of stress concentration at the root of the crack, σ'_0 is nominal fatigue limit, σ is maximum stress, σ' is minimum stress, W is width of specimen, σ_p is maximum plastic stress at root of crack, σ'_p is minimum plastic stress at root of crack, σ_i is instant mean value of internal stress.

Broek and Schijve [BRO 63]	$\frac{da}{dN} = C_1 e^{-C_2 R} \sigma_{\max}^3 \ell^{3/2} \left(1 + 10 \frac{\ell^2}{W^2} \right)$ <p style="text-align: center;">or</p> $\frac{da}{dN} = C_1 \left(\frac{\Delta K}{1-R} \right)^3 \exp(-C_2 R)$ <p style="text-align: center;">or</p> $\frac{da}{dN} = C K_{\max}^2 \Delta K$	<p>[8.136]</p> <p>[8.137]</p> <p>[8.138]</p>	<p>This relation was established to take into consideration a non-zero mean load for aluminum alloys CLAD2024-T3 and 7075-T6.</p> <p>ℓ is half-length of the specimen, W is half-width, σ_{\max} is maximum stress in a cycle ($= \sigma_{\text{mean}} + \sigma_{\text{alternating}}$)</p> <p>$R = \frac{\sigma_{\min}}{\sigma_{\max}}$, $\sigma_{\min} = \sigma_{\text{mean}} - \sigma_a$, C_1 and C_2 are constants.</p>
Krafft [KRA 65]	$\frac{da}{dN} = \frac{A}{E^3 K_{IC}^2 n'} f \left(\frac{\Delta K}{K_{\max}} \right) K_{\max}^4$	[8.139]	n' is stress hardening exponent
Morrow [MOR 64a]	$2N = \left(\frac{\Delta \epsilon_p}{2 \epsilon'_f} \right)^{-(1+5n')} = \left(\frac{\sigma_a}{\sigma'_f} \right)^{-\frac{1+5n'}{n'}}$ <p style="text-align: center;">or, with notations previously used,</p> $\beta = \frac{1}{1+5n'} \text{ and } b = \frac{1+5n'}{n'}$	<p>[8.140]</p> <p>[8.141]</p>	<p>These link the length of the crack to the energy transmitted by cycle (hysteresis) and to the useful lifetime of a cracked part.</p>
Smith [SMI 63a] [SMI 64b]	<p>C.R. Smith proposes two theories:</p> <p>1. Theory of the linear deformation: the root of the notch strain is equal to $K_t \epsilon_{\text{nominal}}$ (after plastic local deformation). With the help of the stress-strain curve, the residual root of the notch stress is determined, hence the root of the notch stress σ</p> $\sigma = K_t \sigma_{\text{nominal}} + \sigma_{\text{residual}} \quad [8.142]$ <p>is calculated. We obtain the number of cycles at fracture N from S-N curves (relative to smooth test bars) for different R values. These numbers of cycles are used with the Miner rule.</p> <p>2. This begins with the idea that the maximum root of the notch stress will be approximately equal to the yield stress as long as a plastic strain occurs. The residual stress involved is directly determined from constant amplitude tests in the specimen tested at the maximum load cycle to apply in the variable amplitude test. The useful lifetime obtained in this test, the hypothesis concerning the maximum stress σ_{\max} at root of notch then indicate, in conjunction with the S-N curve for the smooth specimen, the value of R that applies and thus σ_{\min} at root of notch. This is sufficient to determine the local root of notch stress variation for the variable amplitude test. Knowledge of K_t is not necessary. Again, the Miner rule and fatigue data from the smooth specimen are used.</p> <p>In both cases, C.R. Smith assumes that the material behaves elastically at the root of notch once the residual stress has been introduced by the plastic strain created by the maximum load cycle, and considers that there is no relaxation effect.</p>		

Boettner <i>et al.</i> [BOE 65]	$\frac{da}{dN} = A \left(\epsilon_r \sqrt{a} \right)^m$ <p>hence</p> $\epsilon^2 N = \frac{1}{A} \text{Log} \frac{a_R}{a_i}$	[8.143] [8.144]	Low cycle fatigue, where a is the length of the crack and A is a constant. ϵ_r is total plastic strain (tension-compression), $m \sim 2$, regardless of the material, a_i is initial length of the crack, a_R is length of crack at fracture.
McEvily [MCE 65]	$\frac{da}{dN} = A \frac{(\Delta\sigma \sqrt{a})}{\frac{R_e + R_m}{2} E R_m^2 \epsilon_f}$	[8.145]	R_m is ultimate tensile stress, ϵ_f is ductility, E is Young's modulus, R_e is yield stress.
Weertman [WEE 65]	$\frac{da}{dN} = \frac{(\Delta\sigma \sqrt{a})}{2 \gamma G R_e^2}$	[8.146]	γ is constant linked to the energy of plastic strain, G is shear modulus This relation was established from a infinitesimal dislocation theory, continuously distributed, applied to the propagation of cracks.
Pearson [PEA 66]	$\frac{da}{dN} = 3.43 \cdot 10^7 \left(\frac{K}{E} \right)^{3.6}$	[8.147]	$\frac{da}{dN}$ in inches/cycle K in lb/in ² √in E in lb/inch ²
McClintock [MCC 66]	Correlation of the rate of crack propagation with opening (displacement) of the crack.		
Frost and Dixon [FRO 67]	$\frac{da}{dN} = \frac{\Delta\sigma^2 a}{E^2} \left[\ln \left(\frac{4E}{\Delta\sigma} \right) - 1 \right]$ $\frac{da}{dN} = \frac{32 \Delta\sigma^3 a}{E^2 R_e}$	[8.148] [8.149]	a is half-length of the crack, E is Young's modulus, R_e is yield stress
Forman <i>et al.</i> [FOR 67] [FOR 72] Hudson [HUD 69]	<p>Some relations consider the acceleration of the propagation rate relative to zone III, by leaning $\frac{da}{dN}$ toward infinity when $K_{\max} \rightarrow K_C$, with the help of a multiplying factor of ΔK^m. That is the case for the relation determined by Forman <i>et al.</i>, using value K_C of K at fracture and R:</p> $\frac{da}{dN} = \frac{C \Delta K^m}{(1-R) K_{IC} - \Delta K} = \frac{C \Delta K^m}{(1-R) (K_{IC} - K_{\max})} \quad [8.150]$ <p>or</p> $\frac{da}{dN} = \frac{C \Delta K^m K_{\max}}{K_{IC} - K_{\max}} \quad [8.151]$ <p>$\frac{da}{dN} \rightarrow \infty$ when $\Delta K \rightarrow \Delta K_C$.</p>		

Forman <i>et al.</i> [FOR 67] [FOR 72] Hudson [HUD 69] (cont.)	<p>The authors notice a good correlation with experimental results for aluminum. This point of view is confirmed by other studies [SCH 74], demonstrating that this relation gives the best results for many aeronautical materials.</p> <p>Constants C and m, determined with a single stress amplitude and a single mean value, can be used for other maximum and average stress with low error as long as $R = 0$. For $R \leq 0$, they must be re-evaluated with the help of tests with $R = -1$. Even though it is defined for constant amplitude tests, this relation can be used for variable stress amplitude loads by calculating the propagation cycle by cycle, by ignoring the delay created by high stress cycles [SCH 74]. It is possible, however, to consider this delay, for example with the simple method from Willenborg <i>et al.</i> [WIL 71].</p> <p>We will see that other authors (S. Pearson, followed by e.g. A.J. McEvily) also tried to represent zone III of the propagation curve with the help of a factor close to that of Forman.</p>		
Lardner [LAR 68]	$\frac{da}{dN} = \pi \frac{1-\nu}{4 G R_e} (\Delta K)^2$	[8.152]	This is a model based on the intensity of the plastic strain at the root of the crack. G is shear modulus, ν is Poisson's ratio, R_e is yield stress.
Tomkins [TOM 68]	<p>Low level cycle fatigue:</p> $\frac{da}{dN} = \frac{\pi^2}{8} \left(\frac{k}{2 \bar{T}} \right)^2 \Delta \epsilon_p^{2\beta+1} a$ <p>High level cycle fatigue:</p> $\frac{da}{dN} = \frac{\pi^2}{4} \frac{1}{(k \bar{T})^2} \Delta \sigma^3 \sigma_m a$	<p>[8.153]</p> <p>[8.154]</p>	<p>k, β are constants $\bar{T} = 2 \bar{S}$ where \bar{S} is mean tension stress at fracture in the plastic zone.</p> <p>k is constant, σ_m is mean stress.</p>
Broch [BRO 68a]	$\frac{da}{dN} = C \Delta \epsilon^p a^m$	[8.155]	$\Delta \epsilon$ is range of strain, C is a constant for a given material, m and p are constants (in many cases, $p = 2$ and $m = 1$).
Hahn <i>et al.</i> [HAH 69]	$\frac{da}{dN} = C_1 \frac{\Delta K^2}{E R_e}$ <p>or</p> $\frac{da}{dN} = C_2 \left(\frac{\Delta K}{E} \right)^2$	<p>[8.156]</p> <p>[8.157]</p>	C_1, C_2 are constants, E is Young's modulus, R_e is yield stress.
Walker [WOO 73]	$\frac{da}{dN} = C \left[(1-R)^\ell K_{\max} \right]^m$	[8.158]	This law is sometimes preferred to Forman's as it is closer to experimental results for many materials.

<p>IRSID [LIG 80]</p>	$\frac{da}{dN} = 10^{-4} \left[\frac{\Delta K}{K_0 \left(1 - \frac{R}{2} \right)} \right]^m$	<p>[8.159]</p>	<p>$R = \frac{K_{\min}}{K_{\max}}$ K_0 corresponds to the value of ΔK for $\frac{da}{dN} = 10^{-7}$ mm/cycle in the case where $R = 0$.</p>
<p>Erdogan and Ratwani [ERD 70] Erdogan [ERD 83]</p>	$\frac{da}{dN} = \frac{C (1 + \beta)^\alpha (\Delta K - \Delta K_S)^m}{K_C - (1 + \beta) \Delta K}$	<p>[8.160]</p>	<p>This is a study on cylindrical parts with edge crack, in axial tension (α, m and C are constants). We have $\beta = \frac{1+R}{1-R} = \frac{K_{\max} + K_{\min}}{K_{\max} - K_{\min}}$ $= \frac{2 K_{\text{moy}}}{\Delta K}$ K_S is propagation threshold, K_C is critical intensity factor stress.</p>
<p>Lukas <i>et al.</i> [KLE 71] Lukas and Klesnil [KLE 72]</p>	<p>For steels, $\frac{da}{dN} = C (\Delta K^m - \Delta K_S^m)$ for small values of ΔK and with zero mean load. If ΔK_S is small compared to ΔK, then $\frac{da}{dN} = C \Delta K^m$</p>	<p>[8.161] [8.162]</p>	<p>$m = 2.5$ to 3 depending on the steel $C = \text{constant}$ ΔK_S (equal to $2\text{--}4 \text{ MN m}^{-3/2}$) depends on the mean stress and is considered as a constant for very ductile materials.</p>
<p>Priddle [PRI 72]</p>	$\frac{da}{dN} = C (\Delta K - \Delta K_S)^m$	<p>[8.163]</p>	<p>ΔK_S is a function of R</p>
<p>Lieurade and Rabbe [LIE 72]</p>	$\frac{da}{dN} = 10^{-4} \left(\frac{\Delta K}{\Delta K_0} \right)^m$ <p>In the case where R is non-zero, Lieurade and Rabbe propose:</p> $\frac{da}{dN} = 10^{-4} \left[\frac{\Delta K}{K_0 \left(1 - \frac{R}{2} \right)} \right]^m$	<p>[8.164] [8.165]</p>	<p>ΔK_0 is the abscissa of the point of ordinate 10^{-4} mm/cycle for $R = 0$, m is the slope of the straight line (in logarithmic axes) at this point. If $R < 0$, experience shows that we can use the Paris relation $\frac{da}{dN} = C K_{\max}^m$; Crack rate only depends on the part of the cycle corresponding to tension.</p>

Richards and Lindley [RIC 72]	<p>For steels</p> $\frac{da}{dN} = A \left[\frac{(\Delta K - \Delta K_S)^4}{R_m^2 (\Delta K_C^2 - \Delta K_{\max}^2)} \right]^m$ <p>or sometimes [MCE 73]:</p> $\frac{da}{dN} = A \left[\frac{\Delta K^4}{R_m^2 (K_C^2 - K_{\max}^2)} \right]^m$	<p>[8.166]</p> <p>[8.167]</p>	<p>K_C is the critical stress intensity, K_{\max} is the maximum stress intensity, R_m is the ultimate tensile stress, A is a constant.</p>
Pearson [PEA 72]	$\frac{da}{dN} = C \frac{\Delta K^m}{[(1-R) K_C - \Delta K]^{1/2}}$	[8.168]	This is modification of the Forman expression [FOR 67].
McEvily [MCE 73] [HAU 80] [SIG 73]	<p>For low resilience alloys, current construction steels:</p> $\frac{da}{dN} = \frac{4C}{\pi E \sigma_y} (\Delta K^2 - \Delta K_S^2) \left[1 + \frac{\Delta K}{K_C - \frac{\Delta K}{1-R}} \right]$ $\frac{da}{dN} = \frac{C'}{E^2} (\Delta K - \Delta K_S)^2 \left[1 + \frac{\Delta K}{K_C - \frac{\Delta K}{1-R}} \right]$ <p>These relations are the result of a study based on considerations linked to the crack opening displacement. They introduce the effects of the mean stress with the term</p> $K_{\max} = \frac{\Delta K}{1-R}$ <p>as well as threshold value ΔK_S, assuming that ΔK_S is a function of R given by the following empirical relations:</p> <p>- for expression [8.169]:</p> $\Delta K_S = \frac{1.2 \Delta K_{S0}}{1 + 0.2 \frac{1+R}{1-R}}$ <p>- for expression [8.170]:</p> $\Delta K_S = \left(\frac{1-R}{1+R} \right)^{1/2} \Delta K_{S0}$	<p>[8.169]</p> <p>[8.170]</p> <p>[8.171]</p> <p>[8.172]</p>	<p>σ_y is the rms elastic limit stress, C, C' are constants, K_S is the threshold stress intensity factor, K_C is the critical K value, C is a constant without dimension for a given material.</p> <p>Hausammann [HAU 80] provides some values for different steels.</p> <p>ΔK_{S0} is the threshold value for $R = 0$.</p>
Nicholson [NIC 73]	$\frac{da}{dN} = A \frac{(\Delta K - \Delta K_S)^m}{K_C - K_{\max}}$ <p>When $K_{\max} \rightarrow K_C$, we get farther from the linear law and da/dN rapidly grows to fracture. da/dN increases with the mean stress (with R) for a given ΔK.</p>	[8.173]	Empirical relation established to describe the cracking curve considering the influence of the mean stress.

<p>Sih [SIH 74]</p>	<p>$\frac{da}{dN} = C (\Delta S_{min})^m$</p> <p>$S = r \frac{dW}{dV}$</p> <p>S is the strain energy density per unit of volume at distance r of the head of the crack in the direction defined by both angles ϕ and θ.</p>	<p>[8.174]</p>	<p>m and C are constants, ΔS_{min} is the energy density amplitude of minimal strain.</p>
<div data-bbox="453 451 820 755"></div> <p>Figure 8.27. <i>Element of volume at distance r of the head of the crack</i></p> <p>$\Delta S_{min} = \frac{1}{16 \pi G} \left[a_{11} (K_{I_{max}}^2 - K_{I_{min}}^2) + 2 a_{12} (K_{I_{max}} K_{II_{max}} - K_{I_{min}} K_{II_{min}}) + a_{22} (K_{II_{max}}^2 - K_{II_{min}}^2) \right]$</p> <p>$G = \frac{E}{2(1+\nu)}$ is the shear stress elasticity modulus, ν is Poisson's ratio $a_{11} = (K - \cos \theta)(1 + \cos \theta)$ $a_{12} = (2 \cos \theta - K + 1) \sin \theta$ $a_{22} = (K + 1)(1 - \cos \theta) + (1 + \cos \theta)(3 \cos \theta - 1)$ $K = 3 - 4 \nu$ in the plane strain conditions and $K = \frac{3-\nu}{1+\nu}$ in the case of plane stresses.</p> <p>If the third mode is involved, the term</p> $\frac{a_{33} (K_{III_{max}}^2 - K_{III_{min}}^2)}{16 \pi G}$ <p>must be added to ΔS_{min}.</p> <p>The direction of the crack growth and the fracture toughness in the case where modes I and II coexist are controlled by the critical value of the strain density factor, presumed to be a constant of the material [BAR 80].</p> <p>This method can therefore be used with the three work methods, but does not allow for the superposition of modes III constant and I cyclical (the most frequent case is practice).</p>			

Sullivan and Crooker [SUL 76]	$\frac{da}{dN} = A \left(\frac{1-bR}{1-R} \right)^m \Delta K^m$	[8.176]	For steel, $-2 \leq R \leq 0.75$ b is constant.
Speer [TOP 69a]	$\frac{da}{dN} = C \frac{(\Delta K - \Delta K_S)^m}{(1-R) K_C - \Delta K}$	[8.177]	
Austen [AUS 77] [AUS 78]	$\frac{da}{dN} = \frac{\Delta K^2}{4 \pi R_e E} \left(\frac{\Delta K - \Delta K_S}{K_{IC} - \frac{\Delta K}{1-R}} \right)^{1/2}$	[8.178]	For construction steels $\Delta K_S = \Delta K_{S0} (1-R)^Y$ in units of $\text{MPa m}^{0.5}$ ΔK_{S0} is the value of ΔK_S for $R = 0$ [KLE 72a].
Hobbacher [HOB 77]	$\frac{da}{dN} = \begin{cases} C_0 \Delta K^m & \text{when } \Delta K > \Delta K_S \\ 0 & \text{otherwise} \end{cases}$ <p>or</p> $\frac{da}{dN} = C_0 (\Delta K - \Delta K_S)^m$ <p>Hobbacher writes the Paris law of propagation in the non-dimensional form:</p> $\frac{da}{dN} = \begin{cases} C (\Delta \sigma \sqrt{a})^m & \text{if } \Delta \sigma > \alpha_L \\ 0 & \text{otherwise} \end{cases}$ <p>or</p> $\frac{d\alpha}{dN} = C \Delta \mathfrak{R}^n$ <p>By integration of α between 1 and α_c (infinite), we obtain</p> $N = \frac{2}{(m-2) C \Delta \sigma^m}$	<p>[8.179]</p> <p>[8.180]</p> <p>[8.181]</p> <p>[8.182]</p> <p>[8.183]</p>	<p>This takes into consideration an equivalent of the fatigue limit, defined by a threshold value of the stress intensity factor.</p> <p>$\alpha = \frac{a}{a_i}$ varies by 1 (initial value) at</p> <p>$\alpha_L = \frac{a_c}{a_i}$</p> <p>$a_i$ is the initial size of the crack a_c is the size of crack at fracture $\Delta \mathfrak{R}$ is the standardized stress intensity factor $C = C_0 a_i^{(m-2)/2}$ Threshold value: $\Delta \mathfrak{R}_S = \Delta \sigma \sqrt{\alpha_i} = \Delta \sigma$ since $\sqrt{\alpha_i} = 1$.</p> <p>$\Delta \sigma \sqrt{\alpha} > \alpha_L$</p>
Chakrabarti [CHA 78]	<p>Experimental study on alloy Ti-6Al-2Sn-4Zr-2Mo, based on the hypothesis that the energy received by the component over time Δt during which the crack grows by Δa must be higher than or equal to the sum of the energy transmitted in a calorific form, the plastification energy at root of the crack and the propagation energy of the crack.</p> <p>This method involves numerous factors.</p>		
Davenport and Brook [DAV 79]	<p>The Paris relation</p> $\frac{da}{dN} = C \Delta K^m$ <p>is a straight line in logarithmic axes. In practice, we notice that we obtain a sigmoid instead, because of the presence of higher and lower limits:</p> <p>$\frac{da}{dN} \rightarrow 0$ if $\Delta K \rightarrow \Delta K_S$ (threshold)</p> <p>$\frac{da}{dN} \rightarrow \infty$ when $\Delta K \rightarrow (1-R) \Delta K_C$ (condition of instability).</p>		

<p>Davenport and Brook [DAV 79] (cont.)</p>	<p>Empirical relations were proposed in order to consider this, in order that we can generalize in the form:</p> $\frac{da}{dN} = C \frac{(\Delta K^m - \Delta K_S^m)^p}{[(1-R) K_C - \Delta K]^r} \quad [8.184]$ <p>Often, constants m and r are equal to 1. If $\Delta K_S = 0$, we have Forman's relation [FOR 67]. If $\Delta K_S \neq 0$, $m = 1$, $p = r$ and we obtain Nicholson's relation [NIC 73].</p>		
<p>Oh [OH 80]</p>	<p>K.P. Oh defines a distribution model, taking into account random variations of the characteristics of the material, to calculate the propagation of cracks under random loads and the mean useful lifetime of a component.</p>		
<p>Hausamann [HAU 80]</p>	<p>This was a study on steel specimens, and yielded</p> $\frac{da}{dN} = C_1 (\Delta K^{m_1} - \Delta K_S^{m_1}) \quad [8.185]$ <p>Close to the threshold, $\frac{da}{dN} \rightarrow 0$ when $\Delta K \rightarrow \Delta K_S$, constants C_1 and m_1 are such that, in a given point ΔK_1, rate da/dN is the same as the law of Paris rate and, at this point, the da/dN slope is also that of the Paris curve.</p> <p>Close to the critical zone,</p> $\frac{da}{dN} = C_2 \left[\frac{1}{K_C (1-R) - \Delta K} \right]^{m_2} \quad [8.186]$ <p>and $\frac{da}{dN} \rightarrow \infty$ when $K_{\max} \rightarrow K_C$.</p> <p>At a given point ΔK_2, both curves connect with the same slope (making it possible to calculate constants C_2 and m_2).</p>		
<p>Socie and Kurath [SOC 83]</p>	$\frac{da}{dN} = C \frac{\Delta K^m}{(1-R)^k}$	<p>[8.187]</p>	<p>R is stress ratio, k is a constant function of the material.</p> <p>Stochastic models were more recently developed to consider the random aspect of the propagation of cracks and the dispersion observed on test results [DIT 86] [KOZ 89] [LIN 88] [ORT 88].</p>

Table 8.4. Expressions of the speed of propagation of cracks

8.15. Stress intensity factor

In many cases, crack propagation does not occur with a stress lower than the yield stress as with previous hypotheses; rather it occurs in the plastic domain, as with low cycle fatigue.

A.J. McEvily [MCE 70] defines a strain intensity factor K_ϵ in a similar way to the stress intensity factor. If ϵ_R is the total strain range, then

$$K_\epsilon = \epsilon_R \sqrt{a} \quad [8.188]$$

(similar to $K_\sigma = \sigma \sqrt{a}$) for a plate with a length of $2a$ and infinite width.

The justification of the use of K_ϵ is similar to that of K_σ . Slope m of the curve representative of the straight line (logarithmic axes), expressed

$$\frac{da}{dN} = A \left(\epsilon_R \sqrt{a} \right)^m, \quad [8.189]$$

can vary between 2 and > 6 in the elastic domain. In the plastic domain, m is approximately equal to 2.

McEvily showed that the integration of expression

$$\frac{da}{dN} = A \left(\epsilon_R \sqrt{a} \right)^2 \quad [8.190]$$

leads to a relation in the form of the Manson–Coffin law.

8.16. Dispersion of results

It is not possible to determine in a test the parameters necessary for a correct description of the dispersion occurring in the crack propagation data. The dispersion observed depends in particular on the test method used [POO 76].

An average line can be drawn between the points measured to predict an average fracture time, but the dispersion cannot be evaluated from results of experimental results.

J. Branger [BRA 64] notes that the dispersion observed in notched test bars is substantially smaller than the dispersion viewed with smooth test bars, and that it decreases when the number of notches increases.

The dispersion decreases when the complexity of the specimen increases. This result is masked by the manufacturing tolerances of parts.

8.17. Sample tests: extrapolation to a structure

A.M. Freundenthal [FRE 68] considers that fatigue tests in small samples can only provide generally qualitative and comparative information on the behavior of materials at fatigue.

The comparative study of the emergence of cracks and their speed of propagation requires the use of specimens where the design presents accidents that are important enough and dimensions are sufficiently large.

A.M. Freundenthal highlights the importance of large-scale tests carried out with loads reproducing the distribution of real loads.

Time to fracture during service is also always shorter than for a large-scale test (a test generally carried out on a better structure than on average). The linear accumulation of damages overestimates the real endurance observed in large-scale tests (ratio 2 to 3).

8.18. Determination of the propagation threshold K_S

The propagation threshold can be determined as follows [LIA 73]:

– We apply stress cycles by maintaining the constant R ratio and by slowly decreasing the value of the mean stress, in order to ensure a crack expansion that is not lower than 0.5 mm between each load adjustment. The decrease should be exceed 10% of the previous load. The value of K_S is the value of ΔK corresponding to a propagation speed of 10^{-7} mm/cycle (some authors retain 10^{-8} mm/cycle).

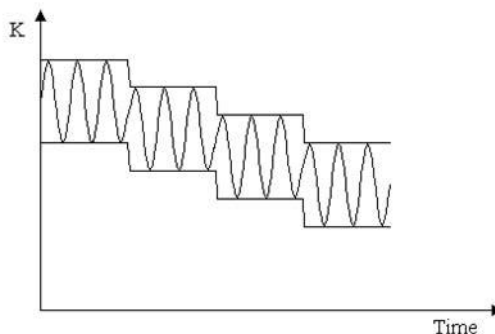


Figure 8.28. *Stress cycles at constant R and decreasing mean*

This method is long and does not consider the material tried.

Other conditions were additionally proposed:

- a minimum expansion of the crack between two load levels should be equal to at least 10 times the size of the plane stress plastic zone of the previous load; or
- ΔK_S is affected by the size of the grain, and a minimum increase of the crack at each level must also be greater than five times the diameter d of the material's grain in order to avoid a possible influence of the crystallographic direction of grains on ΔK_S .

$$\Delta a_i \geq 0.5 \text{ mm}$$

$$\Delta a_i \geq 5 d$$

$$\Delta a_i \geq \frac{10}{\pi} \frac{K_{\max i-1}^2 - K_{\max i}^2}{R_e^2} \quad [8.191]$$

Different methods were used to optimize the test duration [VAN 75].

Different relations were proposed to evaluate the threshold stress intensity factor for any R from this same factor for $R = 0$.

Table 8.5 combines a few expressions

Davenport and Brook [DAV 79]	$\Delta K_S = \Delta K_{S0} \sqrt{1-R}$	[8.192]
Masounave and Bailon [MAS 75]	$\Delta K_S = \Delta K_{S0} (1-R)$	[8.193]
Lukas and Klesnil [KLE 72a]	$\Delta K_S = \Delta K_{S0} (1-R)^\gamma$ with $\gamma \approx 0.71$	[8.194]
McEvily [MCE 77]	$\Delta K_S = \Delta K_{S0} \sqrt{\frac{1-R}{1+R}} \approx \Delta K_{S0} (1-2R)^{1/2}$	[8.195]
Wei and McEvily [WEI 71]	$\Delta K_S = \Delta K_{S0} \frac{K_C (1-R)}{(1-R) K_C + R \Delta K_0}$	[8.196]
	$\Delta K_S = \Delta K_{S0} \left[1 - \frac{R \Delta K_0}{(1-R) K_C} \right]$	[8.197]

Table 8.5. Some expressions for the threshold stress intensity factor

8.19. Propagation of cracks in the domain of low cycle fatigue

The low cycle fatigue process is generally dominated by the crack propagation phenomenon (over 90% of the useful lifetime) [MUR 83].

The theory of crack propagation initially developed in the domain of high cycle fatigue was extended by A.K. Head [HEA 56a] to low cycle fatigue [YAO 62].

The theory is based on idealized material, and shows that:

- cracks can initiate during the first phases of the fatigue test;
- the inverse of the square root of the crack length is a linear function of the number of cycles; and
- the slope of the straight line corresponding to a function of the amplitude of applied stresses.

McClintock [MCC 56] also established that:

- cracks always tend to grow close to the center of the remaining section, closer to the farthest point of open surfaces;
- the propagation of cracks depends on increments of absolute strain integrated without regard to the number of cycles and to the increments of plastic strain;
- cracks propagate faster in the largest of two unspecified specimens, geometrically similar, in the same nominal strain amplitude;
- the initial rate of crack propagation is independent from the angle of the notch.

Cracks appear after a very few cycles and propagate at a generally constant speed until approximately half the useful lifetime of the specimen has passed, then propagation continues with increasing speed [SCH 57].

We show that the law of Manson–Coffin is identical to the law of propagation of micro-cracks (to approximately 1 mm).

The Miner law must be considered on the basis on the micro-crack propagation. It applies to the following conditions [MUR 83]:

- The history of the specimen relative to previously accumulated fatigue in the area where the crack will propagate has no effect on fatigue damage (there is no overload or underload effect), but it greatly influences the propagation speed of subsequent cracks. In order for the Miner law to apply, this prior fatigue should not be considered as fatigue damage.

– The speed of crack propagation is linearly proportional to the length of the crack.

Murakami *et al.* [MUR 83] derive a linear law of propagation by dimensional analysis

$$\frac{da}{dN} = \text{Constant} \times a. \quad [8.198]$$

8.20. Integral J

In the case of large strains producing fractures after a small number of cycles, the above expressions are not precise.

We have implicitly assumed that the plasticity at the top of the crack is so small that the mechanics of the linear elastic fracture applies and that the energy released is not affected by the plastic strain [BRO 78].

A more exact calculation considering plasticity effects was proposed by N.E. Dowling and J.A. Begley [DOW 76] based on the concept of *J integral*. Integral J is initially defined [RIC 68] in the case of non-linear elasticity from the load-deformation curve. For given deformation z_0 , the potential energy variation dU produced by a small increase da of the length of the crack is linked to J by:

$$J = -\frac{1}{B} \frac{dU}{da}, \quad [8.199]$$

where B is specimen size.

If the material has linear behavior, we find

$$J = G = \frac{K^2}{E} \quad [8.200]$$

where G is the rate of linear elastic deformation energy transmitted.

J is linked to K. For elasto-plastic material, U is defined as the energy necessary to deform the specimen in an elasto-plastic manner.

In an approximate way, integral J can be calculated for notched bars in tension and bending by:

$$J = \frac{2}{B b} \int_0^{z_0} P \, dz \quad [8.201]$$

where P is the load.

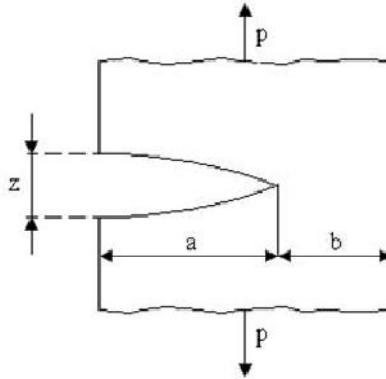


Figure 8.29. *Notched bar*

N.E. Dowling and J.A. Begley [DOW 76] established the relation for steel A-533B:

$$\frac{da}{dN} = 2.13 \cdot 10^{-8} \Delta J^{1.587} \quad [8.202]$$

which can be written in a more general way in the form [MOW 76]:

$$\frac{da}{dN} = C_1 \Delta J^\gamma \quad [8.203]$$

at half-length of the crack, where C_1 and γ are constants for a given material and ΔJ is related to the area under the load-deformation curve by relation [8.201]. This expression agrees with the Paris expression if we consider the relation between J and K^2 .

D.F. Mowbray [MOW 76] shows that this relation can be expressed in the form of the Manson–Coffin equation ($N^{1/\gamma} \epsilon_p = C$). We highlight, however, that an objection exists in applying the concept of integral J to crack propagation: in a strict mathematical sense, this theory is only valid for the theory of plasticity deformations, which does not include discharges.

From a practical point of view, there is only a limited number of cases for which J can be calculated or measured, but any approach taking into account a non-linear behavior of the material would face the same problems [LAM 80a].

R. Tanaka [TAN 83] uses integral J as growth criterion of a fatigue crack. He suggests the generalization of experimental data, available for different materials on the growth of cracks, to derive at a unified formulation from an energy criterion. It links the threshold ΔJ corresponding to ΔK_S to the surface energy of the material, noting that ΔJ should be higher than 4γ (γ is surface energy of the material).

8.21. Overload effect: fatigue crack retardation

We have seen the importance of the sequence of application of loads and increase of useful lifetimes observed during initial overload [SCH 72a]. This overload effect increases when the number of large load cycles grows [PAR 65]. In the cases studied, R.H. Keays observes an increase of the useful lifetime by 20% [KEA 72] and notes that if loads relative to a spectrum are randomly sequenced, the theory predicts an important increase of the number of blocks at fracture.

Different methods were proposed for the consideration of this effect (e.g. Willenborg model [FUC 80], Vorman model [VRO 71], etc.) [BEL 76] [ELB 71] [WIL 71]. Among these methods, we will cite the Wheeler method [BRO 78] [KEA 72] [WHE 72].

The Wheeler model, developed to explain and predict the delay caused by overloads, consists of introducing into the cracking law the relation of two plastic zones [SAN 77]:

- the real plastic zone existing at the root of the crack; and
- a fictional plastic zone that would exist if there was no overload (if the load remained sinusoidal).

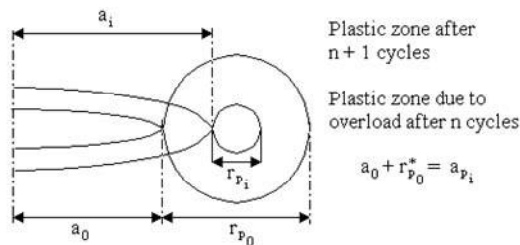


Figure 8.30. Plastic zones

O.E. Wheeler assumes that crack propagation depends on relative sizes of plastic zones during consecutive cycles: if the maximum size of the plastic zone during the first n cycles envelopes that obtained after $n + i$ cycles, there is a cracking retardation [BAR 80].

This delay is proportional to the ratio of the plastic zone size relative to the present level (r_p^*) to the length not yet cracked of the previous plastic zone ($a_{pi} - a_i$).

Hence, by using the Paris law,

$$\frac{da}{dN} = C \Delta K^m \Phi \quad [8.204]$$

where Φ is the *retardation factor*, such that

$$\left\{ \begin{array}{ll} \Phi = \left(\frac{r_{pi}^*}{a_{pi} - a_i} \right)^p & \text{si } a_i + r_{pi}^* < a_{pi} \\ \Phi = 1 & \text{si } a_i + r_{pi}^* \geq a_{pi} \end{array} \right. \quad [8.205]$$

where p is the coefficient function of the nature of the material.

The calculation is done with the help of these relations to follow the propagation of the crack cycle after cycle.

In these expressions,

$$r_{p0} = C \frac{K_0^2}{R_e^2} \quad [8.206]$$

and

$$r_{pi} = C \frac{K_i^2}{R_e^2} . \quad [8.207]$$

We have seen (in relation [8.40]) that, in more precise terms,

$$r_p^* \approx \frac{K_I^2}{6 \pi R_c^2} . \quad [8.208]$$

We should note that negative loads reduce the retardation caused by positive loads.

Limitations [SAN 77]

Limitations include the following:

- β also depends on test conditions;
- this model does not predict that some overloads prevent the crack from propagating later; and
- λ only considers load history after overload and ignores history before overload (even though the retardation is its function).

An improvement of this model was proposed by T.D. Gray and J.P. Callagher [GRA 76], who considered blocking the crack.

8.22. Fatigue crack closure

The phenomenon known as *crack closure* was described by W. Elber [ELB 71] [FUC 80]. He showed experimentally that the tip of a fatigue crack can close before the global effort applied to the specimen cancels out, because of residual strains created by cracking at the root of the crack [SAN 77]. Damage then occurs only in the part of the cycle where the crack is open and not when it is closed (compression).

W. Elber [FUC 80] notes a non-linear behavior in the experimental displacement-load curves and explains it by a physical contact or by an interference of the material zone plastically deformed right after the propagating fatigue crack. He considers that the cyclic growth only occurs when the crack is completely open and develops a relation in the form [ELB 71] [WOO 73]:

$$\frac{\Delta a}{\Delta N} = C (\Delta K_{rms})^m = C (U \Delta K)^m \quad [8.209]$$

where

$$U = \frac{K_{\max} - K_{\text{op}}}{K_{\max} - K_{\min}} = \frac{\Delta K_{\text{rms}}}{\Delta K}, \quad [8.210]$$

where $0 \leq U \leq 1$ and K_{op} is the value of K at the crack opening.

For aluminum alloy 2024-T3, $U = 0.5 + 0.4 R$ ($-0.1 < R < 0.7$).

This is an empirical model using a concept of effective stress range to incorporate the effects of interaction in the estimation of the fatigue useful lifetime with variable amplitude cracking [FUC 80].

W. Elber assumed that the expansion of the crack only happens when the applied stress is larger than the stress necessary for the crack opening. In this way, significant stresses in the propagation process are the maximum stress and the opening stress in a cycle. W. Elber finds that the stress in which the closure occurs is slightly different from the opening stress. This difference is often neglected. He attributes the closure to a zone of residual tension deformation left behind the root of the crack, which interacts with crack root compression stresses.

The stress range contributing to the expansion is called *effective stress range* $\Delta\sigma_{\text{rms}}$ with

$$\Delta\sigma_{\text{eff}} = \sigma_{\max} - \sigma_{\text{op}} \quad [8.211]$$

where σ_{op} is the opening stress experimentally determined.

He defines a *closing factor*

$$C_i = \frac{\sigma_{\text{op}}}{\sigma_{\max}}, \quad [8.212]$$

hence

$$\Delta\sigma_{\text{rms}} = \sigma_{\max} (1 - C_i). \quad [8.213]$$

With the Paris law for example,

$$\frac{da}{dN} = A \Delta K_{\text{rms}}^m \quad [8.214]$$

$$\frac{da}{dN} = A \left(\Delta \sigma_{rms} \sqrt{\pi a} \alpha \right)^m \quad [8.215]$$

and

$$\frac{da}{dN} = A \left[\sigma_{max} (1 - C_i) \sqrt{\pi a} \alpha \right]^m. \quad [8.216]$$

8.23. Rules of similarity

Useful lifetime calculations are always based on the following rules of similarity [SCH 72a]:

- in stress: similar load conditions in critical points for fatigue, in two different specimens composed of a single material, should produce similar results in fatigue;
- in strain: similar strain curves, e.g. at the root of the crack or in a smooth specimen, should produce stresses according to similar times. Another hypothesis is that similar strain curves should also lead to similar useful lifetimes;
- in propagation of crack: K being identical, relation $\frac{da}{dN} = f(K)$ established for a specimen is valid for another type of specimen.

8.24. Calculation of a useful lifetime

The useful lifetime of a part is often calculated by considering [SAN 69]:

- initiation as a short phase in relation to the total lifetime; initiation effects over a useful lifetime are insignificant;
- the behavior in relation to propagation in the micro-crack phase as an extrapolation of the behavior in the macro-crack phase; and
- the final fracture occurs when a critical crack length is reached.

From these hypotheses, the useful lifetime is evaluated by calculating the number of cycles required to grow a crack from a small size to critical length.

The useful lifecycle is therefore characterized by the number of cycles necessary to progress from one crack of initial size a_i (minimum that can be detected) to a critical length a_c for which fracture of the component is almost instant [POO 74].

The law of crack propagation is in the general form

$$\frac{da}{dN} = f(\Delta K, K_{\max}), \quad [8.217]$$

from which we derive

$$N = \int_{a_i}^{a_c} \frac{da}{f(\Delta K, K_{\max})}. \quad [8.218]$$

In the cases where the function $f(\Delta K, K_{\max})$ has a simple form, we can proceed to an analytical integration. Otherwise, we can integrate this expression numerically.

We then replace this integral by a cycle-by-cycle summation such that:

$$a_c - a_i = \sum_{i=1}^N C \Delta K_i^m \Delta n_i. \quad [8.219]$$

For variable amplitude loads, the retardation in crack growth caused by the interaction of loads can be considered with the help of one of the models previously discussed.

For example, the above equation can be written as:

$$a_c - a_i = \sum_{i=1}^N C_{ri} C \Delta K_i^m \Delta n_i \quad [8.220]$$

where C_{ri} is the retardation factor of the Willenborg model.

Example 8.4.

If we estimate that the Paris law $\frac{da}{dN} = C \Delta K^m$ ($\Delta K_S < \Delta K < \Delta K_C$) is the best adapted, for sinusoidal tension excitation such that $\sigma_{\min} = 0$ we have:

$$\Delta K = 2 \sigma \sqrt{\pi a} \quad [8.221]$$

for an infinite plate, where σ = stress amplitude.

Hence [LAM 83]:

$$N = \int_{a_i}^{a_c} \frac{da}{C \Delta K^m} = \frac{1}{C (2 \sigma)^m} \int_{a_i}^{a_c} \frac{da}{(\sqrt{\pi a})^m}, \quad [8.222]$$

$$N = \frac{1}{(2 \sqrt{\pi})^m C \sigma^m} \int_{a_i}^{a_c} \frac{da}{a^{m/2}} = \frac{1}{(2 \sigma \sqrt{\pi})^m C} \left[\frac{a^{1-\frac{m}{2}}}{1-\frac{m}{2}} \right]_{a_i}^{a_c}, \quad [8.223]$$

for $m \neq 2$, hence

$$N = \frac{a_c^{1-\frac{m}{2}} - a_i^{1-\frac{m}{2}}}{(2 \sigma \sqrt{\pi})^m C \left(1 - \frac{m}{2}\right)} \quad [8.224]$$

This relation can be in the form $N \sigma^m = \text{constante}$. The critical size can be calculated from [8.221]:

$$a_c = \left(\frac{\Delta K_c}{2 \sigma \sqrt{\pi}} \right)^2 \quad [8.225]$$

The linear integration (corresponding to the Miner hypothesis), leading to the effects of interaction being neglected, gives a conservative result (shorter useful lifetime than reality). In order to account for these effects, we would have to proceed to a numerical cycle-by-cycle integration by considering the real curve $\frac{da}{dN}(\Delta K)$ which, in logarithmic axes, is not linear in the whole field.

If a load can be broken down into several blocks with S_i amplitude stress with n_i cycles, a rule similar to the Miner rule makes it possible to define the *rate of propagation by block*, i.e.

$$\frac{da}{dB} = \sum_i n_i \left(\frac{da}{dN} \right)_i \quad [8.226]$$

and therefore to calculate the useful lifetime in numbers of blocks [SHE 83a].

NOTE:

Useful lifetime calculated from this model is linked to the length of the crack.

J. Schijve [SCH 70], however, highlights that fatigue damage cannot be completely defined by a single parameter such as this length. Other conditions can also be important, such as the direction of the crack, hardening, residual stresses, etc..

The expansion of a crack during a load cycle will then depend on the prehistory of the fatigue load experienced by the part. This has the consequence of different results begin obtained from a random load and a programmed load.

8.25. Propagation of cracks under random load

The rate of crack propagation under random load is considerably smaller than would be predicted from linear summation of propagation increments based on data obtained by constant amplitude tests [KIR 77].

Crack propagation laws are generally non-linear. It is therefore difficult to transform them prior to using them in the case of random vibrations.

Two types of methods were used to predict the growth of cracks under variable amplitude loads [NEL 78]:

- The rms approach: in this case, we characterize the load spectrum in terms of characteristic parameters such as the rms value. Stress spectra are represented in these studies by a continuous and unimodal distribution, specifically by a Rayleigh distribution (it is a restriction of the method).

- The cycle-by-cycle approach: in these methods, mainly developed for loads measured in aeronautics, we calculate the propagation of the crack cycle-by-cycle and generate the sum [BRU 71] [GAL 74] [KAT 73].

8.25.1. Rms approach

In the case where vibrations are stationary and narrow band, a method may consist of using the Paris law by replacing the stress intensity factor ΔK by its standard deviation.

P.C. Paris [PAR 64] showed that factor K is linked to stress σ by a relation of the form

$$K = \sigma f(a) \quad [8.227]$$

where $f(a)$ is a function of dimension a of the crack.

Since the stress is a function of time, we have

$$K(t) = \sigma(t) f(a). \quad [8.228]$$

As length a varies very little from a stress cycle to the next, $f(a)$ is a factor that also varies very little.

It is therefore possible to calculate the power spectral density (PSD) of $K(t)$:

$$G_K(\Omega) = G_\sigma(\Omega) f^2(a) \quad [8.229]$$

where $G_\sigma(\Omega)$ is the stress PSD, which can in turn be expressed in terms of the excitation at structure input. $G_K(\Omega)$ is therefore, except for the a factor, variable from one moment to the next and identical to $G_\sigma(\Omega)$.

In a given material, the rate of crack propagation produced by a random load $G_\sigma(\Omega)$ is a function of the amplitude of the quasi-stationary power spectrum $G_K(\Omega)$ of factor K .

We can also define the rms value as:

$$\Delta K_{\text{rms}} = \sqrt{\int_0^\infty G_K(\Omega) d\Omega} \quad [8.230]$$

or, in a discrete form [BAR 80]:

$$\Delta K_{\text{rms}} = \sqrt{\sum_{i=1}^n \frac{\Delta K_i^2}{n}} \quad [8.231]$$

where n is the number of cycles.

We therefore obtain the expression of the modified law of Paris, giving the mean value of the cracking rate:

$$\frac{da}{dN} = C (\Delta K_{\text{rms}})^m \quad [8.232]$$

where C and m are constants for a given material [BAR 73] [SMI 66] [SWA 67].

This method cannot be used if $\sigma(t)$ is wide band, since it supposes that the distribution of the peaks of $\sigma(t)$ obeys a Rayleigh law [BAR 76].

The rms value of the variation range of the stress intensity factor then appears as an important parameter for characterizing the rate of crack propagation in the case of complex loads [BER 83] [WEI 78] in an appropriate way. The PSD form also has its importance, but to a lesser degree [SWA 68]. It can be characterized by the irregularity factor r or by $q = \sqrt{1-r^2}$.

The method will therefore consist of replacing ΔK by ΔK_{rms} in useful lifetime calculations already made in the case of a sinusoidal load.

We therefore find that the expression for the propagation rate has already been proposed, as described in the following section.

8.25.1.1. *McEvily expression [MCE 73]*

We have

$$\frac{da}{dN} = \frac{A}{R_e E} (\Delta K_{\text{rms}}^2 - \Delta K_S^2) \quad [8.233]$$

where the term taking into account the mean stress, $\frac{\Delta K}{K_C - K_{\text{max}}}$, is insignificant in the case of steel studied by J.M. Barsom [BAR 76]. This relation leads to results very close to equation [8.232].

8.25.1.2. *Roberts and Erdogan [ROB 67]*

H. Nowack and B. Mukherjee [NOW 63] have modified the law of R. Roberts and F. Erdogan [ROB 67]

$$\frac{da}{dN} = C_1 \Delta K^{k_1} K_{\text{max}}^{k_2} \quad [8.234]$$

where C_1 , k_1 and k_2 are constants depending on

$$\frac{da}{dN} = C_2 \overline{\Delta K}^{k_3} \overline{K_{\max}}^{k_4}, \quad [8.235]$$

$$\overline{K_{\max}} = K_{\text{mean}} + \frac{\overline{\Delta K}}{2} \quad [8.236]$$

where K_{mean} is a stress intensity factor corresponding to the mean stress.

For a Gaussian stationary process,

$$\overline{\Delta K} = \overline{\Delta \sigma'} \sqrt{a} Y \quad [8.237]$$

where Y is a correction factor considering of the finite width of the specimen

$$\overline{\Delta \sigma'} = 2 \pi \sigma_{\text{rms}} r \quad [8.238]$$

where r is the factor of irregularity [SWA 68].

If a_0 is the length of the transition crack (curve bend $\frac{da}{dN}(\Delta K)$), constants C_2 , k_3 and k_4 are listed in Table 8.6, where length is in mm and stress is in kgf/mm^2 .

a_0	C_2	k_3	k_4
< 6 mm	10–11.46	2.16	1.72
> 6 mm	10–20.35	6.06	2.45

Table 8.6. Values of constants C_2 , k_3 and k_4 according to a_0

S.H. Smith [SMI 64c] observed a good correlation between results obtained with constant amplitude loads and random loads when the stress intensity factor was used as the basis of comparison of rate of fatigue crack propagation.

For small K values, random loads lead to greater propagation speeds. For larger K values, random loads lead to shorter propagation speeds than those obtained with constant amplitude load.

For a random load with Rayleigh peak distribution, the speed of crack propagation can be estimated with good precision from a linear summation of propagation speeds obtained in constant amplitude tests, on the condition that the test be done at constant K [SWA 68].

Since rates of propagation for the different levels of stress are determined for constant K , we can calculate, by presuming the Rayleigh peak distribution, the total rate of propagation for a unit length of crack propagation by integrating the curve: percentage of time at a given stress level multiplied by the cracking rate at this stress level.

S.R. Swanson [SWA 68] observes that, for a load and constant K , there is a good agreement between a prediction from a linear calculation and observations. Other authors also agree [CHR 65] [MAY 61].

This linear summation does not use the Miner rule or the S-N curve, for which this could be inadequate.

NOTES:

1. *Since the frequency has very little influence, we show that (stress) 'equivalent' power spectra are those that can be deducted from a given spectrum by an arbitrary linear modification of the scale of frequencies and/or amplitudes* [PAR 62].

2. *Because of a random stress based on time, with a Gaussian distribution of instant values, we can calculate the mean frequency n_0^+ of the signal, the mean frequency of maxima (n_p^+), the mean length \bar{h}_p of ranges (interval between two consecutive extrema), from the PSD of $\sigma(t)$ [POO 79]. If M_n is the order n moment, we show (Volume 3, relations [6.13] and [6.108]) that*

$$n_p^+ = \frac{1}{2\pi} \sqrt{\frac{M_4}{M_2}} \quad [8.239]$$

and

$$\bar{h}_p = \sqrt{2\pi} \frac{M_2}{\sqrt{M_4}}. \quad [8.240]$$

If \bar{h}_k is the mean range of the stress intensity factor relative to $\sigma(t)$, from [8.227], we have [PAR 64]:

$$\bar{h}_k = \bar{h}_p f(a). \quad [8.241]$$

These parameters have an influence on the crack propagation rate [PAR 62].

3. Size of the plastic zone

P.C. Paris [PAR 64] extends the Irwin relation [8.39] in the case of the random and defines the dimension of the plastic zone by

$$r_p = \frac{h_k^2}{8 R_e^2} \quad [8.242]$$

where h_k is the peak-to-peak stress intensity factor (range).

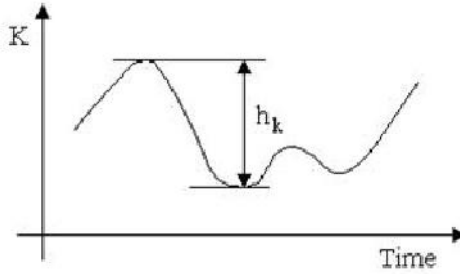


Figure 8.31. Stress intensity factor h_k range

We could calculate statistically the mean rate of crack propagation with the help of the modified Paris relation [BRO 78]:

$$\overline{\frac{d(2a)}{dN}} = C \overline{h_k^4} \quad [8.243]$$

$$h_k = h_p f(a) \quad [8.244]$$

$$\overline{h_k^4} = \int_0^\infty h_k^4 q(h_k) dh_k \quad [8.245]$$

$\overline{h_k^4}$ is the mean of ranges of $K(t)$ to power 4, $K(t)$ being presumed quasi-stationary, and q is the probability density of the ranges h_k of $K(t)$. This density can be calculated from the PSD of $K(t)$, i.e. the stress $\sigma(t)$. The calculation is not however easy, and requires approximations.

8.25.2. Narrow band random loads

L.P. Pook [POO 74] provides a method of analysis that we can consider as an extension of the Miner rule for the mechanics of crack propagation. It takes into consideration the mean stress and gives correlated results by experience [WEI 74].

The analysis is based on fatigue data from constant amplitude tests (welded joints structures).

Because of an “input” load with a Gaussian distribution of instantaneous values, we can often assimilate the distribution of peaks of the response stress in a structure point to a Rayleigh law where the probability density has the form

$$p\left(\frac{\sigma_{\text{peak}}}{\sigma_{\text{rms}}}\right) = \frac{\sigma_{\text{peak}}}{\sigma_{\text{rms}}} \exp\left(-\frac{\sigma_{\text{peak}}^2}{2\sigma_{\text{rms}}^2}\right) \quad [8.246]$$

where σ_{peak} is the stress peak and σ_{rms} is the rms value of stress.

The distribution of ranges between adjacent positive and negative peaks is also close to a Rayleigh law. This distribution is truncated in practice at approximately $5-6 \sigma_{\text{rms}}$. Strictly speaking, a truncated distribution has a smaller rms value σ_{rms} from that of an identical but not truncated distribution. However, as long as the truncation ratio $\sigma_{\text{peak}}/\sigma_{\text{rms}}$ is not too small (lower than 3), the difference is low and can be neglected. For ratios 3, 4 and 5, the differences are 1.1, 0.03 and $4 \times 10^{-4}\%$, respectively [POO 74].

We now assume that each cycle produces the same propagation increment as if it was applied like a part of a constant amplitude load sequence. In this approach, we ignore the effects of interaction that occur when amplitudes vary. In the case of narrow band random loads, a cycle is not much different from the previous cycles, reducing the effects of interaction which are relatively unimportant for low resistance steel.

The damage produced by each cycle in terms of crack propagation is proportional to $(\sigma_{\text{peak}}/\sigma_{\text{rms}})^m$ according to the relation

$$\frac{da}{dN} = C \Delta K^m \quad [8.247]$$

and the relative damage for a sinusoidal load with constant amplitude and similar rms value is equal to

$$\left(\frac{\sigma_{\text{peak}}}{\sigma_{\text{rms}} \sqrt{2}} \right)^m.$$

We define a density function by

$$r\left(\frac{\sigma_{\text{peak}}}{\sigma_{\text{rms}}}\right) = \left(\frac{\sigma_{\text{peak}}}{\sigma_{\text{rms}} \sqrt{2}}\right)^m \frac{\sigma_{\text{peak}}}{\sigma_{\text{rms}}} \exp\left(-\frac{\sigma_{\text{peak}}^2}{2 \sigma_{\text{rms}}^2}\right) \quad [8.248]$$

where $\sigma_{\text{peak}} \leq \sigma_m$, $r\left(\frac{\sigma_{\text{peak}}}{\sigma_{\text{rms}}}\right)$ is the relative probability density of crack propagation due to a peak $\frac{\sigma_{\text{peak}}}{\sigma_{\text{rms}}}$ and σ_m is mean stress.

Figure 8.32 shows the variations of $r\left(\frac{\sigma_{\text{peak}}}{\sigma_{\text{rms}}}\right)$ for different m values. We note

that peaks such as $\frac{\sigma_{\text{peak}}}{\sigma_{\text{rms}}} < \frac{1}{2}$ produce little damage; the maximum is for

$$\frac{\sigma_{\text{peak}}}{\sigma_{\text{rms}}} \approx 2.$$

The area under the relative damage density curve gives the relative damage R_D , which is the ratio of the value of the crack growth produced by the narrow band random load to that produced by a completely tension load with constant amplitude and similar rms stress.

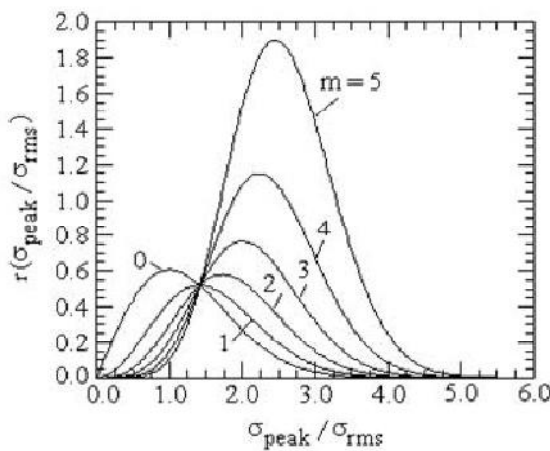


Figure 8.32. Probability density of crack propagation

Relative damage R_D is practically independent from the truncation ratio, as long as this relation is higher than 3.

m	0	2	3	4	5
R_D	Rayleigh	1	1.33	2	3.323

Table 8.7. Relative damage for a few m values

Unless the mean stress σ_m is very high, minima for large value of $\frac{\sigma_{\text{peak}}}{\sigma_{\text{rms}}}$ are below zero. The positive part of a load cycle is the only one creating damage, because it corresponds to a tension opening the crack (a compression maintains the two edges one over the other, without damage). Consequently, the density of relative damage is reduced by correcting the expression above by the factor:

$$\left(\frac{\sigma_m + \sigma_{\text{peak}}}{2 \sigma_{\text{peak}}} \right)^m$$

i.e.

$$r \left(\frac{\sigma_{\text{peak}}}{\sigma_{\text{rms}}} \right) = \left(\frac{\sigma_m + \sigma_{\text{peak}}}{2 \sqrt{2} \sigma_{\text{rms}}} \right)^m \frac{\sigma_{\text{peak}}}{\sigma_{\text{rms}}} \exp \left(- \frac{\sigma_{\text{peak}}^2}{2 \sigma_{\text{rms}}^2} \right) \quad [8.249]$$

where $\sigma_{\text{peak}} \leq \sigma_m$.

Figure 8.33 shows the function thus modified drawn for different values of $\frac{\sigma_m}{\sigma_{\text{rms}} \sqrt{2}}$ ($-\frac{\sqrt{2}}{2}$; 0; $\frac{\sqrt{2}}{2}$; 1; $\sqrt{2}$; 2; ∞) and $m = 3$.

For a constant amplitude sinusoidal load, amplitude σ_a is equal to $\sigma_a = \sigma_{\text{rms}} \sqrt{2}$.

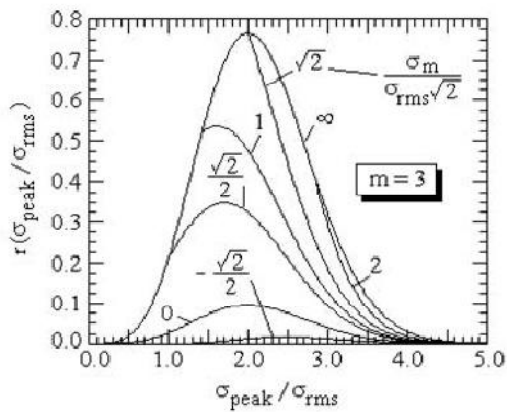


Figure 8.33. Probability density of crack propagation for different values of $\frac{\sigma_m}{\sigma_{\text{rms}} \sqrt{2}}$

Factor $\sqrt{2}$ is then introduced in the diagram of these curves in order to directly compare constant amplitude loads and random loads.

m = 4							
$\frac{\sigma_m}{\sigma_{\text{rms}} \sqrt{2}}$	$-\frac{\sqrt{2}}{2}$	0	$\frac{\sqrt{2}}{2}$	1	$\sqrt{2}$	2	∞
R_D	0.0148	0.125	0.621	0.984	1.487	1.895	2

Table 8.8. Relative damage for a few values of $\frac{\sigma_m}{\sigma_{\text{rms}} \sqrt{2}}$

Even when the mean stress is negative, the largest maxima can be positive and produce damage.

Even though damage R_D is insensitive to small variations of σ_m for large mean values, and the fact that the error is low if the closure does not happen at zero load, R_D greatly depends on σ_m when σ_m is close to zero. Serious mistakes can be made if the crack does not close at zero load.

A fatigue crack of a given length does not grow unless the applied stress exceeds a threshold value $\Delta\sigma_S$ that can be calculated, for given ΔK_S , from

$$\Delta K = \alpha \Delta\sigma \sqrt{\pi a} \quad [8.250]$$

where α is a constant, geometric correction factor, of approximately 1.

The peaks lower than a threshold value of $\frac{\sigma_{\text{peak}} S}{\sigma_{\text{rms}}}$ therefore do not produce damage. The relative damage density curve is truncated and relative damage is decreased. When the crack grows, $\frac{\sigma_{\text{peak}} S}{\sigma_{\text{rms}}}$ decreases according to relation [8.250] and relative damage R_D increases. This phenomenon must be taken into consideration to calculate total useful lifetime.

When the rms value σ_{rms} decreases, $\frac{\sigma_{\text{peak}} S}{\sigma_{\text{rms}}}$ increases and fatigue limit is reached when $\frac{\sigma_{\text{peak}} S}{\sigma_{\text{rms}}}$ is equal to the truncation ratio. In this way, by simply dividing the fatigue limit in constant amplitude by the truncation ratio, we obtain the fatigue limit under narrow band random load.

L.P. Pook then uses relative damage R_D to calculate the number of cycles to fracture:

$$N = \int_{a_i}^{a_c} \frac{10^6}{R} \left(\frac{\Delta K_{10^{-6}}}{2\sqrt{2} K_\sigma} \right)^m \left[P \left(\frac{\sigma_{\text{pic}S}}{\sigma_{\text{eff}}} \right) - P \left(\frac{\sigma_{\text{pic}T}}{\sigma_{\text{eff}}} \right) \right] da \quad [8.251]$$

where a_i is the length of initial crack (Pook uses 4 mm), a_c is the length of critical crack (40 mm), $\Delta K_{10^{-6}}$ is the value of ΔK for a crack propagation rate equal to 10^{-6} m/cycle, K_σ is the rms value of the stress intensity factor for a random load, $\frac{\sigma_{\text{peak S}}}{\sigma_{\text{rms}}}$ is the threshold value of $\frac{\sigma_{\text{peak}}}{\sigma_{\text{rms}}}$, $\frac{\sigma_{\text{peak T}}}{\sigma_{\text{rms}}}$ is the truncation ratio and $P\left(\frac{\sigma_{\text{peak}}}{\sigma_{\text{rms}}}\right)$ is the probability of a peak exceeding $\frac{\sigma_{\text{peak}}}{\sigma_{\text{rms}}}$.

8.25.3. Calculation from a load collective

The calculation of the state of cracks after application of a random vibratory environment can be done from a load collective, evaluated from one of the counting methods presented for traditional fatigue studies.

The resulting load spectrum must be transformed into a horizontal level spectrum on which we can read the number of cycles to associate with each discrete amplitude value.

Example 8.5.

Cracking calculation

We consider that the law of Paris

$$\frac{da}{dN} = C \Delta K^m \quad [8.252]$$

applies with $K = \sigma \sqrt{\pi a}$ and for a minimum crack size detectable of 0.5 mm.

Case where there is no retardation of cracking caused by overloads

Suppose that $C = 2 \times 10^{-9}$ and $m = 4$. The calculation is made by proceeding to a linear numeric integration referring to Table 8.9,

Level of stress (kg/mm ²)	Number of cycles per level (block)	Size of the crack (mm)	ΔK (kg / mm ^{3/2})	$\frac{da}{dN}$ (mm/cycle)	Δa (mm)
12	1	0.5000	15.04	10^{-4}	10^{-4}
10	10	0.5001	12.53	4.9×10^{-5}	4.9×10^{-4}
8	25	0.50059	10.03	2.02×10^{-5}	5.06×10^{-4}

Table 8.9. Example of calculation of the crack size increase

– First line:

$$\Delta K = \sigma \sqrt{\pi a} = 12 \sqrt{\pi 0.5} = 15 \text{ kg} / \text{mm}^{3/2}$$

$$\frac{da}{dN} = C \Delta K^4 = 2 \cdot 10^{-9} (15.04)^4 \approx 10^{-4} \text{ mm} / \text{cycle}$$

Hence the growth of the crack size of

$$\Delta a = \frac{da}{dN} \times \text{number of cycles} = 10^{-4} \times 1 = 10^{-4} \text{ mm} .$$

The size of the crack becomes equal to $0.5 + 0.0001 = 0.5001 \text{ mm}$.

This value is transferred to the second line.

– Second line:

$$\Delta K = \sigma \sqrt{\pi a} = 10 \sqrt{\pi 0.5001} = 12.53 \text{ kg} / \text{mm}^{3/2}$$

$$\frac{da}{dN} = C \Delta K^4 = 2 \cdot 10^{-9} (12.53)^4 \approx 4.9 \cdot 10^{-5} \text{ mm / cycle}$$

For 10 cycles, $\Delta a = 104.9 \times 10^{-5} = 4.9 \times 10^{-4} \text{ mm}$ and the size of the crack tends to $0.5001 + 0.00049 = 0.50049 \text{ mm}$.

Since the load spectrum is broken down into blocks, the calculation is made consecutively for each block, and the number of blocks must be sufficient to limit the effects of overload and correctly distribute the levels.

Calculations are sometimes carried out by considering that the accumulation is broken down into several sequences which, in turn, is made up of blocks as previously described. For each block of the first sequence, the initial size is the same: 0.5 mm in this example (see Table 8.10).

The results obtained with these two methods are similar.

Case where there is retardation of crack

The calculation can be carried out with the Wheeler model, assuming that $p = 1.4$, with

$$r_p^* = \frac{K^2}{6 \pi R_e^2} \quad [8.253]$$

Assuming that $R_e = 60 \text{ kg / mm}^2$, the calculation could be carried out with the previous data, as indicated in Table 8.11. More complex calculations may be necessary if R_D is not constant, with other retardation delay models and more complicated expressions of ΔK .

NOTES:

1. Calculations carried out with these different formulations are never very precise, as in the case of traditional fatigue. We notice that [BRO 78]:

– results are conservative (more severe than in reality) when we do not consider a law of retardation; and

– calculated useful lifetime to experimental useful lifetime ratios are in lower than 2;

– the results can be adjusted with the help of retardations. The Wheeler law is the easiest to use (only one constant). The value of constant p that seems to return the best results is 6; this value leads to results calculated at 30% of experimental results (0.7–1.3);

– results thus obtained are more precise than those derived from laws of fatigue (by proceeding to a few tests to adjust exponent p according to the shape of the excitation spectrum).

2. The retardation model of Willenborg et al. [WIL 71] does not require the use of an arbitrary coefficient compared to that of Wheeler.

3. Most retardation models proposed [BEL 76] [WHE 72] [WIL 71] return satisfying results for the calculation of useful lifetime in random loads, but do not seem as good for “ordered” load spectra [BAD 82] [WEI 78] [WHE 72] [WIL 71]. For these spectra, some authors proposed an iterative procedure retaining the general form of equation [8.222], modified by adding numbers of retardation cycles and defined with periods during which cracks do not propagate, determined experimentally [WEI 78].

Level of stress (kg/mm ²)	Number of cycles	Sequence no. 1				Sequence no. 2			
		Size of the crack (mm)	ΔK (kg / mm ^{3/2})	$\frac{da}{dN}$ (mm / cycle)	Δa_1	Size of the crack (mm)	ΔK (kg / mm ^{3/2})	$\frac{da}{dN}$ (mm / cycle)	Δa_2
12	1	0.5	15.04	10 ⁻⁴	10 ⁻⁴	0.5001	15.0413	1.02 × 10 ⁻⁴	1.02 × 10 ⁻⁴
10	10	0.5	12.53	4.93 × 10 ⁻⁵	4.93 × 10 ⁻⁴	0.5005	12.54	4.95 × 10 ⁻⁵	4.95 × 10 ⁻⁴
8	25	0.5	10.026	2.02 × 10 ⁻⁵	5.05 × 10 ⁻⁴	0.5005	10.031	2.025 × 10 ⁻⁵	5.06 × 10 ⁻⁴
		$\sum \Delta a_1 = 0.001098$				$\sum \Delta a_2 = 0.001103$			
		$a_i + \sum \Delta a_1 = 0.501098$				$a_i + \sum \Delta a_1 + \sum \Delta a_2 = 0.502201$			

Table 8.10. Comparison of two sequences

Level of stress (kg/mm ²)	Number of cycles (n)	Size of crack a_i (mm)	ΔK (kg / mm ^{3/2})	$\frac{da}{dN}$ linear (mm)	r_p^* (mm)	$a + r_p^*$ (mm)	$a + r_{p0}^*$ (mm)	$a + r_{p0}^{*0} - a_i$ (mm)	Φ $=$ $\left(\frac{r_p^*}{a + r_{p0}^* - a_i} \right)^2$	$\frac{da}{dN}$ delayed (mm)	$\Delta a = \frac{da}{dN} \cdot n$ (mm)	New a (mm)
12	1	0.5	15.04	10 ⁻⁴	3.33 × 10 ⁻³	0.50333	0.50333	0.00333	1	10 ⁻⁴	10 ⁻⁴	0.5001
10	10	0.5001	12.53	4.94 × 10 ⁻⁵	2.31 × 10 ⁻⁵	0.5024	0.50333	0.000323	0.627	3.0961 × 10 ⁻⁵	3.096 × 10 ⁻⁴	0.50041
8	25	0.5004	10.0306	2.025 × 10 ⁻⁵	1.48 × 10 ⁻⁵	0.5019	0.50333	2.92 × 10 ⁻³	0.3869	7.83 × 10 ⁻⁶	1.959 × 10 ⁻⁴	0.50061
7	1000	0.5006	8.7785	1.188 × 10 ⁻⁵	1.136 × 10 ⁻⁵	0.5017	0.50333	2.726 × 10 ⁻³	0.2936	3.487 × 10 ⁻⁶	3.487 × 10 ⁻³	0.50409
6	5000	0.5040	7.5506	6.501 × 10 ⁻⁶	8.402 × 10 ⁻⁴	0.5049	0.5049	8.402 × 10 ⁻⁴	1	6.501 × 10 ⁻⁶	3.250 × 10 ⁻²	0.53660

Table 8.11. Example of calculation of the size of the crack in the case of crack retardation

Appendices

A1. Gamma function

A1.1. Definition

The *gamma function* (or *factorial function* or *Euler function-second kind*), $\Gamma(x)$, is defined by [ANG 61]:

$$\Gamma(x) = \int_0^{\infty} \alpha^{x-1} e^{-\alpha} d\alpha \quad [\text{A1.1}]$$

A1.2. Properties

Whatever the value of x , integral or not,

$$\Gamma(1+x) = x \Gamma(x). \quad [\text{A1.2}]$$

If x is a positive integer:

$$\Gamma(1+x) = x! \quad [\text{A1.3}]$$

$$\Gamma\left(\frac{1}{2}+x\right) \Gamma\left(\frac{1}{2}-x\right) = \frac{\pi}{\cos \pi x} \quad [\text{A1.4}]$$

$$\Gamma(x) \Gamma(1-x) = \frac{\pi}{\sin \pi x} \quad [\text{A1.5}]$$

$$\Gamma\left(\frac{1}{2}\right)\Gamma(2x) = 2^{2x-1} \Gamma(x) \Gamma\left(x + \frac{1}{x}\right) \quad [\text{A1.6}]$$

$$\Gamma\left(\frac{1}{2}\right) = \sqrt{\pi} \quad [\text{A1.7}]$$

according to [CHE 66], yielding, for x a positive integer:

$$\Gamma\left(x + \frac{1}{2}\right) = \frac{1.3 \cdots (2x-1)}{2^x} \sqrt{\pi} \quad [\text{A1.8}]$$

$$\Gamma\left(-x + \frac{1}{2}\right) = \frac{(-2)^x}{1.3 \cdots (2x-1)} \sqrt{\pi}. \quad [\text{A1.9}]$$

If x is arbitrarily much higher than 1, we have:

$$\Gamma(1+x) \approx \sqrt{2\pi} (1+x)^{\frac{1+2x}{2}} e^{-(1+x)} \quad [\text{A1.10}]$$

i.e. $\Gamma(x) \approx \sqrt{2\pi} x^{x-\frac{1}{2}} e^{-x}$.

For x an integer, we use relation [A1.3] to calculate $\Gamma(x) = (x-1)!$ or the relation [A1.8] for $\Gamma\left(x + \frac{1}{2}\right)$.

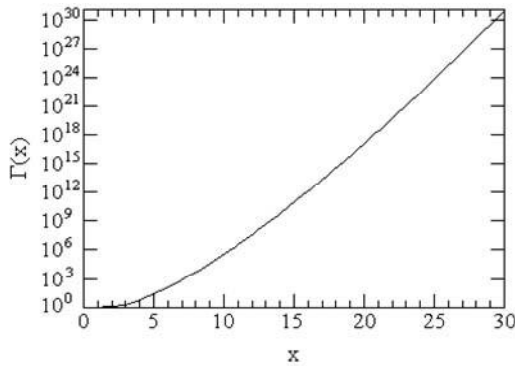


Figure A1.1. Gamma function

For arbitrary x , the relation [A1.2] and Table A1.1 allow $\Gamma(1+x)$ to be determined.

Example A1.1.

$$\Gamma(4.34) = 3.34 \Gamma(3.34)$$

$$\Gamma(4.34) = 3.34 \times 2.34 \times 1.34 \Gamma(1.34)$$

where $\Gamma(1.34)$ is given in Table A1.1.

$$\Gamma(1.34) = \Gamma(1 + 0.34) = 0.8922$$

yielding

$$\Gamma(4.34) = 9.34 .$$

	$\Gamma(1+x)$									
x	0	1	2	3	4	5	6	7	8	9
0.0		0.9943	0.9888	0.9835	0.9784	0.9735	0.9687	0.9642	0.9597	0.9555
0.1	0.9514	0.9474	0.9436	0.9399	0.9364	0.9330	0.9298	0.9267	0.9237	0.9209
0.2	0.9182	0.9156	0.9131	0.9108	0.9085	0.9064	0.9044	0.9025	0.9007	0.8990
0.3	0.8975	0.8960	0.8946	0.8934	0.8922	0.8912	0.8902	0.8893	0.8887	0.8879
0.4	0.8873	0.8868	0.8864	0.8860	0.8858	0.8857	0.8856	0.8856	0.8857	0.8859
0.5	0.8862	0.8866	0.8870	0.8876	0.8882	0.8889	0.8896	0.8905	0.8914	0.8924
0.6	0.8935	0.8947	0.8959	0.8972	0.8986	0.9001	0.9017	0.9033	0.9050	0.9068
0.7	0.9086	0.9106	0.9126	0.9147	0.9168	0.9191	0.9214	0.9238	0.9262	0.9288
0.8	0.9314	0.9341	0.9368	0.9397	0.9426	0.9456	0.9487	0.9518	0.9551	0.9584
0.9	0.9618	0.9652	0.9688	0.9724	0.9761	0.9799	0.9837	0.9877	0.9917	0.9958
1.0	1.0000	1.0043	1.0086	1.0131	1.0176	1.0222	1.0269	1.0316	1.0365	1.0415

Table A1.1. *Values of the gamma function [HAS 55]*

Example A1.2.

$$\Gamma(1 + 0.69) = 0.9068$$

A1.3. Approximations for arbitrary x

For arbitrary x (integer or not) ≥ 1 [LAM 76],

$$\frac{\Gamma(x + \frac{1}{2})}{\Gamma(x)} \approx \sqrt{x - \frac{1}{4}}. \quad [\text{A1.11}]$$

This relation is rather precise for $x > 2$ (better than 0.5%). For x a positive integer, we have, starting from the above relations,

$$\frac{\Gamma(x + \frac{1}{2})}{\Gamma(x)} = \frac{\sqrt{\pi}}{2} \frac{(2x-1)!}{2^{2(x-1)}[(x-1)!]^2} \quad [\text{A1.12}]$$

where $x!$ can be approximated to the Stirling formula

$$x! \approx x^x e^{-x} \sqrt{2\pi x} \quad [\text{A1.13}]$$

or, better, to:

$$x! \approx x^x e^{-x} \sqrt{2\pi x} \left(1 + \frac{1}{12x}\right).$$

A better approximation can be obtained from the relation of Pierrat:

$$\frac{\Gamma(x + \frac{1}{2})}{\Gamma(x)} = \frac{16x-1}{16x+1} \sqrt{x}. \quad [\text{A1.14}]$$

If $0 \leq x \leq 1$, $\Gamma(1+x)$ can be calculated with an error lower than 2×10^{-7} using the polynomial [HAS 55]

$$\Gamma(1+x) = 1 + a_1 x + a_2 x^2 + \dots + a_8 x^8 \quad [\text{A1.15}]$$

where

$$\begin{aligned} a_1 &= -0.5771\ 91652 & a_5 &= -0.7567\ 04078 \\ a_2 &= 0.9882\ 05891 & a_6 &= 0.4821\ 99394 \\ a_3 &= -0.8970\ 56937 & a_7 &= -0.1935\ 27818 \\ a_4 &= 0.9182\ 06857 & a_8 &= 0.0358\ 68343 \end{aligned}$$

A2. Incomplete gamma function

A2.1. Definition

The incomplete gamma function is defined by [ABR 70] [LAM 76]:

$$\gamma(x, T) = \int_0^T x^{\alpha-1} e^{-\alpha} d\alpha \quad [\text{A2.1}]$$

This function is tabulated in various published works [ABR 70] [PIE 48]. Figures A2.1 and A2.2 show the variations of γ with x for given T , then with T for given x .

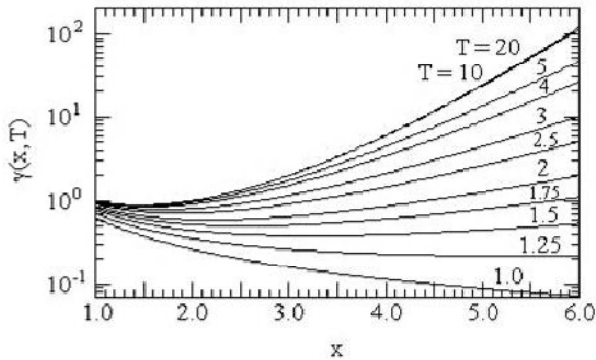


Figure A2.1. Incomplete gamma function versus x

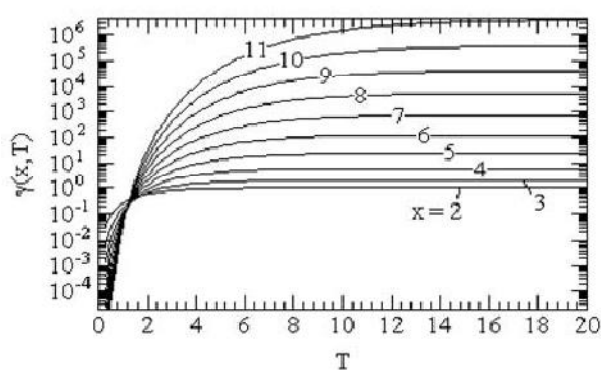


Figure A2.2. Incomplete gamma function versus T

We set:

$$P(x, T) = \frac{1}{\Gamma(x)} \int_0^T e^{-\alpha} \alpha^{x-1} d\alpha. \quad [A2.2]$$

It has been shown that $\gamma(x, T)$ can be written

$$\gamma(x, T) = \Gamma(x) \left[1 - P\left(\frac{\chi^2}{v}\right) \right] \quad [A2.3]$$

where $\chi^2 = 2 T$, $v = 2 x$ and

$$P\left[\frac{\chi^2}{v}\right] = \frac{1}{2^{\frac{v}{2}} \Gamma\left(\frac{v}{2}\right)} \int_0^{\chi^2} t^{\frac{v}{2}-1} e^{-\frac{t^2}{2}} dt, \quad [A2.4]$$

the chi-square probability distribution. The function P is also tabulated [ABR 70].

A2.2. Relation between complete gamma function and incomplete gamma function

We have

$$\int_0^{\infty} \alpha^{x-1} e^{-\alpha} d\alpha = \int_0^T \alpha^{x-1} e^{-\alpha} d\alpha + \int_T^{\infty} \alpha^{x-1} e^{-\alpha} d\alpha$$

yielding

$$\Gamma(x) = \gamma(x, T) + Q(x, T). \quad [A2.5]$$

A2.3. Pearson form of incomplete gamma function

$$I(u, p) = \frac{1}{\Gamma(p+1)} \int_0^{u\sqrt{p+1}} e^{-t} t^p dt \quad [A2.6]$$

$$I(u, p) = P[p+1, u\sqrt{p+1}]$$

$$I(u, p) = P\left(\frac{\chi^2}{v}\right) \quad [A2.7]$$

$$\lambda = 2(p+1)$$

$$\chi^2 = 2u\sqrt{p+1}$$

Tables or abacuses give I varying with u for various values of p [ABR 70] [CRA 63] [FID 75].

A3. Various integrals

A3.1.

$$I_n = \frac{1}{2\pi i} \int_{-\infty}^{\infty} \frac{g_n(x)}{h_n(x) h_{-n}(x)} dx \quad [A3.1]$$

where

$$h_n(x) = a_0 x^n + a_1 x^{n-1} + \dots + a_n$$

$$g_n(x) = b_0 x^{2n-2} + b_1 x^{2n-4} + \dots + b_{n-1}$$

where the roots of $h_n(x)$ are assumed located in the upper half plane for $n \in [1, 7]$.

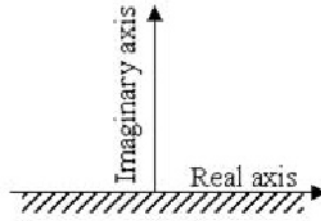


Figure A3.1. Real and imaginary axes

The first values of I_n , extracted from the work of James *et al.* [JAM 47], are the following:

$$I_1 = \frac{b_0}{2 a_0 a_1} \quad [\text{A3.2}]$$

$$I_2 = \frac{-b_0 + \frac{a_0 b_1}{a_2}}{2 a_0 a_1} \quad [\text{A3.3}]$$

$$I_3 = \frac{-a_2 b_0 + a_0 b_1 - \frac{a_0 a_1 b_2}{a_3}}{2 a_0 (a_0 a_3 - a_1 a_2)} \quad [\text{A3.4}]$$

$$I_4 = \frac{b_0 (-a_1 a_4 + a_2 a_3) - a_0 a_3 b_1 + a_0 a_1 b_2 + \frac{a_0 b_3}{a_4} (a_0 a_3 - a_1 a_2)}{2 a_0 (a_0 a_3^2 + a_1^2 a_4 - a_1 a_2 a_3)} \quad [\text{A3.5}]$$

Application

From these expressions, S.H. Crandall and W.D. Mark [CRA 63] and D.E. Newland [NEW 75] deduce the value of the integral

$$I_n = \int_{-\infty}^{+\infty} |H_n(\Omega)|^2 d\Omega \quad [A3.6]$$

where

$$H_n(\Omega) = \frac{B_0 + (i\Omega)B_1 + (i\Omega)^2 B_2 + \cdots + (i\Omega)^{n-1} B_{n-1}}{A_0 + (i\Omega)A_1 + (i\Omega)^2 A_2 + \cdots + (i\Omega)^{n-1} A_n} \quad [A3.7]$$

for $n = 1$,

$$H_1(\Omega) = \frac{B_0}{A_0 + i \Omega A_1}$$

and

$$I_1 = \frac{\pi B_0^2}{A_0 A_1}. \quad [A3.8]$$

For $n = 2$,

$$H_2(\Omega) = \frac{B_0 + i \Omega B_1}{A_0 + i \Omega A_1 - \Omega^2 A_2}$$

$$I_2 = \frac{\pi (A_0 B_1^2 + A_2 B_0^2)}{A_0 A_1 A_2} \quad [A3.9]$$

etc.

A3.2.

$$\left. \begin{aligned} I_1 &= \int e^{a x} \cos b x \, dx = \frac{e^{a x}}{a^2 + b^2} (a \cos b x + b \sin b x) \\ I_2 &= \int e^{a x} \sin b x \, dx = \frac{e^{a x}}{a^2 + b^2} (a \sin b x - b \cos b x) \end{aligned} \right\} \quad [A3.10]$$

These two integrals are calculated simultaneously while multiplying I_2 by i in order to constitute the integral:

$$I = I_1 + I_2 = \int e^{a x} (\cos b x + i \sin b x) dx$$

$$I = \int e^{(a + i b)x} dx = \frac{1}{a + i b} e^{(a + i b)x}$$

$$I = \frac{e^{a x} (\cos b x + i \sin b x) (a - i b)}{a^2 + b^2}$$

$$I = \frac{e^{a x}}{a^2 + b^2} [(a \cos b x + b \sin b x) + i (a \sin b x - b \cos b x)],$$

yielding I_1 and I_2 by separating the real and imaginary parts.

A3.3.

$$\int x e^{ax} dx = \frac{e^{ax}}{a} \left(x - \frac{1}{a} \right) \quad [\text{A3.11}]$$

$$\int_0^\infty x^n \exp\left(-\frac{x^2}{2\sigma^2}\right) dx = \frac{(\sqrt{2}\sigma)^{n+1}}{2} \Gamma\left(\frac{n+1}{2}\right) \quad [\text{A3.12}]$$

[CRA 63], yielding

$$\int_0^\infty \exp\left(-\frac{x^2}{2\sigma^2}\right) dx = \sqrt{\frac{\pi}{2}} \sigma \quad [\text{A3.13}]$$

$$\int_0^\infty x \exp\left(-\frac{x^2}{2\sigma^2}\right) dx = \sigma^2 \quad [\text{A3.14}]$$

$$\int_0^\infty x^2 \exp\left(-\frac{x^2}{2\sigma^2}\right) dx = \sqrt{\frac{\pi}{2}} \sigma^3 \quad [\text{A3.15}]$$

$$\int_0^\infty x^3 \exp\left(-\frac{x^2}{2\sigma^2}\right) dx = 2 \sigma^4 \quad [\text{A3.16}]$$

$$\int_0^\infty x^4 \exp\left(-\frac{x^2}{2\sigma^2}\right) dx = 3\sqrt{\frac{\pi}{2}} \sigma^5 \quad [\text{A3.17}]$$

$$\int_0^x \exp\left(-\frac{u^2}{2\sigma^2}\right) du = \sqrt{\frac{\pi}{2}} \sigma \operatorname{erf}\left(\frac{x}{\sigma\sqrt{2}}\right) \quad [\text{A3.18}]$$

Applications

$$\int_{-\infty}^\infty e^{-\alpha x^2} dx = \sqrt{\frac{\pi}{\alpha}} \quad [\text{A3.19}]$$

[PAP 65]

$$\int_0^\infty x^n \exp\left(-\frac{x^2}{2\sigma^2}\right) dx = \frac{(\sqrt{2}\sigma)^{n+1}}{2} \Gamma\left(\frac{n+1}{2}\right) \quad [\text{A3.20}]$$

[CRA 63]

A3.4.

$$\int_0^{\pi/2} \cos^{2n} \phi \, d\phi = \frac{\sqrt{\pi}}{2} \frac{\Gamma\left(n + \frac{1}{2}\right)}{\Gamma(n+1)} \quad [\text{A3.21}]$$

This result is demonstrated by setting [ANG 61]:

$$\phi = \arccos t^{1/2}$$

yielding

$$\cos^{2n} \phi = t^n$$

and

$$I = \int_0^{\pi/2} \cos^{2n} \phi \, d\phi = \frac{1}{2} \int_0^1 t^{n-\frac{1}{2}} (1-t)^{-1/2} dt.$$

We obtain a Euler integral-first kind of the form

$$B(p, q) = \int_0^1 x^{p-1} (1-x)^{q-1} dx$$

which can be expressed using gamma functions.

A3.5.

$$I_n = \int t^n e^{-\frac{t^2}{2}} dt \quad [A3.22]$$

$$I_n = (n-1) I_{n-2} - t^{n-1} e^{-\frac{t^2}{2}}$$

$$I_1 = -e^{-\frac{t^2}{2}}$$

$$J_n = \int_{-\infty}^{+\infty} t^n e^{-\frac{t^2}{2}} dt \quad [A3.23]$$

$$J_0 = \sqrt{2\pi}$$

$$J_1 = 1$$

$$J_n = (n-1) J_{n-2} \quad [A3.24]$$

If $n = 2m$ (n even),

$$J_{2m} = \frac{(2m)!}{2^m m!} \sqrt{2\pi}$$

If $n = 2m+1$ (n odd),

$$J_{2m+1} = 0$$

A3.6.

$$\left. \begin{aligned} A &= \int_0^{\infty} y^{2k} e^{-a y^2} dy = \sqrt{\pi} \cdot 1.3.5 \dots \frac{(2k-1)}{2^{k+1} a^{k+\frac{1}{2}}} \\ B &= \int_0^{\infty} y^{2k+1} e^{-a y^2} dy = 1.2.3.4 \dots \frac{k}{2 a^{k+1}} \end{aligned} \right\} \quad [A3.25]$$

$$k = 1, 2, 3, \dots$$

Approximations

Integral A can be approximated by the expression:

$$A \approx \frac{(k-1)! \sqrt{k}}{2 a^{k+\frac{1}{2}}} \quad \text{for } k = 2, 3, 4, \dots \quad [A3.26]$$

With this relation, we obtain values a little higher than the true values. The relative error is equal to 6.4% for $k = 2$, to 2.5% for $k = 5$ and to 1.3% for $k = 10$ [DAV 64].

It can be reduced while evaluating $(k-1)!$ using the Stirling formula [A1.13]:

$$(k-1)! = \frac{\sqrt{2\pi} (k-1)^{k-\frac{1}{2}}}{e^{k-1}} \quad (k \geq 2) \quad [A3.27]$$

This error gives a value of the factorial smaller than the true value. For $k = 2$, the relative error is equal to -7.8% . It is equal to -2.1% for $k = 5$ and to -0.9% if $k = 10$. Integral A can then be written, for $(k \geq 2)$,

$$A \approx \sqrt{\frac{\pi k}{2}} \frac{(k-1)^{k-\frac{1}{2}}}{e^{k-1} a^{k+\frac{1}{2}}} \quad [A3.28]$$

The relative error here is equal to -1.94% for $k = 2$, close to $+0.4\%$ for $5 \leq k \leq 10$ and lower than 0.4% if $k > 10$.

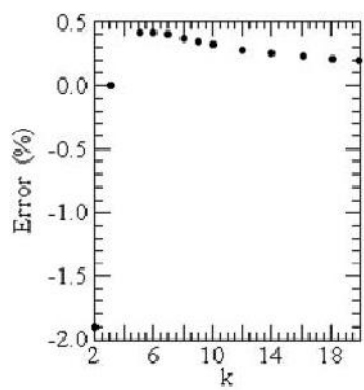


Figure A3.2. *Relative error calculated using the approximate expression for integral A*

Bibliography

- [ABR 70] ABRAMOWITZ M. and STEGUN I., *Handbook of Mathematical Functions*, Dover Publications, Inc., New York, 1970.
- [AGA 75] AGARWAL B.D. and DALLY J.W., “Prediction of low-cycle fatigue behaviour of GFRP: an experimental approach”, *Journal of Materials Science*, 10, 193–199, 1975.
- [ANG 61] ANGOT A., “Compléments de mathématiques à l’usage des ingénieurs de l’électrotechnique et des télécommunications”, *Editions de la Revue d’Optique*, fourth edition, Collection Scientifique et Technique du CNET, 1961.
- [ANG 75] ANG A.H-S. and MUNSE W.H., “Practical reliability basis for structural fatigue”, *ASCE Structural Engineering Conference*, New Orleans, April 1975, Preprint 2494.
- [ASP 63] ASPINWALL D.M., “An approximate distribution for maximum response during random vibration”, *AIAA Simulation for Aerospace Flight Conference*, Columbus, Ohio, 26–28, August 1963, p. 326/330.
- [AST 63] *A Guide for Fatigue Testing and the Statistical Analysis of Fatigue Data*, ASTM Special Technical Publication no. 91-A, 1963.
- [AUS 77] AUSTEN I.M., A basic relationship for the prediction of fatigue crack growth behavior, British Steel Corporation Research, Report PT/6795/8/77, July 1977.
- [AUS 78] AUSTEN I.M., Facteurs affectant la croissance des fissures de fatigue sous corrosion dans les aciers, *European Offshore Steels Research Select Seminar*, U.K., Cambridge, Nov. 1978.
- [BAD 82] BADALIAN R., DILL H.D. and POTTE J.M., “Effects of spectrum variations on fatigue life of composites”, *Composite Materials: Testing and Design*, Sixth Conference, ASTM - STP - 787, pp. 274–286, 1982.
- [BAH 78] BAHUAUD J., MOGUEROU A. and VASSAL R., *Critères de fatigue*, CAST, Fiabilité en mécanique, INSA, Lyon, 1978.
- [BAL 57] BALDWIN E.E., SOKOL G.J. and COFFIN L.F., “Cyclic strain fatigue studies on AISI type 347 stainless steel”, *Proc. ASTM*, Vol. 57, pp. 567–586, 1957.
- [BAR 62] BARENBLATT G.I., “Mathematical theory of equilibrium cracks in brittle fracture”, *Advances in Applied Mechanics*, Vol. VII, Academic Press, New York, 1962.

- [BAR 65] BARNOSKI R.L., The maximum response of a linear mechanical oscillator to stationary and nonstationary random excitation, NASA-CR-340, December 1965.
- [BAR 65a] BARNES J.F. and TILLY G.P., "Assessment of thermal fatigue resistance of high temperature alloys", *Journal of the Royal Aeronautical Society* 69, 343–344, 1965.
- [BAR 68] BARNOSKI R.L., "The maximum response to random excitation of distributed structures with rectangular geometry", *Journal Sound Vib.*, 7(3), 333–350, 1968.
- [BAR 73] BARSOM J.M., Fatigue crack growth under variable amplitude loading in ASTM A514-B Steel, Progress in Flaw Growth and Fracture Toughness Testing, ASTM - STP 536, p. 147, 1973.
- [BAR 76] BARSOM J.M., Fatigue crack growth under variable-amplitude loading in various bridge steels, Fatigue Crack Growth under Spectrum Loads, ASTM STP 595, pp. 217–235, 1976.
- [BAR 77] BARROIS W., "Fiabilité des structures en fatigue basée sur l'utilisation des résultats des essais", Part 1: *L'Aéronautique et l'Astronautique*, 66(5), 51–75, 1977. Part 2: *L'Aéronautique et l'Astronautique* 67(6), 39–56, 1977.
- [BAR 80] BARTHELEMY B., *Notions pratiques de mécanique de la rupture*, Editions Eyrolles, 1980.
- [BAS 10] BASQUIN O.H., "The exponential law of endurance tests", *Proceedings ASTM*, Vol. 10, 625–630, 1910.
- [BAS 75] BASTENAIRE F., "Estimation et prévision statistiques de la résistance et de la durée de vie des matériaux en fatigue", *Journée d'étude sur la Fatigue*, University of Bordeaux I, 29 May 1975.
- [BAU 81] BAUSCHINGER J., "Change of position of the elastic limit under cyclical variations of stress", *Mitteilungen des Mechanisch-Technischen Laboratorium*, Vols 13 and 15, Munich, 1881.
- [BEC 81] BECHER P.E. and HANSEN B., *Statistical Evaluation of Defects in Welds and Design Implications*, Danish Welding Institute, Danish Atomic Energy Commission Research Establishment, 1981.
- [BEL 59] BELCHER P.M., VAN DYKE J.D. Jr. and ESHLEMAN A., "A procedure for designing and testing aircraft structure loaded by jet engine noise", Douglas Aircraft Company, Inc., *Technical Paper no. 893*, March 1959.
- [BEL 76] BELL P.D. and WOLFMAN A., Mathematical modeling of crack growth interaction effects, ASTM STP 595, 157–171, 1976.
- [BEN 46] BENNETT J.A., "A study of the damaging effect of fatigue stressing on X 4130 steel", *Proceedings, American Society for Testing Materials*, Vol. 46, 693–711, 1946.
- [BEN 58] BENHAM P.P., "Fatigue of metals caused by a relatively few cycles of high load or strain amplitude", *Metallurgical Reviews*, 3, 1958, 11.
- [BEN 61] BENDAT J.S., ENOCHSON L.D., KLEIN G.H. and PIERSOL A.G., "The application of statistics to the flight vehicle vibration problem", *ASD Technical Report 61-123*, December 1961.
- [BEN 64] BENDAT J.S., *Probability functions for random responses: prediction of peaks, fatigue damage and catastrophic failures*, NASA CR-33, April 1964.
- [BEN 04] BENASCIUTTI D., Fatigue analysis of andom loadings, PhD Thesis, University of Ferrera, Italy, 2004.

- [BEN 05] BENASCIUTTI D., TOVO R., "Spectral methods for life time prediction under wide-band stationary random processes", *Int. J. Fatigue*, 27(8), 867–877, August 2005.
- [BER 77] BERNSTEIN M., "Single mode stress required for equivalent damage to multimode stress in sonic feature", *ALAA Dynamics Specialist Conference*, San Diego, California, 24–25 March 1977, p. 191–197.
- [BER 83] BERTHEL J.D., CLERIVET A. and BATHIAS C., "On the relation between the threshold and the effective stress-intensity factor range during complex cyclic loading", *Fracture Mechanics: Fourteenth Symposium*, Volume I: Theory and Analysis, ASTM STP 791, pp. I-336–I-379, 1983.
- [BIR 68] BIRNBAUM Z.W. and SAUNDERS S.C., "A probabilistic interpretation of Miner's rule", *SIAM Journal Appl. Math.* 16(3), 637–652, May 1968.
- [BIR 69a] BIRNBAUM Z.W. and SAUNDERS S.C., "A new family of life distributions", *Journal Appl. Prob.* 6, 319–327, 1969.
- [BIR 69b] BIRNBAUM Z.W. and SAUNDERS S.C., "Estimation for a family of life distributions with applications to fatigue", *Journal Appl. Prob.* 6, 328–347, 1969.
- [BIS 95] BISHOP N.W.M., WANG R. and LACK L., "A frequency domain fatigue predictor for wind turbine blades including deterministic components", *Proceedings of the BWEA Conference*, p. 53–58, 1995.
- [BLA 46] BLAND R.B. and PUTNAM A.A., "Cumulative damage in fatigue. Discussion on Ref. {104}", *Journal of Applied Mechanics*, 13, A169–A171, 1946.
- [BLA 69] BLAKE R.E. and BAIRD W.S., "Derivation of design and test criteria", *Proceedings IES*, p. 128–138, 1969.
- [BLA 78] BLANKS H.S., "Exponential excitation expansion: a new method of vibration testing", *Microelectronics and Reliability*, 17, 575–582, 1978.
- [BOE 65] BOETTNER R.C., LAIRD C. and Mc EVILY A., "Crack nucleation and growth in high strain-low cycle fatigue", *Transactions of the Metallurgical Society of AIME*, 233(1), 379–387, Feb. 1965.
- [BOG 78a] BOGDANOFF J.L., "A new cumulative damage model, Part 1", *Trans. of the ASME, Journal of Applied Mechanics*, 45, 246–250, June 1978.
- [BOG 78b] BOGDANOFF J.L. and KRIEGER W., "A new cumulative damage model, Part 2", *Trans. of the ASME, Journal of Applied Mechanics*, 45, 251–257, June 1978.
- [BOG 78c] BOGDANOFF J.L., "A new cumulative damage model, Part 3", *Journal of Applied Mechanics*, 45(4), 733–739, December 1978.
- [BOG 80] BOGDANOFF J.L. and KOZIN F., "A new cumulative damage model, Part 4", *Journal of Applied Mechanics*, 47(1), 40–44, March 1980.
- [BOG 81] BOGDANOFF J.L. and KOZIN F., "On a new cumulative damage model for fatigue", *27th Proc. Ann. Reliability and Maintainability Symposium*, Philadelphia, 27/29 p. 9–18, January 1981.
- [BOL 84] BOLOTIN V.U., *Random Vibrations of Elastic Systems*, Martinus Nishoff Publishers, The Hague, 1984.
- [BOO 66] BOOTH R.T. and WRIGHT D.H., A ten-station machine for variable load fatigue tests, MIRA-Report no. 1966/14, October 1966.

- [BOO 69] BOOTH R.T., WRIGHT D.H. and SMITH N.P., Variable-load fatigue testing. Second report: test with small specimens. A comparison of loading patterns, and the influence of occasional high loads, MIRA Report no. 1969/9, April 1969.
- [BOO 70] BOOTH R.T. and WRIGHT D.H., Variable-load fatigue testing. Fourth report: Tests with small specimens. The influence of high and low loads, and the effect of speed, in stationary-random loading with L736 aluminium alloy, MIRA Report no. 1970/13, September 1970.
- [BOO 76] BOOTH R.T. and KENEFECK M.N., Variable-load fatigue. Sixth report: the effect of amplitude distribution shape in stationary random loading, MIRA Report 1976/2, September 1976.
- [BOU 93] BOUSSY V., NABOISHIKOV S.M. and RACKWITZ R., "Comparison of analytical counting methods for Gaussian processes", *Structural Safety*, 12, 35–57, 1993.
- [BOY 86] BOYER H.E. (ed.) *Atlas of Fatigue Curves*, American Society for Metals, 1986.
- [BRA 64] BRANGER J., Second seminar on fatigue and fatigue design, Tech. Rep. no. 5, Columbia University, Inst. for the Study of Fatigue and Reliability, June 1964.
- [BRA 71] BRANGER J., "The influence of modifications of a fatigue history loading program, Advanced Approaches to Fatigue Evaluation", *Proc. 6th ICAF Symposium*, Miami Beach, NASA SP 309, 1972, 485–540, May 1971.
- [BRA 80a] BRAND A. and SUTTERLIN R., "Calcul des pièces à la fatigue. méthode du gradient", *CETIM*, 1980.
- [BRA 80b] BRAND A., FLAVENOT J.F., GREGOIRE R., TOURNIER C., "Recueil de données technologiques sur la fatigue", *CETIM*, 1980.
- [BRA 81] BRAND A., "Approche classique du problème de fatigue. Définitions. Diagrammes. Facteurs d'influence", *Mécanique-Matériaux-Electricité*, no. 375/376/377, (3-4-5/1981), p. 151/166.
- [BRO 36] BROPHY G.R., "Damping capacity, a factor in fatigue", *Transactions, American Society of Metals*, 24, 154–174, 1936.
- [BRO 63] BROEK D. and SCHIJVE J., "The influence of the mean stress on the propagation of fatigue cracks in aluminum alloy sheets", NLR Report TR M2111, National Aeronautical and Astronautical Research Institute, Amsterdam, January 1963 or "The influence of the mean stress on the propagation of fatigue cracks in light alloy sheet. An investigation into the effect of reducing stress levels on the rate of crack propagation", *Aircraft Engineering* 39, 13–18, March 1967.
- [BRO 68a] BROCH J.T., "On the damaging effects of vibration", *Brüel and Kjaer Technical Review*, no. 4, 1968.
- [BRO 68b] BROCH J.T., "Effets de la fonction de distribution des crêtes sur la fatigue sous sollicitations aléatoires", *Brüel and Kjaer Technical Review*, no. 1, 1968.
- [BRO 70a] BROCH J.T., Peak-distribution effects in random-load fatigue, ASTM-STP 462, 105–126, 1970.
- [BRO 70b] BROWN G.W. and Ikegami R., "The fatigue of aluminum alloys subjected to random loading", *Experimental Mechanics*, 10(8), 321–327, August 1970.
- [BRO 78] BROEK D., *Elementary engineering fracture mechanics*, Sijthoff and Noordhoff, Alphen aan den Rijn, The Netherlands, 1978.

- [BRU 71] BRUSSAT T.R., An approach to predicting to growth to failure of fatigue cracks subjected to arbitrary uniaxial cyclic loading, *Damage Tolerance in Aircraft Structures*, ASTM STP 486, 1971, p. 122.
- [BSI 80] BS 5400: Steel, Concrete and Composite Bridges. 1980. Part 10: Code of practice for fatigue, London, British Standard Institution (BSI).
- [BUC 77] BUCH A., Effect of loading-program modifications in rotating-bending tests on fatigue damage cumulation in aircraft material specimens, TAE no. 325, Technion, Israel Inst. of Technol., no. 78, 25452, November 1977.
- [BUC 78] BUCH A., "The damage sum in fatigue of structure components", *Engineering Fracture Mechanics*, 10, 233–247, 1978.
- [BUI 71] BUI-QUOC T., DUBUC J., BAZERGUI A., BIRON A., "Cumulative fatigue damage under stress-controlled conditions", *Journal of Basic Engineering, Transactions of the ASME*, 93, 691–698, 1971.
- [BUI 80] BUI-QUOC, "Cumul du dommage en fatigue", Chapter 10 of *La fatigue des matériaux et des structures*, Claude Bathias and Jean-Paul Bailon, Maloine SA (ed), 1980.
- [BUI 82] BUI-QUOC T., "Cumulative damage with interaction effect due to fatigue under torsion loading", *Experimental Mechanics*, 180–187, May 1982.
- [BUR 56] BURNS A., Fatigue loadings in flight: loads in the tailplane and fin of a varsity, Aeronautical Research Council Technical Report CP 256, London, 1956.
- [BUR 01] BURTON T., SHARPE D., JENKINS N., BOSSANYI E., *Wind Energy Handbook*, John Wiley & Sons, 2001.
- [BUS 67] BUSSA S.L., *Fatigue Life of a Low Carbon Steel Notched Specimen under Stochastic Conditions*, Advanced Test Engineering Department, Ford Motor Company, 1967.
- [BUS 72] BUSSA S.L., SHETH N.J. and SWANSON R.S., "Development of a random load life prediction model", *Materials Research and Standard*, 12(3), 31–43, March 1972.
- [BUX 66] BUXBAUM O., *Statistische Zählverfahren als Bindeglied zwischen Beanspruchungsmessung und Betriebsfestigkeitsversuch*, LBF Bericht, Nr TB.65, 1966.
- [BUX 73] BUXBAUM O., "Methods of stress-measurement analysis for fatigue life evaluation", AGARD Lecture Series, no. 62, *Fatigue Life Prediction For Aircraft Structures and Materials, N73-29924 to 29934*, May 1973.
- [CAR 73] CARTWRIGHT D.J. and ROOKE D.P., Methods of determining stress intensity factors, RAE – Technical Report 73031, 1973.
- [CAR 73a] CARDRICK A.W., "Fatigue in carbon fibre reinforced plastic structures – A review of the problems", RAE Technical Report 73183, Dec. 1973, *Proc. of the Seventh ICAF Symposium*, London, July 1973.
- [CAR 74] CARMAN S.L., "Using fatigue considerations to optimize the specification of vibration and shock tests", *IES Proceedings*, 83–87, 1974.
- [CAR 74a] CARTWRIGHT D.J. and ROOKE D.P., "Approximate stress intensity factors compounded from know solutions", *Engng Fracture Mech.*, 6, 563, 1974.
- [CAU 61] CAUGHEY T.K. and STUMPF H.J., "Transient response of a dynamic system under random excitation", *Transactions of the ASME, Journal of Applied Mechanics*, 28, 563–566, December 1961.

- [CAZ 69] CAZAUX R, POMEY G., RABBE P., JANSSEN Ch., *La fatigue des matériaux*, Dunod, 1969.
- [CHA 74] CHABOCHE J.L., "Une loi différentielle d'endommagement de fatigue avec cumulation non linéaire", *Revue Française de Mécanique*, 50–51, 71–78, 1974.
- [CHA 78] CHAKRABARTI A.K., "An energy-balance approach to the problem of fatigue-crack growth", *Engineering Fracture Mechanics*, 10, 469–483, 1978.
- [CHA 85] CHAUDHURY G.K. and DOVER W.D., "Fatigue analysis of offshore platforms subject to sea wave loadings", *International Journal of Fatigue*, 7(1), 13–19, January 1985.
- [CHE 66] CHENG D.K., *Analysis of Linear Systems*, Addison Wesley Publishing Company, Inc., 1966.
- [CHR 65] CHRISTENSEN R.H., "Growth of fracture in metal under random cyclic loading", *International Conference on Fracture*, Sendai, Japan, September 1965.
- [CLA 70] CLARK W.G. and WESSEL E.T., "Application of fracture mechanics technology to medium-strength steels", *Review of Developments in Plane Strain Fracture Toughness Testing*, ASTM STP 463, 160–190, 1970.
- [CLE 65] CLEVENSON S.A. and STEINER R., "Fatigue life under various random loading spectra", *The Shock and Vibration Bulletin*, no. 35, Part II, 1965, p. 21–31, or "Fatigue life under random loading for several power spectral shapes", *Technical Report NASA-R-266*, September 1967.
- [CLE 66] CLEVENSON S.A. and STEINER R., "Fatigue life under various random loading spectra", *The Shock and Vibration Bulletin*, no. 35, Part 2, 21–31, January 1966.
- [CLE 77] CLEVENSON S.A. and STEINER R., "Fatigue life under random loading for several power spectral shapes", NASA, TR-R-266, September 1977.
- [CLI 64] Mc CLINTOCK F.A. and IRWIN G.R., Plasticity aspects of fracture mechanics. Symposium on Fracture Toughness, June 1964, A.S.T.M. STP 381, pp. 84/113.
- [COF 54] COFFIN L.F., "A study of the effects of cyclic thermal stresses on a ductile metal, Transactions", *American Society of Mechanical Engineers*, TASMA, 76, 931–950, 1954.
- [COF 62] COFFIN L.F., "Low cycle fatigue: a review", *Applied Materials Research*, 1(3), 129–141, October 1962.
- [COF 69] COFFIN L.F., "Predictive parameters and their application to high-temperature low-cycle fatigue", *Proc. 2nd Int. Conf. Fracture*, Brighton, 13/18 April 1969, 643–654, Chapman and Hall, London, 1969.
- [COF 69a] COFFIN L.F., "A generalized equation for predicting high-temperature, low-cycle fatigue including hold time", General Electric Research and Development Center, report 69-C-401, Dec. 1969.
- [COF 69b] COFFIN L.F., "The effect of frequency on high-temperature, low-cycle fatigue", *Proc. of the Air Force Conference on Fatigue and Fracture Aircraft Structures and Materials*, Miami Beach, Florida, 15-18 December 1969, 301–311, AFFDL TR 70-144, 1970.
- [COF 71] COFFIN L.F. Jr., "A note on low cycle fatigue laws", *Journal of Materials*, 6(2), 388–402, 1971.
- [COL 65] COLES A. and SKINNER D., "Assessment of thermal fatigue resistance of high temperature alloys", *Journal of the Royal Aeronautical Society* 69, 53–55, 1965.

- [CON 78] CONLE A. and TOPPER T.H., "Evaluation of small cycle omission criteria for shortening of fatigue", *Proceedings SEEEO, Soc. Environ. Engr. Fat. Grp.*, 1978, p. 10.1/10.17.
- [COP 80] COPE R. and BALME A., "Le comportement en fatigue des polyesters renforcés de fibres de verre", *Cahiers du Centre Scientifique et Technique du Batiment*, no. 212, September 1980, Cahier 1663.
- [COR 56] CORTEN H. and DOLAN T., "Cumulative fatigue damage", *IME-ASME Int. Conf. on Fatigue of Metals*, London, September 235–246, 1956.
- [COR 59] CORTEN H. and DOLAN T., "Progressive damage due to repeated loading", *Fatigue of Aircraft Structures. Proc.*, WADC-TR-59.507, August 1959.
- [COS 69] COST T.B., *Cumulative Structural Damage Testing*, Naval Weapons Center, TP 4711, October 1969.
- [CRA 62] CRANDALL S.H., MARK W.D. and KHABBAZ G.R., The variance in Palmgren-Miner damage due to random vibration, AFOSR 1999, January 1962, ASTIA: AD 271151, or *Proceedings, US National Congress of Applied Mechanics*, Berkeley, California, 119–126, June 1962.
- [CRA 63] CRANDALL S.H. and MARK W.D., *Random Vibration in Mechanical Systems*, Academic Press, 1963.
- [CRA 66] CRANDALL S.H., CHANDIRAMANI K.L. and COOK R.G., "Some first-passage problems in random vibration", *Transactions of the ASME, Journal of Applied Mechanics*, 532–538, September 1966.
- [CRA 70] CRANDALL S.H., "First-crossing probabilities of the linear oscillator", *Journal Sound Vib.*, 12(3), 285–299, 1970.
- [CRE 56a] CREDE C.E., "Concepts and trends in simulation", *The Shock and Vibration Bulletin*, 23, 1–8, June 1956.
- [CRE 56b] CREDE C.E. and LUNNEY E.J., "Establishment of vibration and shock tests for missile electronics as derived from measured environment", *WADC Tech. Report 56-503*, WADC Patterson AFB, Ohio, 1956.
- [CRE 57] CREDE C.E., "Criteria of damage from shock and vibration", *The Shock and Vibration Bulletin*, 25, Part II, 227–232, 1957.
- [CUR 71] CURTIS A.J., TINLING N.G. and ABSTEIN H.T., *Selection and Performance of Vibration Tests*, The Shock and Vibration Information Center, SVM 8, 1971, United States Department of Defence.
- [CUR 82] CURTIS A.J., MOITE S.M., "The effects of endurance limit and crest factor on time to failure under random loading", *The Shock and Vibration Bulletin*, 52, Part 4, 21–24, May 1982.
- [CZE 78] CZECHOWSKI A. and LENK A., "Miner's rule in mechanical tests of electronic parts", *IEEE Transactions on Reliability*, R27(3), 183–190, August 1978.
- [DAV 64] DAVENPORT A.G., "Note on the distribution of the largest value of a random function with application to gust loading", *Proceedings Institution of Civil Engineers*, 28, 187–196, London, 1964.
- [DAV 79] DAVENPORT R.T. and BROOK R., "The threshold stress intensity range in fatigue", *Fatigue of Engineering Materials and Structures*, 1(2), 151–158, 1979.

- [DEI 72] DEITRICK R.E., "Confidence in production units based on qualification vibration (U)", *The Shock and Vibration Bulletin*, Part 3, 42, 99–110, 1972.
- [DEJ 70] DE JONGE J.B., "The monitoring of fatigue loads", *International Council of the Aeronautical Sciences 7th*, Rome, Italy, 14–18 Paper ICAS 70-31, September 1970.
- [DEN 62] DENEFF, G. V., *Fatigue Prediction Study*, WADD TR-61-153 (AD-273 894), January 1962.
- [DEN 71] DENGEL D., *Einige grundlegende Gesichtspunkte für die Planung und Auswertung von Dauerschwingversuchen*, Material Prüfung 13, no. 5, 145–180, 1971.
- [DER 79] DER KIUREGHIAN A., "On response of structures to stationary excitation", *Earthquake Engineering Research Center Report no. UCB/EERC 79/32*, College of Engineering, University of California, Berkeley, December 1979.
- [DES 75] *Design against fatigue*, Basic design calculations, Engineering Sciences Data Unit, Data Item no. 75022, 1975.
- [DEV 86] DE VIS D., SNOEYS R. and SAS P., "Fatigue lifetime estimation of structures subjected to dynamic loading", *AIAA Journal*, 24(8), 1362–1367, August 1986.
- [DEW 86] DE WINNE J., "Equivalence of fatigue damage caused by vibrations", *IES Proceedings*, 227–234, 1986.
- [DIR 85] DIRLIK T., Application of computers in fatigue analysis, University of Warwick, Ph.D. Thesis, 1985.
- [DIT 86] DITLEVSEN O. and OLESEN R., "Statistical analysis of the Virkler data on fatigue crack growth", *Engineering Fracture Mechanics*, 25(2), 177–195, 1986.
- [DOL 49] DOLAN T.J., RICHART F.E. and WORK C.E., "The influence of fluctuations in stress amplitude on the fatigue of metals", *Proceedings ASTM*, 49, 646–682, 1949.
- [DOL 52] DOLAN T.J. and BROWN H.F., "Effect of prior repeated stressing on the fatigue life of 75S-T aluminum", *Proceedings ASTM*, 52, 1–8, 1952.
- [DOL 57] DOLAN T.J., "Cumulative damage from vibration", *The Shock and Vibration Bulletin*, no. 25, Part 2, 200–220, 1957.
- [DOL 59] DOLAN T.J., "Basic concepts of fatigue damage in metals", *Metal Fatigue*, McGraw-Hill, New York, 39–67, 1959.
- [DON 67] DONELY P., JEWEL J.W. and HUNTER P.A., "An assessment of repeated loads on general aviation and transport aircraft", *Proceedings 5th ICAF Symposium "Aircraft Fatigue—Design Operational and Economic Aspects"*, Melbourne, Australia, May 1967.
- [DOW 72] DOWLING N.E., "Fatigue failure predictions for complicated stress-strain histories", *Journal of Materials*, 7(1), 71–87, March 1972, or University of Illinois, Urbana, Dept. of Theoretical and Applied Mechanics, Report no. 337, 1971.
- [DOW 76] DOWLING N.E. and BEGLEY J.A., "Fatigue crack growth during gross plasticity and the J-integral", *Mechanics of Crack Growth*, ASTM-STP 590, 83–103, 1976.
- [DOW 82] DOWNING S.D. and SOCIE D.F., "Simple rainflow counting algorithms", *International Journal of Fatigue*, 4, 31–40, January 1982.
- [DOW 87] DOWNING S.D. and SOCIE D.F., "Simple rainflow counting algorithms", *International Journal of Fatigue*, 9(2), 119–121, 1987.

- [DUB 71] DUBUC J., BUI-QUOC T., BAZERGUI A., and BIRON A., *Unified Theory of Cumulative Damage in Metal Fatigue*, Weld. Res. Council, WRC Bulletin 162, 1–20, June 1971.
- [DUB 71a] DUBUC J., BAZERGUI A. and BIRON A., “Cumulative fatigue damage under strain controlled conditions”, *Journal of Materials*, 6(3), 718–737, Sept. 1971.
- [DUN 68] DUNEGAN H.L., HARRIS D.O. and TATRO C.A., “Fracture analysis by use of acoustic emission”, *Engineering Fracture Mechanics*, 1(1), 105–122, June 1968.
- [ECK 51] ECKEL J.F., “The influence of frequency on the repeated bending life of acid lead”, *Proceedings ASTM*, 51, 745–760, 1951.
- [EFT 72] EFTIS J. and LIEBOWITZ H., “On the modified Westergaard equations for certain plane crack problems”, *Int. J. Fracture Mech.* 8(4), 383–392, Dec. 1972.
- [ELB 71] ELBER W., The significance of fatigue crack closure, Damage Tolerance in Aircraft Structures, ASTM STP 486, 230–242, 1971.
- [ELD 61] ELDRED K., ROBERTS W.M., and WHITE R., Structural vibrations in space vehicles, WADD Technical Report 61–62, December 1961.
- [END 67] ENDO T. and MORROW J.D., *Cyclic Stress Strain and Fatigue Behavior of Representative Aircraft Metals*, American Society for Testing and Materials, 70th Annual Meeting, Boston, Mass., June 1967.
- [END 74] ENDO T., MITSUNAGA K., TAKAHASHI K., KOBAYASHI K. and MATSUISHI M., “Damage evaluation of metals for random or varying loading. Three aspects of rain flow method”, *Proceedings 1974, Symp. Mech. Behaviour Matls Soc*, Material Sci. I., Japan, 371–380, 1974.
- [EPR 52] EPREMIAN E. and MEHL R.F., Investigation of statistical nature of fatigue properties, NACA Technical Note 2719, June 1952.
- [ERD 67] ERDOGAN F., Crack propagation theories, NASA CR 901, 1967.
- [ERD 68] ERDOGAN F., “Cracks-propagation theories”, *Fracture – An advanced treatise*, Edited by H. LIEBOWITZ. Vol. II, Academic Press, 497–590, 1968.
- [ERD 70] ERDOGAN F., RATWANI M., “Fatigue and fracture of cylindrical shells containing a circumferential crack”, *Int. Journal Fracture Mech.*, 6, 379–392, 1970.
- [ERD 83] ERDOGAN F., “Stress intensity factors”, *Transactions of the ASME, Journal of Applied Mechanics*, 50(4b), 992–1002, December 1983.
- [EDW 77] EDWARDS P.R., RYMAN R.J. and COOK R., “Fracture mechanics prediction of fretting fatigue”, *Proceedings of the 9th ICAF Symposium “Fatigue Life of Structures under Operational Loads”*, Darmstadt, May 11–12, 1977, LBF Report NO. TR 136, 1977, pp. 4.6.1/4.6.46.
- [ESH 59] ESHLEMAN A.L., VAN DYKE J.D. and BELCHER P.M., A procedure for designing and testing aircraft structure loaded by jet engine noise, Douglas Engineering Paper no. 692, Douglas Aircraft Co, Long Beach, California, March 1959.
- [ESH 64] ESHLEMAN A.L. and VAN DYKE J.D., A rational method of analysis by matrix methods of acoustically-loaded structure for prediction of sonic fatigue strength, Douglas Engineering Paper no. 1922, April 1964.
- [ESI 68] ESIN A., “The microplastic strain energy criterion applied to fatigue”, *Transactions ASME*, 28–36, March 1968.

- [EST 62] *Establishment of the Approach to, and Development of, Interim Design Criteria for Sonic Fatigue*, Aeronautical Systems Division, Flight Dynamics Laboratory, Wright-Patterson, Air Force Base, Ohio, ASD-TDR 62-26, AD 284 597, June 1962.
- [EUG 65] EUGENE J., "Statistical theory of fatigue crack propagation", *Current Aeronautical Fatigue Problems*, Pergamon Press, Inc. New York, 215, 1965.
- [EUR 93] EUROCODE 3, Design of Steel Structures, 1993, Part 1–9: Fatigue strength of steel structures, European Norm EN 1993-1-9.
- [EXP 59] Experimental investigation of effects of random loading on the fatigue life of notched cantilever-beam specimens of 7075-T6 aluminium alloy, NASA Memo 4-12-59L, June 1959.
- [FAC 72] FACKLER W.C., *Equivalence Techniques for Vibration Testing*, NRL, Technical Information Division, SVM 9, 1972.
- [FAT 77] *Fatigue Life Estimation under Variable Amplitude Loading*, Engineering Sciences Data Unit, 77 004, London, 1977.
- [FAT 93] *Fatigue sous sollicitations d'amplitude variable. Méthode Rainflow de comptage des cycles*, Norme AFNOR A 03-406, November 1993.
- [FED 67] FEDDERSEN C.E., Plane strain crack toughness testing of high strength metallic materials, ASTM - STP 410, 77–79, 1967.
- [FEL 59] FELTNER C.E., Strain hysteresis, energy and fatigue fracture, TAM Report 146, University of Illinois, Urbana, June 1959.
- [FEO 69] FEODOSSIEV V., *Résistance des matériaux*, Editions de la Paix, Moscow, 1969.
- [FER 55] FERRO A. and ROSSETTI U., "Contribution à l'étude de la fatigue des matériaux avec essais à charge progressive", *Colloque de Fatigue*, Springer Verlag, Berlin, 24–34, 1955.
- [FID 75] FIDERER L., "Dynamic environment factors in determining electronic assembly reliability", *Microelectronics and Reliability*, 14, 173–193, 1975.
- [FOR 61] FORD D.G., GRAFF D.G. and PAYNE A.O., "Some statistical aspects of fatigue life variation. Fatigue of Aircraft Structures", edited by Barrois and E.L. Ripley, *Proceedings 2nd ICAF Symposium*, Paris, 179–208, 16/18 May 1961.
- [FOR 62] FORREST P.G., *Fatigue of Metals*, Pergamon Press, London, 1962.
- [FOR 67] FORMAN R.G., KEARNEY V.E. and ENGLE R.M., "Numerical analysis of crack propagation in cyclic-loaded structures", *Journal of Basic Engineering* 89(3), 459–464, Sept. 1967.
- [FOR 72] FORMAN R.G., "Study of fatigue crack initiation from flaws using fracture mechanics theory", *Engng. Fract. Mech.*, 4, 333–345, 1972.
- [FOR 74] FORREST P.G., *Fatigue of Metals*, Pergamon Press, Oxford, 1974.
- [FRA 59] FRALICH R.W., Experimental investigation of effects of random loading on the fatigue life of notched cantilever-beam specimens of 7075-T6 aluminium alloy, NASA, 4-12-59L, 1959.
- [FRA 61] FRALICH R.W., Experimental investigation of effects of random loading on the fatigue life of notched cantilever-beam specimens of SAE 4130 normalized steel, NASA TND 663, February 1961.
- [FRE 53] FREUDENTHAL A.M. and GUMBEL E.J., "On the statistical interpretation of fatigue tests", *Proceedings of the Royal Society of London*, Ser. A, 216, 309–322, 1953.

- [FRE 55] FREUDENTHAL A.M., "Physical and statistical aspects of cumulative damage", *IUTAM Colloquium on Fatigue*, edited by Weihill and Odqvist, Stockholm, 1955.
- [FRE 56] FREUDENTHAL A.M., "Cumulative damage under random loading", *IME-ASME – Conference on Fatigue of Metals*, Session 3, Paper 4, 257–261, 1956.
- [FRE 58] FREUDENTHAL A.M. and HELLER R.A., *On Stress Interaction in Fatigue and a Cumulative Damage Rule*, WADC-TR-58-69, Wright-Patterson AFB, Ohio, June 1958, or *Journal Aerospace Science*, 26(7), 431–442, July 1959.
- [FRE 60] FREUDENTHAL A.M., *Fatigue of Structural Metals under Random Loading*, ASTM 67b, 1960.
- [FRE 61] FREUDENTHAL A.M., *Fatigue of Materials and Structures under Random Loading*, WADC-TR-59-676, Wright-Patterson AFB, Ohio, March 1961.
- [FRE 68] FREUDENTHAL A.M., "Some remarks on cumulative damage in fatigue testing and fatigue design", *Welding in the World*, 6(4), Document 11s-311-68, 1968.
- [FRO 58] FROST N.E. and DUGSDALE D.S., "The propagation of fatigue cracks in sheet specimen", *Journal of the Mechanics and Physics of Solids*, 6, 92–110, 1958.
- [FRO 67] FROST N.E. and DIXON J.R., "A theory of fatigue crack growth", *Int. J. Fracture Mech.*, 3, 301–316, 1967.
- [FRO 75] FROST N.E., "The current state of the art of fatigue: its development and interaction with design", *Journal of the Society of Environmental Engineers*, 14(65), 21–28, June 1975.
- [FUC 77] FUCHS H.O., NELSON D.V., BURKE M.A. and TOOMAY T.L., *Shortcuts in Cumulative Damage Analysis, Fatigue Under Complex Loading*, 145–162, SAE 1977.
- [FUC 80] FUCHS H.O. and STEPHENS R.I., *Metal Fatigue in Engineering*, John Wiley & Sons, 1980.
- [FUL 61] FULLER J.R., "Cumulative fatigue damage due to variable-cycle loading", *Noise Control*, July/August 1961, or *The Shock and Vibration Bulletin*, Part IV, no. 29, 253–273, 1961.
- [FUL 62] FULLER R.J., "Research on techniques of establishing random type fatigue curves for broad band sonic loading", ASTIA – The Boeing Co Report no. ASD-TDR-62-501, October 1962, or *National Aero Nautical Meeting*, SAE Paper 671C, April 1963.
- [FUL 63] FULLER J.R., Research on Techniques of Establishing Random Type Fatigue Curves for Broad Band Sonic Loading, Society of Automotive Engineers, SAE Paper 671C, National Aeronautical Meeting, Washington, DC, 8/11 April 1963.
- [GAL 74] GALLAGHER J.P. and STALNAKER H.D., "Methods for analyzing fatigue crack growth rate behavior associated with flight-by-flight loading", *AIAA/ASME/SAE, 15th Structures, Structural Dynamics and Materials Conf.*, Las Vegas, April 1974.
- [GAS 65] GASSNER E. and SCHÜTZ W., "Assessment of the allowable design stresses and the corresponding fatigue life", *Proceedings of the 4th Symposium of the International Committee on Aeronautical Fatigue* (Fatigue Design Procedures), Munich, edited by E. Gassner and W. Schütz, Pergamon Press, June 1965.
- [GAS 72] GASSNER E., "Fatigue resistance of various materials under random loading", *Fatigue Life of Structures under Operational Loads, Proceedings of the 9th ICAF Symposium*, Darmstadt, 11–12 May 1972, *LBF Report NO. TR 136*, 1977, p. 3.5.1/3.5.34.

- [GAS 76] GASSNER E., LOWAK H. und SCHÜTZ D., *Bedeutung des Unregelmäßigkeit Gauß'scher Zufallsfolgen für die Betriebsfestigkeit*, Laboratorium für Betriebsfestigkeit, Darmstadt, Bericht Nr. FB-124, 1976.
- [GAS 77] GASSNER E., "Fatigue resistance of various materials under random loading", *LBF Report*, 1977.
- [GAT 61] GATTS R.R., "Application of a cumulative damage concept to fatigue", *Transactions ASME, Journal of Bas. Eng.*, 83, 529–540, 1961.
- [GAT 62a] GATTS R.R., "Cumulative fatigue damage with random loading", *ASME Transactions, Journal Basic Eng.*, 84(3), 403–409, September 1962.
- [GAT 62b] GATTS R.R., "Cumulative fatigue damage with progressive loading", *ASME Paper 62-WA-292*, 1962.
- [GER 59] GERBERICH W.W., Syracuse University Research Institute, Report no. MET 575-5961, 1959.
- [GER 61] GERTEL M., "Specification of laboratory tests", *Shock and Vibration Handbook*, edited by C.M. HARRIS and C.E CREDE, Vol. 2, no. 24, McGraw-Hill, 1961.
- [GER 62] GERTEL M., "Derivation of shock and vibration tests based on measured environments", *The Shock and Vibration Bulletin*, Part II, no. 31, 1962, p. 25/33, or *The Journal of Environmental Sciences*, 14–19, December 1966.
- [GER 66] GERKS I.F., *Optimization of Vibration Testing Time*, Collins Radio Company, June 1966.
- [GER 74] GERBER W., "Bestimmung der Zulässigen Spannungen in Eisen Constructionen", *Z. Bayer Arch. Ing. Ver.*, 6, 1874.
- [GER 82] GERHARZ J.J., "Prediction of fatigue failure", *AGARD Lecture Series*, 124, 8.1–8.22, September 1982.
- [GOE 60] GOEPFERT W.P., Variation of mechanical properties in aluminum products, Statistical Analysis Dept., Alcoa, Pittsburgh, Penn., 1960.
- [GOL 58] GOLUEKE C.A., "What to do about airborne electronic component failure", *SAE Journal*, 66(12), 88–90, 1958.
- [GOO 30] GOODMAN J., *Mechanics Applied to Engineering*, Longmans Green, London, ninth edition, Vol. 1, 1930.
- [GOO 73] GOODWILLIE A.G., A comparison of flight loads counting methods and their effects on fatigue life estimates using data from Concorde, ARC–CP no. 1304, December 1973.
- [GOP 89] GOPALAKRISHNA H.S. and METCALF J., "Fatigue life assessment of a leaded electronic component under a combined thermal and random vibration environment", *IES Proc.*, 110–118, 1989.
- [GOU 24] GOUGH H.J., *The Fatigue of Metals*, Scott, Greenwood and Sons, London, 113–136, 1924.
- [GRA 76] GRAY T.D. and CALLAGHER J.P., Predicting fatigue crack retardation following a single overload using a modified Wheeler model, ASTM-STP 589, 1976, pp. 331/344.
- [GRE 81] GREGOIRE R., "La fatigue sous charge programmée", *CETIM*, Note Technique, no. 20, May 1981.
- [GRI 21] GRIFFITH A.A., "The phenomena of rupture and flow in solids", *Phil. Trans. Roy. Soc. of London*, A221, 163–197, 1921.

- [GRI 25] GRIFFITH A.A., "The theory of rupture", *Proc. 1st Int. Congress Appl. Mech.*, pp. 55–63, Biezeno and Burgers Ed. Waltman, 1925.
- [GRO 55] GROSS J.H. and STOUT R.D., "Plastic fatigue properties of high-strength pressure-vessel steels", *The Welding Journal* 34(4), Research Suppl., 161s–166s, 1955.
- [GRO 59] GROVER H., *Cumulative Damage Theories*, WADC 59-507, Wright Patterson AFB, Ohio, August 1959.
- [GRO 60] GROVER H., An observation concerning the cycle ratio in cumulative damage, ASTM – STP 247, p. 120, 1960.
- [GUR 48] GURNEY C. and PEARSON S., "Fatigue of mineral glass under static and cyclic loading", *Proceedings Royal Society*, 192, 537–544, 1948.
- [GUR 68] GURNEY T.R., *Fatigue of Welded Structures*, Cambridge University Press, England, 1968.
- [GUR 79] GURNEY T.R., *Fatigue of Welded Structures*, Cambridge University Press, London, 1979.
- [HAA 62] HAAS T., "Loading statistics as a basis of structural and mechanical design", *The Engineer's Digest*, 23(4), 81–85, April 1962 and 23(3), 79–84, March 1962 and 23(5), 79–83, May 1962.
- [HAA 98] HAAGENSEN P.J., STATNIKOV E.S. and LOPEZ-MARTINEZ L., Introductory fatigue tests on welded joints in high strength steel and aluminium improved by various methods including ultrasonic impact treatment (UIT), International Institute of Welding, IIW Doc. XIII-1748-98, p. 1/12, 1998.
- [HAH 69] HAHN G.T., SARRAT H. and ROSENFELD A.R., The nature of the fatigue crack plastic zone, AFFDL Technical Report 70-144, 1970, pp. 425/450 or *Air Force Conf. on Fatigue and Fracture*, 1969.
- [HAI 70] HAIBACH E., *Modifizierte lineare Schadensakkumulations-Hypothese zur Berücksichtigung des Dauerfestigkeitsabfalls mit fortschreitender Schädigung*, LBF Technische Mitteilungen TM Nr 50/70, 1970.
- [HAI 78] HAIBACH E., "The influence of cyclic materials properties on fatigue life prediction by amplitude transformation", *Proceedings SEECO, Soc. Environ. Engr. Fat. Grp*, p. 11.1/11.25, 1978.
- [HAL 61] HALFORD G.R., MORROW J.T. and MORROW A.M., Low cycle fatigue in torsion, University of Illinois, Rep. no. 203, October 1961.
- [HAL 78] HALLAM M.G., "Fatigue analysis of offshore oil platforms", *Proceedings SEECO 78, Soc. Environ. Engr. Fat. Grp*, 17.1–17.16, April 1978.
- [HAR] HARRIS D.O., DUNEGAN H.L. and TETELMAN A.S., Prediction of fatigue lifetime by combined fracture mechanics, DUNEGAN/ENDEVCO Technical Bulletin DRC-105, UCRL-71760.
- [HAR 60] HARDRATH H.F. and NAUMANN E.C., Variable amplitude fatigue tests of aluminium alloy specimens, ASTM STP 274, 125, 1960.
- [HAR 61] HARRIS W.J., *Metallic Fatigue*, Pergamon Press, London, 1961.
- [HAR 63] HARDRATH H.F., "A unified technology plan for fatigue and fracture design", *RAE Technical Report 73183*, December 1963, Seventh ICAF Symposium, London, July 1973.

- [HAR 70] HARRISON J.P., "An analysis of data on non-propagation fatigue cracks on a fracture mechanics basis", *Metal Construction and British Welding Journal* 2(3), 93–98, March 1970.
- [HAR 83] HARRIS D.O. and LIM E.Y., Applications of a probabilistic fracture mechanics model to the influence of in-service inspection on structural reliability, Probabilistic Fracture Mechanics and Fatigue Methods: Applications for Structural Design and Maintenance, ASTM - STP 798, 19–41, 1983.
- [HAS 55] HASTINGS C., Jr, *Approximations for Digital Computers*, Princeton University Press, 1955.
- [HAS 64] HASSLACHER G.J. and MURRAY H.L., "Determination of an optimum vibration acceptance test", *Shock, Vibration and Associated Environments Bulletin*, Part III, 33, 183–188, March 1964.
- [HAS 77] HASHIN Z. and ROTOM A., A cumulative damage theory of fatigue failure, Air Force Office of Scientific Research, Grant ASFOSR76-3014, Scientific Report no. 3, Tel Aviv University, Israel, February 1977.
- [HAU 69] HAUGEN E.B. and HRITZ J.A., "A re-definition of endurance life design strength criteria by statistical methods", *Proceedings of the Air Force Conference on Fatigue and Fracture of Aircraft Structures and Materials*, Miami Beach, Florida, p. 685–697, 15–18 December 1969, AFFDL TR 70-144, 1970.
- [HAU 80] HAUSAMMANN H., Influence of fracture toughness on fatigue life of steel bridges, PhD thesis, Lehigh University, Bethlehem, Pennsylvania, July 1980.
- [HEA 53] HEAD A.K., "The mechanism of fatigue of metals", *Journal of the Mechanics and Physics of Solids*, 1, 134–141, 1953.
- [HEA 53a] HEAD A.K., "The growth of fatigue cracks", *The Philosophical Magazine*, 44(7), 925–938, 1953.
- [HEA 56] HEAD A.K. and HOOKE F.H., "Random noise fatigue testing", *International Conference on Fatigue of Metals*, London, ASME-IME, Session 3, 301–303, September 1956.
- [HEA 56a] HEAD A.K., "Propagation of fatigue cracks", *Journal of Applied Mechanics*, 23(3), 407–410, 1956.
- [HEL 65] HELLER R.A. and HELLER A.S., A probabilistic approach to cumulative fatigue damage in redundant structures, Department of Civil Engineering and Engineering Mechanics, Columbia University of the City of New York, T.R. no. 17, March 1965.
- [HEN 55] HENRY D.L., "A theory of fatigue-damage accumulation in steel", *Transactions of the ASME*, 77, 913–918, 1955.
- [HEN 03] HENDERSON A. R., PATEL M. H., "On the Modelling of a Floating Offshore Wind Turbine", *Wind Energy*, 6, 53–86, 2003.
- [HEY 70] HEYER R.H. and Mc CABE D.E., Evaluation of a method of test for plane strain fracture toughness using a bend specimen, Review of Developments in Plane Strain Fracture Toughness Testing, ASTM STP 463, 22–41, Sept. 1970.
- [HIL 70] HILLBERRY B.M., Fatigue life of 2024 T3 aluminium alloy under narrow- and broad-band random loading. Effects of environment and complex load history on fatigue life, ASTM-STP 462, 167–183, 1970.

- [HOB 77] HOBACHER A., "Cumulative fatigue by fracture mechanics", *Journal of Applied Mechanics*, 769–771, vol. 44, Dec. 1977.
- [HOF 68] HOFER K.E., "Equations for fracture mechanics", *Machine Design*, 1968.
- [HOL 73] HOLLINGER D. and MUELLER A., "Accelerated fatigue-testing improvements from road to laboratory", Society of Automotive Engineers, *SAE Paper 730564*, Automobile Engineering Meeting, Detroit, Mich., 14/18 May 1973.
- [HON 83] HONG I., "Frequency effects on fatigue life: a survey of the state of the art, random fatigue life prediction", *4th National Congress on Pressure Vessel and Piping Technology*, Portland, Oregon, 19–24 June 1983, *ASME, PVP*, 72, 121–133.
- [HOP 12] HOPKINSON B. and TREVOR-WILLIAMS G., "The elastic hysteresis of steel", *Proceedings of the Royal Society of London, Series A*, 87, 502, 1912.
- [HUD 69] HUDSON C.M., Effect of stress ratio on fatigue crack growth in 7075-T6 and 2024-T3 aluminum alloy specimen, NASA TND 5390, August 1969.
- [IMP 65] IMPELLIZERI L.F., "Development of a scatter factor applicable to aircraft life", *Structural Fatigue in Aircraft, ASTM Special*, Technical Publication, no. 404, November 136–157, 1965.
- [ING 13] INGLIS C.E., "Stresses in a plate due to the presence of cracks and sharp corners", *Trans. Inst. Naval Architects*, 55, 219–241, 1913.
- [ING 27] INGLIS N.P., "Hysteris and fatigue of Woehler rotating cantilever specimen", *The Metallurgist*, 23–27, February 1927.
- [INV 60] Investigation of thermal effects on structural fatigue. Part I, Douglas Aircraft Company Inc., WADD TN R60-410, 1960.
- [IRW 57] IRWIN G.R., "Analysis of stresses and strains near the end of a crack traversing a plate", *Journal of Applied Mechanics*, 24(3), 361–364, 1957.
- [IRW 58] IRWIN G.R., *Fracture, Handbuch der Physik*, Vol. VI, Springer, 551–590, 1958.
- [IRW 58a] IRWIN G.R., "Fracture mechanics", *Proc. Symposium on Naval Structural Mechanics*, Stanford University, 557–594, Aug. 11, 1958.
- [IRW 60] IRWIN G.R., "Fracture mode transition for a crack traversing a plate", *Journal of Basic Engineering*, Series D, 82(2), 417, June 1960.
- [IRW 60a] IRWIN G.R., "Plastic zone near a crack and fracture toughness", *Proc. 7th Sagamore Conf.*, p. IV - 63, 1960.
- [ISI 55] ISIDA M., "On the tension of a strip with a central elliptic hole, Part I and Part II.", *Nihon Kikai Gakkai Ronbunshu*, 21, 507–513 and 514–518, 1955.
- [JAC 56] JACOBSON R.H., Vibration and shock evaluation of airborne electronic component parts and equipments, WADC Technical Report 56-301, ASTIA-AD 123 658, December 1956.
- [JAC 66] JACOBY G., Application of microfractography to the study of crack propagation under fatigue stresses, AGARD Report 541, NATO Advisory Group for Aerospace Research and Development, 1966.
- [JAC 68] JACOBY G., "Comparison of fatigue life estimation processes for irregularly varying loads", *Proceedings 3rd Conference of Dimensioning*, Budapest, 81–95, 1968.

- [JAC 69] JACOBY G., *Vergleich der Lebensdauer aus Betriebsfestigkeits-, Einzelflug- und digital programmierten Random-Versuchen sowie nach der linearen Schadenakkumulations-hypothese*, Fortschritt Bericht, VDI-Z, Reihe 5, Nr. 7, 63, 1969.
- [JAC 72] JACOBY G., *Le problème de la fatigue en construction automobile*, INSA, CAST, Lyon, 1972.
- [JAM 47] JAMES H.M., NICHOLS N.B. and PHILLIPS R.S., *Theory of Servomechanisms*, MIT Radiation Laboratory Series, Vol. 25, McGraw-Hill, 1947.
- [JEN 25] JENKIN C.F., "High frequency fatigue tests", *Proceedings Roy. Soc.*, London, A.109, 119–143, 1925.
- [JOH 78] JOHNSON T.M., "Fatigue life prediction of automotive - type load histories", *Fatigue Under Complex Loading: Analyses and Experiments*, R.M. Wetzel (ed), The Society of Automotive Engineers, 85–93.
- [JOH 53] JOHNSON A.I., Strength, safety and economical dimensions of structures, Division of Building Statics and Structural Engineering, Royal Institute of Technology, Stockholm, Report 12, 1953.
- [JOH 82] JOHNSTON G.O., "A review of probabilistic fracture mechanics literature", *Reliability Engineering* 3, 423–448, 1982.
- [JOH 83] JOHNSTON G.O., Statistical scatter in fracture toughness and fatigue crack growth rate data, Probabilistic Fracture Mechanics and Fatigue Methods: Applications for Structural Design and Maintenance, ASTM - STP 798, 42–66, 1983.
- [JU 69] JU F.D., YAO J.T.P. and LIU T.T., "On the criterion of low-cycle shear fracture", *Proc. of the Air Force Conference on Fatigue and Fracture of Aircraft Structures and Materials*, Miami Beach, Florida, 265–269, 15-18 December 1969, AFFDL TR70-144, 1970.
- [KAC 76] KACENA W.J. and JONES P.J., "Fatigue prediction for structures subjected to random vibration", *The Shock and Vibration Bulletin*, 3(46), 87–96, August 1976.
- [KAR 66] KARNOPP D. and SCHARTON T.D., "Plastic deformation in random vibration", *Journal of the Acoustical Society of America*, 39(6), 1154–1161, 1966.
- [KAT 73] KATCHER M., "Crack growth retardation under aircraft spectrum loads", *Engr. Frac. Mech.*, 5, 793, 1973.
- [KEA 72] KEAYS R.H., Numerical evaluation of Wheeler's model of fatigue crack propagation for programmed load spectra, Australian Defense Scientific Service, Aeronautical Research Laboratories, Structure and Materials, Note ARL/SM 376, April 1972.
- [KEN 82] KENEFECK M.N., Variable load fatigue tenth report: speed of testing and the exclusion of low and high stress peaks, The Motor Industry Research Association, MIRA Report no. 1982/1.
- [KID 77] KIDDLE F.E. and DARTS J., "The effects on fatigue life of omitting small loads, large loads and loads dwells from a loading spectrum", *Proceedings of the 9th ICAF Symposium*, Darmstadt, May 1977, LBF Report no. TR-136, "Fatigue Life of Structures under Operational Loads", p. 3.3/1, 3.3/33.
- [KIK 71] KIKUKAWA M. and JONO M., "Cumulative damage and behavior of plastic strain in high and low cycle fatigue", *Proceedings of International Conference on Mechanical Behavior of Materials*, Vol. 11, 458–468, 1971.

- [KIM 26] KIMBALL A.L. and LOVELL D.E., "Internal friction in solids", *Transactions, ASME*, 48(2016), 479–500, 1926.
- [KIR 65a] KIRKBY W.T. and EDWARDS P.R., "Constant amplitude or variable amplitude tests as a basis for design studies", *Fatigue Design Procedures – Proceedings of the 4th Symposium of the International Committee on Aeronautical Fatigue*, Munich, E. Gassner and W. Schütz (eds), Pergamon Press, June 1965.
- [KIR 65b] KIRKBY W.T., *Constant amplitude or variable amplitude tests as a basis for design studies*, Royal Aircraft Establishment, ICAF, Fatigue Design Procedures, Munich, June 1965.
- [KIR 72] KIRKBY W.T., "Some effects of change in spectrum severity and spectrum shape on fatigue behaviour under random loading", *Symposium on Random Load Fatigue*, AGARD – CP, no. 118, AD.752.369, 2.1–2.19, October 1972.
- [KIR 77] KIRKBY W.T., "Some research problems on the fatigue of aircraft structures", *Journal of the Society of Environmental Engineers*, 16(2), 7–24, June 1977.
- [KIT 71] KITAGAWA H. *et al.*, *Trans. Japan Soc. Mech. Engr.*, 49, 714–810, 1971.
- [KLE 71] KLESNIL M. LUKAS P. and RYS P., Inst. of Phys. Met. Czech Academy of Sciences, Report, Brno, 1971.
- [KLE 72] KLESNIL M. and LUKAS P., "Influence of strength and stress history on growth and stabilisation of fatigue cracks", *Engineering Fracture Mechanics*, 4, 77–92, 1972.
- [KLE 72a] KLESNIL M. and LUKAS P., "Effect of stress cycle asymmetric on fatigue crack growth", *Mater. Sci. Engng.*, 9, 231–240, 1972.
- [KLI 81] KLIMAN V., "To the estimation of fatigue life based on the Miner rule", *Strojnicky Casopis*, 32(5), 559–610, 1981.
- [KOM 45] KOMMERS J., "The effect of overstress in fatigue on the endurance life of steel", *ASTM Proceedings*, 45, 532–541, 1945.
- [KON 56] KONISHI I. and SHINOZUKA M., "Scatter of fatigue life of structural steel and its influence on safety of structures", *Memoirs Fac. Engng.*, Kyoto University, 28, 73–83, 1956.
- [KOS 74] KOSHIGA F., KAWAHARA M., A proposed design basis with special reference to fatigue crack propagation, Technical Research Center, Nippon KOKAN KK, Kawasaki, Japan, Doc. IIS XIII, 738-74, May 1974.
- [KOW 59] KOWALEWSKI J., "On the relation between fatigue lives under random loading and under corresponding program loading", *Proceedings of Symposium on Full-scale Fatigue Testing of Aircraft Structure*, Amsterdam, 1959, p. 60/75, F.J. Plantema and J. Schijve (eds), Pergamon Press, 1961.
- [KOW 61] KOWALEWSKI J., *Full-scale Testing of Aircraft Structures*, F.J. Plantema and J. Schijve (eds), Pergamon Press, 1961, p. 60/75.
- [KOW 63] KOWALEWSKI J., *Über die Beziehungen zwischen der Lebensdauer von Bauteilen bei unregelmäßig schwankenden und bei geordneten Belastungsfolgen*, DVL-Bericht Nr 249, PORZ-WAHN, September 1963.
- [KOZ 68] KOZIN F. and SWEET A.L., "Investigation of a random cumulative damage theory", *Journal of Mater.*, 3(4), 802–823, December 1968.
- [KOZ 89] KOZIN F. and BOGDANOFF J.L., "Recent thoughts on probabilistic fatigue crack growth", *Appl. Mech. Rev.*, 42(11), Part 2, 5121–5127, Nov. 1989.

- [KRA 65] KRAFFT J.M., "A comparison of cyclic fatigue crack propagation with single cycle crack toughness and plastic flow", *Transactions Quarterly, American Society for Metals*, ASMQA 58, 691, 1965.
- [KRE 83] KREE P. and SOIZE C., *Mécanique aléatoire*, Dunod, Bordas, Paris, 1983.
- [KUH 64] KUHN P., The prediction of notch and crack strength under static and fatigue loading, SAE-ASME Meeting, New York, SAE Paper 843C, April 27-30, 1964.
- [LAI 66] LAIRD C., The influence of metallurgical structure on the mechanisms of fatigue crack propagation, ASTM STP 415, 131–180, 1966.
- [LAL 82] LALANNE C., "Les vibrations sinusoïdales à fréquence balayée", CESTA/EX no. 803, 8/6 June 1982.
- [LAL 87] LALANNE C., *Specifications d'essais en environnement et coefficients de garantie*, DAM/DT/EX/MEV 1089, 18 November 1987.
- [LAL 92] LALANNE C., *Fatigue des matériaux*. Stage « Environnements Vibratoires Réels-Analyse et Spécifications », Intespace, Toulouse, France, March 1992.
- [LAL 94] LALANNE C., *Vibrations aléatoires - Dommage par fatigue subi par un système mécanique à un degré de liberté*, CESTA/EX no. 1019/94, 1994.
- [LAM 73] LAMBERT J.A.B., "The use of counting accelerometer data in fatigue life predictions for aircraft flying in complex roles", AGARD - Lecture Series no. 62, *Fatigue Life Prediction for Aircraft Structures and Materials*, N 73 29924 to 29934, May 1973.
- [LAM 76] LAMBERT R.G., "Analysis of fatigue under random vibration", *The Shock and Vibration Bulletin*, 46(3), 55–72, August 1976.
- [LAM 78] LAMBERT R.G., "Fracture mechanics applied to step-stress fatigue under sine/random vibration", *The Shock and Vibration Bulletin* 48(3), 93–101, Sept. 1978.
- [LAM 80] LAMBERT R.G., "Criteria for accelerated random vibration tests", *Proceedings IES*, 71–75, May 1980.
- [LAM 80a] LAMBERT R.G., Accelerated fatigue test rationale, General Electric Company, AESD, AD-A103212, March 1980.
- [LAM 82] LAMBERT R.G., "Fatigue life prediction for various random stress peak distributions", *The Shock and Vibration Bulletin*, 52(4), 1–10, May 1982.
- [LAM 83] LAMBERT R.G., Application of fatigue analytical methods for random stress with stress-strength variances, "Random Fatigue Life Prediction", *4th National Congress on Pressure Vessel and Piping Technology*, Portland, Oregon, June 19-24 1983, ASME - PVP, Vol. 72, 135–140.
- [LAM 88] LAMBERT R.G., "Plastic work interaction damage rule applied to narrow-band gaussian random stress situations", *Journal of Pressure Vessel Technology, Transactions of the ASME*, 110, 88–90, February 1988.
- [LAM 93] LAMBERT R.G., "Fatigue damage prediction for combined random and static mean stresses", *Journal of the IES*, XXXVI(3), 25–32, May/June 1993, or *IES Proceedings*, 2, 289–296, 1992.
- [LAN 37] LANGER B.F., "Fatigue failure from stress cycles of varying amplitude", *J. App. Mech.*, 4(4), A.160–A.162, December 1937.
- [LAN 72] LANDGRAF R.W., MITCHELL M.R. and LAPOINTE N.R., Monotonic and cyclic properties of engineering materials, Metallurgical Dept., Scientific Research Staff, Ford Motor Company, Dearborn, Mich., June 1972.

- [LAR 66] LARDNER R.W., "Crack propagation under random loading", *Journal of Mech. Phys. Solids*, 14, Pergamon Press Ltd., 141–150, 1966.
- [LAR 68] LARDNER R.W., "A dislocation model for fatigue crack growth in metals", *Phil. Mag.* 17, 71–78, 1968.
- [LAS 05] LASSEN T., DARCIS Ph., and N. RECHO N., "Fatigue Behavior of Welded Joints Part I: Statistical Methods for Fatigue Life Prediction", Supplement to the *Welding Journal*, vol. 84, supplement, 183s–187s, December 2005.
- [LAV 69] LA VERNE ROOT, "Fatigue design of electronic equipment", *The Shock and Vibration Bulletin*, 40(4), 97–101, December 1969.
- [LAZ 68] LAZAN B.J., *Damping of Materials and Members in Structural Mechanics*, Pergamon Press, 1968.
- [LEI 69] LEIS H. und SCHÜTZ W., Bruchzähigkeit und Rißfortschritt von Titanlegierungen, *Luftfahrttechnik-Raumfahrttechnik*, Bd. 15, no. 7, 1969.
- [LEI 70] LEIS H. und SCHÜTZ W., Bewertung neuer Flugzeugbauwerkstoffe mit den Methoden der Bruchmechanik, *Luftfahrttechnik-Raumfahrttechnik*, Bd. 16, no. 10, 1970.
- [LEI 78] LEIS B.N., "Fatigue-life prediction for complex structure", *Journal of Mechanical Design, Trans. ASME*, 100, 2–9, January 1978.
- [LEI 81] LEIS B.N. and BROEK D., "The role of similitude in fatigue crack growth analyses", *Shock and Vibration Digest*, 13(8), 15–28, August 1981.
- [LEM 70] LEMAITRE J., MORCHOISNE Y., MONTHULET A., NOPPE J.M. and RIVIERE C., "Influence de l'endommagement de fatigue sur les caractéristiques de résistance des matériaux", *Rech. Aéronautique*, 5, September/October 1970.
- [LEN 68] LENZEN K.H., YEN B.T., NORDMARK G.E., YAO J.T.P. and MUNSE W.H., "Analysis and interpretation of fatigue data", *Journal of the Structural Division, Proceedings of the ASCE*, 94(ST12), Proc. Paper 6283, 2665–2677, December 1968.
- [LEV 55] LEVY J.C., "Cumulative damage in fatigue. A method of investigation economical in specimens", *Engineering*, 179, 724–726, June 1955.
- [LEV 57] LEVY J.C., "Cumulative damage in fatigue – A design method based on the S-N curves", *J. Roy. Aeronaut. Soc.*, 61(559), 585–591, July 1957.
- [LEY 63] LEYBOLD H.A. and NAUMANN E.C., "A study of fatigue life under random loading", *Am. Soc. Test. Mat., Proc.*, Reprint no. 70 - B., Vol. 63, 717–734, June 1963.
- [LEY 65] LEYBOLD H.A., Techniques for examining statistical and power-spectral properties of random time histories, NASA-TND-2714, March 1965 (MS Dissertation, VPI, May 1963).
- [LIA 73] LIARD F. and MARCOUX C., "Influence of the degree of fail-safe achieved, using the internal pressure indicator (BIM), on the flight safety during a specified life of main rotor blades of SA321 and SA 330 helicopters", RAE Technical Report 73183, Dec. 1973, *Proceedings of the Seventh ICAF Symposium*, London, July 1973, A.M. STAGG (ed).
- [LIE 72] LIEURADE H.P., RABBE P., "Etude, à l'aide de la mécanique de la rupture, de la vitesse de fissuration en fatigue d'une gamme étendue d'aciers", *Mémoires Scientifiques de Métallurgie* LXIX(9), 605–621, 1972.
- [LIE 78] LIEURADE H.P., Comportement mécanique et métallurgique des aciers dans le domaine de la fatigue oligocyclique. Etude des phénomènes et application à la croissance des fissures, PhD thesis, University of Metz, September 1978.

- [LIE 80] LIEURADE H.P., "Estimation des caractéristiques de résistance et d'endurance en fatigue", Chapter 2, *La fatigue des matériaux et des structures*, Claude Bathias and Jean Paul Bailon (ed), Maloine SA, 1980.
- [LIE 82] LIEURADE H.P., *La pratique des essais en fatigue*, PYC Edition, 1982.
- [LIE 82a] LIEURADE H.P., Les essais de fatigue sous sollicitations d'amplitude variable, Chapitre 11 in *La Fatigue des Matériaux et des Structures*, Claude Bathias and Jean-Paul Bailon (ed), Maloine SA, 1982.
- [LIE 91] LIEURADE H.P., "Rôle des principaux paramètres de résistance à la fatigue des aciers", *Mécanique-Matériaux-Electricité*, 440, 29–35, September 1991.
- [LIG 80] LIGERON J.C., *Méthodes pratiques d'utilisation en fiabilité mécanique des nouveaux concepts de mécanique de la rupture*, CNET Lannion, Colloque International sur la Fiabilité et la Maintainabilité, Communication V A-1, 117–124, 1980.
- [LIN 67] LIN Y.K., *Probabilistic Theory of Structural Dynamics*, McGraw-Hill, 1967.
- [LIN 72] LINSLEY R.C. and HILLBERRY B.M., "Random fatigue of 2024-T3 aluminium under two spectra with identical peak-probability density functions", *Probabilistic Aspects of Fatigue*, ASTM STP 511, 156–167, 1972.
- [LIN 87] LINDGREN G. and RYCHLIK I., "Rain flow cycle distributions for fatigue life prediction under gaussian load processes", *Journal of Fatigue and Fracture of Engineering Materials and Structure*, 10(3), 251–260, 1987.
- [LIN 88] LIN Y.K. and YANG J.N., "On statistical moments on fatigue crack propagation", *Engineering Fracture Mechanics*, 18(2), 243–256, 1988.
- [LIU 48] LIU S.I., LYNCH J.J., RIPPLING E.J. and SACHS G., "Low cycle fatigue on aluminium alloy 24S-T in direct stress", *Trans. Am. Inst. Mining Metallurgical Engrs.*, Metals Div., 469, Feb. 1948.
- [LIU 59] LIU H.W. and CORTEN H.T., Fatigue damage during complex stress histories, NASA TN D-256, November 1959.
- [LIU 60] LIU H.W. and CORTEN H.T., Fatigue damage under varying stress amplitudes, NASA TN D-647, November 1960.
- [LIU 61] LIU H.W., "Crack propagation in thin metal sheet under repeated loading", *Journal of Basic Engineering*, Series D, 83, 23–31, 1961.
- [LIU 63] LIU H.W., "Fatigue crack propagation and applied stress range. An energy approach", *Journal of Basic Engineering*, Series D, 85, 116, 1963.
- [LIU 63a] LIU H.W., Size effects on fatigue crack propagation, GALCIT-SM 63-7, March 1963.
- [LIU 69] LIU S.I. and SACHS G., "The flow and fracture characteristics of the aluminium alloy 24 ST after alternating tension and compression", *Trans. Am. Inst. Mining Metallurgical Engineers*, Metals Div, 193, 1969.
- [LLO 63] LLOYD KAECHLE, Review and analysis of cumulative fatigue damage theories, The Rand Corp. Memorandum RM 3650 PR, August 1963.
- [LOM 56] LOMAS T.W., WARD J.O., RAIT J.R. and COLBECK E.W., "The influence of frequency of vibration on the endurance limit of ferrous alloys at speeds up to 150 000 cycles per minute using a pneumatic resonance system", *International Conference on Fatigue of Metals*, Inst. of Mech. Engrs and ASME, London, 375–385, 1956.

- [LOW 62] LOWCOCK M.T. and WILLIAMS T.R.G., Effects of random loading on the fatigue life of aluminium alloy L73, University of Southampton, Department of Aeronautics and Astronautics, AASU Report, no. 225, July 1962.
- [LUN 55] LUNDBERG B., "Fatigue life of airplane structures", *J. Aeron. Sci.*, 22(6), 349–402, June 1955.
- [LUN 58] LUNNEY E.J. and CREDE C.E., Establishment of vibration and shock tests for airborne electronics, WADC 57-75, ASTIA Doc. 142349, January 1958.
- [LUN 64] LUNDBERG B.O.K. and EGGWERTZ S., *A Statistical Method of Fail Safe Design with Respect to Aircraft Fatigue*, Flygtekniska Försöksanstalten Meddelande 99, 1964.
- [MAC 49] MACHLIN E.S., Dislocation theory of the fatigue of metals, NACA Report 929, 1949.
- [MAN 04] MANN T., B. TVEITEN W. and HÄRKEGÅRD G., "Fatigue of welded aluminium T-joints", *15th European Conference of Fracture*, ECF15, Advanced Fracture Mechanics for Life and Safety Assessments, European Structural Integrity Society (ESIS), Stockholm, Sweden, August 11-13, 2004.
- [MAN 54] MANSON S.S., Behaviour of materials under conditions of thermal stress, NACA Tech. Note 2933, 1954.
- [MAN 65] MANSON S.S., "Fatigue: a complex subject - some simple approximations", *Experimental Mechanics*, 5(7), 193–226, July 1965.
- [MAN 67] MANSON S., FRECHE J. and ENSIGN C., Application of a double linear rule to cumulative damage, NASA-TN-D 3839, April 1967.
- [MAR 54] MARCO S.M. and STARKEY W.L., "A concept of fatigue damage", *Trans. Am. Soc. Mech. Engrs.*, 76(4), 627–632, 1954.
- [MAR 56] MARIN J., "Interpretation of fatigue strengths for combined stresses", *International Conference on Fatigue of Metals*, IME–ASME, 1956.
- [MAR 58] MARTIN D.E. and SINCLAIR G.M., "Crack propagation under repeated loading", *Proceedings of the Third U.S. National Congress of Applied Mechanics*, 595–604, June 1958.
- [MAR 61] MARK W.D., The inherent variation in fatigue damage resulting from random vibration, PhD Thesis, MIT, Cambridge, Mass., August 1961.
- [MAR 61a] MARTIN D.E., "An energy criterion for low-cycle fatigue", *Journal of Basic Eng.*, 83, 565–571, 1961.
- [MAR 65] MARSH K.J., Direct stress cumulative fatigue damage tests on mild-steel and aluminum alloy specimens, Nat. Engineering Lab. Glasgow, NEL Report, no. 204, 1965.
- [MAR 66] MARSH K.J. and MAC KINNON J.A., Fatigue under random loading, NEL Report, no. 234, July 1966.
- [MAR 68] MARSH K.J. and MACKINNON J.A., "Random-loading and block-loading fatigue tests on sharply notched mild steel specimens", *Journal Mechanical Engineering Science*, 10(1), 48–58, 1968.
- [MAR 76] MARSHALL W., An assessment of the integrity of PWR pressure vessels, H.M. Stationery Office, London, England, 1976.
- [MAS 66a] MASRI S.F., "Cumulative damage caused by shock excitation", *The Shock and Vibration Bulletin*, 35(3), 57–71, January 1966.

- [MAS 66b] MASRI S.F., "Cumulative fatigue under variable-frequency excitation", *SAE Paper*, no. 660720, 1966.
- [MAS 75] MASOUNAVE J. and BAILON J.P., "The dependance of the threshold stress intensity on the cyclic stress ratio in fatigue of ferritic-pearlite steels", *Scripta Metall.*, 723–730, 1975.
- [MAT 68] MATSUISKI M. and ENDO T., *Fatigue of Metals Subjected to Varying Stress*, Kyushu District Meeting of the Japan Society of Mechanical Engineers, Fukuoka, Japan, March 1968.
- [MAT 69] MATOLCSY M., "Logarithmic rule of fatigue life scatters", *Materialprüf.*, 11(6), 196–200, June 1969.
- [MAT 71] MATTHEWS W.T., BARATTA F.I. and DRISCOLL G.W., "Experimental observation of a stress intensity history effect upon fatigue crack growth rate", *International Journal of Fracture Mechanics*, 7(2), 224–228, 1971.
- [MAY 61] MAY A.N., "Fatigue under random loads", *Nature*, 192(4798), 158, October 14, 1961.
- [MCC 56] McCLINTOCK F.A., "The growth of fatigue cracks under plastic torsion", *International Conference on Fatigue of Metals*, IME and ASME, 538, 1956.
- [MCC 63] McCLINTOCK F.A., "On the plasticity of the growth of fatigue cracks", in D.C. Drucker and J.J. Gilman (eds), *Fracture of Solids*, Interscience Publishers, John Wiley, New York, 65, 1963.
- [MCC 64] McCLINTOCK F.A. and IRWIN G.R., "Plasticity aspects of fracture mechanics", *Symposium on Fracture Toughness*, 84–113, June 1964, ASTM STP 381.
- [MCC 64a] McClymonds J.C. and GANOUNG J.K., "Combined analytical and experimental approach for designing and evaluating structural systems for vibration environments", *The Shock and Vibration Bulletin*, 34(2), 159–175, December 1964.
- [MCC 66] McCLINTOCK F.A., Fatigue Crack Propagation, Discussion, ASTM - STP - 415, 170–174, 1966.
- [MCE 58] McEVILY A.J. and ILLG W., The rate of fatigue – crack propagation in two aluminum alloys, NACA TN 4394, Sept. 1958.
- [MCE 63] McEVILY A.J. and BOETTNER R.C., "On the fatigue crack propagation in FCC metals", *Acta Metallurgica*, II(7), 725–743, July 1963.
- [MCE 65] McEVILY A.J. and JOHNSTON T.L., "The role of cross-slip in brittle fracture and fatigue", *Proc. 1st Int. Conf. Fracture*, Vol. II, Japanese Society for Strength and Fracture of Materials, Sendai, Japan, 515–546, 12/17 Sept. 1965.
- [MCE 70] McEVILY A.J., "Fatigue crack growth and the strain intensity factor", *Proc. of the Air Force Conference on Fatigue and Fracture of Aircraft Structures and Materials*, Miami Beach, 15-18 December 1969, pp. 451/458, AFFDL TR 70-144, 1970.
- [MCE 73] McEVILY A.J., "Phenomenological and microstructural aspects of fatigue", The Institute of Metals and the Iron and Steel Institutes, *Third International Conference on the Strength of Metals and Alloys*, 1973, Publication 36(2), 204–225, 1974.
- [MCE 77] McEVILY A.J., "Current aspects of fracture", Metals Society, *Conf. Proc. "Fatigue 77"*, Cambridge, UK, 1–9, 1977.
- [MCG 57] McGALLEY R.B., Jr., "The evaluation of random-noise integrals", *The Shock and Vibration Bulletin*, II(25), 243–252, 1957.

- [MEA 54] "Measuring fatigue", *The Aeroplane*, 86, 478–479, 16 April 1954.
- [MEH 53] MEHLE R.F. and EPREMIAN E., "Investigation of statistical nature of fatigue properties", *ASTM – STP*, no. 137, 25, 1953 (or *NACA-TN-2719*, June 1952).
- [MET 76] Metallic materials and elements for aerospace vehicle structures, Military Standardization Handbook, MIL-Hdbk-5c, US Department of Defense and Federal Aviation Agency, 15 Sept. 1976.
- [MIL 53] MILES J.W., An approach to the buffeting of aircraft structures by jets, Douglas Report, no. SM-14795, June 1953.
- [MIL 54] MILES J.W., "On structural fatigue under random loading", *Journal of the Aeronautical Sciences*, 21, 753–776, November 1954.
- [MIL 61] MILES J.W. and THOMSON W.T., "Statistical concepts in vibration", *Shock and Vibration Handbook*, Vol. 1-11, edited by C.M. HARRIS and C.E. CREDE, McGraw-Hill, 1961.
- [MIL 67] McMILLAN T.S. and PELLOUX R.M.N., Fatigue crack propagation under programmed and random loads, ASTM STP 415, 1967 or Boeing Research Lab., Doc. D-1829558, July 1966.
- [MIL 82] MILET-OTVA B., "Facteurs d'influence sur l'endurance des aciers", *Revue Pratique de Contrôle Industriel*, 114, 60–62, April 1982.
- [MIN 45] MINER M.A., "Cumulative damage in fatigue", *Journal of Applied Mechanics, Trans. ASME*, 67, A159–A164, 1945.
- [MOO 27] MOORE H.F. and KOMMERS J.B., *The Fatigue of Metals*, McGraw-Hill, New York, 1927.
- [MOR 63] MORROW C.T., *Shock and Vibration Engineering*, John Wiley and Sons, Inc., Vol. 1, 1963.
- [MOR 64] MORROW J., Meeting of Division 4 of the SAE Iron and Steel Technical Committee, 4 November 1964.
- [MOR 64a] MORROW J. D., Cyclic plastic strain energy and fatigue of metals, Internal Friction, Damping and Cyclic Plasticity, ASTM-STP 378, 45–97, 1964.
- [MOR 67] MORTON W.W. and PECKHAM C.G., Structural flight loads data from F-5A aircraft, Technical Report SEG-TR-66-51, 1967.
- [MOR 83] MORROW J.D., KURATH P., SEHITOGLU H., DEVES T.J., "The effect of selected subcycle sequences in fatigue loading histories", *Random Fatigue Life Predictions, ASME Publication Pressure Vessel and Piping*, 72, 43–60, 1983.
- [MOR 90] MORGAN C.A. and TINDAL A.J., "Further analysis of the Orkney MS-1 data", Proceedings of the BWEA Conference, p. 325/330, 1990.
- [MOW 76] MOWBRAY D.F., "Derivation of a low-cycle fatigue relationship employing the J-integral approach to crack growth", *Cracks and Fracture*, ASTM-STP 601, 33–46, 1976.
- [MUR 52] MURRAY W.M. (Editor), *Fatigue and Fracture of Metals*, Paper no. 4, John Wiley and Sons, Inc., New York, 1952.
- [MUR 83] MURAKAMI Y., HARADA S., ENDO T., TANI-ISHI H. and FUKUSHIMA Y., "Correlations among growth law of small cracks, low-cycle fatigue law and applicability of Miner's rule", *Engineering Fracture Mechanics*, 18(5), 909–924, 1983.

- [MUS 60] MUSTIN G.S. and HOYT E.D., Practical and theoretical bases for specifying a transportation vibration test, Bureau of Naval Weapons, ASTIA AD 285 296, Wash. 25, DC, Project RR 1175 - P6, 25 February 1960, or *Shock, Vibration and Associated Environments*, Bulletin no. 30, Part III, 122–137, February 1962.
- [NAU 59] NAUMANN E.C. and HARDRATH H.F., Axial load fatigue tests of 2024-T3 loads, NASA, TN, D.212, 1959.
- [NAU 64] NAUMANN E.C., Evaluation of the influence of load randomization and of ground-air-ground cycles on fatigue life, NASA-TND 1584, October 1964.
- [NAU 65] NAUMAN E.C., Fatigue under random and programmed loads, NASA TN D2629, February 1965.
- [NEA 66] McNEAL R.H., BARNOSKI R.L. and BAILIE J.A., “Response of a simple oscillator to nonstationary random noise”, *J. Spacecraft*, 3(3), 441–443, March 1966, or *Computer Engineering Assoc.*, Report ES 182-6, 441–443, March 1962.
- [NEL 77] NELSON D.V. and FUCHS H.O., *Predictions of cumulative fatigue damage using condensed load histories*, *Fatigue Under Complex Loading*, SAE, 163–188, 1977.
- [NEL 78] NELSON D.V., Cumulative fatigue damage in metals, PhD thesis, Stanford University, California, 1978.
- [NEU 91] NEUGEBAUER J. and BLOXSOM K., “Fatigue-sensitive editing reduces simulation time for automotive testing”, *Test Engineering and Management*, 53(5), 10–14, October/November 1991.
- [NEW 75] NEWLAND, *An Introduction to Random Vibrations and Spectral Analysis*, Longman, London, 1975.
- [NIC 73] NICHOLSON C.E., “Influence of mean stress and environment on crack growth”, *Proceedings of BSC Conference on Mechanics and Mechanisms of Crack Growth*, Churchill College, Cambridge, 226–243, April 1973.
- [NIS 77] NISHIOKA K., HIRAKAWA K. and KITaura I., “Fatigue crack propagation behaviors of various steels”, *The Sumitomo Search* 17, 39–55, May 1977.
- [NOL 76] NOLTE K.G. and HANSFORD J.E., “Closed-form expressions for determining the fatigue damage of structures due to ocean waves”, *Proceedings of the Offshore Technology Conference*, Paper Number OTC 2606, 861–872, May 1976.
- [NOW 63] NOWACK H. and MUKHERJEE B., Effect of mean stress on crack propagation under random loading, RAE Technical Report 73183, Dec. 1963, Seventh ICAF Symposium, London, July 1963, A.M. STAGG (ed).
- [OH 80] OH K.P., “The prediction of fatigue life under random loading: a diffusion model., *Int. J. Fatigue*, 2, 99–104, July 1980.
- [OHJ 66] OHJI K., MILLER W.R., MARIN J., “Cumulative damage and effect on mean strain in low-cycle fatigue of a 2024-T351 aluminium alloy”, *Trans. ASME, J.I. of Basic Eng.*, 88, 801–810, Dec. 1966.
- [ORO 52] OROWAN E., “Stress concentrations in steel under cyclic loading”, *Welding Journal*, Research Supplement, 31(6), 273s–282s, 1952.
- [ORT 88] ORTIZ K. and KIREMIDJIAN A.S., “Stochastic modeling of fatigue crack growth”, *Engineering Fracture Mechanics*, 29(3), 317–334, 1988.
- [OSG 69] OSGOOD C.C., “Analysis of random responses for calculation of fatigue damage”, *The Shock and Vibration Bulletin*, 40(2), 1–8, December 1969.

- [OSG 82] OSGOOD C.C., *Fatigue design*, Pergamon Press, 1982.
- [PAL 24] PALMGREN A., "Die Lebensdauer von Kugellagern", *VDI Zeitschrift*, 339–341, 1924.
- [PAL 65] PALFALVI I., *The effect of load frequency on the fatigue test results*, GEP, no. 11, 1965.
- [PAP 65] PAPOULIS A., *Probability Random Variables and Stochastic Processes*, McGraw-Hill, 1965.
- [PAR 57] PARIS P.C., A note on the variables affecting the rate of crack growth due to cyclic loading, The Boeing Company, Document no. D-17867, Addendum N, September 12, 1957.
- [PAR 59] PARZEN E., On models for the probability of fatigue failure of a structure, Stanford University Technical Report, no. 45, 17 April 1959.
- [PAR 61] PARIS P.C., GOMEZ M.P. and ANDERSON W.E., "A rational analytic theory of fatigue", *The Trend in Engineering*, 13(1), 9–14, Jan. 1961.
- [PAR 62] PARIS P.C., The growth of cracks due to variations in loads, PhD thesis, Lehigh University, Bethlehem, Pennsylvania, 1962 (AD63-02629).
- [PAR 63] PARIS P., ERDOGAN F., "A critical analysis of crack propagation laws", *Journal of Basic Engineering* 85, 528–534, Dec. 1963.
- [PAR 64] PARIS P.C., "The fracture mechanics approach to fatigue", *Proc. 10th Sagamore Army Mater. Res. Conf.*, Syracuse University Press, Syracuse, N.Y., 107–132, 1964.
- [PAR 65] PARIS P.C. and SIH G.C., Stress analysis of cracks, ASTM - STP 391, 1965, pp. 30/81.
- [PEA 66] PEARSON B.S., "Nature", *NATUA*, 211, 1077–1078, 1966.
- [PEA 72] PEARSON S., "The effect of mean stress on fatigue crack propagation in half-inch (13.7 mm) thick specimens of aluminum alloys of high and low fracture toughness", *Engineering Fracture Mechanics*, 4, 9–24, 1972.
- [PEL 70] PELLOUX R.M., "Review of theories and laws of fatigue crack propagation", *Proc. of the Air Force Conference on Fatigue and Fracture of Aircraft Structures and Materials*, Miami Beach, 409–416, 15–18 December 1969, AFFDL TR 70-144, 1970.
- [PER 74] PERRUCHET C. and VIMONT P., *Résistance à la fatigue des matériaux en contraintes aléatoires*, ENICA, 1974.
- [PET 99] PETRUCCI G. and ZUCCARELLO B., "On the estimation of the fatigue cycle distribution from spectral density data", *J. Mech. Engng. Sci.* C213, 819–631, 1999.
- [PET 00] PETRUCCI G., DI PAOLO M. and ZUCCARELLO B., "On the characterisation of dynamic properties of random processes by spectral parameters", *J. Appl. Mech.* 67, 519–526, 2000.
- [PET 04] PETRUCCI G. and ZUCCARELLO B., "Fatigue life prediction under wide band random loading", *Fatigue Fract. Engng Mater. Struct.* 27, 1183–1195, 2004.
- [PHI 65] PHILLIPS E.P., Fatigue of RENE'41 under constant and random-amplitude loading at room and elevated temperatures, NASA-TND-3075, 1965.
- [PHI 76] PHILIPPIN G., TOPPER T.H. and LEIPHOLZ H.H.E., "Mean life evaluation for a stochastic loading programme with a finite number of strain levels using Miner's rule", *The Shock and Vibration Bulletin*, 46(3), 97–101, 1976.

- [PIE 48] PIERSON K., *Tables of the Incomplete Gamma Function*, Cambridge University Press, New York, 1948.
- [PIE 64] PIERSON A.G., The measurement and interpretation of ordinary power spectra for vibration problems, NASA-CR 90, 1964.
- [PIE 04] PIERRAT L., “Une approximation analytique nouvelle du dommage par fatigue subi par un système linéaire du second ordre soumis à une vibration aléatoire gaussienne”, *Essais Industriels* 30, 14–18, September 2004.
- [PIN 80] PINEAU A. et PETREQUIN P., “La fatigue plastique oligocyclique”, Chapter 4 of *La fatigue des matériaux et des structures*, Claude Bathias and Jean Paul Baillon (eds), Maloine SA, 1980.
- [PLE 68] PLENARD E., “Intérêt pratique d'une nouvelle caractéristique mécanique: la limite d'accommodation”, *Revue de Métallurgie*, 845–862, December, 1968.
- [PLU 66] PLUNKETT R. and VISWANTHAN N., “Fatigue crack propagation rates under random excitation”, *ASME Paper*, no. 66-WA/Met. 3, November 1966.
- [POO 70] POOK L.P., Linear fracture mechanics – What it is, what it does, N.E.L. Report no. 465, East Kilbridge, Glasgow, National Engineering Laboratory, 1970.
- [POO 74] POOK L.P., “Fracture mechanics analysis of the fatigue behaviour of welded joints”, *Welding Research International*, 4(3), 1–24, 1974.
- [POO 76] POOK L.P., “Basic statistics of fatigue crack growth”, *Journal of the Society of Environmental Engineers*, 15(4), 3–10, Dec. 1976.
- [POO 78] POOK L.P., “An approach to practical load histories for fatigue testing relevant to offshore structures”, *Journal of the Society of Environmental Engineers*, 17-1(76), 22–35, March 1978.
- [POO 79] POOK L.P. and GREENAN A.F., “The effect of narrow-band random loading on the high cycle fatigue strength of edge-cracked mild steel plates”, *Int. J. Fatigue*, 1, 17–22, January 1979.
- [POP 62] POPPLETON E., On the prediction of fatigue life under random loading, UTIA Report, no. 82, University of Toronto, Institute of Aerophysics, February 1962.
- [POT 73] POTTER J.M., An experimental and analytical study of spectrum truncation effects, AFFDL-TR-73-117, September 1973.
- [POW 58] POWELL A., “On the fatigue failure of structures due to vibrations excited by random pressure fields”, *The Journal of the the Acoustical Society of America*, 30(12), 1130–1135, December 1958.
- [PRI 72] PRIDDLE E.K., Constant amplitude fatigue crack propagation in a mild steel at low stress intensities: the effect of mean stress on propagation rate, Central Electricity Generating Board, CEGB Report RD/B/N 2233, May 1972.
- [PRO 48] PROT E.M., “Une nouvelle technique d'essai des matériaux: l'essai de fatigue sous charge progressive”, *Revue de Métallurgie*, XLV, no. 12, 481–489, December 1948 or Fatigue testing under progressive loading – A new technique for testing materials, WADC - TR 52-148, Sept. 1952.
- [PUL 67] PULGRANO L.J., Distribution of damage in random fatigue, Grumman Aerospace Corp., Report LDN 1159-148, July 1967.
- [PUL 68] PULGRANO L.J. and ABLAMOWITZ M., “The response of mechanical systems to bands of random excitation”, *The Shock and Vibration Bulletin*, 39(III), 73–86, 1968.

- [RAB 80] RABBE P., *La fatigue des matériaux et des structures*, Claude BATHIAS and Jean-Paul BAILON (eds), Editions Hermès, Chapter 1 ; Mécanismes et mécanique de la fatigue, 1980.
- [RAD 80] RADHAKRISHNAN V.M., "Quantifying the parameters in fatigue crack propagation", *Engng. Fract. Mech.* 13(1), 129–141, 1980.
- [RAN 43] RANKINE W.J., "On the cause of the unexpected breakage of the journals of railway axles and on the means of preventing such accidents by observing the law of continuity in their construction", *Proc. Inst. Civil Engrs.*, 2, 105, 1843.
- [RAN 49] RANSOM J.T. and MEHL R.F., "The statistical nature of the endurance limit", *Metals Transactions*, 185, 364–365, June 1949.
- [RAV 70] RAVISHANKAR T.J., *Simulation of random load fatigue in laboratory testing*, University of Toronto, March 1970.
- [RIC 48] RICHART F.E. and NEWMARK N.M., "An hypothesis for the determination of cumulative damage in fatigue", *Proceedings, Am. Soc. Testing Mats.*, 48, 767, 1948.
- [RIC 64] RICE J.R. and BEER F.P., "On the distribution of rises and falls in a continuous random process", *Trans. ASME, J. Basic Eng.*, Paper 64 WA/Met. 8, 1964.
- [RIC 65a] RICE J.R., BEER F.P. and PARIS P.C., "On the prediction of some random loading characteristics relevant to fatigue", *Acoustical Fatigue in Aerospace Structures*, Syracuse University Press, 121–144, 1965.
- [RIC 65b] RICHARDS C.W., *La science des matériaux de l'ingénieur*, Dunod, 1965.
- [RIC 68] RICE J.R., *Fracture - An Advanced Treatise*, Vol. II, Mathematical Press, New York, 1968.
- [RIC 72] RICHARDS C.E. and LINDLEY T.C., "The influence of stress intensity and microstructure on fatigue crack propagation in ferritic materials", *Engineering Fracture Mechanics*, 4, 951–978, 1972.
- [RIC 74] RICHARDS F., LAPOINTE N. and WETZEL R., A cycle counting algorithm for fatigue damage analysis, Paper no. 74 0278, SAE Automotive Engineering Congress, Detroit, Michigan, 1974.
- [RID 77] RIDER C.K., ANDERSON B.E. and SPARROW J.G., "An investigation of the fighter aircraft flight load spectrum", *Proceedings of the 9th ICAF Symposium "Fatigue Life of Structures under Operational Loads"*, Darmstadt, 11/12 May 1977, LBF Report no. TR 136, 2.2/2–2.2/9, 1977.
- [ROB 66] ROBERTS J.B., "The response of a single oscillator to band-limited white noise", *J. Sound Vib.*, 3(2), 115–126, 1966.
- [ROB 67] ROBERTS R. and ERDOGAN F., "The effect of mean stress on fatigue crack propagation in plates under extension and bending", *Trans. ASME, Journal of Basic Engineering*, 89, 885–892, 1967.
- [ROO 64] ROOT L.W., "Random-sine fatigue data correlation", *The Shock and Vibration Bulletin*, 33(II), 279–285, February 1964.
- [ROO 76] ROOKE D.P. and CARTWRIGHT D.J., *Compendium of stress intensity factors*, Procurement Executive, Ministry of Defense, London Her Majesty's Stationery Office, Hillingdon Press, London, 1976.
- [ROW 13] ROWETT F.E., "Elastic hysteresis in steel", *Proceedings of the Royal Society of London*, Series A, 89, 528–543, 1913.

- [RUD 75] RUDDER F.F. and PLUMBEE H.E., *Sonic fatigue design guide for military aircraft*, Technical Report AFFDL - TR 74 112, May 1975.
- [RYC 87] RYCHLIK I., "A new definition of the rainflow counting method", *Int. J. Fatigue*, 9(2), 119–121, 1987.
- [SAL 71] SALKIND M.J., "Fatigue of composites", *Advanced Approaches to Fatigue Evaluation, Proc. 6th ICAF Symposium*, Miami Beach, May 1971, or NASA SP 309, 333–364, 1972.
- [SAN 69] SANGA R.V. and PORTER T.R., "Application of fracture mechanics for fatigue life prediction", *Proc. of the Air Force Conference on Fatigue and Fracture of Aircraft Structures and Materials*, Miami Beach, 595–610, 15 Dec. 1969, AFFDL TR 70-144, 1970.
- [SAN 77] SANZ G., "Développements récents dans le domaine de la mécanique de la rupture", *Revue de Métallurgie*, 74(11), 605–619, Nov. 1977.
- [SAU 69] SAUNDERS S.C., A probabilistic interpretation of Miner's rule, II Boeing Scientific Research Laboratories. Mathematics Research Laboratory, Math. Note no. 617 (D1.82.0899), July 1969.
- [SCH 57] SCHEVEN G., SACHS G. and TONG K., "Effects of hydrogen on low-cycle fatigue of high strength steels", *Proc. ASTM* 57, 682, 1957.
- [SCH 58] SCHJELDERUP H.C., *Structural acoustic proof testing*, Douglas Aircraft Company, Inc., Technical Paper, no. 722, November 1958.
- [SCH 59] SCHJELDERUP H.C., "The modified Goodman diagram and random vibration", *Journal of the Aerospace Sciences*, vol. 26, 686, October 1959.
- [SCH 61a] SCHJELDERUP H.C. and GALEF A.E., Aspects of the response of structures subject to sonic fatigue, Air Force Flight Dynamics Laboratory, USAF, WADD T.R. 61-187, July 1961.
- [SCH 61b] SCHJELDERUP H.C., *A new look at structural peak distributions under random vibration*, WADC-TR-676, Ohio, AD 266374, March 1961.
- [SCH 61c] SCHIJVE J., BROEK D. and DE RIJK P., The effect of the frequency of an alternating load on the crack rate in a light alloy sheet, National Luchtvaart Laboratorium, NRL TN M-2092, September, 1961.
- [SCH 63] SCHIJVE J., *The analysis of random load-time histories with relation to fatigue tests and life calculations*, *Fatigue of Aircraft Structures*, Pergamon, 1963, p. 115–149, or National Luchtvaart Laboratorium, NLL Report MP 201, October 1960.
- [SCH 70] SCHIJVE J., "Cumulative damage problems in aircraft structures and materials", *The Aeronautical Journal of the Royal Aeronautical Society*, 74(714), 517–532, June 1970.
- [SCH 71] SCHIJVE J., "Fatigue tests with random flight-simulation loading, Advanced Approaches to Fatigue Evaluation", *Proc. 6th ICAF Symposium*, Miami Beach, 253–274, May 1971, NASA SP 309, 1972.
- [SCH 72a] SCHIJVE J., *The Accumulation of Fatigue Damage in Aircraft Materials and Structures*, AGARDograph, AG. 157, January 1972.
- [SCH 72b] SCHUTZ W., "The fatigue life under three different load spectra. Tests and calculations", *Symposium on Random Load Fatigue*, AGARD, CP.118, AD. 752 369, 7-1–7-11 October 1972.

- [SCH 72c] SCHIJVE J., "Effects of test frequency on fatigue crack propagation under flight – simulation loading", *Symposium on Random Load Fatigue*, AGARD CD no. 118, 4-1-4-1, 7 October 1972, AD 752369.
- [SCH 74] SCHUTZ W., "Fatigue life prediction of aircraft structures. Past, present and future", *Engineering Fracture Mechanics*, 6, 745–773, 1974.
- [SER 64] SERENSEN S.V., *Fatigue damage accumulation and safety factors under random variable loading*, Fatigue Resistance of Materials and Metal Structural Parts, A. BUCH (ed), Pergamon Press, 34–43, 1964.
- [SES 63] SESSLER J.G. and WEISS V., "Low cycle fatigue damage in pressure-vessel materials", *Journal of Basic Engineering*, 85, 539–547, Dec. 1963.
- [SEW 72] SEWELL R., *An investigation of flight loads, counting methods, and effects on estimated. fatigue life*, Soc. of Automotive Engineers, SAE Paper 720 305, National Business Aircraft Meeting, 15–17 March 1972, or *SAE 1412, LTR-ST 431*, October 1970.
- [SHA 52] SHANLEY F.R., *A theory of fatigue based on unbonding during reversed slip*, The Rand Corporation, Tech. Note P350, 11 November 1952.
- [SHA 59] SHANLEY F.G., "Discussion of methods of fatigue analysis", *WADC Symposium*, WADC TR 59-507, 182–206, 1959.
- [SHE 05] SHERRATT F., BISHOP N.W.M. and DIRLIK T., "Predicting fatigue life from frequency-domain data: current methods, Part A: Design requirements and modern methods", *Journal of the Engineering Integrity Society*, 18, 12–16, September 2005.
- [SHE 82] SHERRATT F., "Fatigue life estimation: a review of traditional methods", *Journal of the Society of Environmental Engineers*, 21-4(95), 23–30, December 1982.
- [SHE 83] SHERRAT F., "Vibration and fatigue: basic life estimation methods", *Journal of the Society of Environmental Engineers*, 22-4(99), 12–17, December 1983.
- [SHE 83a] SHERRATT F., "Fatigue life estimation using simple fracture mechanics", *Journal of the Society of Environmental Engineers*, 22(1), 23–35, March 1983.
- [SHI 66] SHINOZUKA M., Application of stochastic processes to fatigue, creep and catastrophic failures, Seminar in the Application of Statistics in Structural Mechanics, Department of Civil Engineering, Columbia University, 1 November 1966.
- [SHI 72] SHIGLEY J.E., *Mechanical Engineering Design*, McGraw-Hill, New York, 458–581, 1972.
- [SHI 80] SHIMOKAWA T. and TANAKA S., "A statistical consideration of Miner's rule", *Int. J. Fatigue*, 2(4), 165–170, October 1980.
- [SHI 83] SHIN Y.S. and LUKENS R.W., "Probability based high-cycle fatigue life prediction", *Random Fatigue Life Prediction, The 4th National Congress on Pressure Vessel and Piping Technology*, 72, 73–87, Portland, Oregon, 19–24 June 1983.
- [SIH 73] SIH G.C., *Handbook of Stress Intensity Factors for Researchers and Engineers*, Institute of Fracture and Solid Mechanics, Lehigh University, Bethlehem, 1973.
- [SIH 74] SIH G.C., "Strain-energy density factor applied to mixed mode crack problems", *International Journal of Fracture*, 10(3), 305–321, Sept. 1974.
- [SIN 53] SINCLAIR G.M. and DOLAN T.J., "Effect of stress amplitude on statistical variability in fatigue life of 75S-T6 Aluminium alloy", *Trans. ASME*, 75, 687–872, 1953.

- [SMA 65] SMALL E.F., "A unified philosophy of shock and vibration testing for guided missiles", *Proceedings IES*, 277–282, 1965.
- [SMI 42] SMITH J.O., The effect of range of stress on the fatigue strength of metals, University of Illinois, Engineering Experiment Station, Urbana, Bulletin no. 334, February 1942.
- [SMI 58] SMITH C.R., "Fatigue - service life prediction based on tests at constant stress levels", *Proc. SESA*, 16(1), 9, 1958.
- [SMI 63] SMITH P.W. and MALME C.I., "Fatigue tests of a resonant structure with random excitation", *Journal of the Acoustical Society of America*, 35(1), 43–46, January 1963.
- [SMI 63a] SMITH C.R., "Small specimen data for predicting life of full-scale structures", *Symp. Fatigue Tests of Aircraft Structures: Low-cycles Full-Scale and Helicopters*, Am. Soc. Testing Mats., STP 338, 241–250, 1963.
- [SMI 64a] SMITH K.W., "A procedure for translating measured vibration environment into laboratory tests", *Shock, Vibration and Associated Environments Bulletin*, 33(III), 159–177, March 1964.
- [SMI 64b] SMITH C.R., Linear strain theory and the SMITH method for predicting fatigue life of structures for spectrum type loading, Aerospace Research Laboratories, ARL 6455, AD 600 879, April 1964.
- [SMI 64c] SMITH S.H., "Fatigue crack growth under axial narrow and broad band random loading", in W.J. TRAPP and D.M. FORNEY Jr (eds), *Acoustical Fatigue in Aerospace Structures*, May 1964, Syracuse University Press, 331–360, 1965.
- [SMI 66] SMITH S.H., Random-loading fatigue crack growth behavior of some aluminum and titanium alloys, Structure Fatigue in Aircraft, ASTM STP 404, 74, 1966.
- [SMI 69] SMITH K.N., WATSON P. and TOPPER T.H., "A stress strain function for the fatigue of metals", Report 21, Solid Mechanics Division, University of Waterloo, Waterloo, Ontario, Canada, October 1969 or *J. of Mater.*, 5(4), 767–778, Dec. 1970.
- [SNE 46] SNEDDON I.N., "The distribution of stress in the neighbourhood of a crack in a elastic solid", *Proc. Royal Soc. of London*, A187, 229–260, 1946.
- [SOB 92] SOBCZYK K. and SPENCER B.F., *Random Fatigue: From Data to Theory*, Academic Press, Inc., 1992.
- [SOC 77] SOCIE D.F., "Fatigue-life prediction using local stress/strain concept", *Experimental Mechanics*, 17(2), 50–56, 1977.
- [SOC 83] SOCIE D.F. and KURATH P., "Cycle counting for variable-amplitude crack growth", *Fracture Mechanics: Fourteenth Symposium, Vol. II: Testing and Applications*, ASTM STP 791, p. II.19/II.32, 1983.
- [SOR 68] SORENSEN A., A general theory of fatigue damage accumulation, ASME 68, WA/MET-6, December 1968.
- [STA 57] STARKEY W.L. and MARCO S.M., "Effects of complex stress time cycles on the fatigue properties of metals", *Trans. ASME*, 79, 1329–1336, August 1957.
- [STE 73] STEINBERG D.S., *Vibration Analysis for Electronic Equipment*, John Wiley, 1973.
- [STR 14] STROMEYER C.E., "The determination of fatigue limits under alternating stress conditions" *Proc. Roy. Soc. London*, A90, 411–25, 1914.
- [STR 73] STRATTING J., Fatigue and stochastic loadings, Stevin Laboratory, Department of Civil Engineering, ICAF Doc. 683, 1973.

- [SUL 76] SULLIVAN A.M. and CROOKER T.W., "Analysis of fatigue-crack growth in a high-strength steel, Part I: Stress level and stress ratio effects at constant amplitude, Part II: Variable amplitude block loading effects", *Journal of Pressure Vessel Technology*, vol. 98, 179–184, 208–212, May 1976.
- [SVE 52] SVENSON O., „Unmittelbare Bestimmung der Grösse und Häufigkeit von Betriebsbeanspruchungen", *Transactions of Instruments and Measurements Conference*, Stockholm, 1952.
- [SWA 63] SWANSON S.R., An investigation of the fatigue of aluminum alloy due to random loading, Institute of Aerophysics, University of Toronto, UTIA Report, no. 84, AD 407071, February 1963.
- [SWA 67] SWANSON S.R., CICCIO F. and HOPPE W., "Crack propagation in Clad 7079-T6 aluminum alloy sheet under constant and random amplitude fatigue loading", *Fatigue Crack Propagation*, ASTM STP 415, 312, 1967.
- [SWA 68] SWANSON S.R., "Random load fatigue testing: a state of the art survey", *Materials Research and Standards*, ASTM, 8(4), April 1968.
- [SWA 69] SWANSON S.R., "A review of the current status of random load testing in America", *Proceedings of the 11th ICAF Meeting*, Stockholm, 2-3-1, 2-3-17, 1969.
- [SYL 81] SYLWAN O., Study in comparing the severity of design and test load spectra, Final Report, Work Package 1, Survey of Comparison Methods, Rept ESA-CR(8)1618, CTR-EXTEC 4627/81, November 1981, N83-13157/3.
- [TAD 73] TADA H., PARIS P.C. and IRWIN G.R., *The Stress Analysis of Cracks Handbook*, Del Research Corporation, Hellertown, Pennsylvania, June 1973.
- [TAN 70] TANG J.P. and YAO J.T.P., Random fatigue, A literature review, Bureau of Engineering Research, University of New Mexico, Albuquerque, TR-CE-22(70)-NSF-065, July 1970 (The Department of Civil Engineering).
- [TAN 72] TANAKA S. and AKITA S., "Statistical Aspects of Fatigue Life of Metals under Variable Stress Amplitudes", *Transactions of the Society of Mechanical Engineers Japan*, 38(313), 2185–2192, 1972.
- [TAN 75] TANAKA S. and AKITA S., "On the Miner's damage hypothesis in notched specimens with emphasis on scatter of fatigue life", *Eng. Fracture Mech.*, 7, 473–480, 1975.
- [TAN 78] TANG JHY-PYNG, "Prediction of structural random fatigue life", *Proc. Natl. Sci. Council*, ROC, 2(3), 300–307, 1978.
- [TAN 80] TANAKA S., ICHIKAWA M. and AKITA S., "Statistical aspects of the fatigue life of nickel-silver wire under two-level loading", *Int. J. Fatigue*, 2(4), 159–163, October 1980.
- [TAN 83] TANAKA K., "The cyclic J-integral as a criterion for fatigue crack growth", *International Journal of Fracture*, 22(2), 91–104, 1983.
- [TAV 59] TAVERNELLI J.F. and COFFIN L.F., "A compilation and interpretation of cyclic strain fatigue tests on metals", *Transactions, Am. Soc. Metals*, 51, 438–453, 1959.
- [TAV 62] TAVERNELLI J.F. and COFFIN L.F., "Experimental support for generalized equation predicting low cycle fatigue", *Journal of Basic Engineering, Transactions of the ASME*, 84, 533–541, Dec. 1962.
- [TAY 50] TAYLOR J., *Design and Use of Counting Accelerometers*, Aeronautical Research Council 2812, 1950.

- [TAY 53] TAYLOR J., "Measurement of gust loads in aircraft", *Journal of the Royal Aeronautical Society*, 57, 78–88, February 1953.
- [TED 73] TEDFORD J.D., CARSE A.M. and CROSSLAND B., "Comparison of component and small specimen block load fatigue test data", *Engineering Fracture Mechanics*, 5, 241–258, 1973.
- [TEI 41] TEICHMANN A., *Grundsätzliches zum Betriebsfestigkeitsversuch*, Jahrbuch der deutschen Luftfahrtforschung, p. 467, 1941.
- [TEI 55] TEICHMANN A., *The Strain Range Counter*, Vickers-Armstrong (Aircraft Ltd), Weybridge, Technical Office, VTO/M/46, April 1955.
- [THR 70] THROOP J.F. and MILLER G.A., "Optimum fatigue crack resistance" in *Achievement of High Fatigue Resistance in Metals and Alloys*, ASTM STP 467, pp. 154–168, 1970.
- [TIF 65] TIFFANY C.F. and MASTERS J.N., *Applied fracture mechanics*, ASTM STP 381, 249–278, 1965.
- [TIM 53] TIMOSHENKO S.P., *History of Strength of Materials*, McGraw-Hill, New York, 1953.
- [TOM 68] TOMKINS B., "Fatigue crack propagation – An analysis", *Phil. Mag.* 18, 1041–1066, 1968.
- [TOM 69] TOMKINS B. and BIGGS W.D., "Low endurance fatigue in metals and polymers, Part 3: The mechanisms of failure", *Journal of Materials Science*, 4, 544–553, 1969.
- [TOP 69] TOPPER T.H., SANDOR B.I. and MORROW J.D., "Cumulative fatigue damage under cyclic strain control", *Journal of Materials*, 4(1), 189–199, March 1969.
- [TOP 69a] TOPPER T.H., WETZEL R.M. and MORROW J.D., "Neuber's notch rule applied to fatigue of notched specimens", *ASTM Journal of Materials*, 4(1), 200–209, March 1969.
- [TOP 70] TOPPER T.H. and SANDOR B.I., Effects of mean stress and prestrain on fatigue damage summation, ASTM STP 462, 93–104, 1970.
- [TUC 74] TUCKER L.E., LANDGRAF R.W. and BROSE W.R., Proposed technical report on fatigue properties for the SAE Handbook, SAE Paper no. 740279, Feb. 1974.
- [TUC 77] TUCKER L., BUSSA S., *Fatigue Under Complex Loading: Analysis and Experiments*, 1st Edn. Society of Automotive Engineers, AE 6, Warrendale Pa., 1977, pp. 3–14.
- [TRO 58] TROTTER W.D., Fatigue of 2024.T3 Aluminium sheet under random loading, Boeing Airplane Co, Test Report no. T2.1601, November 1958.
- [TVE 03] TVEITEN B. W., The Fatigue Strength of RHS T-joints, SINTEF report STF24 A03220, Trondheim, 2003.
- [VAL 61a] VALLURI S.R., A theory of cumulative damage in fatigue, Report ARL 182, Calif. Inst. of Technol., December 1961.
- [VAL 61b] VALLURI S.R., "A unified engineering theory of high stress level fatigue", *Aerosp. Eng.*, 20, 18–19, 68–69, October 1961.
- [VAL 63] VALLURI S.R., GLASSCO T.B. and BROCKRATH G.E., "Further considerations concerning a theory of crack propagation in metal fatigue", *Trans. SAE*, Paper 752A, September 1963, Los Angeles, Douglas Aircraft Company, Inc., Engineering Paper no. EP-1695, Calif. Inst. of Technology, GalcIT SM 63 - 16, July 1963.

- [VAL 64] VALLURI S.R., GLASSCO T.B. and BROCKRATH G.E., "Further considerations concerning a theory of crack propagation in metal fatigue, engineering consequences especially at elevated temperatures", *AIAA*, Paper no. 64 - 443, Washington D.C., 29 June - 2 July 1964.
- [VAL 81] VALANIS K.C., "On the effect of frequency on fatigue life", in *Mechanics of Fatigue*, Winter Annual Meeting of the ASME, Washington D.C., AMD 47, T. Mura (ed), 21-32, Nov. 15-20, 1981.
- [VAN 71] VAN DIJK G.M., "Statistical load information processing. Advanced Approaches to Fatigue Evaluation", *Proc. 6th ICAF Symposium*, Miami Beach, May 1971, or NASA SP 309, 565-598, 1972.
- [VAN 72] VANMARCKE E.H., "Properties of spectral moments with applications to random vibration", *Journal of Engineering Mechanics Division*, ASCE, 98, 425-446, 1972 [AMR 26, 1973, Rev. 259].
- [VAN 75] VAN DIJK G.M. and DE JONGE J.B., "Introduction to a fighter aircraft loading standard for fatigue evaluation "FALSTAFF", Part I", *Proc. 8th ICAF Symp. Problems with Fatigue Aircraft*, Lausanne, or National Aerospace Laboratory, NRL MP 75017U, The Netherlands, 1975.
- [VER 56] VERHAGEN C.J.D.M. and DE DOES J.C., "A special stress analyser for use on board ship", *International Shipbuilding Progress*, Rotterdam, May 1956.
- [VIR 78] VIRKLER D.A., HILLBERRY B.M. and GOEL P.K., The statistical nature of fatigue crack propagation, AFFDL-TR-78-43, Air Force Flight Dynamics Laboratory, April 1978.
- [VIT 53] VITOVEC F.H. and LAZAN B.J., Review of previous work on short-time tests for predicting fatigue properties of materials, Wright Air Development Center, Tech. Report no. 53-122, August 1953.
- [VRO 71] VROMAN G.A., Analytical predictions of crack growth retardation using a residual stress intensity concept, North American Rockwell Co. Report, May 1971.
- [WAD 56] WADE A.R. and GROOTENHUIS P., "Very high-speed fatigue testing", *Internat. Conf. on Fatigue of Metals*, Inst. of Mech. Engrs and ASME, London, 361-369, 1956.
- [WAL 58] WALKER W.G. and COPP M.R., *Summary of VGH and V-G data obtained from piston-engine transport airplanes from 1947 to 1958*, NASA - TN D-29, September 1959.
- [WAL 83] WALKER E.K., Exploratory study of crack-growth-based inspection rationale, Probabilistic Fracture Mechanics and Fatigue Methods: Applications for Structural Design and Maintenance, ASTM-STP 798, 116-130, 1983.
- [WAT 62] WATERMAN L.T., "Random versus sinusoidal vibration damage levels", *The Shock and Vibration Bulletin*, 30(4), 128-139, 1962.
- [WAT 76] WATSON P. and DABELL B.J., "Cycle counting and fatigue damage", *Journal of the Society of Environmental Engineers*, 15.3(70), 3-8, September 1976.
- [WEB 66] WEBBER D., "Working stresses related to fatigue in military bridges", *Proc. Stresses in Service*, Institution for Civil Engineers, London, 237-247, 1966.
- [WEE 65] WEERTMAN J., "Rate of growth of fatigue cracks calculated from the theory of infinitesimal dislocations distributed on a plane", *Proc. 1st Int. Conf. Fracture*, Vol. 1, Japanese Society for Strength and Fracture Materials, Sendai, Japan, 153-164, 1965.

- [WEI 49] WEIBULL W., "A statistical representation of fatigue failures in solids", *Trans. Roy., Swed. Inst. Tech.* 27, 1949.
- [WEI 52] WEIBULL W. and WALODDI, "Statistical design of fatigue experiments", *Journal of Applied Mechanics*, 19(1), March 1952.
- [WEI 54] WEIBULL W., The propagation of fatigue cracks in light-alloy plates, SAAB Aircraft Co T.N. 25, Linköping, Sweden, Jan. 12, 1954.
- [WEI 60] WEIBULL W., Size effects on fatigue-crack initiation and propagation in aluminum sheet specimens subjected to stress of nearly constant amplitude, F.F.A. Report 86, Stockholm, June 1960.
- [WEI 71] WEI R.P. and Mc EVILY A.J., "Fracture mechanics and corrosion fatigue", NACE, *Conf. Proc. "Corrosion Fatigue"*, Storrs, Conn., USA, 381–395, 1971.
- [WEI 74] WEI R.P. and SHIH T.T., "Delay in fatigue crack growth", Noordhoff International Publishing, Leyden, *International Journal of Fracture*, 10(1), 77–85, March 1974.
- [WEI 78] WEI R.P., "Fracture mechanics approach to fatigue analysis in design", *Journal of Engineering Materials and Technology*, 100, 113–120, April 1978.
- [WEL 65] WELLS H.M., "Flight load recording for aircraft structural integrity", *AGARD Symposium on Flight Instrumentation*, Paris, September 1965, p. 127/140.
- [WES 39] WESTERGAARD H.M., "Bearing pressures and cracks", *Journal of Applied Mechanics*, 6, A49–A54, 1939.
- [WHE 72] WHEELER O.E., "Spectrum loading and crack growth", *Journal of Basic Engineering*, 94, 181–186, March 1972.
- [WHI 61] WHITMAN J.G., "Repeated rest periods in fatigue of mild steel bar", *The Engineer*, London, 211(5501), 1074–1076, 30 June 1961.
- [WHI 69] WHITE D.J., "Effect of truncation of peaks in fatigue testing using narrow band random loading", *International Journal of Mechanical Sciences*, 11(8), 667–675, August 1969.
- [WHIT 69] WHITTAKER I.C. and BESUNER P.M., *A reliability analysis approach to fatigue life variability of aircraft structures*, Wright Patterson Air Force Base, Technical Report AFML-TR-69-65, April 1969.
- [WHIT 72] WHITTAKER I.C., Development of titanium and steel fatigue variability model for application of reliability approach to aircraft structures, AFML-TR-72-236, Wright Patterson AFB, Ohio, October 1972.
- [WIL 57] WILLIAMS M.L., "On the stress distribution at the base of a stationary crack", *Journal of Applied Mechanics*, 24(1), 109–114, March 1957.
- [WIL 71] WILLENBORG J., ENGLE R.M. and WOOR H.A., A crack growth retardation model using an effective stress concept, Air Force Dynamics Laboratory, Wright-Patterson AFB, AFFDL Technical Memorandum 71-1-FBR, Jan. 1971.
- [WIR 76] WIRSCHING P.H. and YAO J.T.P., "A probabilistic design approach using the Palmgren-Miner hypothesis, methods of structural analysis", *ASCE*, 1, 324–339, 1976.
- [WIR 77] WIRSCHING P.H. and SHERATA A.M., "Fatigue under wide band random stresses using the rain-flow method", *Journal of Engineering Materials and Technology*, ASME, 99(3), 205–211, July 1977.
- [WIR 79] WIRSCHING P.H., *Fatigue reliability in welded joints of offshore structures*, Offshore Technology Conference, OTC 3380, 197–206, 1979.

- [WIR 80a] WIRSCHING P.H., "Digital simulation of fatigue damage in offshore structures", *Winter Annual Meeting of ASME*, Chicago, Ill, 16/21 November 1980, *ASME*, New York, 37, 69–76, 1980.
- [WIR 80b] WIRSCHING P.H., "Fatigue under wide band random stresses", *ASCE J. Struct. Div.*, 106(7), July 1980.
- [WIR 80c] WIRSCHING P.H., "Fatigue reliability in welded joints of offshore structures", *Int. J. Fatigue*, 2(2), 77–83, April 1980.
- [WIR 81] WIRSCHING P.H., The application of probabilistic design theory to high temperature low cycle fatigue, NASA.CR 165488, N.82-14531/9, November 1981.
- [WIR 82] WIRSCHING P.H. and YAO J.T.P., "Fatigue reliability: introduction", *ASCE Journal of the Structural Division*, 108(ST1), 3–23, January 1982.
- [WIR 83a] WIRSCHING P.H., Statistical summaries of fatigue data for design purposes, NASA - CR 3697, 1983.
- [WIR 83b] WIRSCHING P.H., Probability based fatigue design criteria for offshore structures, Final Project Report API-PRAC 81-15, The American Petroleum Institute, Dallas, TX, January 1983.
- [WIR 83c] WIRSCHING P.H. and WU Y.T., "A review of modern approaches to fatigue reliability analysis and design, 'Random Fatigue Life Prediction'", *The 4th National Congress on Pressure Vessel and Piping Technology*, Portland, Oregon, ASME - PVP, 72, 107–120, 19–24 June 1983.
- [WÖH 60] WÖHLER A., "Versuche über die Festigkeit der Eisenbahnwagen-Achsen", *Zeitschrift für Bauwesen*, 1860.
- [WÖH 70] WÖHLER A., "Über die Festigkeitsversuche mit Eisen und Stahl", *Zeitschrift für Bauwesen* 20, 1870.
- [WOO 71] WOOD H.A., "Fracture control procedures for aircraft structural integrity", *Advanced Approaches to Fatigue Evaluation, Proc. 6th ICAF Symposium*, Miami Beach, May 1971, 437–484, NASA SP 309, 1972.
- [WOO 73] WOOD H.A., "A summary of crack growth prediction techniques", *Agard Lecture Series* no. 62, *Fatigue Life Prediction for Aircraft Structures and Materials*, no. 73 29924 to 29934, May 1973.
- [WRI] WRISLEY D.L. and KNOWLES W.S., *Investigation of fasteners for mounting electronic components*, Report on Contract no. DA-36-039 SC-5545 between the Calidyne Co and SCEL, Ft. Monmouth, N.J.
- [YAN 72] YANG J.N., "Simulation of random envelop processes", *Journal of Sound and Vibrations*, 21, 73–85, 1972.
- [YAO 62] YAO J.T.P. and MUNSE W.H., "Low-cycle fatigue of metals. Literature review", *Welding Research Supplement*, 41, 182s–192s, April 1962.
- [YAO 62a] YAO J.T.P. and MUNSE W.H., Low-cycle axial fatigue behavior of mild steel, ASTM STP 338, 5–24, 1962.
- [YAO 72] YAO J.T.P. and SHINOZUKA., "Probabilistic structural design for repeated loads", *ASCE, Specialty Conference on Safety and Reliability of Metals Structures*, Pittsburgh, Pennsylvania, 371–397, 2–3 November 1972.
- [YAO 74] YAO J.T.P., "Fatigue reliability and design", *Journal of the Structural Division ASCE*, 100(ST 9), 1827–1836, September 1974.

- [YOK 65] YOKOBORI T., “The strength, fracture and fatigue of materials”, in *Strength, Fracture and Fatigue of Materials*, P. Noordhoff (ed), Groningen, Netherlands, 1965.
- [ZHA 92] ZHAO, W.W., BAKER M.J., “On the probability density function of rainflow stress range for stationary Gaussian processes”, *Int. J. Fatigue*, 14(2), 121–135, 1992.

Index

A

accommodation, 256
accumulation of fatigue damage, 47
acoustic transmission, 334
alternating
 stress, 4
 symmetric cycle, 4

B

b parameter, 199
Basquin, 265
 curve, 265
 relation, 22, 74, 129, 133, 143
Baushinger effect, 250
breaking
 materials, 325
 rupture, 294
brittle material, 12

C

closing factor, 362
coefficient
 C, 143
 K, 143
Coffin law, 266

Coffin-Manson curves, 264
combined steady and cyclic stress, 5
composite material, 290
constraint
 ratio, 3
 variation rate, 3
Corten-Dolan's law, 235
count method
 level-crossing, 100
 level-restricted peak, 79
 method, 71
 pair, 87, 92
 range-mean, 87, 246

 restricted peak, 79
 time spent at given level, 123
 zero crossings, 166
crack
 initiation, 296, 297
 propagation, 373
 propagation law, 336
 root of, 303, 311
cracking
 delay, 377, 359
 resistance, 325
Crandall's method, 150
critical value, 316, 333

curve

- endurance, 294
- resistance to fatigue, 264

cycle coefficient, 3

cyclic

- constraint, 2
- strain hardening coefficient, 263
- strain hardening, 251

D

damage, 47

- accumulation, 284
- accumulation law, 48
- failure, 147
- scatter, 53
- standard deviation, 205, 210

dampening energy, 28, 271

delay, 380

- cracking, 377, 359

diagram, Goodman, 107

Dirlik's probability density, 172

dispersion, 353

distribution

- factor, 33, 34
- law of peaks of response, 242
- fatigue strength, 16

E

elimination of small variations, 83

endurance

- curve, 10
- distribution, 14
- limit, 11
- ratio, 12
- zone, 15

energy dissipated by cycle, 272

equivalent narrow band noise, 153

error function, 141

expected fatigue life, 133

exponential distribution, 241, 244

F

failure

- cycles to, 146
- probability, 217

fatigue, 1

- ductility, 267
- failure, 180
- generalized, 283
- in composite materials, 46
- life, 45, 144, 187, 199
- limit, 11, 31, 75, 193, 229, 249

- notch sensitivity, 34

- oligocyclic, 249

- real corrosion, 330

- strength, 16

fatigue damage, 7, 72, 129, 205, 229

PSD, 132

- signal versus time, 130

fatigue-meter method, 80, 109

field of constraint, 4

fracture mechanics, 293

frequency 208

- influence of 280

- stresses, 35

G

gamma function, 140, 150, 383

- incomplete, 193, 231, 387

Gaussian distribution, 180, 241

Gerber parabola, 40

Goodman diagram

- modified, 239, 247

- line, modified, 40

Griffith criterion, 323

H

Haigh diagram, 40

- statistical, 45

hardening, 257

Hayes counting method, 96

Henry's method, 63

- modified 65

hysteresis, 7
 loop, 252
 hysteretic damping, 248

I

incomplete gamma function, 193,
 231, 387
 index
 damage to failure, 55
 fatigue curve, 23
 initiating, 256
 initiation of the crack, 296
 integral J, 357
 irregularity factor, 161

L

law, Paris, 333, 342
 level-crossing count method, 100
 level-restricted peak count method,
 79
 lifetime, 363, 379
 limited endurance zone, 11
 load
 collection, 377
 spectrum, 71
 low cycle fatigue, 9, 10, 249, 356,
 domain, 248
 low variations elimination, 125

M

mean damage per maximum, 146
 Miner, 49
 Miner's rule, 49, 57, 68, 129, 132,
 284
 modified, 59
 mode
 I, 301, 304
 II, 307
 III, 307
 Mohr circle, 309

N

narrow band, 372
 noise, 144, 191
 response, 140, 144, 153
 non-Gaussian distribution, 241
 non-linear damage accumulation,
 132, 235
 non-zero mean
 random vibration, 239
 stress, 36, 85
 normal distribution, 76
 notched test-bar, 34
 NRL counting method, 120
 nucleation, 296

O

oligocyclic fatigue, 249
 ordered overall range counting
 method, 97
 overload, 33
 effect, 359

P

PVP method, 104
 Pagoda roof method, 111
 parameter
 b, 24, 167
 r, 167, 189
 Paris
 law, 362
 relation, 335
 peak
 counting, 75
 distribution, 370
 histogram, 72
 truncation, 189
 plastic
 fracture, 294
 zone, 310, 371
 probability density
 crack propagation, 373
 ranges, 161
 propagation threshold, 354

PSD shape, 189
pulsating cycle, 4

R

RMS approach, 366
rainflow, 96
 method, 130, 153, 161, 166
 counting method, 111,
random load, 2, 6, 366
range
 count method, 84
 counting, 89
restricted peak count method, 79
range-mean count method, 87, 246
 pair count, 87, 92
rate
 deformation energy, 357
 elastic energy, 325
 propagation by block, 365
Rayleigh distribution, 154, 244, 247,
 366
 modified, 157
Rayleigh's probability density, 162
real corrosion fatigue, 330
relative damage, 373
repeated stress, 5
resistance
 cracking, 325
 fracture, 299
root of the crack, 303, 311

S

scale effect, 32
signal truncation, 195
similarity rules, 363
skewed alternating stress, 6
small variation elimination, 73, 78,
 86, 90
smooth test bar, 33
S-N curve, 10, 22, 129, 143, 179,
 184, 229
 layout for truncated distribution,
 199

 random, 126
 statistical, 220
Söderberg line, 40
softening, 257
specific dampening energy, 28, 271
spectral moment, 172
speed of propagation, 330
standard deviation of damage, 205,
 210

statistical Haigh diagram, 45
strain
 corrosion fatigue, 330
 deformation curve, 251
 gradient, 296
 hardening curve, 262
 intensity factor, 314, 352
stress spectrum, 71
stress peaks, 190
swept sine, 187
symmetric cycle, 4

T

temperature, influence of 280
test acceleration, 124
threshold, propagation, 332
threshold strain, intensity 332
truncation, 374
 stress peaks, 190

V

variation coefficient, 55, 212, 214
 damage, 206
 fatigue strength, 17
 number of cycles to failure, 15

W

Weibull distribution, 243
white noise, 143, 144
wide-band response, 138
Wöhler, 22, 294

Fatigue Damage: Second Edition – Volume 4

Christian Lalanne

Copyright © 2009, ISTE Ltd.

Summary of Other Volumes in the Series

Summary of Volume 1

Sinusoidal Vibration

Chapter 1. The Need

- 1.1. The need to carry out studies into vibrations and mechanical shocks
- 1.2. Some real environments
 - 1.2.1. Sea transport
 - 1.2.2. Earthquakes
 - 1.2.3. Road vibratory environment
 - 1.2.4. Rail vibratory environment
 - 1.2.5. Propeller airplanes
 - 1.2.6. Vibrations caused by jet propulsion airplanes
 - 1.2.7. Vibrations caused by turbofan aircraft
 - 1.2.8. Helicopters
- 1.3. Measuring vibrations
- 1.4. Filtering
 - 1.4.1. Definitions
 - 1.4.2. Digital filters
- 1.5. The frequency of a digitized signal
- 1.6. Reconstructing the sampled signal
- 1.7. Characterization in the frequency domain
- 1.8. Elaboration of the specifications
- 1.9. Vibration test facilities
 - 1.9.1. Electro-dynamic exciters
 - 1.9.2. Hydraulic actuators

Chapter 2. Basic Mechanics

- 2.1. Basic principles of mechanics
 - 2.1.1. Principle of causality

- 2.1.2. Concept of force
- 2.1.3. Newton's First law (inertia principle)
- 2.1.4. Moment of a force around a point
- 2.1.5. Fundamental principle of dynamics (Newton's second law)
- 2.1.6. Equality of action and reaction (Newton's third law)
- 2.2. Static effects/dynamic effects
- 2.3. Behavior under dynamic load (impact)
- 2.4. Elements of a mechanical system
 - 2.4.1. Mass
 - 2.4.2. Stiffness
 - 2.4.3. Damping
 - 2.4.4. Static modulus of elasticity
 - 2.4.5. Dynamic modulus of elasticity
- 2.5. Mathematical models
 - 2.5.1. Mechanical systems
 - 2.5.2. Lumped parameter systems
 - 2.5.3. Degrees of freedom
 - 2.5.4. Mode
 - 2.5.5. Linear systems
 - 2.5.6. Linear one-degree-of-freedom mechanical systems
- 2.6. Setting an equation for n degrees-of-freedom lumped parameter mechanical system
 - 2.6.1. Lagrange equations
 - 2.6.2. D'Alembert's principle
 - 2.6.3. Free-body diagram

Chapter 3. Response of a Linear One-Degree-of-Freedom Mechanical System to an Arbitrary Excitation

- 3.1. Definitions and notation
- 3.2. Excitation defined by force versus time
- 3.3. Excitation defined by acceleration
- 3.4. Reduced form
 - 3.4.1. Excitation defined by a force on a mass or by an acceleration of support
 - 3.4.2. Excitation defined by velocity or displacement imposed on support
- 3.5. Solution of the differential equation of movement
 - 3.5.1. Methods
 - 3.5.2. Relative response
 - 3.5.3. Absolute response
 - 3.5.4. Summary of main results
- 3.6. Natural oscillations of a linear one-degree-of-freedom system

- 3.6.1. Damped aperiodic mode
- 3.6.2. Critical aperiodic mode
- 3.6.3. Damped oscillatory mode

Chapter 4. Impulse and Step Responses

- 4.1. Response of a mass–spring system to a unit step function (step or indicial response)
 - 4.1.1. Response defined by relative displacement
 - 4.1.2. Response defined by absolute displacement, velocity or acceleration
- 4.2. Response of a mass–spring system to a unit impulse excitation
 - 4.2.1. Response defined by relative displacement
 - 4.2.2. Response defined by absolute parameter
- 4.3. Use of step and impulse responses
- 4.4. Transfer function of a linear one-degree-of-freedom system
 - 4.4.1. Definition
 - 4.4.2. Calculation of $H(h)$ for relative response
 - 4.4.3. Calculation of $H(h)$ for absolute response
 - 4.4.4. Other definitions of the transfer function

Chapter 5. Sinusoidal Vibration

- 5.1. Definitions
 - 5.1.1. Sinusoidal vibration
 - 5.1.2. Mean value
 - 5.1.3. Mean square value – rms value
 - 5.1.4. Periodic vibrations
 - 5.1.5. Quasi-periodic signals
- 5.2. Periodic and sinusoidal vibrations in the real environment
- 5.3. Sinusoidal vibration tests

Chapter 6. Response of a Linear One-Degree-of-Freedom Mechanical System to a Sinusoidal Excitation

- 6.1. General equations of motion
 - 6.1.1. Relative response
 - 6.1.2. Absolute response
 - 6.1.3. Summary
 - 6.1.4. Discussion
 - 6.1.5. Response to periodic excitation
 - 6.1.6. Application to calculation for vehicle suspension response
- 6.2. Transient response
 - 6.2.1. Relative response

- 6.2.2. Absolute response
- 6.3. Steady state response
 - 6.3.1. Relative response
 - 6.3.2. Absolute response
- 6.4. Responses $\left| \frac{\omega_0 \dot{z}}{\ddot{x}_m} \right|$, $\left| \frac{\omega_0 z}{\dot{x}_m} \right|$ and $\frac{\sqrt{k m} \dot{z}}{F_m}$
 - 6.4.1. Amplitude and phase
 - 6.4.2. Variations of velocity amplitude
 - 6.4.3. Variations in velocity phase
- 6.5. Responses $\frac{k z}{F_m}$ and $\frac{\omega_0^2 z}{\ddot{x}_m}$
 - 6.5.1. Expression for response
 - 6.5.2. Variation in response amplitude
 - 6.5.3. Variations in phase
- 6.6. Responses $\frac{y}{x_m}$, $\frac{\dot{y}}{\dot{x}_m}$, $\frac{\ddot{y}}{\ddot{x}_m}$ and $\frac{F_T}{F_m}$
 - 6.6.1. Movement transmissibility
 - 6.6.2. Variations in amplitude
 - 6.6.3. Variations in phase
- 6.7. Graphical representation of transfer functions

Chapter 7. Non-Viscous Damping

- 7.1. Damping observed in real structures
- 7.2. Linearization of non-linear hysteresis loops – equivalent viscous damping
- 7.3. Main types of damping
 - 7.3.1. Damping force proportional to the power b of the relative velocity
 - 7.3.2. Constant damping force
 - 7.3.3. Damping force proportional to the square of velocity
 - 7.3.4. Damping force proportional to the square of displacement
 - 7.3.5. Structural or hysteretic damping
 - 7.3.6. Combination of several types of damping
 - 7.3.7. Validity of simplification by equivalent viscous damping
- 7.4. Measurement of damping of a system
 - 7.4.1. Measurement of amplification factor at resonance
 - 7.4.2. Bandwidth or $\sqrt{2}$ method
 - 7.4.3. Decreased rate method (logarithmic decrement)
 - 7.4.4. Evaluation of energy dissipation under permanent sinusoidal vibration

- 7.4.5. Other methods
- 7.5. Non-linear stiffness

Chapter 8. Swept Sine

- 8.1. Definitions
 - 8.1.1. Swept sine
 - 8.1.2. Octave – number of octaves in frequency interval (f_1 , f_2)
 - 8.1.3. Decade
- 8.2. ‘Swept sine’ vibration in the real environment
- 8.3. ‘Swept sine’ vibration in tests
- 8.4. Origin and properties of main types of sweepings
 - 8.4.1. The problem
 - 8.4.2. Case 1: sweep where time Δt spent in each interval Δf is constant for all values of f_0
 - 8.4.3. Case 2: sweep with constant rate
 - 8.4.4. Case 3: sweep ensuring a number of identical cycles ΔN in all intervals Δf (delimited by the half-power points) for all values of f_0

Chapter 9. Response of a One-Degree-of-Freedom Linear System to a Swept Sine Vibration

- 9.1. Influence of sweep rate
- 9.2. Response of a linear one-degree-of-freedom system to a swept sine excitation
 - 9.2.1. Methods used for obtaining response
 - 9.2.2. Convolution integral (or Duhamel’s integral)
 - 9.2.3. Response of a linear one-degree-of freedom system to a linear swept sine excitation
 - 9.2.4. Response of a linear one-degree-of-freedom system to a logarithmic swept sine
- 9.3. Choice of duration of swept sine test
- 9.4. Choice of amplitude
- 9.5. Choice of sweep mode

Appendix: Laplace Transformations

Vibration Tests: a Brief Historical Background

Bibliography

Index

Summary of Volume 2

Mechanical Shock

Chapter 1. Shock Analysis

- 1.1. Definitions
 - 1.1.1. Shock
 - 1.1.2. Transient signal
 - 1.1.3. Jerk
 - 1.1.4. Simple (or perfect) shock
 - 1.1.5. Half-sine shock
 - 1.1.6. Versed sine (or haversine) shock
 - 1.1.7. Terminal peak sawtooth (TPS) shock
(or final peak sawtooth (FPS))
 - 1.1.8. Initial peak sawtooth (IPS) shock
 - 1.1.9. Square shock
 - 1.1.10. Trapezoidal shock
 - 1.1.11. Decaying sinusoidal pulse
 - 1.1.12. Bump test
 - 1.1.13. Pyroshock
- 1.2. Analysis in the time domain
- 1.3. Fourier transform
 - 1.3.1. Definition
 - 1.3.2. Reduced Fourier transform
 - 1.3.3. Fourier transforms of simple shocks
 - 1.3.4. What represents the Fourier transform of a shock?
 - 1.3.5. Importance of the Fourier transform
- 1.4. Energy spectrum
 - 1.4.1. Energy according to frequency
 - 1.4.2. Average energy spectrum
- 1.5. Practical calculations of the Fourier transform
 - 1.5.1. General

- 1.5.2. Case: signal not yet digitized
- 1.5.3. Case: signal already digitized
- 1.5.4. Adding zeros to the shock signal before the calculation of its Fourier transform
- 1.6. The interest of time-frequency analysis
 - 1.6.1. Limit of the Fourier transform
 - 1.6.2. Short term Fourier transform (STFT)
 - 1.6.3. Wavelet transform

Chapter 2. Shock Response Spectrum

- 2.1. Main principles
- 2.2. Response of a linear one-degree-of-freedom system
 - 2.2.1. Shock defined by a force
 - 2.2.2. Shock defined by an acceleration
 - 2.2.3. Generalization
 - 2.2.4. Response of a one-degree-of-freedom system to simple shocks
- 2.3. Definitions
 - 2.3.1. Response spectrum
 - 2.3.2. Absolute acceleration SRS
 - 2.3.3. Relative displacement shock spectrum
 - 2.3.4. Primary (or initial) positive SRS
 - 2.3.5. Primary (or initial) negative SRS
 - 2.3.6. Secondary (or residual) SRS
 - 2.3.7. Positive (or maximum positive) SRS
 - 2.3.8. Negative (or maximum negative) SRS
 - 2.3.9. Maximax SRS
- 2.4. Standardized response spectra
 - 2.4.1. Definition
 - 2.4.2. Half-sine pulse
 - 2.4.3. Versed sine pulse
 - 2.4.4. Terminal peak sawtooth pulse
 - 2.4.5. Initial peak sawtooth pulse
 - 2.4.6. Square pulse
 - 2.4.7. Trapezoidal pulse
- 2.5. Choice of the type of SRS
- 2.6. Comparison of the SRS of the usual simple shapes
- 2.7. SRS of a shock defined by an absolute displacement of the support
- 2.8. Influence of the amplitude and the duration of the shock on its SRS
- 2.9. Difference between SRS and extreme response spectrum (ERS)
- 2.10. Algorithms for calculation of the SRS
- 2.11. Subroutine for the calculation of the SRS

- 2.12. Choice of the sampling frequency of the signal
- 2.13. Example of use of the SRS
- 2.14. Use of SRS for the study of systems with several degrees of freedom

Chapter 3. Properties of Shock Response Spectra

- 3.1. Shock response spectra domains
- 3.2. Properties of SRS at low frequencies
 - 3.2.1. General properties
 - 3.2.2. Shocks with zero velocity change
 - 3.2.3. Shocks with $\Delta V = 0$ and $\Delta D \neq 0$ at the end of a pulse
 - 3.2.4. Shocks with $\Delta V = 0$ and $\Delta D = 0$ at the end of a pulse
 - 3.2.5. Notes on residual spectrum
- 3.3. Properties of SRS at high frequencies
- 3.4. Damping influence
- 3.5. Choice of damping
- 3.6. Choice of frequency range
- 3.7. Choice of the number of points and their distribution
- 3.8. Charts
- 3.9. Relation of SRS with Fourier spectrum
 - 3.9.1. Primary SRS and Fourier transform
 - 3.9.2. Residual SRS and Fourier transform
 - 3.9.3. Comparison of the relative severity of several shocks using their Fourier spectra and their shock response spectra
- 3.10. Care to be taken in the calculation of the spectra
 - 3.10.1. Main sources of errors
 - 3.10.2. Influence of background noise of the measuring equipment
 - 3.10.3. Influence of zero shift
- 3.11. Use of the SRS for pyroshocks

Chapter 4. Development of Shock Test Specifications

- 4.1. Introduction
- 4.2. Simplification of the measured signal
- 4.3. Use of shock response spectra
 - 4.3.1. Synthesis of spectra
 - 4.3.2. Nature of the specification
 - 4.3.3. Choice of shape
 - 4.3.4. Amplitude
 - 4.3.5. Duration
 - 4.3.6. Difficulties
- 4.4. Other methods
 - 4.4.1. Use of a swept sine
 - 4.4.2. Simulation of SRS using a fast swept sine

- 4.4.3. Simulation by modulated random noise
- 4.4.4. Simulation of a shock using random vibration
- 4.4.5. Least favorable response technique
- 4.4.6. Restitution of an SRS by a series of modulated sine pulses
- 4.5. Interest behind simulation of shocks on shaker using a shock spectrum

Chapter 5. Kinematics of Simple Shocks

- 5.1. Introduction
- 5.2. Half-sine pulse
 - 5.2.1. General expressions of the shock motion
 - 5.2.2. Impulse mode
 - 5.2.3. Impact mode
- 5.3. Versed sine pulse
- 5.4. Square pulse
- 5.5. Terminal peak sawtooth pulse
- 5.6. Initial peak sawtooth pulse

Chapter 6. Standard Shock Machines

- 6.1. Main types
- 6.2. Impact shock machines
- 6.3. High impact shock machines
 - 6.3.1. Lightweight high impact shock machine
 - 6.3.2. Medium weight high impact shock machine
- 6.4. Pneumatic machines
- 6.5. Specific testing facilities
- 6.6. Programmers
 - 6.6.1. Half-sine pulse
 - 6.6.2. TPS shock pulse
 - 6.6.3. Square pulse – trapezoidal pulse
 - 6.6.4. Universal shock programmer

Chapter 7. Generation of Shocks Using Shakers

- 7.1. Principle behind the generation of a signal with a simple shape versus time
- 7.2. Main advantages of the generation of shock using shakers
- 7.3. Limitations of electrodynamic shakers
 - 7.3.1. Mechanical limitations
 - 7.3.2. Electronic limitations
- 7.4. Remarks on the use of electrohydraulic shakers
- 7.5. Pre- and post-shocks
 - 7.5.1. Requirements

- 7.5.2. Pre-shock or post-shock
- 7.5.3. Kinematics of the movement for symmetric pre- and post-shock
- 7.5.4. Kinematics of the movement for a pre-shock or post-shock alone
- 7.5.5. Abacuses
- 7.5.6. Influence of the shape of pre- and post-pulses
- 7.5.7. Optimized pre- and post-shocks
- 7.6. Incidence of pre- and post-shocks on the quality of simulation
 - 7.6.1. General
 - 7.6.2. Influence of the pre- and post-shocks on the time history response of a one-degree-of-freedom system
 - 7.6.3. Incidence on the shock response spectrum

Chapter 8. Control of a Shaker Using a Shock Response Spectrum

- 8.1. Principle of control using a shock response spectrum
 - 8.1.1. Problems
 - 8.1.2. Parallel filter method
 - 8.1.3. Current numerical methods
- 8.2. Decaying sinusoid
 - 8.2.1. Definition
 - 8.2.2. Response spectrum
 - 8.2.3. Velocity and displacement
 - 8.2.4. Constitution of the total signal
 - 8.2.5. Methods of signal compensation
 - 8.2.6. Iterations
- 8.3. D.L. Kern and C.D. Hayes' function
 - 8.3.1. Definition
 - 8.3.2. Velocity and displacement
- 8.4. ZERD function
 - 8.4.1. Definition
 - 8.4.2. Velocity and displacement
 - 8.4.3. Comparison of ZERD waveform with standard decaying sinusoid
 - 8.4.4. Reduced response spectra
- 8.5. WAVSIN waveform
 - 8.5.1. Definition
 - 8.5.2. Velocity and displacement
 - 8.5.3. Response of a one-degree-of-freedom system
 - 8.5.4. Response spectrum
 - 8.5.5. Time history synthesis from shock spectrum
- 8.6. SHOC waveform
 - 8.6.1. Definition
 - 8.6.2. Velocity and displacement

- 8.6.3. Response spectrum
- 8.6.4. Time history synthesis from shock spectrum
- 8.7. Comparison of WAVSIN, SHOC waveforms and decaying sinusoid
- 8.8. Use of a fast swept sine
- 8.9. Problems encountered during the synthesis of the waveforms
- 8.10. Criticism of control by SRS
- 8.11. Possible improvements
 - 8.11.1. IES proposal
 - 8.11.2. Specification of a complementary parameter
 - 8.11.3. Remarks on the properties of the response spectrum
- 8.12. Estimate of the feasibility of a shock specified by its SRS
 - 8.12.1. C.D. Robbins and E.P. Vaughan's method
 - 8.12.2. Evaluation of the necessary force, power and stroke

Chapter 9. Simulation of Pyroshocks

- 9.1. Simulations using pyrotechnic facilities
- 9.2. Simulation using metal to metal impact
- 9.3. Simulation using electrodynamic shakers
- 9.4. Simulation using conventional shock machines

Appendix: Similitude in Mechanics

Mechanical Shock Tests: A Brief Historical Background

Bibliography

Index

Summary of Volume 3

Random Vibration

Chapter 1. Statistical Properties of a Random Process

- 1.1. Definitions
 - 1.1.1. Random variable
 - 1.1.2. Random process
- 1.2. Random vibration in real environments
- 1.3. Random vibration in laboratory tests
- 1.4. Methods of random vibration analysis
- 1.5. Distribution of instantaneous values
 - 1.5.1. Probability density
 - 1.5.2. Distribution function
- 1.6. Gaussian random process
- 1.7. Rayleigh distribution
- 1.8. Ensemble averages: through the process
 - 1.8.1. n order average
 - 1.8.2. Centered moments
 - 1.8.3. Variance
 - 1.8.4. Standard deviation
 - 1.8.5. Autocorrelation function
 - 1.8.6. Cross-correlation function
 - 1.8.7. Autocovariance
 - 1.8.8. Covariance
 - 1.8.9. Stationarity
- 1.9. Temporal averages: along the process
 - 1.9.1. Mean
 - 1.9.2. Quadratic mean – rms value
 - 1.9.3. Moments of order n
 - 1.9.4. Variance – standard deviation
 - 1.9.5. Skewness

- 1.9.6. Kurtosis
- 1.9.7. Temporal autocorrelation function
- 1.9.8. Properties of the autocorrelation function
- 1.9.9. Correlation duration
- 1.9.10. Cross-correlation
- 1.9.11. Cross-correlation coefficient
- 1.9.12. Ergodicity
- 1.10. Significance of the statistical analysis (ensemble or temporal)
- 1.11. Stationary and pseudo-stationary signals
- 1.12. Summary chart of main definitions
- 1.13. Sliding mean
- 1.14. Identification of shocks and/or signal problems
- 1.15. Breakdown of vibratory signal into “events”: choice of signal samples
- 1.16. Interpretation and taking into account of environment variation

Chapter 2. Random Vibration Properties in the Frequency Domain

- 2.1. Fourier transform
- 2.2. Power spectral density
 - 2.2.1. Need
 - 2.2.2. Definition
- 2.3. Cross-power spectral density
- 2.4. Power spectral density of a random process
- 2.5. Cross-power spectral density of two processes
- 2.6. Relationship between the PSD and correlation function of a process
- 2.7. Quadspectrum – cospectrum
- 2.8. Definitions
 - 2.8.1. Broad band process
 - 2.8.2. White noise
 - 2.8.3. Band-limited white noise
 - 2.8.4. Narrow band process
 - 2.8.5. Pink noise
- 2.9. Autocorrelation function of white noise
- 2.10. Autocorrelation function of band-limited white noise
- 2.11. Peak factor
- 2.12. Effects of truncation of peaks of acceleration signal on the PSD
- 2.13. Standardized PSD/density of probability analogy
- 2.14. Spectral density as a function of time
- 2.15. Relationship between the PSD of the excitation and the response of a linear system
- 2.16. Relationship between the PSD of the excitation and the cross-power spectral density of the response of a linear system
- 2.17. Coherence function

2.18. Transfer function calculation from random vibration measurements

- 2.18.1. Theoretical relations
- 2.18.2. Presence of noise on the input
- 2.18.3. Presence of noise on the response
- 2.18.4. Presence of noise on the input and response
- 2.18.5. Choice of transfer function

Chapter 3. Rms Value of Random Vibration

- 3.1. Rms value of a signal as a function of its PSD
- 3.2. Relationships between the PSD of acceleration, velocity and displacement
- 3.3. Graphical representation of the PSD
- 3.4. Practical calculation of acceleration, velocity and displacement rms values
 - 3.4.1. General expressions
 - 3.4.2. Constant PSD in frequency interval
 - 3.4.3. PSD comprising several horizontal straight line segments
 - 3.4.4. PSD defined by a linear segment of arbitrary slope
 - 3.4.5. PSD comprising several segments of arbitrary slopes
- 3.5. Rms value according to the frequency
- 3.6. Case of periodic signals
- 3.7. Case of a periodic signal superimposed onto random noise

Chapter 4. Practical Calculation of the Power Spectral Density

- 4.1. Sampling of signal
- 4.2. PSD calculation methods
 - 4.2.1. Use of the autocorrelation function
 - 4.2.2. Calculation of the PSD from the rms value of a filtered signal
 - 4.2.3. Calculation of the PSD starting from a Fourier transform
- 4.3. PSD calculation steps
 - 4.3.1. Maximum frequency
 - 4.3.2. Extraction of sample of duration T
 - 4.3.3. Averaging
 - 4.3.4. Addition of zeros
- 4.4. FFT
- 4.5. Particular case of a periodic excitation
- 4.6. Statistical error
 - 4.6.1. Origin
 - 4.6.2. Definition
- 4.7. Statistical error calculation
 - 4.7.1. Distribution of the measured PSD
 - 4.7.2. Variance of the measured PSD
 - 4.7.3. Statistical error

- 4.7.4. Relationship between number of degrees of freedom, duration and bandwidth of analysis
- 4.7.5. Confidence interval
- 4.7.6. Expression for statistical error in decibels
- 4.7.7. Statistical error calculation from digitized signal
- 4.8. Influence of duration and frequency step on the PSD
 - 4.8.1. Influence of duration
 - 4.8.2. Influence of the frequency step
 - 4.8.3. Influence of duration and of constant statistical error frequency step
- 4.9. Overlapping
 - 4.9.1. Utility
 - 4.9.2. Influence on the number of dofs
 - 4.9.3. Influence on statistical error
 - 4.9.4. Choice of overlapping rate
- 4.10. Information to provide with a PSD
- 4.11. Difference between rms values calculated from a signal according to time and from its PSD
- 4.12. Calculation of a PSD from a Fourier transform
- 4.13. Amplitude based on frequency: relationship with the PSD
- 4.14. Calculation of the PSD for given statistical error
 - 4.14.1. Case study: digitization of a signal is to be carried out
 - 4.14.2. Case study: only one sample of an already digitized signal is available
- 4.15. Choice of filter bandwidth
 - 4.15.1. Rules
 - 4.15.2. Bias error
 - 4.15.3. Maximum statistical error
 - 4.15.4. Optimum bandwidth
- 4.16. Probability that the measured PSD lies between \pm one standard deviation
- 4.17. Statistical error: other quantities
- 4.18. Peak hold spectrum
- 4.19. Generation of random signal of given PSD
 - 4.19.1. Random phase sinusoid sum method
 - 4.19.2. Inverse Fourier transform method
- 4.20. Using a window during the creation of a random signal from a PSD

Chapter 5. Statistical Properties of Random Vibration in the Time Domain

- 5.1. Distribution of instantaneous values
- 5.2. Properties of derivative process
- 5.3. Number of threshold crossings per unit time

- 5.4. Average frequency
- 5.5. Threshold level crossing curves
- 5.6. Moments
- 5.7. Average frequency of PSD defined by straight line segments
 - 5.7.1. Linear-linear scales
 - 5.7.2. Linear-logarithmic scales
 - 5.7.3. Logarithmic-linear scales
 - 5.7.4. Logarithmic-logarithmic scales
- 5.8. Fourth moment of PSD defined by straight line segments
 - 5.8.1. Linear-linear scales
 - 5.8.2. Linear-logarithmic scales
 - 5.8.3. Logarithmic-linear scales
 - 5.8.4. Logarithmic-logarithmic scales
- 5.9. Generalization: moment of order n
 - 5.9.1. Linear-linear scales
 - 5.9.2. Linear-logarithmic scales
 - 5.9.3. Logarithmic-linear scales
 - 5.9.4. Logarithmic-logarithmic scales

Chapter 6. Probability Distribution of Maxima of Random Vibration

- 6.1. Probability density of maxima
- 6.2. Expected number of maxima per unit time
- 6.3. Average time interval between two successive maxima
- 6.4. Average correlation between two successive maxima
- 6.5. Properties of the irregularity factor
 - 6.5.1. Variation interval
 - 6.5.2. Calculation of irregularity factor for band-limited white noise
 - 6.5.3. Calculation of irregularity factor for noise of form
 $G = \text{Const. } f b$
 - 6.5.4. Case study: variations of irregularity factor for two narrow band signals
- 6.6. Error related to the use of Rayleigh's law instead of a complete probability density function
- 6.7. Peak distribution function
 - 6.7.1. General case
 - 6.7.2. Particular case of a narrow band Gaussian process
- 6.8. Mean number of maxima greater than the given threshold (by unit time)
- 6.9. Mean number of maxima above given threshold between two times
- 6.10. Mean time interval between two successive maxima
- 6.11. Mean number of maxima above given level reached by signal excursion above this threshold
- 6.12. Time during which the signal is above a given value

- 6.13. Probability that a maximum is positive or negative
- 6.14. Probability density of the positive maxima
- 6.15. Probability that the positive maxima is lower than a given threshold
- 6.16. Average number of positive maxima per unit of time
- 6.17. Average amplitude jump between two successive extrema

Chapter 7. Statistics of Extreme Values

- 7.1. Probability density of maxima greater than a given value
- 7.2. Return period
- 7.3. Peak ℓ_p expected among N_p peaks
- 7.4. Logarithmic rise
- 7.5. Average maximum of N_p peaks
- 7.6. Variance of maximum
- 7.7. Mode (most probable maximum value)
- 7.8. Maximum value exceeded with risk α
- 7.9. Application to the case of a centered narrow band normal process
 - 7.9.1. Distribution function of largest peaks over duration T
 - 7.9.2. Probability that one peak at least exceeds a given threshold
 - 7.9.3. Probability density of the largest maxima over duration T
 - 7.9.4. Average of highest peaks
 - 7.9.5. Mean value probability
 - 7.9.6. Standard deviation of highest peaks
 - 7.9.7. Variation coefficient
 - 7.9.8. Most probable value
 - 7.9.9. Median
 - 7.9.10. Value of density at mode
 - 7.9.11. Expected maximum
 - 7.9.12. Average maximum
 - 7.9.13. Maximum exceeded with given risk α
- 7.10. Wide band centered normal process
 - 7.10.1. Average of largest peaks
 - 7.10.2. Variance of the largest peaks
 - 7.10.3. Variation coefficient
- 7.11. Asymptotic laws
 - 7.11.1. Gumbel asymptote
 - 7.11.2. Case study: Rayleigh peak distribution
 - 7.11.3. Expressions for large values of N_p
- 7.12. Choice of type of analysis
- 7.13. Study of the envelope of a narrow band process
 - 7.13.1. Probability density of the maxima of the envelope
 - 7.13.2. Distribution of maxima of envelope
 - 7.13.3. Average frequency of envelope of narrow band noise

Chapter 8. Response of a One-Degree-of-Freedom Linear System to Random Vibration

- 8.1. Average value of the response of a linear system
- 8.2. Response of perfect bandpass filter to random vibration
- 8.3. The PSD of the response of a one-dof linear system
- 8.4. Rms value of response to white noise
- 8.5. Rms value of response of a linear one-dof system subjected to bands of random noise
 - 8.5.1. Case where the excitation is a PSD defined by a straight line segment in logarithmic scales
 - 8.5.2. Case where the vibration has a PSD defined by a straight line segment of arbitrary slope in linear scales
 - 8.5.3. Case where the vibration has a constant PSD between two frequencies
 - 8.5.4. Excitation defined by an absolute displacement
 - 8.5.5. Case where the excitation is defined by PSD comprising n straight line segments
- 8.6. Rms value of the absolute acceleration of the response
- 8.7. Transitory response of a dynamic system under stationary random excitation
- 8.8. Transitory response of a dynamic system under amplitude modulated white noise excitation

Chapter 9. Characteristics of the Response of a One-Degree-of-Freedom Linear System to Random Vibration

- 9.1. Moments of response of a one-degree-of-freedom linear system: irregularity factor of response
 - 9.1.1. Moments
 - 9.1.2. Irregularity factor of response to noise of a constant PSD
 - 9.1.3. Characteristics of irregularity factor of response
 - 9.1.4. Case of a band-limited noise
- 9.2. Autocorrelation function of response displacement
- 9.3. Average numbers of maxima and minima per second
- 9.4. Equivalence between the transfer functions of a bandpass filter and a one-dof linear system
 - 9.4.1. Equivalence suggested by D.M. Aspinwall
 - 9.4.2. Equivalence suggested by K.W. Smith
 - 9.4.3. Rms value of signal filtered by the equivalent bandpass filter

Chapter 10. First Passage at a Given Level of Response of a One-Degree-of-Freedom Linear System to a Random Vibration

- 10.1. Assumptions
- 10.2. Definitions

- 10.3. Statistically independent threshold crossings
- 10.4. Statistically independent response maxima
- 10.5. Independent threshold crossings by the envelope of maxima
- 10.6. Independent envelope peaks
 - 10.6.1. S.H. Crandall method
 - 10.6.2. D.M. Aspinwall method
- 10.7. Markov process assumption
 - 10.7.1. W.D. Mark assumption
 - 10.7.2. J.N. Yang and M. Shinozuka approximation
- 10.8. E.H. Vanmarcke model
 - 10.8.1. Assumption of a two state Markov process
 - 10.8.2. Approximation based on the mean clump size

Appendices

Bibliography

Index

Summary of Volume 5

Specification Development

Chapter 1. Extreme Response Spectrum of a Sinusoidal Vibration

- 1.1. The effects of vibration
- 1.2. Extreme response spectrum of a sinusoidal vibration
 - 1.2.1. Definition
 - 1.2.2. Case of a single sinusoid
 - 1.2.3. Case of a periodic signal
 - 1.2.4. General case
- 1.3. Extreme response spectrum of a swept sine vibration
 - 1.3.1. Sinusoid of constant amplitude throughout the sweeping process
 - 1.3.2. Swept sine composed of several constant levels

Chapter 2. Extreme Response Spectrum of a Random Vibration

- 2.1. Unspecified vibratory signal
- 2.2. Gaussian stationary random signal
 - 2.2.1. Calculation from peak distribution
 - 2.2.2. Use of the largest peak distribution law
 - 2.2.3. Response spectrum defined by k times the rms response
 - 2.2.4. Other ERS calculation methods
- 2.3. Limit of the ERS at the high frequencies
- 2.4. Response spectrum with up-crossing risk
 - 2.4.1. Complete expression
 - 2.4.2. Approximate relation
 - 2.4.3. Calculation in a hypothesis of independence of threshold overshoot
 - 2.4.4. Use of URS
- 2.5. Comparison of the various formulae
- 2.6. Effects of peak truncation on the acceleration time history

- 2.6.1. Extreme response spectra calculated from the time history signal
- 2.6.2. Extreme response spectra calculated from the power spectral densities
- 2.6.3. Comparison of extreme response spectra calculated from time history signals and power spectral densities
- 2.7. Sinusoidal vibration superimposed on a broad band random vibration
 - 2.7.1. Real environment
 - 2.7.2. Case of a single sinusoid superimposed to a wide band noise
 - 2.7.3. Case of several sinusoidal lines superimposed on a broad band random vibration
- 2.8. Swept sine superimposed on a broad band random vibration
 - 2.8.1. Real environment
 - 2.8.2. Case of a single swept sine superimposed to a wide band noise
 - 2.8.3. Case of several swept sines superimposed on a broad band random vibration
- 2.9. Swept narrow bands on a wide band random vibration
 - 2.9.1. Real environment
 - 2.9.2. Extreme response spectrum

Chapter 3. Fatigue Damage Spectrum of a Sinusoidal Vibration

- 3.1. Fatigue damage spectrum definition
- 3.2. Fatigue damage spectrum of a single sinusoid
- 3.3. Fatigue damage spectrum of a periodic signal
- 3.4. General expression for the damage
- 3.5. Fatigue damage with other assumptions on the S–N curve
 - 3.5.1. Taking account of fatigue limit
 - 3.5.2. Cases where the S–N curve is approximated by a straight line in log-lin scales
 - 3.5.3. Comparison of the damage when the S–N curves are linear in either log-log or log-lin scales
- 3.6. Fatigue damage generated by a swept sine vibration on a single degree-of-freedom linear system
 - 3.6.1. General case
 - 3.6.2. Linear sweep
 - 3.6.3. Logarithmic sweep
 - 3.6.4. Hyperbolic sweep
 - 3.6.5. General expressions for fatigue damage
- 3.7. Reduction of test time
 - 3.7.1. Fatigue damage equivalence in the case of a linear system
 - 3.7.2. Method based on fatigue damage equivalence according to Basquin's relationship
- 3.8. Remarks on the design assumptions of the ERS and FDS

Chapter 4. Fatigue Damage Spectrum of a Random Vibration

- 4.1. Fatigue damage spectrum from the signal as function of time
- 4.2. Fatigue damage spectrum derived from a power spectral density
- 4.3. Simplified hypothesis of Rayleigh's law
- 4.4. Calculation of the fatigue damage spectrum with Dirlik's probability density
- 4.5. Reduction of test time
 - 4.5.1. Fatigue damage equivalence in the case of a linear system
 - 4.5.2. Method based on a fatigue damage equivalence according to Basquin's relationship taking account of variation of natural damping as a function of stress level
- 4.6. Truncation of the peaks of the 'input' acceleration signal
 - 4.6.1. Fatigue damage spectra calculated from a signal as a function of time
 - 4.6.2. Fatigue damage spectra calculated from power spectral densities
 - 4.6.3. Comparison of fatigue damage spectra calculated from signals as a function of time and power spectral densities
- 4.7. Sinusoidal vibration superimposed on a broad band random vibration
 - 4.7.1. Case of a single sinusoidal vibration superimposed on broad band random vibration
 - 4.7.2. Case of several sinusoidal vibrations superimposed on a broad band random vibration
- 4.8. Swept sine superimposed on a broad band random vibration
 - 4.8.1. Case of one swept sine superimposed on a broad band random vibration
 - 4.8.2. Case of several swept sines superimposed on a broad band random vibration
- 4.9. Swept narrow bands on a broad band random vibration

Chapter 5. Fatigue Damage Spectrum of a Shock

- 5.1. General relationship of fatigue damage
- 5.2. Use of shock response spectrum in the impulse zone
- 5.3. Damage created by simple shocks in static zone of the response spectrum

Chapter 6. Influence of Calculation Conditions of ERSs and FDSs

- 6.1. Variation of the ERS with amplitude and vibration duration
- 6.2. Variation of the FDS with amplitude and duration of vibration
- 6.3. Should ERSs and FDSs be drawn with a linear or logarithmic frequency step?
- 6.4. With how many points must ERSs and FDSs be calculated?
- 6.5. Difference between ERSs and FDSs calculated from a vibratory signal according to time and from its PSD

- 6.6. Influence of the number of PSD calculation points on ERS and FDS
- 6.7. Influence of the PSD statistical error on ERS and FDS
- 6.8. Influence of the sampling frequency during ERS and FDS calculation from a signal based on time
- 6.9. Influence of the peak counting method
- 6.10. Influence of a non-zero mean stress on FDS

Chapter 7. Tests and Standards

- 7.1. Definitions
 - 7.1.1. Standard
 - 7.1.2. Specification
- 7.2. Types of tests
 - 7.2.1. Characterization test
 - 7.2.2. Identification test
 - 7.2.3. Evaluation test
 - 7.2.4. Final adjustment/development test
 - 7.2.5. Prototype test
 - 7.2.6. Pre-qualification (or evaluation) test
 - 7.2.7. Qualification
 - 7.2.8. Qualification test
 - 7.2.9. Certification
 - 7.2.10. Certification test
 - 7.2.11. Stress screening test
 - 7.2.12. Acceptance or reception
 - 7.2.13. Reception test
 - 7.2.14. Qualification/acceptance test
 - 7.2.15. Series test
 - 7.2.16. Sampling test
 - 7.2.17. Reliability test
- 7.3. What can be expected from a test specification?
- 7.4. Specification types
 - 7.4.1. Specification requiring *in situ* testing
 - 7.4.2. Specifications derived from standards
 - 7.4.3. Current trend
 - 7.4.4. Specifications based on real environment data
- 7.5. Standards specifying test tailoring
 - 7.5.1. The MIL-STD 810 standard
 - 7.5.2. The GAM.EG 13 standard
 - 7.5.3. STANAG 4370
 - 7.5.4. The AFNOR X50–410 standard

Chapter 8. Uncertainty Factor

- 8.1. Need – definitions
- 8.2. Sources of uncertainty
- 8.3. Statistical aspect of the real environment and of material strength
 - 8.3.1. Real environment
 - 8.3.2. Material strength
- 8.4. Statistical uncertainty factor
 - 8.4.1. Definitions
 - 8.4.2. Calculation of uncertainty factor
 - 8.4.3. Calculation of an uncertainty coefficient when the real environment is only characterized by a single value

Chapter 9. Aging Factor

- 9.1. Purpose of the aging factor
- 9.2. Aging functions used in reliability
- 9.3. Method for calculating aging factor
- 9.4. Influence of standard deviation of the aging law
- 9.5. Influence of the aging law mean

Chapter 10. Test Factor

- 10.1. Philosophy
- 10.2. Calculation of test factor
 - 10.2.1. Normal distributions
 - 10.2.2. Log-normal distributions
 - 10.2.3. Weibull distributions
- 10.3. Choice of confidence level
- 10.4. Influence of the number of tests n

Chapter 11. Specification Development

- 11.1. Test tailoring
- 11.2. Step 1: Analysis of the life cycle profile. Review of the situations
- 11.3. Step 2: Determination of the real environmental data associated with each situation
- 11.4. Step 3: Determination of the environment to be simulated
 - 11.4.1. Need
 - 11.4.2. Synopsis methods
 - 11.4.3. The need for a reliable method
 - 11.4.4. Synopsis method using power spectrum density envelope
 - 11.4.5. Equivalence method of extreme response and fatigue damage
 - 11.4.6. Synopsis of the real environment associated with an event (or sub-situation)

- 11.4.7. Synopsis of a situation
- 11.4.8. Synopsis of all life profile situations
- 11.4.9. Search for a random vibration of equal severity
- 11.4.10. Validation of duration reduction
- 11.5. Step 4: Establishment of the test program
 - 11.5.1. Application of a test factor
 - 11.5.2. Choice of the test chronology
- 11.6. Applying this method to the example of the 'round robin' comparative study
- 11.7. Taking environment into account in project management

Chapter 12. Influence of Calculation Conditions of Specification

- 12.1. Choice of the number of points in the specification (PSD)
- 12.2. Influence of Q factor on specification (outside of time reduction)
- 12.3. Influence of Q factor on specification when duration is reduced
- 12.4. Validity of a specification established for Q factor equal to 10 when the real structure has another value
- 12.5. Advantage in the consideration of a variable Q factor for the calculation of ERSs and FDSs
- 12.6. Influence of the value of parameter b on the specification
 - 12.6.1. Case where test duration is equal to real environment duration
 - 12.6.2. Case where duration is reduced
- 12.7. Choice of the value of parameter b in the case of material made up of several components.
- 12.8. Influence of temperature on parameter b and constant C
- 12.9. Importance of a factor of 10 between the specification FDS and the reference FDS (real environment) in a small frequency band
- 12.10. Validity of a specification established by reference to a 1 dof system when real structures are multi dof systems

Chapter 13. Other Uses of Extreme Response Up-Crossing Risk and Fatigue Damage Spectra

- 13.1. Comparisons of the severity of different vibrations
 - 13.1.1. Comparisons of the relative severity of several real environments
 - 13.1.2. Comparison of the severity of two standards
 - 13.1.3. Comparison of seism severity
- 13.2. Swept sine excitation – random vibration transformation
- 13.3. Definition of a random vibration with the same severity as a series of shocks

13.4. Writing a specification only from an ERS (or a URS)

13.4.1. Matrix inversion method

13.4.2. Method by iteration

13.5. Establishment of a swept sine vibration specification

Appendices

Formulae

Index